Petrology and Geochemistry of Upper Carboniferous – Lower Permian Volcanic Rocks in Scotland

Susan M. Wallis

Thesis submitted for the degree of Doctor of Philosophy

University of Edinburgh

1989

DECLARATION

I declare that this thesis is my own work except where otherwise stated.

Susan M. Wallis

ABSTRACT

The volcanic rocks considered in this thesis represent the later stages of a volcanic event which affected southern Scotland throughout the Carboniferous and early Permian. Magmatism was dominated by alkaline to transitional compositions, with a short tholeiitic period in the late Stephanian - early Permian. Both groups are relatively unevolved: the alkaline samples range from basalt and basanite to hawaiite, and the quartz dolerites from basalt to rare basaltic andesite.

Phenoncryst assemblages comprise olivine $\pm$ clinopyroxene with occasional plagioclase in the more evolved samples. Clinopyroxenes are diopsidic salites or augites and many show appreciable Ca-Tschermak's molecule substitution reflecting the degree of magma undersaturation. Al^{iv}/Al^{vi} ratios attest to a range of crystallisation pressures with the highest pressures (10-20kb) indicated by clinopyroxenes from the Highland dykes and Fife & Lothian basanites. The preservation of high-pressure phenocrysts and olivine and clinopyroxene xenocrysts indicates high rates of ascent for many of the magmas, with little or no residence time in high level magma reservoirs. Major and compatible trace element concentrations have been controlled by fractional crystallisation, constrained by calculations to <36%.

Incompatible trace element and REE concentrations indicate a narrow range of melting for the alkaline samples. Y and HREE concentrations suggest buffering by residual garnet, and pronounced negative K and Rb chondrite-normalised anomalies imply that phlogopite was also a minor residual phase. Flatter chondrite-normalised profiles for the quartz dolerites indicate a larger degree of melting for these magmas, although average Y and HREE contents are very similar to those of the alkaline samples, suggesting that melting had not proceeded to a point at which garnet was consumed. However, a trend of increasing Ce/Y with increasing Zr/Nb for these samples apparently contradicts this observation.

Partial melting models suggest that the post-Dinantian suite must represent the result of mixing between melts from at least two sources. The absence of a hot-spot trail across the Midland Valley despite a long period of intraplate volcanism and rapid plate movements argues against the involvement of a deep-seated mantle plume. Lithospheric mantle sources require impossibly

large degrees of melting to produce realistic incompatible element concentrations (and are unlikely to melt without melting of the asthenosphere). By elimination it is suggested that the post-Dinantian basalts represent partial melts from a heterogeneous (streaky) asthenospheric source.

Relatively low $^{87}Sr/^{86}Sr_t$ ratios (0.7032-0.7049) and high $^{143}Nd/^{144}Nd_t$ ratios (0.5122-0.5126) indicate that crustal contamination has been of minor importance. Isotopic and elemental variations within the post-Dinantian samples are consistent with variable degree melting of a heterogeneous (streaky) asthenospheric mantle source. However, trends of increasing $^{87}Sr/^{86}Sr$ and decreasing $^{143}Nd/^{144}Nd$ with progressive melting suggest minor lithospheric contributions to the Mauchline melts.

Comparison of the post-Dinantian compositions with data for the Dinantian groups allows the identification of a lithospheric component in many of these older lavas. It is suggested that they represent the result of mixing between small degree (<3%) partial melts from the asthenosphere and even smaller degree melts (<1%) from the lithosphere. A synthesis of magmatism in the Midland Valley throughout the Carboniferous and Permian suggests that during the Dinantian, asthenospheric melts were affected by significant lithospheric mantle interaction. The younger larger-scale melting event which produced the quartz dolerites effectively exhausted any remaining enrichments at the base of the lithosphere leaving only refractory phases less likely to contribute to the late Stephanian - Permian melts. The absence of quartz dolerites in Ayrshire allowed the preservation of isotopic enrichments at the base of the lithosphere which were sampled by some of the Mauchline magmas.

ACKNOWLEDGEMENTS

This research was carried out during the tenure of a studentship from NERC, receipt of which is gratefully acknowledged. For their supervision and direction, thanks are extended to Brian Upton and Godfrey Fitton.

Brian Upton and Peder Aspen are thanked for introducing me to the igneous rocks of the Midland Valley - their knowledge of specific localities has been invaluable and both of them provided me with much appreciated field assistance and sherpa services!

Invaluable analytical assistance and advice was provided by Dodie James and Godfrey Fitton (XRF); Pete Hill, Stuart Kearns and John Craven (electron Microprobe); the staff of the Radiogenic Isotope Unit SURRC, East Kilbride (Sr, Nd & Ar mass spectrometry); and Nick Walsh and the staff of the Geochemistry Lab at Royal Holloway and Bedford New College (I.C.P. analysis). Pete Winterburn is especially thanked for his help with sample preparation.

Diane Batty and Yvonne Cooper are thanked for their advice and help concerning drafting and all things photographic; and for patient, good humoured help with the plotting of 'not more graphs', Pete Lithgrow, John Clarke, Dave Milne and Lilas Howarth (E.R.C.C. Job reception staff) are also thanked.

This research has benefited greatly from informal discussions with many people, most notably, Dodie James, Dave Latin, Hugh Nicholson, Pauline Smedley and Pete Winterburn (as well as Brian and Godfrey!); and Gordon Biggar is thanked for his reorganisation of Chapter 4.

A cast of many, starring in order of appearance, the Bethunes, Schulgas, Mackenzies, Simpsons and Vandersteens is thanked for proof-reading - no more problems with insomnia! For dotting the Figs. tabulating appendices, and sorting out references in the last minute rush, family (Mum, Dad, Liz and Anne) and friends (Nicola Dobie, Hugh Nicholson and Johanna Thorlacius) are thanked. Photocopying services were expertly provided by Kenneth and Jennifer Beall at 'Print on Tyne Ltd'.

Special appreciation is extended to my 'office-mates' Claire Linklater, Edward Follows and Johanna Thorlacius for making Research Room IV such a memorable experience; and to Hazel Barr, Andy Poole, Dave Walker, Dave Whitmarsh, Tracy Watson, Nana Kolocotroni, Pete Clift, and many of the

previously mentioned people, whose friendship and good humour have made the Grant Institute such an enjoyable place in which to work.

Last, but by no means least, a thank you to the Mackenzie Family (Colin, Rosemary, Morag, Donald and Iain) for sharing their home with me for my last two months in Edinburgh.

This thesis is dedicated to my parents with appreciation for their constant love, support and encouragement.

TABLE OF CONTENTS

CHAPTER 1

INTRODUCTION

1.1. Overview

A common aim of all petrogenetic studies of temporally and spatially related igneous suites is the evaluation of the processes involved in their genesis. Partial melting processes are of fundamental interest; however, their modelling is only possible if the post-melting effects of fractional crystallisation, magma mixing, contamination and alteration can be constrained. Trace element and isotope data allow the assessment of such processes, and provide some insight into the chemical and isotopic nature of the mantle.

The Scottish post-Dinantian rocks comprise a suite of transitional to alkaline basalts, basaltic hawaiites, hawaiites and basanites. Their restricted range of differentiation and the frequent occurrence of included mantle xenoliths attest to their primitive nature. As such they lend themselves to a detailed petrogenetic study, allowing constraints to be placed on partial melting processes.

Carboniferous - Permian igneous rocks in Scotland outcrop in a province which comprises the Southern Uplands, the Midland Valley and the Western Highlands. However, this chapter concentrates on the Midland Valley Suite since magmatic activity was at its greatest here. Outcrops from north and south of the area are described in chapter 2.

The Midland Valley of Scotland is approximately 65km wide, bounded to the north and south by the Highland Boundary and Southern Uplands faults respectively. It has maintained an aspect of low relief in comparison to the Grampian Highlands and Southern Uplands from its initiation as a graben structure in the late Silurian or early Devonian. It was the site of spasmodic magmatic activity through the Carboniferous and early Permian, and it is the igneous rocks from the latter part of this period (Silesian to Autunian) which form the basis of this thesis. They outcrop in two main areas within the Midland Valley. Exposure in the east is confined to the Regions of Fife and Lothian, and in the west, to the southern part of the Strathclyde Region. In this account the latter area is referred to by its older name of Ayrshire. The following sections describe first the general plate tectonic environment of

northern Europe through Carboniferous and early Permian times. The volcano-tectonic environment of the Midland Valley is then outlined in more detail; this is followed by a description of the outcrops and a discussion of nomenclature. The final section gives a brief account of previous research.

1.2. European volcano-tectonic setting

Tectonic processes in the Midland Valley during the Upper Palaeozoic have been related to the suturing of Laurasia and then Pangaea. These processes were intermittently active until early Permian times (Ziegler, 1978, 1982, 1984) and are outlined below.

East-west convergence of the Laurentian-Greenland (Laurentia) and Fennoscandian-Russian (Baltica) cratons during the late Silurian resulted in the closure of the Iapetus Ocean, and the formation of the new continent of Laurasia. Subduction appears to have given way to transcurrent faulting with the development of the Arctic-North Atlantic wrench system in the Devonian (Ziegler, 1982). In Britain this is represented by the Great Glen Fault, although it is possible that transcurrent movements at this time also initiated or reactivated faulting along the Southern Upland and Highland Boundary Faults (Kennedy, 1958; George, 1960; Ziegler, 1978; Bluck, 1978, 1980). Whether the Midland Valley developed as a graben in response to post-orogenic differential uplift and subsidence (Kennedy, 1958; George, 1960; Leeder, 1976; Francis, 1978a,b; Ziegler, 1978), or was superimposed on a late Silurian fore-arc basin (Leeder, 1982; Ziegler, 1982), it was clearly a subsiding basin by early Devonian times. Subsidence of the northern British basins was accompanied by extensive calc-alkaline magmatism (Francis, 1978a; Ziegler, 1978, 1982), some of which is thought to pre-date the cessation of active subduction (Thirlwall, 1981; Leeder, 1982), and the Southern Uplands and Scottish Highlands were sites of plutonic activity.

Basin subsidence continued throughout the Devonian with maximum rates of subsidence in the early Carboniferous. The major tectonic influences on the Arctic - North Atlantic craton (and therefore Britain) during the Carboniferous originated far to the south. They were the result of collision between Africa (Gondwanaland) and Euro-North America (Laurasia) (Leeder, 1988b; Ziegler, 1982,1984).

Continued northerly subduction of the Proto-Tethys plate beneath northern

Europe resulted in subsidence and rifting of the Cornwall-Rhenish and Central Armorican-Saxothuringian back-arc basins (Leeder, 1976, 1982; Ziegler, 1978, 1982, 1984). Volcanic activity in these basins was at its most intense during the mid-Devonian, with the extrusion of submarine alkaline felsic and mafic lavas. It abated in the late Devonian (Ziegler, 1978), to be resumed again during the Dinantian. This renewal of volcanic activity correlates with the onset of magmatism in the Arctic-North Atlantic Craton (Fig. 1.1). Outcrops in England (Midlands and Derbyshire) preserve records of both alkaline and tholeiitic magma types (Upton, 1982; Kirkton, 1984; Macdonald *et al*, 1984). However, further away from the European collision zone, in the Northumberland-Solway Basin, Dublin Trough and Midland Valley, magmatism was confined to transitional and alkaline types (Upton, 1982; Smedley, 1986a,b). The Proto-Tethys Ocean had been consumed at its western limits by late Visean to early Namurian times and the Laurasian and Gondwanan continents began to collide (Ziegler, 1982). Advancing thrust sheets transformed the Cornwall-Rhenish and Central Amorican-Saxthuringian back-arc basins into fore-deep basins, heralding the onset of the main Variscan orogenic phase (Ziegler, 1982).

The tectonic influences of this orogeny on the northern foreland have been debated by many authors. Some have proposed oblique closure of the Proto-Tethys Ocean with Africa sliding dextrally past Europe (Arthaud & Matte, 1977; Badham, 1982; Dewey, 1982), others favour a rifting setting during the Carboniferous. Leeder (1976, 1982) and Leeder & McMahon (1978) attributed Dinantian magmatism to N-S back-arc tension, which reactivated Caledonian NE/SW faults and created new E-W faults. Their attribution of late Carboniferous subsidence to thermal cooling fails to explain the continuation of alkali basalt volcanism during the Upper Carboniferous and early Permian (Figs. 1.2-1.4). Russell (1976) recognised that many Carboniferous ore deposits and some basins were sited on N-S structures, and proposed that E-W stresses dominated throughout this period. Evidence from these structures, and from the abundant alkali basalt volcanism, marine transgressions, basin types and orientations was used by Russell (1976), Russell & Smythe (1983) and Haszeldine (1984) to propose the opening of the northern North Atlantic during the late Westphalian.

The development of a complex E-W fault system across much of the northern foreland towards the end of the Carboniferous was accompanied by the

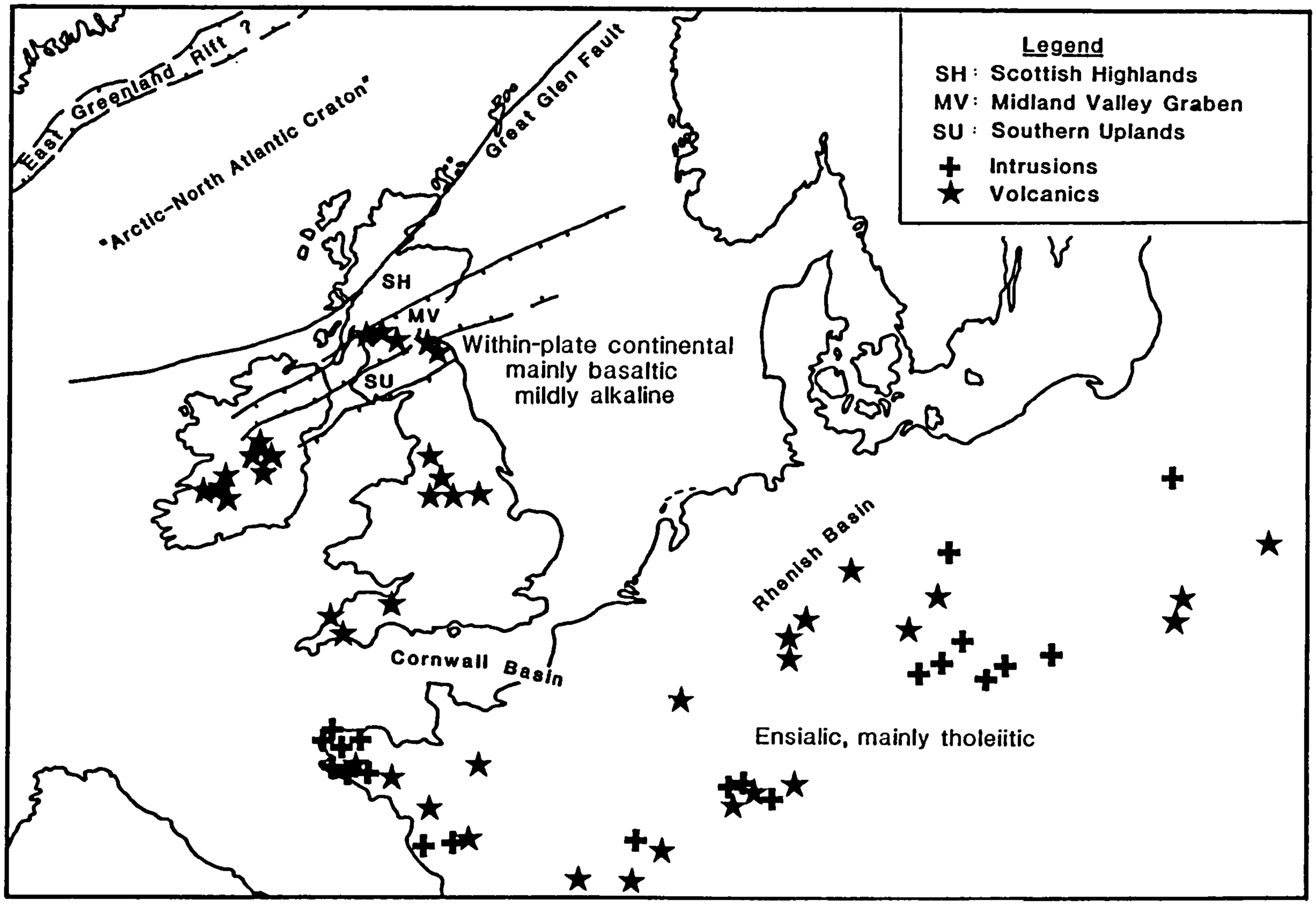

Fig. 1.1 Dinantian magmatism in Northern Europe (after Ziegler, 1982 and Francis, 1988).

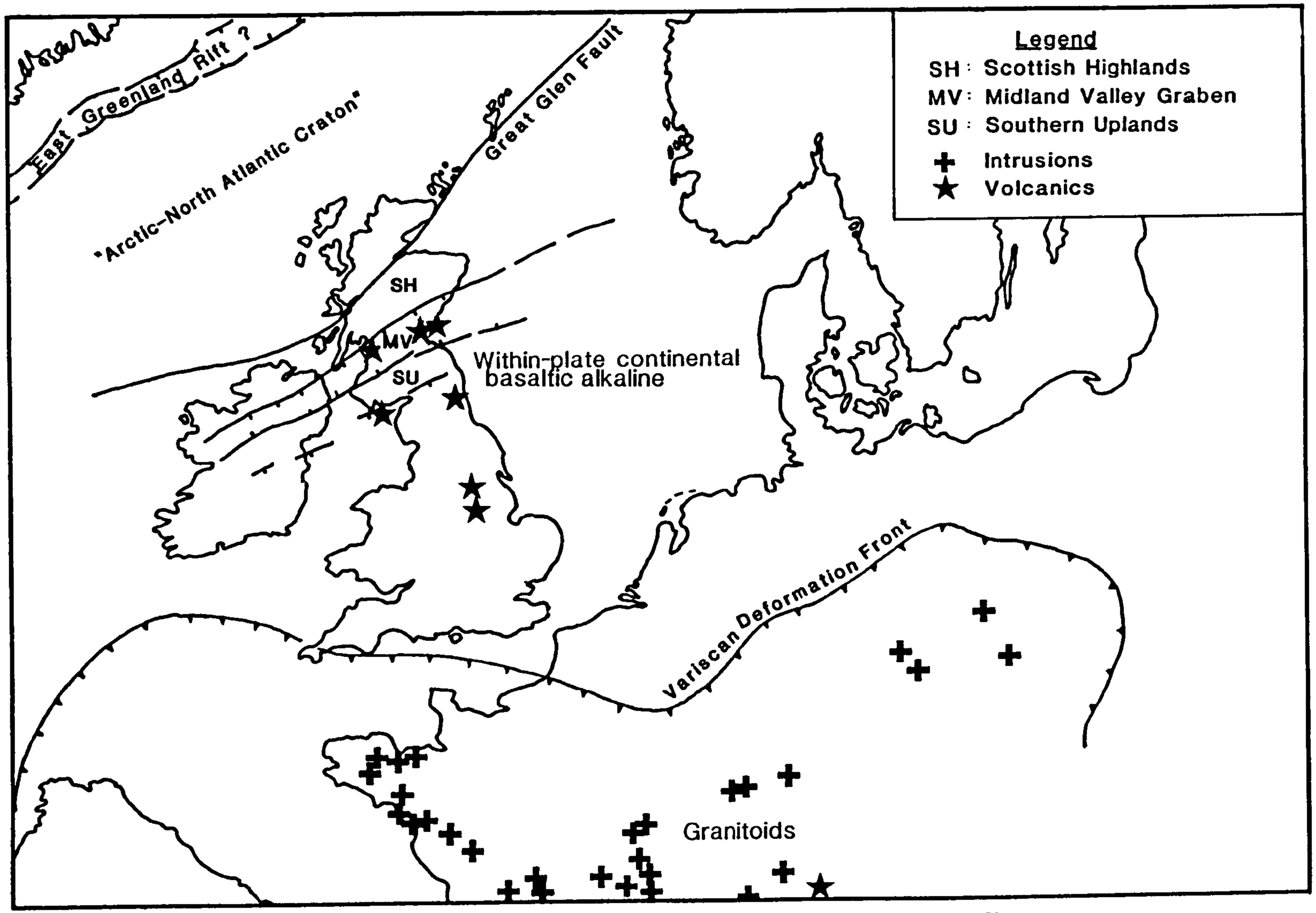

Fig. 1.2 Namurian magmatism in Northern Europe (after Ziegler, 1982 and Francis, 1988).

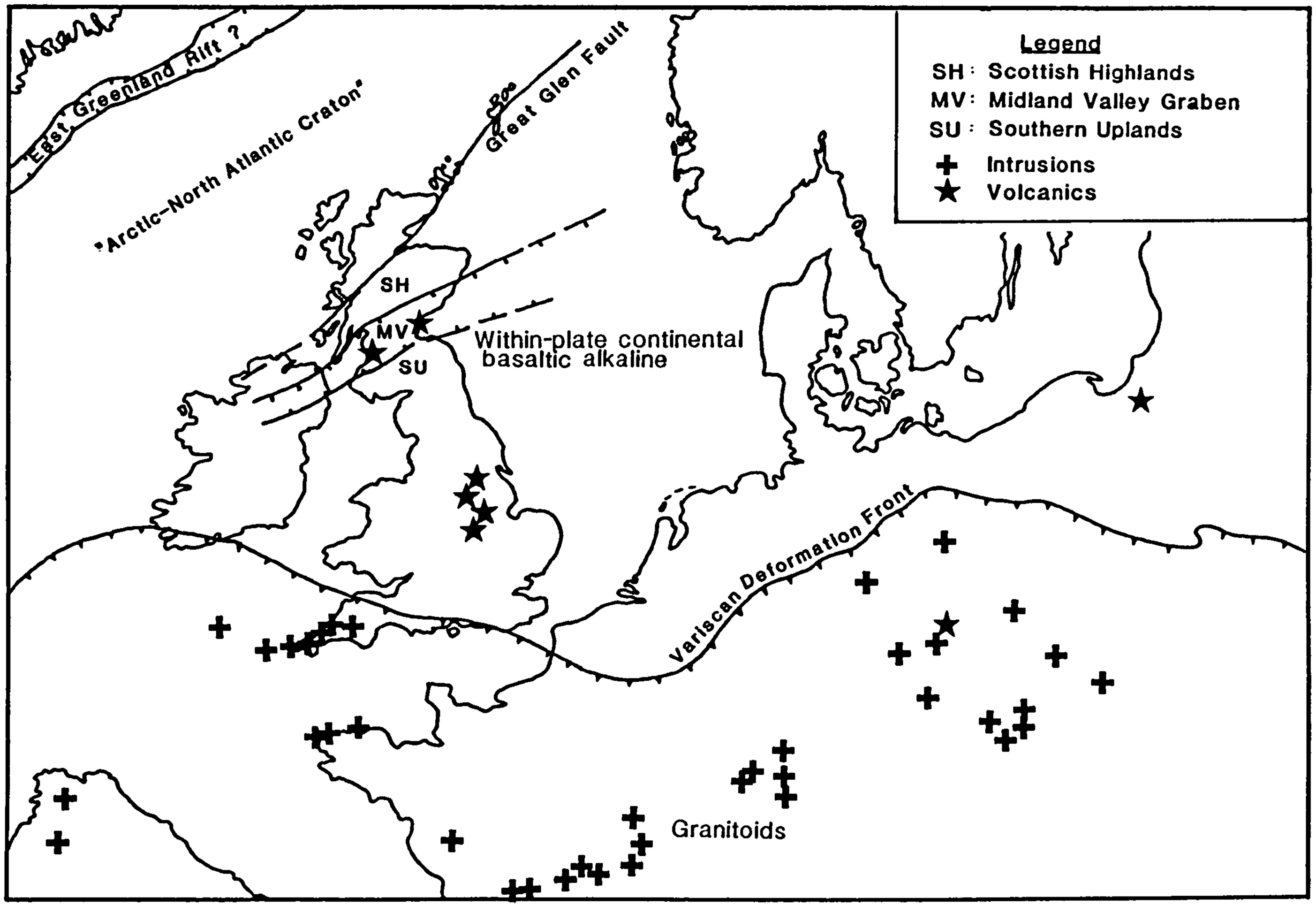

Fig. 1.3 Westphalian magmatism in Northern Europe (after Ziegler, 1982 and Francis, 1988).

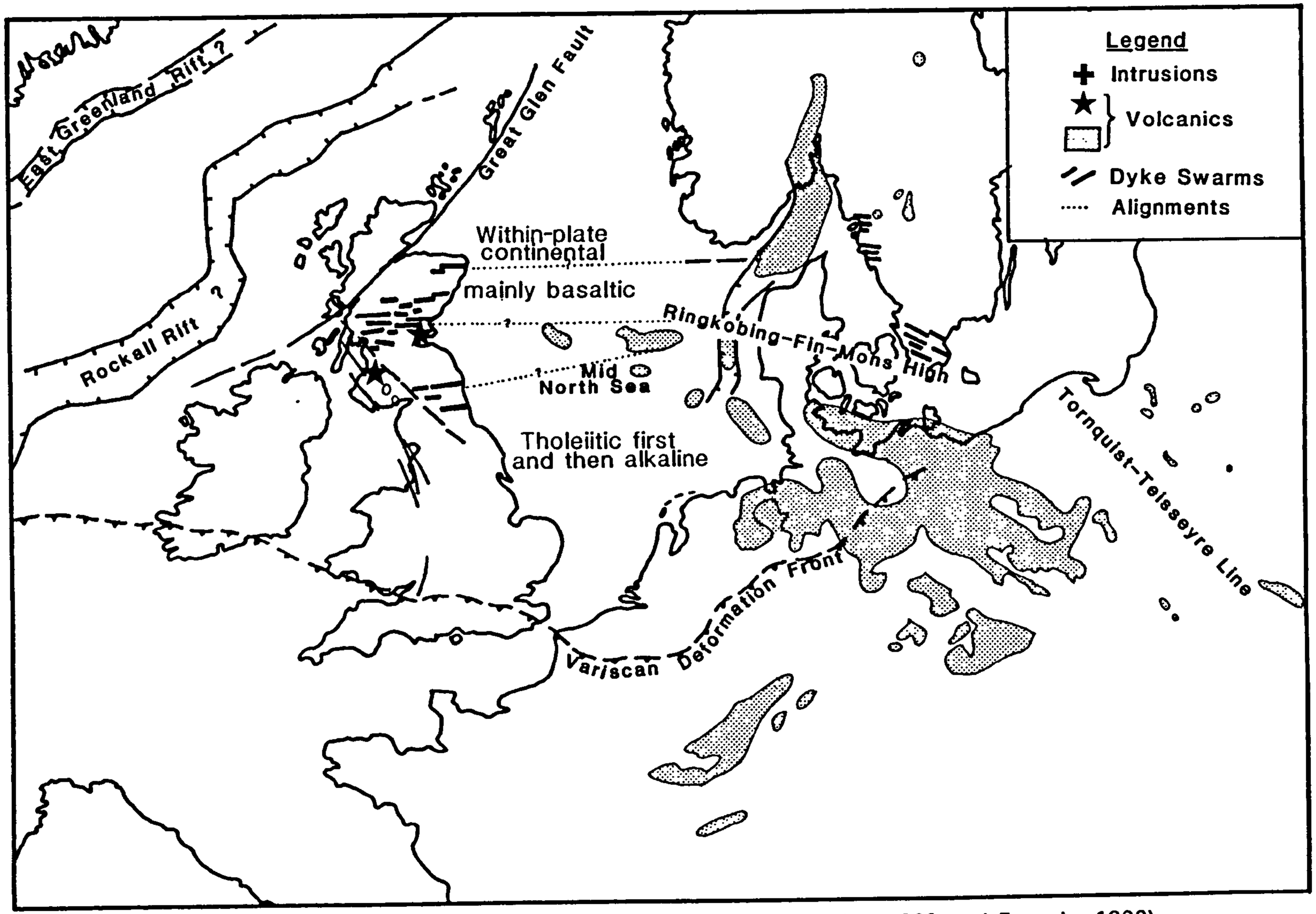

Fig. 1.4 Stephanian – Autunian magmatism in Northern Europe (after Ziegler, 1982 and Francis, 1988).

intrusion of a tholeiite dyke swarm dated at c.300 Ma (Fig. 1.4). Dykes outcrop in the Midland Valley and the Northumberland Basin where large sill complexes are also developed (Francis, 1978b). Magnetic anomalies indicate the continuation of dykes offshore on the British side of the North Sea Central Graben (Russell & Smythe, 1983) and they have been correlated with similar intrusions in southern Sweden. The only known extrusive expression of the tholeiitic event is provided by the oldest of the Oslo Rift lavas (Macdonald *et al*, 1981).

Alkaline magmatism during the late Carboniferous and Permian was associated with the development of a series of intermontane troughs across Europe. The area of trough formation extends north-westwards from the Oslo Graben to Scotland, south-eastwards to the southern European coast, south-westwards into Spain and Morocco, and to the north-east it is bounded by the Tournquist line (Lorenz & Nicholls, 1976). The earliest troughs formed in central Europe (southern Poland to Massif Central) in the late Viséan and the Namurian (Lorenz & Nicholls, 1976), and appear to be associated with ongoing subduction close to the region (Francis, 1988). In early Permian times volcanism spread over the whole province, and in northern Europe, formed a belt of intraplate alkaline magmatism (Fig 1.4).

Hydrocarbon exploration has shown the most extensive volcanic field extending northwards from outcrop in the Saar-Nahe and Halle districts of mid Germany, beneath Holland and the North German Plain, to the northern flank of the mid North Sea Ringkobing Fin high (Francis, 1988). Volcanics in the Horn Graben and Bramble Trough are coeval with rifting and magmatism in the Oslo Graben (Ziegler, 1978). Igneous rocks in these areas are transitional to alkaline in chemistry and display a marked mafic-felsic bimodality (Oftedahl, 1978; Dixon *et al*, 1981). In areas of maximum extension (e.g. Oslo Graben and Saar-Nahe trough) later flows were tholeiitic (Dixon *et al*, 1981; Nicholls & Lorenz, 1973).

Contemporaneous basin subsidence occured in Northern Britain (Francis 1978a,b) and on the continental shelf west of Britain (McLean, 1978). British Permian magmatism is mafic and in the Mauchline, Thornhill and Sanquhar basins is of a highly alkaline to transitional composition (Chapter 5). Volcanism to the east of the Midland Valley is solely alkaline in composition.

Many models have been proposed to explain the volcano-tectonic regime of

late Carboniferous - Permian northern Europe. Three are described below: Lorenz & Nicholls (1976) emphasised the similarities between the magmatism and tectonics of Permian northern Europe, and the late Cenozoic Basin and Range province of the western United States. Their model attributed magmatism to the post-orogenic release of compressive forces and they concluded that volcanism resulted from lateral movement of a subduction-initiated upper mantle diapir.

Dixon *et al.* (1981) concurred with the Basin and Range analogy but suggested that basin formation was related to strike-slip movement along faults. Major dextral NW-SE faults parallel to the Tornquist line are a prominent feature of late Carboniferous/early Permian European tectonics (Ziegler, 1978). If faulting is largely post-extensional then rifting and basinal subsidence could be attributed to local pull-apart effects caused by irregularities in these major faults (Dixon *et al*, 1981).

Only the North Atlantic rifting model of Russell (1976), Russell & Smythe (1983) and Haszeldine (1984) (mentioned earlier in this section) accounts for the quartz dolerite dykes and sills. It interprets them as the result of tension focused around the final rupture of continental crust.

1.3. Volcano-tectonic history of the Midland Valley

Magmatic activity in the Dinantian was voluminous and gave rise to c.6000km^3 of lavas over much of the Midland Valley (Tomkeieff, 1937), although variations of thickness and basalt type indicate that there were several principal volcanic fields (Francis, 1983) (Fig. 1.5). The majority of the lavas (c. 85%) were mildly undersaturated basalts, the remainder comprising undersaturated and saturated trachytic differentiates and subordinate rhyolites. Whether eruptions were via central volcanoes (Whyte & MacDonald, 1974; Craig & Hall, 1975) or fissures (Francis *et al*, 1970), it is clear that localisation of eruption was in many instances provided by reactivated NE-SW Caledonian basement structures (Cameron & Stephenson, 1985).

These thick piles of early lavas had some control on the disposition of the Midland Valley sedimentary basins, and deposition was concentrated in three areas: the Ayrshire basin to the south of the Clyde Plateau lavas, and the Central-Stirling-Clackmannon and East Fife-Midlothian basins to the east. The latter two were separated by the Burntisland Anticline which coincides with,

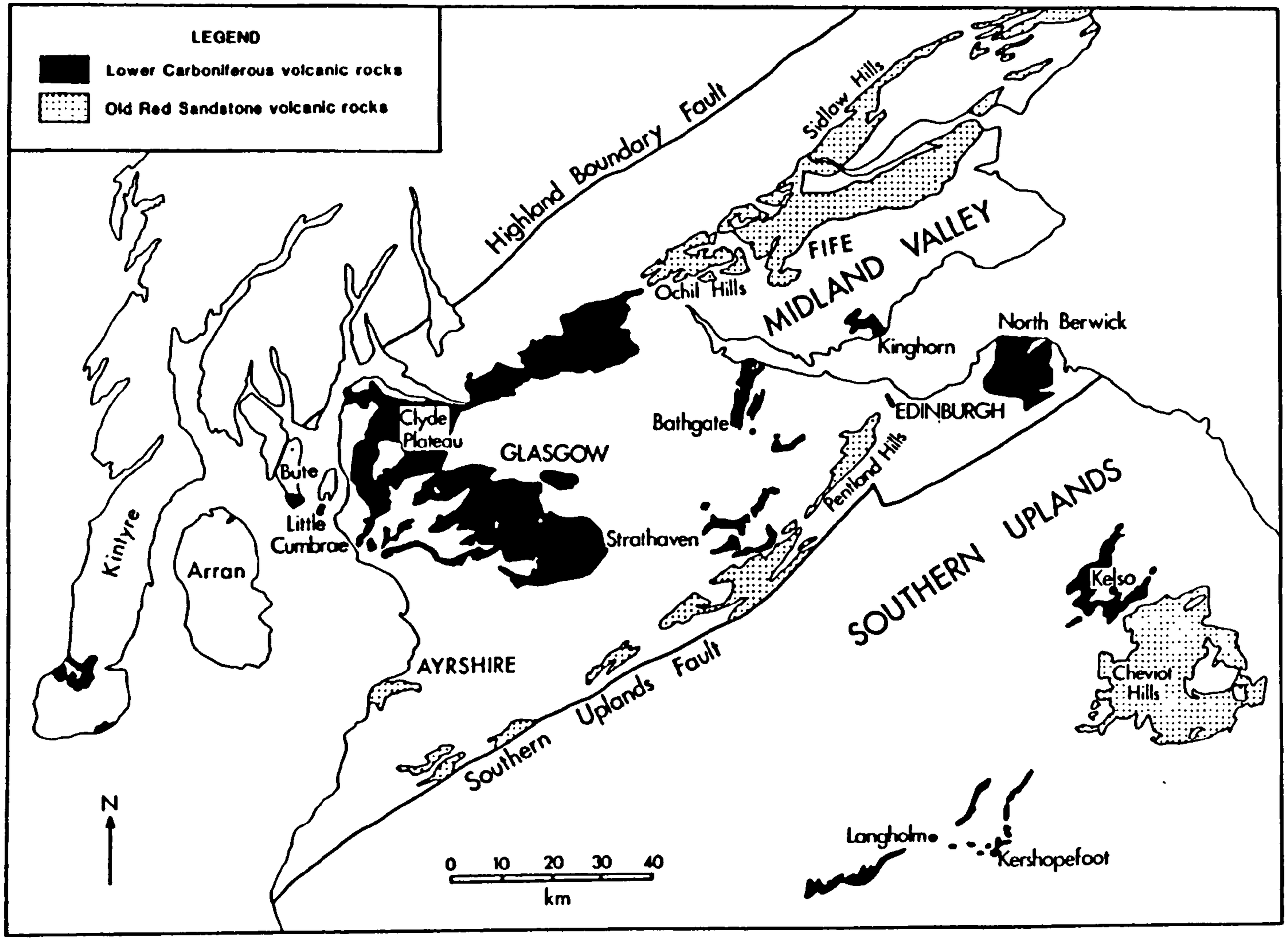

Fig. 1.5 Regional distribution of Dinantian and ORS lavas in Southern Scotland (from Smedley, 1986b).

and is probably a consequence of, thick lava piles (Cameron & Stephenson, 1985).

The widespread Dinantian volcanism had diminished by the early Namurian, and volcanism continued throughout the Silesian at a much less productive level. There was some decline in the influence of the NE volcano-tectonic controls as NW-SE lineaments became increasingly important (Hall, 1974; Cameron & Stephenson, 1985; Read, 1988). Volcanic activity, often phreatic, centred on numerous short-lived vents producing abundant pyroclastic deposits, interbedded with shallow-water sedimentary deposits (Cameron & Stephenson, 1985). Although it is impossible to locate all centres of explosive activity either at outcrop or through mining activity, their presence can be inferred from tuff layers. Large volumes of magma were intruded as sills, partly a result of increased sediment thicknesses in the basins, and the only lava flows of any consequence outcrop in Ayrshire.

A restricted compositional range of basalts and basanites with basaltic hawaiites and some hawaiites, is in marked contrast to the wide range of differentiates in most Dinantian sequences.

A brief chronology of intrusive and extrusive events is outlined below and summarised in Table 2.1. A more detailed discussion of age controls is given in chapter 2. Figs. 1.6-1.8 show the regional distribution of late-Palaeozoic igneous rocks in the Midland Valley. In the Bathgate area of Lothian, Dinantian basalt extrusion continued into the Namurian, and basalts replace much of the Limestone Coal Group in this area. Eruptive sequences in West Fife (around Saline) at this time, were dominated by tuffs with subordinate lavas accumulated from several necks (Francis, 1961). Pyroclastic activity on a smaller scale continued through the Limestone Coal and Upper Limestone Groups in much of Fife. It culminated near Largo Law with the extrusion of two lava flows (the Blindwells Quarry lavas) and at Westfield with an episode which produced five pillow lava flows associated with tuffs and hyaloclastites (Francis, 1983). At the same time the Fife and Lothian area underwent a long period of intrusive activity which may have continued into the Westphalian. Phraeatic activity continued in Fife until the Late Namurian (Passage Group).

In Ayrshire, particularly in the Dalry area, tuffs occur at several levels in the Limestone Coal Group and extend up into the Upper Limestone Group (Richey

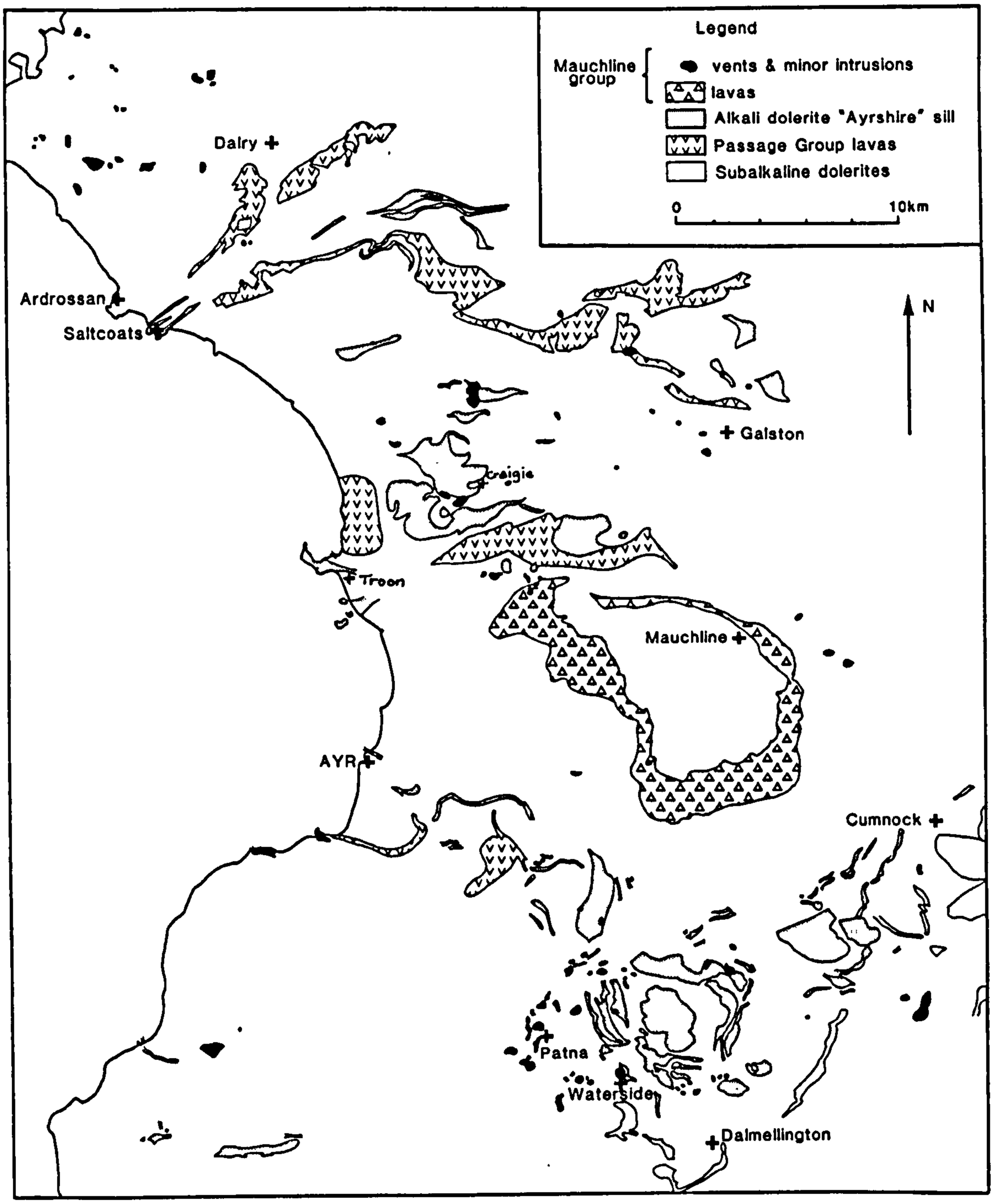

Fig. 1.6 Late-Palaeozoic igneous outcrops in Ayrshire.

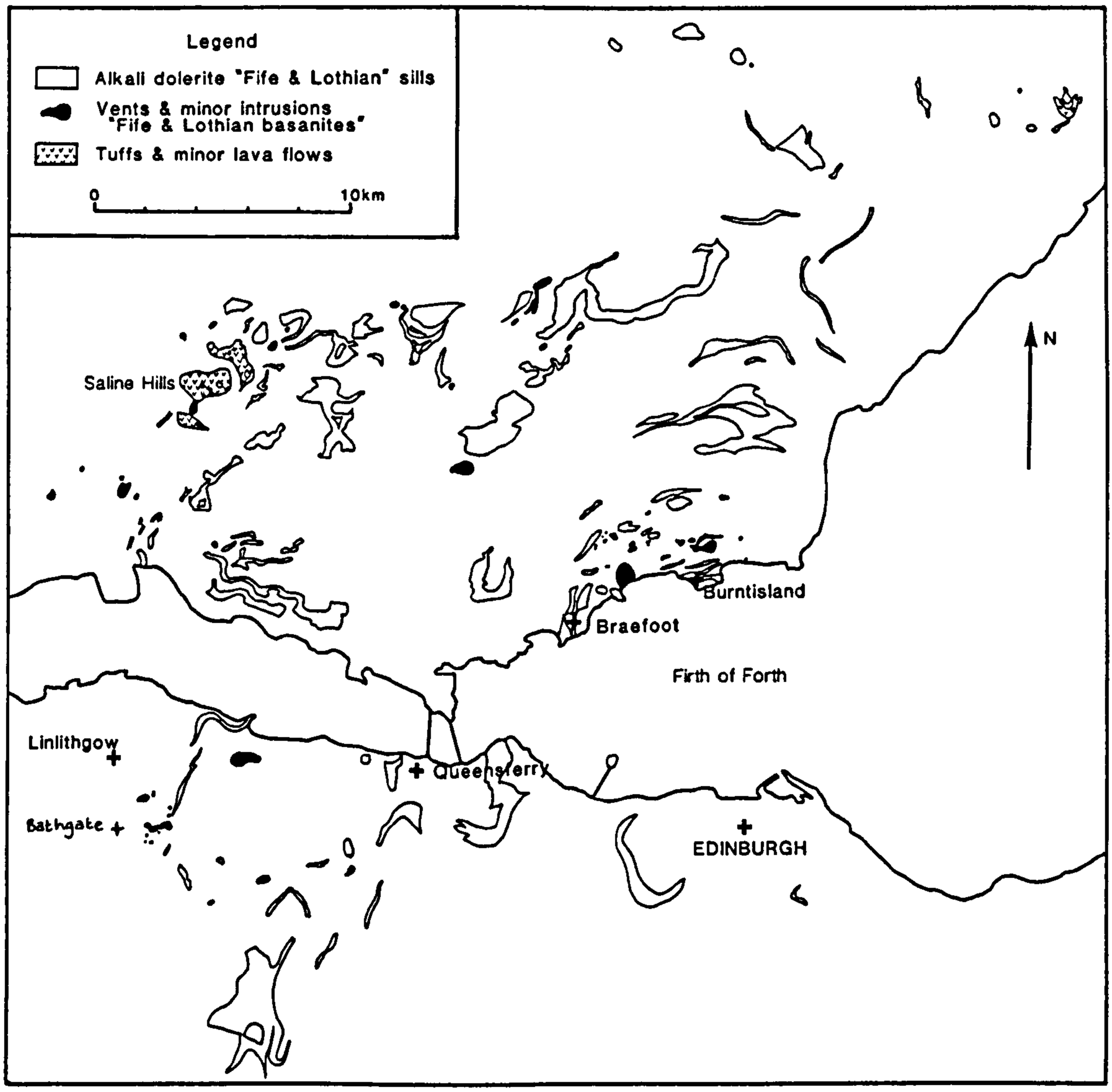

Fig. 1.7 Late-Palaeozoic igneous outcrops in west Fife & Lothian.

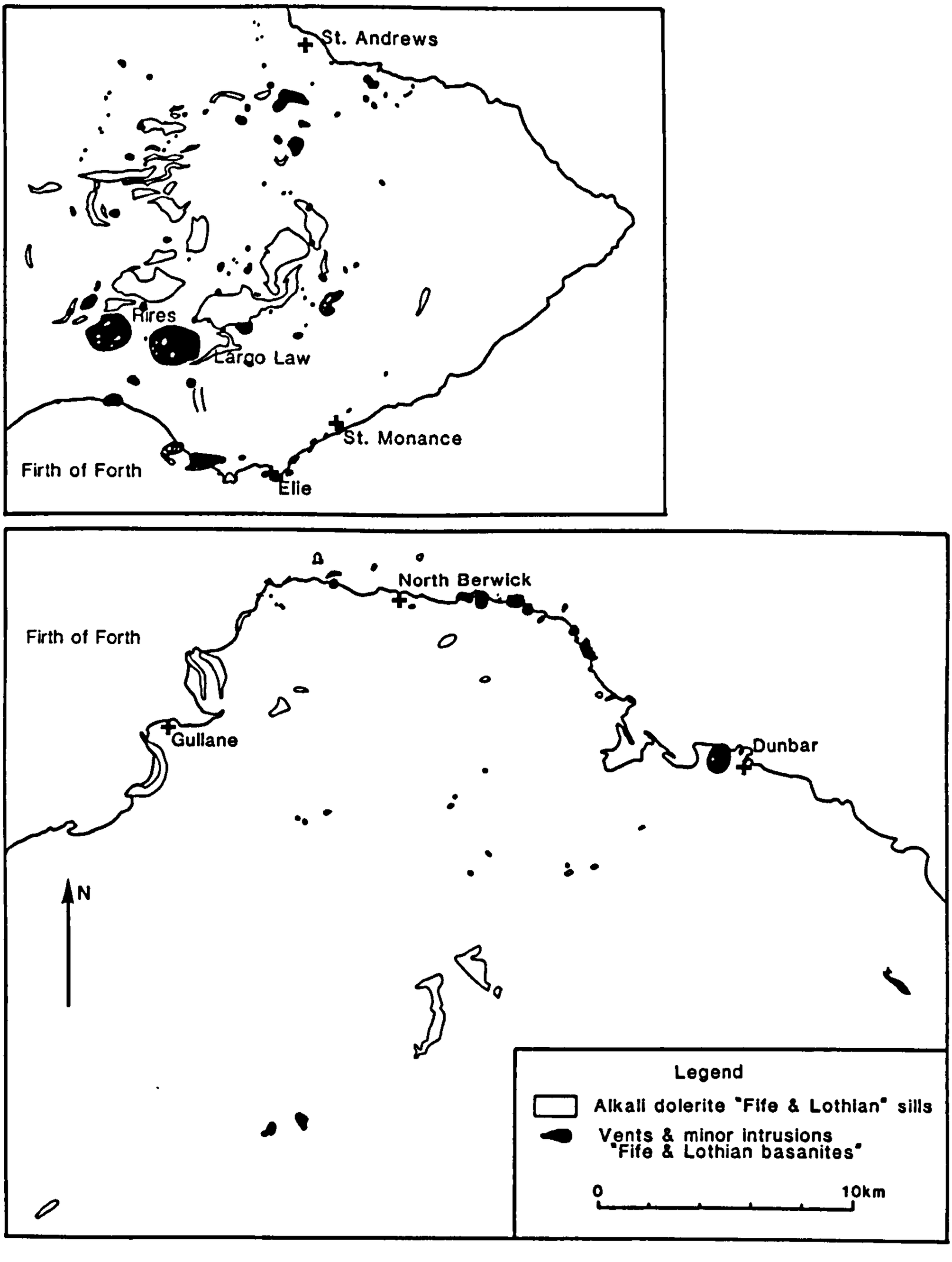

Fig. 1.8 Late-Palaeozoic igneous outcrops in east Fife & Lothian.

et al, 1930; Francis, 1983). Volcanism in the late Namurian produced the first post-Dinantian flows of any consequence: the Passage Group lavas, which possibly extend up into the very earliest Westphalian. Westphalian extrusive activity in Fife is concentrated to the east in a belt of pyroclastic rocks stretching southwards from Largo Law, beneath the Firth of Forth. Some of the sills of the Fife/Lothian region are possibly early Westphalian in age (see chapter 2), but the area of most magmatic activity was in Ayrshire where sills were intruded from Westphalian to early Permian.

The steadily decreasing NE controls of volcanic activity were apparently terminated abruptly in the late Westphalian - early Stephanian with the emplacement of numerous E-W faults cutting across all earlier structures, and the associated intrusion of a tholeiitic suite of dykes, and a sill complex. The intrusion of alkali dolerite sills may have continued throughout this phase in Ayrshire which lay too far south to be affected by this magmatic phase. The area was also remote from the Northumberland - Durham region of tholeiitic magmatism.

Permian volcanism and sedimentation in the Mauchline Basin was controlled by a NW-SE system of fractures (Mykura, 1967). Similar fault-bounded basins formed in the Southern Uplands (Sanquhar and Thornhill) and in Northern England (Vale of Eden). These are all coeval with the North Sea Permian Basins and the Oslo Graben and the NW-SE trending Ardgour dyke swarm of the Scottish Highlands (Baxter & Mitchell, 1984).

Permian lavas and numerous small feeder-vents are preserved in and around the Mauchline Basin. In Fife and Lothian many small vents were also active, and there are indications that some basanite intrusions cut Dinantian vents (Martin, 1955). There are no lavas or tuffs of Permian age in the geological record of Fife and Lothian.

1.4. Field setting

Over 600 samples were collected from the post-Dinantian lavas and supposed post-Dinantian intrusions and vents of the Midland Valley, (sample localities are marked on the maps in the back pocket of this thesis). The numerous tuff occurrences have been mentioned in section 1.3, but for the purposes of this project they were ignored because of their unsuitability for geochemical analysis. Exposure varies considerably from area to area, and collection was

often dependent on the existence of old quarries and river sections. The following sections describe the general field characteristics of the lavas, sills and vents of the Midland Valley.

1.4.1. Lavas

The only two significant lava successions outcrop in Ayrshire. They are the Passage Group and Mauchline lavas.

1.4.1.1. Passage Group lavas

The Passage Group lavas occupy a position between sediments of the Passage Group and Lower Coal Measures. The thickness of the whole suite varies from 9m to a maximum of 170m in the Barassie inlier near Troon (Richey *et al.* 1930; Cameron & Stephenson, 1985). The maximum thickness of 9m for a single flow was recorded by Richey *et al.* (1930). The lavas probably underlie most of the Ayrshire Coalfield Basin (Richey *et al.*, 1930; Cameron & Stephenson, 1985), but their original extent is unclear. On the basis of scattered exposures Richey *et al.* (1930) indicated that the Passage Group lava fields covered a pear-shaped area extending southwards to Stranraer and westwards across southern Arran, parts of Kintyre, and possibly to Ballycastle in Northern Ireland. Today the main area of lavas is north of the Mauchline Basin between Craigie and Dalry, with two smaller outcrops immediately ESE of Ayr (Fig. 1.6).

Most of the flows sampled were exposed in river sections or small cuttings and are sparsely amygdaloidal. Columnar jointing is often developed - an indication of slow cooling and hence thick flows. Freshness varies quite considerably over a small distance, and it is not uncommon to find severely spheroidally-weathered outcrops.

The lavas are thought to have been extruded as sub-horizontal flows on a slowly sinking surface (Richey *et al.*, 1930). Considerable time-lapses between flows are indicated by the presence of intercalated sediments; and indications of long inter-eruption periods of weathering in a hot, humid climate are provided by ferruginous and aluminous clays (Cameron & Stephenson, 1985). A prolonged period of emergence and deep weathering gave rise to the Ayrshire bauxitic clay which attains a thickness of 9m in the north of the area.

1.4.1.2. Mauchline lavas

The Mauchline lavas outcrop in a ring around the edge of the Mauchline Basin, and underlie Permian aeolian sandstones (Fig. 1.6). The junction between Coal Measures sediments and the lavas is unconformable (Eyles *et al*, 1949). The lava sequence thickens eastwards from 100 to 238m, although flows rarely exceed 2m in thickness. Scoriaceous tops are common, with calcite and zeolite amygdales and occasionally the larger cavities and fissures in the slaggy tops are filled with sandstone (Eyles *et al*, 1949). Most of the exposure is confined to sections along the Ayr and Lugar rivers.

Underlying the lavas are tuffs intercalated with sandstones and occasional marly shales and mudstones (Eyles *et al*, 1949). The tuffs are rarely exposed, but have been proved in numerous bore holes. They are basaltic and usually fine-grained, and often host large (up to 15cm), rounded blocks of basalt (eg SW71a-m). The lavas themselves contain intercalated sediment and tuff, of both subaqueous and subaerial origin.

The characteristic red speckled appearance of the Mauchline lavas is caused by the near-complete haematisation of olivine.

1.4.2. Vents

1.4.2.1. General information

With the exception of the Largo Law and Rires vents in Fife, most of the Midland Valley vents are between 50-600m in diameter. The two exceptions are c. 2km diameter. Most necks are sub-circular in plan, and in section have a tendency to taper downwards (Eyles *et al*, 1949; Forsyth & Chisholm, 1977). Numerous data from mining and borehole sections in Fife suggest that the margins are essentially ring-fractures inclined inwards at angles of 45° to 80° with frequent narrow crush zones (Forsyth & Chisholm, 1977). The necks are filled by fragmental material which can be both sedimentary and igneous in origin The former is derived by comminution of the sediments pierced by the necks and ranges in size from large blocks several metres across, down to dust. The igneous material is from two sources. Most is juvenile, represented by blocks and bombs (several cm to >1m) and lapilli, derived from the parent magmas. Of secondary importance are 'accidental' blocks from older flows or intrusions.

The size distribution of particles composing the vent varies between localities: some are composed almost entirely of tuffaceous fragments (<1cm) and others contain high concentrations of blocky material. Tuffs and agglomerates can be unbedded or bedded and some necks include both types. The descriptions of some of the structures associated with bedding in the East Fife vents (Forsyth & Chisholm, 1977) can be applied to the necks of the other regions. These authors suggested that the lithologies and textures of the bedded rocks conform almost entirely to criteria for Surtseyan-type deposits, where water has free access to the vent.

Geikie (1900) suggested a fourfold division for the vents in Central Fife which is useful as an indication of the range of exposure-types encountered:

1. Vent-filling dominated by non-volcanic material
2. Vent-filling dominated by tuff and/or agglomerate
3. Dyke(s) and/or plug(s) intruding vent
4. Neck dominated by basaltic intrusions. No remaining record of original (if any) pyroclastic material.

Many of the necks are intruded by basalt. Plugs are the commonest type of intrusion, but dykes and more rarely sills are also present. Forsyth & Chisholm (1977) described tuffisite intrusions in some of the vents of East Fife.

1.4.2.2. Ayrshire

Over sixty volcanic vents occur within a 20km radius of the centre of the Mauchline Basin. The only obvious grouping of the vents is in the south around Patna (Eyles *et al*, 1949). In most instances the vents are obvious as small hills, and exposure (if any) is confined to small hollows around the hillside. Central plugs are rare, dykes are more common. Many of the vents and small intrusions host cognate and accidental xenoliths and xenocrysts.

1.4.2.3. Fife & Lothian

At least thirty vents of Dinantian and post-Dinantian age outcrop in Lothian. More than half of these are concentrated along the coast of east Lothian, with the remainder to the west between Linlithgow and Queensferry. There is no

surface exposure of vents in Midlothian. To the east the vents pierce the Dinantian lavas and tuffs and Calciferous Sandstone Measures, except around Dunbar where the Upper Old Red Sandstone sediments are intruded. To the west the necks cut the Upper Oil Shale Group and Lower Limestone sediments.

The main concentration of vents in Fife is found to the east where over 80 have been recorded. Exposure today is confined to hillsides and coastal sections where the vents intrude sediments between Calciferous Sandstone Measures and Upper Limestone Group. Vents in Burntisland and West Fife total about twenty and intrude Carboniferous sediments up to the Limestone Coal Group. As with Lothian, there is a central belt with no surface exposure of vents. This corresponds to a major syncline affecting a belt across the Firth of Forth, which was a depositional basin in the Namurian and the Westphalian. Whether this distribution of vents is real or only a reflection of exposure is unclear.

1.4.3. Sills

Numerous alkali dolerite sills outcrop in both the east and the west of the Midland Valley. Petrographic affinities and field relationships indicate that many of the sills are part of larger complexes. This has been proved by Francis and Walker (1987) for the West Fife sills. Some of the sills comprise rock types indicative of crystal accumulation and some are composite intrusions (Francis, 1983). For example, the Lugar Sill in Ayrshire displays evidence of multiple injections of successively less-evolved alkali basaltic magmas from a deeper magma chamber, followed by a larger pulse of liquid carrying abundant olivine phenocrysts. The latter, intruded into the central part of the sill, shows evidence for *in situ* differentiation (Henderson & Gibb, 1987). The Braefoot Outer Sill in Fife provides an example of simple gravitational sinking of olivine (Campbell *et al*, 1932, 1934; Francis, 1983).

1.4.3.1. Ayrshire

Sills of alkali dolerite outcrop in much of Ayrshire. They intrude sediments from the Limestone Coal Group to the Upper Coal Measures, but the majority are concentrated within the Coal Measures sediments. Thicknesses vary from <1m to >30m (Richey *et al*, 1930) with borehole records suggesting that the thinner sheets follow coal seams. A complete section through possibly the largest sill (Lugar) proved a thickness of 49m (Henderson & Gibb, 1987). The maximum

areal extent of individual sills at outcrop is between 3-4km^2.

1.4.3.2. Fife & Lothian

As with the vents of this region, two main areas of outcrop can be identified - one to the east and one to the west - leaving a central belt with little evidence of intrusive activity. Records of the east Fife intrusions indicate thicknesses in excess of 60m. In east Lothian, only one borehole has proved the total thickness of any intrusion, that is the Spilmerford intrusion at 114.5m (McAdam, 1974). In West Lothian the maximum recorded thickness for a sill is 137m (Peach *et al*, 1910) and in west Fife, 190m for the Parkhill- Cowdenbeath-Kinglassie Sill (Francis & Walker, 1987). Maximum extents for single sills are between 5-6km^2.

1.4.4. Relationship between lavas, sills and vents

1.4.4.1. Ayrshire

The relationship between vents and lavas in Ayrshire is generally unambiguous. Petrographic and geochemical considerations suggest that the vents acted as feeders to the lavas. A possible exception to this involves a group of vents to the NW of the area, which has been described by Wilson (1916) and Richey *et al.* (1930). Wilson (1916) suggested on the basis of the similarity of ashes in these vents to those interbedded with Lower Millstone Grit in the nearby Dalry Basin that the vents fed the latter. Richey *et al.* (1930) were of the opinion that most of the vents were Permian in age, the only possible exception being the Holmbyre vent which they considered to be Namurian. No feeders for the Passage Group lavas have yet been identified.

The large size of some of the Ayrshire sills, the fact that crystal (olivine) accumulation has clearly been an important process in some (see chapter 3), and the petrographic similarities between some of the sills and vents suggests that some sills may have acted as shallow magma chambers feeding material to the surface. This has been indicated by Francis (1968) for some of the Namurian sills of Fife and is discussed below.

1.4.4.2. Fife & Lothian

In contrast with Ayrshire there are few lava flows in Fife and Lothian and all are intimately related to phases of pyroclastic activity. Although it is clear from stratigraphical records that pyroclastic activity ensued throughout the Namurian and Westphalian, it is seldom possible to correlate a bedded tuff with a specific neck (Forsyth & Chisholm, 1977). Dating of supposed cognate inclusions from the Elie Ness and Kincraig vents by Macintyre *et al.* (1981) suggested a late Namurian magmatic event in the area which has no surface expression.

Francis (1968) suggested that magma rising beneath a thick cover of weakly consolidated sediments would form shallow-depth sill complexes which could act as reservoirs for tuff eruption through vents. Continuous magma pulsation supplying one sill complex could account for tuffaceous sediments through the stratigraphical pile (Francis, 1968). The phreatic explosions from magma/water interaction necessary to feed pipes from high-level reservoirs (Francis, 1968) were considered unlikely by Francis & Walker (1987). They suggested that magma ascended as dykes along E-W and NE-SW basement faults underlying the synsedimentary basins. From these dyke bodies, pipes were drilled upwards through wet sediments, and phreatic explosions were generated by magma-water interaction. Sills would be intruded when vents choked by debris and solidified plugs caused the lateral movement of degassed magma through the walls of necks or along minor fractures radial and concentric to the necks. The relationships between the Chapel Ness Sill and a basaltic plug in the Craigforth neck (east Fife) (Forsyth & Chisholm, 1977) were used to support this model.

There is one region in Fife where post-Dinantian volcanic activity has been demonstrably linked to tectonic activity, namely along the Ardross Fault. Francis & Hopgood (1970) outlined a volcano-tectonic history which invoked relatively early emplacement of tuffs, breccias and agglomerates and later major dextral movement along the fault.

Some of the vents along the Lothian coast acted as feeders for the Dinantian lavas in the area (Martin, 1955; Davies *et al.*, 1986; McAdam & Tulloch, 1985). Martin (1955) divided the vents of east Lothian into two groups: an older Red Group and a younger Green Group. He demonstrated that the Red Group vents were active prior to Dinantian lava eruption, whereas the Green Group vents cut strata near the top of the volcanic succession. This allows two

possibilities: that they were initiated in the Silesian to early Permian by the basanitic phase, or that they are older vents intruded by younger bodies. The fact that none of the Red Group has been similarly intruded perhaps suggests the former option.

This section has concentrated on outcrops of volcanic rocks in the Midland Valley. However, it should be emphasised that although the Midland Valley was the main focus for post-Dinantian volcanism, it was by no means the only one. Samples have been collected from Permian lavas and intrusions in the Thornhill and Sanquhar basins of the Southern Uplands (Fig. 1.9). North of the Midland Valley and coeval with this Permian activity are the dykes of the Ardgour Swarm (Baxter & Mitchell, 1984: Fig. 1.10). Samples were collected from six of these dykes.

1.5. Classification and nomenclature

There are problems of nomenclature with fine-grained, sometimes glassy rocks in which modal mineralogy is difficult or impossible to assess. To this end many authors have used classification schemes based on chemical criteria. Since no major geochemical study of the Midland Valley post-Dinantian suite has been undertaken until now, previous classifications have relied almost totally on petrographic considerations. In contrast, this study adopts some of the well-established chemical criteria for classification (see chapter 5). This section reviews the modal and chemical classification schemes which have been employed.

1.5.1. Modal classifications

Alkaline rocks in general are those which contain an excess of Na_2O and K_2O with respect to available SiO_2 and/or Al_2O_3. The excess which cannot be accommodated by feldspar, is commonly taken up by feldspathoids, sodic pyroxenes and amphiboles (Fitton & Upton, 1987).

A spectrum of rocks exists with increasing silica-undersaturation from alkali basalt (no modal feldspathoid) through basanite and basanitic foidite to foidite (no modal plagioclase). The modal proportions of felsic constituents changes between each of these groups (Streckeisen, 1979), and each will display its own fractionation trend (Coombs & Wilkinson, 1969).

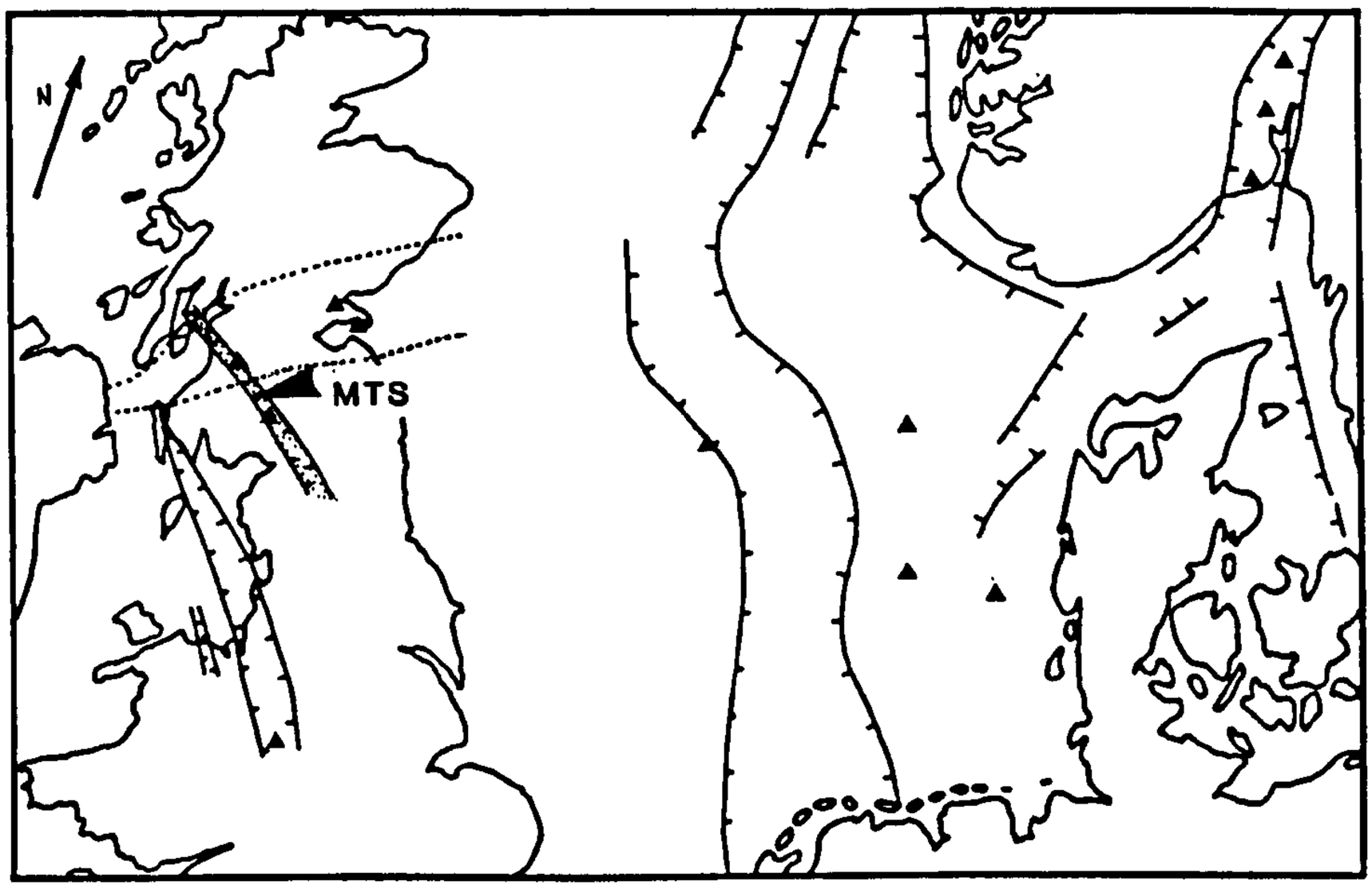

Fig. 1.9 Map showing Permian rifting in north west Europe. The relationship between the Mauchline, Thornhill and Sanquhar basins is highlighted - **MTS** (from Francis, 1978b).

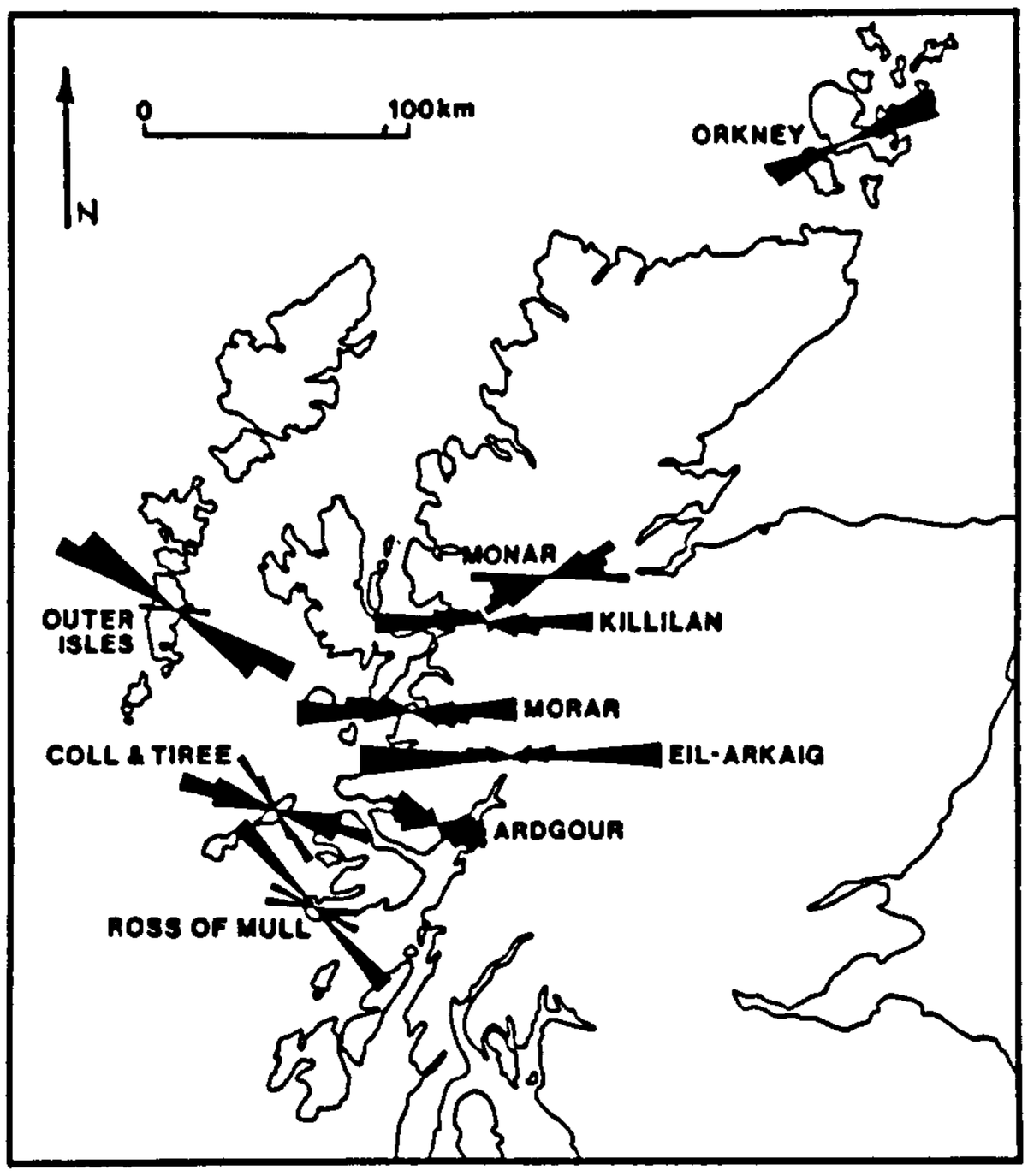

Fig. 1.10 Location and distribution of the main Scottish Highland dyke swarms. The Highland Dykes trend NW-SE (from Baxter, 1986; after Rock, 1983).

Most accounts of the Midland Valley volcanic suite have used these definitions correctly. However, through much of the literature there is frequent misuse of the term 'monchiquite' to describe olivine and/or augite-phyric rocks with groundmasses including nepheline, analcime, feldspar and glass. These are actually analcime-basanites (Rock, 1977; Forsyth & Chisholm, 1977). A monchiquite *(sensu stricto)* is a lamprophyre containing phenocrysts of ol+cpx ±bi±amph in an often highly altered groundmass of glass or analcime (Bates & Jackson, 1980).

A complex nomenclature has developed for the coarser-grained rocks under study, usually in an attempt to classify a sample on the basis of the type of feldspathoid present. Nepheline-dolerites have been referred to as theralites and analcime-dolerites as teschenites, with kyalite and crinanite for respective olivine-rich varieties (Sørenson, 1974, Streckeisen, 1979). Since analcime is almost certainly a deuteric alteration product of nepheline (Henderson & Gibb, 1983) and the amount of olivine present can be accounted for by the variable efficiency of phenocryst concentration during emplacement (Murata & Richter, 1966) the term dolerite (with 'nepheline' or 'analcime' prefixes) is preferred.

1.5.2. Chemical classifications

Whole-rock geochemical characteristics have been used both as an aid to the classification of fine-grained and glassy rocks (Le Bas *et al*, 1986, Le Bas, in press), and in the identification of fractionation trends or lineages (Thornton & Tuttle, 1960; Coombs & Wilkinson, 1969; Wilkinson, 1986).

The total alkali-silica (TAS) diagram (Le Bas *et al*, 1986) provides the basis for a non-genetic classification of volcanic rocks which is in good accord with the QAPF modal classification of Streckeisen (1979). It must however be treated with some caution when dealing with altered rocks and when trying to apply it to coarser-grained rocks which will have compositions differing in various degrees from that of a magmatic liquid.

The boundary dividing the field of foidites from that of basanite plus tephrite in TAS is known to be unsatisfactory. Because of this a classification based on the CIPW norm has been devised by Le Bas (in press) who defines basanites as having >5% normative *ab* and between 5 and 20% normative *ne*. Coombs & Wilkinson (1969) indicated that chemical analyses of rocks may contain as much as 5% *ne* before feldspathoid is unequivocally identifiable and that, for

rocks with more than 8% normative *ne,* modal nepheline or analcime is usually present in appreciable amounts. The term basanitoid for rocks with greater than 5% normative *ne* but no modal nepheline (Macdonald & Katsura, 1964; Green & Ringwood, 1967; Coombs & Wilkinson, 1969) has been discarded (Wilkinson, 1986).

Nephelinitic rocks can be divided into three groups (Le Bas, in press).

1. **Melanephelinites** contain abundant pyroxene phenocrysts, few or no olivine phenocrysts and little modal nepheline.

2. **Olivine nephelinites** are rich in olivine, mostly as phenocrysts. Pyroxene is restricted to the groundmass.

3. **'Simple' nephelinites** have an abundance of nepheline often as phenocrysts as well as in the groundmass, and pyroxene, sometimes as phenocrysts but more often only in the groundmass. Feldspar and olivine are absent.

Olivine nephelinites and melanephelinites have <5% normative *ab* and between 5 and 20% normative *ne,* and can be distinguished from one another on the basis of MgO content. The former has MgO >10wt% and the latter MgO <10wt%. Nephelinites proper have > 20% normative *ne.*

Chemical fractionation trends using the differentiation index (D.I. = *q+or+ab+ne+lc)* (Thornton & Tuttle, 1960) and normative plagioclase composition *[an = 100an/(an+ab)]* (Coombs & Wilkinson, 1969) have been used by many petrologists. However, the latter has drawbacks when applied to alkaline suites. The increased content of aluminium in pyroxenes of undersaturated rocks such as basanite, tends to enhance normative *an,* so partly compensating for *ab* in alkali feldspars (Wilkinson, 1986).

1.6. Previous research

Archibald Geikie was the first to focus attention on the late Palaeozoic volcanic rocks of the Midland Valley, with his descriptions of the "Ancient Volcanoes" (Geikie 1866,1880,1892,1897). The early years of the 20th century saw numerous contributions to the geological literature on these rocks, in papers which provide a wealth of detailed field and petrographic information. A bibliography is provided in Appendix VIII.

1.6.1. Age constraints

There has always been debate over the ages of the Midland Valley intrusions. The east Fife vents have posed a problem because of the paucity of lava flows in the stratigraphic succession of the area, making correlation with a particular volcanic event impossible. Geikie (1897) proposed a Permian age, but Balsillie (1923, 1927) discussed evidence which suggested Namurian activity. The vents were probably active from the Namurian through the Westphalian (and possibly the Stephanian (see chapter 2)) to early Permian times.

In Ayrshire much discussion has taken place over the ages of the sills. Eyles *et al.* (1949) and Richey *et al.* (1930) attempted to assess the chronology for central and north Ayrshire respectively. They based their work on the cross-cutting relationships of intrusions and faults, maintaining the subdivision of the alkali dolerites on the basis of feldspathoid content (Tyrrell, 1909; see chapter 2).

The Permian age of the Mauchline lavas was thrown into doubt by Mykura (1965) with the discovery of plants of supposed Westphalian D age in thin sediments near the base of the lavas. This was disputed by Wagner (1966) who suggested an Upper Stephanian, and then (1983) Permian age for the flora.

In Fife and Lothian recent discussion over the age of the vents has centred around possible correlations of tuffs in the sedimentary sequence with the vents which pierce it. Forsyth & Chisholm (1977) and McAdam & Tulloch (1985) presented some K-Ar age determinations for the Fife and Lothian intrusions respectively, and these combined with the results of De Souza's research, (1979) provide a reasonable control on the age of volcanism.

1.6.2. Geochemistry

Major element analyses often accompanied the early field and petrological accounts of individual intrusions. Tomkeieiff (1937) produced the first geochemical review of late Palaeozoic magmatism, and this was discussed further by Macgregor (1948). Enlarging on Tomkieiff's work he produced a complete synthesis of Carboniferous-Permian igneous activity involving fusion of crustal layers of different composition. Discussion rested there until Macdonald (1975) reviewed the petrochemistry of the Dinantian lavas, making brief mention of the nature of post-Dinantian volcanism of the Midland Valley.

Macdonald *et al.* (1977) presented 39 new major element analyses of basalts, basanites and basaltic hawaiites from the Midland Valley province with the aim of filling in the data gaps which existed in the post-Dinantian sequences. Consideration of the degree of silica-saturation as a function of stratigraphic position distinguished two thermal cycles, each starting with *hy*-normative magmatism and progessing towards increasingly silica-undersaturated types. The second cycle comprised all the late-Palaeozoic samples and started with the *hy*-normative Passage Group lavas. These authors indicated that post-Dinantian magmatism was predominantly silica-undersaturated, tending towards nephelinites in extreme cases in the late Carboniferous and early Permian. With the exception of the Passage Group lavas and quartz dolerites, *hy*-normative rocks were thought uncommon in post-Dinantian sequences.

Several authors have presented trace element analyses of individual intrusions, either as part of the Geological Survey descriptions (e.g. Forsyth & Chisholm, 1977) or as part of xenolith studies (e.g. Chapman, 1974; Hunter & Upton, 1987); and the Namurian sills of west Fife have been analysed as part of a larger project on the emplacement mechanism of high-level dolerite sills (Walker, 1986). The first (and to date, only) regional review based the trace-element compositions was provided by Macdonald (1980). He attributed the *hy*-normative/*ne*-normative range in composition to various degrees of equilibrium partial melting of a phlogopite-peridotite mantle with strong partitioning of Ba, Ce, Nb, P, Sr and Zr into the liquid. K and Rb were retained, for small degrees of melting, by residual phlogopite. The mantle source was attributed characteristics broadly similar to an ocean island basalt source, and shown to be heterogeneous with respect to incompatible trace elements.

Russell (1985) has provided the only mineral chemistry data for the late-Palaeozoic suite. He concentrated on rocks of Dinantian age but eight Silesian - early Permian samples were included in the data set.

1.6.3. Xenolith inclusions

Individual occurrences of xenolith-bearing intrusions and lavas have often been mentioned in the literature, particularly in the more recent Geological Survey memoirs for each area (e.g. Eyles *et al.*, 1949; Richey *et al.*, 1930; Forsyth & Chisholm, 1977; McAdam & Tulloch, 1985; Davies *et al.*, 1986). Chapman (1974, 1976) and Chapman & Powell (1976) made a comprehensive study of the

xenoliths and megacrysts from some of the tuff pipes and minor intrusions of Fife and Lothian. With additional experimental data he was able to present a petrogenetic model for the area involving deep-level (at least 70km) pyrope/augite fractionation from an alkaline magma, with shallower-level clinopyroxene-olivine fractionation (<35km) producing cumulates. These were fragmented by a later magma of alkaline affinity and carried to the surface as xenolithic inclusions (Macintyre *et al*, 1981).

Upton *et al.* (1983) recognised that these isolated xenolith occurrences constituted a broad 'nodule province' embracing much of northern and western Britain. On the basis of their observations an extremely heterogeneous upper mantle below a high-grade (granulite facies) feldspathic basement was inferred to underlie all the major north British structural provinces. Further discussion of the geochemical characteristics of some of these xenolithic suites was provided by Hunter & Upton (1987).

1.7. Summary

1. Post-Dinantian magmatic activity in the Midland Valley was of a restricted compositional range, producing basalts, basanites and basaltic hawaiites with rare hawaiites and nephelinitic samples.

2. The largest volumes of magma were intruded as sills: volcanic activity was of a phreato-magmatic nature except in Ayrshire where Namurian and Permian lavas outcrop.

3. Mantle melting has been attributed to the orogenic effects associated with the suturing of Pangaea and to possible rifting of the Arctic-North Atlantic craton in the Westphalian. Within the Midland Valley three broad tectonic phases controlled volcanism (1) NW-SE (Dinantian-late Westphalian) (2) E-W (late Westphalian/Stephanian) and (3) N-S - NE-SW (Permian).

4. Samples have been collected from lava flows, sills, minor intrusions and blocks from vents, and have been classified using chemical criteria.

5. Much work has been carried out on the igneous rocks of the area in the past. It has concentrated on detailed accounts of individual

localities, radiometric age determinations, and mantle xenolith studies. The present study represents the first geochemical study of the post-Dinantian suite.

CHAPTER 2

AGE RELATIONSHIPS

2.1. Introduction

Any attempt to quantify magma evolution relies on the ability to place the rocks under study within a chronological framework. This is harder to achieve for the Silesian-Autunian igneous rocks of the Midland Valley than for those of the Dinantian, because of the higher ratio of intrusive to extrusive rocks. The framework established in this thesis is based on K-Ar ages from a number of sources including this work.

Regional tectonic interpretations of magmatic events are constrained to a certain degree by the time scale used. The most widely quoted time scale is that of Harland *et al.* (1982) which places the beginning of the Silesian at 333 Ma and the Carboniferous/Permian boundary at 286 Ma. The more recent scale of Forster & Warrington (1985) indicates a Silesian time-span of 325-290 Ma. Midland Valley lavas span the Dinantian/Namurian, Namurian/Westphalian and Stephanian/Permian boundaries (see Table 2.1), and K-Ar age-dating by De Souza (1979, 1982) was used by Forster & Warrington (1985) to constrain these boundaries. Both these scales (Harland *et al*, 1982; Forster & Warrington, 1985) suffer from a paucity of calibration points in the Silesian. This has been overcome significantly by recent $^{40}Ar/^{39}Ar$ age determinations on sanidine crystals separated from central European Silesian tonsteins (Lippolt *et al*, 1984; Hess *et al*, 1985). The tonsteins are interbedded with biostratigraphically well-dated coal-bearing facies, and the age determinations obtained are considered to provide the best inter-Silesian time constraints to date (Leeder, 1988b). The revised time scale used by Leeder (1988b) and Leeder & MacMahon (1988) places the Silesian between 326-300 Ma, ending c.10 Ma before the date suggested by Forster & Warrington (1985). The greater precision of the $^{40}Ar/^{39}Ar$ technique over K/Ar dating, combined with more accurate results expected from sanidine separates than from whole-rock analyses, provides a strong basis for accepting the new time scale of Lippolt *et al.* (1984) and Hess *et al.* (1985).

Adoption of this time scale obviously has profound implications for late Carboniferous crustal and magmatic events in north west Europe. Most notably these are (summarised from Leeder, 1988b):

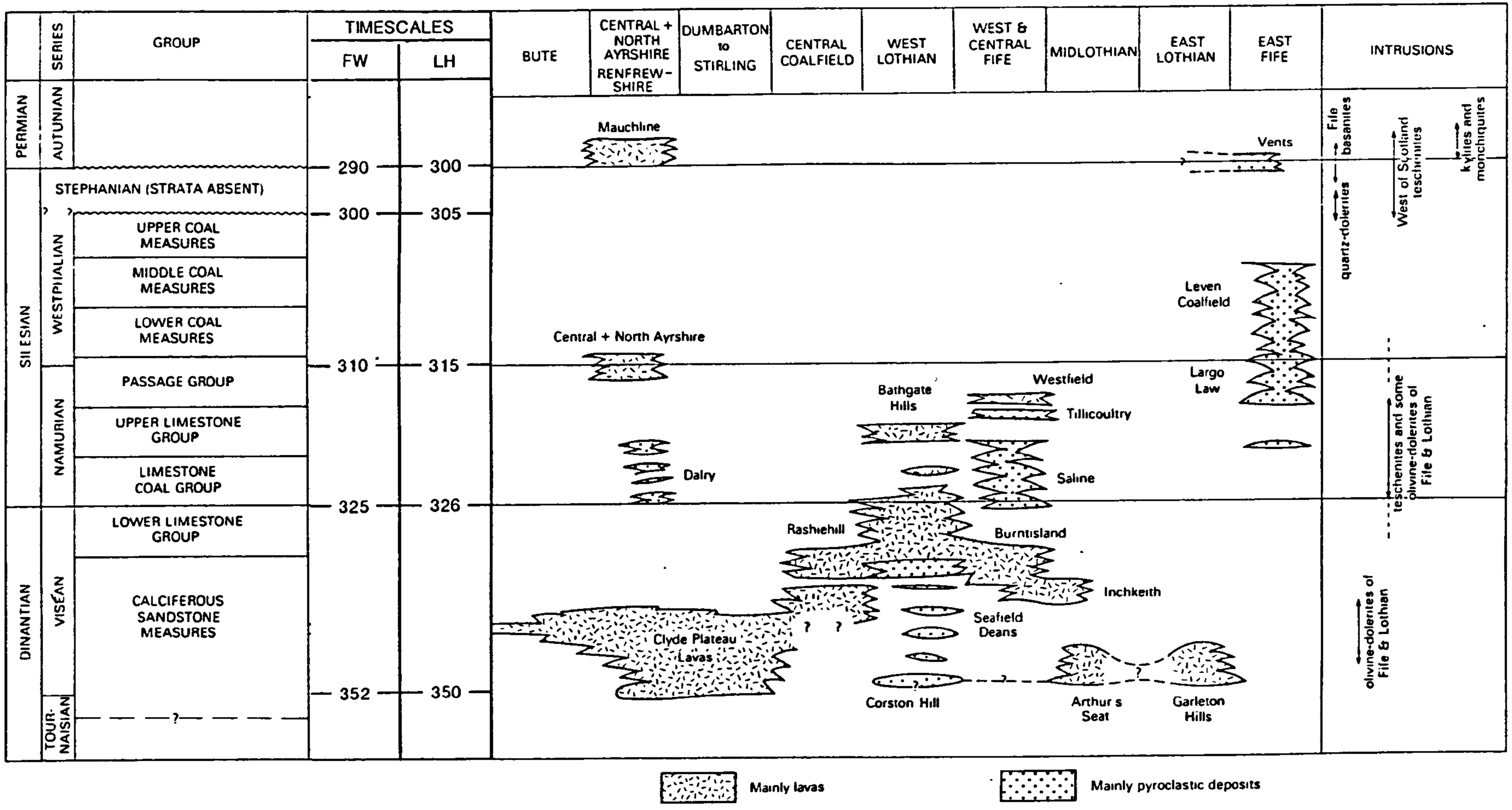

Table 2.1 Diagrammatic representation of geographical and stratigraphical distribution of Carboniferous and Permian igneous rocks of the Midland Valley. The time scales of Forster & Warrington (1985) [FW] and Lippolt *et al.* (1984) & Hess *et al.* (1985) [LH] are shown for comparison. (Adapted from Cameron & Stephenson, 1985)

1. The intrusion of the quartz dolerite sills and dykes in the early Permian rather than the Stephanian. Similarly, the Mauchline, Thornhill and Sanquhar lavas, the Ayrshire sills, many of the Fife & Lothian minor intrusions and the Highland dykes must also represent a magmatic event of Permian age.

2. The age of any possible North Atlantic rifting (Russell & Smythe, 1983) must be older than lower Permian, since the quartz dolerite suite and equivalent intrusions in the Oslo Graben have been used to date the event.

In the following account the implications of both the Forster & Warrington (FW) and Lipolt/Hess (LH) time scales are emphasised.

Published ages have been converted when necessary to ages compatible with the standard decay constants and abundances recommended by the IUGS subcommission on Geochronology (Steiger & Jager, 1977). The tables used for this conversion can be found in Harland *et al.* (1982). Table 2.2 lists known age determinations for post-Dinantian rocks.

The following sections outline the magmatic histories of Ayrshire, and Fife and Lothian, treating them as two distinct areas. Subsequent sections comment on the tholeiitic rocks of the region, on Permian activity outside the Midland Valley, and on the ages determined as part of this project. The final section discusses briefly some of the apparently anomalous age determinations.

2.2. Ayrshire

2.2.1. Passage Group activity

The Dinantian in north Ayrshire drew to a close with the extrusion of the pre-Brigantian Clyde Plateau lavas, dated by De Souza (1979) at $327^{+}_{-}7$ Ma. Igneous activity in the west appears to have abated for nearly 15 million years (with the exception of subordinate tuffs in the Limestone Coal and Upper Limestone Groups of the Dalry Basin) until the eruption of the Passage Group lavas in the late Namurian. These occur between mid-Namurian A and Westphalian A sediments (De Souza, 1979) and have been assigned a minimum age of $305^{+}_{-}6$ Ma by De Souza (1979,1982). On the Lippolt/Hess time scale the

Table 2.2 (See foot for details)

AYRSHIRE			
Passage Group Lavas			
Annick Water, Rashiehall	NS 382430	304±6	E
Carmel Water, Kilmaurs	NS 425417	(271±6)	E
Auchenharvie Castle	NS 363443	(289±7)	E
		(300±5)	A
Annick Water Mill	NS 374423	299±3	E
Mauchline Lavas			
Tarbolton Station	NS 445254	(255±7)	E
River Ayr nr Stair	NS 454245	281±8	E
Howford Bridge	NS 517254	278±8	E
Minor intrusions			
Patna Hill dyke	NS 406109	256±7	E
Ashentree Glen	NS 435137	295±6	J
Carskeoch vent nr Patna	NS 411093	288±9	E
Major intrusions			
Benbeoch Crags	NS 496083	(232±6)	E
Craigs of Kyle	NS 434151	(246±6)	E
Kilmein Hill	NS 452112	282±6	E
Carskeoch	NS 411093	291±7	E
		291±5	E
Lugar Sill	NS 600215	297±7	E
		288±6	H
Howford Bridge	NS 515254	58.4±1.4	E
Polnessan Burn	NS 430114	(254±9)	E
Craigens–Avisyard	NS 587181	303±7	E
Castle Craig	NS 226416	278±7	E
Polbaith Gorge, Galston	NS 488392	(262±7)	E
Boulder nr Craigie	NS 429329	282±7	E
Craigie Hill Quarrie	NS 425326	292±7	E
Lennoxtown Glasgow)	NS 628794	276±7	E
Craigmaddie, Milngavie	NS 566759	252±7	E
Necropolis, Glasgow	NS 605655	279±9	E
Cathcart Castle, Glasgow	NS 587600	276±8	E
Barshaw nr Paisley		276±8	E
FIFE			
Minor intrusions			
Lundin Links	NO 411024	(244±6)	D
Coalyard Hill	NO 513008	(259±7)	D
Kinaldy	NO 510101	(272±7)	D
St. Monance	NO 523013	288±6	D
Chapel Ness	NT 480993	288±6	D
		245±5	J
Davie's Rock	NO 521013	290±6	D
Largo Law	NO 427104	295±6	D
Craig Rock, Largo Law	NO 433049	295±6	D
Kincraig	NT 466997	(117±3)	E
		138±4	J

Rires Craig	NO 456043	287±7	E
Ruddon's Point	NO 455006	260±5	J
Elie Harbour	NO 493996	270±4	G
Elie Ness	NO 497993	279±4	G
East Lomond	NO 245062	277±8	A
Green Hill	NO 222068	282±8	A
		277±6	A
Cowden Hill Intrusion	NT 112964	259±5	J
The Binn	NT 235868	209±8	E
	NT 235870	290±8	E
Glenshee Ruin	NT 205871	241±5	J
Major intrusions			
Greigston	NO 445108	(267±6)	D
Newbiggin of Craighall	NO 423104	(288±6)	D
Drumcarrow Craig	NO 460131	240±6	D
Laeddie	NO 445131	294±6	D
Baldutho Quarrie	NO 499063	304±6	D
Kilbrackmont Quarry	NO 472064	310±6	D
Dunicher Law	NO 451083	280±8	D
Cassindonald	NO 462124	289±6	D
Lavas			
Blindwell's Quarry	NO 418039	(272±6)	D
		281±7	E
Largo House	NO 418039	298±6	D
LOTHIAN			
Minor intrusions			
Yellow Craig	NT559853	354±9	B
St. Baldred's Cradle	NT635815	302±7	B
		235±5	J
Fidra	NT 513868	241±5	J
		335±8	J
Yellow Craig Plantation	NT 519858	299±6	C
Dyke nr Leithes	NT 574854	293±7	J
Gin Head	NT 592852	267±5	J
Gin Head Sill		239±7	C
Gin Head Dyke		278±7	C
Oldhamstocks	NT 737706	295±6	J
Major intrusions			
Ravensheugh stock	NT 631814	319±9	B
Gosford Bay	NT 440776	313±5	B
Corstorphine Sill	NT 201755	317±9	E
R. Almond, Cramond	NT 193772	316±7	E
Mons Hill	NT 147793	308±7	E
GLAS EILEAN LAVA			
		284±6	I
HIGHLAND DYKES			
		288±4	F
		263±4	F
		292±4	F

	286±4	F
	286±4	F
	273±4	F
	294±4	F
	274±4	F
QUARTZ DOLERITES		
Linlithgow Sill	302±7	A
Dyke, Campsie Fells	305±7	A
Sill, Lomond Hills	280±9	A
Sill, Lomond Hills	(277±6)	A
Dyke, Carleton Hill	294±7	B

Table 2.2 K-Ar age determinations for Scottish post-Dinantian igneous rocks. Letters A-J refer to the source of the date. Low ages are bracketed where the author concerned felt there was some explanation for loss of Ar e.g. sample alteration, high glass and/or analcime content.

A Fitch *et al.* 1970; **B** De Souza 1974; **C** Snelling & Chan 1976; **D** Forsyth & Rundle 1978; **E** De Souza 1979; **F** Speight & Mitchell 1979; **G** Macintyre *et al.* 1981 **H** Henderson & Gibb 1987; **I** Upton *et al.* 1987; **J** This study.

stratigraphic position indicates an age of c. 320–315 Ma. There are no exposures of lava south of the NE-trending Kerse Loch Fault, However there is a series of decomposed quartz-bearing dolerite sills and De Souza (1979) obtained a minimum age of $307^{+}_{-}7$ Ma for a biotite separate from the Craigens–Avisyard sill complex. On the basis of this and their gross geochemical similarity (both are subalkaline in character, and some of the lavas are quartz-normative), he suggested that these dolerites were intrusive equivalents to the Passage Group lavas. Subsidence and sedimentation south of the Kerse Loch Fault would have inhibited extrusive activity, and high-level sills were emplaced in which alteration was promoted by the relatively wet sediments (De Souza, 1979).

2.2.2. Westphalian–early Permian and Tertiary sills

The alkali dolerite sills of Ayrshire represent a period of intrusive activity from the Westphalian to early Permian. Early workers on the alkaline dolerite sills of Ayrshire (Tyrrell, 1909; Eyles *et al*, 1949) divided them into two main groups: intrusions of kylitic and teschenitic affinity. Some members of the teschenitic group intrude the Mauchline lavas, and because of their petrographic resemblance to the Inner Hebridean Tertiary crinanites were assigned a Tertiary age (Eyles *et al*, 1949). A K–Ar determination of $58.4^{+}_{-}1.4$ Ma for the Howford Bridge sill beside the River Ayr (De Souza, 1979) substantiates this. Palaeomagnetic work (Armstrong, 1957) suggested that the Howford Bridge sill is part of a larger sill complex which stretches from the coast near Prestwick, eastwards to Catrine.

The kylites and remaining teschenites were distinguished from one another on the basis of petrography (Eyles *et al*, 1949), and evidence for their relative ages sought. Both intrude sediments as young as Westphalian Coal Measures and members of both are pierced by Permian vents. However, because the teschenites always precede the prominent NW and WNW phase of faulting in the area, while the kylitic intrusions straddle it, Eyles *et al.* (1949) suggested that the kylitic intrusions post-date the teschenitic dolerites. De Souza (1979) apparently confirmed this with a K–Ar minimum age of $297^{+}_{-}7$ Ma from an amphibole separate from the teschenitic Lugar sill, and one of $282^{+}_{-}6$ Ma from the kylitic–essexite intrusion of Kilmein Hill. These, he suggested, indicated two phases of intrusion: an earlier teschenitic one between the Passage Group and Mauchline activity, and a later kylitic episode, which may be coeval with the

Mauchline lavas.

Recently, Henderson *et al.* (1987) dated a kaersutite separate from the main theralite-picrite unit of the Lugar Sill, using the incremental heating $^{40}Ar/^{39}Ar$ method. The mean plateau age obtained was $288^{+}_{-}6$ Ma, i.e. some 10 Ma younger than De Souza's (1979) age for the same sill, and strengthens the case for contemporaneity with the Mauchline lavas.

Henderson *et al.* (1987) further pointed out that a kylite/teschenite division is based purely on petrography, in particular on the amount of olivine, and on whether the dominant feldspathoid is nepheline or analcime. With this in mind, and because of the geochemical similarity of the two groups (see chapter 5), no distinction is drawn between them in this study.

2.2.3. Mauchline group

The Mauchline volcanic group composes the second major post-Dinantian extrusive sequence in Ayrshire. On the basis of identification of Rotliegende flora in intercalated sediments (Wagner, 1983), and a minimum age determination of $286^{+}_{-}7$ Ma for the lavas (De Souza, 1979,1982), the Carboniferous/Permian boundary was redefined as $290^{+}_{-}5$ Ma (Forster & Warrington, 1985; De Souza, 1982). The Mauchline lavas are therefore at least early Permian in age (FW) and possibly as young as mid-Lower Permian (LH).

Igneous fragments from the vents around the Mauchline Basin generally resemble the Mauchline lavas, leaving little doubt of their affinity. Basaltic intrusions piercing the vents were most likely feeders for the lavas. A K-Ar determination of $288^{+}_{-}9$ Ma for a basanite dyke cutting the Carskeoch vent near Patna (De Souza, 1979) and one of $295^{+}_{-}6$ Ma for a sheet intruding the Ashentree vent (Table 2.3) substantiate this belief.

2.3. Fife & Lothian

2.3.1. Early Silesian activity

The oldest Silesian volcanic rocks in the eastern part of the Midland Valley are the Bathgate and Linlithgow lavas of west Lothian. They straddle the Viséan/Namurian boundary, are of Brigantian-Namurian A age, and are thought to have been fed by some of the numerous vents in the area. Alteration of

these and the early Namurian Saline tuffs (west Fife) has made K-Ar dating impossible. There are no extensive lavas in west Fife, but a series of alkali dolerite sills outcrop in the area. The consanguinity of the intrusions and tuffs is inferred from several lines of evidence:

1. Petrographic similarity of some of the incorporated basaltic plugs to some of the marginal facies of the sills (Francis, 1968).

2. Evidence that the west Fife sills were intruded into wet sediments, and therefore must be of Namurian age, (since the sediments they intrude are very early Namurian), (Francis, 1968).

3. Close spatial association of the sills and extrusive rocks.

4. Comparability of sill and rare lava trace element ratios e.g. Zr/Nb and clinopyroxene compositions (Walker, 1986).

Further confirmation of an early Silesian (Namurian) intrusive event is obtained from radiometric age determinations of Lothian and east Fife sills. Both sets bear a marked petrographic similarity to the west Fife intrusions.

The oldest dates obtained from samples from the east Fife complex are $310^{+}_{-}6$ Ma and $304^{+}_{-}6$ Ma (Forsyth & Rundle, 1978). De Souza's (1974, 1979) work yielded a mean apparent age (seven samples) of $306^{+}_{-}12$ Ma for the Lothian alkali dolerites. If there has not been significant argon loss from these samples there remains the possibility that emplacement continued into the Westphalian (FW) and possibly until late Westphalian times (LH).

2.3.2. Late Silesian activity

Pyroclastic activity in east Fife continued through to the mid-Westphalian (Forsyth & Chisholm, 1977; chapter 1). Many discussions have assumed that the vents in the region acted as feeders for the extrusive materials. However, radiometric dates for eight of the minor intrusions (Forsyth & Rundle, 1978) have suggested a younger age for at least some of them. The five oldest results (288-295 Ma) are indistinguishable within the limits of analytical error, providing a best minimum estimate for the time of emplacement of $295^{+}_{-}10$ Ma, i.e. late Silesian to early Permian (FW) or early to mid Lower Permian (LH).

Further evidence for small-volume late magmatic activity in Fife is provided by minimum ages of 276$^{+}_{-}$4 Ma for intrusions in the Elie Harbour and Elie Ness vents (Macintyre *et al*, 1981) and by radiometric age determinations of the East Lomond and Green Hill intrusions of Central Fife (Fitch *et al*, 1970). The latter two yielded ages of 277$^{+}_{-}$8 Ma and 282$^{+}_{-}$8 Ma respectively and are considered by the authors to be a good approximation to the date of intrusion.

Along the Lothian coast west of Eyebroughy are numerous volcanic vents all of which either predate or are contemporaneous with the Dinantian Garleton Hill volcanic rocks (Martin, 1955; McAdam & Tulloch, 1985 Davies *et al*, 1986). Associated with some of these vents is a group of minor intrusions, some of comparable lithology to the Dinantian lavas, but many of a more silica-poor type similar to those of the Fife Silesian - Permian vents. K-Ar analyses of these basanites (see Table 2.2 for sources of dates) yielded ages in the range 293$^{+}_{-}$7 Ma - 229$^{+}_{-}$6 Ma. In the absence of information to the contrary and on the basis of geochemical similarities of these and the Fife intrusions (this study), a Lower Permian age has been asigned to the Lothian intrusions.

2.4. Tholeiitic interlude

All of the magmatism in the Midland Valley considered so far comprises alkaline basaltic compositions. However, a brief tholeiitic interlude occurred in late Carboniferous times resulting in the Midland Valley sill complex, believed to be contemporaneous with the Whin Sill of NE England. Associated with it are the E-W trending dykes up to 30km in length which cross-cut the major NE-SW tectonic features of the region.

From field evidence and by analogy with the Whin Sill of Northern England (Fitch et al., 1970) the dykes and sills have always been regarded as post-Wesphalian but pre-Permian in age (Francis, 1983). Fitch *et al*, (1970) determined ages for four members of the tholeiitic suite. Of these, two were fresh enough to yield ages considered to be a close approximation to the actual time of intrusion. On the basis of these the sills and dykes have been assigned an age of approximately 301 Ma (straddling the Westphalian - Stephanian boundary) (FW) or the Stephanian - Autunian boundary (LH).

2.5. Scottish Permian igneous activity outside the Midland Valley

Permian lavas also outcrop outside the Midland Valley. Those south of the Southern Uplands Fault from the Thornhill and Sanquhar basins are petrographically and geochemically similar to the Mauchline lavas (Fig. 1.9). North of the Highland Boundary Fault the Glas Eilean lavas between Islay and Jura have yielded a mean age of 285$^{+}_{-}$6 Ma (Upton *et al*, 1987), and the Duncansby Ness vent in Caithness has an apparent age of 267$^{+}_{-}$1 Ma (Macintyre *et al*, 1981).

A suite of late-Palaeozoic silica-undersaturated basic dykes outcrops throughout the Scottish Highlands and Islands (Baxter & Mitchell, 1984: Fig. 1.10). K-Ar age determinations by Speight & Mitchell (1979) and Baxter & Mitchell (1984) indicated three tectono-magmatic events:

1. Late Visean (324$^{+}_{-}$9 Ma) E-W Eil-Arkaig and Monar swarms.
2. Stephanian (FW)/ Permian (LH) (291$^{+}_{-}$5 Ma) NW-SE Ardgour swarm.
3. Late Permian (258$^{+}_{-}$10 Ma) NE-SW Orkney swarm.

The second of these, the Ardgour dyke swarm was probably co-magmatic with the Mauchline, Thornhill-Sanquhar and Glas Eilean lavas.

2.6. New K-Ar age determinations

2.6.1. Analytical procedure

Argon analyses were carried out at the Scottish Universities Research and Reactor Centre, East Kilbride by the isotope dilution method using ^{38}Ar as a spike. The procedure has been described by De Souza (1979). Ratios were measured statically on an MS10 mass spectrometer. Potassium concentrations were obtained by conversion of wt% oxide concentrations measured by XRF analysis at Edinburgh University. K-Ar ages were calculated using the standard decay constants and abundances recommended by the IUGS Subcommision on Geochronology (Steiger & Jager, 1977). Results are outlined in Table 2.3.

Sample	Locality	wt%K	^{40}Ar	$\frac{^{40}Ar^*}{^{40}Ar_T}$	Age
SW9	Ruddon's Point [NO 455006]	0.952	4.625	0.925	$260^{+}_{-}5$
SW452	Kincraig [NT 467998]	0.565	1.410	0.524	$138^{+}_{-}4$
SW456	Chapel Ness [NT 475996]	1.175	5.351	0.795	$245^{+}_{-}5$
SW472	Cowden Hill [NT 112964]	1.046	5.061	0.884	$259^{+}_{-}5$
SW536	Glenshee Ruin [NT 205871]	0.697	3.120	0.699	$241^{+}_{-}6$
SW8	Fidra [NT 513868]	0.749	3.347 4.788	0.722 0.691	$241^{+}_{-}5$ $335^{+}_{-}8$
SW25	Oldhamstocks [NT 737706]	1.034	5.749	0.912	$295^{+}_{-}6$
SW557	St Baldred's Cradle [NT 635815]	1.381	3.617 5.999	0.777 0.922	$145^{+}_{-}3$ $234^{+}_{-}5$
SW560	Gin Head Dyke [NT 592852]	2.240	1.195	0.945	$267^{+}_{-}5$
SW562	Yellow Man Dyke [NT 574854]	1.679	9.274	0.927	$293^{+}_{-}7$
PA01	Ashentree Glen [NS 435137]	0.794	4.300 4.328	0.848 0.897	$288^{+}_{-}6$ $294^{+}_{-}6$

Table 2.3 K-Ar whole-rock isotopic data and ages for samples anaysed as part of this project.

Explanation: $^{40}Ar^*$ = radiogenic argon 40; $^{40}Ar_T$=Total argon 40.

2.6.2. Discussion of results

2.6.2.1. Fife

Five vent intrusions from Fife were analysed and, with the exception of the Cowden Hill intrusion (SW472, with a measured age of 291$^{+}_{-}$6) Ma they have yielded dates between 260$^{+}_{-}$5 Ma and 241$^{+}_{-}$6 Ma. The late Permian - early Triassic dates determined for the four minor intrusions from Ruddon's Point (SW9), Chapel Ness (SW456), Cowden Hill (SW472) and Glenshee Ruin (SW536) are puzzling, since volcanic activity in the area is thought not to have extended beyond the early Permian. The Chapel Ness intrusion was analysed by Forsyth & Rundle (1978) and their age of 288$^{+}_{-}$6 Ma is now held to be a good approximation to the date of intrusion. This suggests that there has been significant Ar loss from SW456. However, the rock is fresh with little groundmass analcime or glass. There does however, remain the possibility that Ar could have been lost during an event associated with the few thin zeolite veins which dissect the rock.

There are no previous age determinations with which dates for the other two intrusions can be compared. SW9 (Ruddon's Point) is a fine-grained olivine-phyric basanite. There are some patches of analcime in its fine-grained glassy groundmass, otherwise, with the exception of incipient serpentinisation of olivine along fractures, it is fresh. The Glenshee Ruin intrusion (SW536) was analysed in an attempt to throw light on the age of the Burntisland minor intrusions. It had been assumed on the basis of petrography that they were emplaced during the period of lava extrusion in the late Dinantian (Allan, 1924; Cameron & Stephenson, 1985). However De Souza (1979) obtained a date of 284$^{+}_{-}$8 Ma for a fresh intrusion in the Binn vent, and could not rule out the possibility that it post-dated the Dinantian activity. The date of 241$^{+}_{-}$6 Ma determined for SW536 must be treated with some caution since the sample, has quite a glassy groundmass. However, because of geochemical evidence (the majority of Dinantian lavas are *hy*-normative and the smaller vent-intrusions are *ne*-normative), and on the basis of the date quoted for the Binn vent intrusion, it is felt that this set of intrusions is probably co-magmatic with the late-Silesian - early Permian activity in Fife and Lothian.

2.6.2.2. Lothian

Dates determined from the five Lothian intrusions display variations both between and within samples.

Analysis of a sample from the Fidra intrusion (SW8) has yielded two dates of $335^{+}_{-}8$ Ma and $312^{+}_{-}7$ Ma. If the older date is correct then a late Dinantian age must be inferred for Fidra. However, the date of $312^{+}_{-}7$ indicates a possible Namurian-Westphalian age.

The intrusion at St. Baldred's Cradle was dated by De Souza (1974) and yielded a minimum age of $296^{+}_{-}7$ Ma. This conflicts with Clough *et al.* (1910) and Davies *et al.* (1986) who maintained on the basis of petrography, that the intrusion was a feeder for some of the Dinantian lavas. Two dates have been obtained for the intrusion as part of this project: $214^{+}_{-}4$ and $234^{+}_{-}5$ Ma. Both are significantly different from De Souza's value of $296^{+}_{-}7$ Ma. Geochemically SW557 is dissimilar to the post-Dinantian intrusions of the area, and it is felt that it probably is Dinantian. Argon must therefore have been lost from the sample.

Two intrusions which yield dates comparable to those obtained by Forsyth & Rundle (1978) for some of the Fife vent intrusions are the Oldhamstocks sill (SW25) and the Yellow Man Dyke (SW562) with ages of $295^{+}_{-}6$ Ma and $293^{+}_{-}7$ Ma respectively. Both are fresh ol-cpx-phyric basanites, containing small amounts of analcime. In addition SW562 has a fine-grained glassy groundmass.

The final intrusion considered is a dyke from near Gin Head. Petrographically it is very different from any of the other intrusions sampled, with a notable absence of olivine phenocrysts. As well as subhedral augite phenocrysts, it contains elongate plagioclase and augite, indicating rapid crystallisation. The date of $267^{+}_{-}5$ Ma must be considered a minimum age if the dyke is related to the Permian basanite activity. Snelling & Chan (1976) dated a dyke from Gin Head at $272^{+}_{-}7$ Ma. Since it is uncertain whether this is the same intrusion, direct comparison is not possible.

2.6.2.3. Ayrshire

The geochronology of the Ayrshire intrusions and lavas has been constrained by De Souza (1979). However one additional analysis was made as part of this project. The age of $291^{+}_{-}6$ Ma for the Ashentree Glen vent intrusion is consistent with its having been a feeder to the early Permian Mauchline lavas.

2.7. General Discussion

From preceeding sections it is clear that there is often some doubt concerning the ages obtained using K-Ar isotope analysis. Problems include loss of argon from analcime, altered plagioclase and glassy groundmasses, and in extreme cases, gain of potassium in alteration products. (These are discussed more fully by De Souza, 1979). The literature is sometimes inconclusive about why certain samples are rejected as having lost argon, and others accepted as representative of the true age when they are petrographically similar. There are some examples where no discussion of petrography is given. This makes division of the post-Dinantian samples into well-defined geographic - age groups difficult. Seven groups have been created as a result of combined age, petrographical and geochemical considerations. The three Ayrshire groups comprise the Passage Group lavas, the Ayrshire sills, and the Mauchline group. Included in the Mauchline group are the Mauchline lavas, and samples from their feeder vents, as well as the coeval and geochemically similar Thornhill, Sanquhar and Glas Eilean samples. The east Midland Valley samples are less easily divided into groups. Based on some often poorly constrained K-Ar ages and on petrographic and geochemical considerations the consensus in the literature (section 2.3.1) is for a Namurian - Westphalian age for the majority of alkaline dolerite sills. Similarly, a late Silesian - early Permian age has been proposed for many of the minor intrusions in vents. The arbitrary nature of this division is acknowledged, but in the absence of any clearer criterion for division, it has been maintained, giving the Fife & Lothian sill and the Fife & Lothian basanite groups. The term basanite is used in this instance to emphasise the undersaturated composition of the group as a whole. Individual members may not be basanites *sensu stricto*. In cases where a relationship has been proved between particular sills and vent intrusions, the samples from the vent intrusion have been included in the sill group. Similarly some small sills have been included in the basanite group. Whereas the latter form a coherent geochemical group (see chapter 5), the same cannot be said for the former. Approximately half the sills have geochemical characteristics comparable to the basanitic intrusions of Fife & Lothian whilst the remainder are less undersaturated.

It was mentioned in section 2.6.2.1 that there has in the past been some ambiguity concerning the ages of the Burntisland intrusions. It is clear from geochemical comparisons with the Dinantian lavas that the intrusions did not

Locality	wt%K	Age	
Ludin Links [NO 411024]	0.950	$239^{+}_{-}6$	D
Coalyard Hill [NO 513008]	1.540	$254^{+}_{-}7$	D
Kinaldy [NO 510101]	1.550	$267^{+}_{-}7$	D
Yellow Craig [NT 559835]		$224^{+}_{-}6$	C
Gin Head sill [NT 592852]		$234^{+}_{-}7$	C
Gin Head dyke . [NT 592852]		$272^{+}_{-}7$	C
Gin Head dyke [NT 592852]	2.240	$267^{+}_{-}5$	J
Ruddon's Point [NO 455006]	0.952	$260^{+}_{-}5$	J
Chapel Ness [NT 480992]	1.175	$245^{+}_{-}5$	J
Cowden Hill [NT 112964]	1.046	$259^{+}_{-}5$	J
Glenshee Ruin [NT 205871]	0.697	$241^{+}_{-}6$	J
Patna Hill [NS 406109]	1.169	$251^{+}_{-}7$	E

Table 2.4 Minor intrusions with apparent minimum ages between 270 and 250 Ma. Letters refer to source of age (see table 2.2).

act as feeders for the lavas, and they must therefore be assigned to either the Fife & Lothian sill group, the Fife & Lothian basanite group or to a new group of a different age. The minor intrusions are petrographically similar to the ol^{+} _cpx-phyric basanites of Lothian (lacking only the high-pressure clinopyroxene phenocrysts and xenocrysts of the other Fife samples), and the sills are similar to those elsewhere in Fife and Lothian. The Burntisland samples have therefore been assigned to one or other of these groups.

A final consideration concerns the handful of fresh samples which have low ages. Table 2.4 lists the twelve minor intrusions which record ages younger than 270 Ma. Undoubtedly some of these ages can be attributed to loss of Argon: those determined as part of this project have been discussed already, and those from other sources are samples for which the analyst has either made no comment about, or could find no cause for, Ar loss. Nine of the intrusions fall within the age range of 249-268$^{+}_{-}$4 Ma determined by Baxter & Mitchell (1984) for the Orkney monchiquite dykes. It is possible that because of their differing K contents (a range of 0.95-2.24 wt% K) the dates reflect the true ages of the intrusions since systematic Ar-loss would be unlikely (R. Macintyre, pers. comm., 1988). There therefore remains the possibility that they represent a magmatic event younger than any so far recorded in the Midland Valley, contemporaneous with intrusion of the Orkney monchiquite dykes (Baxter & Mitchell, 1984) and with waning magmatism in the Oslo Graben (Sundvoll, 1978).

2.8. Summary

1. The post-Dinantian alkaline magmatic evolution of the Fife and Lothian region can be summarised as follows:

   - During early Silesian times there was extrusive activity in the west (lavas in Lothian and pyroclastics in Fife) with associated intrusion of alkali dolerite sills throughout the whole region. This intrusive activity commenced in the early Namurian and may have continued into the Westphalian.

   - Alkaline igneous activity apparently abated for at least 15 million years and resumed on a smaller scale during the Silesian to early Permian (c.290 Ma). Minor intrusions of basanitic affinity are of

particular importance in the eastern parts of Fife and Lothian. An age of $312^{+}_{-}7$ for the Fidra intrusion (SW8) suggests that some basanitic minor intrusions may be coeval with the alkali dolerite sills.

2. The post-Dinantian alkaline magmatic evolution of Ayrshire can be summarised as follows:

   - Late Namurian/early Westphalian (c.310 Ma) extrusion of the Passage Group lavas north of the Kerse Loch Fault, and intrusion of an assumed co-eval set of sills in the thicker sediments to the south of the fault.

   - A phase of alkali dolerite intrusion during Westphalian and Stephanian times which continued into the early Permian.

   - Permian (c.290) extrusion of the Mauchline lavas and associated neck intrusions.

3. The youngest magmatic event in Ayrshire is of Tertiary age (c.58 Ma), producing the Prestwick-Mauchline sill complex and probably related to similar activity in Arran.

4. Permian igneous activity outside the Midland Valley produced the Thornhill-Sanquhar lavas and minor intrusions south of the Southern Upland Fault, and the Glas Eilean lavas, the Highland (Ardgour) dyke swarm and the Duncansby Ness Vent north of the Highland Boundary Fault. Lavas in the North Sea (Viking Graben) and southern Norway (Oslo Graben) are also related to this magmatic event.

5. Much of the region was affected by a brief tholeiitic event at the end of the Westphalian.

6. K-Ar ages of 270-250 Ma for nine of the minor intrusions suggests that magmatism might have continued on a small scale into the mid- late-Lower Permian.

7. Samples have been allocated to seven groups:

- Passage Group lavas
- Ayrshire sills
- Mauchline group (comprising Mauchline lavas and samples from feeder vents, as well as samples from the Thornhill and Sanquhar basins and the Glas Eilean lavas).
- Fife & Lothian sills
- Fife & Lothian basanites
- Quartz dolerites
- Highland dykes (comprising samples from the Ardgour dyke swarm).

CHAPTER 3

PETROGRAPHY

3.1. Introduction

Apart from segregations within the larger intrusions (mainly sills), the rocks are entirely of basaltic or doleritic composition, i.e. are composed largely of basic plagioclase and augitic pyroxene $\pm$ olivine, opaque oxide (with some feldspathoid).

Previous descriptions of the late-Palaeozoic igneous rocks of the Midland Valley by the Geological Survey and others have resulted in a plethora of names, particularly for the doleritic varieties (see section 1.5.1). Since these classifications are largely based upon the recognition of different proportions of feldspar to feldspathoid within a spectrum of rocks which changes little in phenocryst assemblage, the differences are rarely emphasised below. It should be remembered therefore when reading the following account that, with the exception of the Passage Group Lavas and the quartz dolerites, there exists a gradation in the alkali olivine basalts and dolerites in which the proportion of feldspathoid increases at the expense of feldspar. This is often accompanied by an increase in the modal proportion of augite and brown interstitial glass in the groundmass.

In the following section the features characteristic of the late-Palaeozoic suite as a whole are described. Subsequent sections deal with each group in turn, with descriptions of general characteristics of the group, and phenocryst assemblages.

3.2. Features common to all groups

3.2.1. Recognition of phenocrysts

Cox *et al*, (1979) defined a phenocryst or intratelluric crystal assemblage as a solid phase that was in equilibrium with the liquid before quenching. Phenocrysts are identified on the basis of their greater size relative to groundmass phases, and their euhedral to subhedral shape. This is obvious in extrusive and small-volume intrusive rocks, but is less clear in larger-volume intrusive rocks. Identification of possible phenocryst phases in samples from sills has generally been made on the basis of there being two generations of

the phase concerned, a smaller one consistent with groundmass crystal sizes and a larger one. The latter are not always euhedral to subhedral in outline and the rocks are often better described as sub-porphyritic.

Large anhedral and/or skeletal crystals can be the result of at least three causes:

1. Shallow-level resorption of original deeper-level phenocrysts.
2. Rapid growth during quenching of liquid.
3. Xenocrystal origin.

There are however many instances where it is difficult or impossible to decide with any certainty which process may have given rise to a particular large crystal.

3.2.2. Grain-size and texture descriptions

All fine- to medium-grained samples contain at least one identifiable phenocryst phase. In this account the term phenocryst is used to describe crystal sizes in excess of 0.5 milimetres and microphenocryst for those less than 0.5mm.

Groundmasses vary from glassy through fine-grained (<0.1mm) to medium-grained (0.1-0.3mm) for extrusive and small-volume intrusive rocks; and from medium- to coarse-grained (>0.3mm) for the larger-volume intrusive rocks.

3.2.3. Augite segregations

These consist of rounded irregular patches up to a few mm across which contain a higher concentration of augite than the groundmass (plate 3.4a). Other groundmass components are usually present as 'accessory phases'. A variety of textures are displayed. Often the augite is granular and shows a decrease in grain-size towards the centre of the segregation. Rarely the patches possess a central area which is occupied by felsic material e.g sodic plagioclase or a zeolite, suggesting a late-stage infilling, but usually augite ($\pm$ minor plagioclase, opaque oxides, glass) continues to the centre. In one

example (SW158: plate 3.4b) a segregation has a 'euhedral' equant outline suggesting a possible pseudomorphous relationship with a previous mineral. Reaction relationships are suggested by rounded examples (e.g. SW404) composed of rims of small granular augite and interiors of elongate bladed augite radiating into the centre. There often appears to be a narrow zone of groundmass alteration surrounding these. Similar features are described by Forsyth & Chisholm (1977) from some of the Fife intrusions, and attributed by them to reaction of host magma with quartz xenocrysts.

3.2.4. Alteration

De Souza (1979) outlined five stages of alteration within Scottish Carboniferous and Permian igneous rocks. This is adapted below for the post-Dinantian suite:

1. Minor alteration of olivine. Clinopyroxene phenocrysts and groundmass remain fresh.

2. Olivine partly or wholly altered. Pseudomorphs include red-brown iddingsite, green bowlingite, chlorite, serpentine, carbonate and more rarely opaque oxides. Clinopyroxene still fresh, but small amounts of interstitial chlorite may be present in the groundmass.

3. Olivine totally altered; feldspar sericitised along cracks; incipient alteration of clinopyroxene; chloritic mesostasis.

4. Pseudomorphed olivine; feldspars turbid and sericitised along cracks; more extensive alteration of clinopyroxenes than in (3), often along cleavages. Calcite, chlorite and zeolites may be present in groundmass.

5. Mafic minerals almost completely replaced; feldspars albitised; groundmass cloudy.

3.2.5. Inclusions

Xenoliths have been identified in some of the finer-grained samples. Fragments of sedimentary rocks include shale, sandstone and limestone, all showing evidence of reaction with the liquid. Xenoliths and xenocrysts of a suspected mantle origin, or representative of a previous magmatic event, have

been identified in blocks from vents and minor intrusions throughout the whole region, and more rarely in lava flows and tuffs of the Mauchline Basin.

The information in the following account of inclusion lithology is extracted from Upton *et al.* (1983), Hunter *et al.* (1984), Upton *et al.* (1984), and Hunter & Upton (1987).

Upton *et al.* (1983), listed eleven classes of inclusions:

1. Magnesian peridotites (lherzolites & harxburgites)
2. Dunites & wehrlites
3. 'Anhydrous pyroxenites'
4. Kaersutite-pyroxenites
5. Lherzites & glimmerites
6. Magnetite-apatite ($^{+}_{-}$ biotite) rocks
7. Feldspar rocks (anorthosites & anorthoclastites)
8. Basic granulites
9. Quartzo-feldspathic gneisses
10. Miscellaneous plutonic xenoliths of presumed igneous origin
11. Megacrysts

The three dominant lithologies are the magnesian peridotites (1), the wehrlite-clinopyroxenite series (2&3) and the basic granulites (8). Of the magnesian-peridotites, spinel lherzolites are the commonest. They are composed of olivine (70-90%), orthopyroxene (10-20%) and clinopyroxene and spinel (1-10%), and together with the harzburgites, display a range of deformation and recrystallisation textures. The compositional range of lherzolitic olivines and clinopyroxenes from five Midland Valley localities is given in Table 4.2. Mineral grains are essentially unzoned, and compositions within individual inclusions are homogeneous except where there has been localised interaction with the host magma.

In the wehrlite-clinopyroxenite suite, the wehrlites comprise discrete olivine and spinel grains set in clinopyroxene oikocrysts up to 1cm in size. With

decreasing olivine, these grade into spinel-clinopyroxenites (plate 3.4c). The suite does not normally possess deformed metamorphic fabrics, although locally they are annealed and thermally re-equilibrated. Compositionally, the constituent minerals are distinct from those in the magnesian peridotites: clinopyroxenes are generally richer in Fe, TiO_2, Al_2O_3 and poorer in Na_2O and Cr_2O_3 (see Table 3.1), the olivines are more fayalitic and the spinels poorer in Mg and Cr.

Members of the basic granulite (metagabbro) suite have primary mineral assemblages composed of plag + cpx + mt $\pm$ opx $\pm$ ap ($\pm$ gt). Modal proportions are variable, with plagioclase forming up to 85% of the mode. Textures range from relict igneous (metagabbro) to thoroughly recrystallised metamorphic fabrics. Modification of primary mineralogies has been achieved by (a) annealing and recrystallisation, particularly along grain boundaries, (b) exsolution of spinel and/or pyroxene from primary pyroxene, (c) marginal zoning in plagioclases (and pyroxenes) and (d) growth of new, texturally distinct phases, principally olivine and/or orthoclase. The ranges in clinopyroxene chemistry for this group are outlined in Table 3.1.

Xenoliths are often accompanied by large (up to 10cm) discrete crystals which can be strongly out of equilibrium with their hosts. These megacrysts sometimes contain inclusions of other phases, and are sometimes found as crystal aggregates which may indicate a direct linkage to various of the xenolith types. The commonest megacryst species are alkali feldspars, clinopyroxenes (plate 3.4e), amphiboles, micas and magnetites.

3.2.6. Amygdales

Little comment can be made concerning amygdale characteristics since the emphasis of sample collection was on obtaining material suitable for geochemical analysis, consequently non-amygdaloidal material was preferentially sampled. Amygdale compositions appear to be dominated by calcite or zeolites, and more rarely chloritic assemblages.

	Pyroxenite–wehrlite		Granulite
	Olivine	Clinopyroxene	Clinopyroxene
$Mg/Mg+Fe^{2+}$	0.74–0.81	0.68–0.86	0.61–0.81
NiO	0.18–0.27		
Ca/Ca+Mg+Fe		0.39–0.50	0.44–0.48
Al_2O_3		4.2–9.3	2.0–5.6
Cr_2O_3		0.21–0.57	
TiO_2		0.51–0.91	0.21–1.18
Na_2O		0.21–1.18	0.40–1.03

Table 3.1 Olivine and clinopyroxene compositional parameters from the Fidra pyroxenite–wehrlite and granulite suites. (Data from Hunter *et al*, 1984).

Plate 3.1

a. Typical Passage Group lava with pseudomorphed olivine phenocrysts in a groundmass of plagioclase, augite, opaque oxides and chloritised glass [SW243b, PP].

b. Olivine- augite- plagioclase-phyric Passage Group lava [SW307, XP]

c. Mauchline lava with reasonably fresh olivine phenocrysts in a groundmass of plagioclase, augite, olivine, opaque oxides and glassy mesostasis. Such fresh olivine is rare in these lavas and phenocrysts are usually completely pseudomorphed by iddingsite (e.g. plates 3.1d & e) [SW124, PP].

d. Hawaiitic Mauchline lava with augite glomerocrysts and iddingsite pseudomorphs after olivine. There is a high concentration of alkali feldspar in the trachytoid-textured groundmass [SW134, XP].

e. Feldspathoidal Mauchline lava, with pseudomorphed (iddingsite) olivine microphenocrysts in a groundmass of augite, olivine and feldspathoid. Plagioclase is present only in accessory amounts [SW202, PP].

f. Olivine-phyric basanite from the Ashentree Glen intrusion in the Mauchline Basin. The irregular olivine in the bottom left of the field of view has strained extinction and is possibly a xenocryst [PA01, PP].

Plate 3.2

a. Olivine-phyric member of the Ayrshire sill group with euhedral phenocrysts and an irregular xenocryst with strained extinction (bottom left corner). Some of the phenocrysts show evidence of zoning, this is clearer in plate 3.2b [SW299, XP].

b. Zoned subhedral olivine phenocryst from one of the Ayrshire sills [SW297, XP].

c. Olivine- clinopyroxene-phyric dolerite from the Ayrshire sill group. The clinopyroxene phenocrysts have distinct titanaugite rims. This is a common feature of many clinopyroxenes from the post-Dinantian suite [SW105, PP].

d. Accumulations of olivine and clinopyroxene in one of the most porphyritic Ayrshire sills [SW91, XP].

e. Biotite and kaersutite in the Saltcoats sill, Ayrshire. The turbid colourless patches are plagioclase; non-turbid patches are analcime [SW363b, PP].

f. Olivine- clinopyroxene-phyric minor intrusion from Largo Law, Fife. Subhedral olivine phenocrysts show incipient bowlingite alteration along cracks. The groundmass comprises augite, opaque oxides, olivine, plagioclase and brown, slightly turbid glass [SW39, PP].

Plate 3.3

a. Olivine- clinopyroxene-phyric intrusion from Fife [SW442, PP].

b. Sub-ophitic alkaline dolerite from Fife, with variably altered olivine phenocrysts [SW414, XP]

c. 'Non-ophitic' olivine- clinopyroxene-phyric alkaline dolerite from Fife [SW468, PP].

d. Quartz dolerite comprising plagioclase, clinopyroxene, opaque oxides and brown turbid glass [RM63, PP].

e. Altered olivine and variably preserved clinopyroxene phenocrysts and fragments in a plagioclase-free glassy groundmass: Highland dyke [SW115, XP].

f. Felsic ocellus containing needles of augite and small laths of biotite: Highland dyke [SW114, PP].

Plate 3.4

a. Augite 'segregation' with decreasing clinopyroxene crystal size from margin to centre [Mauchline lava: SW173, XP].

b. 'Euhedral' segregation comprising augite with a plagioclase filled central area [SW158, XP].

c. Part of a clinopyroxenite inclusion [Fife basanite: SW493, XP].

d. Rounded clinopyroxenite fragment of assumed xenolithic origin [Fife basanite: SW427, XP].

e. Anhedral, partly resorbed clinopyroxene megacryst with reaction rim [Mauchline diatreme block: SW335, PP].

f. Large partly resorbed olivine xenocryst [Fife basanite: SW456, PP].

Plate 3.5

a. Anhedral olivine fragment of supposed xenocrystal origin [Fife basanite: SW45, PP].

b. Clinopyroxene with sieve-textured core, of assumed xenocrystal origin [SW428, XP].

c. Anhedral, twinned clinopyroxene phenocryst with sieve-textured core [Fife basanite: SW442, XP].

d. Sieve-textured clinopyroxene phenocryst with titanaugite rim [Fife basanite: SW403, PP].

e. Euhedral clinopyroxene with sieve-textured core [Fife basanite: SW442, PP].

f. g. Clinopyroxene phenocrysts with anhedral core regions and euhedral rims. The cores are probably partly resorbed high-pressure phenocrysts or xenocrysts [Fife basanite: SW493, XP].

h. Clinopyroxene with green anhedral core (partly resorbed fassaitic augite) mantled by augite zoning to titanaugite [Fife basanite: SW429, XP].

3.3. Ayrshire samples

3.3.1. Passage Group lavas

These lavas which range in composition from basalts to basaltic hawaiites, contain pseudomorphed olivine phenocrysts in a groundmass of plagioclase, augite, opaque oxides and a chloritised glass (plate 3.1a). The presence or absence of olivine as a groundmass phase is difficult to assess because of alteration. Augite and more rarely plagioclase are present as microphenocryst phases in some samples.

Modal concentrations of olivine phenocrysts vary between 2-10% but are commonly around 5%. The olivines range in size from 0.5-4mm but are generally <2mm. Subhedral shapes dominate. Augite microphenocrysts are never present in concentrations >2%, and are rarely bigger than 0.25mm. Larger crystals are euhedral, and there is a tendency towards glomeroporphyritic texture. Some of the larger crystals show continuous concentric zonations: some however, show sector-zoning. They are occasionally twinned.

One sample (SW307: plate 3.1b) contains phenocrysts of plagioclase (0.5-1mm) with variably-sieved, often rounded cores, and euhedral rims. It displays a general seriate texture from groundmass to microphenocryst. Individual crystals show differing degrees of zonation from cores of An_{65} to rims of (the most extreme example) An_{47}

3.3.2. Mauchline group

This group includes samples of lavas, small hypabyssal intrusions, and blocks in diatremes from the Mauchline, Sanquhar and Thornhill Basins. The lavas range in composition from basalts to basaltic hawaiites, with rare hawaiites and basanites. They are invariably porphyritic to some degree (e.g. plate 3.1c), containing (pseudomorphed) olivine phenocrysts $\pm$ augite phenocrysts. Groundmasses are composed of varying proportions of plagioclase, augite, olivine, analcime, nepheline, opaque oxides and a glassy mesostasis (or chloritised alteration thereof), with accessory alkali feldspar and apatite. Samples containing phenocrysts of olivine but little or no augite can be divided into two groups on the basis of the ratio of felsic to mafic material in the groundmass. Those in which felsic material dominates are nearly always

hy-normative whereas those with abundant augite are generally *ne*-normative. This distinction becomes less clear as the concentration of augite phenocrysts increases.

The hawaiitic samples (SW132-SW145 e.g. plate 3.1d) are noteworthy because of their trachytoid textures and the high concentration of groundmass alkali feldspar, up to 50%.

Olivine is a ubiquitous phenocryst phase with size-ranges typically between 0.25-1.25mm, but exceptionally ranging up to as much as 4mm. Modal concentrations vary from <4% in the hawaiites to >15% in basaltic and basanitic samples. Consequently many of the lava samples could be described as picritic. Crystals are usually euhedral to subeuhedral with less frequent skeletal examples. Fresh olivine is uncommon and the reddening characteristic of this group of rocks is largely due to haematitic alteration of the olivines. When fresh they have homogeneous cores surrounded by normally-zoned rims.

Modal concentrations of augite phenocrysts vary between 0-4%. In samples with concentrations <1% the augites are usually <0.25mm in diameter and are generally euhedral. Clusters of smaller crystals give rise to glomeroporphyritic texture. There is a tendency for the size of the phenocrysts to increase as the mode increases and in some samples they are as big as or bigger than coexisting olivines. In the more augite-phyric samples the sizes of the augite phenocrysts tend to be bimodal at around 0.5mm and 1.5mm respectively. Their shapes range from euhedral to rounded, and glomeroporphyritic texture is still common (plate 3.1d). The larger crystals are usually more complexly zoned than the smaller ones, with normal, oscillatory, patchy and/or sector zoning evident. Occasionally there are darker pinkish-brown rims to the augites, similar in colour to groundmass pyroxene. This late-stage zoning to titanaugite is a much commoner occurrence in the hawaiitic samples in which the largest (up to 4mm) augite phenocrysts are found.

Lava sample SW202 (plate 3.1e) from the Mauchline Basin is notably feldspathoidal. Similar samples were collected from intrusions and blocks from the Mauchline Basin and Sanquhar Basin vents. All contain olivine microphenocrysts (0.25-0.5mm) in groundmasses of augite, olivine and feldspathoid. Plagioclase is either absent or present only in accessory ammounts. Two of the Mauchline Basin minor intrusions (SW370 and PA01

from Hellenton Mains and Ashentree Glen (plate 3.1f) respectively) resemble some of the samples from the Fife and Lothian minor intrusions described in section 3.4.2. Some of the olivine microphenocrysts appear broken, display strained extinction, and may be xenocrysts. Both samples contain rare augites (c.3mm) with sieve-textured cores, showing strained extinction.

Xenoliths of spinel lherzolite, wehrlite and granulite, and megacrysts of clinopyroxene and olivine were found in a Mauchline lava near Ochiltree (P. Aspen pers. comm., 1988). Peridotite xenoliths and megacrysts of anorthoclase, augite, spinel and hornblende are recorded from many of the vents and minor intrusions (Eyles *et al*, 1949; Upton *et al*, 1983; P. Aspen, pers. comm., 1988).

Samples of blocks in diatremes are assumed to be accidental and unrelated inclusions when they are found in small numbers and cannot be matched with any of the lavas or intrusions of the area. They include trachytes, a plagioclase-phyric basalt, some ol-cpx-plag-micropyhric basalts, and some altered dolerites.

3.3.3. Sills

These are divided on the basis of age into those believed to be coeval with the Mauchline Basin volcanic activity (see chapter 2) and a group of supposed Tertiary age. The latter have been included in this study for comparative purposes.

3.3.3.1. Late-Palaeozoic 'Ayrshire' sills

The medium- to coarse-grained groundmasses of these samples consist of normally-zoned plagioclase with intergranular augite and olivine (plate 3.2a). Bulk compositions are predominantly basaltic but range to hawaiitic. Biotite, apatite, opaque oxides, alkali feldspar and nepheline are present in accessory amounts. Analcime occurs interstitially and kaersutite is an essential phase in the Lugar and Saltcoats sills (plate 3.2e).

All the analysed samples are ol$^{+}_{-}$cpx-phyric. Olivine phenocrysts (up to 2mm) are euhedral to anhedral, and are often fresh. They have homogeneous cores and normally-zoned rims (plate 3.2b). Modal proportions vary considerably from c.8% in the least porphyritic samples, to 35-40% in the most porphyritic (eg

SW68, SW91: plate 3.2d).

Augite phenocryst abundances generally vary between 0-8% although in samples with high concentrations of olivine, modal abundances are as high as (and sometimes higher than) the olivine (35-40%). The augites are rarely euhedral, and although they can attain sizes comparable with the olivines (1.5-2mm) they are usually <1mm. Zoning from colourless or pale pink cores to darker pinkish-brown rims is common (plate 3.2c).

3.3.3.2. Tertiary sills

Fine-grained varieties of this group are usually plagioclase-microphyric and sparsely olivine-phyric, with a groundmass of plagioclase, magnetite, augite and olivine, although small grainsize and alteration make this difficult to assess. Sometimes the plagioclase demonstrates seriate texture. Coarse-grained varieties comprise sub-ophitic augite, plagioclase, magnetite and olivine with accessory biotite and amphibole. Olivine rarely takes on the proportions of a phenocryst phase, and analcime is present in accessory amounts.

3.4. Fife samples

3.4.1. Lavas

Late-Palaeozoic lava flows are rare in Fife and Lothian. Two samples have been collected from a possible flow which outcrops to the south west of Largo Law (Fife) in Blindwell's Quarry. This was described as a lava of Passage Group age by Forsyth & Chisholm (1977). However, De Souza (1979) considered that the field and petrographic evidence was not convincing and suggested that it was an intrusion coeval with the Fife neck intrusions.

Both samples collected are olivine-phyric with medium-grained groundmasses dominated by plagioclase, with augite, olivine, opaque oxides, and a small amount of chlorite probably after glass. Olivine phenocrysts compose c.15% and 10% of samples SW571 and SW572 respectively. They range in size up to 2mm and are euhedral to subhedral.

3.4.2. Fife & Lothian basanites

This group comprises samples from small hypabyssal intrusions and blocks from vents. Whereas the proportion of groundmass phases varies from sample to sample, the mineralogy remains essentially constant. Common to many sections is a brown isotropic, slightly turbid glass. Plagioclase is present in varying proportions in all but the most glassy or the most undersaturated samples, and small, prismatic, pink augites, and rounded opaque oxides are ubiquitous. Olivine is difficult to distinguish from clinopyroxene in the fresh samples, but with increasing alteration coloured pseudomorphs after olivine make it more obvious. Irregular patches of analcime and small apatite needles are common. Nepheline has been tentatively identifed in one sample.

Modal concentrations of olivine phenocrysts are usually between 10-15% and can be as high as 25%. Phenocryst sizes vary between 0.25-1.5mm, and exceptionally up to 3mm. Shapes vary from euhedral to anhedral, (examples of the latter can be rounded or crenulate) to skeletal (Plates 3.2f, 3.3a, 3.4f, 3.5a). Individual samples often contain at least two generations of olivine (defined by shape), and it is not uncommon to see euhedral and skeletal crystals in the same rock.

Unaltered olivine is commonly seen to be zoned and in fresh samples it is possible to distinguish between phenocrysts and possible xenocrysts of olivine. The latter are often (although not always) fragmental in outline and larger (up to 4.5mm) than coexisting phenocrysts. If tentative identification of pseudomorphed examples based on larger size and more irregular shape than coexisting phenocrysts is well-founded, it can be assumed that nearly half the group contain small proportions of xenocryst olivine possibly derived from disaggregation of peridotite xenoliths.

Augite is present as a phenocryst in concentrations of 0-7% and rarely as high as 15% (SW442). Two types can be identified. The first consists of small (0.25-0.75mm) generally euhedral crystals which are unzoned or continuously zoned from core to rim. They are sometimes mantled by a simple outer titanaugite rim and are occasionally sector-zoned. The second type shows greater variation: individual phenocrysts are larger than the first group (0.5-1mm) and show varying degrees of embayment, sieving and zoning, as a result of resorption (e.g. plates 3.5b-g). This second genaration of augite phenocrysts is rarely present in the minor intrusions of Burntisland and Lothian.

Clinopyroxenite fragments are abundant (plate 3.4d). These augite clusters vary in size up to 7mm diameter, but are commonly between 2-4mm, with individual crystals between 0.25-7mm. Interlocking crystals give a 'jigsaw' appearance to crystal boundaries. Individual members of a cluster are often strained, and sieve textures are common. Many of these clusters have been identified as xenoliths, however, caution must be exercised with such identifications since some clusters represent glomeroporphyritic segregations of phenocrysts.

'Free-floating' anhedral clinopyroxenes with strained extinction and sieve-textured cores have been identified as clinopyroxenite fragments on the basis of their similarity to the xenolithic pyroxenes.

In addition to the clinopyroxenite and peridotitic fragments described, fragments of polymineralic assemblages have been identified. These are listed below:

1. Basic granulite with zoned plagioclase, altered clinopyroxenes and orthopyroxenes (SW22).

2. Amphibole-olivine clinopyroxenite with brown pleochroic kaersutitic amphibole, sieve-textured clinopyroxene, altered olivines and apatite (SW429).

3. Wehrlitic fragments with varying proportions of olivine and clinopyroxene.

Single megacrysts include:

1. Magnetite.

2. Feldspar (?)anorthoclase, showing strained extinction.

3. Orthopyroxene tentatively identified on the basis of its alteration to dark striated pseudomorphs. (This is similar to the type of marginal alteration observed in a lherzolite xenolith from Fidra).

3.4.3. Fife & Lothian sills

Two divisions are recognised (although gradational varieties occur): a sub-ophitic (plate 3.3b) and a non-ophitic (plate 3.3c) group. Matrix phases within each group are similar and comprise plagioclase, clinopyroxene, opaque oxides, pseudomorphed olivine and analcime. In the coarser-grained non-ophitic examples kaersutite and accessory biotite occur.

Using the criteria of section 3.2.1 to identify phenocryst phases, it appears that both the non-ophitic and sub-ophitic varieties contain aphyric members. In porphyritic samples, olivine phenocrysts are commonly between 0.5-2mm. Concentrations vary between 4-15% (usually c.7%) in non-ophitic samples, and are around 10% in sub-ophitic samples. There are some euhedral crystals, but most are anhedral, the rounded crystals often forming glomerocrysts. Fresh examples show zoning.

Seriate-textured augites in non-ophitic examples can attain sizes of up to 0.5mm and concentrations of c.10% (range 1-10%). Continuous zoning is common and some crystals are sector-zoned.

Two samples (SW459 and SW545) contain (micro)phenocrysts of plagioclase (up to 1mm).

3.5. Highland dykes

Only six samples have been collected. Descriptions for each of these are given below. For more extensive descriptions of the suite as a whole, reference should be made to Rock (1983).

In all the samples olivine is pseudomorphed by chlorite, bowlingite or serpentine.

SW111 and SW112 (from Smearisary) are both porphyritic with pseudomorphs after olivine up to 0.5mm in diameter. Modal concentrations are c.5% in SW111 and approach 8% in SW112. The groundmass compositions are augite, opaque oxides, feldspathoid, brown glass and accessory apatite and biotite.

SW113 (from Smearisary) contains microphenocrysts of olivine, augite and plagioclase in a groundmass similar to SW111 and SW112. Olivine phenocrysts comprise c.2% of the rock, augite c.1% and plagioclase <<1%

SW114 (from Streap Comhlaidh) and **SW116** (from Brain Choille) contain the highest concentration of olivine phenocrysts (c.20%) in this group of rocks. The euhedral to subhedral pseudomorphs are set in a very fine groundmass which appears to consist of augite, opaque oxides, olivine and feldspathoid, Felsic ocelli are present as irregular patches between 0.5-1mm containing needles of augite and small biotite laths (plate 3.3f). Amygdales contain chlorite, and a wehrlitic xenolith has been identified.

SW115 (from Achnanellan) (plate 3.3e) is the only sample with augite phenocrysts, which are present in higher concentrations than olivine (25% c.f. 15%). Both are euhedral to subhedral, the former ranging in size between 0.5-2mm and the latter showing a seriate texture up to 2mm. Augite cores are sieve-textured and the rims a deeper pinkish-brown compared to the cores. Some crystals cluster in glomerocrysts. The groundmass consists of augite, olivine, opaque oxides and an alteration product of (?)nepheline.

3.6. Quartz dolerites

The quartz dolerites represent a major tholeiitic interlude in the middle of the late-Palaeozoic alkaline phase of magmatism. The twelve samples analysed were provided by R. Macdonald of Lancaster University as representing the geochemical variation within the suite. The account which follows is based on five thin sections provided by him, and on the descriptions of Macdonald *et al.* (1981).

The mineralogy of the dykes is dominated by plagioclase, augite and opaque oxides (plate 3.3d). Hypersthene, pigeonite, olivine, hornblende, biotite and apatite are common, minor constituents. Olivine and orthopyroxene are nearly always pseudomorphed. In the sections provided by R. Macdonald grain-sizes are medium to coarse.

The low pressure evolution of the magmas was controlled by fractionation of olivine-plagioclase-pyroxene-oxide assemblages from more magnesian magmas, and by removal of plagioclase-pyroxene-oxide-apatite assemblages from intermediate compositions (Macdonald *et al*, 1981). Olivine nodules in a magnesian basalt dyke from Fife indicate a possible higher pressure stage of fractionation dominated by olivine (Macdonald *et al*, 1981).

3.7. Discussion

Russell (1985) suggested that the limited size range of phenocrysts in the post-Dinantian suite was indicative of rapid crystallisation from magmas during ascent from the upper mantle. The size, limited species variation and the paucity of resorptional textures (in all but basanitic samples from Fife) suggests that high-level magma chambers were typically absent.

It is common for alkali basaltic rocks to contain clinopyroxene of varied origin (e.g. Binns *et al*, 1970; Irving, 1974a, 1974b; White, 1966; Kuno, 1964; Wass, 1979; Wass & Irving, 1976; Dobosi, 1989). Wass (1979) described four modes of origin:

1. Cr-diopsides: as xenocrysts derived from accidentally included mantle xenoliths.

2. Al-augites: as accidentally included xenoliths of basaltic composition, from intrusions solidified in the mantle from an earlier magmatic episode.

3. Al-augites: as discrete megacrysts or in xenoliths, representing high-pressure crystallisation products of alkali basaltic melts contemporaneous with the magmatic episode producing the host rocks.

4. Phenocrysts and quench pyroxenes which crystallised at low pressure and thus show no reaction or rimming relationships.

Augites fitting the descriptions of groups 2-4 have been identified in the Fife vent intrusions and blocks. The high pressure Al-augites described by Wass appear to be represented by members of the second group of phenocrysts described in section 3.4.2, and the low pressure phenocrysts by the first group. It is possible that the cores of the second group represent partial resorption of both xenolithic fragments and high-pressure phenocrysts. There are obvious examples of xenocrystal material with non-euhedral later rims, but it is not inconceivable that more complex resorption would yield the smaller amoeboid cores described in section 3.4.2. The Fife basanites appear therefore to have experienced polybaric crystallisation, which is reflected in complex zoning and resorption textures in many of the pyroxene crystals.

Petrographic considerations indicate that the parent liquids to the Midland

Valley suite sat within the primary phase field of olivine, and in many cases fractionation proceeded to reach the ol-cpx cotectic boundary and more rarely the ol-cpx-plag cotectic. The presence of skeletal olivines and sector-zoned augites is indicative of late-stage fast growth (Donaldson, 1976; Drever & Johnston, 1957; Wass, 1973) Sector-zoning in clinopyroxenes is generally attributed to disequilibrium crystallisation during rapid growth (Nakamura, 1973; Leung, 1974; Shimizu, 1981). The suggestion by Strong (1969) that they originated as swallow-tailed skeletal crystals with later infilling of hollows, has been discounted by the recognition of concentric zoning continuous through all sectors (Wass, 1973; Downes, 1974; Russell, 1985). Hence initial crystal growth is considered to have been rapid relative to ionic diffusion in the melt, resulting in variations of chemistry in different growth directions (Wass, 1973).

Rapid ascent is also indicated by the presence of deep-seated xenolithic inclusions within many of the basanitic samples, and by the retention of amoeboid, assumed high-pressure cores in augite phenocrysts in the Fife basanites. Xenolithic fragments possibly represent cumulates from liquids which failed to reach to the surface. These may or may not be cognate with the host liquids. Macintyre *et al.* (1981) discussed the probability of Namurian subsurface magmatic activity in Fife resulting in lower crustal (>35km) cumulates (Chapman, 1975), which were then sampled by the later basanitic magmas.

3.8. Summary

The following generalisations can be made concerning the late Palaeozoic volcanic rocks of the Midland Valley.

1. Olivine is a nearly ubiquitous phenocryst phase. A spectrum exists with increasing concentration and size of augite phenocrysts, from samples which are devoid of augite phenocrysts, to those which can be described as ol-cpx-phyric.

2. The only other phenocryst phase encountered is plagioclase. This is only present as (micro)phenocrysts in a few samples.

3. Phenocrysts seldom attain sizes greater than 2mm, resulting in the description of the suite as microporphyritic (Macdonald, 1975;

Russell, 1985) and suggesting rapid rates of magma ascent with little or no residence time in magma chambers. Olivines are usually larger than co-existing clinopyroxenes and may be presumed to have commenced crystallisation earlier.

4. Xenoliths and xenocrysts are common in the small intrusions and diatremes of Fife and Lothian, and have been found in several vent intrusions and one lava flow in the Mauchline Basin.

5. Clinopyroxene phenocrysts with sieve-textured $\pm$ complexly-zoned cores are commonly found in the basanites of Fife. Such sieving and embayment are associated with the resorption of xenoliths or high-pressure phenocrysts. The basanites also contain an additional generation of smaller and simpler augite phenocrysts which are present in the minor intrusions of Burntisland and Lothian.

6. Phenocrysts of ol$\pm$cpx have been identified in the Midland Valley alkaline sills. They are recognised on the basis of shape and/or a bimodal size distribution, indicating both phenocryst and groundmass generations.

7. Skeletal crystals of olivine commonly occur with euhedral crystals within the same sample, and sector-zoned clinopyroxenes are common.

CHAPTER 4

MINERAL CHEMISTRY

4.1. Introduction

With the exception of the quartz dolerites, mineral analyses have been determined for each of the late-Palaeozoic groups outlined in chapter 2. Phases analysed are pyroxene, olivine and feldspar, and data for these are recorded in Appendix II. However, because of alteration it has not been possible to obtain olivine analyses for Highland dyke or Passage Group lava samples. Feldspar compositions are presented for information only (see section 4.4) and the rest of this chapter is devoted to presentation and discussion of the clinopyroxene and olivine data. Inter-element diagrams distinguish cores and rims of supposed phenocrysts and xenocrysts. The phenocryst-xenocryst distinctions are based on petrographic observations (see chapter 3), and do not reflect subsequent re-identification on the basis of chemistry. This is discussed further in section 4.5.

4.2. Clinopyroxenes

4.2.1. Introduction

Element concentrations and distributions within clinopyroxenes are principally controlled by the silica activity of the magma, its degree of differentiation, and the temperature and pressure of crystallisation. Their effects are discussed below.

4.2.1.1. Major element variations Mg, Fe, Ca

Increasing Fe (& Mn) concentrations in pyroxenes at the expense of Mg reflect the well-established major element trends associated with the evolution of most magmas. However, variations in Ca-concentration are not so easily attributed to differentiation processes alone. Gibb (1973) and Larsen (1976) showed an inverse relationship between Si activity of a magma and the Ca content of its clinopyroxenes. This has been emphasised more recently by Sack & Carmichael (1984) who showed a trend of increasing Ca with increasing Si-deficiency in the tetrahedral site. It reflects the importance of Ca-Tschermak's molecule ($CaAl(AlSi)_2O_6$) substitution with increasing degrees of silica undersaturation. Therefore the Ca concentration is influenced by the

silica activity of the magma, which changes with magma differentiation.

4.2.1.2. Al and Ti linked substitutions

Al provides the major compensation for Si deficiency in the tetrahedral site of silica undersaturated pyroxenes. (In rare cases of Al deficiency Fe^{3+} and less commonly Ti^{4+} will provide the needed substitution (Hartman, 1969; Sack & Carmichael, 1984)). Incorporation of Ti in the M1 site provides the main charge balance for tetrahedral substitution, and consequently Ti contents are also inversely related to the degree of Si saturation (Le Bas, 1962; Sack & Carmichael, 1984). The effects of magma differentiation on Al concentration depends on the silica activity of the magma. In Si saturated and oversaturated magmas the proportion of the Z group filled by Al atoms decreases as Si in the magma increases with differentiation and for Si undersaturated rocks the reverse is true (Le Bas, 1962). Ti increases in concentration in both cases (Le Bas, 1962).

Experimental data have suggested that some of the variations in Al and Ti content must be attributed to variations in temperature and pressure. Ti increases with decreasing pressure (Yagi & Onuma, 1967; Edgar *et al.* 1980) accounting for the greater solubility of Ti-Tschermak's molecule at low pressures, and suggesting that most titanaugites are comparatively low pressure phases (Wilkinson, 1974). An increase in Ti content should also be expected with increasing temperature (Akella & Boyd, 1973; Gamble & Taylor, 1980), although the inverse relationship has been indicated by the experiments of Thompson (1974). Thompson (1974) also suggested that Al in liquidus clinopyroxenes rises with increasing temperature and pressure. However, this conflicts with Wass (1979) who showed that the total Al_2O_3 of low-pressure clinopyroxenes overlapped and was commonly higher than that of high-pressure clinopyroxenes. She suggested that the Al^{iv}/Al^{vi} ratio provides the best (albeit qualitative) indication of pressure of crystallisation, since there is a gradual shift in co-ordination from Al^{iv} to Al^{vi} with increasing pressure (Aoki & Kushiro, 1968, Aoki & Shiba, 1973, Velde & Kushiro, 1978). (Al^{iv} is here calculated as 2-Si, and Al^{vi} as $\Sigma Al - Al^{iv}$). Although the overall trend is independent of the composition of the parent liquid (Wass, 1979) it would appear from Thompson's (1974) experimental work on pyroxenes that absolute Al^{iv}/Al^{vi} ratios are composition-dependent. Caution is also necessary since Al_2O_3 content in pyroxenes has been shown to increase with temperature

(Thompson, 1974), and Al^{iv} shown to increase with H_2O content of the magma at constant temperature and pressure (Dolfi & Trigila, 1983).

4.2.1.3. Variations in Na and Cr

The high crystal field stabilisation energy of Cr ensures its rapid depletion in fractionating magmas. Campbell & Borley (1974) indicated that Cr^{3+} would be preferentially partitioned into early forming crystals to give charge balance for Al substitution in the tetrahedral site. It is replaced by Ti^{4+} as the melt becomes depleted in Cr.

The Na concentration of clinopyroxenes increases with magma differentiation (Irving, 1974b) and is reflected in the increasing importance of the acmite molecule in more evolved magmas. Increasing Na content with increasing pressure is reflected in jadeite substitution.

4.2.2. Analysed compositions

All analyses have been recast with respect to Fe^{2+} and Fe^{3+} on the basis of stoichiometry (4 cations to 6 oxygens, e.g. Droop, 1987), using software written by A. Walker (Edinburgh University). This calculation is very sensitive to the quality of the SiO_2 analysis: an increase of 1% in measured SiO_2 can more than halve the calculated Fe^{3+} cation proportion. A smaller increase in calculated Al^{vi} (up to 30%) should also be expected.

4.2.2.1. Inter-element variations

The general pattern within all the groups is one of decreasing Si, Cr and Mg with increasing Ti, Fe, and Mn from core to rim in a given phenocryst. Ca relationships are variable with no clear zonations in phenocrysts, and Al generally increases between core and rim in all but the Passage Group lavas where it decreases. Inter-element relationships are outlined in more detail below.

There is generally a spread in Ca concentrations for a given Mg/(Mg+Fe+Mn) ratio except for the Ayrshire sill pyroxenes which have Ca contents between 0.89-0.92 cations per formula unit (CFU). A rough assessment of the relationship between initial Ca content and degree of silica-saturation can be made by comparing the range of core Ca contents for the transitional Passage Group lavas and the basanitic intrusions of Fife & Lothian. The majority of

Passage Group cores have Ca contents between 0.76–0.89 CFU whereas they fall between 0.80–0.93 CFU for the basanites, confirming a crude correlation between Ca content and Si–activity. There is no clear correlation between Ca and Al^{vi}, contrary to the suggestions of section 4.2.1.1.

Fig 4.1 indicates the variation of Cr using Mg/(Mg+Fe+Mn) as a differentiation index. For Mg/(Mg+Fe+Mn) values >0.85 CFU a crude positive correlation is apparent, but for values <0.85 CFU Cr–contents are generally below the limits of detection. Graphs of Ti against Mg/(Mg+Fe+Mn) (Fig. 4.2), show a negative correlation as Ti–content increases with differentiation from core to rim. With TiO_2 contents up to 6wt% (0.17 CFU) many of the pyroxenes are titaniferous augites or titanaugites, following the nomenclature of Yagi & Onuma (1967).

Fig 4.3 indicates the relationship between Al and Ti. Although at first glance it would appear that cores are generally more aluminous than rims, examination of particular core–rim pairs shows that, except for the Passage Group lavas, this is not so. In all but this group the rims are generally more aluminous and titaniferous than the cores.

Al^{vi} is plotted against Al^{iv} in Fig. 4.4 with the qualititative pressure fields of Aoki & Kushiro (1968) indicated. The data show that, as may be expected, groundmass and rim compositions of all groups plot within the field of 'igneous rocks'. However, core compositions from the Highland Dyke group lie exclusively in the field of 'granulites and inclusions in basaltic rocks' whereas those from the Fife & Lothian sills lie almost exclusively within the field of 'igneous rocks'. Core compositions from the remaining groups spread across both fields.

4.2.2.2. End–member compositions

Fig 4.5 shows all pyroxene compositions plotted in the traditional pyroxene quadrilateral. Most fall into the diopsidic salite or augite fields. However, the fact that many plot above the 50% wollastonite line indicates the presence of 'non–quadrilateral' components since M1 site occupancy by R^{3+} and R^{4+} ions increases the Ca/(Ca+Mg+Fe) ratio (Robinson, 1980). Possible additional components can be represented by two end–member groups: (1) the alkali pyroxenes – jadeite and acmite, and (2) the Tschermak's molecules – Ca–ferriTschermak's, Ca–Ti–Tschermak's and Ca–Tschermak's. Both jadeite and acmite contain Na in the M2 site, so their importance in pyroxene solid

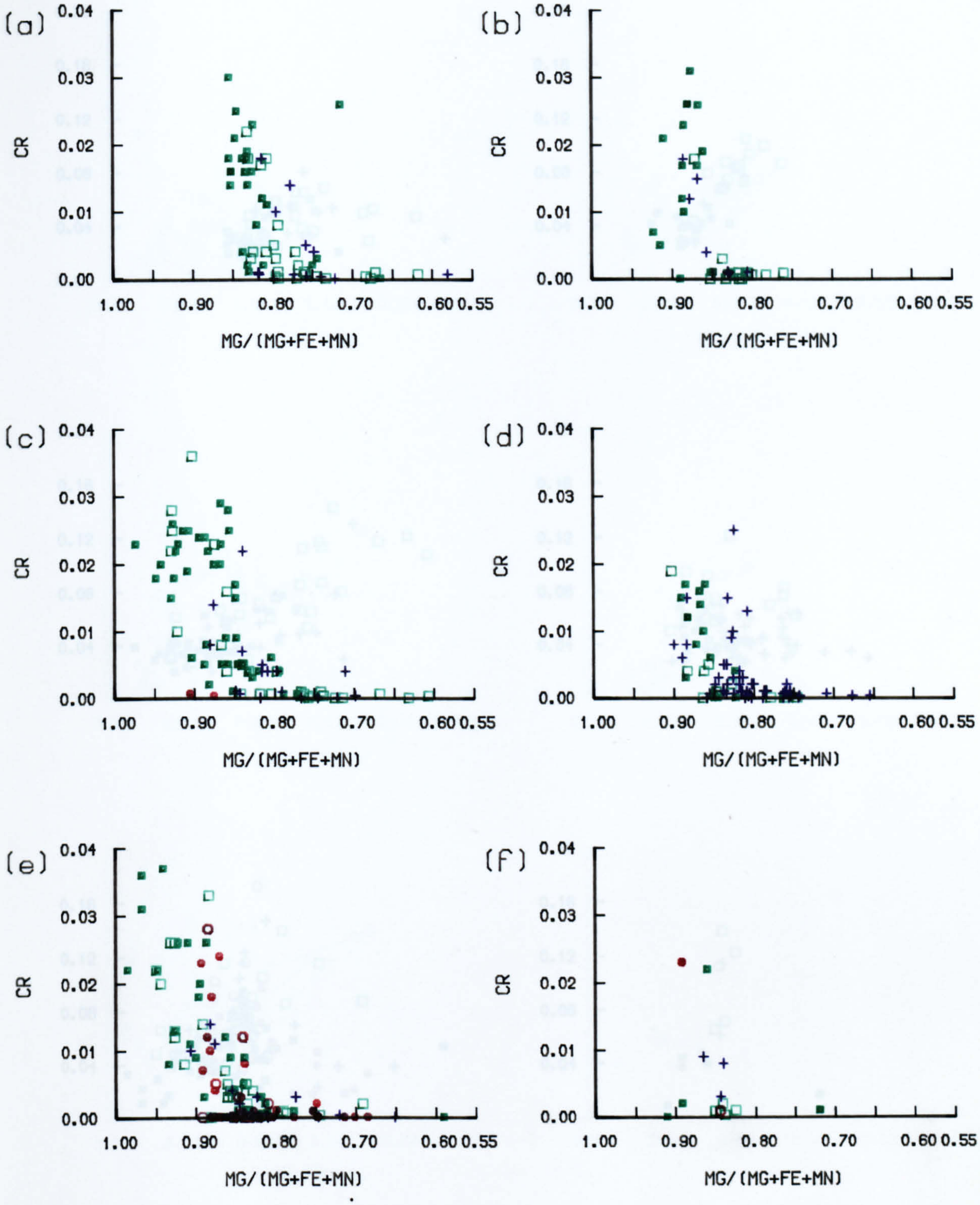

Fig. 4.1 Cr variation against Mg/(Mg+Fe^{2+}+Mn) for clinopyroxenes from (a) Passage Group lavas (b) Ayrshire sills (c) Mauchline group (d) Fife & Lothian sills (e) Fife & Lothian basanites (f) Highland dykes. Element concentrations expressed as cations per formula unit.

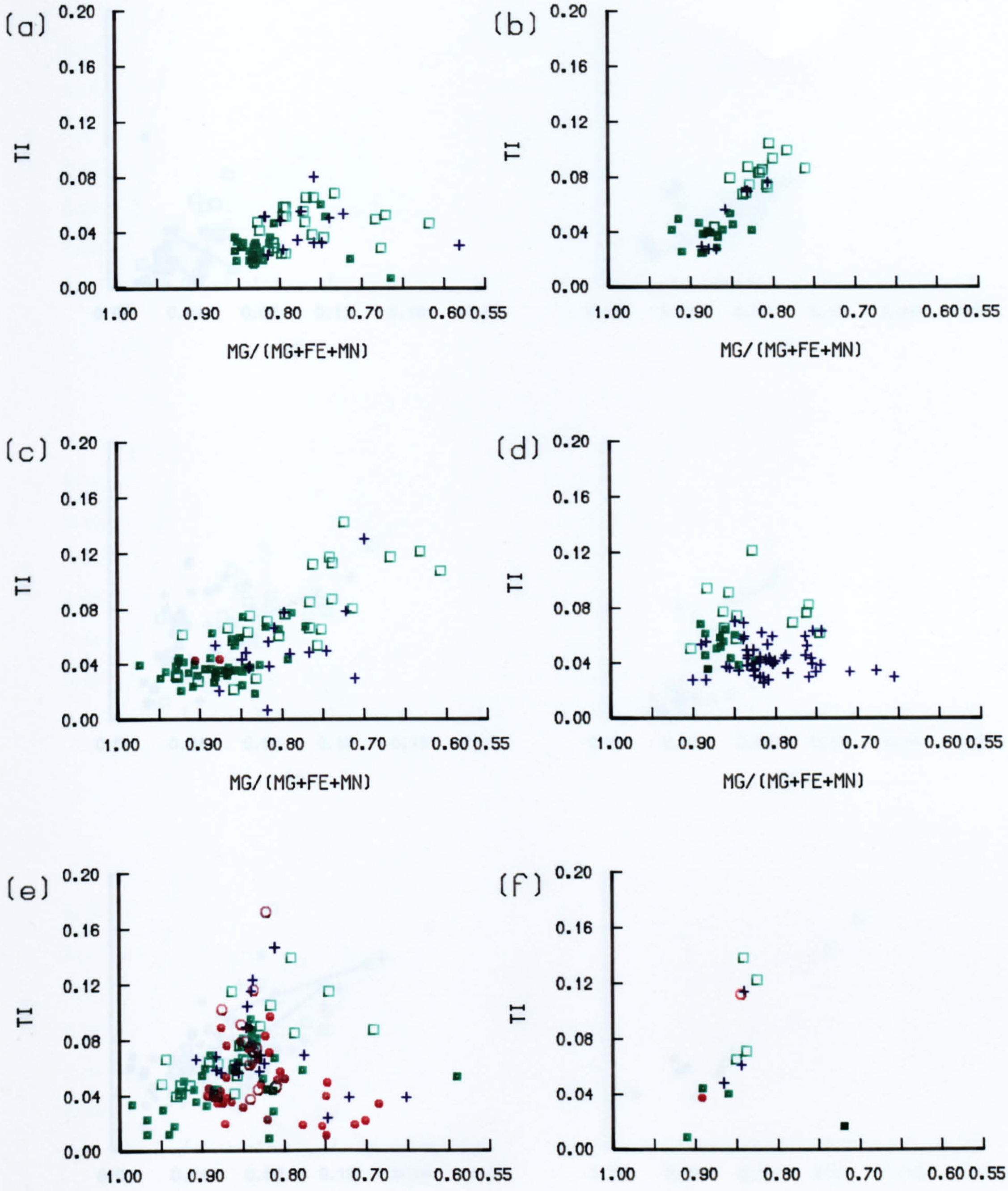

Fig. 4.2 Ti variation against Mg/(Mg+Fe^{2+}+Mn) for clinopyroxenes from (a) Passage Group lavas (b) Ayrshire sills (c) Mauchline group (d) Fife & Lothian sills (e) Fife & Lothian basanites (f) Highland dykes. Element concentrations expressed as cations per formula unit.

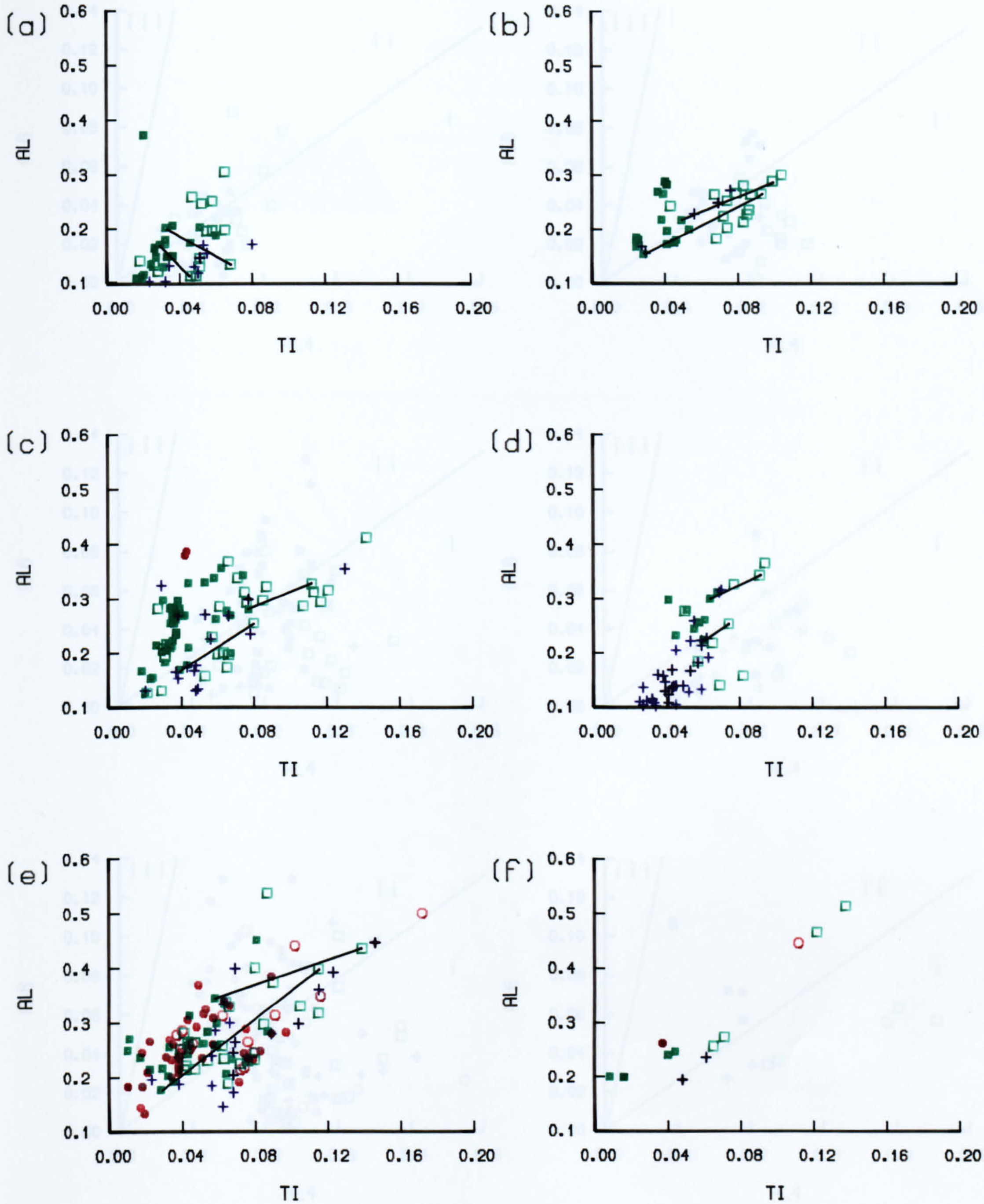

Fig. 4.3 Al variation against Ti for clinopyroxenes from
(a) Passage Group lavas (b) Ayrshire sills (c) Mauchline group (d) Fife & Lothian sills (e) Fife & Lothian basanites (f) Highland dykes. Element concentrations expressed as cations per formula unit. Two phenocryst core–rim pairs are shown in each plot.

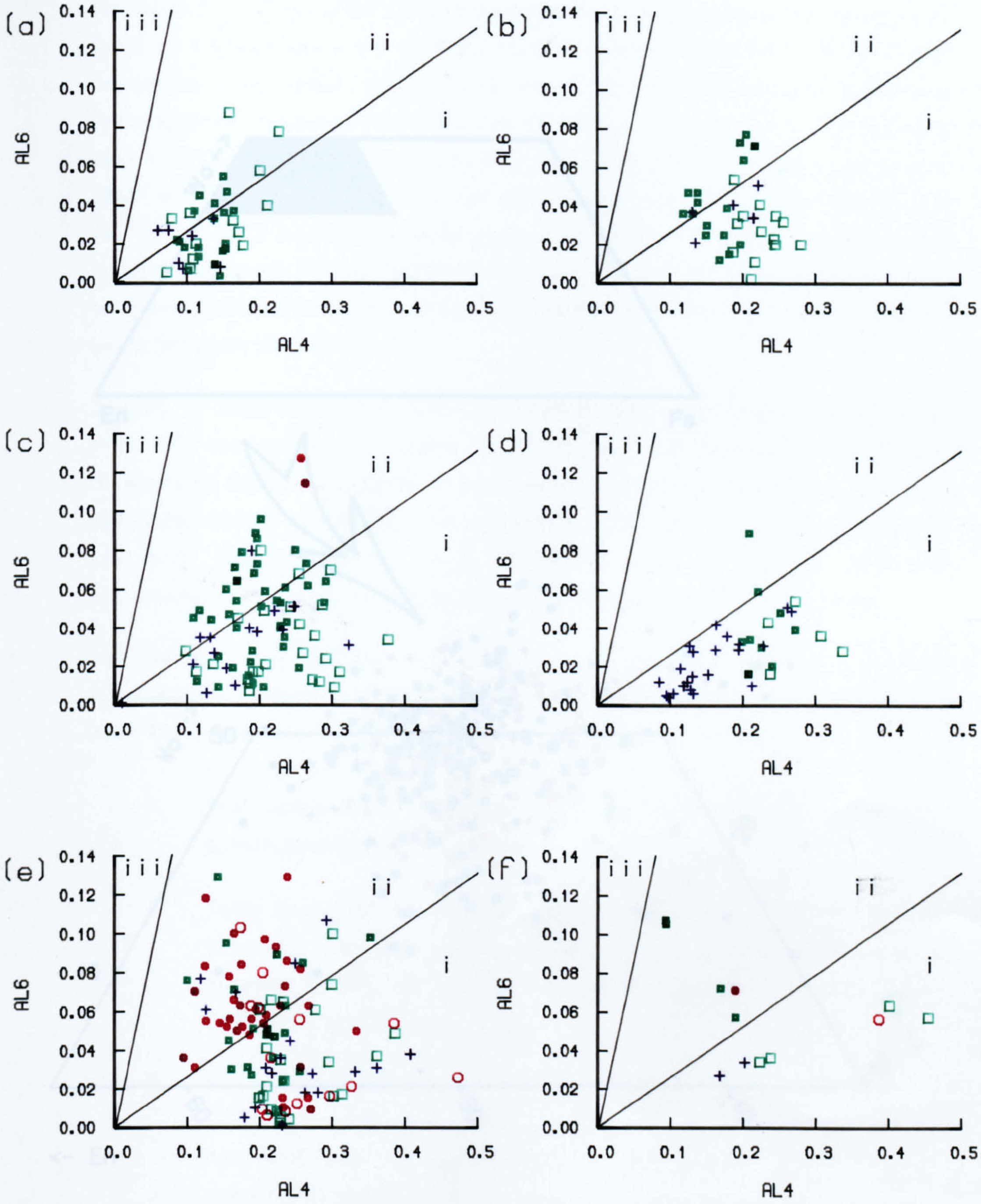

Fig. 4.4 Al^{VI} and Al^{IV} variations for clinopyroxenes from
(a) Passage Group lavas (b) Ayrshire sills (c) Mauchline group (d) Fife & Lothian sills (e) Fife & Lothian basanites (f) Highland dykes. Element concentrations expressed as cations per formula unit. Fields (i), (ii) and (iii) from Aoki & Kushiro (1968): (i) igneous rocks; (ii) granulites & xenoliths in basalts; (iii) eclogites.

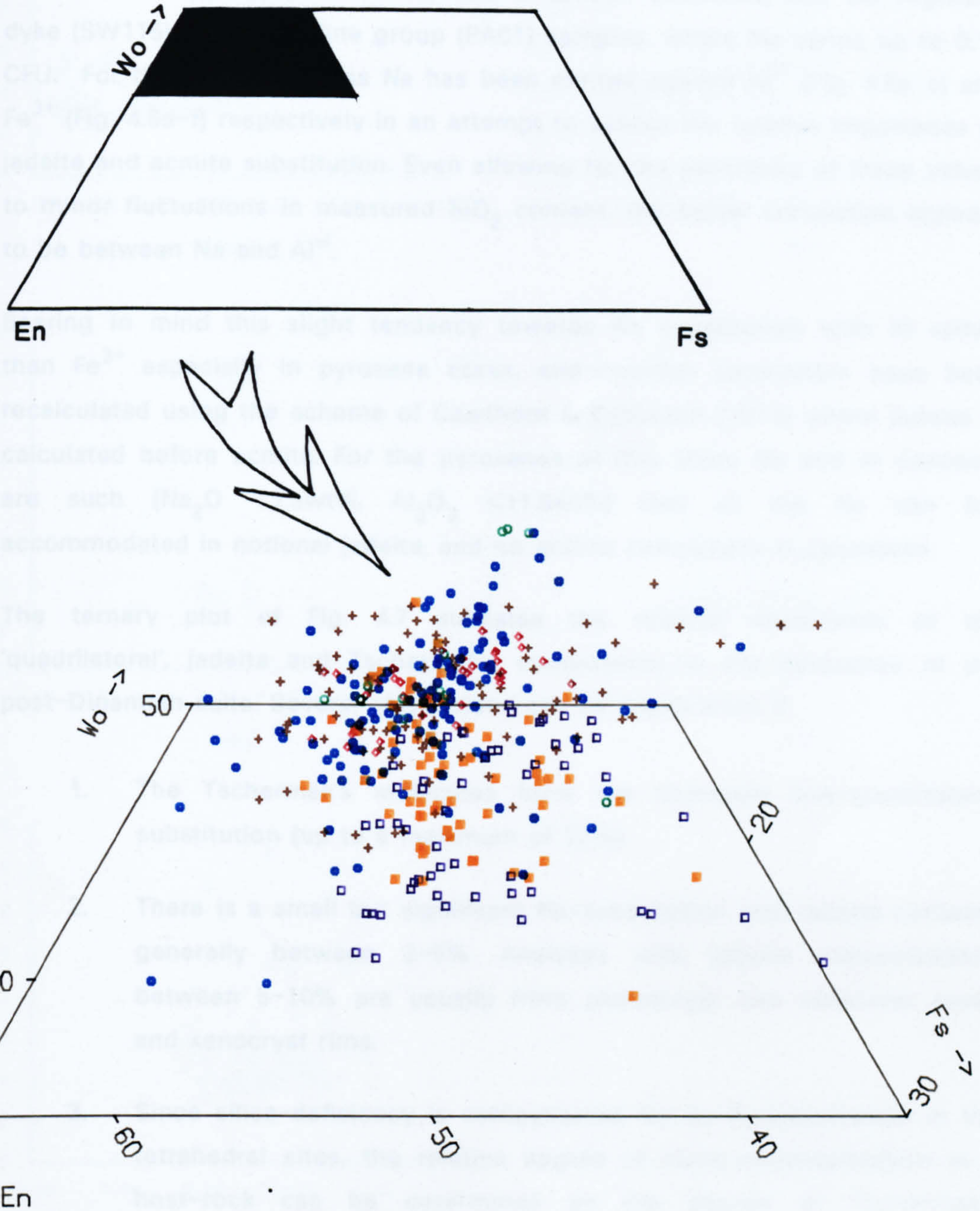

Fig. 4.5 Pyroxene compositions plotted in terms of Ca–Mg–Fe^{2+} (Wo–En–Fs) for all groups.

solutions should be reflected in increasing Na concentrations. Na contents of most of the pyroxenes are uniform, varying only between 0.03-0.06 CFU, and suggesting that these substitutions are relatively unimportant. Exceptions include some pyroxenes from the Fife & Lothian basanites, and the Highland dyke (SW115) and Mauchline group (PA01) samples, where Na varies up to 0.15 CFU. For these three groups Na has been plotted against Al^{vi} (Fig. 4.6a-c) and Fe^{3+} (Fig. 4.6d-f) respectively in an attempt to assess the relative importance of jadeite and acmite substitution. Even allowing for the sensitivity of these values to minor fluctuations in measured SiO_2 content, the better correlation appears to be between Na and Al^{vi}.

Bearing in mind this slight tendency towards Na substitution with Al rather than Fe^{3+} especially in pyroxene cores, end-member parameters have been recalculated using the scheme of Cawthorn & Collerson (1974) where jadeite is calculated before acmite. For the pyroxenes of this study Na and Al contents are such (Na_2O <1.5wt%, Al_2O_3 <11.5wt%) that all the Na can be accommodated in notional jadeite, and no acmite component is calculated.

The ternary plot of Fig. 4.7 indicates the relative importance of the 'quadrilateral', jadeite and Tschermak's components in the pyroxenes of the post-Dinantian suite. Several conclusions can be drawn from it:

1. The Tschermak's molecules form the dominant non-quadrilateral substitution (up to a maximum of 27%).

2. There is a small but significant Na-substitution with jadeite contents generally between 2-5%. Analyses with jadeite concentrations between 5-10% are usually from phenocryst and xenocryst cores and xenocryst rims.

3. Since silica-deficiency is compensated for by Al-substitution in the tetrahedral sites, the relative degree of silica-undersaturation in a host-rock can be determined by the degree of Tschermak's substitution displayed by its pyroxene phenocrysts.

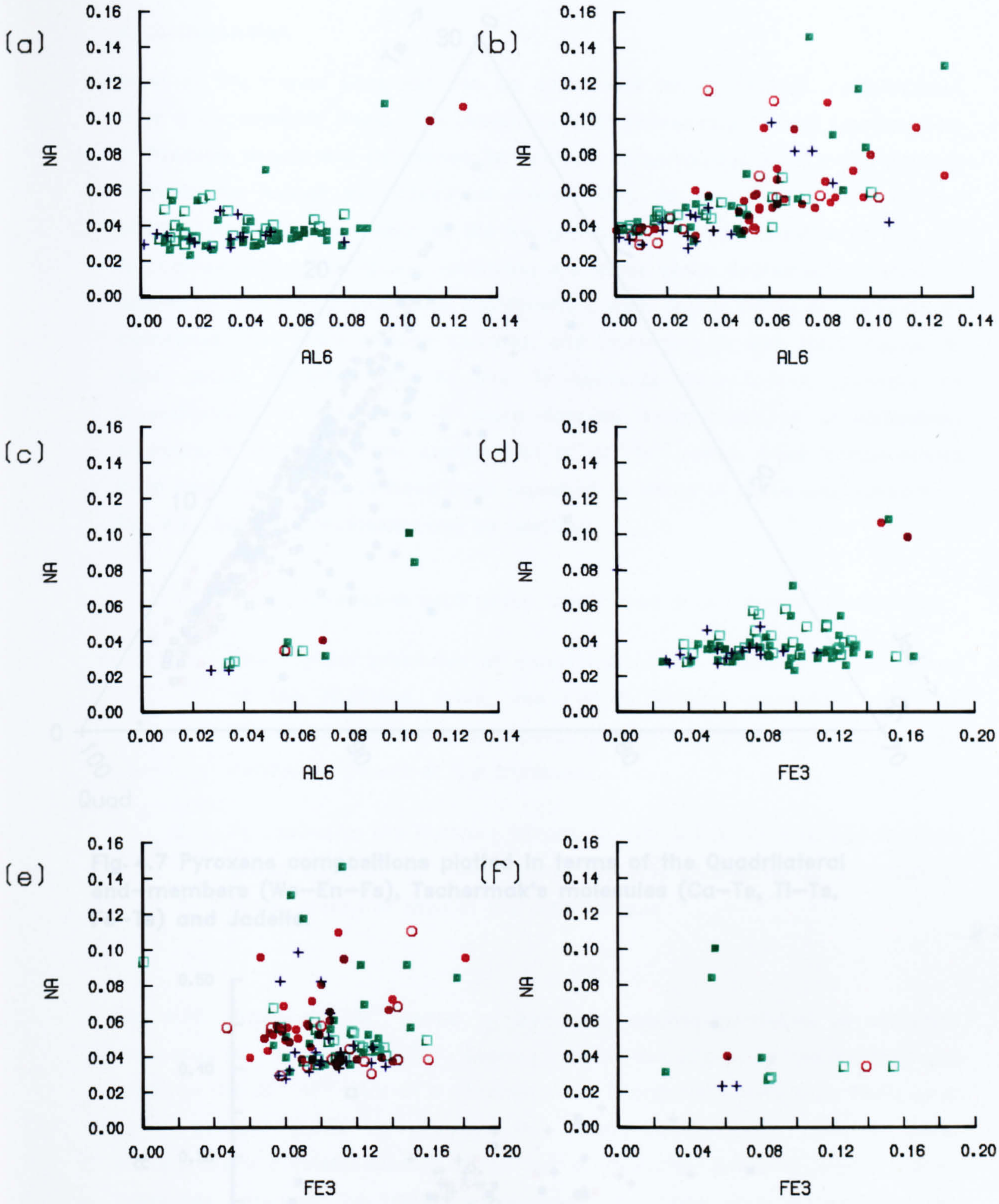

Fig. 4.6 Na variation against Al^{iv} (a–c) and against Fe^{3+} (d–f) for clinopyroxenes from (a,d) Mauchline group (b,e) Fife & Lothian basanites (c,f) Highland dykes. Element concentrations expressed as cations per formula unit.

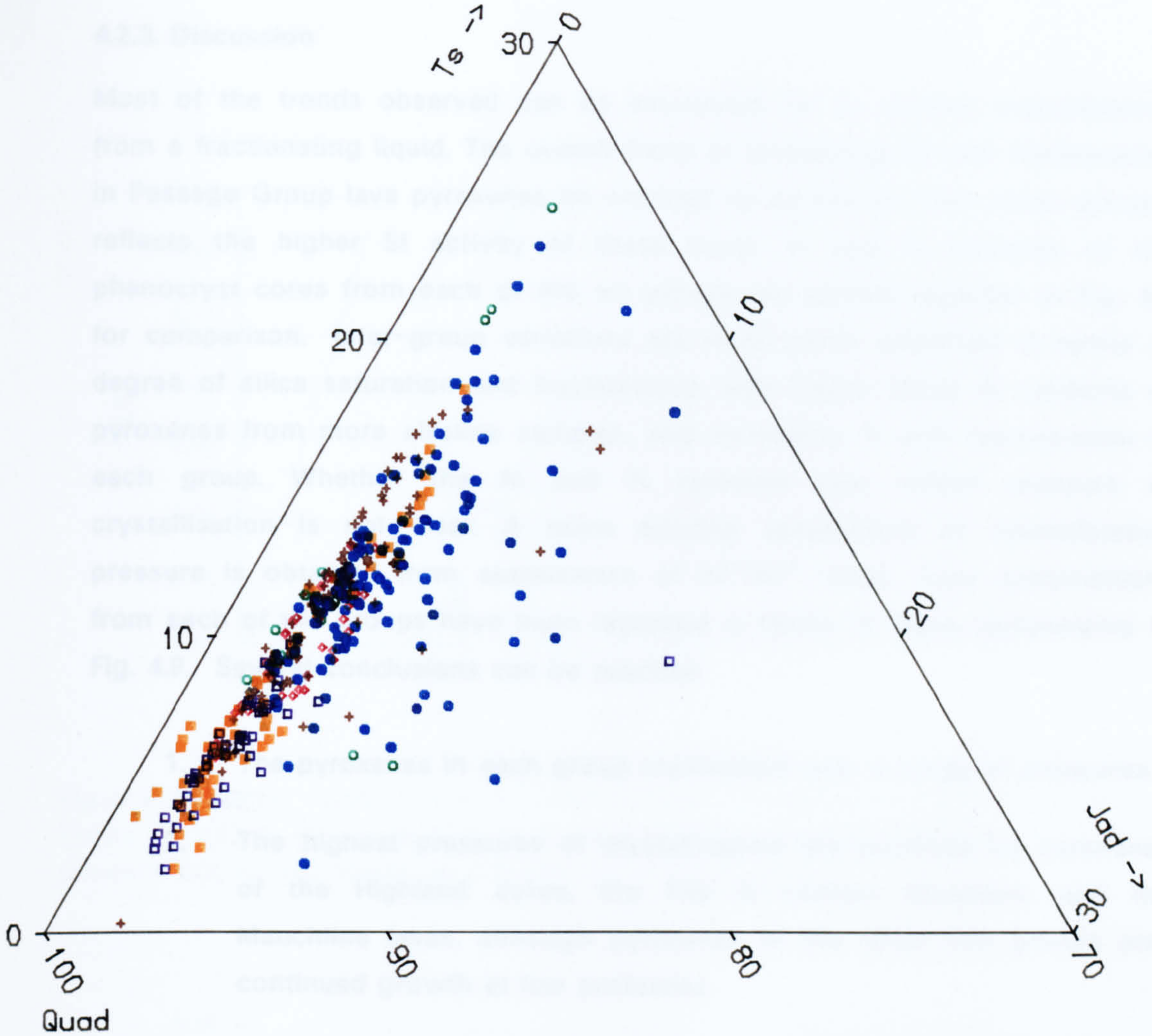

Fig. 4.7 Pyroxene compositions plotted in terms of the Quadrilateral end-members (Wo-En-Fs), Tschermak's molecules (Ca-Ts, Tl-Ts, Fe-Ts) and Jadeite.

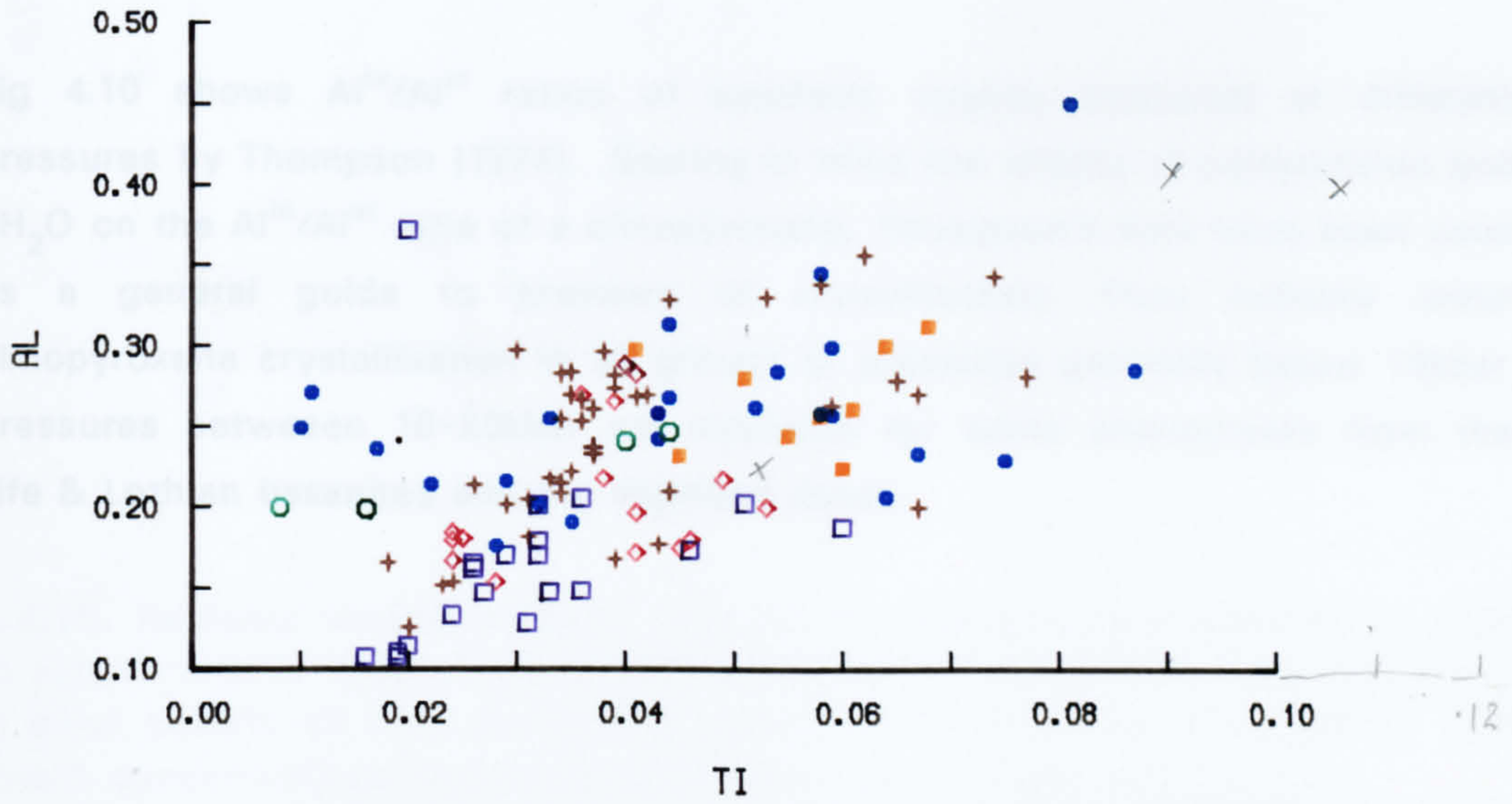

Fig. 4.8 Regional variations in Al and Ti for clinopyroxene phenocryst cores. Element concentrations expressed as cations per formula unit.

4.2.3. Discussion

Most of the trends observed can be accounted for by normal crystallisation from a fractionating liquid. The overall trend of decreasing Al with fractionation in Passage Group lava pyroxenes (in contrast to pyroxenes from other groups) reflects the higher Si activity of these lavas. Al and Ti contents of the phenocryst cores from each of the six groups are plotted together in Fig. 4.8 for comparison. Inter-group variations are most easily explained in terms of degree of silica saturation and fractionation, with higher initial Al contents of pyroxenes from more alkaline samples, and increasing Ti with fractionation in each group. Whether the Al and Ti contents also reflect pressure of crystallisation is not clear. A more detailed assessment of crystallisation pressure is obtained from examination of Al^{iv}/Al^{vi} ratios. Core compositions from each of the groups have been replotted in terms of these components in Fig. 4.9. Several conclusions can be reached:

1. The pyroxenes in each group crystallised over a range of pressures.
2. The highest pressures of crystallisation are recorded by pyroxenes of the Highland dykes, the Fife & Lothian basanites, and the Mauchline lavas, although pyroxenes in the latter two groups also continued growth at low pressures.
3. Pyroxenes in the Ayrshire intrusions, Fife & Lothian sills and Passage group lavas reflect more closely isobaric crystallisation, generally at lower pressures than in the other groups.

Fig 4.10 shows Al^{iv}/Al^{vi} ratios of synthetic augites produced at different pressures by Thompson (1974). Bearing in mind the effects of composition and pH_2O on the Al^{iv}/Al^{vi} ratio of a clinopyroxene, Thompson's data have been used as a general guide to pressure of crystallisation. They indicate initial clinopyroxene crystallisation in all groups at pressures generally below 10kbar. Pressures betweeen 10-20kbar are indicated for some phenocrysts from the Fife & Lothian basanites and the Highland dykes.

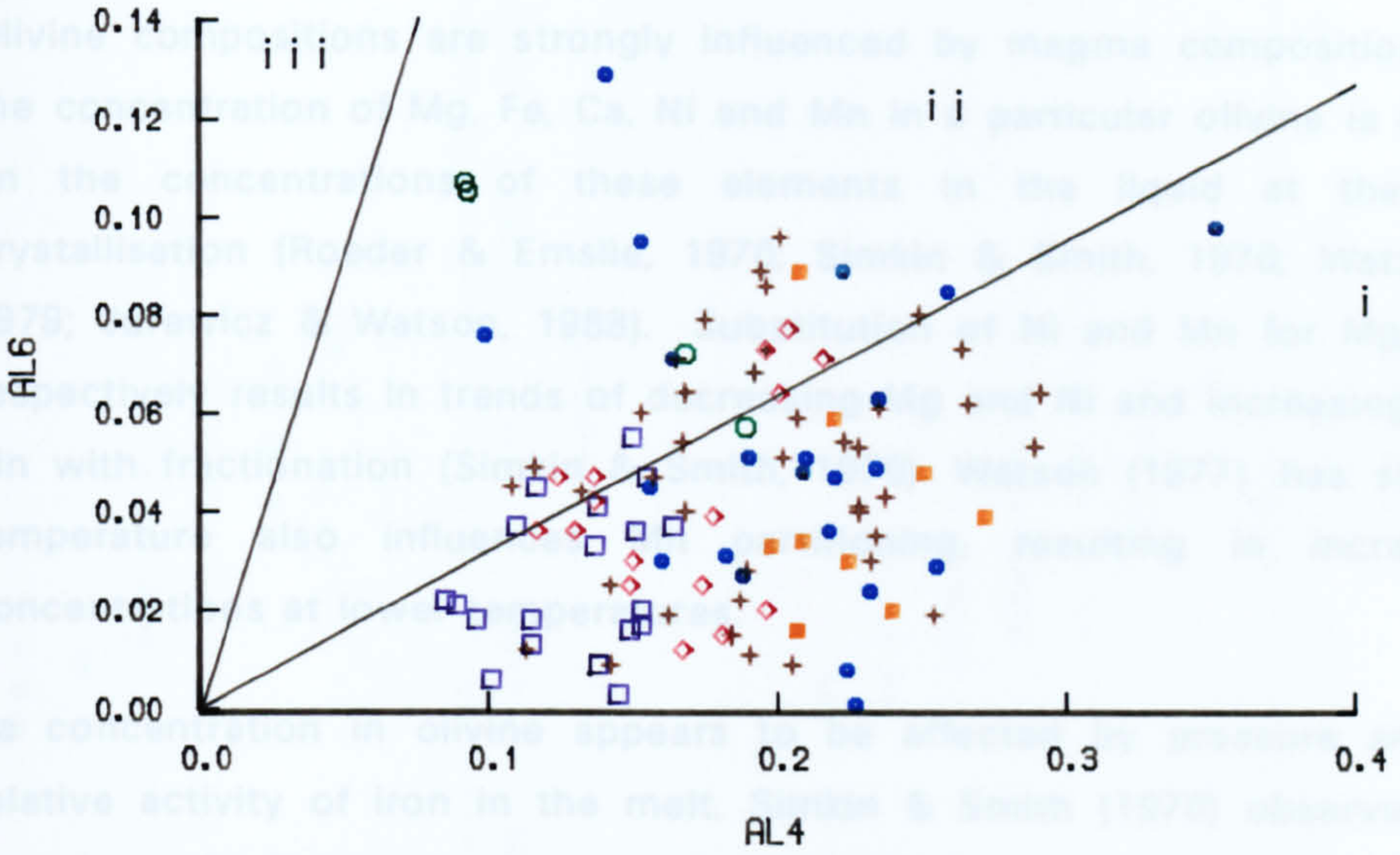

Fig. 4.9 Regional variations in Al^{VI} and Al^{IV} for clinopyroxene phenocryst cores. Fields (i), (ii) & (iii) from Aoki & Kushiro (1968) (See fig 4.4). Element concentrations expressed as cations per formula unit.

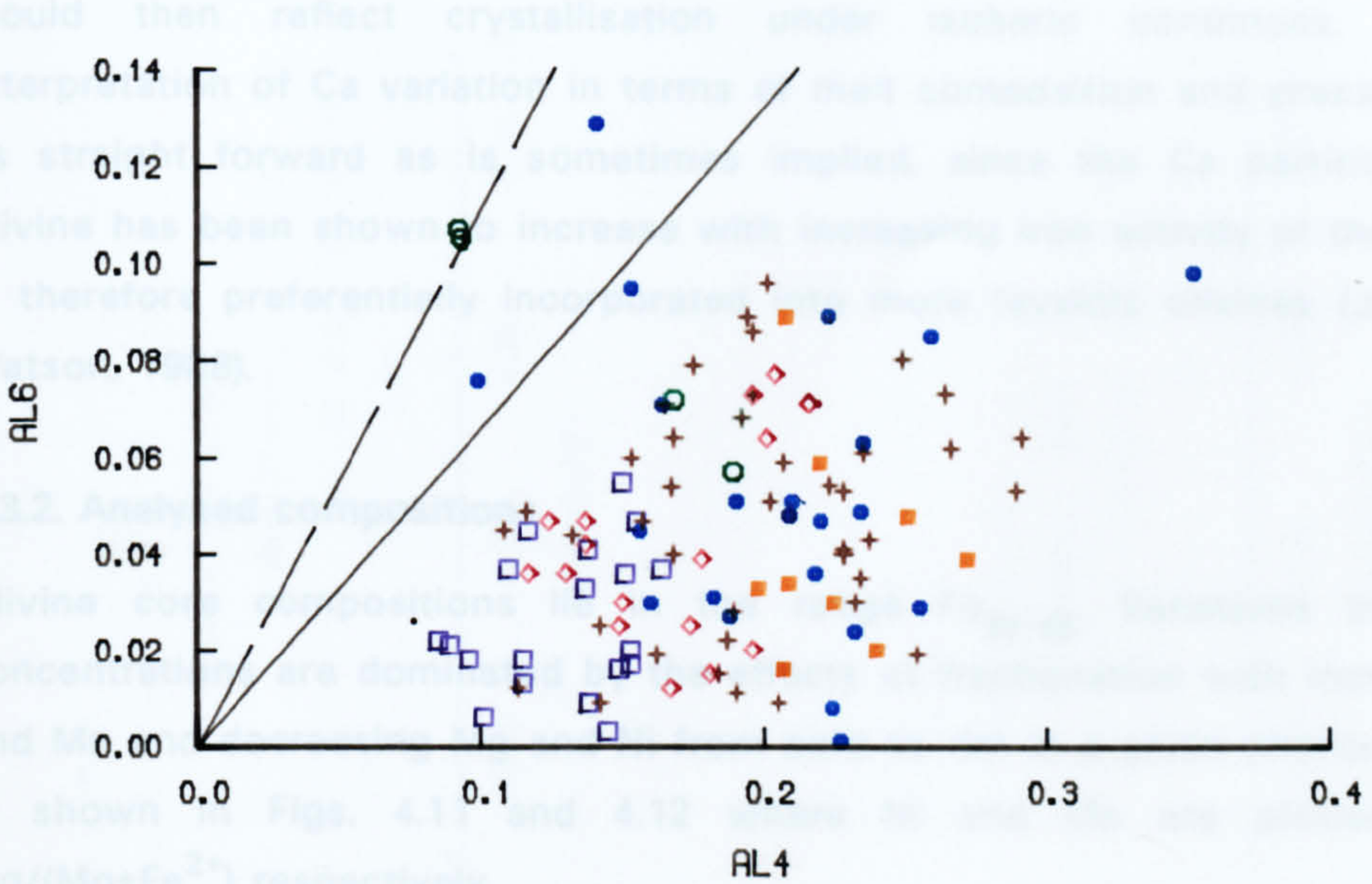

Fig. 4.10. Regional variations in Al^{IV} and Al^{VI} for clinopyroxene phenocryst cores. with experimentally determined Al^{VI}/Al^{IV} ratios for clinopyroxenes from olivine–rich alkali basalts at 10kb (solid line) and 20kb (dashed line) (Thompson, 1974). Element concentrations expressed as cations per formula unit.

4.3. Olivine

4.3.1. Introduction

Olivine compositions are strongly influenced by magma composition, so that the concentration of Mg, Fe, Ca, Ni and Mn in a particular olivine is dependent on the concentrations of these elements in the liquid at the time of crystallisation (Roeder & Emslie, 1970; Simkin & Smith, 1970; Watson, 1977, 1979; Jurewicz & Watson, 1988). Substitution of Ni and Mn for Mg and Fe^{2+} respectively results in trends of decreasing Mg and Ni and increasing Fe^{2+} and Mn with fractionation (Simkin & Smith, 1970). Watson (1977) has shown that temperature also influences Mn partitioning, resulting in increased Mn concentrations at lower temperatures.

Ca concentration in olivine appears to be affected by pressure and by the relative activity of iron in the melt. Simkin & Smith (1970) observed that Ca contents of olivines from deep-seated plutonic and ultramafic rocks were generally lower (<0.1wt%) than those of olivines from extrusive and hypabyssal rocks (>0.1wt%). Stormer (1973) suggested that zonal trends towards calcium enrichment in olivine phenocrysts may be a response to pressure release during crystallisation. A normal Mg to Fe trend with no increase in calcium would then reflect crystallisation under isobaric conditions. However, interpretation of Ca variation in terms of melt composition and pressure is not as straight forward as is sometimes implied, since the Ca partitioning into olivine has been shown to increase with increasing iron activity of the melt. Ca is therefore preferentially incorporated into more fayalitic olivines (Jurewicz & Watson, 1988).

4.3.2. Analysed compositions

Olivine core compositions lie in the range Fo_{90-65}. Variations in element concentrations are dominated by the effects of fractionation with increasing Fe and Mn and decreasing Mg and Ni from core to rim in a given phenocryst. This is shown in Figs. 4.11 and 4.12 where Ni and Mn are plotted against $Mg/(Mg+Fe^{2+})$ respectively.

Inspection of these diagrams and individual analyses shows that:

1. The least evolved olivines are from the Fife & Lothian basanites and

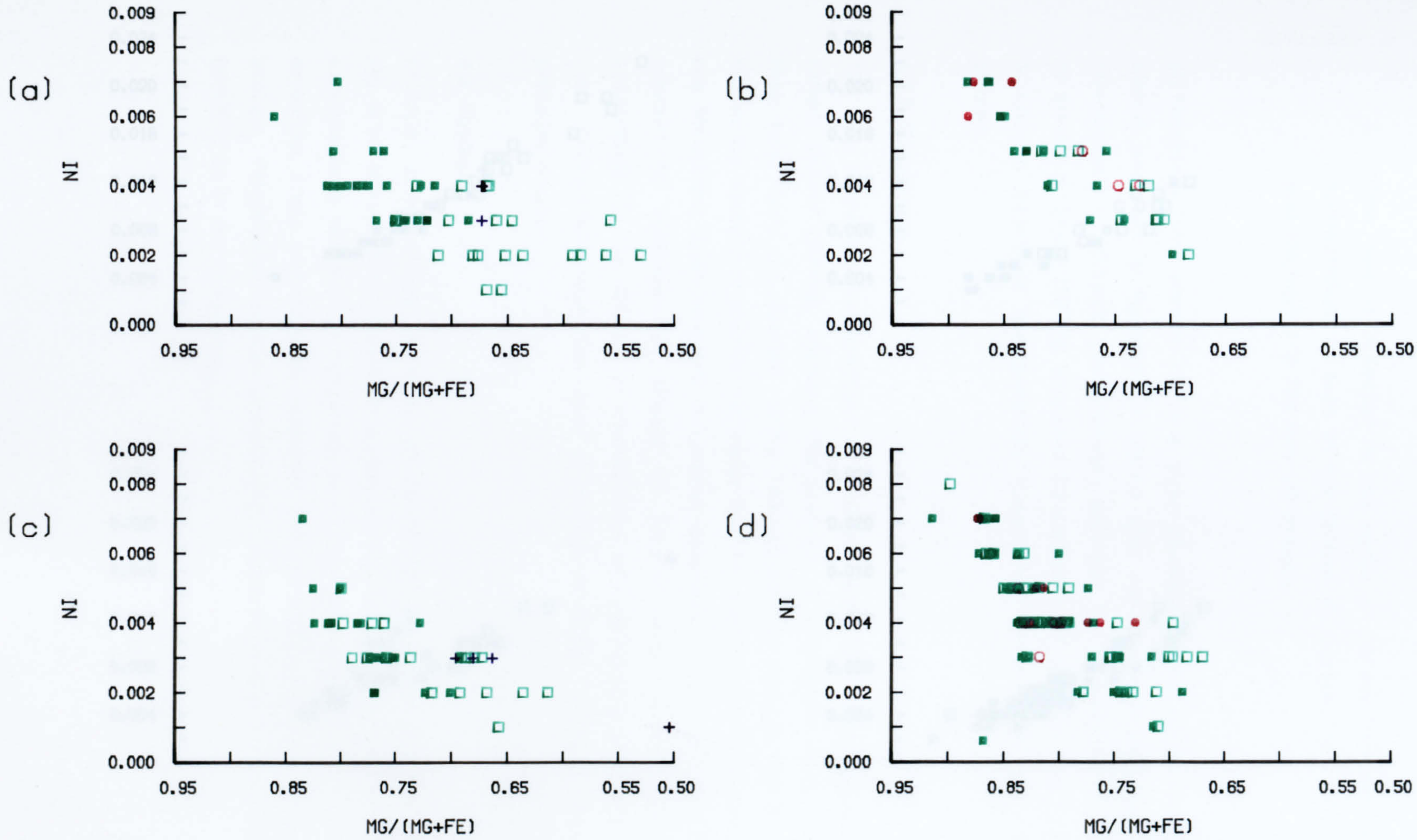

Fig. 4.11 Variations in Ni and Mg/(Mg+Fe^{2+}) for olivines from (a) Ayrshire sills (b) Mauchline group (c) Fife & Lothian sills (d) Fife & Lothian basanites.

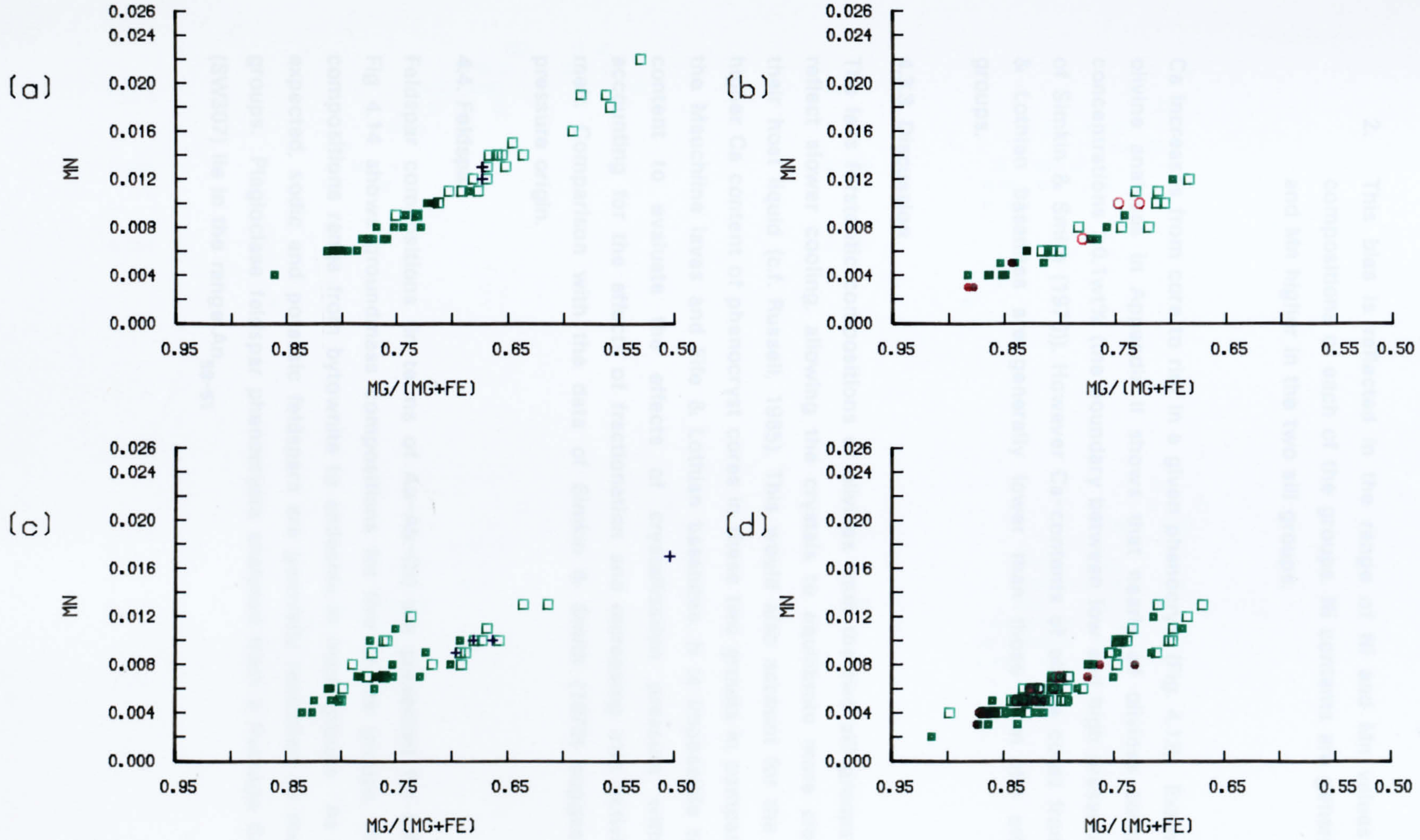

Fig. 4.12 Variations in Mn and Mg/(Mg+Fe^{2+}) for olivines from (a) Ayrshire sills (b) Mauchline group (c) Fife & Lothian sills (d) Fife & Lothian basanites.

the Mauchline lavas, with the Ayrshire and Fife & Lothian sills having a higher proportion of olivine cores with lower Mg-values.

2. This bias is reflected in the range of Ni and Mn values for core compositions of each of the groups. Ni contents are generally lower and Mn higher in the two sill groups.

Ca increases from core to rim in a given phenocryst (Fig. 4.13). Examination of olivine analyses in Appendix II shows that nearly all olivines contain Ca in concentrations >0.1wt% (the boundary between low and high pressure olivines of Simkin & Smith (1970)). However Ca-contents of olivine cores from the Fife & Lothian basanites are generally lower than those from the other three groups.

4.3.3. Discussion

The less forsteritic compositions of olivines from the two sill groups probably reflect slower cooling, allowing the crystals to equilibrate more closely with their host liquid (c.f. Russell, 1985). This would also account for the generally higher Ca content of phenocryst cores in these two groups in comparison with the Mauchline lavas and Fife & Lothian basanites. It is impossible to use Ca content to evaluate the effects of crystallisation pressure without first accounting for the effects of fractionation and increasing iron activity in the melt. Comparison with the data of Simkin & Smith (1970) suggests a low pressure origin.

4.4. Feldspar

Feldspar compositions (in terms of An-Ab-Or) are presented for information. Fig 4.14 shows groundmass compositions for five of the groups. Plagioclase compositions range from bytownite to andesine in most groups. As might be expected, sodic and potassic feldspars are generally restricted to the two sill groups. Plagioclase feldspar phenocrysts analysed from a Passage Group lava (SW307) lie in the range An_{59-51}

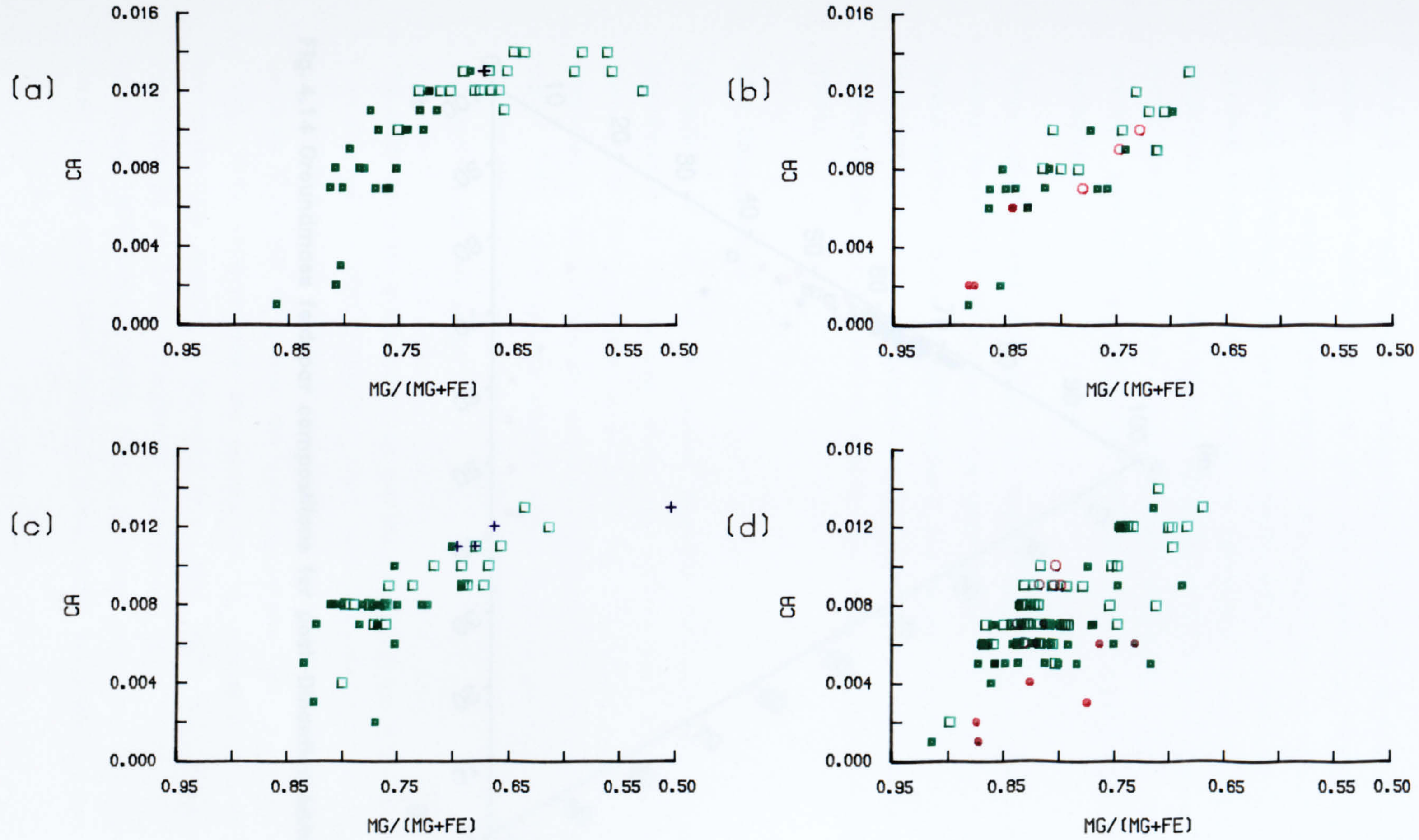

Fig. 4.13 Variations in Ca and Mg/(Mg+Fe^{2+}) for olivines from (a) Ayrshire sills (b) Mauchline group (c) Fife & Lothian sills (d) Fife & Lothian basanites.

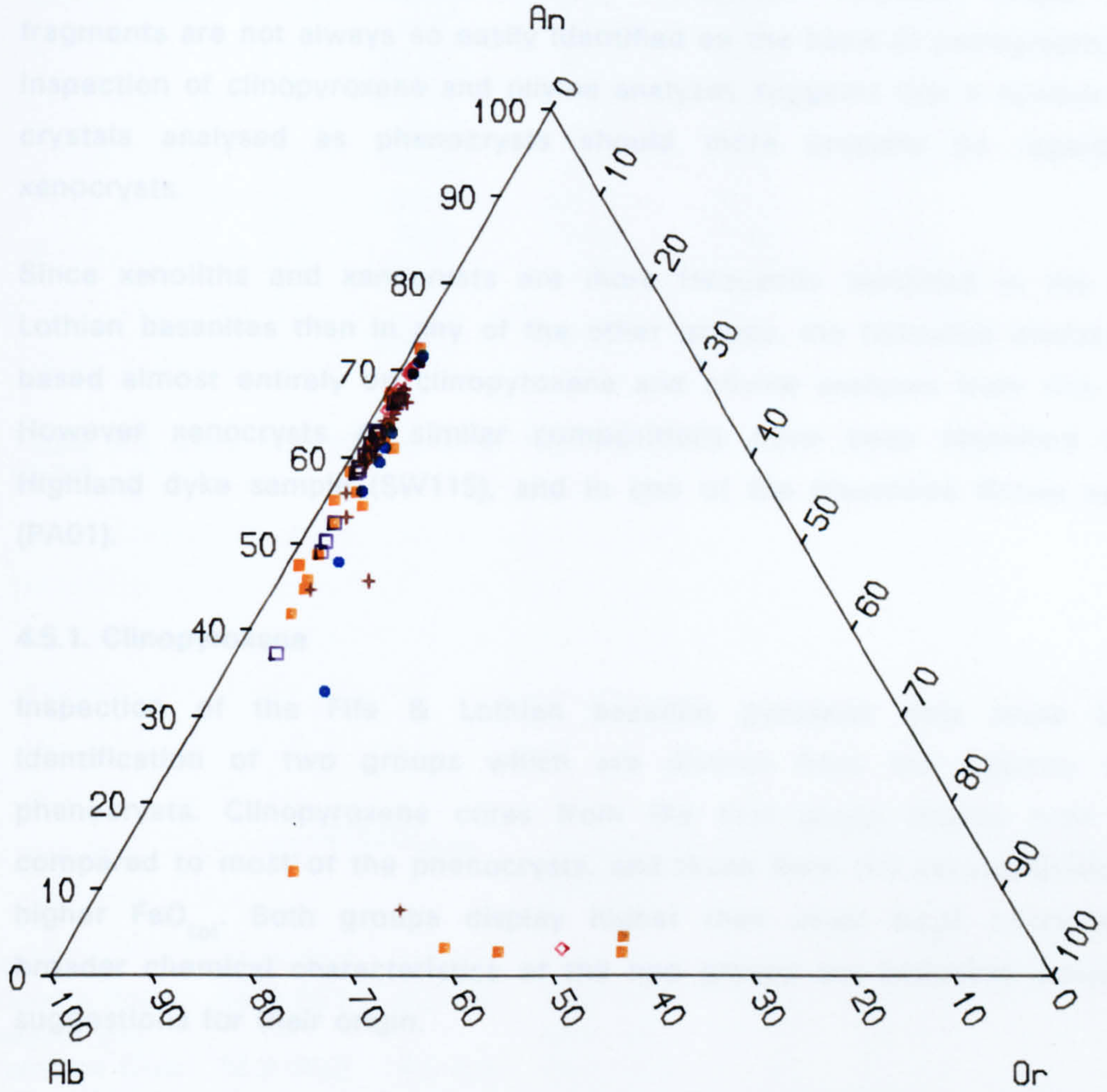

Fig. 4.14 Groundmass feldspar compositions for post–Dinantian samples.

4.5. Xenolith compositions

It is clear from chapter 3 that a significant number of the post-Dinantian igneous rocks host a variety of xenolithic inclusions. Polymineralic xenoliths are usually easily identified as such, and those comprising clinopyroxene and/or olivine can often be distinguished from phenocryst aggregates because of textural differences: e.g. they are commonly anhedral, fragmented crystals with strained extinction and evidence of resorption. However, single crystal fragments are not always so easily identified on the basis of petrography alone. Inspection of clinopyroxene and olivine analyses suggests that a number of the crystals analysed as phenocrysts should more properly be regarded as xenocrysts.

Since xenoliths and xenocrysts are more frequently identified in the Fife & Lothian basanites than in any of the other groups, the following discussion is based almost entirely on clinopyroxene and olivine analyses from this group. However xenocrysts of similar compositions have been identified in the Highland dyke sample (SW115), and in one of the Mauchline Group samples (PA01).

4.5.1. Clinopyroxene

Inspection of the Fife & Lothian basanite pyroxene data leads to the identification of two groups which are distinct from the majority of the phenocrysts. Clinopyroxene cores from the first group display high Cr_2O_3 compared to most of the phenocrysts, and those from the second group have higher FeO_{tot}. Both groups display higher than usual Na_2O contents. The broader chemical characteristics of the two groups are described below with suggestions for their origin.

The three analyses which compose the **high Cr** group are from SW20, a block from the Ardross Vent, (Table 4.1). They have distinctly higher Cr_2O_3 and Na_2O concentrations (1.07–1.33 wt% and 0.7–1.85 wt% respectively), and lower TiO_2 contents (0.38–0.80 wt%) than the other pyroxenes. Mg-values are also high (>95). Their compositions are comparable to clinopyroxenes from spinel lherzolites (e.g. Kutolin & Frovola, 1970; Best, 1974; Frey & Green, 1974; Hutchison *et al*, 1975; Littlejohn & Greenwood, 1975; Varne, 1977; Duda & Schminke, 1985; Dobosi, 1989). Spinel lherzolite pyroxenes from the Midland Valley (Hunter *et al*, 1984; Hunter & Upton, 1987), are slightly poorer in Cr_2O_3

	1	2	3
SiO_2	50.84	51.22	49.23
TiO_2	0.38	0.42	0.80
Al_2O_3	5.78	6.30	4.90
Cr_2O_3	1.33	1.27	1.07
FeO	2.91	3.53	4.87
MnO	0.11	0.12	0.17
MgO	16.31	15.52	15.71
CaO	19.64	19.09	21.27
Na_2O	1.66	1.85	0.73
total=	98.96	99.32	98.75

Table 4.1 Core compositions of high Cr_2O_3 clinopyroxene phenocrysts from SW20.

Locality	Olivine		Clinopyroxene				
	Fo	NiO	$\frac{100Ca}{(Ca+Mg+Fe)}$	Al_2O_3	Cr_2O_3	Na_2O	TiO_2
Fidra	88.0–91.0	0.3–0.4	45.0–49.0	6.3–7.6	0.5–0.8	1.0–1.9	0.4–0.8
Ruddon's Point	88.8–90.1	0.2–0.4	43.6–48.8	2.8–7.4	0.5–0.9	0.9–2.0	0.2–0.7
Coalyard Hill	–	–	46.2–48.2	5.6–7.5	0.6–0.7	1.7–1.9	0.2–0.6
Ashentree Glen	88.9–89.6	0.2–0.3	46.2–46.8	6.4–6.8	0.5–0.6	1.4–1.7	0.6–0.7
Baidland Hill	–	–	46.9	5.8	1.1	1.2	0.7

Table 4.2 Compositional parameters of olivine and clinopyroxene from spinel lherzolite xenoliths. (Data from Hunter & Upton, 1987).

and richer in Na_2O than the SW20 pyroxenes (compare Tables 4.1 and 4.2). Despite this, the similarities with spinel lherzolite pyroxenes suggest that the cores of these three crystals were derived from disaggregated spinel lherzolite xenoliths which acted as nucleation sites for subsequent clinopyroxene crystallisation (c.f. Dobosi, 1989).

The **high Fe** group (Table 4.3) comprises 13 core analyses of xenocrysts and supposed phenocrysts. They are characterised by FeO contents in the range 8.11–12.95 wt% and high Na_2O (0.80–2.03 wt%), moderate to low TiO_2 (0.29–1.87 wt%), and very low Cr_2O_3 (<0.09 wt%). Mg-values are in the range 51–84. They are chemically similar to some of the megacrysts and xenocrysts from minor intrusions in the Highlands (Streap Comlaidh, Stob a' Ghrianian and Colonsay, (P. Aspen & B.G.J. Upton, pers. comm., 1988; compare Tables 4.3 and 4.4). The high Fe pyroxenes are also comparable to the fassaitic augites of Duda & Schminke (1985) and Dobosi (1989).

4.5.2. Olivine

Identification of olivine xenocrysts on the basis of chemistry is not easy. Those identified as xenocrysts on the basis of morphology are not always compositionally distinct from the phenocrysts. Six crystals analysed as xenocrysts show distinct reversed-zoning with cores more Fe-rich and Mg-poor than rims (compared to normally zoned phenocrysts) FeO contents of 16.6–28.11wt% are comparable to phenocryst rims of olivines from the Fidra wehrlite–clinopyroxenite suite (P. Aspen & B.G.J. Upton pers. comm., 1988; compare Table 4.5 with Table 4.6). An additional five phenocrysts can be assigned to the xenocryst group using these chemical criteria.

4.6. Discussion

Clinopyroxene phenocryst compositions are similar to those from many other alkaline provinces (e.g. Fodor *et al.*, 1975; Wass, 1979; Cundari & Ferguson, 1982; Almond, 1988; Farone *et al.*, 1988; Cundari & Salviulo, 1989; Dobosi, 1989). However, the high Al_2O_3 and TiO_2 contents of clinopyroxene rims of some of the Fife & Lothian basanite and the Highland dyke samples are notable. Bedard *et al.* (1988) showed a positive relationship between Al^{iv} + Ti and Mg-number for clinopyroxenes in intermediate and leucocratic dykes of the Monteregian alkaline province, Southern Quebec which they attributed to fractionation of Ti-rich phases from the magma. The more common inverse relationship

	1	2	3	4	5	6	7	8
SiO_2	50.45	51.03	50.03	47.52	47.09	43.98	50.12	50.90
TiO_2	0.35	0.66	0.73	1.77	1.15	2.87	0.65	0.60
Al_2O_3	4.07	5.61	4.68	8.41	5.95	10.18	4.09	3.21
Cr_2O_3	nd	nd	nd	nd	nd	0.03	nd	0.03
FeO	10.97	8.53	11.18	9.38	12.95	9.08	11.24	10.73
MnO	0.40	0.27	0.36	0.17	0.31	0.18	0.38	0.36
MgO	12.99	13.08	10.60	11.66	9.26	10.57	2.18	13.25
CaO	18.54	19.89	20.75	20.46	21.30	21.35	20.62	20.43
Na_2O	1.29	1.33	1.50	0.95	1.29	1.15	0.80	0.84
total=	99.06	100.40	99.83	100.32	99.30	99.39	100.08	100.35

	9	10	11	12	13
SiO_2	53.54	51.40	46.90	47.88	48.22
TiO_2	0.29	1.00	2.09	1.85	1.87
Al_2O_3	0.71	4.02	7.87	7.21	5.97
Cr_2O_3	0.09	0.06	0.03	0.05	nd
FeO	8.92	8.17	0.47	8.54	8.80
MnO	0.51	0.25	0.25	0.18	0.17
MgO	13.92	11.82	11.74	12.70	13.22
CaO	21.91	21.13	19.69	20.36	20.56
Na_2O	1.28	2.03	1.26	0.98	0.96
total=	101.17	99.88	100.30	99.75	99.77

Table 4.3 Core compositions of high FeO clinopyroxenes. (1-4) SW6; (5,6) SW9; (7,8) SW25; (9-11) SW40; (12,13) SW442.

	1	2	3	4	5	6	7	8	9	10
SiO_2	48.17	47.89	47.40	47.40	50.21	50.40	49.41	51.23	50.47	49.36
TiO_2	1.63	1.49	1.56	1.58	1.06	0.97	1.08	0.75	0.88	3.82
Al_2O_3	7.72	7.61	7.87	5.38	4.47	4.68	3.21	4.44	5.03	3.82
FeO	11.72	11.88	11.77	10.70	12.52	12.14	12.51	11.33	12.02	13.00
MnO	0.23	0.25	0.22	0.12	0.30	0.27	0.26	0.16	0.15	0.24
MgO	8.98	9.10	8.86	11.21	9.60	9.92	11.61	10.92	10.24	10.26
CaO	19.56	19.75	19.71	23.48	20.17	20.20	21.77	20.06	19.76	21.09
Na_2O	2.13	2.21	2.08	0.33	2.16	1.90	0.77	1.87	2.13	1.19
total=	100.14	100.18	99.47	100.20	100.49	100.48	100.62	100.76	100.68	102.78

Table 4.4 Clinopyroxene megacryst and xenolith compositions from Highland intrusions: (1-4) Colonsay; (5,6) Stob a' Ghrianain; (7-10) Streap Comlaidh.

	1	2	3	4	5	6	7	8
SiO_2	38.38	39.21	37.48	37.41	39.24	38.00	38.90	36.79
Al_2O_3	0.08	0.08	0.05	0.08	0.04	0.07	0.05	0.04
FeO	17.62	19.95	19.42	28.11	17.47	24.35	21.87	23.00
MnO	0.25	0.27	0.23	0.47	0.23	0.37	0.35	0.33
NiO	0.20	0.12	0.17	0.09	0.24	0.18	0.19	0.11
MgO	43.07	40.54	41.43	34.83	43.04	37.27	39.75	38.90
CaO	0.19	0.17	0.22	0.31	0.24	0.22	0.23	0.21
total=	99.79	100.34	99.00	101.30	100.50	100.46	101.34	99.38

	9	10	11
SiO_2	38.45	38.49	39.93
Al_2O_3	0.05	0.07	0.07
FeO	16.60	20.86	16.87
MnO	0.26	0.31	0.25
NiO	0.22	0.17	0.25
MgO	44.55	40.23	43.73
CaO	0.14	0.10	0.22
total=	100.27	100.23	101.32

Table 4.5 Olivne core compositions of possible pyroxenite-wehrlite xenoliths: (1) SW6; (2) SW9; (3,4) SW40; (5-8) SW442; (9-11) SW526.

	1	2	3	4
SiO_2	38.84	37.99	39.09	38.62
Al_2O_3	0.11	-	-	-
FeO	21.05	23.68	21.87	24.17
MnO	0.34	0.41	0.37	0.38
NiO	0.20	-	0.18	0.16
MgO	39.57	37.56	39.28	37.95
CaO	0.33	0.47	0.21	0.36
total=	100.44	100.11	101.00	101.64

Table 4.6 Olivine core compositions from Fidra pyroxenite-wehrlite xenoliths. (Unpublished data from P. Aspen & B.G.J. Upton, pers. comm., 1989).

between Al^{iv} + Ti and Mg-number for the post-Dinantian clinopyroxene phenocrysts confirms the petrographic observation that Fe-Ti-oxide fractionation has been insignificant.

The discrete Cr-diopside crystals analysed in this study are probably remnants of spinel lherzolite inclusions. It would appear that on disaggregation, orthopyroxene and spinel react rapidly with the host magma and are wholly resorbed. Although olivine would remain stable, olivine xenocrysts would be expected to re-equilibrate rapidly with the host magma, and rarely be recognisable.

The olivine xenocrysts of Table 4.5 have compositions similar to those of the Fidra wehrlite xenoliths. Xenoliths of the Fidra suite bear a petrographical and mineralogical resemblance to Al-augite-bearing xenoliths from other parts of the world (Hunter *et al*, 1984). Wass (1979) identified two types of Al-augite xenocryst: (1) 'Accidental' xenocrysts totally unrelated to the magmatic episode represented by the host alkali basalt, and (2) 'Cognate' xenocrysts resulting from high-pressure crystallisation of alkali basaltic melts contemporaneous with the host magma. Wass (1979) showed that the two were compositionally and often petrographically indistinct. It is therefore possible that some of the augites identified as high-pressure phenocrysts in this study, are not actually cognate with the host magma. Hunter *et al.* (1984) indicated a possible cumulate origin for the wehrlite-clinopyroxenite suite. They suggested that such high-pressure cumulates could have precipitated from magmas similar in composition to the host basanite. However, the range of textures from igneous to re-equilibrated (metamorphosed), implies that magmatism must have extended over a considerable time.

The Fe-rich clinopyroxenes of some of the Fife & Lothian basanites resemble the fassaitic augites of Duda & Schminke (1985) and Dobosi (1989) (see section 3.5.1). Fe-rich clinopyroxenes are a common occurrence in alkali basalts throughout the world (Brooks & Printzlau, 1978) and Duda & Schminke (1985) offer two possible origins:

1. They are cognate, with inverse zoning caused by increasing fO_2. This could be caused by resorption of kaersutite at low pressure (Frisch & Schminke, 1969) or by sinking of the crystal in a convecting magma chamber (Borley *et al*, 1971). Alternatively the

green cores represent a high-pressure differentiation trend (Wilkinson, 1975; Wass, 1979).

2. They are xenocrysts representing either wall-rock debris entrained by the rising magma (Barton & vanBergman, 1981; Lloyd, 1981), or crystallisation products of an evolved magma which subsequently mixed with a more primitive magma (Thompson, 1977; Barton *et al*, 1982; Brooks & Prinzlau, 1978; Wass *et al*, 1980).

Non-equilibrium between pyroxenes of these compositions and alkali basalts (Duda & Schminke, 1985; Dobosi, 1989) suggests that the Fe-rich clinopyroxenes are xenocrysts, but whether they are from disaggregated metasomatised mantle xenoliths or whether they represent high-pressure phenocrysts from more fractionated magmas encountered by, and intermingled with, the ascending alkali basalt magmas, is not clear.

Mantle metasomatism beneath the Midland Valley has been proposed by Upton *et al.* (1984), who suggested a metasomatic origin for the biotite- and kaersutite-pyroxenites of the region, with mantle infiltration by K- Fe- and Ti-rich fluids. However because of the compositional similarity between the intercumulus kaersutite and some of the 'intermediate' members of the Fife basanites, Chapman (1974, 1976) suggested that the former represents a frozen trapped basanitic liquid. More extreme fractionation would produce more evolved rocks represented by xenoliths containing biotite, Na-amphibole and albite, and by the anorthoclase megacrysts of the region (Chapman, 1974, 1976) all of which are possibly genetically related to the Fe-rich clnopyroxenes.

Further work on the anorthoclase megacrysts (Aspen *et al*, in press), has shown that they did not crystallise from their host magmas, and in some cases they are in isotopic disequilibrium with the host basalt. Aspen *et al.* suggested that the alkali feldspars crystallised from highly evolved felsic (trachytic) magmas, the ultimate origin of which is unclear. Interception of a wholly crystalline felsic body or partly crystalline porphyritic felsic magma by a fast-moving alkali basalt magma would result in the entrainment of xenoliths/xenocrysts and phenocrysts respectively. In the latter case some degree of magma mixing must be inferred. However, the Fife & Lothian basanite whole-rock compositions can be explained in terms of variable degree melting

of an upper mantle source (chapter 6), and the whole-rock geochemistry gives no reason to invoke magma mixing. Therefore the preferred interpretation for the Fe-rich clinopyroxene megacrysts is that they represent disaggregated metasomatised mantle.

4.7. Summary

1. The post-Dinantian igneous rocks of the Midland Valley contain a wide variety of olivine and pyroxene phenocrysts and xenocrysts. Distinctions between the phenocrysts and xenocrysts have been made on the basis of geochemistry.

2. Olivine phenocrysts are virtually ubiquitous. Cores range between Fo_{90-65} and display trends of increasing Fe and Mn with decreasing Mg and Ni. More evolved compositions for olivine cores in the two sill groups may be due to slower cooling and longer equilibration times than those of the lavas and minor intrusions. Ranges in Ca content suggest that olivines of the Fife & Lothian basanites began growing at higher pressures than those of the Mauchline lavas, and Ayrshire and Fife & Lothian sills.

3. Clinopyroxene phenocrysts have diopsidic salite or augite compositions and many show appreciable Tschermak's-molecule substitution reflecting the degree of magma undersaturation. Variations in Al and Ti reflect melt compositions and fractionation effects. With fractionation Ti and Al contents increase in all except the transitional Passage Group lavas where Al decreases. Al^{iv}/Al^{vi} ratios show that pyroxenes in each group crystallised over a range of pressures, and that all groups contain examples of low pressure clinopyroxenes. The highest crystallisation pressures (10-20 kb), are indicated by clinopyroxenes from the Highland Dykes and the Fife basanites. Ca shows a broad correlation with melt composition, with higher concentrations in clinopyroxenes from undersaturated rocks. There generally appears to be a positive relationship between host-rock alkalinity and the observed maximum depth of initial clinopyroxene crystallisation.

4. Plagioclase feldspar phenocrysts analysed from one Passage Group

lava lie in the range An_{59-51}.

5. Xenocrysts have been allocated to one of three groups. Reverse-zoned olivines with FeO-rich cores (16.60-28.11wt% FeO; Fo_{83-68}) resemble olivines from the Fidra pyroxenite-wehrlite suite. Clinopyroxenes with higher-than-normal Cr_2O_3 and Na_2O contents (1.07-1.33wt% and 0.17-1.85wt% respectively) resemble Cr-diopsides from spinel-lherzolite xenoliths, and high FeO - high Na_2O clinopyroxenes (8.11-12.95wt% and 0.80-2.03 wt% repectively) are geochemically similar to pyroxene megacrysts and xenocrysts from minor intrusions in the Highlands.

CHAPTER 5

WHOLE-ROCK GEOCHEMISTRY

5.1. Introduction

Approximately 400 samples from the post-Dinantian Scottish suite have been analysed by X-Ray fluorescence for major and trace elements. In an attempt to limit the effects of alteration only samples in which the clinopyroxene was relatively unaltered (alteration stages 1-3 of section 3.2.4) were analysed. LOI values are therefore with few exceptions, less than 6 wt%. Six Highland dyke samples were analysed as part of this project. The additional analyses are from Baxter (1986) and Morrison *et al.* (1986). Ranges in element concentrations for each of the seven groups are outlined in Table 5.1.

It is common practice to display element variations against wt% MgO as an index of differentiation, since this will decrease rapidly with olivine and pyroxene fractionation from a magma. However, experimental studies have suggested that the MgO content of primary magmas may also reflect the pressure of melting. Such studies by Thompson *et al.* (1983) indicated a range in primary melt MgO content from c.8% at 10kb to c.25% at 40kb. A similar relationship has been observed in mid-ocean ridge basalts where calculated mean primary magmas range in composition between 10-15 wt% MgO, the more magnesian compositions correlating with greater depth and degree of melting (Klein & Langmuir, 1987). However, it is usual in geochemical studies to assume that although the individual distribution coefficients of Fe^{2+} and Mg^{2+} are sensitive to changes in temperature, pressure, oxygen fugacity and composition, their ratio remains constant. This assumption has allowed the calculation of a range of Mg-values for primary magmas in equilibrium with mantle olivine (Fo_{94-90}), (Roeder & Emslie, 1970; Basaltic Volcanism Study Project, 1981). However, the assumption may not be strictly valid. Experiments imply both a pressure (Bender *et al.*, 1978; Takahashi & Kushiro, 1983) and a composition (Longhi *et al.*, 1978) dependence for the distribution coefficient ratios. Variations should also be expected under high pressure hydrous conditions and with changing Mg-value of the source peridotite (Nicholls, 1974; Mysen, 1975; Wilkinson & Le Maitre, 1987). Because of these influences it is difficult to justify the selection of a specific range in Mg-values which might correctly discriminate between primary and fractionated mafic compositions (see Wilkinson & Le Maitre (1987) for further discussion). However, Beattie *et*

	1 (24)		2 (28)		3 (147)		4 (54)		5 (89)		6 (20)		7 (12)	
	m	sd	m	sd	m	sd	m	sd	m	sd	m	sd	m	sd
SiO_2	48.0	3.5	46.7	3.3	46.3	3.8	47.9	3.8	45.3	3.2	43.3	3.7	50.6	2.7
Al_2O_3	15.0	1.2	14.5	4.1	14.3	1.8	15.0	2.2	14.3	1.8	13.4	2.2	14.0	1.2
Fe_2O_3	12.4	1.5	11.9	3.0	12.3	1.6	12.1	2.1	12.4	1.9	12.2	2.5	13.4	2.2
MgO	7.0	2.3	10.8	8.1	10.2	3.9	8.2	3.5	8.8	3.1	9.3	4.2	5.7	2.7
CaO	10.7	2.9	9.4	2.3	10.0	2.2	8.9	2.7	9.9	2.3	10.9	2.7	9.7	2.7
Na_2O	2.7	0.6	3.2	1.7	2.6	1.3	3.3	1.5	3.4	1.4	2.7	1.8	2.3	0.6
K_2O	1.0	0.3	1.3	0.9	1.1	0.6	1.4	1.2	1.3	1.1	1.9	1.8	1.0	1.6
TiO_2	2.0	0.3	1.6	0.7	1.1	0.5	1.4	1.0	2.8	0.5	2.5	0.7	2.5	0.8
MnO	0.1	0.06	0.2	0.03	0.2	0.1	0.2	0.1	0.3	0.3	0.2	0.1	0.2	0.1
P_2O_5	0.5	0.2	0.3	0.2	0.4	0.3	0.5	0.4	0.7	0.3	0.8	0.5	0.3	0.2
Ni	178	72	239	303	275	186	154	140	208	120	192	191	65	60
Cr	245	103	404	475	442	259	268	263	292	195	331	327	102	141
V	217	34	229	65	258	61	214	77	244	53	*267	533	358	58
Sc	24	7	24	9	25	8	21	8	21	10	23	8	31	6
Cu	55	32	63	38	40	42	48	27	54	31	*54	24	98	121
Zn	165	204	85	24	107	138	103	49	170	368	*106	18	128	120
Sr	496	260	497	244	558	297	621	586	911	493	1014	784	365	233
Rb	21	7	27	17	24	20	29	29	25	28	51	41	20	24
Zr	172	50	123	63	151	66	190	123	289	106	237	197	199	87
Nb	34	18	26	16	36	27	41	44	68	33	*86	47	16	6
Ba	586	633	497	384	645	553	776	1551	1076	1233	*1979	2763	269	324
La	23	15	15	13	23	24	32	34	51	33	51	48	32	21
Ce	54	33	40	27	54	41	66	70	108	58	*128	66	54	45
Nd	27	14	20	13	26	16	30	27	47	20	*56	24	30	20
Y	25	4	20	8	23	5	26	6	29	6	27	9	32	11

Table 5.1 Mean (m) and 2σ (sd) for samples from each group: (1) Passage Group lavas; (2) Ayrshire sills; (3) Mauchline group; (4) Fife & Lothian sills; (5) Fife & Lothian basanites; (6) Highland dykes; (7) Quartz dolerites. Number of samples shown in brackets at the top of each column. Asterisked Highland dyke analyses are the mean of 6 samples.

al. (pers.comm 1989) have shown a linear relationship between the partition coefficients of Mg and Fe^{2+} for olivine, over a range of pressures. It therefore appears that the thermodynamic constraints are such that a Kd_{Fe}/Kd_{Mg} ratio of $0.33^{+}_{-}0.03$ can be assumed. The majority of post-Dinantian samples have MgO contents in the range 2-16 wt%, and in the absence of any contrary indications, it has been assumed that the MgO variation is dominated by the effects of fractional crystallisation. Consequently element variations can be plotted against wt% MgO as an index of differentiation (Figs. 5.1-5.24). Linear trends on such diagrams are interpreted in terms of simple fractionation processes. However, such well-defined trends are rare and scatter can be attributed to a combination of causes which are discussed below.

Only scatter which is greater than the precision of the analytical technique can be confidently attributed to natural processes. In an attempt to assess this range for the Midland Valley suite, six separate glass discs and pressed powder pellets were made from SW161C, the sample closest in composition to the mean for the whole suite (excluding the quartz dolerites). The results are displayed in Appendix VI. They show that with the exception of Na_2O, the percentage error (two standard deviations expressed as a percentage of the mean) for the major elements, is less than 1%. With the exceptions of Pb, Th, La, Ce and Nd, 2-sigma for trace element analyses are generally less than 3% of the respective element mean. However the scatter for all elements is outwith that which can be attributed purely to analytical precision.

Some element variations are undoubtedly inherited from weathering and alteration processes. In general the mobility of an element in an aqueous fluid can be assessed from its ionic potential. Elements with low (<3) and very high (>12) ionic potentials are usually mobile, and those intermediate to these values, immobile (Keller, 1957; Pearce, 1983). On this basis Ca^{2+}, Na^{+}, K^{+}, Sr^{2+}, Rb^{+} and Ba^{2+} and to a lesser extent Mn^{2+}, Cu^{2+} and Zn^{2+} would be expected to show some degree of mobility. Because element concentrations are expressed as weight fractions (% or ppm), decreasing mobile major element concentrations (e.g. Na_2O, K_2O) will be reflected in apparent increasing concentrations of the immobile elements (e.g. TiO_2, P_2O_5 and immobile trace elements). Hence alteration may also effect immobile element variation.

The relationship between LOI and major element oxide variations has been studied by Latin *et al.* (in press,a) for a North Sea ankaramite flow. Their data

suggested that significant variations in element concentrations should be expected at LOI values in excess of 10%. However, LOI values up to 6wt% for some of the post-Dinantian samples emphasise the influence of alteration processes in some cases, and therefore movement (loss or gain) of the more mobile elements should be expected. In an attempt to distinguish between scatter due to alteration and that produced by other processes, samples from the Midland Valley volcanic province have been compared to a geochemically similar suite of rocks from the Basin and Range province in the south west United States (J.G. Fitton, pers. comm., 1988). These rocks are young, and have therefore experienced little if any alteration. Statistical comparisons between the Basin & Range and Midland Valley samples are not possible since differences in degree of partial melting and differentiation affects the range of element concentrations. However, visual comparisons suggest that for most elements the scatter is no larger than that expected for a suite of unaltered samples. In general, the majority of Midland Valley samples define a reasonably coherent grouping for each element, from which only a few samples (generally different for each element) deviate. This is particularly noticeable for MnO concentrations (Fig 5.8) in the Fife & Lothian basanites and Mauchline group, and for Zn ranges (Fig 5.15) in the Passage Group lavas and Fife & Lothian basanites. A significant number of 'deviant' samples in the basanite and Mauchline groups are blocks from vents, and as such are likely to have been more susceptible to alteration processes than their associated lavas and intrusions, or to represent exotic and irrelevant samples e.g. from the ORS or Dinantian. In these two groups there is no correlation between LOI and degree of scatter. However the Passage Group lavas with the greatest Zn concentrations are generally those with highest LOI values. Ba concentrations (Fig. 5.20) in all groups are generally <2000ppm. However, some samples, (noticeably from the sill and basanite groups of Fife & Lothian, and from the Highland dyke group), have Ba contents in excess of this. There is no correlation between Ba concentration and either LOI or degree of silica saturation, and it is possible that both alteration and partial melting processes have contributed to these high concentrations.

It is obvious that neither analytical imprecision nor alteration can explain the variable element concentrations at a given MgO concentration. Some scatter, particularly for the more incompatible elements, will be the result of variable degrees of partial melting at different depths in the mantle. Variations in mantle

composition and mineralogy, the type of melting and the activity of volatile species will also influence the composition of the initial melt.

Variable element concentrations acquired during melting will be enhanced during crystal fractionation, since phase compositions and degree of crystallisation will vary with pressure, volatile activity and the rate of magma ascent. Additionally, *in situ* differentiation within sills may result in vertical and lateral heterogeneity producing a range of compositions from the least evolved chilled margins, to the most evolved syenite veins (Walker, 1986). (These processes are more obviously reflected in the sills of Fife & Lothian than in those from Ayrshire).

A minor cause of scatter in these diagrams is the analysis of variably porphyritic samples. It is clear that several of the Ayrshire sill and Mauchline Group samples have accumulated olivine (chapter 3). This is reflected in increased MgO contents (up to 20wt%), and in trends at an angle to linear fractionation trends. (These samples have been omitted from the diagrams).

5.2. Summary of element variations with MgO

Some caution must be exercised in the identification of trends. There are some inter-element plots in which most of the samples clump together in a group, but a few extraneous samples plotting away from the main group produce a 'pseudo trend' which may not be explicable in terms of crystal fractionation processes.

5.2.1. Major elements

Major element correlations with MgO are shown in Figs. 5.1-5.9 and are summarised for each group in Table 5.2. The two elements which show the best correlations for all groups are Al_2O_3 (Fig. 5.2) and Na_2O (Fig. 5.5). Both these oxides increase with decreasing MgO. Fe_2O_{3tot} (Fig. 5.3) appears to decrease with decreasing MgO in the Passage Group lavas and Ayrshire sills and to a lesser extent in the sills and basanites of Fife & Lothian. The Ayrshire sills show the best correlation with MgO for all the oxides.

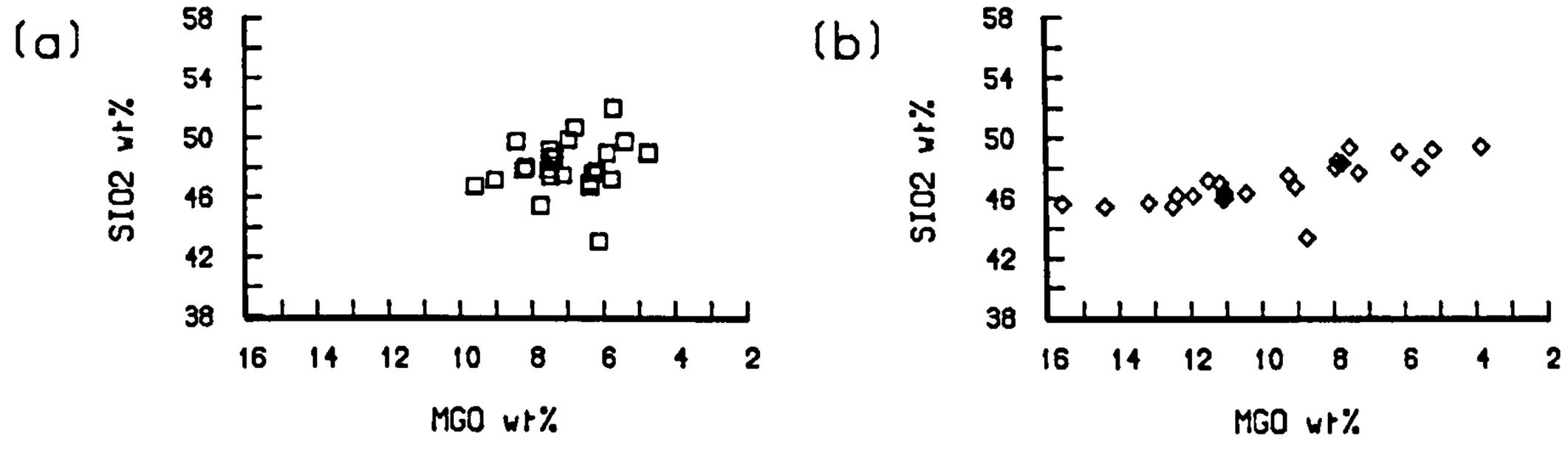

Fig.5.1 SiO_2 against MgO for all groups

(a) Passage Group lavas (b) Ayrshire Sills (c) Mauchline Group
(d) Fife & Lothian sills (e) Fife & Lothian basanites (f) Highland Dykes
(g) Quartz dolerites and (h) Basin & Range for comparison.

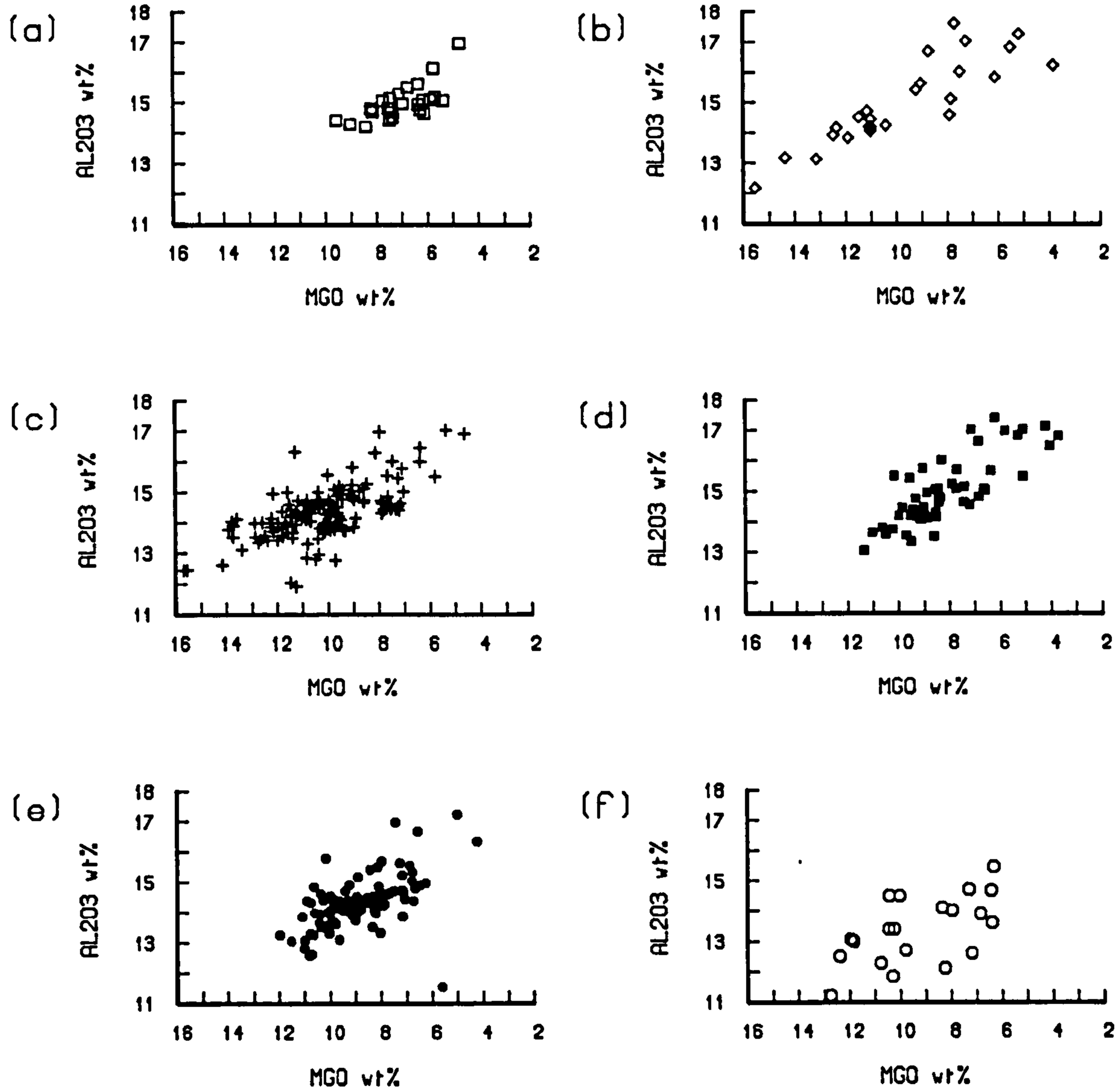

Fig.5.2 Al_2O_3 against MgO for all groups

(a) Passage Group lavas (b) Ayrshire Sills (c) Mauchline Group
(d) Fife & Lothian sills (e) Fife & Lothian basanites (f) Highland Dykes
(g) Quartz dolerites and (h) Basin & Range for comparison.

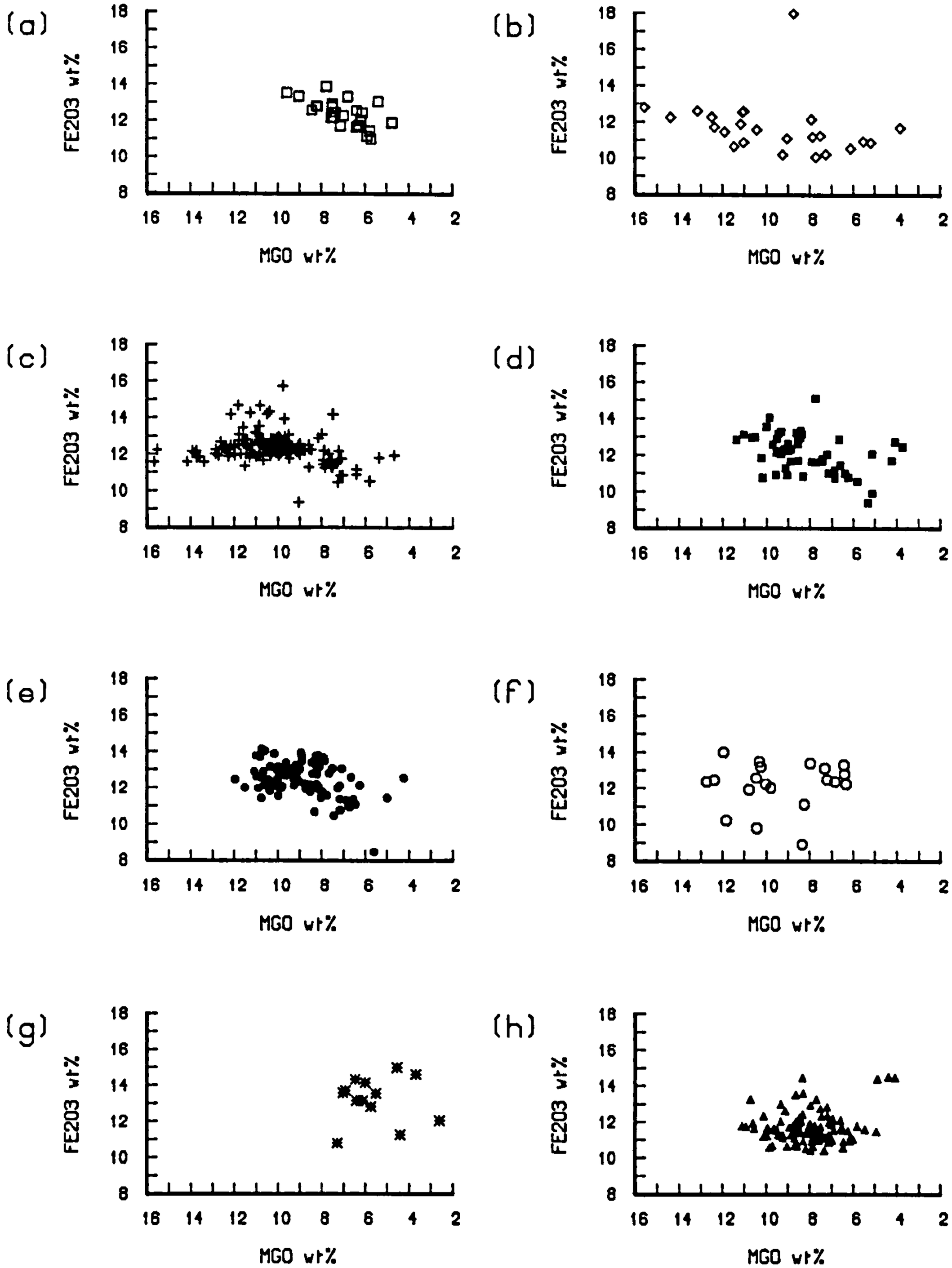

Fig.5.3 Fe_2O_{3tot} against MgO for all groups

(a) Passage Group lavas (b) Ayrshire Sills (c) Mauchline Group
(d) Fife & Lothian sills (e) Fife & Lothian basanites (f) Highland Dykes
(g) Quartz dolerites and (h) Basin & Range for comparison.

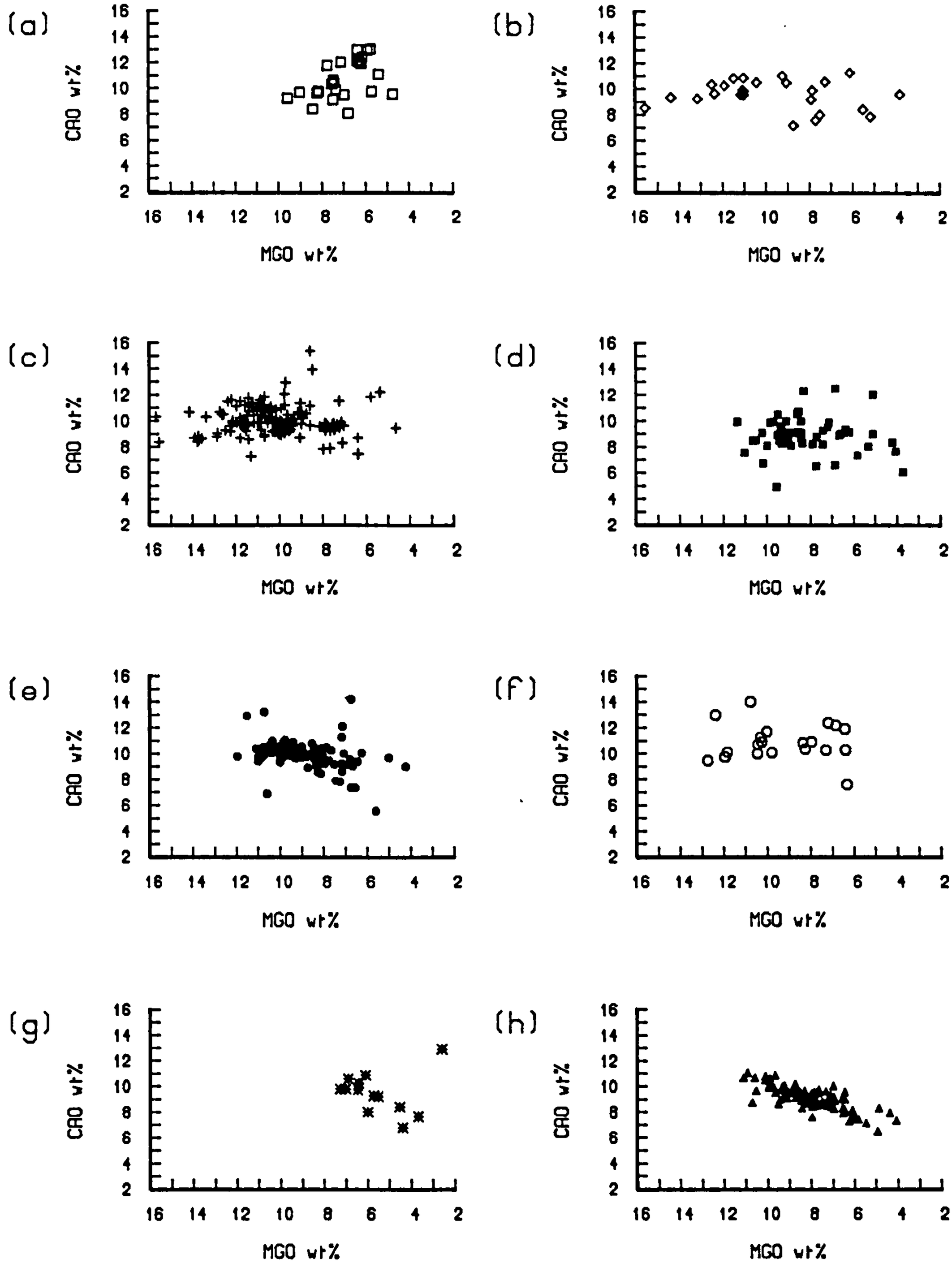

Fig.5.4 CaO against MgO for all groups

(a) Passage Group lavas (b) Ayrshire Sills (c) Mauchline Group
(d) Fife & Lothian sills (e) Fife & Lothian basanites (f) Highland Dykes
(g) Quartz dolerites and (h) Basin & Range for comparison.

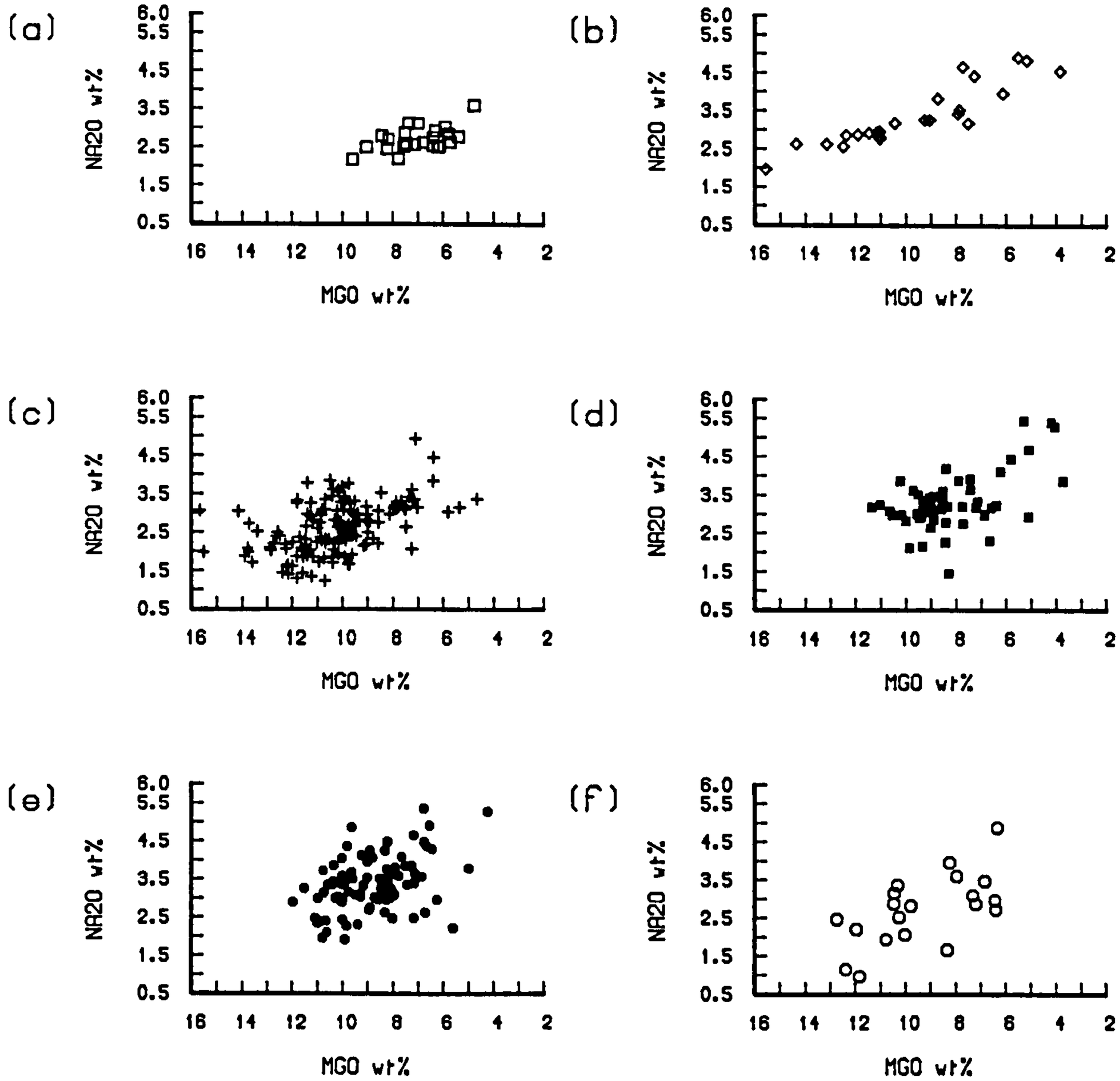

Fig.5.5 Na_2O against MgO for all groups

(a) Passage Group lavas (b) Ayrshire Sills (c) Mauchline Group
(d) Fife & Lothian sills (e) Fife & Lothian basanites (f) Highland Dykes
(g) Quartz dolerites and (h) Basin & Range for comparison.

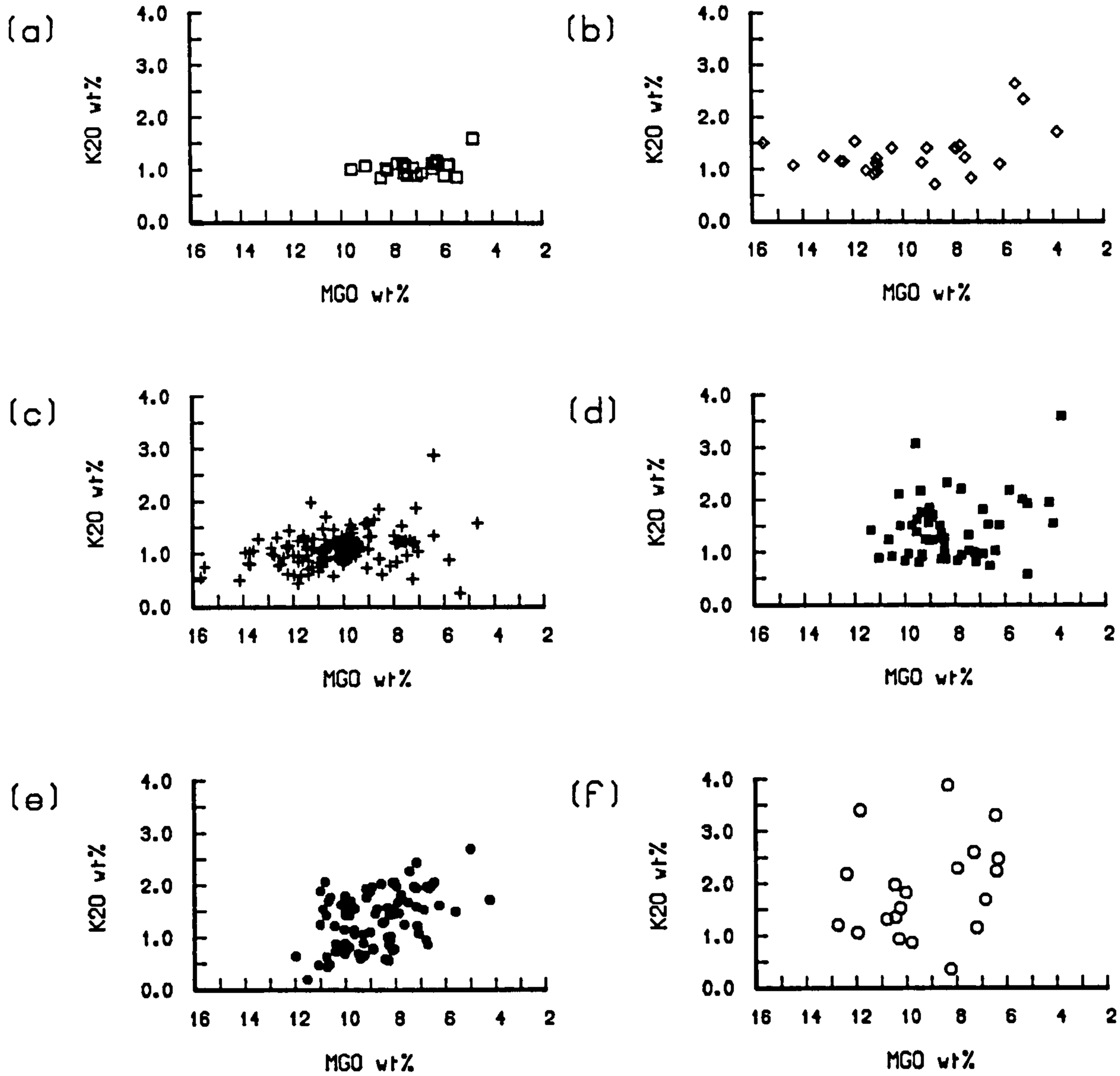

Fig.5.6 K_2O against MgO for all groups

(a) Passage Group lavas (b) Ayrshire Sills (c) Mauchline Group
(d) Fife & Lothian sills (e) Fife & Lothian basanites (f) Highland Dykes
(g) Quartz dolerites and (h) Basin & Range for comparison.

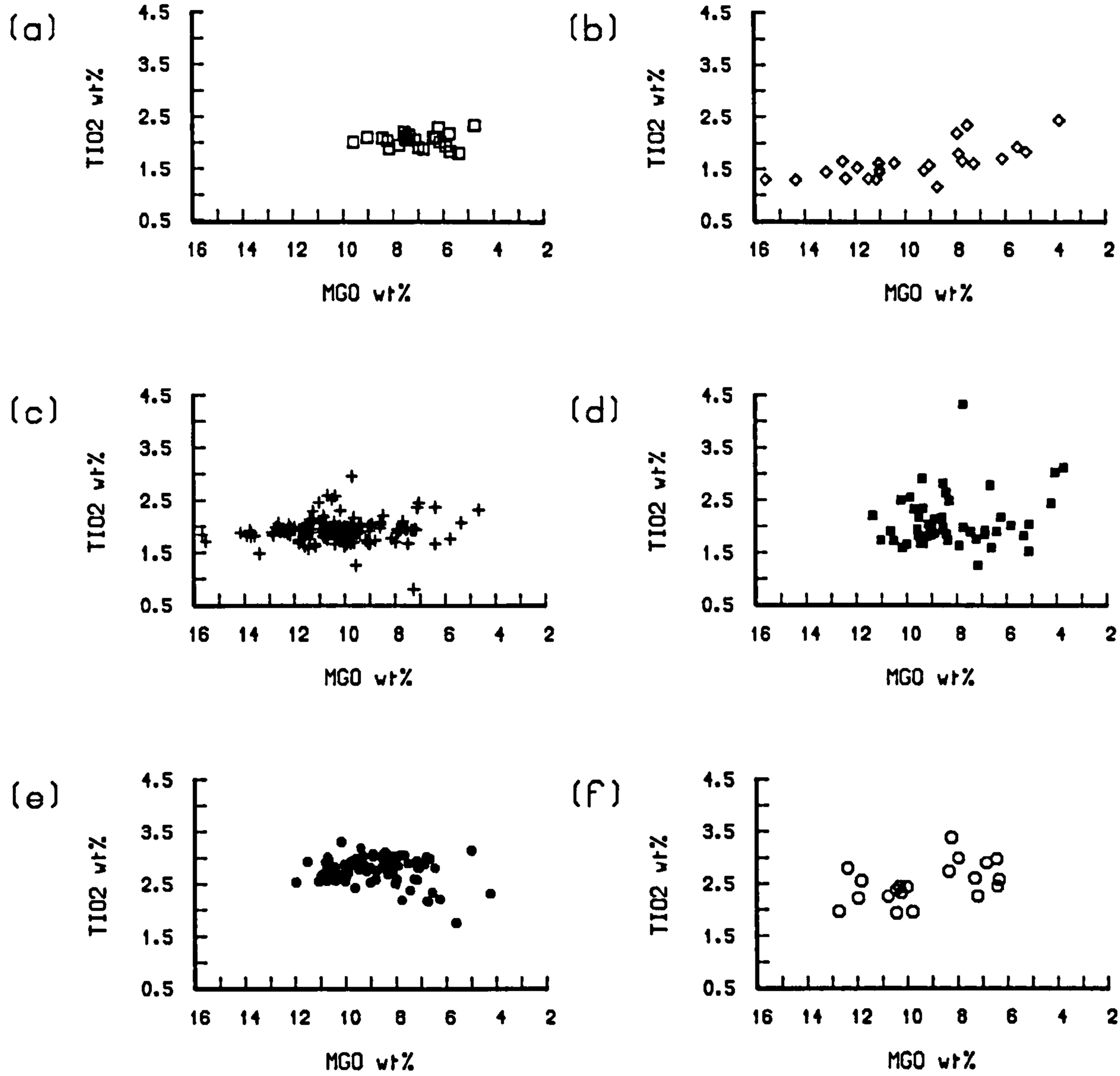

Fig.5.7 TiO_2 against MgO for all groups

(a) Passage Group lavas (b) Ayrshire Sills (c) Mauchline Group
(d) Fife & Lothian sills (e) Fife & Lothian basanites (f) Highland Dykes
(g) Quartz dolerites and (h) Basin & Range for comparison.

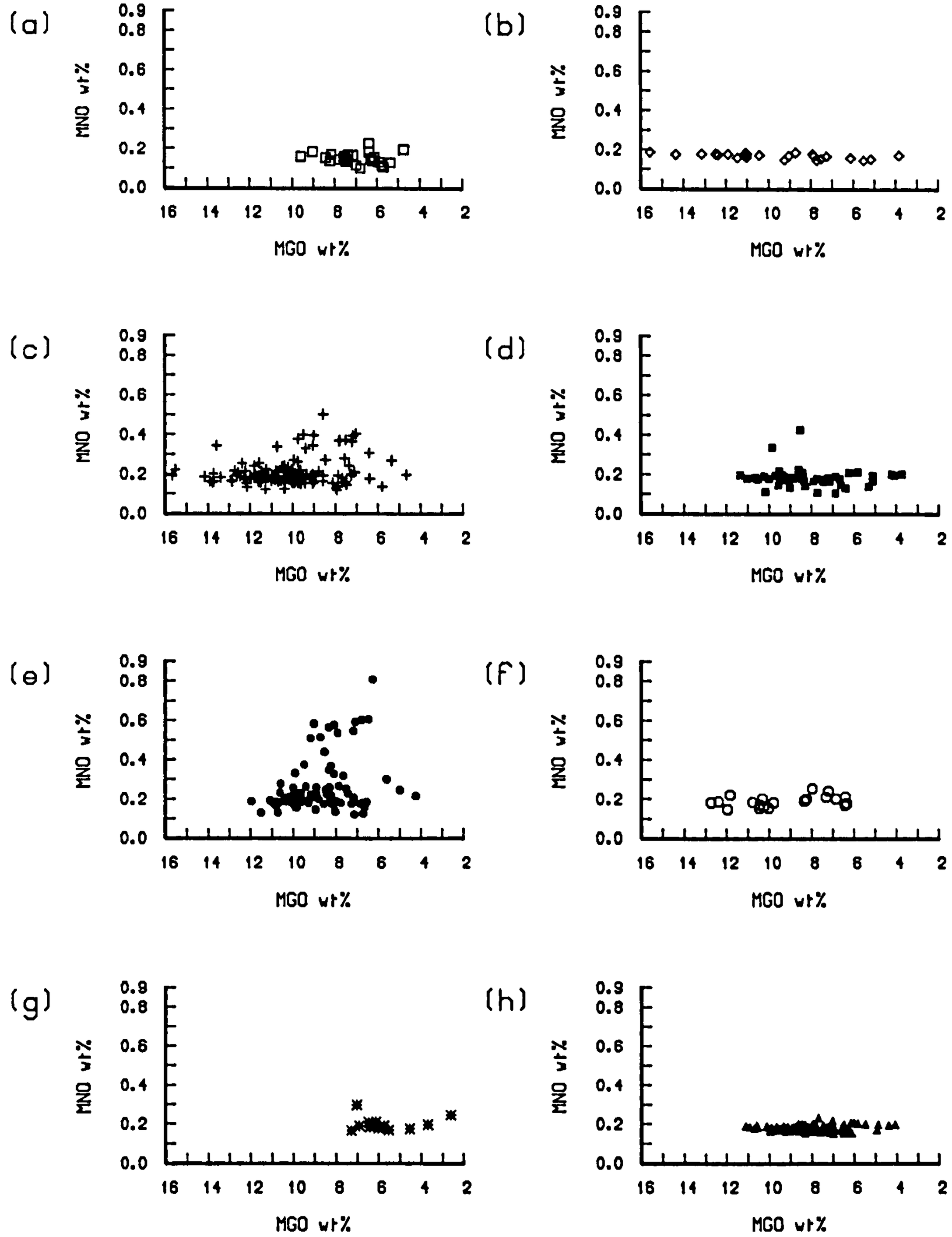

Fig.5.8 MnO against MgO for all groups

(a) Passage Group lavas (b) Ayrshire Sills (c) Mauchline Group
(d) Fife & Lothian sills (e) Fife & Lothian basanites (f) Highland Dykes
(g) Quartz dolerites and (h) Basin & Range for comparison.

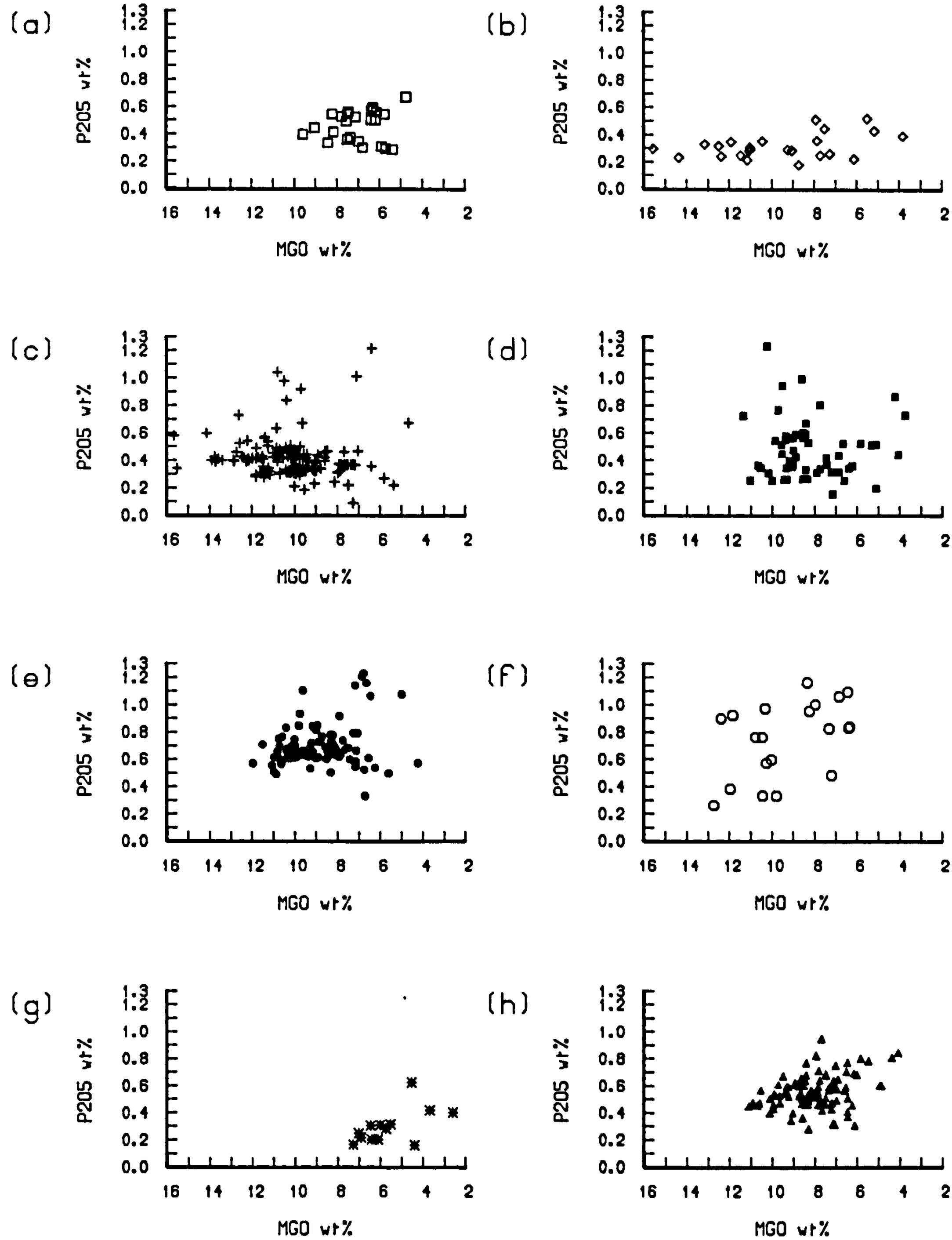

Fig.5.9 P_2O_5 against MgO for all groups

(a) Passage Group lavas (b) Ayrshire Sills (c) Mauchline Group
(d) Fife & Lothian sills (e) Fife & Lothian basanites (f) Highland Dykes
(g) Quartz dolerites and (h) Basin & Range for comparison.

	1	2	3	4	5	6	7
SiO_2	+	+	+	+	+		
Al_2O_3	+	+	+	+	+	+	+
Fe_2O_3	−	−		−	−		
CaO	+						−
Na_2O	+	+	+	+	+	+	+
K_2O					+		+
TiO_2	+					+	
Ni	−	−	−	−	−	−	−
Cr	+	−	−	−	−	−	−
V	+	+			−		
Sc	−				−	−	

Table 5.2 Summary of major and compatible trace element variations with decreasing MgO content for each group: (1) Passage Group lavas; (2) Ayrshire sills; (3) Mauchline group; (4) Fife & Lothian sills; (5) Fife & Lothian basanites; (6) Highland dykes; (7) Quartz dolerites.

5.2.2. Trace elements

Compatible trace element correlations with MgO for each group are also summarised in Table 5.2 and displayed in Figs. 5.10–5.24. Again, the best element–MgO correlations are provided by the Ayrshire sills. The plots indicate a marked decrease in Ni concentrations with decreasing MgO content (Fig. 5.10) for all groups. The same is true for Cr (Fig. 5.11) in all but the Passage Group lavas, where element concentrations increase with fractionation. V concentrations (Fig. 5.12) are buffered in the Mauchline Group, Fife & Lothian sill, Highland Dyke and quartz dolerite samples. However the Passage Group lavas and Ayrshire sills display trends of increasing V with fractionation, and for the Fife & Lothian basanites the reverse is true. Sc concentrations (Fig. 5.13) appear to be buffered for the Mauchline Group and the Ayrshire and Fife & Lothian sills. They increase with fractionation in the Passage Group lavas, and decrease in the Fife & Lothian basanites and Highland dykes. Those elements incompatible with phenocryst phases (Sr, Rb, Zr, Nb, Ba, Ce, Nd and Y) display a range of concentrations for given MgO content. However broad trends of increasing concentration with decreasing MgO content are evident.

5.2.3. Discussion

Trace element trends appear consistent with fractional crystallisation processes. Decreasing Ni concentrations indicate partitioning of this element into olivine, and Cr and Sc variations show evidence of partitioning into clinopyroxene. The apparent lack of correlation between Cr and MgO, and the negative correlation between Sc and MgO in the Passage Group lavas confirms the petrographic observation that clinopyroxene was generally a minor fractionating phase in these lavas.

V appears to be compatible only in the Fife & Lothian basanites. If this is indicative of Fe–Ti oxide fractionation (not observed petrographically) then a similar correlation between Ti and MgO would be expected. This is not apparent. Increasing concentrations of Al_2O_3 with decreasing MgO in all groups is probably a reflection of ol$^{+}_{-}$cpx crystallisation, leaving a residual magma more enriched in Al_2O_3.

Decreasing Fe_2O_{3tot} with decreasing MgO (Passage Group lavas, Ayrshire sills, Fife & Lothian samples) would normally be attributed to crystallisation of titanomagnetite. However, this is not indicated in TiO_2 trends which are

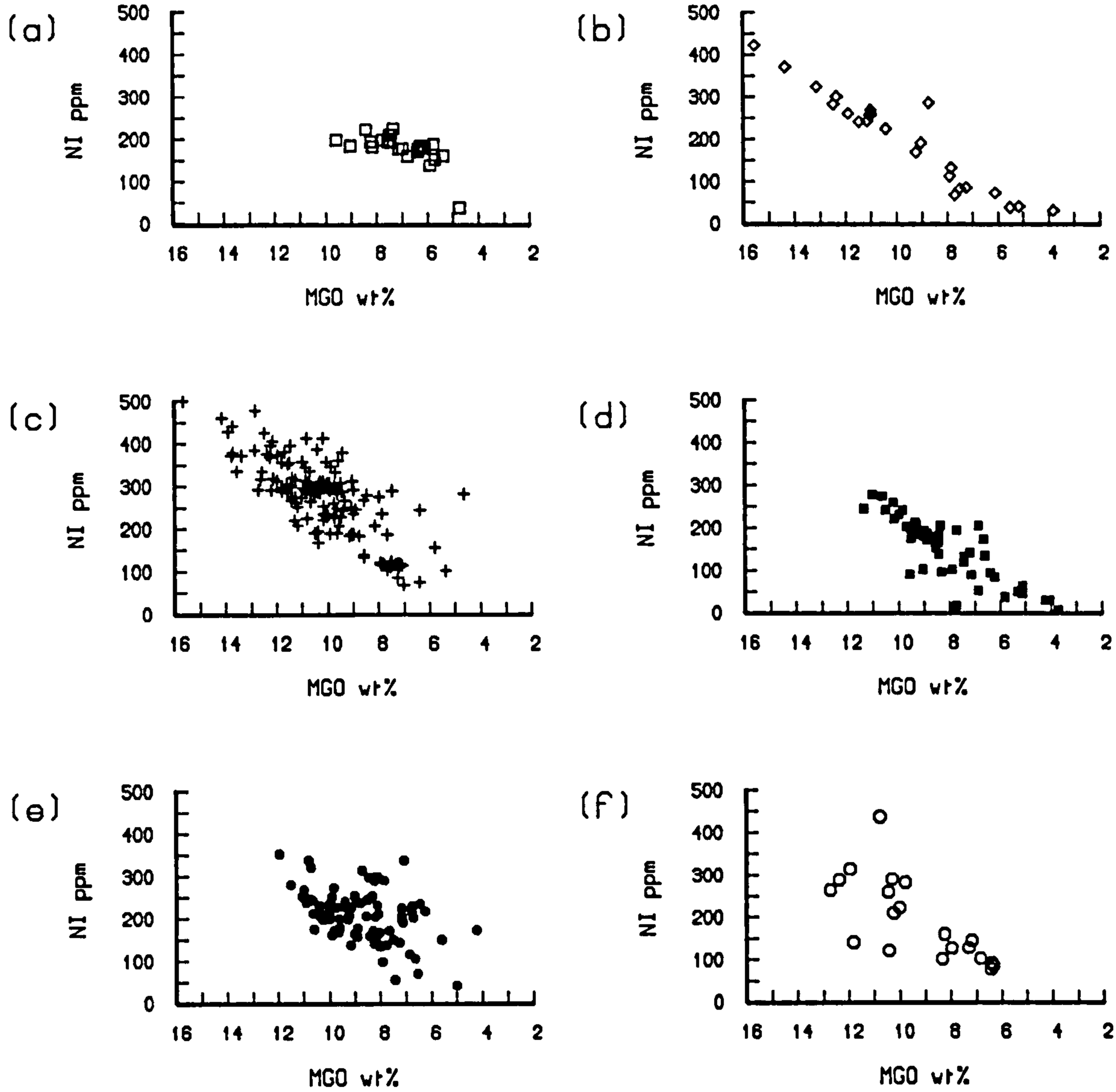

Fig.5.10 NI against MgO for all groups

(a) Passage Group lavas (b) Ayrshire Sills (c) Mauchline Group
(d) Fife & Lothian sills (e) Fife & Lothian basanites (f) Highland Dykes
(g) Quartz dolerites and (h) Basin & Range for comparison.

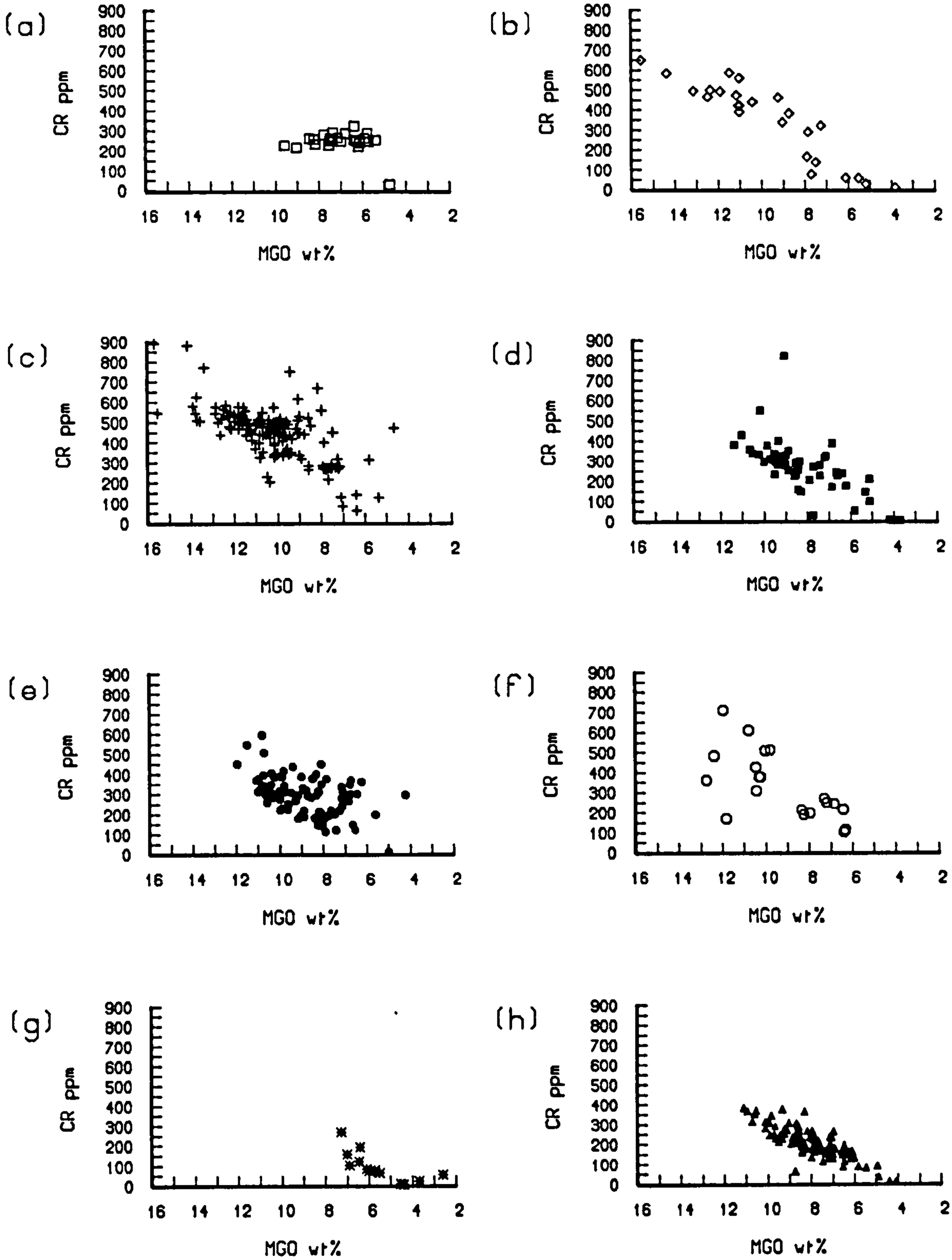

Fig.5.11 Cr against MgO for all groups

(a) Passage Group lavas (b) Ayrshire Sills (c) Mauchline Group
(d) Fife & Lothian sills (e) Fife & Lothian basanites (f) Highland Dykes
(g) Quartz dolerites and (h) Basin & Range for comparison.

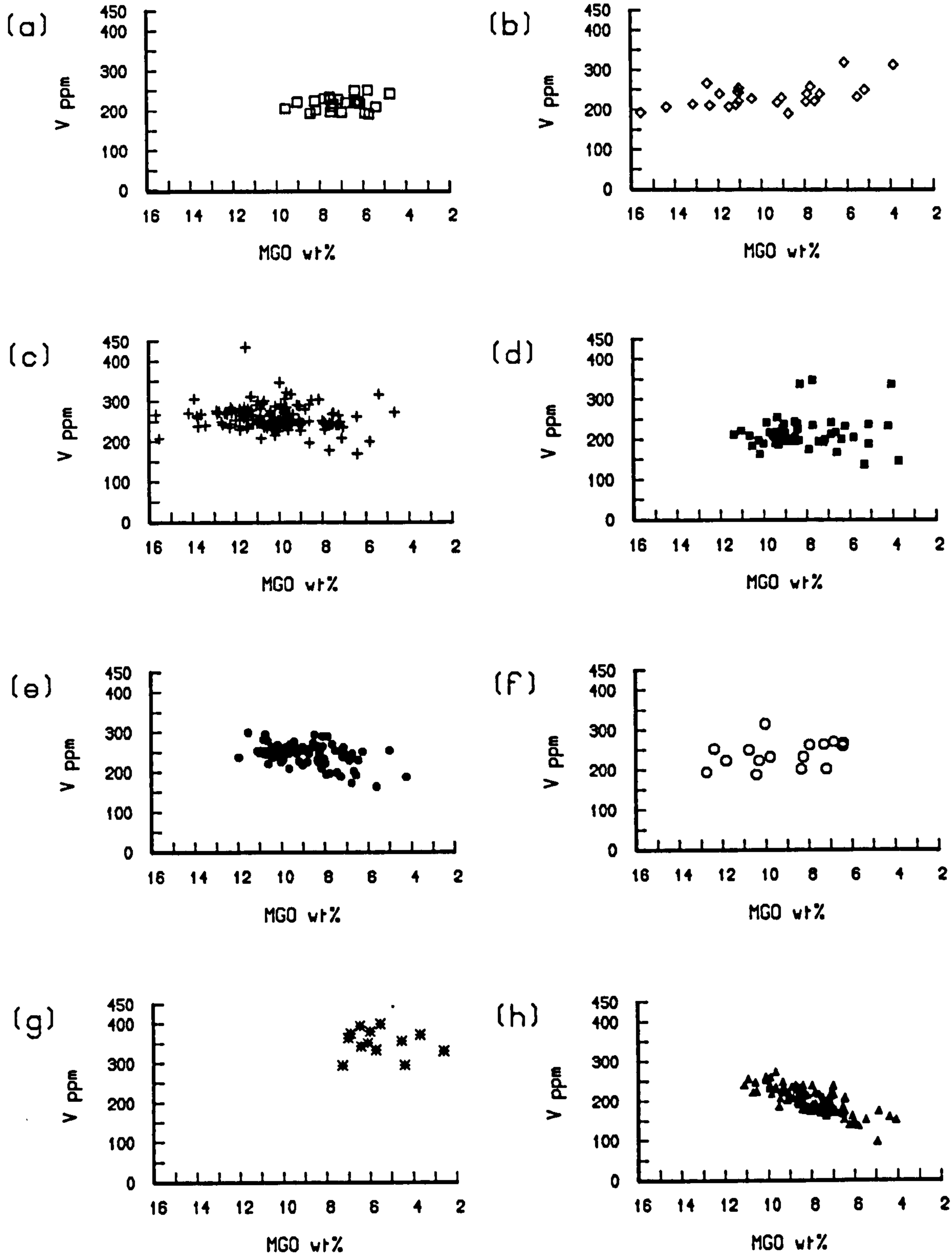

Fig.5.12 V against MgO for all groups

(a) Passage Group lavas (b) Ayrshire Sills (c) Mauchline Group
(d) Fife & Lothian sills (e) Fife & Lothian basanites (f) Highland Dykes
(g) Quartz dolerites and (h) Basin & Range for comparison.

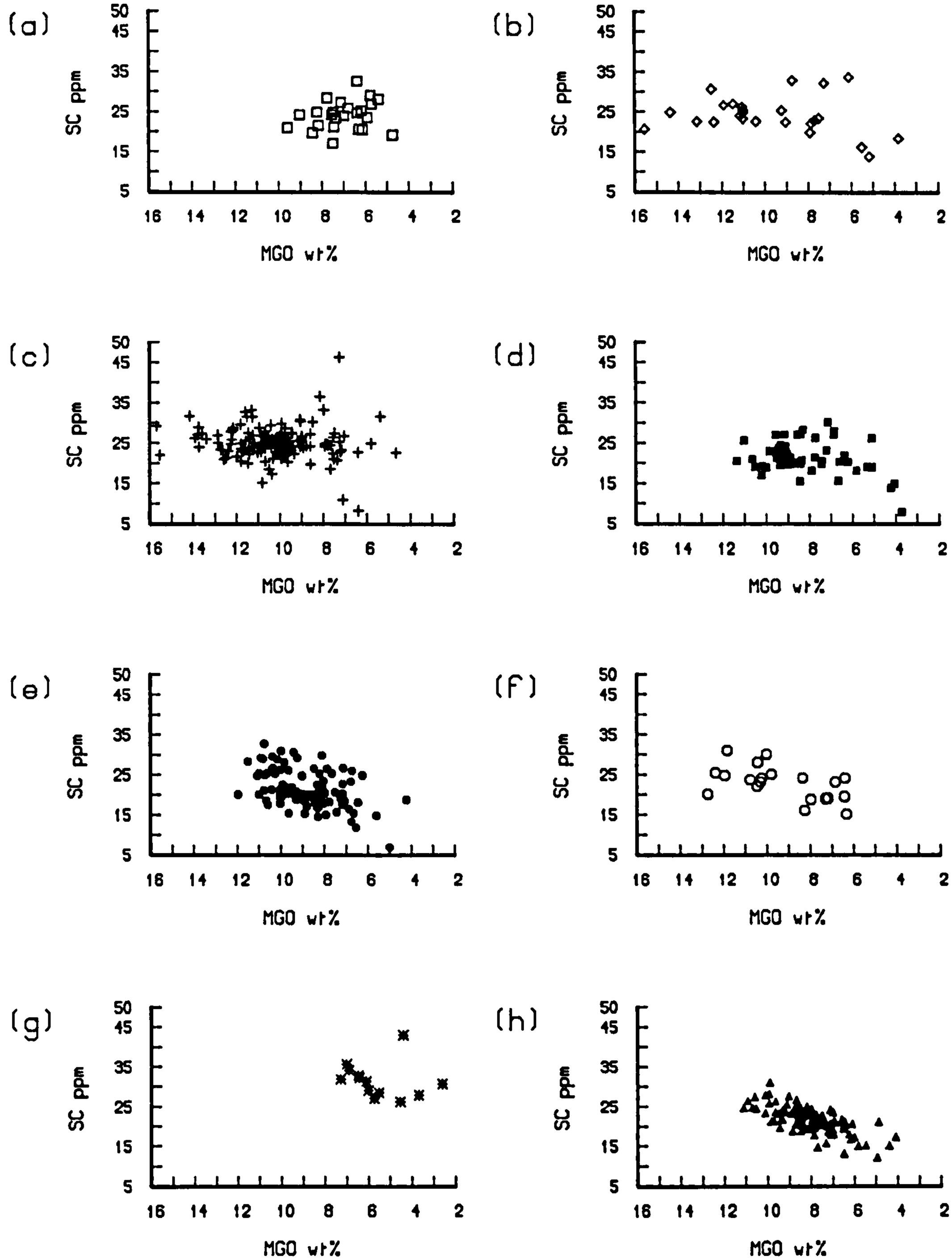

Fig.5.13 Sc against MgO for all groups

(a) Passage Group lavas (b) Ayrshire Sills (c) Mauchline Group
(d) Fife & Lothian sills (e) Fife & Lothian basanites (f) Highland Dykes
(g) Quartz dolerites and (h) Basin & Range for comparison.

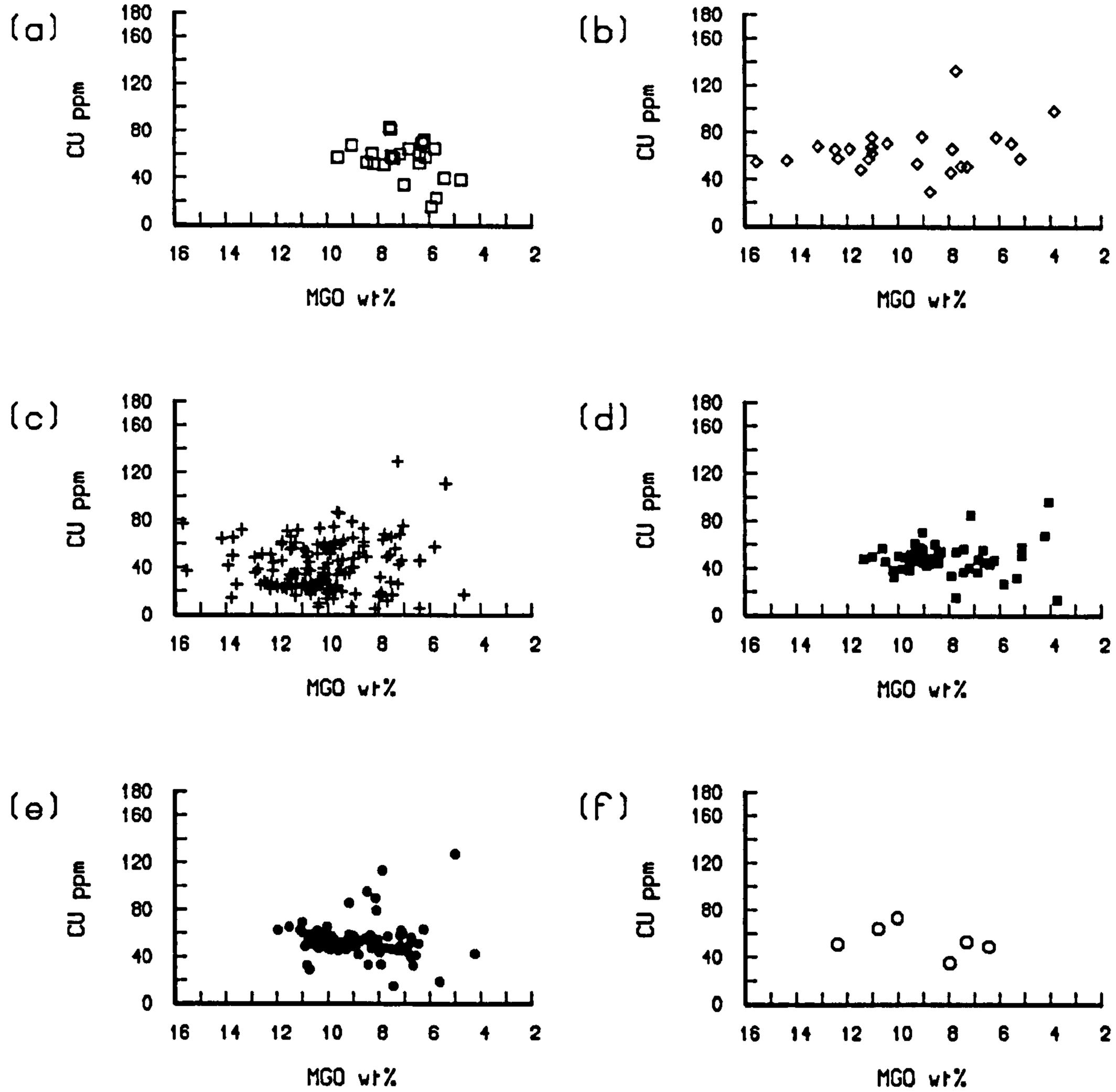

Fig.5.14 Cu against MgO for all groups

(a) Passage Group lavas (b) Ayrshire Sills (c) Mauchline Group
(d) Fife & Lothian sills (e) Fife & Lothian basanites (f) Highland Dykes
(g) Quartz dolerites and (h) Basin & Range for comparison.

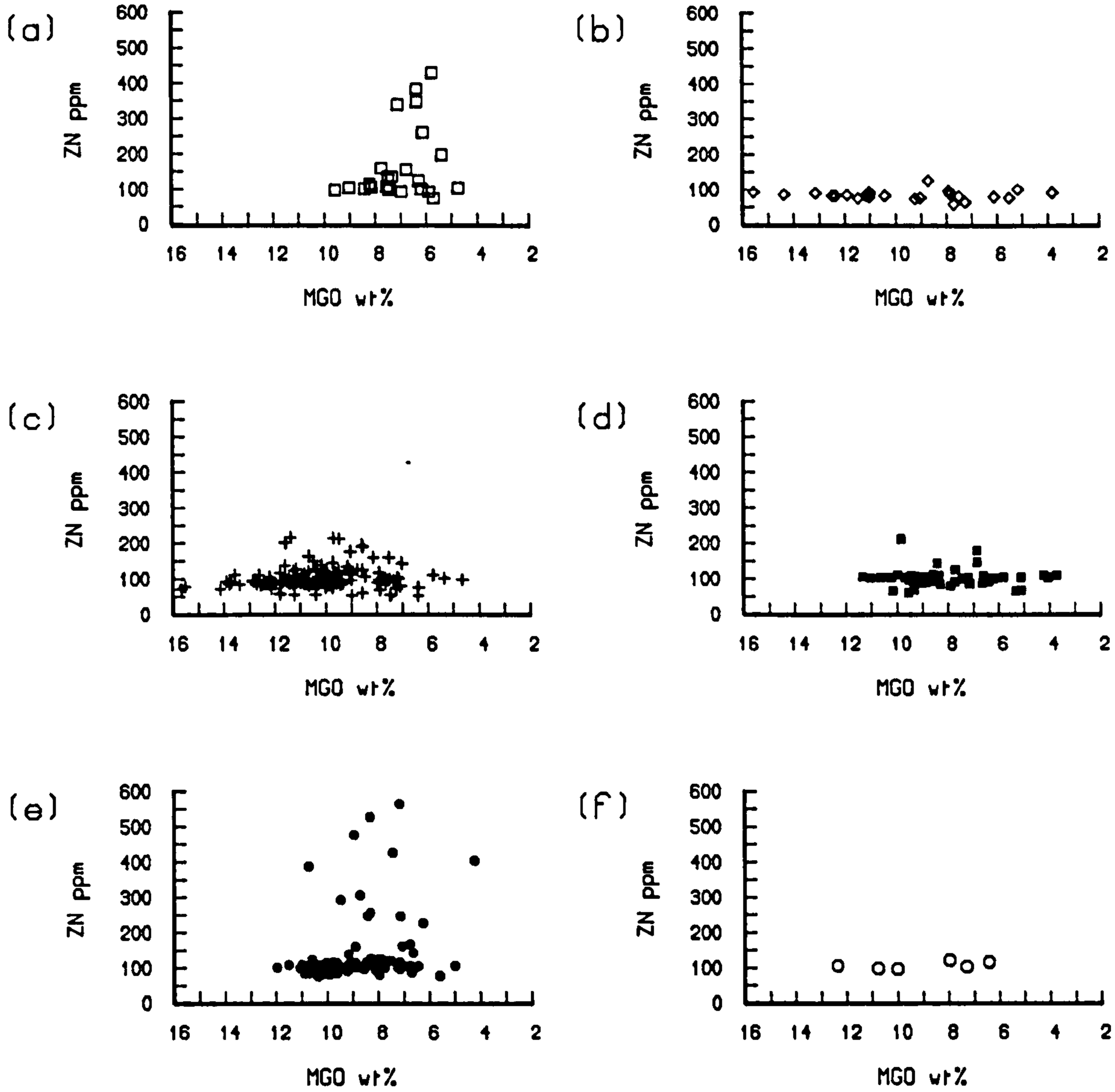

Fig.5.15 Zn against MgO for all groups

(a) Passage Group lavas (b) Ayrshire Sills (c) Mauchline Group
(d) Fife & Lothian sills (e) Fife & Lothian basanites (f) Highland Dykes
(g) Quartz dolerites and (h) Basin & Range for comparison.

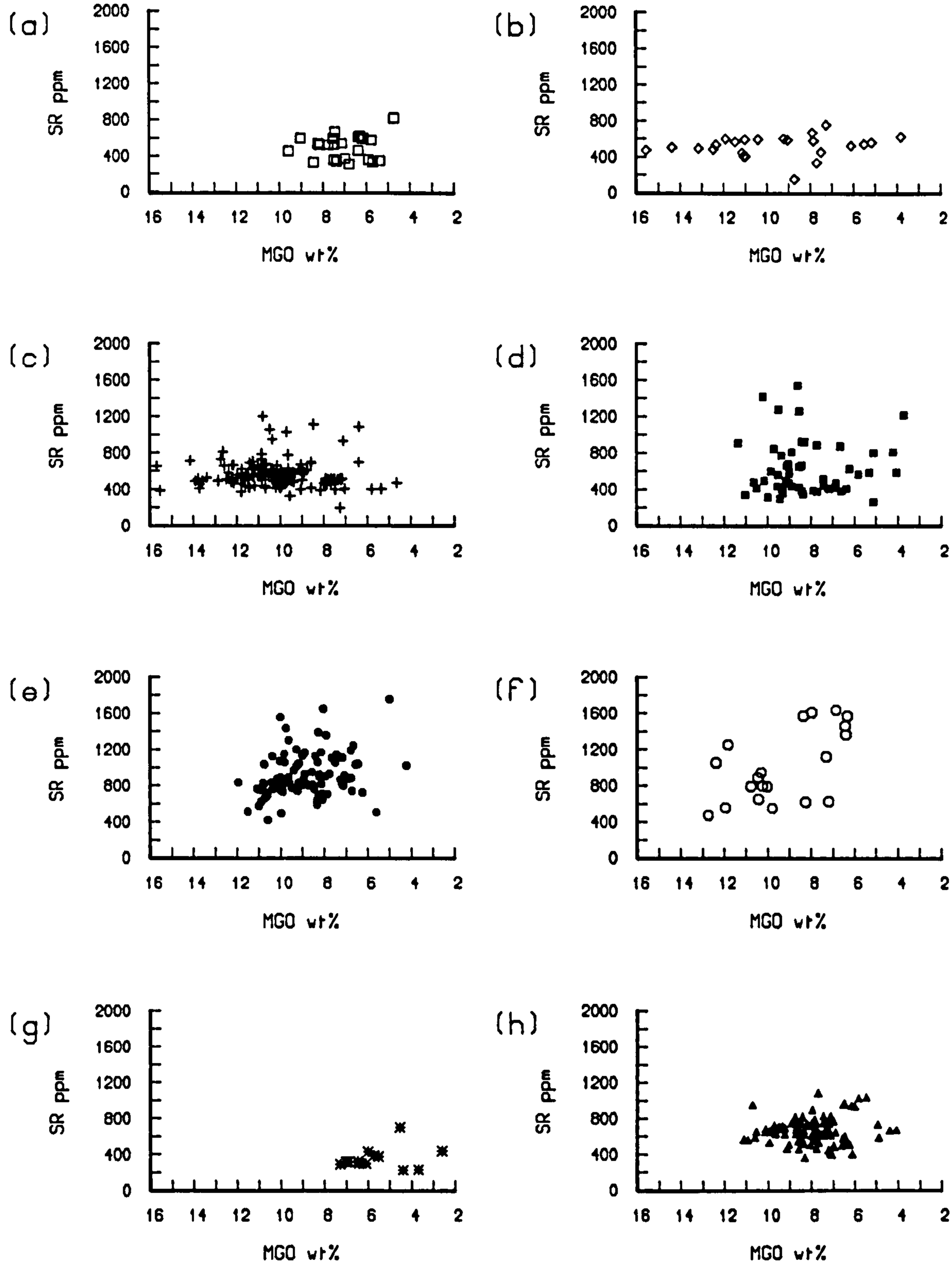

Fig.5.16 Sr against MgO for all groups

(a) Passage Group lavas (b) Ayrshire Sills (c) Mauchline Group
(d) Fife & Lothian sills (e) Fife & Lothian basanites (f) Highland Dykes
(g) Quartz dolerites and (h) Basin & Range for comparison.

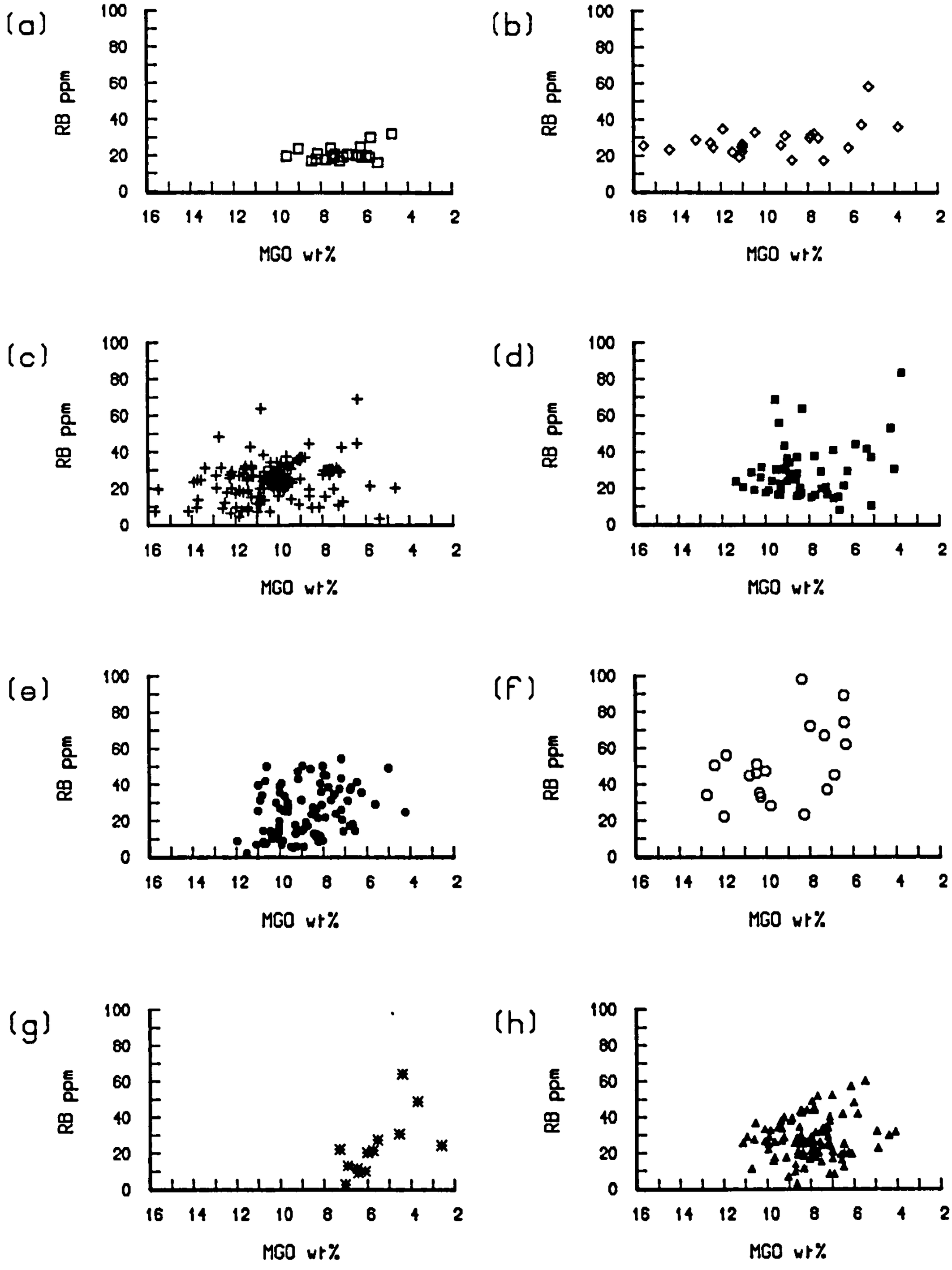

Fig.5.17 Rb against MgO for all groups

(a) Passage Group lavas (b) Ayrshire Sills (c) Mauchline Group
(d) Fife & Lothian sills (e) Fife & Lothian basanites (f) Highland Dykes
(g) Quartz dolerites and (h) Basin & Range for comparison.

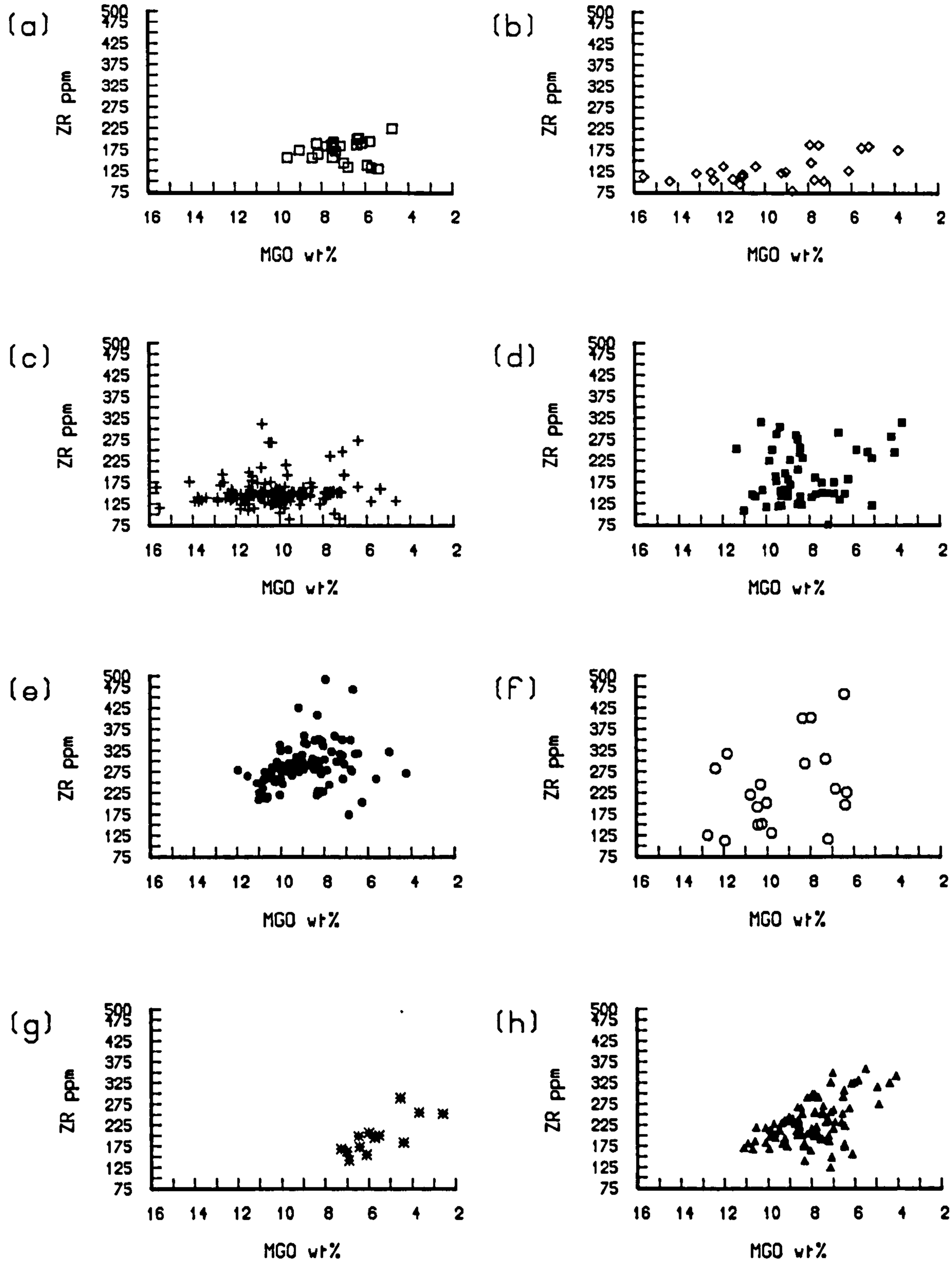

Fig.5.18 Zr against MgO for all groups

(a) Passage Group lavas (b) Ayrshire Sills (c) Mauchline Group
(d) Fife & Lothian sills (e) Fife & Lothian basanites (f) Highland Dykes
(g) Quartz dolerites and (h) Basin & Range for comparison.

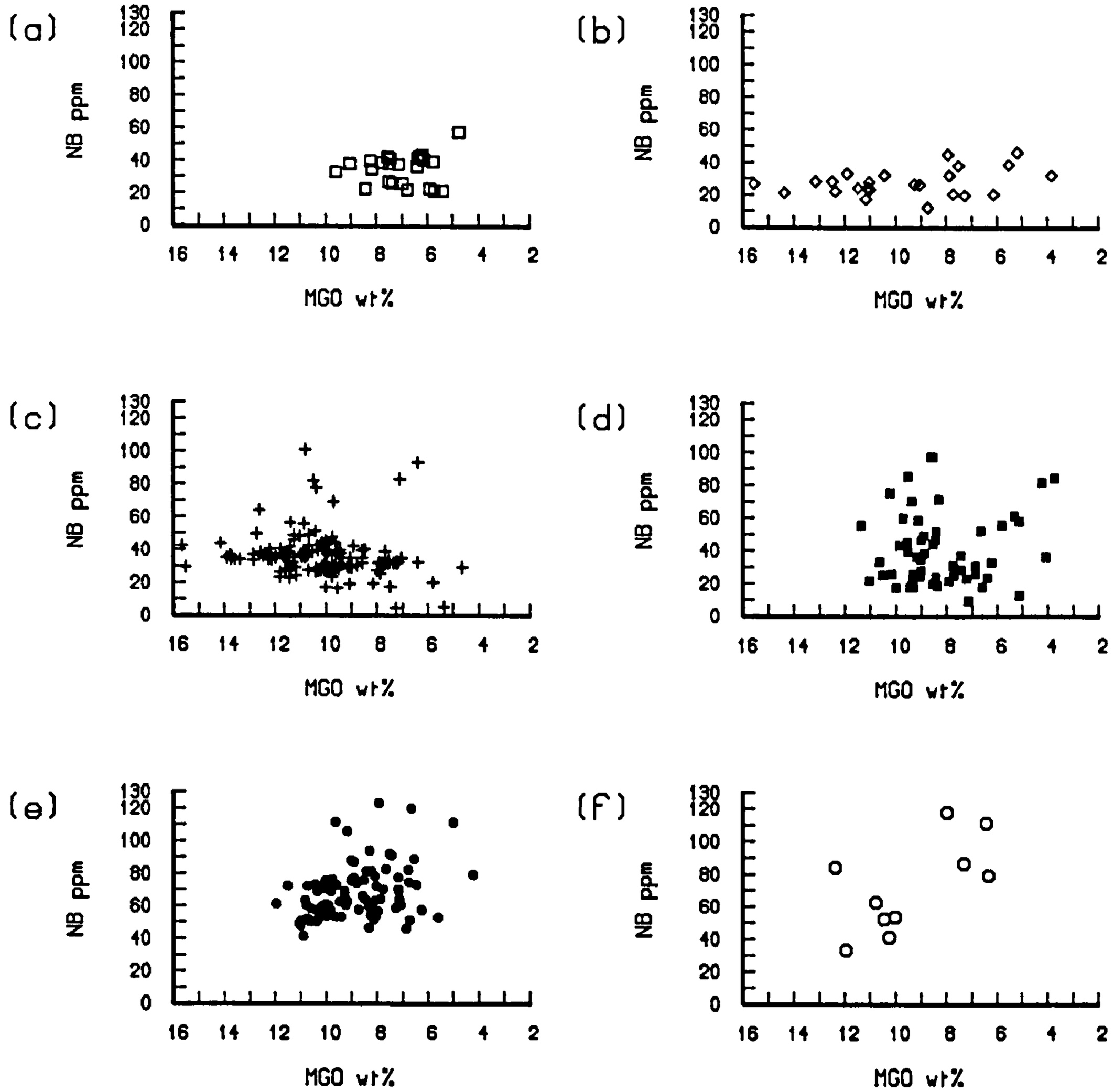

Fig.5.19 Nb against MgO for all groups

(a) Passage Group lavas (b) Ayrshire Sills (c) Mauchline Group
(d) Fife & Lothian sills (e) Fife & Lothian basanites (f) Highland Dykes
(g) Quartz dolerites and (h) Basin & Range for comparison.

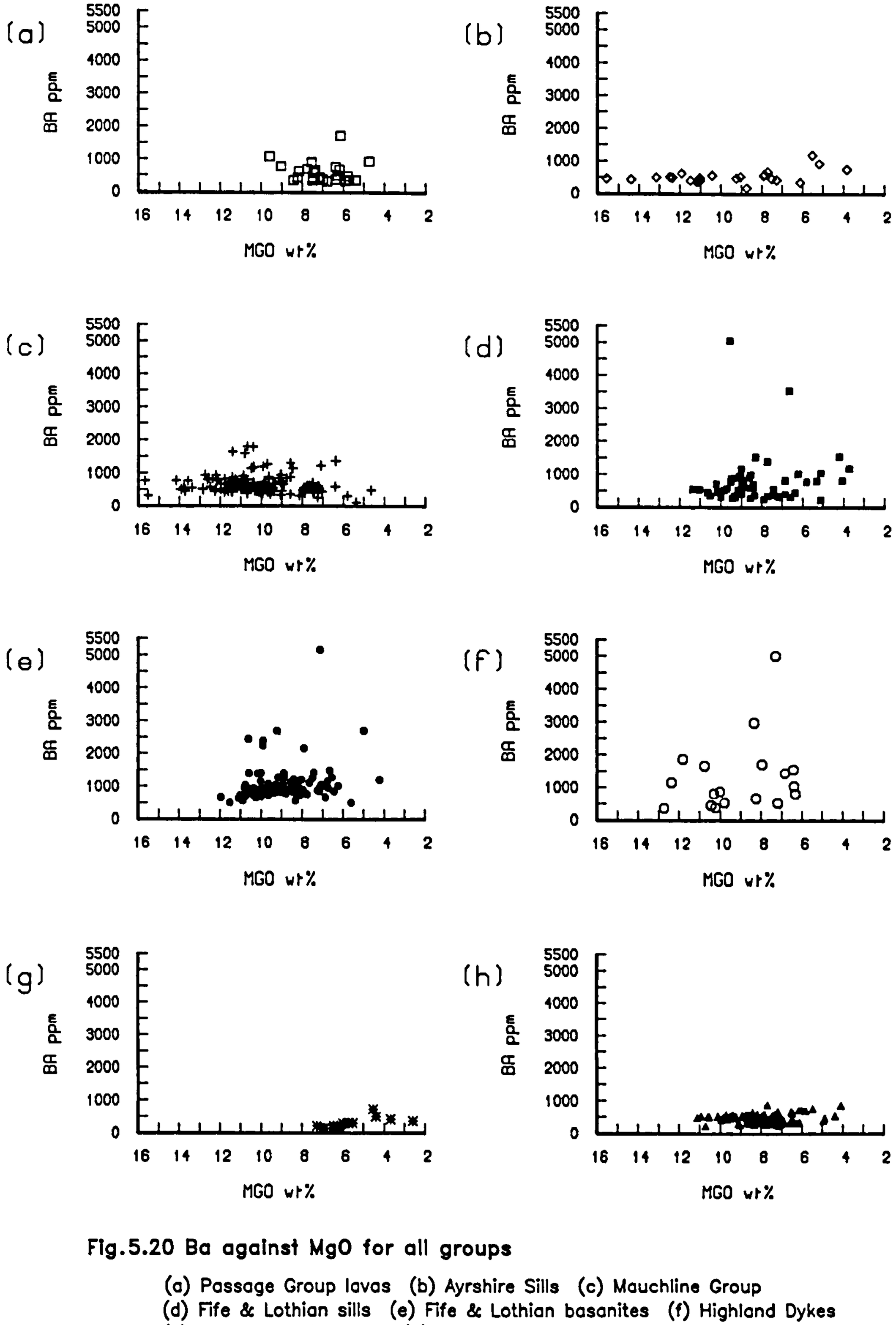

Fig.5.20 Ba against MgO for all groups

(a) Passage Group lavas (b) Ayrshire Sills (c) Mauchline Group
(d) Fife & Lothian sills (e) Fife & Lothian basanites (f) Highland Dykes
(g) Quartz dolerites and (h) Basin & Range for comparison.

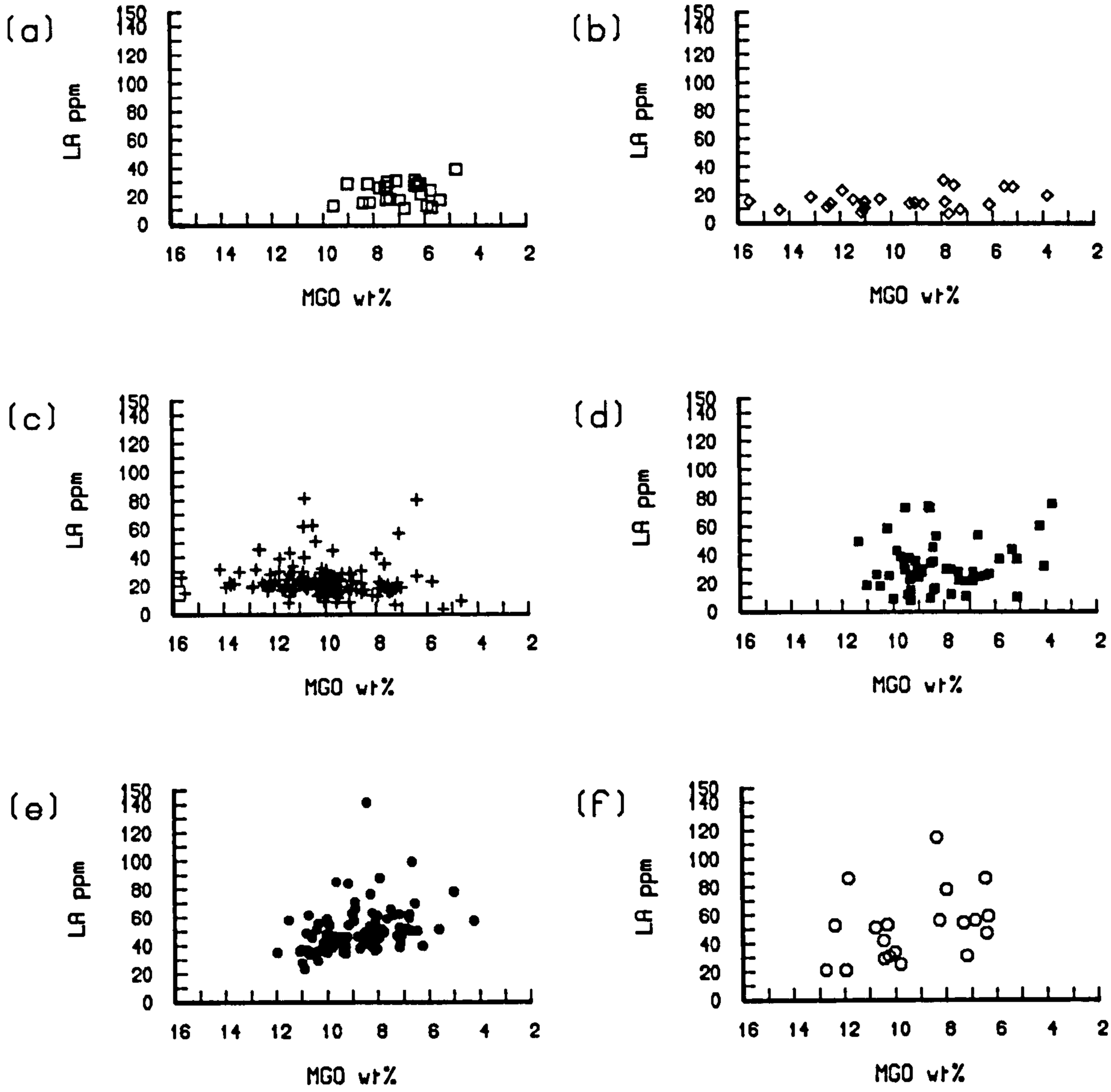

Fig.5.21 La against MgO for all groups

(a) Passage Group lavas (b) Ayrshire Sills (c) Mauchline Group
(d) Fife & Lothian sills (e) Fife & Lothian basanites (f) Highland Dykes
(g) Quartz dolerites and (h) Basin & Range for comparison.

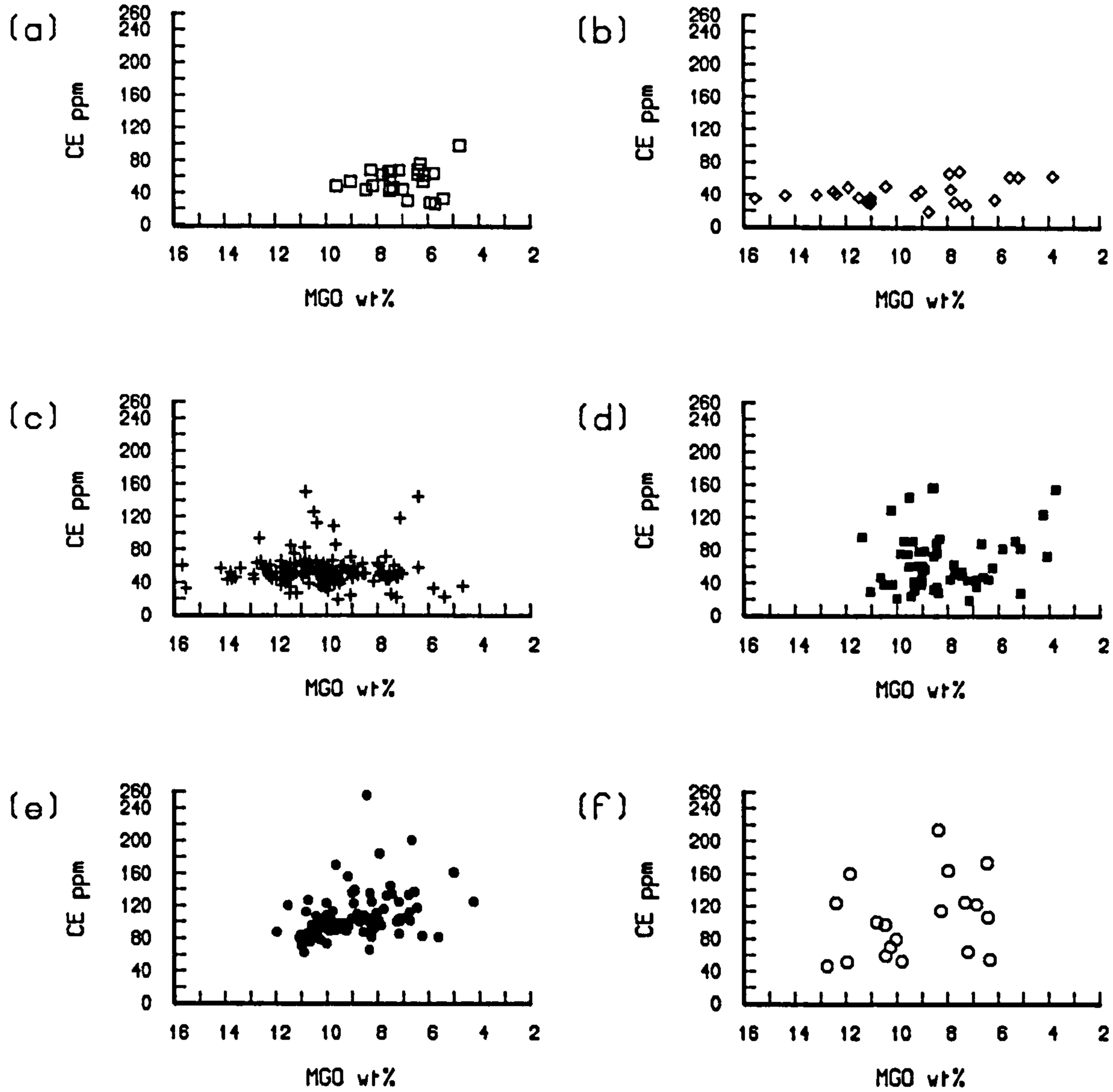

Fig.5.22 Ce against MgO for all groups

(a) Passage Group lavas (b) Ayrshire Sills (c) Mauchline Group
(d) Fife & Lothian sills (e) Fife & Lothian basanites (f) Highland Dykes
(g) Quartz dolerites and (h) Basin & Range for comparison.

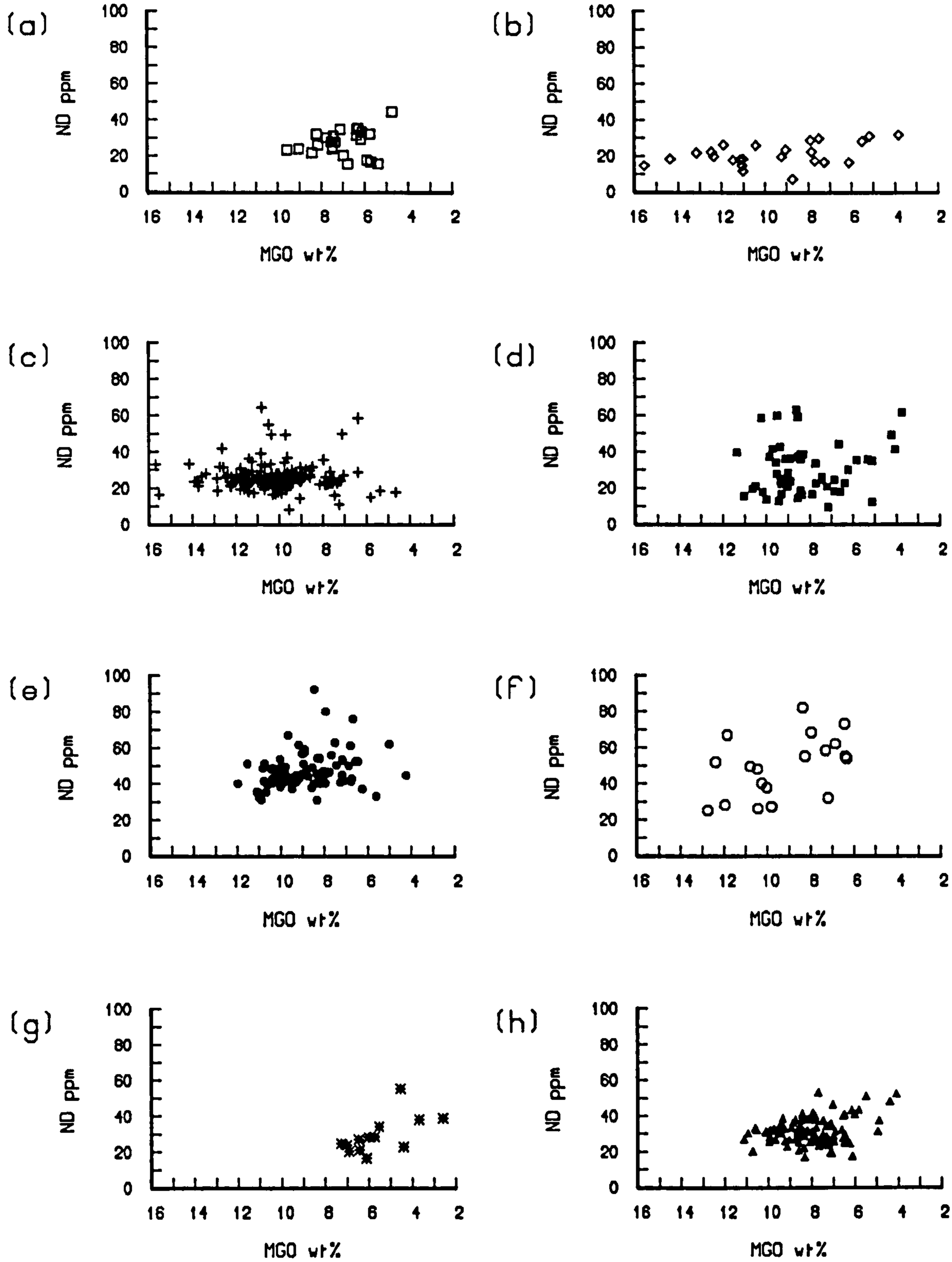

Fig.5.23 Nd against MgO for all groups

(a) Passage Group lavas (b) Ayrshire Sills (c) Mauchline Group
(d) Fife & Lothian sills (e) Fife & Lothian basanites (f) Highland Dykes
(g) Quartz dolerites and (h) Basin & Range for comparison.

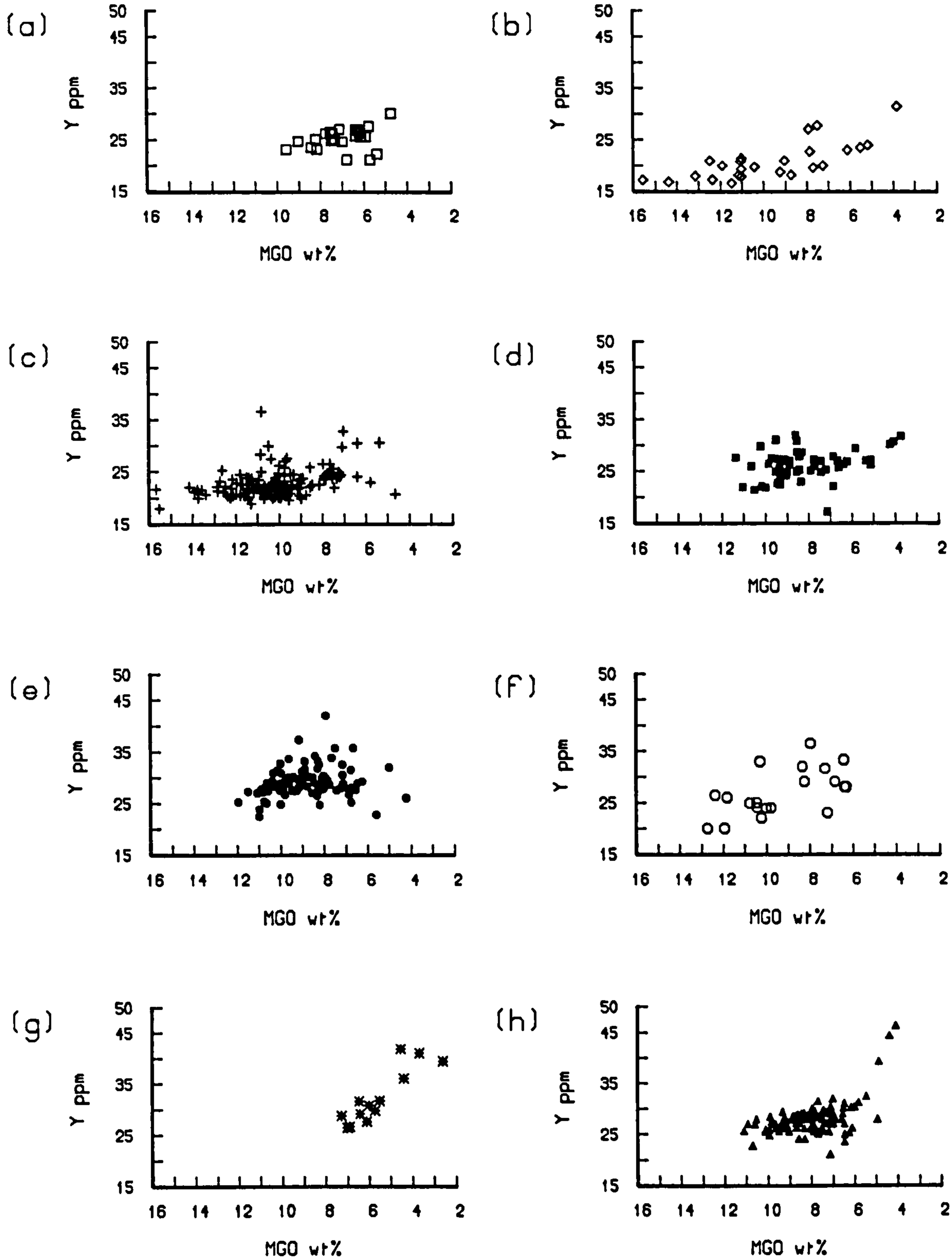

Fig.5.24 Y against MgO for all groups

(a) Passage Group lavas (b) Ayrshire Sills (c) Mauchline Group
(d) Fife & Lothian sills (e) Fife & Lothian basanites (f) Highland Dykes
(g) Quartz dolerites and (h) Basin & Range for comparison.

buffered or increase with differentiation. Fe_2O_{3tot} variations may be attributed to fractionation of more Fe-rich olivine in basaltic hawaiites and hawaiites (Smedley, 1986b) or they possibly represent multiple liquid lines of descent.

Examination of incompatible element concentrations in each of the groups allows the identification of two broad geochemical groups for post-Dinantian igneous rocks of the Midland Valley: a less and a more enriched group. The first (Group A) comprises most of the Mauchline lavas, all of the Passage Group lavas and Ayrshire sills, and approximately half of the Fife & Lothian sills. The second (Group B) comprises the Fife & Lothian basanites, most of the Highland dykes, the remaining Fife & Lothian sills and a handfull of the Mauchline group samples. Rough boundaries between the two groups for each of the incompatible elements under consideration are given by: P_2O_5=0.5wt%, Zr=200ppm, Nb=45ppm La=35ppm, Ce=70ppm, Nd=30ppm, Y=25ppm. The division is also reflected in Sr (Group A < 600ppm, Group B > 600ppm) and to a lesser extent by TiO_2.

5.3. Classification

The majority of the rocks under study (c. 75%) are fine-grained and many have glassy groundmasses. This makes classification on the basis of modal mineralogy difficult, so chemical classification schemes have been adopted. For the sake of consistency, the coarser-grained rocks have been classified on the same basis.

The Ti-Zr-Y discrimination diagram of Pearce & Cann (1973) (Fig. 5.25) confirms the within-plate origin of the post-Dinantian samples. Plots of P_2O_5 v Zr and Nb/Y v Zr/P_2O_5 (Figs. 5.26a,b; Floyd & Winchester, 1975) show the alkali basaltic characteristics of all but the quartz dolerites. The tholeiitic nature of these latter samples is obvious.

The predominently ne-normative character of the suite as a whole is highlighted in Fig. 5.29. 'Q' is normative quartz + quartz in hypersthene, and is given by:

$$'Q' = (hy/\text{mol wt hy}) \times 0.5 \text{ mol wt qz} + qz$$

where mol wt hy approximates as: 0.5(mol wt en + mol wt fs). The line ne=0

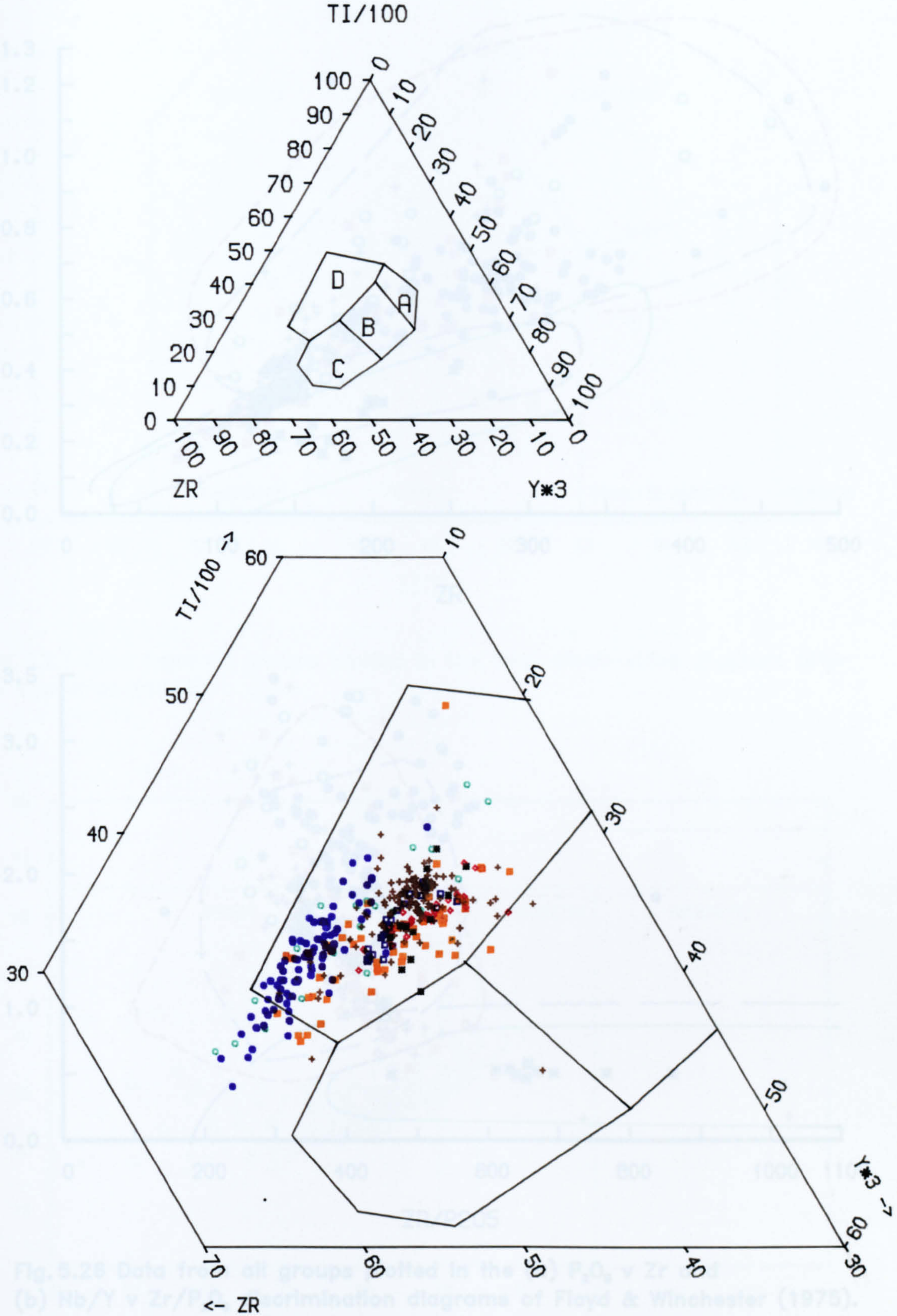

Fig. 5.25 Data from all groups plotted in the Ti–Zr–Y discrimination diagram of Pearce & Cann (1973).

Field A – Low potassium tholeiites; B– low potassium tholeiites & calc–alkaline basalts; C– calc–alkaline basalts; D– Oceanic and continental within–plate basalts.

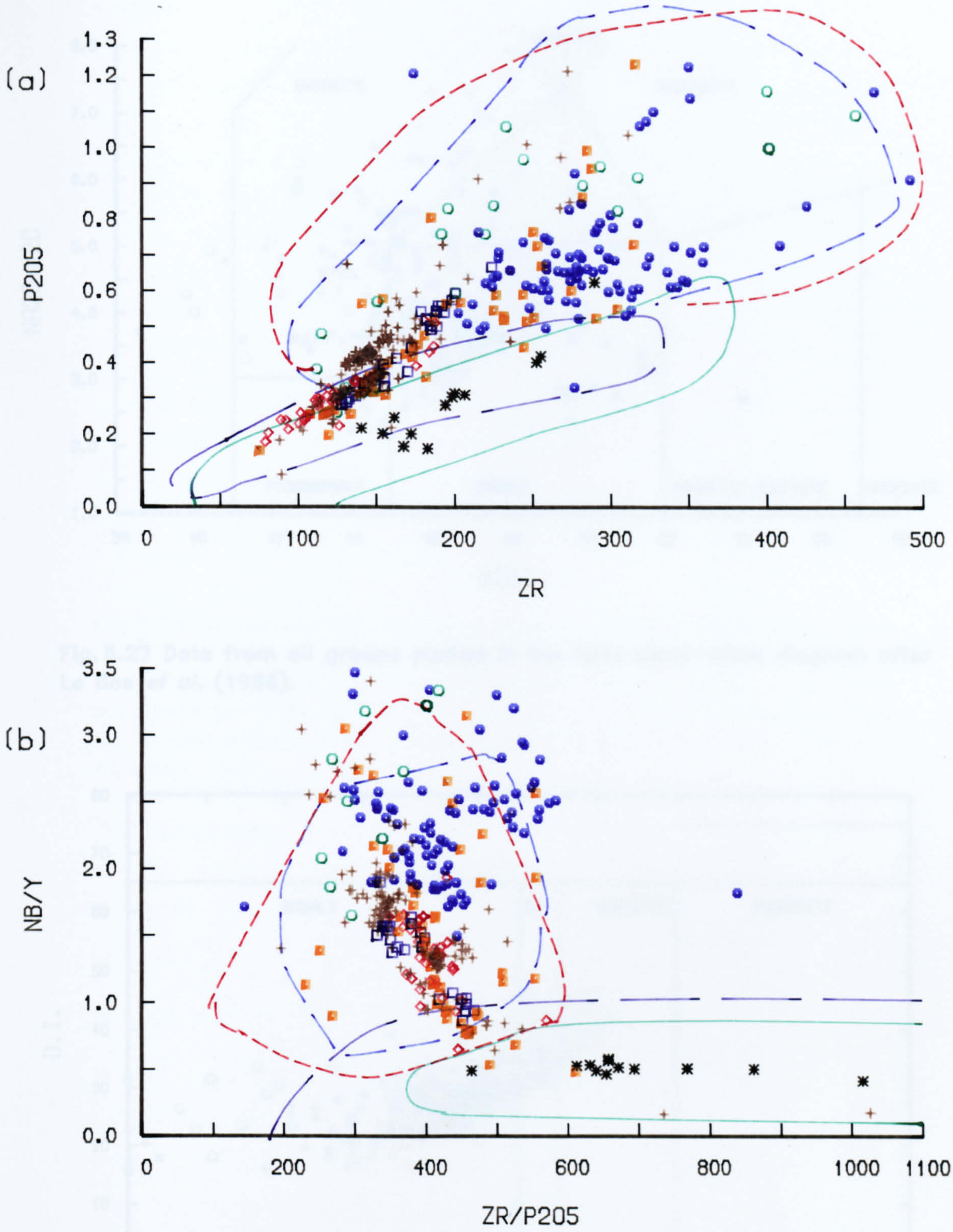

Fig. 5.26 Data from all groups plotted in the (a) P_2O_5 v Zr and (b) Nb/Y v Zr/P_2O_5 discrimination diagrams of Floyd & Winchester (1975).

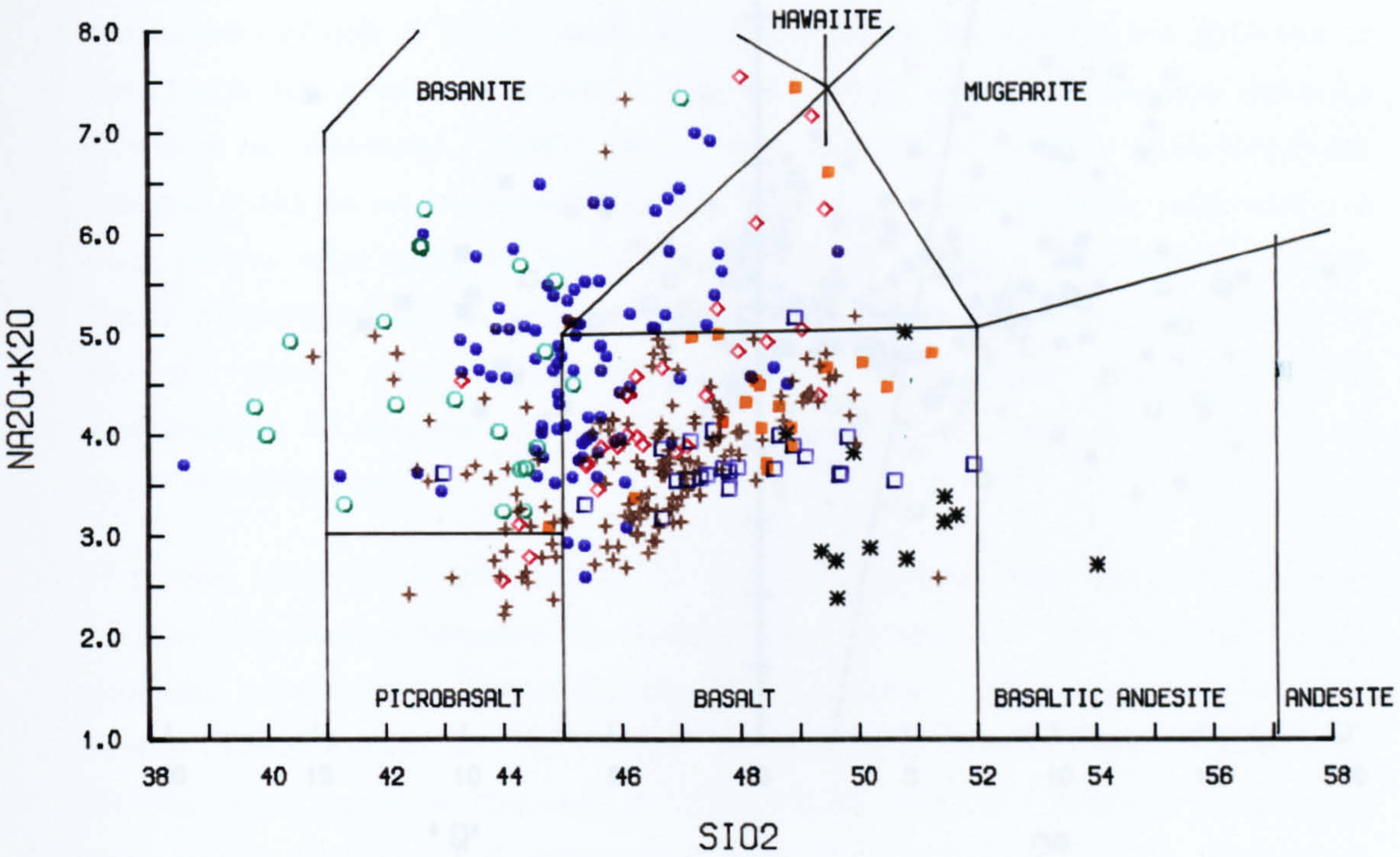

Fig. 5.27 Data from all groups plotted in the total alkali–silica diagram after Le Bas *et al.* (1986).

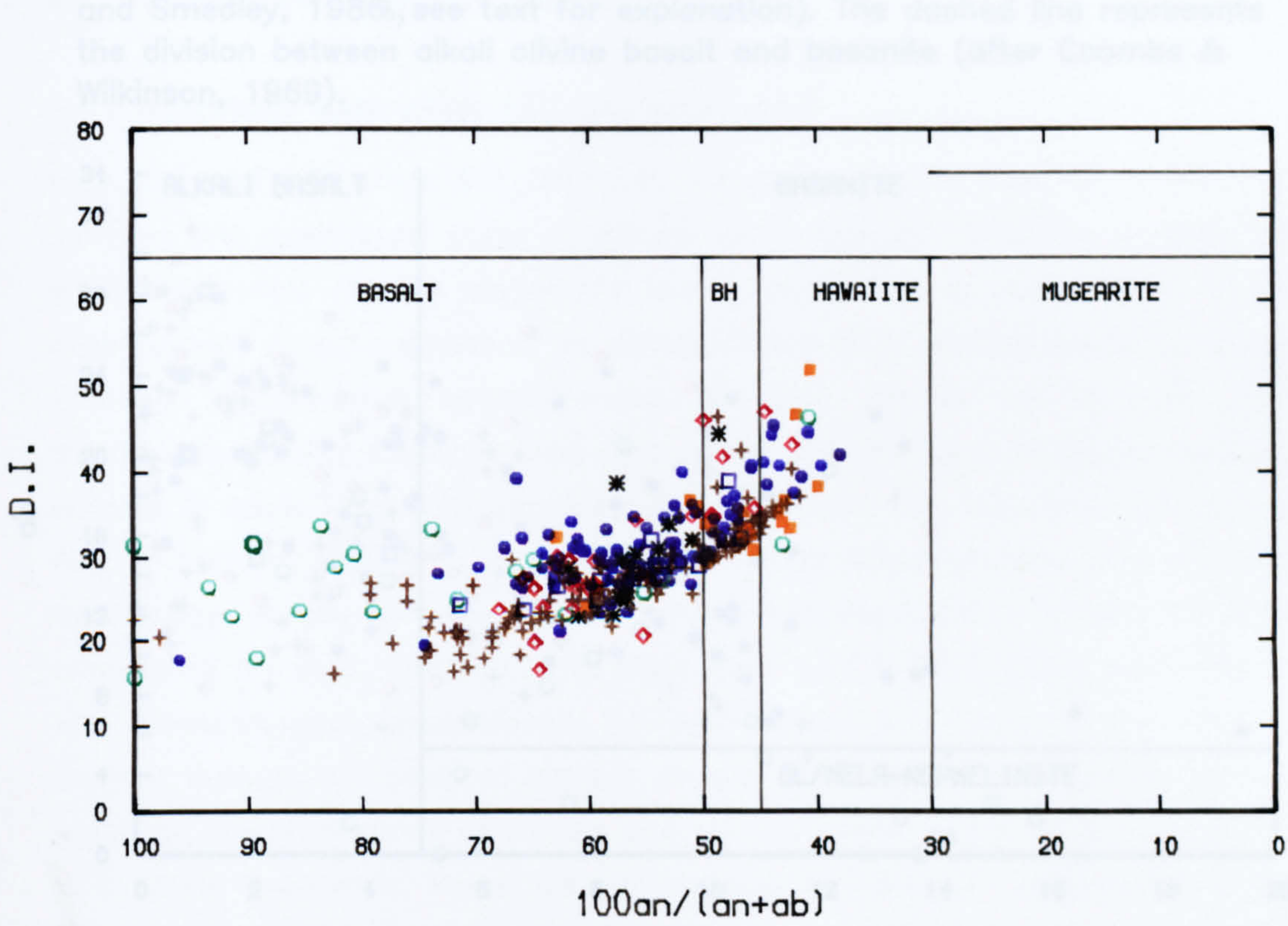

Fig. 5.28 Normative plagioclase composition (100an/(an+ab)) plotted against differentiation index (D.I.) for all groups.
Classification scheme after Thornton & Tuttle (1960), Coombs & Wilkinson (1969) and Macdonald (1975).

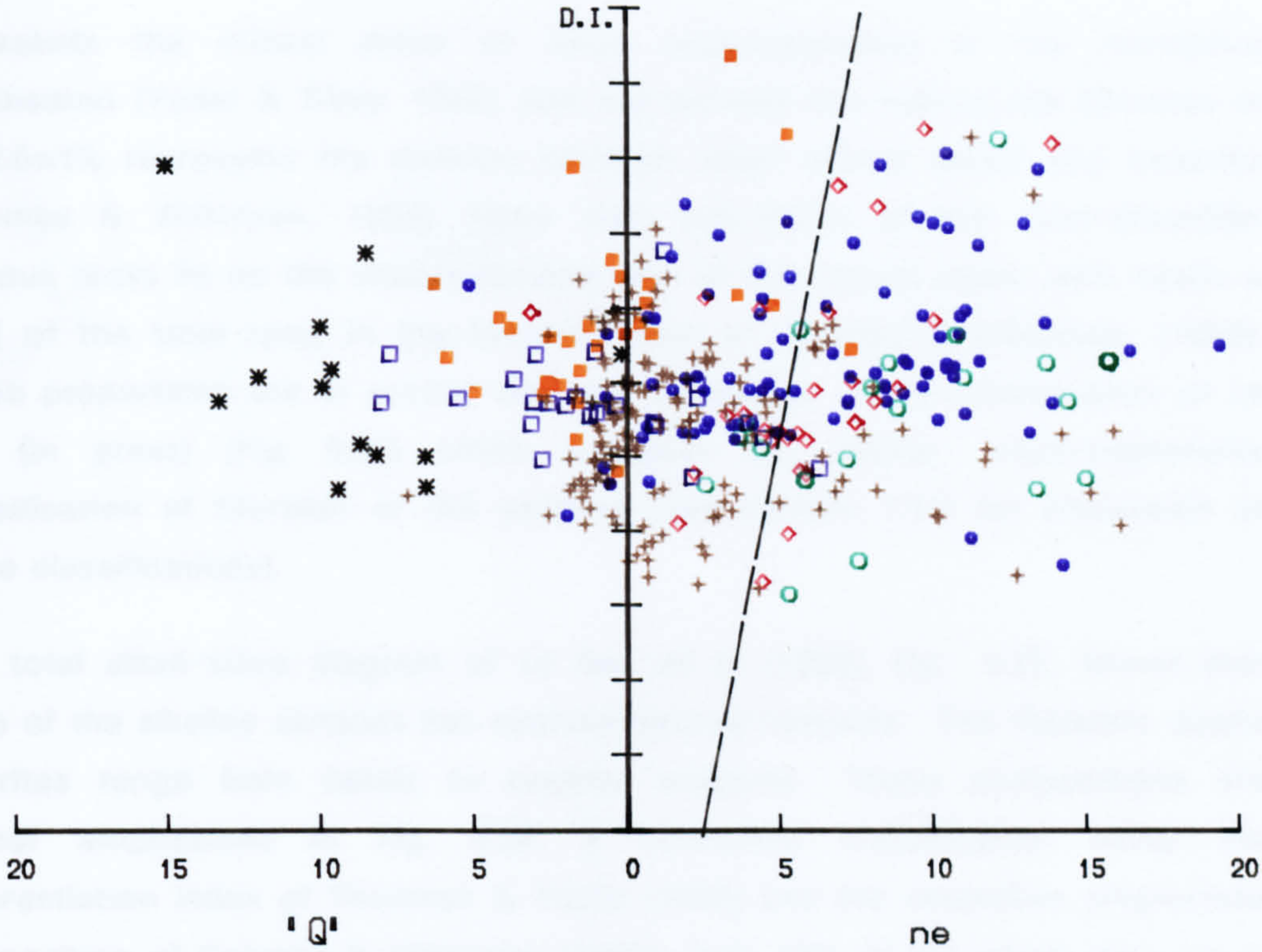

Fig. 5.29 Degree of silica saturation plotted against differentiation index (D.I.) for all groups.

'Q' is normative *q* + quartz in *hy* (modified after Thompson *et al.*, 1972 and Smedley, 1986b, see text for explanation). The dashed line represents the division between alkali olivine basalt and basanite (after Coombs & Wilkinson, 1969).

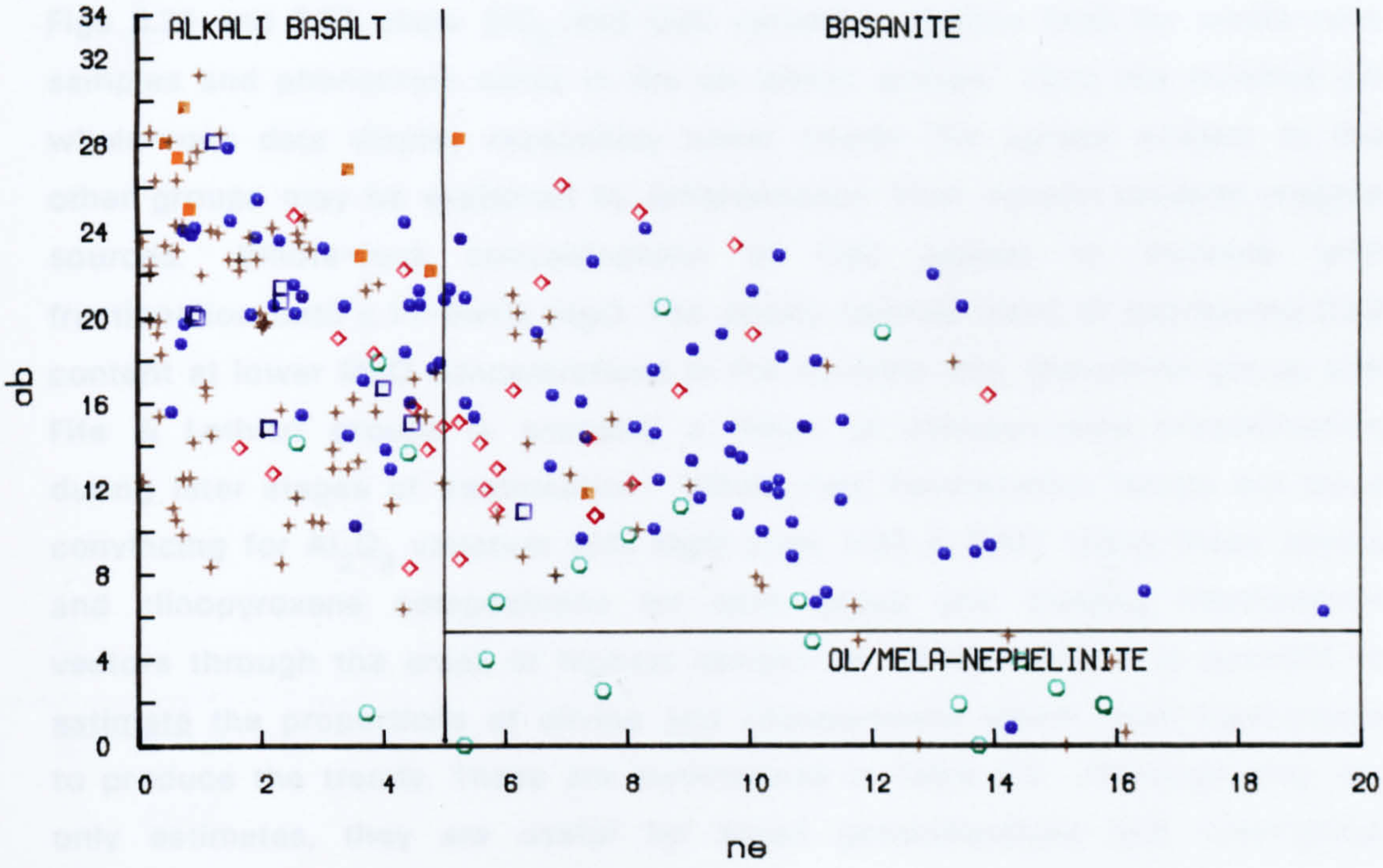

Fig. 5.30 CIPW normative plot of *ab* against *ne* for all samples (after Le Bas, in press**).**

represents the critical plane of silica undersaturation in the normative tetrahedron (Yoder & Tilley, 1962), and the inclined line cutting the abscissa at *ne*=2.5wt% represents the division between alkali olivine basalt and basanite (Coombs & Wilkinson, 1969). More than two-thirds of the post-Dinantian igneous rocks lie on the undersaturated side of the critical plane, with nearly a third of the total lying in the basanite field of Coombs & Wilkinson, (1969). These proportions are in accord with the normative *ab-ne* classification of Le Bas (in press) (Fig. 5.30) which indicates the olivine- mela-nephelinite classification of fourteen of the samples (see section 1.5.2 for discussion of these classifications).

The total alkali-silica diagram of Le Bas *et al.* (1986), Fig. 5.27, shows that none of the alkaline samples has evolved beyond hawaiite. The tholeiitic quartz dolerites range from basalt to basaltic andesite. These compositions are further emphasised in Fig. 5.28, a normative classification using the differentiation index of Thornton & Tuttle (1960) and the normative plagioclase composition of Coombs & Wilkinson (1969). Only 10% of the whole data set is more evolved than basaltic hawaiite.

5.4. Fractional crystallisation patterns

5.4.1. Inferences from whole-rock and probe data

Figs 5.31 and 5.32 show SiO_2 and CaO variations against MgO for whole-rock samples and phenocryst cores in the six alkalic groups. Only the Ayrshire sill whole-rock data display reasonably linear trends The spread evident in the other groups may be explained by differentiation from several parental magma sources. Whole-rock concentrations of CaO appear to increase with fractionation until c.11-8wt% MgO. The poorly-defined trend of decreasing CaO content at lower MgO concentrations in the Ayrshire sills, Mauchline group, and Fife & Lothian groups is probably a result of clinopyroxene crystallisation during later stages of fractionation. Whole-rock fractionation trends are more convincing for Al_2O_3 variation with MgO (Figs. 5.33 & 5.34). Using mean olivine and clinopyroxene compositions for each group and drawing fractionation vectors through the areas of highest density for whole-rocks, it is possible to estimate the proportions of olivine and clinopyroxene which have fractionated to produce the trends. These are summarised in Table 5.3. Although they are only estimates, they are useful for broad generalisations and inter-group

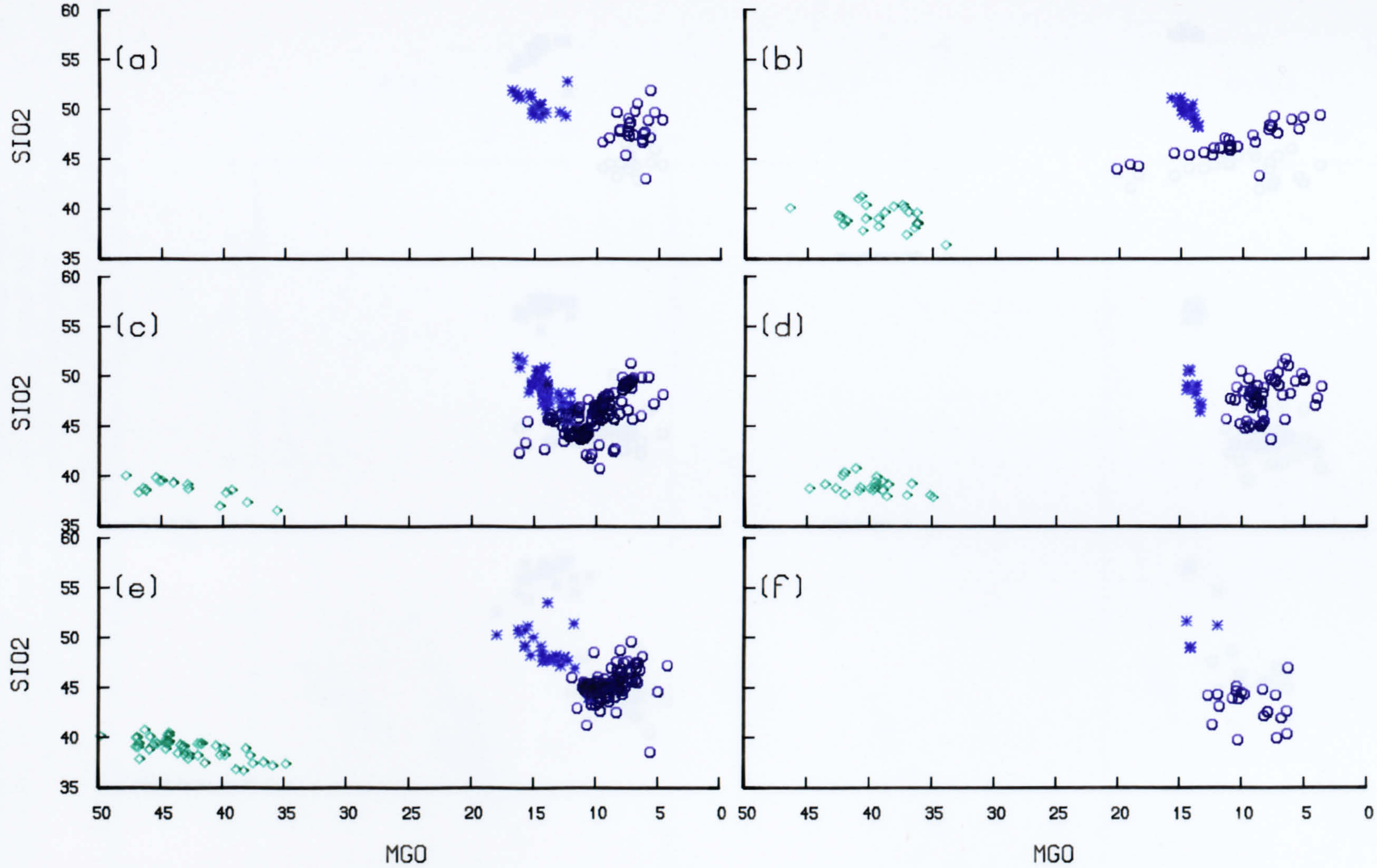

Fig. 5.31. SiO_2 and MgO variations in clinopyroxene ✳ and olivine ◇ phenocryst cores, and whole rocks ○ for: (a) Passage Group lavas; (b) Ayrshire sills; (c) Mauchline Group; (d) Fife & Lothian sills; (e) Fife & Lothian basanites; (f) Highland dykes.

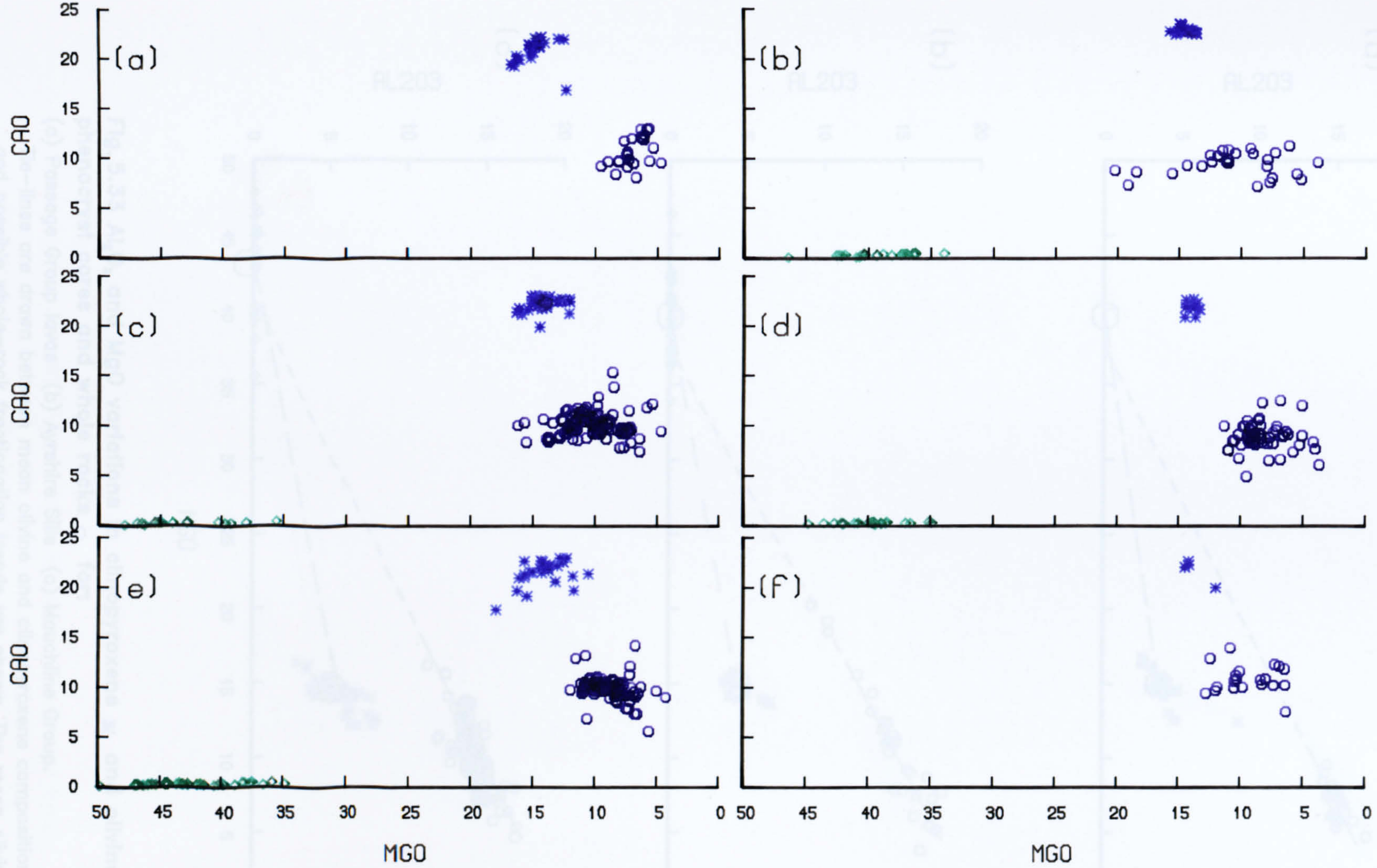

Fig. 5.32. CaO and MgO variations in clinopyroxene ✳ and olivine ◇ phenocryst cores, and whole rocks ○ for: (a) Passage Group lavas; (b) Ayrshire sills; (c) Mauchline Group; (d) Fife & Lothian sills; (e) Fife & Lothian basanites; (f) Highland dykes.

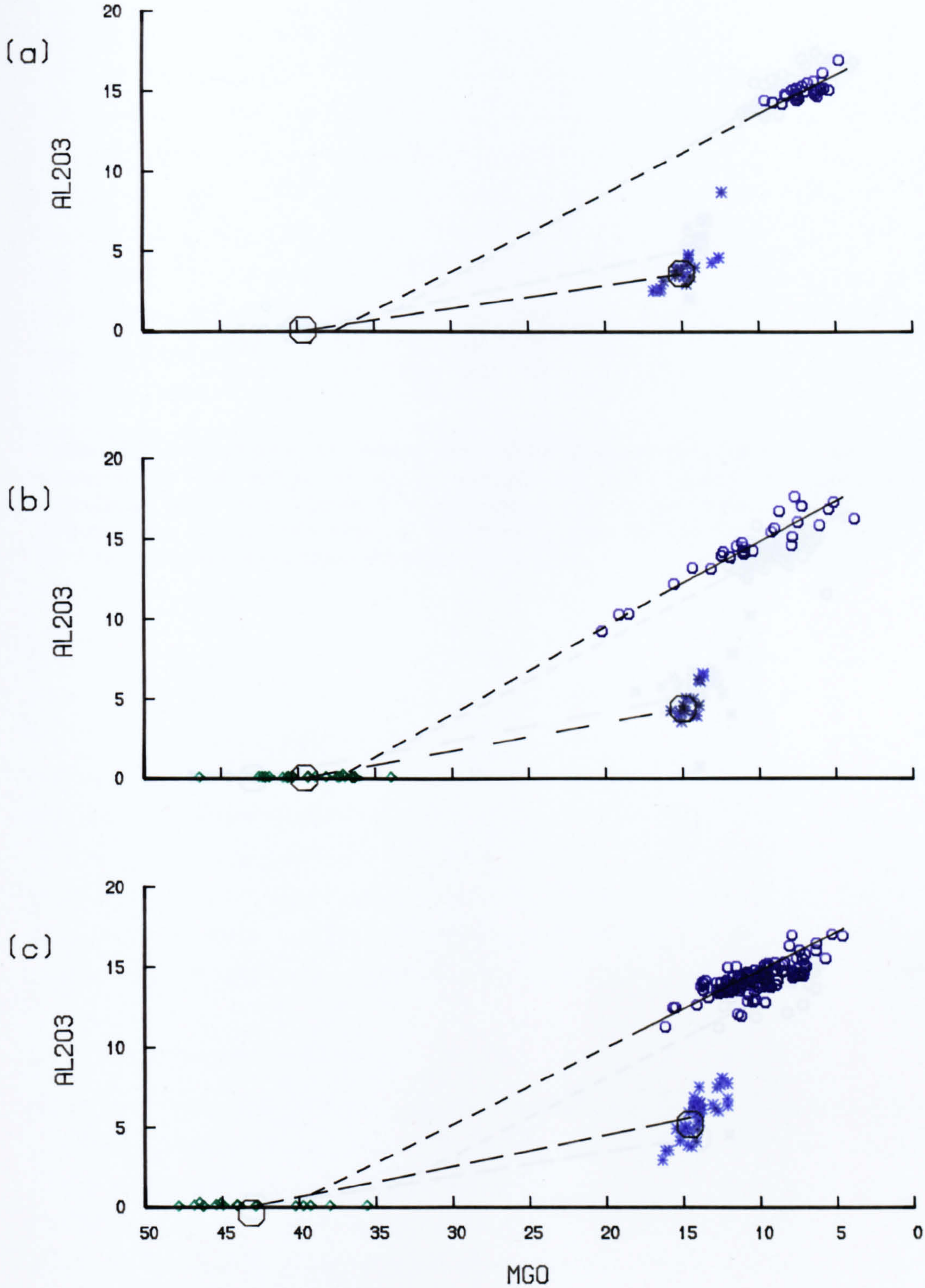

Fig. 5.33 Al_2O_3 and MgO variations in clinopyroxene ✳ and olivine ◇ phenocryst cores and whole rocks ○ for:

(a) Passage Group lavas (b) Ayrshire Sills (c) Mauchline Group.
Tie–lines are drawn between mean olivine and clinopyroxene compositions, and possible whole–rock fractionation trends are shown. The mean olivine composition for the Passage Group lavas is substituted from the Ayrshire sill data.

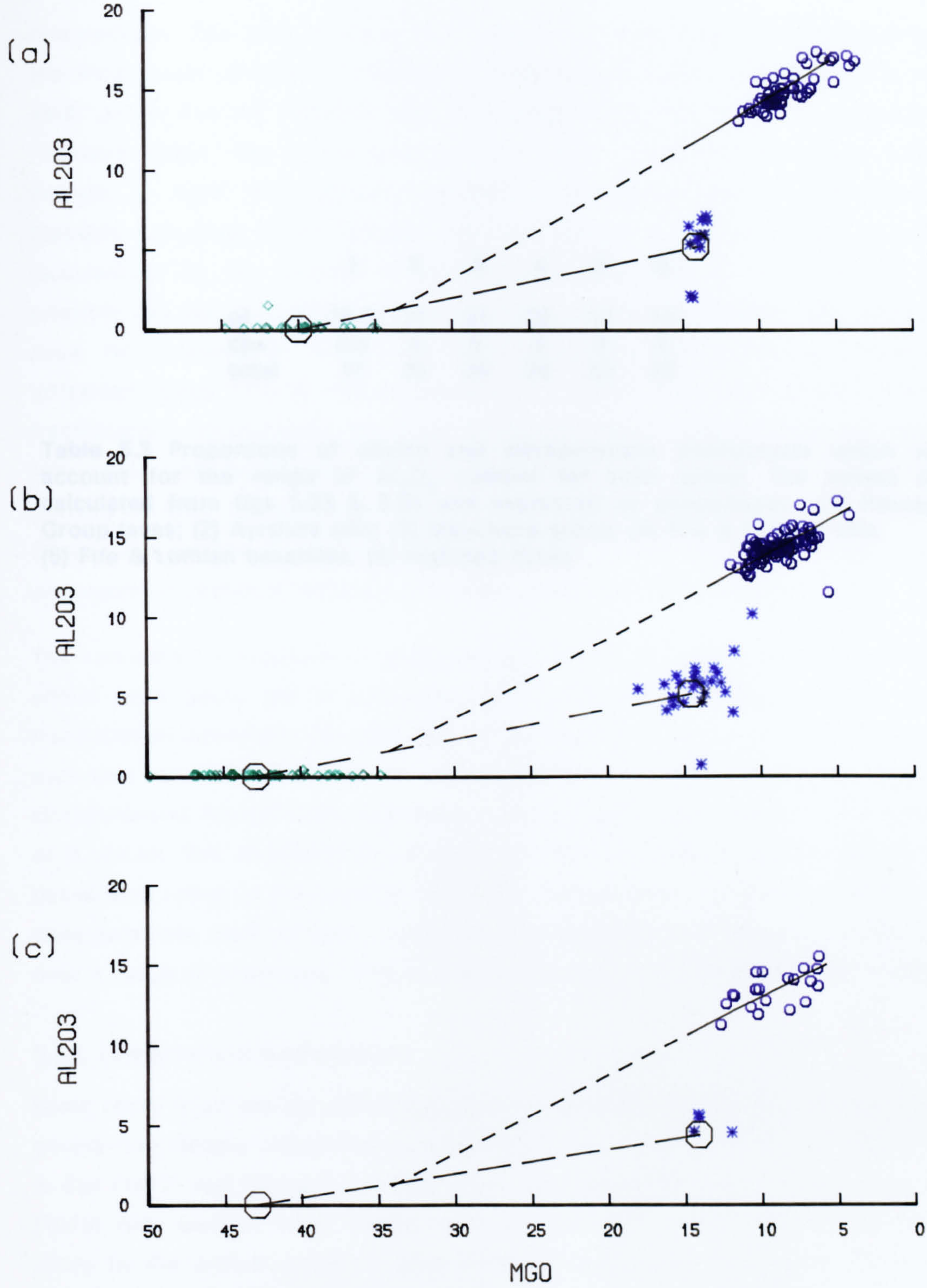

Fig. 5.34 Al_2O_3 and MgO variations in clinopyroxene ✳ and olivine ◇ phenocryst cores and whole rocks ○ for:

(a) Fife & Lothian sills (b) Fife & Lothian Basanites (c) Highland Dykes. Tie–lines are drawn between mean olivine and clinopyroxene compositions, and possible whole–rock fractionation trends are shown. The mean olivine composition for the Highland Dykes is substituted from the Fife & Lothian basanite data.

	1	2	3	4	5	6
ol	16.5	31	31	20	17	18
cpx	0.5	4	5	6	8	8
total	17	35	36	26	25	26

Table 5.3 Proportions of olivine and clinopyroxene phenocrysts which will account for the range of Al_2O_3 content for each group. The values are calculated from figs 5.33 & 5.34 and expressed as percentages. (1) Passage Group lavas; (2) Ayrshire sills; (3) Mauchline group; (4) Fife & Lothian sills; (5) Fife & Lothian basanites; (6) Highland dykes.

comparisons. The data indicate that between 17-36% crystal fractionation of the most basic samples is required to produce the most evolved samples in each group. For the Ayrshire sills, Mauchline Group, Fife & Lothian sills and Highland dykes, the most basic samples have calculated Mg-values high enough to have been primary magmas in equilibrium with mantle olivine (Basaltic Volcanism Study Project, 1981; see section 5.1 for discussion of this calculation), so the degrees of fractionation calculated for these groups is possibly not too unrealistic. (The three most magnesian Ayrshire sill samples have Ni contents in excess of primary magma concentrations (Basaltic Volcanism Study Project 1981; & section 5.1), and so have been ignored in the fractionation calculations). The most magnesian Fife & Lothian basanites have Mg-values c.65 suggesting that their compositions are not far removed from primary magma compositions. However the highest Mg-value for a Passage Group lava sample is c.58, suggesting that the Passage Group magmas have undergone a degree of fractionation much larger than the calculated 17%.

The calculated proportions of ol:cpx required to account for chemical variation within each group are in agreement with petrographic observations. Olivine fractionation dominated the evolution of the Passage Group lavas almost to the exclusion of clinopyroxene. In the Ayrshire sills and Mauchline group, clinopyroxene fractionation was more important with cpx:ol ratios of the order of 0.14:0.86. This is further increased in the two Fife groups and the Highland dykes with ratios of the order of 0.32:0.68. Petrographic and mineral chemistry considerations have already suggested that fractional crystallisation operated over a range of pressures. This is discussed further in the following sections.

5.4.2. Low pressure fractionation

Basic rocks from the six alkalic groups have been plotted in the 1 atmosphere olivine-plagioclase-clinopyroxene (ol-pl-cpx) phase diagram (Fig. 5.35) after Cox & Bell (1972) and Cox *et al.* (1979). Following the criteria set out by Cox *et al.* (1979) only basaltic rocks *(an/(an+ab)*>50) with K_2O c.1% or less, which plot close to the critical plane of silica undersaturation are represented. Samples from the Ayrshire sills, Mauchline Group, Fife & Lothian basanites and Highland Dykes all sit within the primary phase field of olivine, and in the first three cases, show scattered trends towards plagioclase. However, a significant number of the samples contain both olivine and clinopyroxene phenocrysts (and only rarely plagioclase). The Passage Group lava and the Fife & Lothian

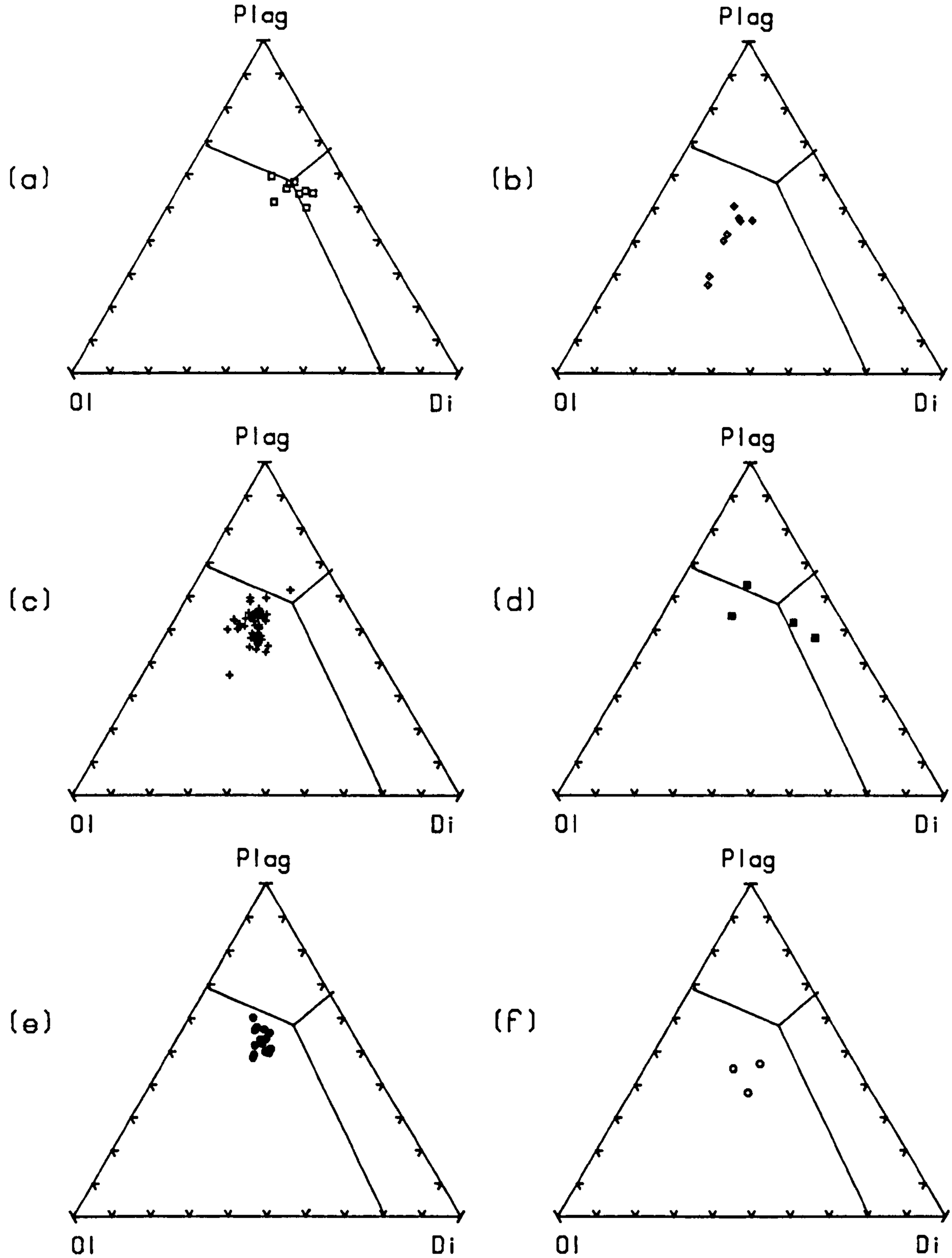

Fig.5.35 Normative projections from *ne* and *q* into *Ol–Pl–Cpx* (wt) for basalts from all alkaline groups.

(a) Passage Group lavas (b) Ayrshire Sills (c) Mauchline Group
(d) Fife & Lothian sills (e) Fife & Lothian basanites (f) Highland Dykes
1atm phase boundaries from Cox & Bell (1972).

sill samples spread about the ol-pl-cpx cotectic, but the phenocryst assemblages of the samples represented are dominated by olivine. The contradiction between observed phenocryst assemblages and those inferred from the diagrams of Fig. 5.35 suggest that the trends cannot be entirely (if at all) attributed to low pressure fractional crystallisation.

5.4.3. Polybaric fractionation

In an attempt to elucidate the polybaric nature of fractionation, samples from each of the groups have been plotted in projections from O'Hara's (1968) natural basalt phase diagram, for pressures up to 30 kb. These diagrams are subject to uncertainties through lack of experimental data and because of solid solutions involving garnet and aluminous pyroxene (Cox *et al*, 1979), no unique interpretation of natural rock data is possible from individual projections. However, they provide the basis for some useful qualitative comments. Since olivine and clinopyroxene are the principal phenocryst phases, the projections chosen are olivine into CS-MS-A and diopside into C_3A-M-S. Phase boundaries are taken from O'Hara (1968) and Cox *et al.* (1979), and the whole-rock paramaters were calculated assuming $Fe_2O_3/(FeO+Fe_2O_3) = 0.13$ (Brooks, 1976).

The projection from diopside into C_3A-M-S (Fig. 5.36) shows clearly the projections of the critical plane of silica undersaturation and the plane of silica saturation, (the olivine- and hypersthene-gabbro planes). It emphasises the predominently silica-undersaturated nature of the Ayrshire sills, Fife & Lothian basanites, Highland dykes and most of the Mauchline samples; the transitional nature of the Passage Group lavas and some of the Fife & Lothian sills; and the silica-saturated compositions of the quartz dolerites. The ol$^{+}_{-}$cpx phenocryst assemblages of the majority of samples in the six alkalic groups suggest that the 1 atmosphere phase boundaries are the most appropriate. However, they cannot be entirely so, since a significant number of samples then plot within the plagioclase field. With increasing pressure the olivine field contracts and the spinel field begins to impinge on that of plagioclase, so that at 10kb many samples plot within the diopside + spinel field - equally unacceptable on a petrographic basis. Most of the quartz dolerites plot within the di+pl or di+opx fields at 10kb.

Figs 5.37 & 5.38 show the olivine into CS-MS-A projection for the seven groups. The elongate trends common to each group are the result of the

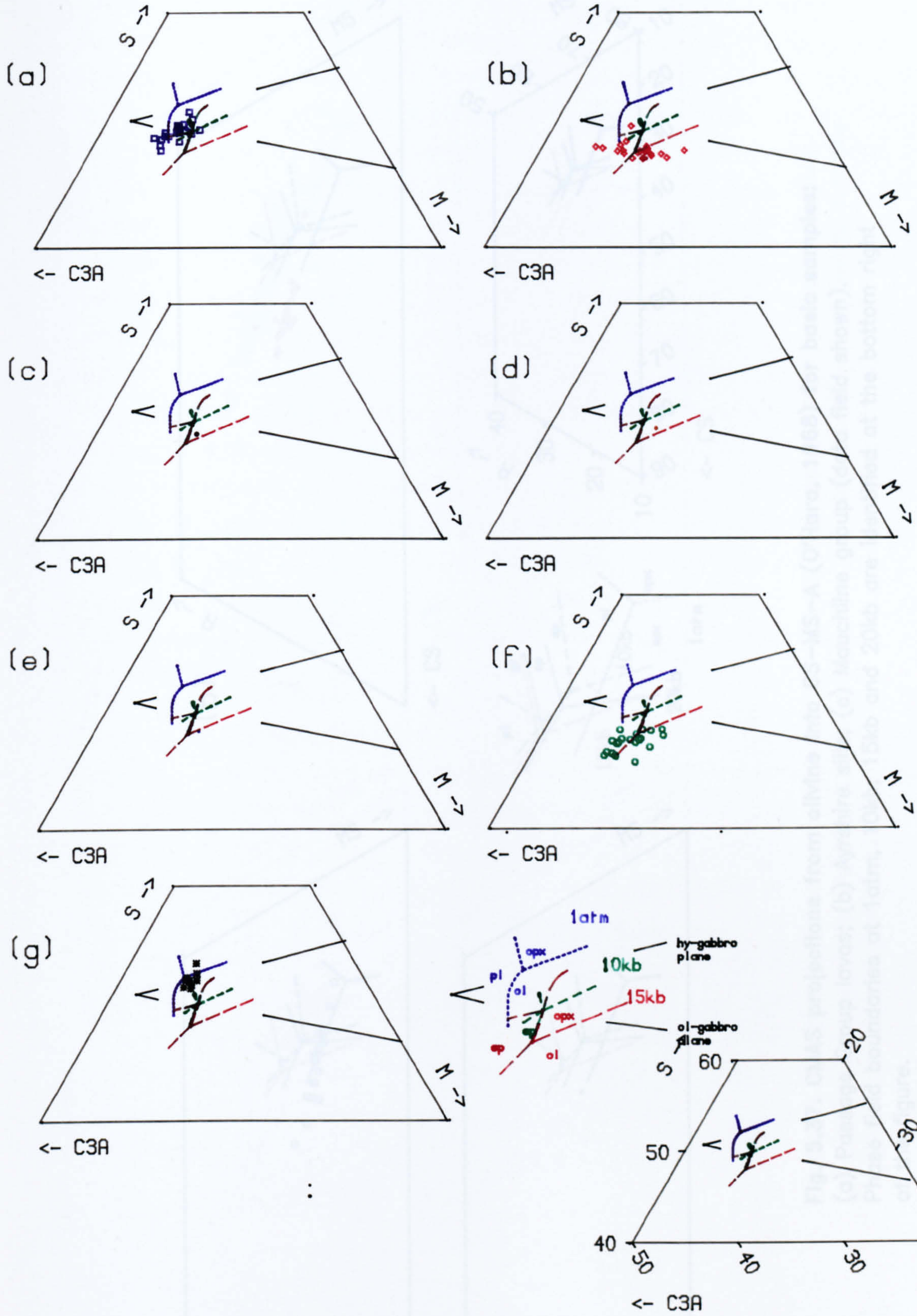

Fig. 5.36. CMAS projections from diopside into C_3A–M–S (O'Hara, 1968) for basic samples from all groups.

(a) Passage Group lavas (b) Ayrshire Sills (c) Mauchline Group
(d) Fife & Lothian sills (d) Fife & Lothian basanites (e) Highland Dykes
(g) Quartz dolerites. Figs c–e show data fields only. Phase stability fields at 1atm, 10kb and 15kb identified at bottom right of figure.

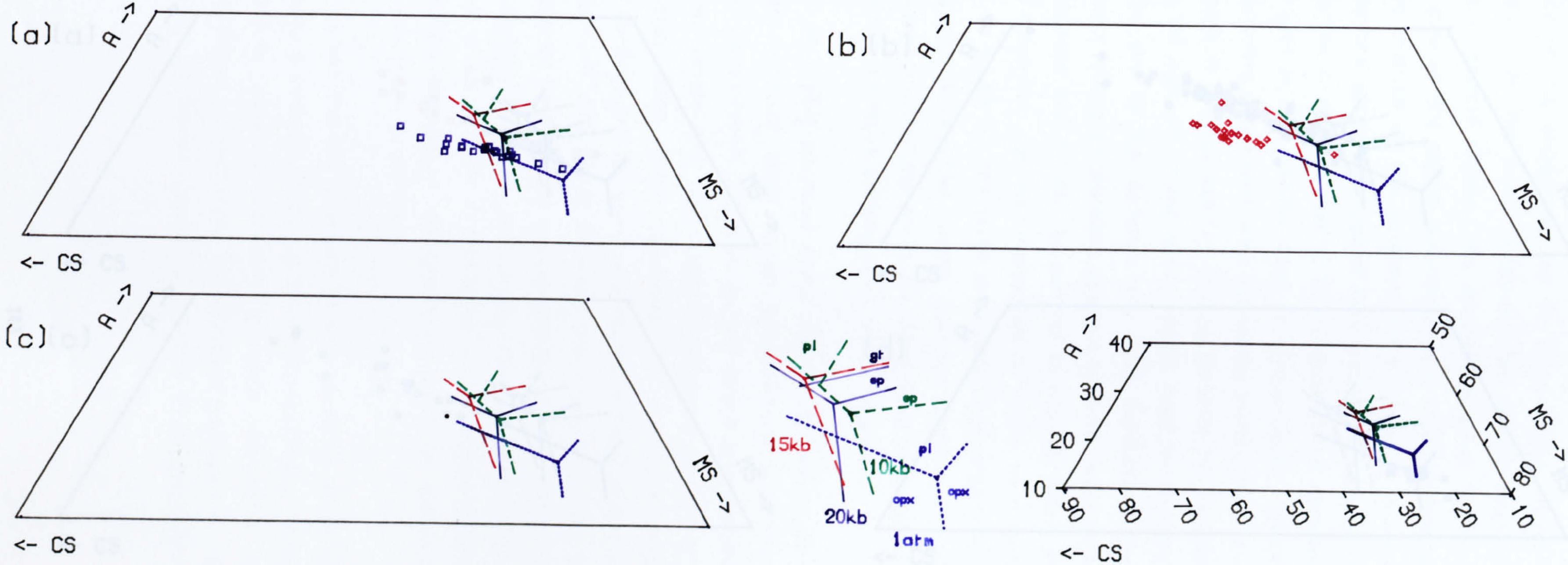

Fig. 5.37. CMAS projections from olivine into CS–MS–A (O'Hara, 1968) for basic samples: (a) Passage Group lavas; (b) Ayrshire sills; (c) Mauchline group (data field shown). Phase field boundaries at 1atm, 10kb, 15kb and 20kb are identified at the bottom right of the figure.

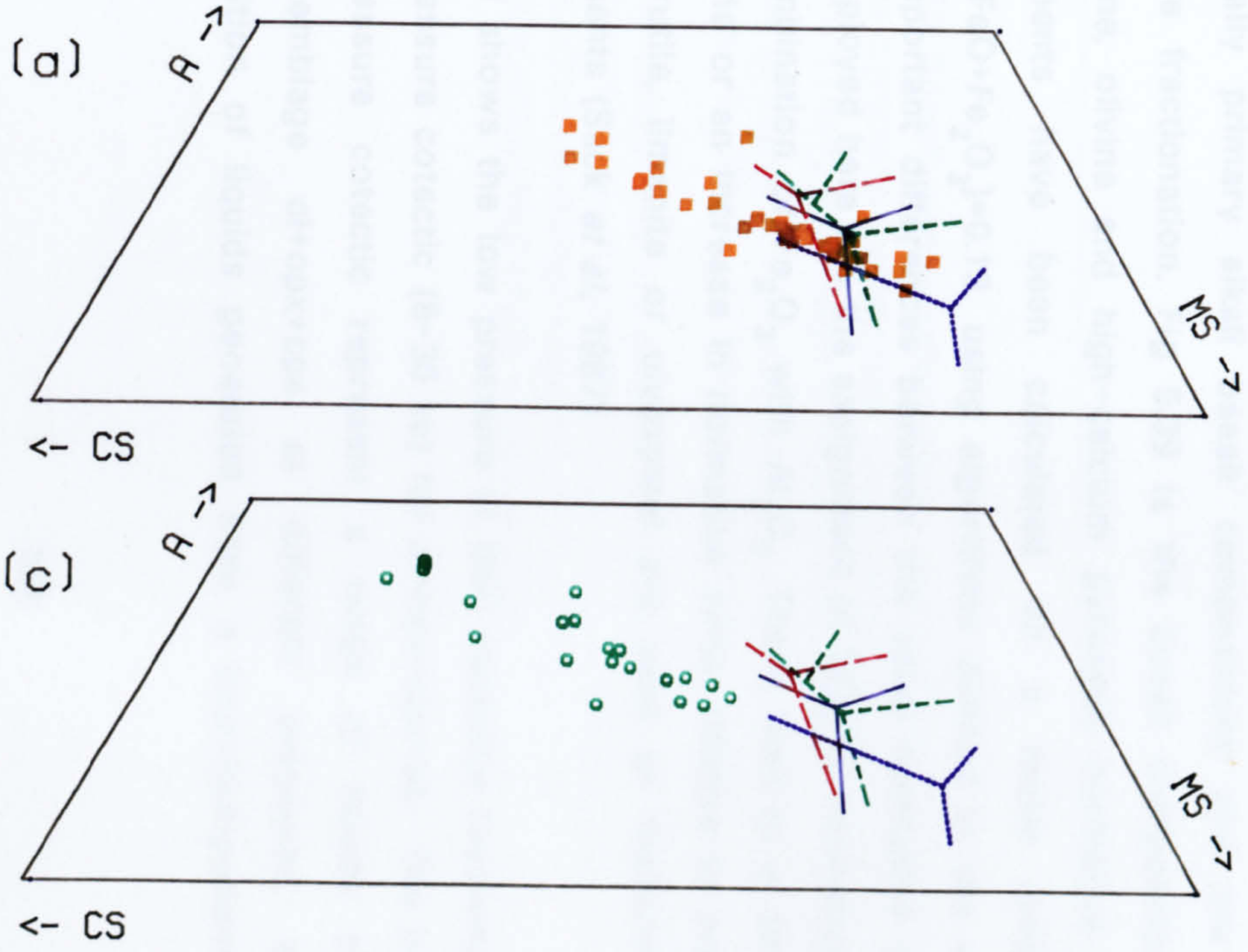

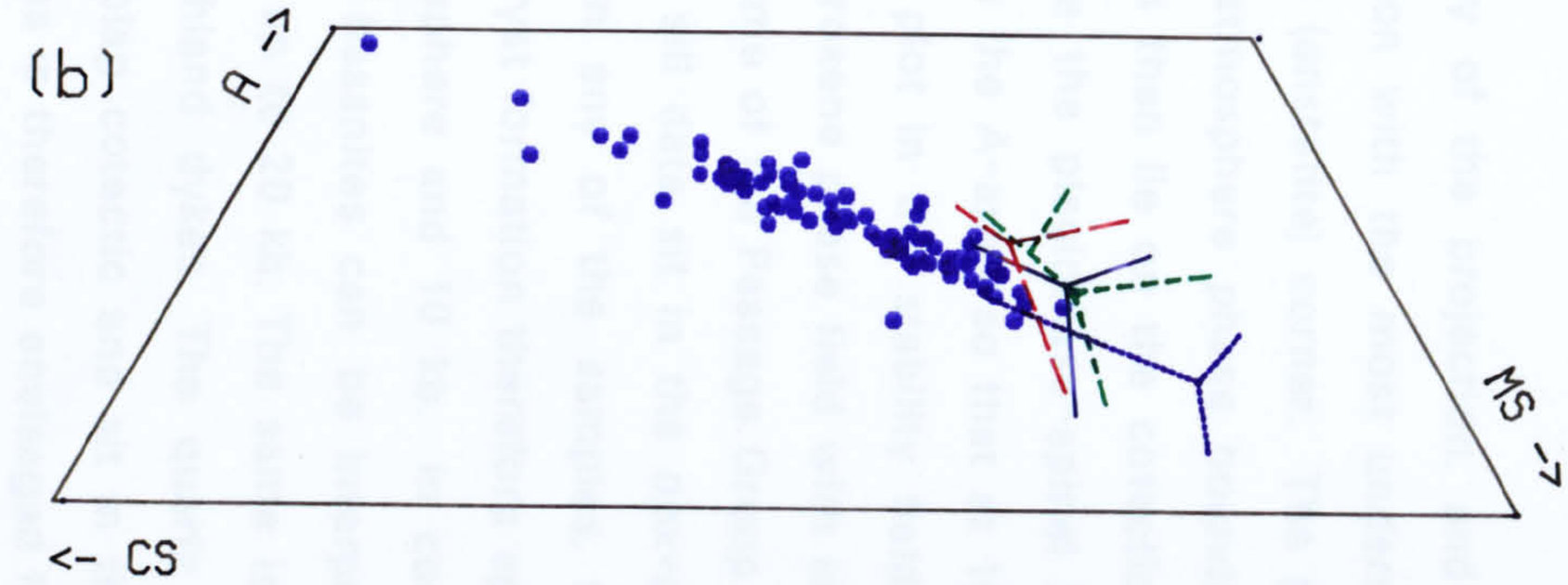

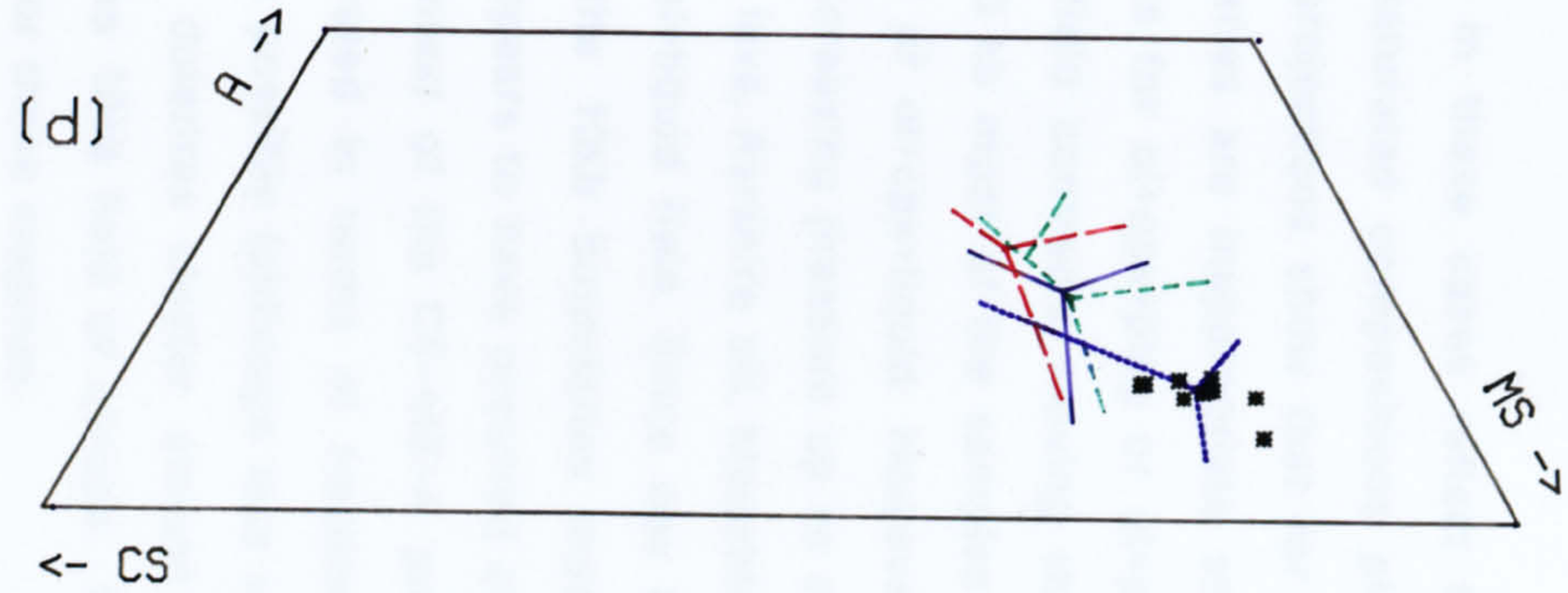

Fig. 5.38. CMAS projections from olivine into CS–MS–A (O'Hara, 1968) for basic samples: (a) Fife & Lothian sills; (b) Fife & Lothian basanites (c) Highland dykes; (d) Quartz dolerites. (See fig 5.37 for annotation).

obliquity of the projection, and in these cases reflect the degree of silica saturation with the most undersaturated compositions plotting furthest from the MS (enstatite) corner. The projections show that for each of the groups the 1 atmosphere phase boundaries are inappropriate since the majority of samples then lie on the cotectics for ol+cpx+plag or ol+plag. With increasing pressure the plagioclase-spinel field contracts moving the plag-cpx cotectic towards the A-apex so that at 10 kb most of the samples from the six alkalic groups plot in the stability field of ol+cpx+liquid. However, expansion of the orthopyroxene phase field with increasing pressure up to c.15kb means that at 10kb some of the Passage Group lava, Ayrshire sill, Mauchline group and Fife & Lothian sill data sit in the opx+ol+liquid field. Since opx is not a phenocryst phase in any of the samples, the 10kb boundaries must be inappropriate. Phenocryst formation therefore appears to have occurred at pressures between 1 atmosphere and 10 kb. In context of the CS-MS-A projection, the Fife & Lothian basanites can be interpreted in terms of fractionation at pressures varying up to 20 kb. The same is possibly (although less convincingly) true of the Highland dykes. The quartz dolerites cluster around the 1 atmosphere ol+cpx+plag cotectic and sit in the 10kb field of ol+opx. Fractionation at low pressures is therefore envisaged for these magmas.

Sack *et al.* (1987) provided some useful constraints for the assessment of potentially primary alkali basalt compositions and the processes of low pressure fractionation. Fig 5.39 is the basalt composition plane defined by nepheline, olivine and high-calcium pyroxene normative components. These components have been calculated on a molar oxide basis assuming $Fe_2O_3/(FeO+Fe_2O_3)=0.13$, using algorithms defined in the caption to Fig. 5.39. Two important differences between the usual normative calculations and the one employed here are the assignment of TiO_2 to normative clinopyroxene, and the combination of Fe_2O_3 with Al_2O_3. These lead to a decrease in normative nepheline or an increase in normative silica, relative to projection schemes in which rutile, ilmenite or ulvospinel are used as titanium-bearing normative components (Sack *et al*, 1987).

Fig 5.39 shows the low pressure (1 bar) cotectics involving pl-ol-di-ne, and a high-pressure cotectic (8-30 kb) for ol+opx+cpx+sp. The points plotted on the high-pressure cotectic represent a range of liquids coexisting with the sub-assemblage ol+opx+cpx at different pressures, and therefore the composition of liquids generated from a four-component mantle source at

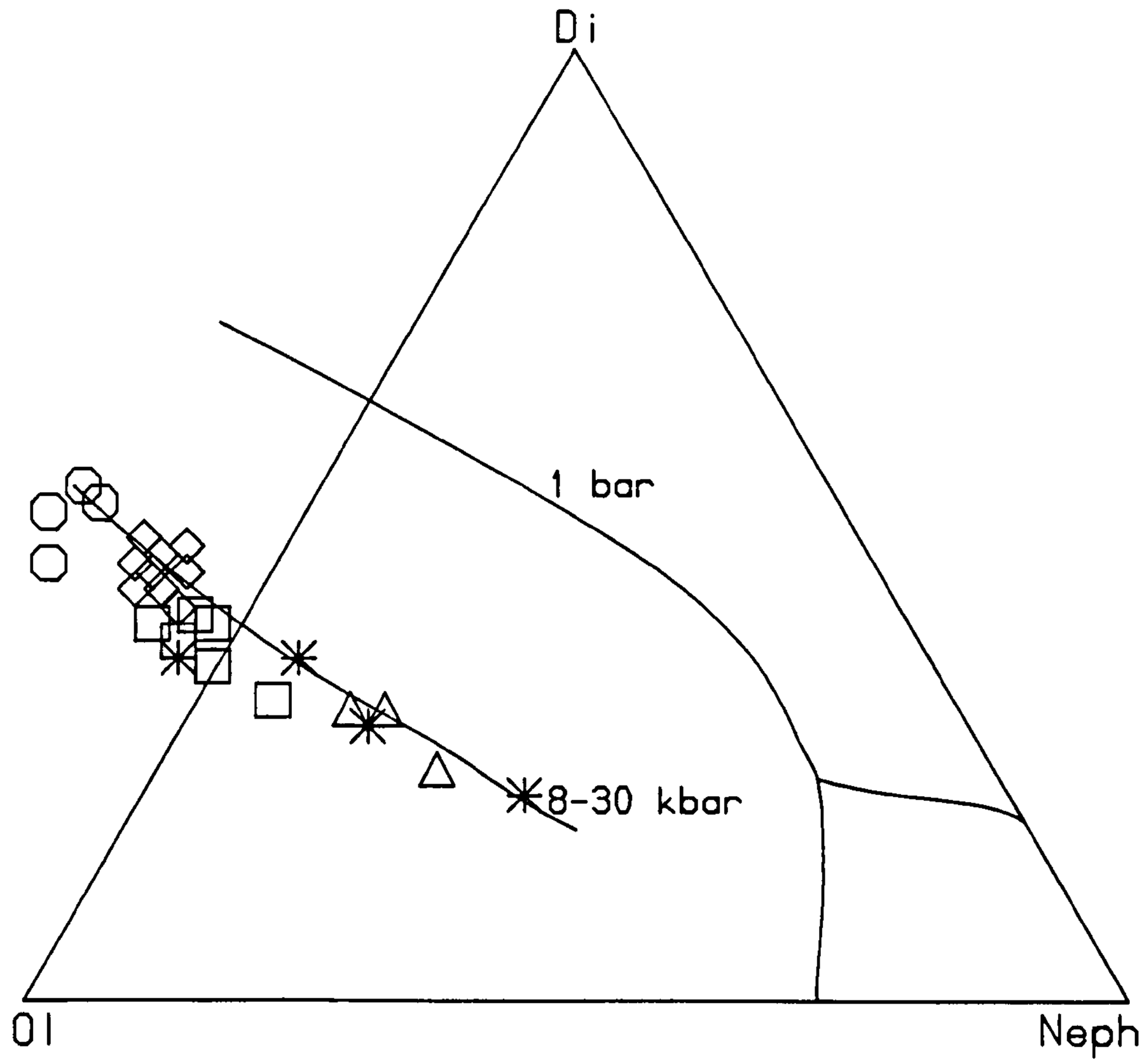

Fig.5.39 Basalt composition plane defined by nepheline, olivine and high-calcium pyroxene normative components after Sack *et al.* (1987), with low pressure (1bar) and high pressure (8-30kbar) cotectics drawn.

Pressures of liquids co-existing with the sub-assemblage of ol+opx+cpx are indicated as:
○ 8kbars, ◇ 10kbars, □ 15kbars, ✳ 20kbars, △ 30kbars.

Normative components are defined by the expressions:

Neph= $0.25(11Na_2O+11K_2O+3CaO+Al_2O_3+Fe_2O_3+FeO+MnO+MgO) - 0.5(SiO_2+2TiO_2)$

Ol= $0.5(FeO+MnO+MgO+Al_2O_3+Fe_2O_3-CaO-Na_2O-K_2O)$

Di= $(CaO+TiO_2+Na_2O+K_2O) - (Al_2O_3+Fe_2O_3)$

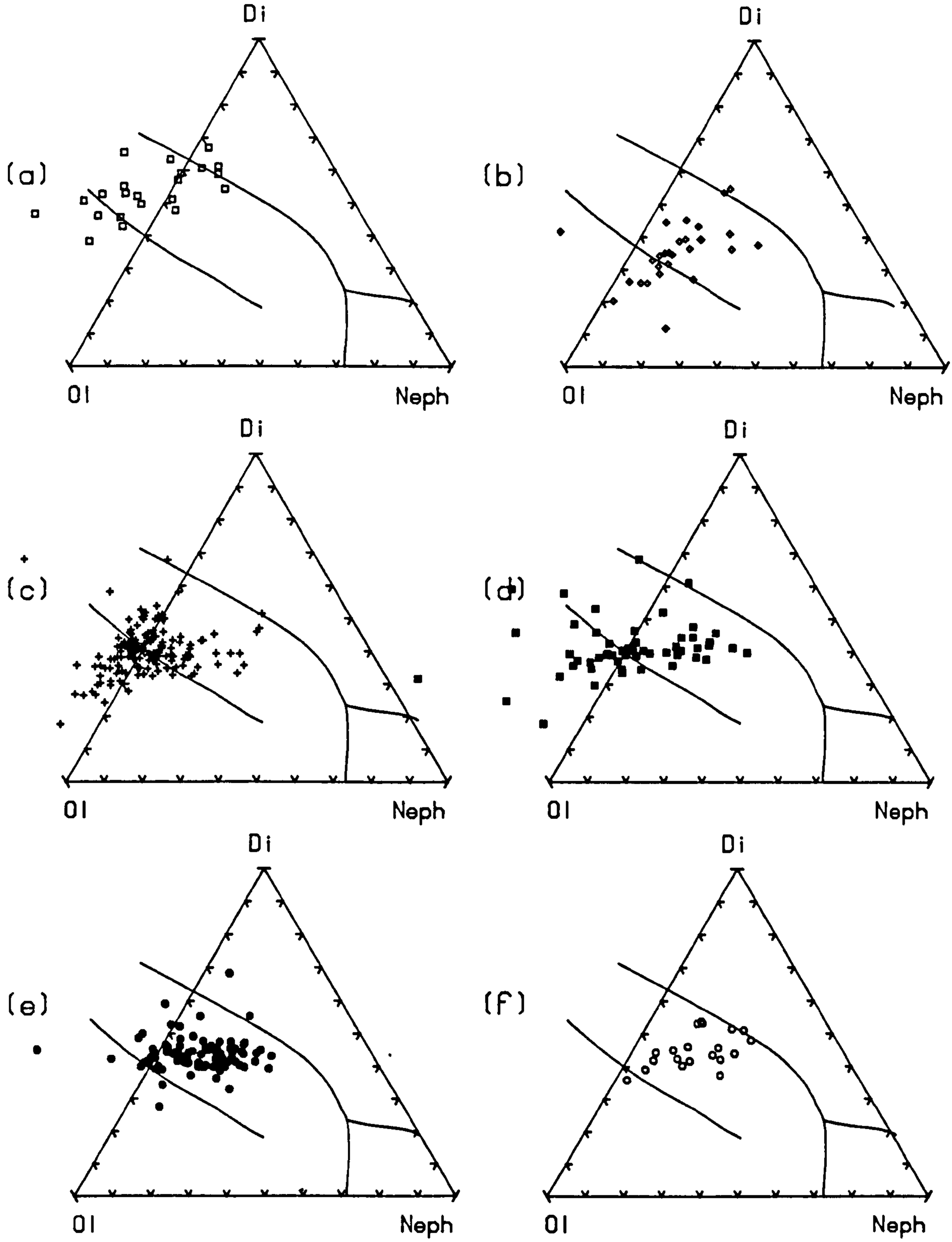

Fig.5.40 Data from all alkaline groups plotted in the basalt composition plane of Sack *et al.* (1987). (For explanation see fig 5.39). (a) Passage Group lavas, (b) Ayrshire sills, (c) Mauchline group, (d) Fife & Lothian sills, (e) Fife & Lothian basanites, (f) Highland dykes.

various pressures (Data summarised by Sack *et al.* (1987) from Stolper, 1980; Takahashii & Kushiro, 1983; Fujii & Scarfe, 1985). The diagram shows that the liquids on the cotectic define a band which becomes narrower with increasing neph/(neph+ol+di) and increasing pressure.

Figs 5.40a–f show the same diagram with data from each of the six alkalic groups superimposed. Comparison of these diagrams with Fig. 5.39 suggests that the most primitive Passage Group lavas could have been in equilibrium with mantle assemblages at pressures between 8–10 kb. The basanites and sills from Fife & Lothian, the Highland dykes and the majority of primitive Mauchline Group lavas indicate a pressure range of 10–15 kb although some of the Mauchline Group samples cluster around the cotectic in the vicinity of the 20kb samples of Sack *et al.* (1987). The Ayrshire sills appear to have been in equilibrium with mantle assemblages at pressures between 15 and 20 kb. However, accumulated olivine might have dragged the compositions of some samples towards the olivine apex. Although neither this nor the CMAS projections should be treated as fully quantitative indicators of fractionation pressure, they provide confirmation of the polybaric nature of fractionation in the post-Dinantian samples.

5.5. Incompatible element variations

5.5.1. Spiderdiagrams

Elements incompatible in the phenocryst assemblage of ol+cpx have been normalised to chondrite (Sun, 1980) and plotted on 'spiderdiagrams' in order of increasing compatibility (left to right) (Fig. 5.41). Alternative choices of normalising factors have been discussed by Wilson (1989). Their adoption has little effect on the overall shape of the spiderdiagrams except in the region of Rb, Ba and K. For example normalisation of the post-Dinantian suite using Thompson's (1982) data set (a factor of 6.9 for Ba as opposed to Sun's (1980) factor of 3.8) causes a flattening of profiles in the region of Rb, Ba and K for the Ayrshire sills, Fife & Lothian Group A sills and the Passage Group lavas. Although the Passage Group lavas still retain minor negative K and Rb anomalies, the same is not true for the Ayrshire sills. Using Thompson's data they would display a slight negative Ba anomaly which becomes more pronounced in the quartz dolerites. These effects should be borne in mind during the following discussions.

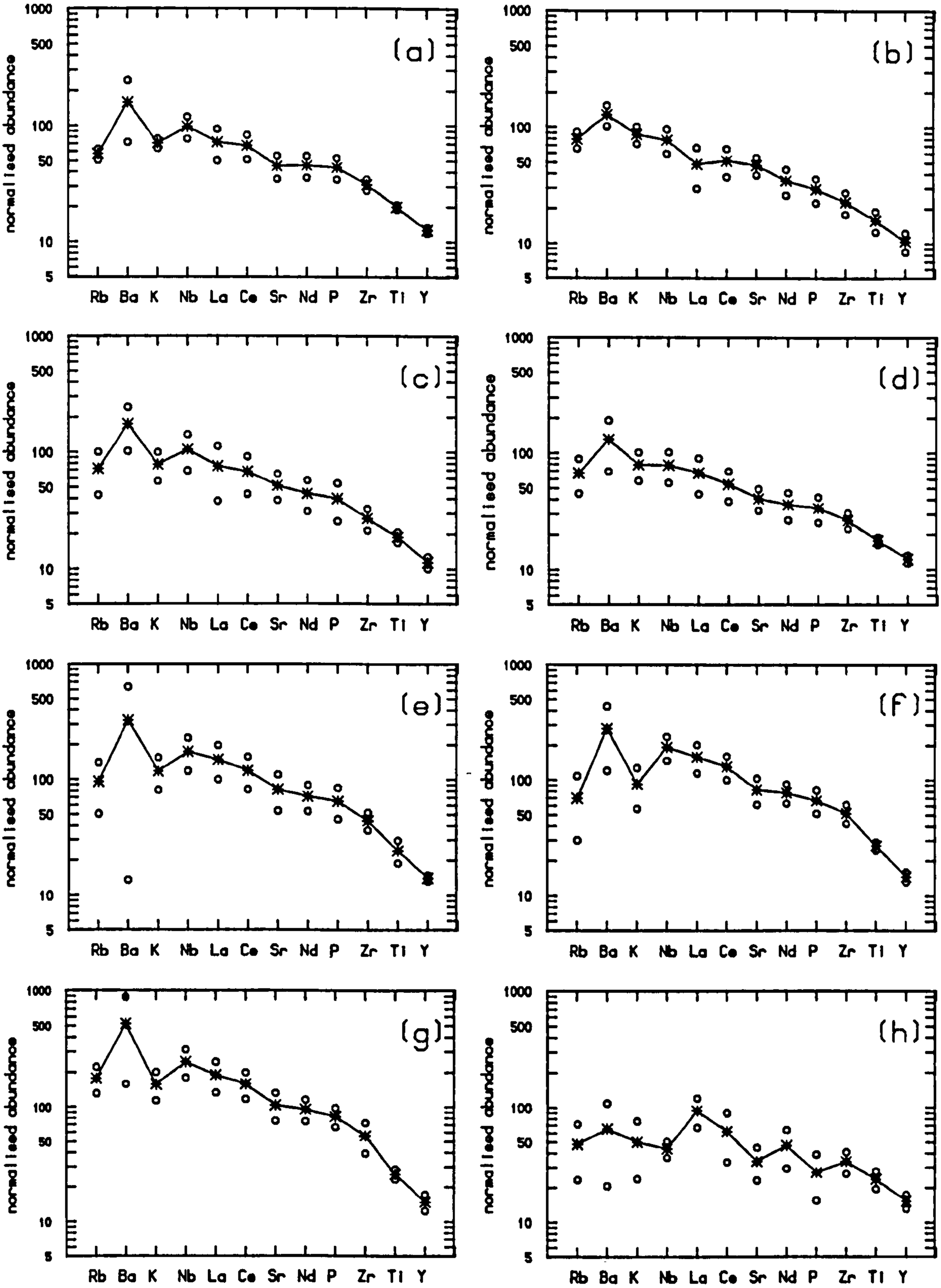

Fig.5.41. Mean chondrite normalised incompatible element profiles (spiderdiagrams) for basic samples with >6wt% MgO, (Quartz dolerites >4wt% MgO). The maximum and minimum point plotted for each element represents the mean ± 1 standard deviation. The number of analyses in each group is indicated below in square brackets.

(a) Passage Group lavas [20] (b) Ayrshire Sills [21] (c) Mauchline Group [136] (d) Fife & Lothian Group A sills [26] (e) Fife & Lothian Group B sills [17] (f) Fife & Lothian basanites [85] (g) Highland Dykes [6] (h) Quartz dolerites [10]

Spiderdiagrams of alkali basalts are characterised by general negative slopes from the more to less incompatible elements, the gradients of which decrease with increasing degrees of melting. This effect is particularly sensitive to small changes in melt fraction at low degrees of partial melting. Incompatible trace element concentrations are also enriched during fractional crystallisation, but because of the large melt fraction the effects on element concentration are less than those of partial melting. This was shown graphically by Fitton & Dunlop (1985) for basic (>4wt% MgO, with phenocryst phases of ol+cpx) rocks of the Cameroon Line, where profiles retain their overall shape and increase only slightly in steepness with decreasing MgO. At MgO contents c.4-6wt% plagioclase, hornblende, apatite or magnetite may join olivine and augite on the liquidus (Smedley, 1986b; Fitton, 1987), so that Rb, Ba, K, Sr, P and Ti may become compatible, producing troughs on spiderdiagrams. Accumulation of any of these crystals will increase the concentration of their compatible elements producing peaks rather than troughs. However accumulation of olivine and clinopyroxene will 'dilute' the concentration of the 'spiderdiagram elements' since they are all incompatible in these two phases, and the effect on the spiderdiagram profile will be antithetic to those of fractional crystallisation.

It is therefore likely that incompatible element concentrations have been most strongly influenced by partial melting processes. To aid intergroup comparisons and minimise the effects of spurious inflections due to within group variations in partial melting and fractional crystallisation, average profiles have been calculated for each group (Fig. 5.41). To avoid the effects of more extreme fractionation, only basic samples (>6wt% MgO for the alkaline groups; >4wt% for the quartz dolerites) have been included. Anomalous samples from each group are considered separately. The Fife & Lothian sills have been split into the two subgroups indicated in section 5.2.3. The second of these (referred to as Group B sills) are those which are geochemically similar to the Fife & Lothian basanites. Only the Highland dykes collected as part of this project have been plotted because of incomplete analyses of some of the spiderdiagram elements in samples included from Baxter (1986) and Morrison *et al.* (1986).

For ease of comparison, average profiles for the Midland Valley alkaline rocks are plotted together in Fig. 5.42a. The quartz dolerites and Highland dykes are shown in Fig. 5.42b. The following observations can be made concerning

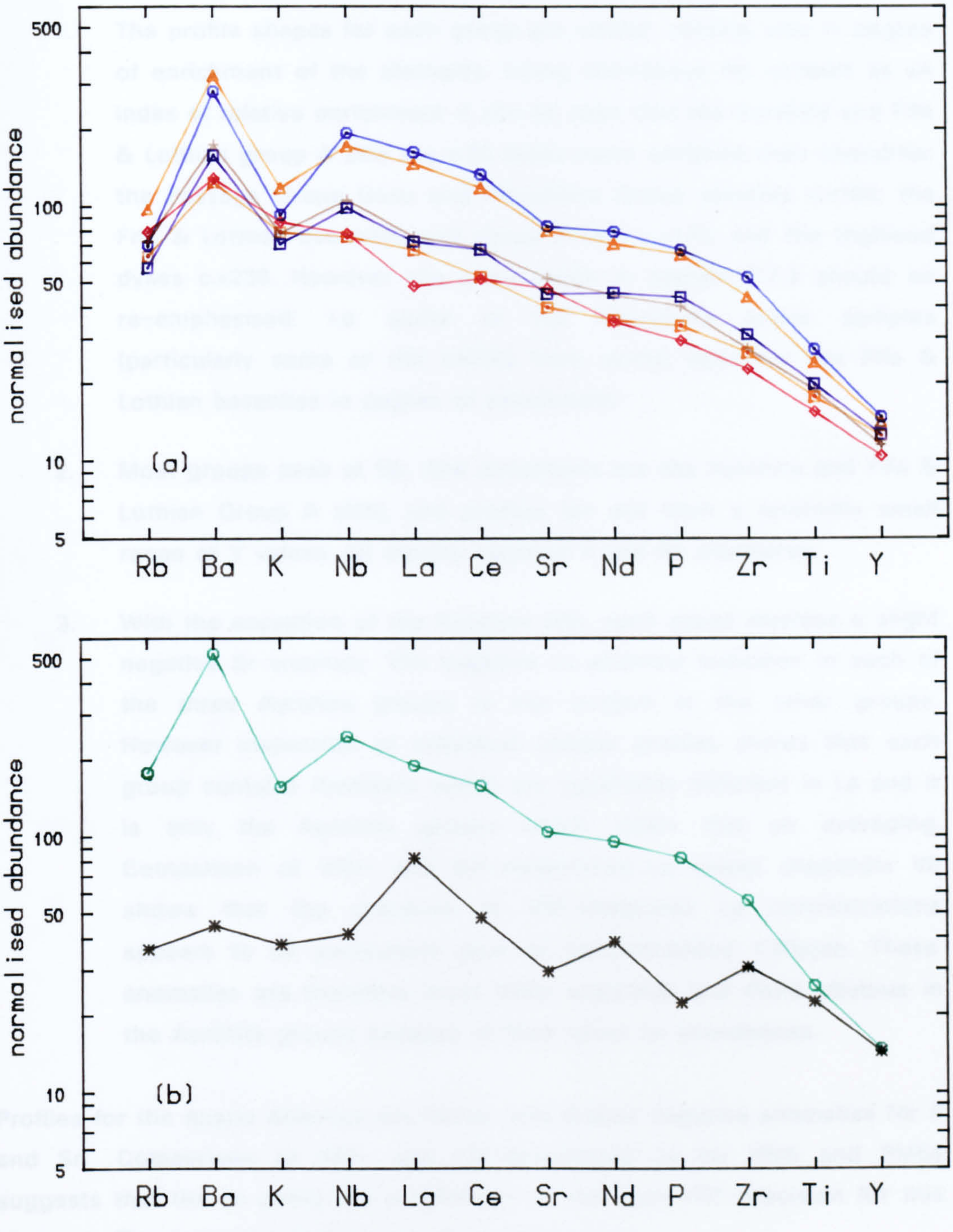

Fig. 5.42 Mean chondrite normalised spiderdiagram plots for basic samples from (a) Midland Valley alkaline suite (b) Highland dykes & Quartz dolerites.

- □ Passage Group lavas
- \+ Mauchline group
- △ Fife & Lothian Group B sills
- ○ Highland dykes
- ◇ Ayrshire sills
- □ Fife & Lothian Group A sills
- ○ Fife & Lothian basanites
- ✳ Quartz dolerites

the alkaline samples:

1. The profile shapes for each group are similar, varying only in degree of enrichment of the elements. Using normalised Nb content as an index of relative enrichment it can be seen that the Ayrshire and Fife & Lothian group A sills are c.80 times more enriched than chondrite; the Passage Group lavas and Mauchline Group samples c.x100; the Fife & Lothian basanites and group B sills c.x170; and the Highland dykes c.x230. However the point made in section 5.2.3 should be re-emphasised: i.e. some of the Mauchline group samples (particularly some of the blocks from vents) approach the Fife & Lothian basanites in degree of enrichment.

2. Most groups peak at Nb, (the exceptions are the Ayrshire and Fife & Lothian Group A sills), and profiles fan out from a relatively small range of Y values. All display negative K and Rb anomalies.

3. With the exception of the Ayrshire sills, each group displays a slight negative Sr anomaly. The negative La anomaly indicated in each of the three Ayrshire groups is not evident in the other groups. However inspection of individual sample profiles shows that each group contains members which are apparently deficient in La and it is only the Ayrshire groups which retain this on averaging. Comparison of XRF- and ICP-determined La values (Appendix VI) shows that the precision in XRF-measured La concentrations appears to be particularly poor at concentrations <30ppm. These anomalies are therefore most likely analytical and more obvious in the Ayrshire groups because of their lower La abundances.

Profiles for the quartz dolerites are flatter, and display negative anomalies for P and Sr. Comparison of XRF- and ICP-determined La for RM5 and RM64 suggests that the La peaks are a reflection of the poor XRF-precision for this element. The corrected profiles are much flatter at La.

Anomalous basic samples for each group are plotted in Fig. 5.43. SW84, SW100 and SW376 are all samples from the Ayrshire sills. SW84 is depleted in Nd, Sr, Ce and Nb relative to the majority of Ayrshire sill samples. It was collected from within 0.5m of the sedimentary contact and has therefore possibly been

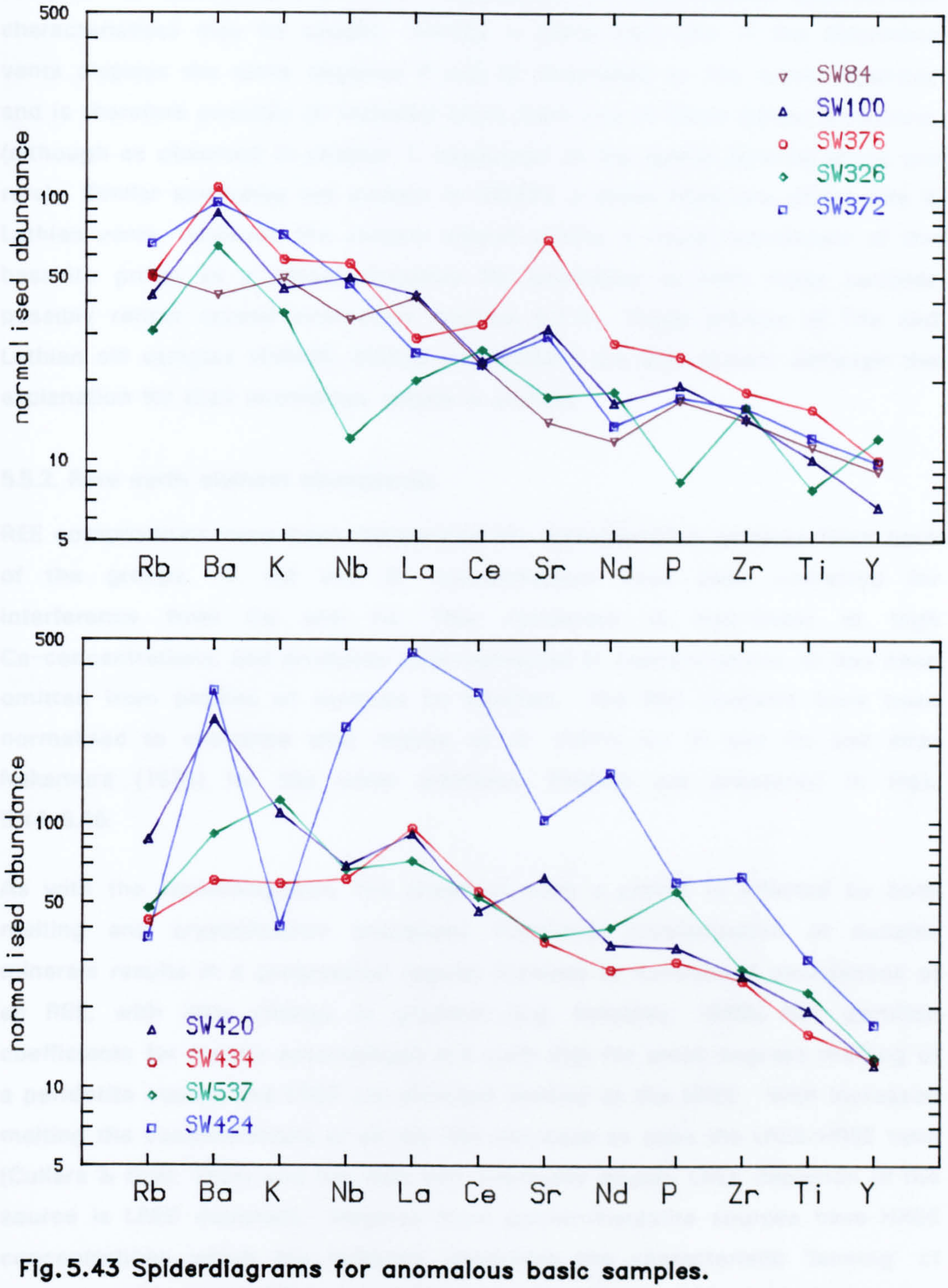

Fig. 5.43 Spiderdiagrams for anomalous basic samples.
Ayrshire sills: SW84, SW100, SW376; Mauchline group: SW326, SW372; Fife & Lothian Group A sills: SW420, SW434, SW537; Fife & Lothian basanite: SW424.

effected by crustal assimilation. The field relationships of the other two samples are unclear and a similar explanation for their deviant geochemical characteristiscs may be sought. SW326, a block from one of the Mauchline vents displays the same negative P and Sr anomalies as the quartz dolerites and is therefore possibly an included block from one of these earlier intrusions, (although as observed in chapter 1, exposures of the quartz dolerite group are rare). Similar anomalies are evident in SW424, a block from one of the Fife & Lothian vents. However, the steeper overall profile is more reminiscent of the basanite group as a whole. Negative Nb anomalies in both these samples possibly reflect crustal interaction (section 6.1.3). Three profiles of Fife and Lothian sill samples (SW420, SW434 and SW537) are also shown, although the explanation for their anomalous nature is unclear.

5.5.2. Rare earth element abundances

REE compositions have been determined for representative samples from each of the groups. Pr, Gd and Er concentrations have been corrected for interference from Ca and Fe. This correction is non-linear at high Ca-concentrations, and produces over-corrected Er concentrations. Er has been omitted from profiles of samples so affected. The REE contents have been normalised to chondrite after Watika *et al.* (1971) for Pr and Ho and after Nakamura (1974) for the other elements. Profiles are presented in Figs. 5.44–5.46.

As with the spiderdiagrams, the shape of such a profile is affected by both melting and crystallisation processes. Fractional crystallisation of basaltic minerals results in a progressive regular increase in normalised abundances of all REE, with little change in gradient (e.g. Smedley, 1986b). REE partition coefficients for mantle assemblages are such that for small degrees melting of a peridotite source, the LREE are enriched relative to the HREE. With increased melting the concentrations of all the REE decrease as does the LREE/HREE ratio (Cullers & Graf, 1984) and the melt will eventually display LREE depletion (if the source is LREE depleted). Magmas from garnet-lherzolite sources have HREE concentrations which are buffered, producing the characteristic 'fanning' of profiles about the HREEs, with variation in degree of melting. Examination of Figs. 5.44–5.46 indicates that the within-group ranges reflect both the effects of partial melting and fractional crystallisation, and that the former has been of greater influence (see section 5.5.1).

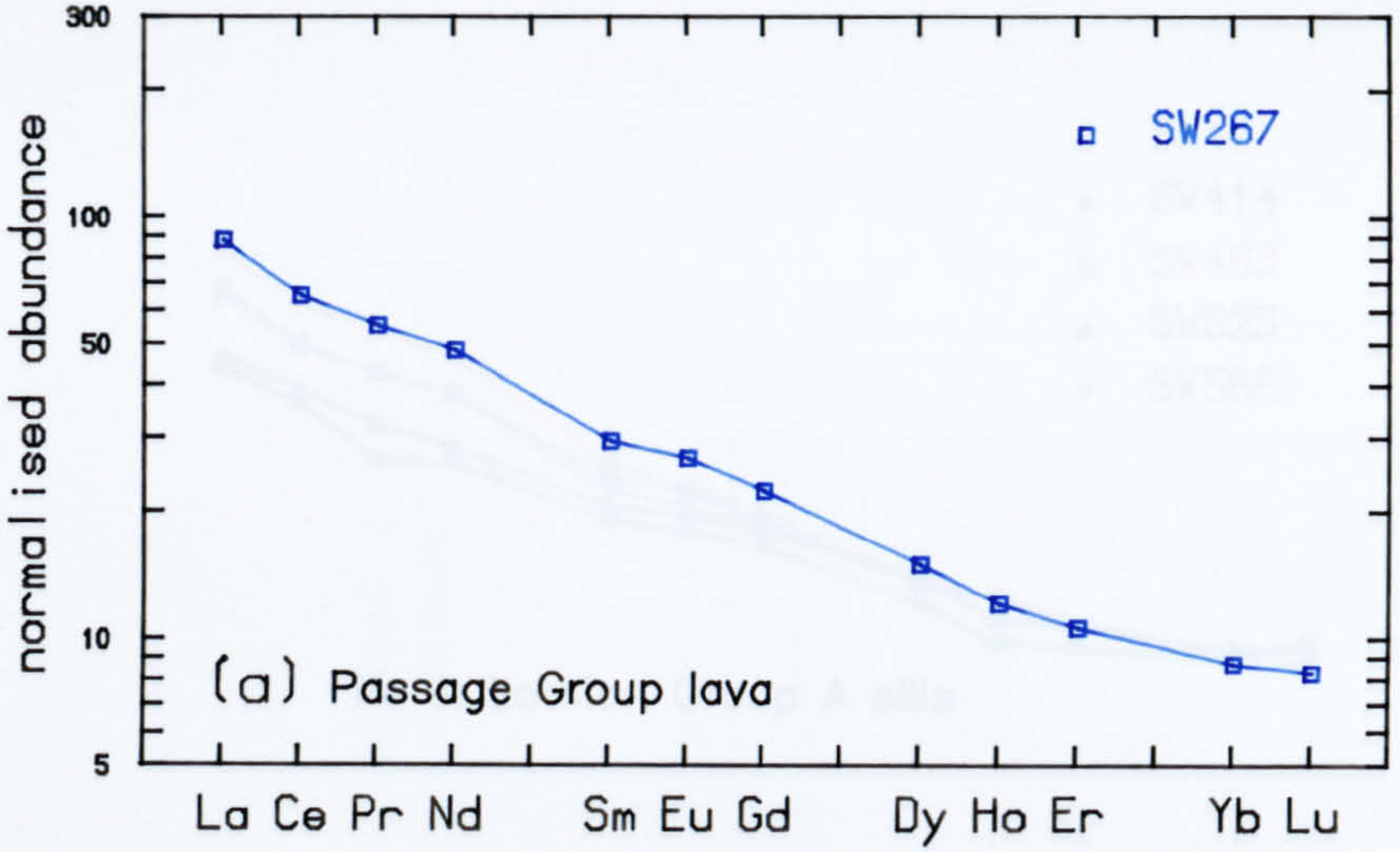

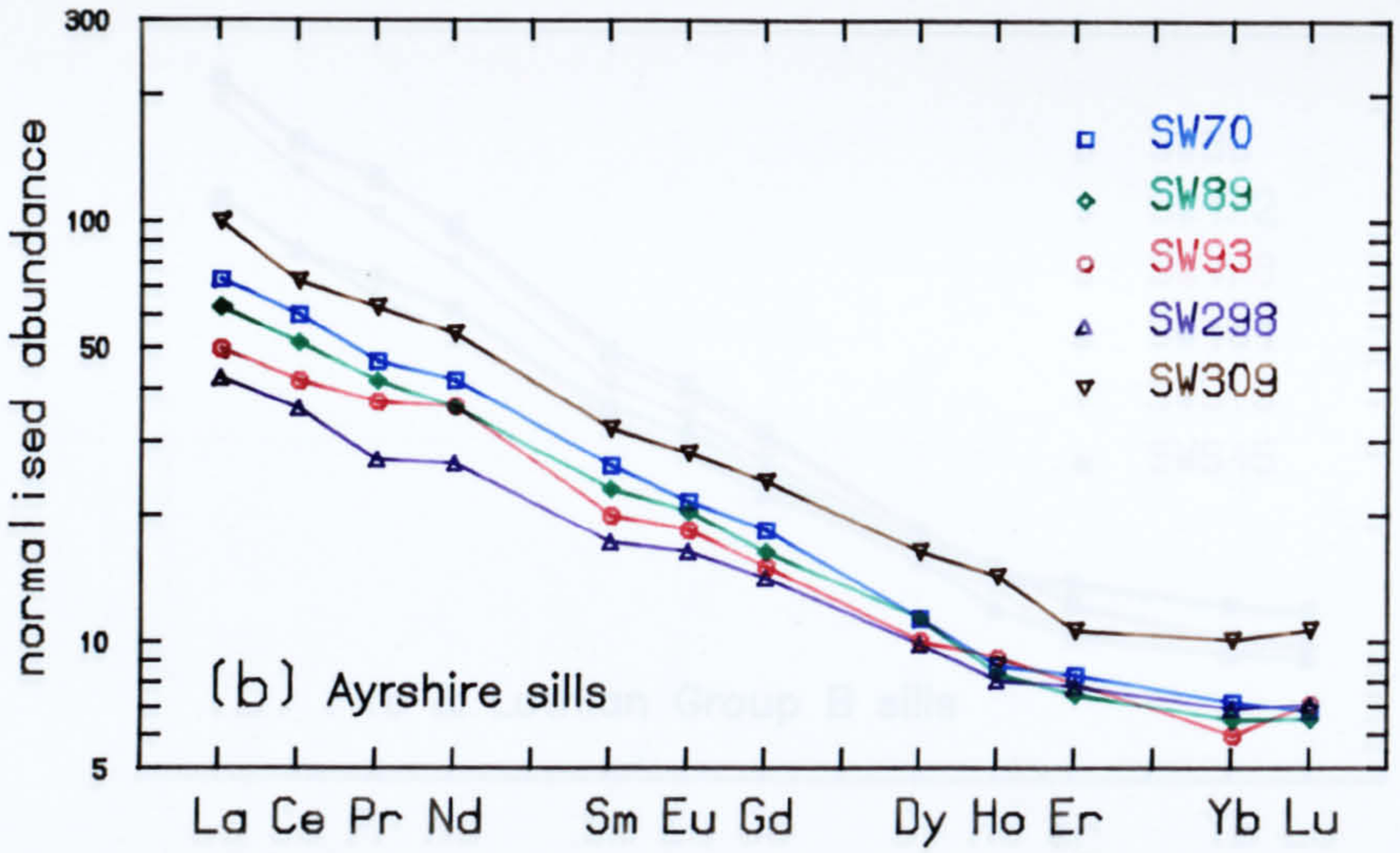

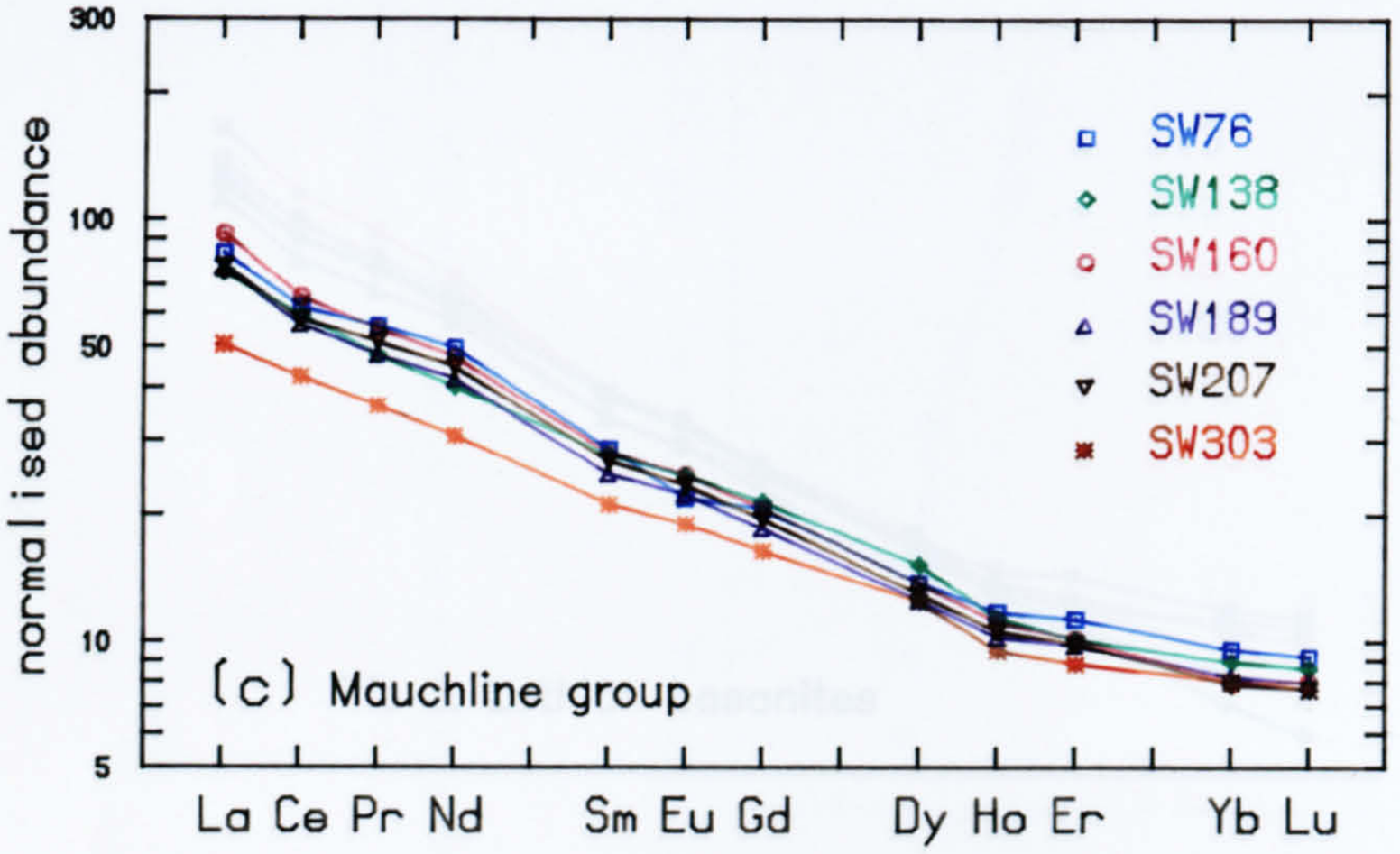

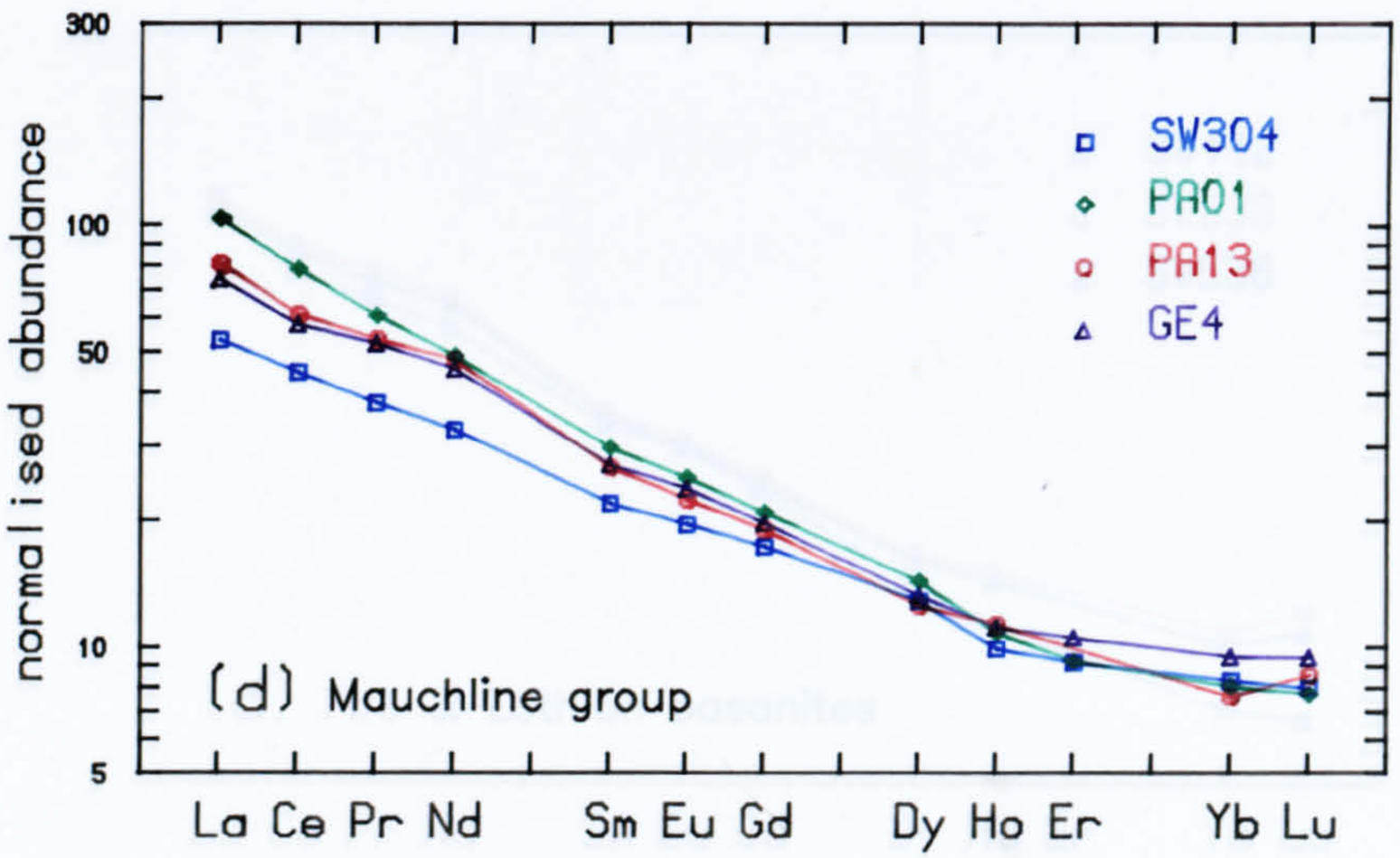

Fig. 5.44 Chondrite normalised REE abundances for samples from (a) Passage Group lavas (b) Ayrshire sills (c),(d) Mauchline group

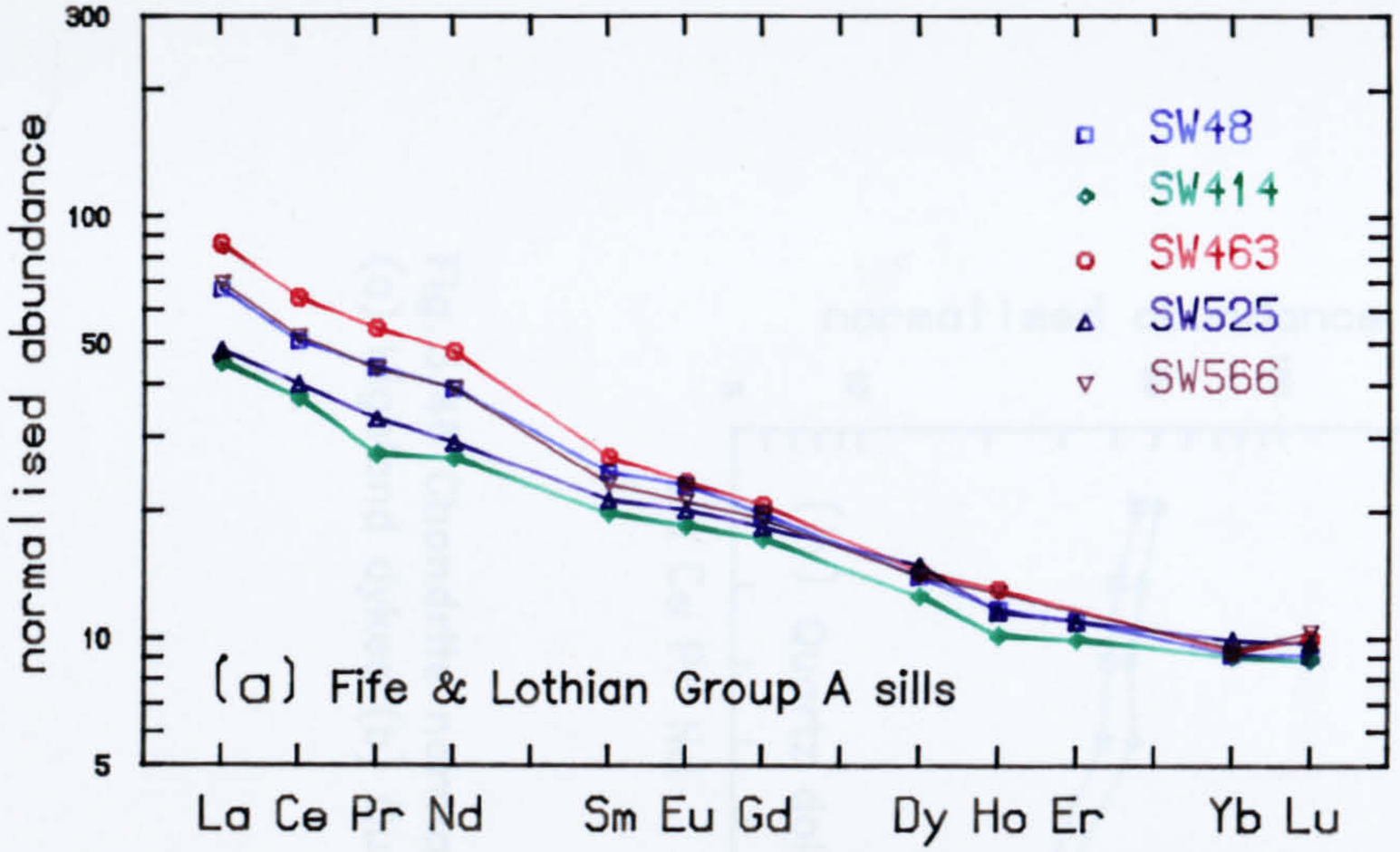

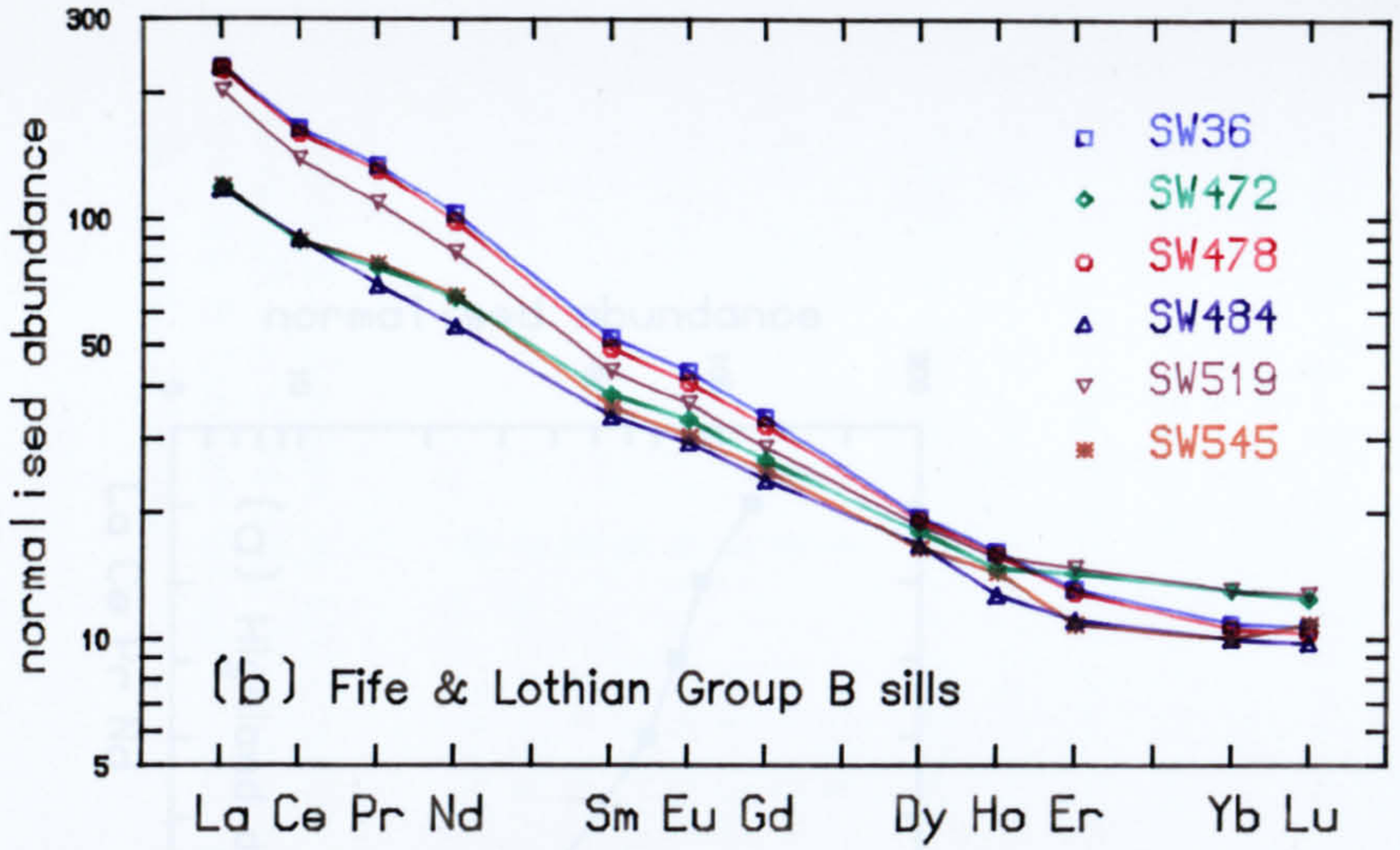

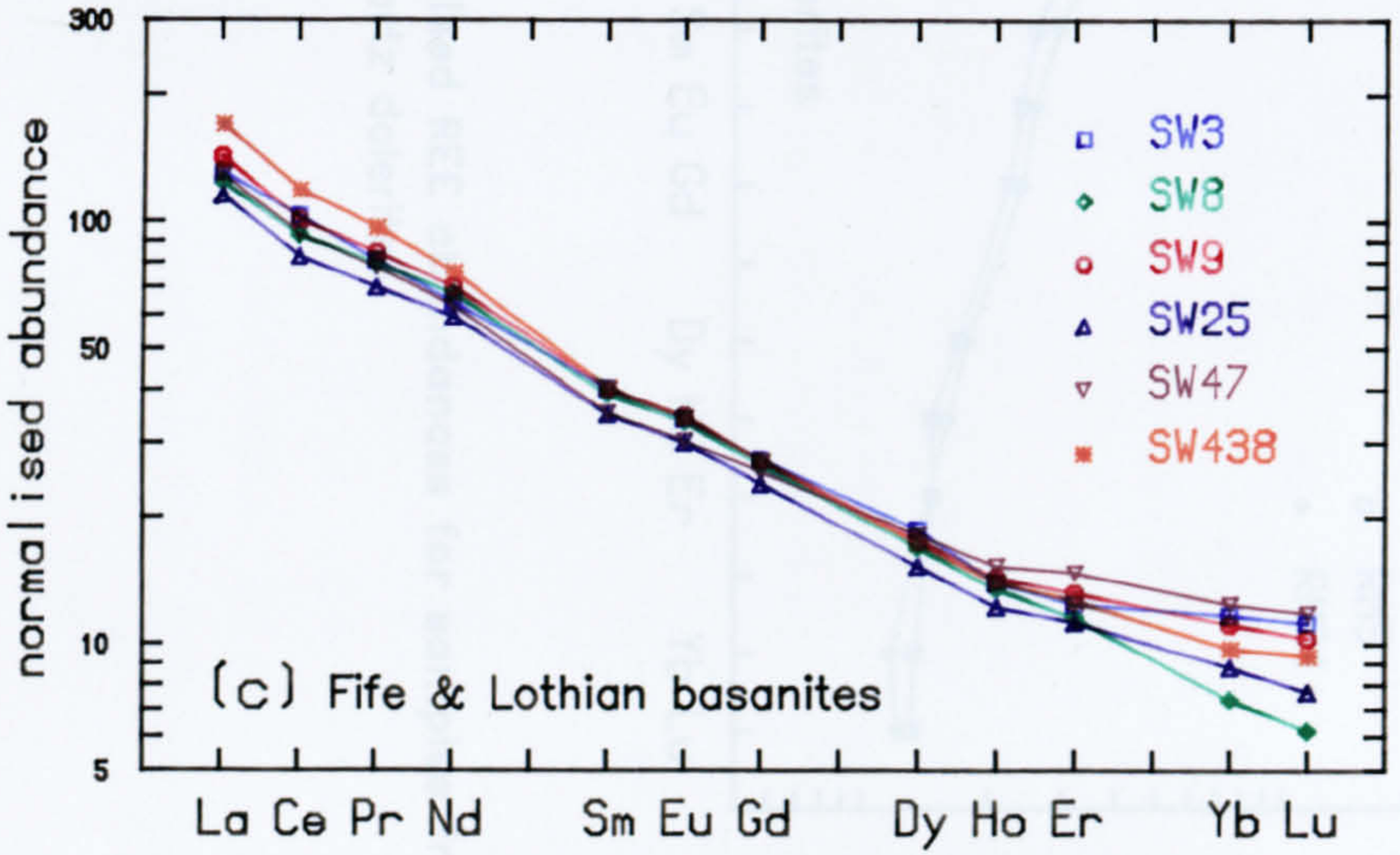

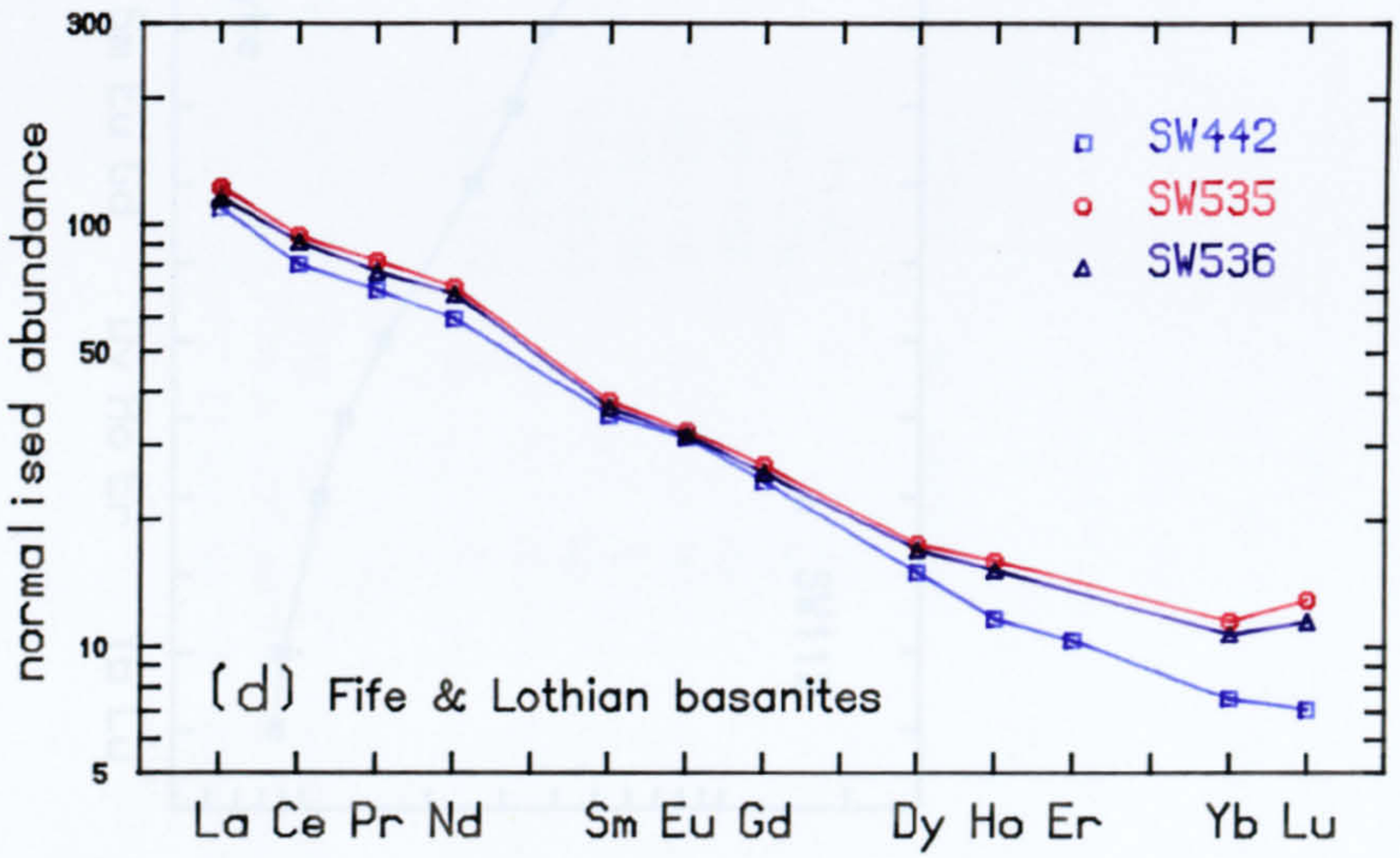

Fig. 5.45 Chondrite normalised REE abundances for samples from (a) Fife & Lothian Group A sills (b) Fife & Lothian Group B sills (c),(d) Fife & Lothian basanites.

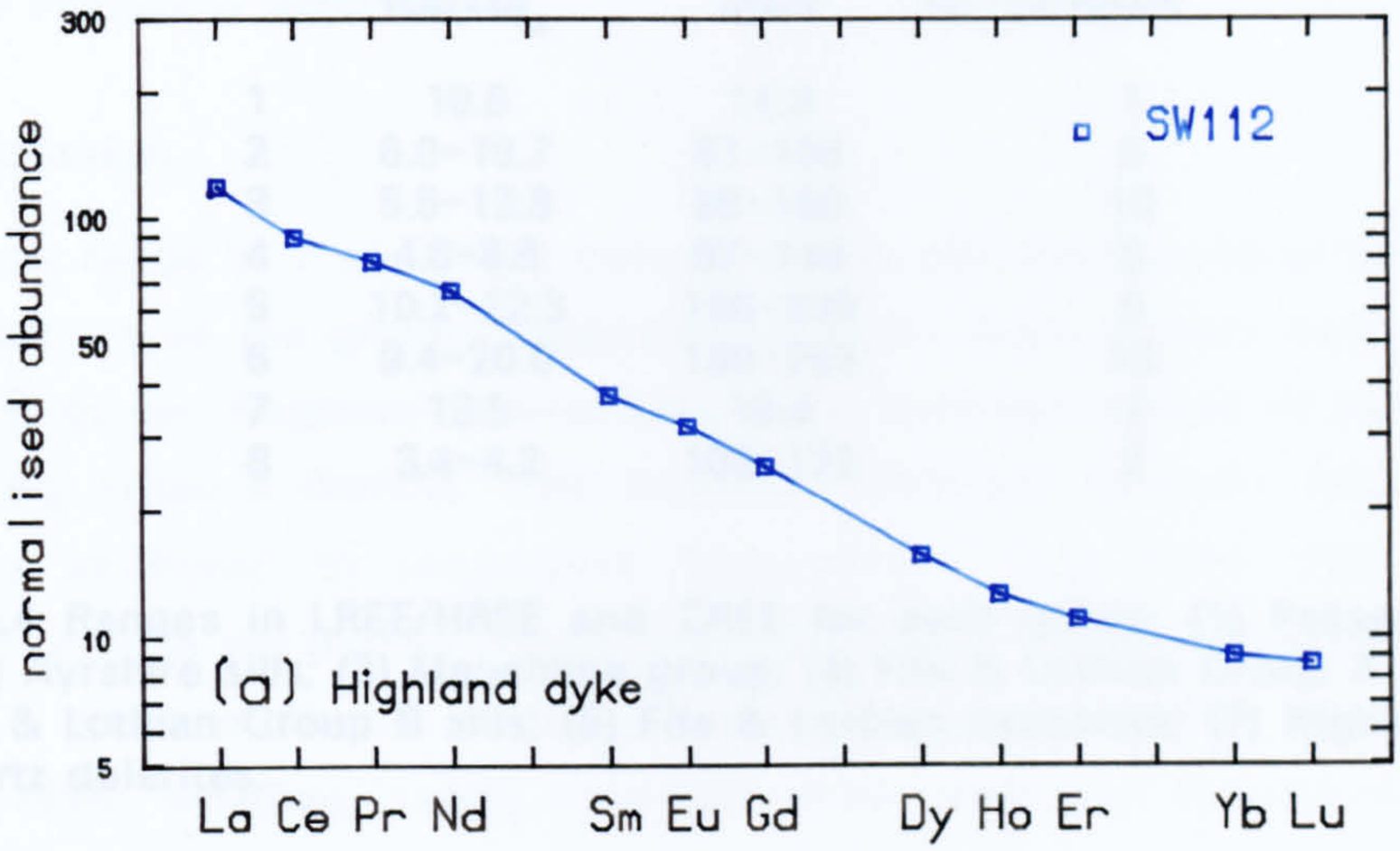

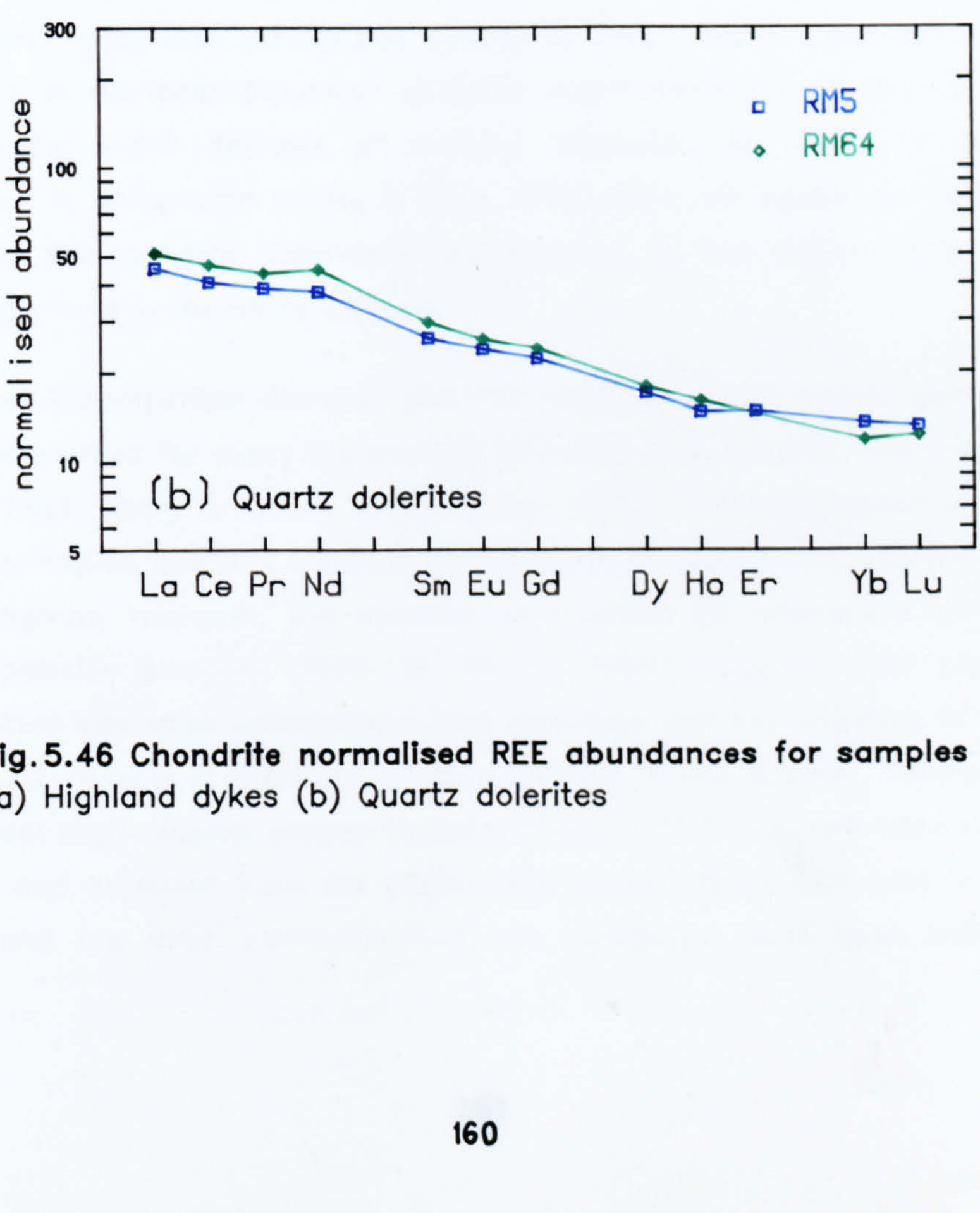

Fig. 5.46 Chondrite normalised REE abundances for samples from (a) Highland dykes (b) Quartz dolerites

	$(La/Lu)_n$	ΣREE	no. samples
1	10.6	14.9	1
2	6.0–10.7	81–166	5
3	5.5–13.8	98–160	10
4	4.6–8.6	87–149	5
5	10.2–22.3	186–339	5
6	9.4–20.0	180–253	10
7	13.5	19.4	1
8	3.4–4.2	106–122	2

Table 5.4 Ranges in LREE/HREE and ΣREE for each group: (1) Passage Group lava; (2) Ayrshire sills; (3) Mauchline group; (4) Fife & Lothian Group A sills; (5) Fife & Lothian Group B sills; (6) Fife & Lothian basanites; (7) Highland dyke; (8) Quartz dolerites.

Samples from all groups display LREE enrichment and ranges in ΣREE content and LREE/HREE are shown in Table 5.4. Comparison of these with the classification of Cullers & Graf (1984) indicates a transitional-alkaline composition for the Ayrshire samples and Group A sills from Fife & Lothian, and an alkaline-nephelinitic composition for the remaining Fife & Lothian samples and the one analysed Highland dyke. It also reflects the tholeiitic nature of the quartz dolerites.

5.5.3. Discussion

The narrow range in Y and HREE concentrations and the light-over-heavy REE enrichments in all the groups suggests that melts were derived from sources containing garnet. Negative Sr anomalies are a common feature of many alkali basalts (e.g. Fitton & Dunlop, 1985; Smedley, 1986b) and for basic samples can rarely be attributed to plagioclase fractionation. They most likely reflect depletion of Sr in the mantle source (Smedley, 1986b). Negative K-anomalies are similarly a common feature of Si-undersaturated basic magmas (e.g. Fitton & Dunlop, 1985; Smedley, 1986b). They are often attributed to retention of a K-bearing phase such as phlogopite or amphibole in the source for low degrees of partial melting. Rb is relatively incompatible in amphibole, but is easily partitioned into phlogopite (Irving & Frey, 1984). The coupled Rb-K depletions in the post-Dinantian samples might therefore indicate phlogopite retention for small degrees of melting. However, Ba which is also very compatible in phlogopite (Irving & Frey, 1984) does not appear to be depleted in any of the samples. Confident identification of the nature of a possible K-bearing phase is therefore difficult.

The flatter incompatible element and REE profiles for the quartz dolerites are typical of profiles for many continental tholeiites (e.g. Basaltic Volcanism Study Project, 1981; Norry & Fitton, 1983; Wilson, 1989). The pronounced negative P and Sr anomalies possibly indicate fractionation of apatite and plagioclase from these magmas. However, the absence of negative Eu anomalies for the two quartz dolerite samples (RM5 & RM24) might suggest that plagioclase fractionation has been unimportant, and therefore that the negative Sr anomaly of Fig. 5.42 reflects a depletion of this element in the source. Alternatively it may reflect high magma oxygen fugacity (Drake, 1975) in which case Eu will be trivalent and excluded from the plagiaclase crystal lattice. Of note is the fact that Y and the HREE concentrations still appear to have been buffered by

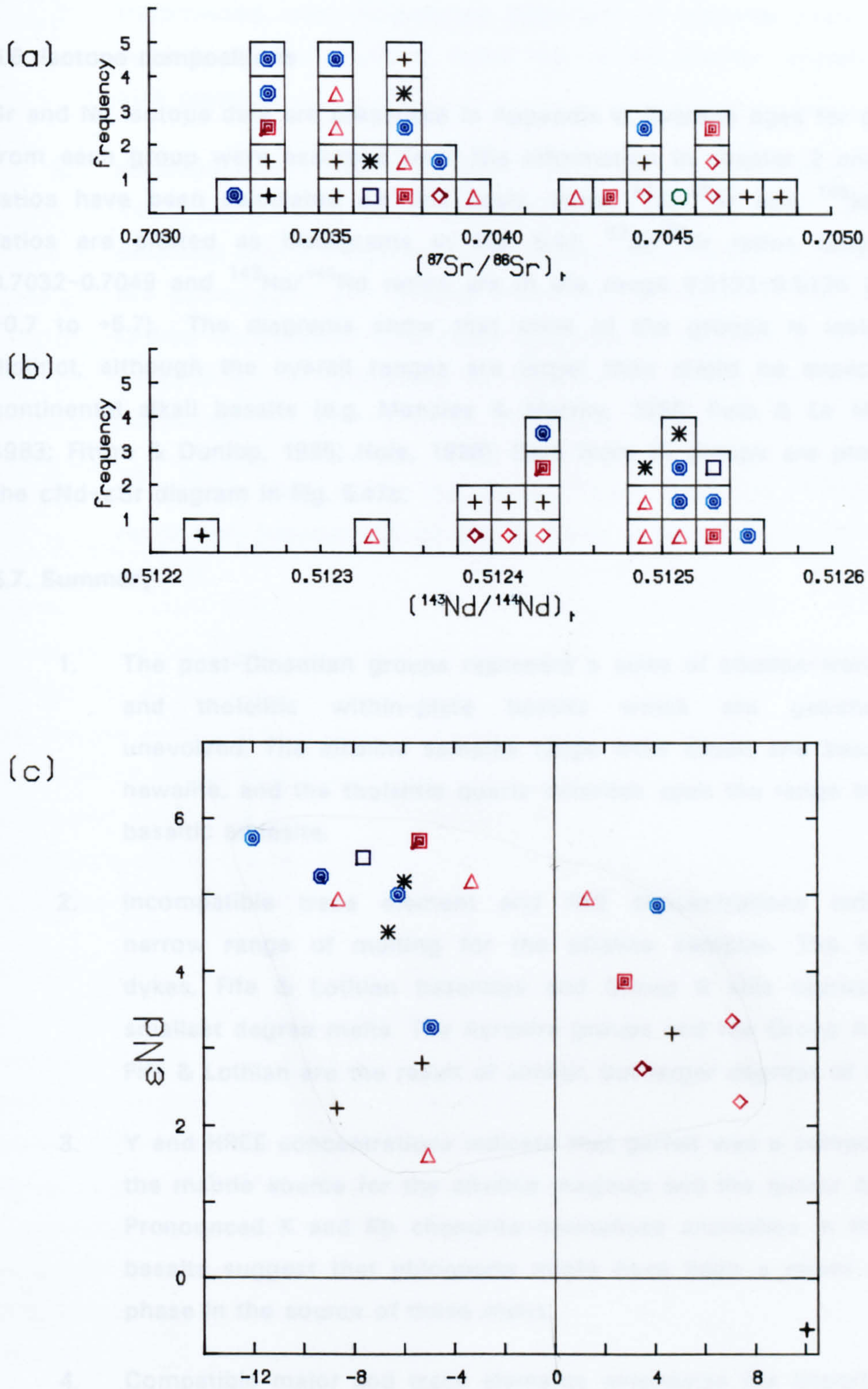

Fig. 5.47. Histograms for (a) $(^{87}Sr/^{86}Sr)_t$ and (b) $(^{143}Nd/^{144}Nd)_t$ for samples from all groups; and (c) isotope data plotted in terms of ε–units.

garnet, and there appear to be no marked depletions in Nb.

5.6. Isotope compositions

Sr and Nd isotope data are presented in Appendix V. Average ages for samples from each group were assumed from the information in chapter 2 and initial ratios have been calculated on this basis. Initial $^{87}Sr/^{86}Sr$ and $^{143}Nd/^{144}Nd$ ratios are plotted as histograms in Fig. 5.47. $^{87}Sr/^{86}Sr$ ratios range from 0.7032–0.7049 and $^{143}Nd/^{144}Nd$ ratios are in the range 0.5122–0.5126 (εNd of -0.7 to +5.7). The diagrams show that none of the groups is isotopically distinct, although the overall ranges are larger than might be expected for continental alkali basalts (e.g. Menzies & Murthy, 1980; Futa & Le Masurier, 1983; Fitton & Dunlop, 1985; .Hole, 1988). Data from all groups are plotted on the εNd–εSr diagram in Fig. 5.47c.

5.7. Summary

1. The post-Dinantian groups represent a suite of alkaline–transitional, and tholeiitic within–plate basalts which are geochemically unevolved. The alkaline samples range from basalt and basanite to hawaiite, and the tholeiitic quartz dolerites span the range basalt to basaltic andesite.

2. Incompatible trace element and REE concentrations indicate a narrow range of melting for the alkaline samples. The Highland dykes, Fife & Lothian basanites and Group B sills represent the smallest degree melts. The Ayrshire groups and the Group A sills of Fife & Lothian are the result of similar, but larger degrees of melting.

3. Y and HREE concentrations indicate that garnet was a component of the mantle source for the alkaline magmas and the quartz dolerites. Pronounced K and Rb chondrite–normalised anomalies in the alkali basalts suggest that phlogopite might have been a minor residual phase in the source of these melts.

4. Compatible major and trace elements emphasise the importance of crystal fractionation involving ol$^{+}_{-}$cpx. Variations in Al_2O_3 with MgO in whole–rock, olivine and clinopyroxene phenocrysts constrain fractional crystallisation to <36%, and indicate the dominance of

olivine fractionation in the Ayrshire samples. Clinopyroxene fractionation was increasingly important in samples from Fife & Lothian and the Highland dykes (i.e. in the smaller degree partial melt products).

5. Projections into the ol-pl-cpx (Cox & Bell, 1972), CMAS (O'Hara, 1969) and ne-ol-di (Sack *et al*, 1987) phase diagrams confirm the polybaric nature of the fractional crystallisation which is indicated in the petrography and mineral chemistry of many of the samples. Crystal fractionation took place at pressures between 0-10 kb, and exceptionally at pressures as high as 20 kb (some of the Fife basanites).

6. $(^{87}Sr/^{86}Sr)_t$ ratios are in the range 0.7032-0.7049 and $(^{143}Nd/^{144}Nd)_t$ ratios vary between 0.5122-0.5126. None of the groups is isotopicaly distinct.

CHAPTER 6

PETROGENESIS

6.1. Basalt genesis

The previous chapter outlined the geochemical characteristics of the post-Dinantian igneous suite. The alkali basalt affinities of all but the quartz dolerites were noted. The following sections present a short digression into some of the broader geochemical aspects of basalt genesis with emphasis on alkali basalts. Three 'popular' models for the generation of OIB are presented and the effects of lithospheric and crustal interaction are discussed. Succeeding sections discuss the inferred effects of these processes on the post-Dinantian magmas.

6.1.1. Compositional constraints

Efforts to quantify the composition of the Earth's mantle through analysis of the basaltic products of partial melting have met with some success over the last decade. If consideration is limited to oceanic volcanism it can be assumed that magma compositions reflect the composition of a sub-lithospheric source with little or no additional lithospheric or crustal components. This is because all oceanic plates are young (<200Ma) and comprise uncomplicated refractory lithospheric mantle, underlying a structurally and lithologically simple basaltic crust (Norry & Fitton, 1983).

Oceanic basalts can be divided into two groups: MORB and OIB. The more voluminous is MORB. Trace element and experimental studies (e.g. Gast, 1968; Jaques & Green, 1980) have shown MORB to be the result of 20-30% partial melting of a lherzolite source. Depletions in LILE associated with inferred ancient melting events producing low Rb/Sr and Nd/Sm ratios, are coupled with non-radiogenic $^{87}Sr/^{86}Sr$ and radiogenic $^{143}Nd/^{144}Nd$ ratios. The MORB source is therefore thought to represent the depleted mantle residue left after the extraction of continental crust. Various models (e.g. De Paolo & Wasserburg, 1976; Jacobsen & Wasserburg, 1979; O'Nions *et al*, 1979; De Paolo, 1980) have proposed that primitive mantle began to differentiate between 1 and 3.5 by ago. Calculations indicate that c.50% of the mantle has been depleted in this way (Ringwood, 1975; O'Nions *et al*, 1979; Anderson, 1982b; Hofmann *et al*, 1986).

However, Pb isotope compositions indicate that a single stage closed-system evolutionary model is not completely satisfactory. If it was, the resulting MORB mantle source should show depletion in U/Pb (since U is more incompatible than Pb, (Tatsumoto, 1978)), and $^{206}Pb/^{204}Pb$ and $^{207}Pb/^{204}Pb$ for MORB would fall to the left of the primary geochron and below the mantle growth curve (Anderson, 1982a) rather than to the right. Various authors have attributed this 'Pb paradox' to processes such as core formation, influx of meteoric material after core formation, multistage mantle evolution, secular increase of U/Pb ratio, mantle mixing or continuous input of crustal radiogenic Pb (summarised by Sun, 1980).

In contrast to MORB, OIB show enrichments in LILE. However this is not reflected in their isotopic compositions, which imply a time-integrated depletion in Rb and Nd with respect to Sr and Sm. So, compared to the MORB source, the OIB source is characterised by more radiogenic Pb and Sr and less radiogenic Nd (Wilson, 1989). Early considerations of Sr and Nd isotope compositions led to the suggestion of mixing between OIB and MORB sources to produce the so-called 'mantle array'. However, as isotopic data have increased, it has become apparent that there is more than one OIB source. Weaver *et al.* (1987) summarised four hypothetical sources for the origin of OIB.

1. Primordial lower mantle which has undergone little or no chemical fractionation since shortly after the fractionation of the Earth (Schilling, 1973; Sun & Hanson, 1975; Dupre & Allègre, 1980; Allègre, 1982).

2. Subducted ocean crust which has had a considerable residence time at the core/mantle boundary or at the boundary between the upper and lower mantle (Hofmann & White, 1982; Ringwood, 1982; Vollmer, 1983; White, 1985).

3. Material which was originally part of the subcontinental lithospheric mantle, but which is now resident in the asthenosphere (McKenzie & O'Nions, 1983; Cohen *et al*, 1984).

4. A mantle source which has been contaminated by recycled continental crustal material (Hawkesworth *et al*, 1979; Cohen &

O'Nions, 1982; White, 1985).

Zindler & Hart (1986) and Hart (1988) suggested three major enriched mantle components:

1. The uranium-rich component (HIMU) with high U/Pb ratios. Processes to account for this include the extraction of Pb into the core (Vollmer, 1977; Vidal & Dosso, 1978), recycling of ancient continental crust (Allègre & Turcotte, 1985), recycling of ancient oceanic crust (Chase, 1981; Zindler *et al.*, 1982; Hofmann & White, 1982) and intra-mantle metasomatism (Hart *et al.*, 1986; Zindler & Hart, 1986).

2. Enriched mantle 1 (EM1) with radiogenic Sr, very unradiogenic $^{206}Pb/^{204}Pb$ (rivalled only by a few MORB samples), and the lowest $^{143}Nd/^{144}Nd$ present in the oceans. Hart (1988) assigned a metasomatic origin to EM1 and suggested that EM1 and HIMU may be complementary parts of the same metasomatic process (infiltrate versus residue).

3. Enriched mantle 2 (EM2) with the highest $^{87}Sr/^{86}Sr$ of all oceanic mantle, coupled with intermediate $^{206}Pb/^{204}Pb$ and $^{143}Nd/^{144}Nd$. The most popular models accounting for EM2 invoke the subduction and recycling of continental material (e.g. Hofmann & White, 1982; Chase, 1981; White & Hofmann, 1982).

6.1.2. Mantle models

Although it seems likely that the OIB source has experienced various (often ancient) contamination events, in the long term it must have evolved in isolation from the MORB source. This has led to the development of numerous models which can be summarised under three headings: (1) Stratified mantle, (2) Heterogeneous (streaky) mantle, (3) Metasomatised mantle.

6.1.2.1. Stratified mantle

Most stratified mantle models propose an undifferentiated lower mantle below c.600km (OIB source) with a differentiated upper mantle (MORB source) above 600km. One exception to this is Anderson's (1982a) model. He proposed an upper anciently enriched and a lower anciently depleted layer. He showed how magmas from such an enriched reservoir could mix with magmas from a depleted reservoir and still maintain LILE enrichment patterns whilst displaying isotopic ratios which ranged from depleted to enriched in composition. The low-viscosity zone differentiation model of Green (1971) also placed the OIB source at a shallower level than the MORB source. The continuous upward migration of small amounts of silica-undersaturated melt enriched in incompatible elements was thought to cause depletion through most of the low velocity zone (LVZ), creating the MORB source. Re-precipitation of these elements at higher, cooler levels enriched the potential OIB source.

However, the recognition of mantle xenoliths in OIB which contain an established 'old' MORB component with 'recent' additions of OIB-like material (Menzies & Hawkesworth, 1987) implies that OIB are derived from greater depths than MORB. Most authors have now relegated the OIB source to the lower mantle, from where melts are derived by mantle plume activity (e.g. Sun & Hanson, 1975; Allègre *et al*, 1981,1982; Thompson *et al*, 1984; Menzies & Hawkesworth, 1987).

The possible primordial nature of the OIB source has been debated. The identification of high $^{3}He/^{4}He$ ratios in young OIB (Kurz *et al*, 1982) indicates a primordial component in their genesis. (^{3}He in mantle gases is mostly primordial whereas ^{4}He is primarily radiogenic, produced by the decay of ^{238}U, ^{235}U and ^{232}Th (Kurz *et al*, 1982)). Alternatively, Hofmann *et al*, (1986), have used Nb/U and Ce/Pb ratios to suggest that a primordial origin is not tenable. Their argument was based on the similarity of Nb/U and Ce/Pb ratios for OIB and MORB, which are different from chondritic abundances. They advocated a three stage mantle evolution model: (1) Chemical depletion of the mantle by removal of incompatible elements during crustal fractionation; (2) homogenisation of the mantle through efficient convection; (3) internal differentiation via the processes of subduction and recycling to produce separate OIB and MORB sources. During these secondary differentiation processes the bulk partition coefficients of Nb and Ce must have been very

similar to those of U and Pb respectively.

6.1.2.2. Heterogeneous mantle

In contrast to the stratified mantle models are models involving asthenosphere which is heterogeneous on a small scale (<10m) (e.g. Sun, 1980; Zindler *et al*, 1984; Sleep, 1984; Fitton & Dunlop, 1985; Fitton & James, 1986). Small degrees of melting will preferentially sample pods or streaks of more enriched mantle producing the characteristic LILE-enriched compositions of OIB. More extreme melting eliminates these differences to produce MORB. Fitton & Dunlop (1985) proposed the presence of numerous enriched streaks within the asthenosphere. These represent pockets of ancient enriched magmas (Fitton & Dunlop, 1985) or patches of subducted ocean floor (Fitton & James, 1986). Enriched in LILE compared to their MORB source, they would both evolve over geological time to higher $^{87}Sr/^{86}Sr$ and $^{206}Pb/^{204}Pb$ ratios and lower $^{143}Nd/^{144}Nd$ ratios than the bulk asthenosphere. Convection would cause large-scale mantle homogenisation, with the persistence of small-scale (m-km) homogeneities for long periods (Olsen *et al*, 1984). Fitton & Dunlop (1985) calculated that the Cameroon Line Lavas represented <0.34% batch melting of such a source. They showed how a magma produced by 10% partial melting of a depleted mantle source could assume the trace element content of a 0.2% equilibrium partial melt via the process of grain boundary percolation. This process depends on trace elements being concentrated at grain boundaries (Kleeman *et al*, 1969; Basu & Murthy, 1977; Stosch & Seck, 1980), and melt migrating rapidly along such boundaries instead of through large conduits. This will be achieved if, as suggested by Mckenzie (1985), the amount of melt present in the mantle is always restricted to <3%.

6.1.2.3. Metasomatised mantle

The need to account for recent LREE enrichment without appealing to 'impossibly small' degrees of partial melting has attracted many authors to models proposing mantle metasomatism as a precursor to alkaline magmatic activity (e.g. Lloyd & Bailey, 1975; Boettcher & O'Neil, 1980; Menzies & Murthy, 1980; Wass, 1980; Futa & Le Masurier, 1983; Roden *et al*, 1984; Bailey, 1987). A general sequence of events would involve:

1. Non-uniform enrichment of depleted lithospheric mantle in LREE, Ti,

Al, Fe, Ca, Na, K, H_2O, CO_2, Rb, Sr, Y, Zr, Nb, Ba and La by the infiltration of volatile-rich fluids or melts.

2. Later fusion initiated by either: (a) increasing the volatile concentration and hence lowering the mantle solidus or (b) increasing the mantle geotherm (e.g. perturbation due to upwelling of asthenospheric mantle).

The resulting liquid would be one of alkali basalt affinity, enriched in the elements listed above. There would be no need however, to limit melting to less than 1-2%. Enriched LILE concentrations would be achieved by 5-11% melting which is thought by many authors to be more acceptable, and correlates well with experimental determinations. However, McKenzie (1984, 1985, 1987) has shown that the extraction of small degree partial melts need not be a problem. Under volatile-rich conditions, melt segregation can take place when the melt fraction is as low as 0.1%.

6.1.3. Wall-rock interaction

Observations on the similarities of OIB and continental alkali basalts (Allegre *et al*, 1981; Norry & Fitton, 1983; Fitton & Dunlop, 1985; Menzies, 1987) bear witness to a common source in the underlying asthenosphere or mesosphere. It therefore negates the necessity for mantle metasomatism as a precursor to all alkaline magmatism. Although magma may interact with lithospheric mantle and crust in an oceanic setting, the effects on magma composition will be insignificant because of their depleted nature. However, the continental crust and lithosphere have both experienced a long and complicated tectonic and magmatic history (Norry & Fitton, 1983), and long-term stability of the mantle immediately beneath continents helps preserve the trace element heterogeneities that have allowed isotopic variations to develop. As a result, assimilation processes might be expected to affect the geochemical characteristics of magmas.

The extent of magma/wall-rock interaction is dependent on several factors: the temperature, composition and rate of ascent of the magma, its mode of transport through the lithosphere and crust, and the composition of the wall-rocks. Huppert & Sparks (1985) emphasised two styles of contamination:

assimilation and fractional crystallisation (AFC) in magma chambers, and contamination during ascent. AFC processes are possibly of relevance when considering the large quartz dolerite sill complex. However small phenocryst sizes, the presence of mantle xenoliths in many samples and the unevolved compositions of all of the alkaline post-Dinantian lavas indicate rapid rates for magma ascent, with little or no residence times in magma chambers. (Calculations by Spera (1984) based on the preservation of garnet megacrysts in the Fife basanites, indicated ascent velocities of 2-5ms^{-1} for these magmas, from depths of c.75km). When flow is entirely laminar some magma solidifies on the conduit wall preventing contamination of the remaining magma (Huppert & Sparks, 1985). Turbulent flow increases the likelihood of contamination. It is likely that the post-Dinantian alkaline magmas ascended with laminar flow.

Rocks with low fusion temperatures will be selectively melted. In the lithosphere mantle these are likely to be secondary metasomatic and magmatic veins and patches; in the continental crust silica-rich rocks such as pegmatite and granite will be particulary prone to melting, as opposed to rocks with more refractory compositions (gabbros, amphibolites and ultramafites). However, the enrichment of alkali basalts in strongly incompatible elements makes them relatively insensitive to the addition of small amounts of material enriched in these elements. The compositions of many continental flood basalts are thought to represent the extreme of expected lithospheric mantle and/or crustal interaction. This is reflected by high Ba, Rb, Th, K and LREE contents and $^{87}Sr/^{86}Sr$ ratios, and in negative Nb and Ta anomalies, compared to those of ocean island tholeiites.

The inferred effects of lithospheric mantle and crustal interaction on post-Dinantian samples are discussed in section 6.2.2.

6.2. Modelling the post-Dinantian suite: post-partial melting processes

The previous sections have shown that the geochemical characteristics of a primary basaltic magma are inherited from its source and are dependant on the degree of melting and extraction proccess, and the mineralogical and chemical characteristics of the source. However, subsequent chemical changes depend on a variety of processes operating on the magma up to its consolidation, as well as proccesses affecting its solidified products. The more common of these processes are fractional crystallisation, lithospheric/crustal assimilation, and

alteration. The inferred effects of each of these processes on the post-Dinantian samples are discussed below, prior to discussion of partial melting processes.

6.2.1. Alteration and fractional crystallisation

The effects of alteration were discussed in section 5.1 where it was indicated that there is no correlation between LOI and element concentration. It was therefore concluded that the effects of alteration were (with a few stated exceptions) minimal.

Phenocryst phases in the basaltic (>6wt% MgO) members of the post-Dinantian suite are limited to ol$^{+}_{-}$cpx. Since none of the 'spiderdiagram elements' (Rb, Ba, K, Nb, La, Ce, Sr, Nd, P, Zr, Ti, & Y) are notably compatible in either of these phases, their concentrations would be expected to increase with fractionation, whilst approximately maintaining inter-element ratios. However, if one element is more easily partitioned into one of the phenocryst phases than another, inter-element fractionation will result. This is demonstrated using P_2O_5 and TiO_2 which are plotted for each sample in Fig. 6.1.

Two observations can be made:

1. The six alkaline groups overlap to some extent with the highest TiO_2 and P_2O_5 concentrations displayed by the Fife & Lothian sills and basanites, and the Highland dykes. The quartz dolerites plot in a compositionally distinct group.

2. The Passage Group lavas, Ayrshire sills and most of the Mauchline group samples are reasonably tightly constrained groups in terms of P_2O_5 and TiO_2. The reverse is true of the Fife & Lothian basanites and sills and the Highland dykes which show a greater degree of scatter.

Fig 6.2 shows the same diagram with fields marked for the alkaline and tholeiitic samples. Superimposed on it is a melting curve for a MORB source (see discussion in section 6.3.1), calculated using the D-values of Fitton & James (1986). The position of such melting curves in compositional space is

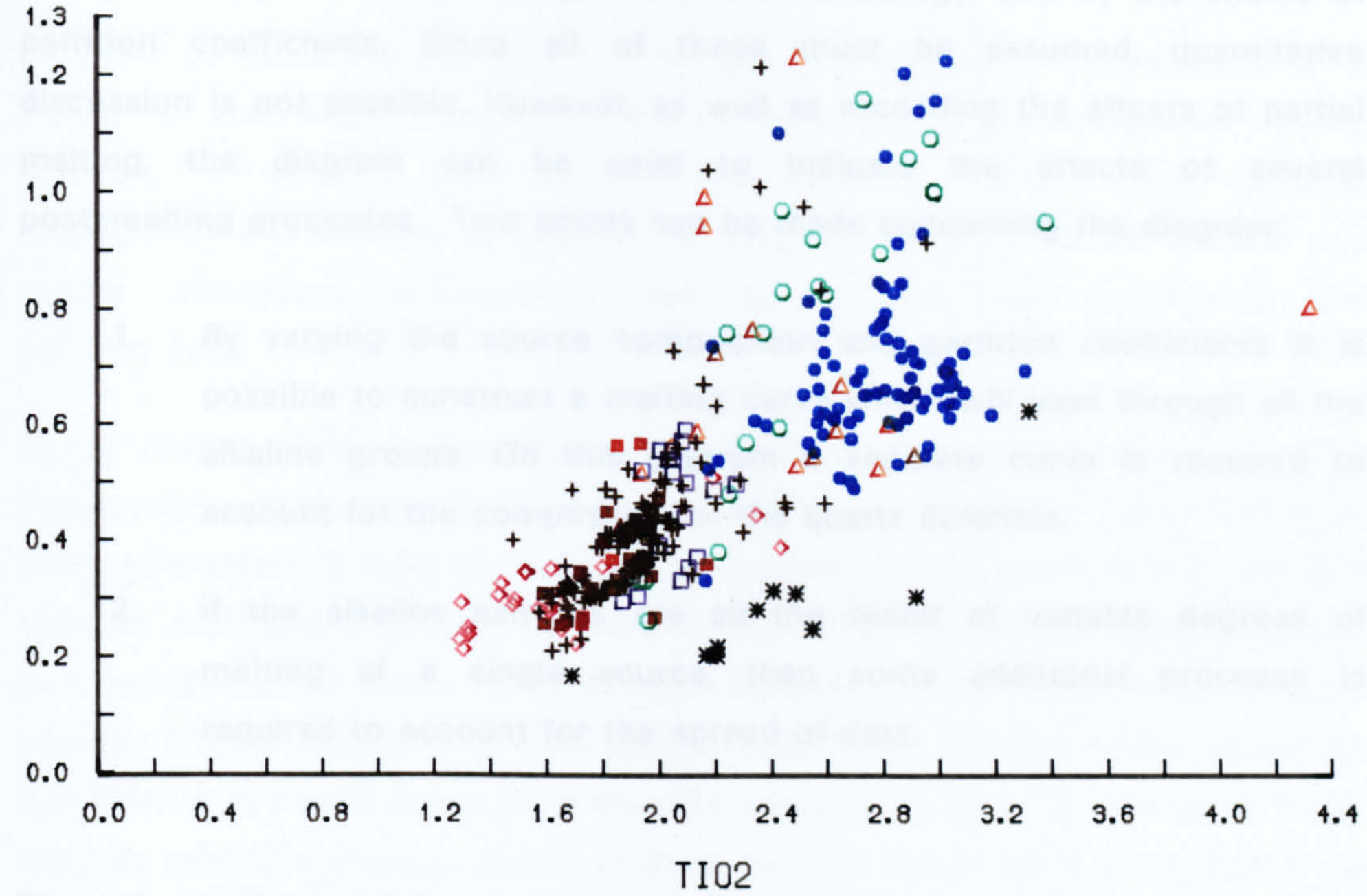

Fig. 6.1 P_2O_5 plotted against TiO_2 for samples from all the groups.

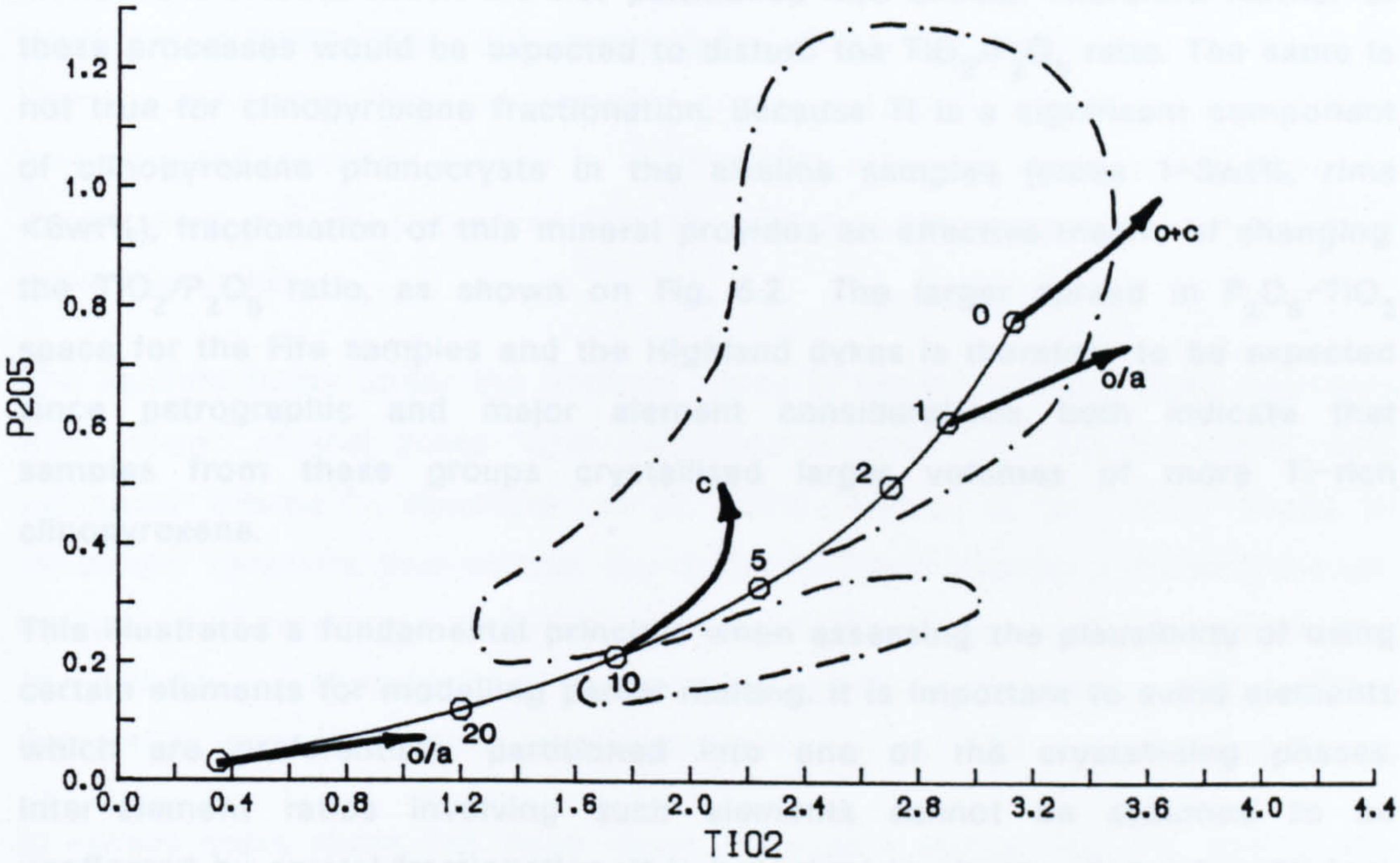

Fig. 6.2 MORB source melting curve superimposed on the P_2O_5 v TiO_2 plot.
Numbers refer to % partial melting. D values for the melting curve are from Fitton & James (1986): D_{Ti}=0.111, D_P=0.0353. The vectors represent the effects of olivine fractionation and/or alteration (o/a), clinopyroxene fractionation (c), and ol+cpx fractionation (ol+cpx) in the proportion 75:25.

constrained by the source composition and mineralogy, and by the choice of partition coefficients. Since all of these must be assumed, quantitative discussion is not possible. However, as well as modelling the effects of partial melting, the diagram can be used to indicate the effects of several post-melting processes. Two points can be made concerning the diagram:

1. By varying the source composition and partition coefficients it is possible to construct a melting curve which will pass through all the alkaline groups. On this diagram a separate curve is required to account for the composition of the quartz dolerites.

2. If the alkaline samples are all the result of variable degrees of melting of a single source, then some additional proccess is required to account for the spread of data.

The effects of crystal fractionation (ol & cpx) and alteration are indicated by vectors on Fig. 6.2. They show that it is impossible to distinguish between the effects of alteration and olivine fractionation since TiO_2 and P_2O_5 are both immobile elements which are not partitioned into olivine. Therefore neither of these processes would be expected to disturb the TiO_2/P_2O_5 ratio. The same is not true for clinopyroxene fractionation. Because Ti is a significant component of clinopyroxene phenocrysts in the alkaline samples (cores 1-3wt%, rims <6wt%), fractionation of this mineral provides an effective means of changing the TiO_2/P_2O_5 ratio, as shown on Fig. 6.2. The larger spread in P_2O_5-TiO_2 space for the Fife samples and the Highland dykes is therefore to be expected since petrographic and major element considerations both indicate that samples from these groups crystallised larger volumes of more Ti-rich clinopyroxene.

This illustrates a fundamental principle when assessing the plausibility of using certain elements for modelling partial melting. It is important to avoid elements which are preferentially partitioned into one of the crystallising phases. Inter-element ratios involving such elements cannot be assumed to be unaffected by crystal fractionation. It is important to choose elements with low, but different, partition coefficients.

6.2.2. Lithospheric mantle and crustal assimilation

In order to assess more properly the possible effects of assimilation, it is helpful to have some indication of the compositions of the lithospheric mantle and crust. Information about upper crustal rocks is relatively easily obtained through surface outcrop and borehole data. Evidence for lower crustal and mantle lithosphere compositions must be inferred from geophysical and xenolith data.

Upper crustal rocks in the Midland Valley and Southern Uplands are mainly Palaeozoic sediments. North of the Highland Boundary fault Dalradian metasediments dominate the succession. Seismic studies north of the Southern Uplands fault (LISPB profile: Bamford *et al*, 1976, 1977, 1978) have identified two lower crustal layers: a basal unit between 7 and 15km thick (P-wave velocity c.7kms^{-1}) extending from depths c.18-23km, and above this at depths c.6-14km, a granulite facies layer (P-wave velocity >6.4kms^{-1}). This upper layer reaches relatively shallow depths (7-8km) beneath the Midland Valley (Upton *et al*, 1983).

The identification of basic and acid granulite xenoliths as inclusions in Midland Valley vents has been used to substantiate the two layer lower crustal model. Upton *et al.* (1983, 1984) and Hunter *et al.* (1984) suggested that the one- or two-pyroxene granulites are samples of the deeper layer. On the assumption that chemical zonation results in increasingly siliceous rocks with decreasing depth, these authors suggested that the acid gneisses were derived from more superficial layers.

The seismic Moho under the Midland Valley is sharp, implying rapid transition from lower crustal rocks with velocities c.7kms^{-1} to mantle rocks with velocities c.8kms^{-1}. (Bamford *et al*, 1978; Hunter *et al*, 1984). Study of ultramafic xenoliths implies that the Scottish Upper mantle is heterogeneous: composed of tectonised lherzolite and harzburgite cross-cut by younger bodies of wehrlite, websterite, clinopyroxenite, garnet pyroxenite and various kaersutite- and biotite-rich ultramafites (Upton *et al*, 1983, see also chapter 3).

In recent years there has been much discussion concerning the age of the lower crust and lithosphere beneath Scotland. The granulite basement beneath the Midland Valley was assumed to be of Lewisian age. However, Hunter *et al*, (1984) noted a chemical distinction between basic pyroxene granulites of the

Midland Valley, and those of the Lewisian Complex of north west Scotland. Recent isotopic data have indicated significantly younger ages c.1100-1000 Ma ((Grenvillian) Aftalion *et al*, 1984; Davies *et al*, 1984) or perhaps younger than this (Halliday *et al*, 1985). Other evidence has been sought from the late Caledonian granites. Combined Sr, Nd, Pb and O isotope data have confirmed the importance of continental lithosphere in the generation of the granites (Blaxland *et al*, 1979; Halliday *et al*, 1979; Harmon & Halliday, 1980). The more radiogenic Pb compositions of Southern Uplands granites compared with those of north-west Scotland have been interpreted as indicating a younger crustal layer in the south of Scotland. Zircons extracted from the late Caledonian granites north-west of the Highland Boundary fault have a marked isotopic Pb memory which is absent from zircons in granites to the south-east (i.e. those of the Southern Uplands: Pidgeon & Aftalion, 1978). A similar NW-SE division has been identified for the Nd-isotope compositions of these granites (Halliday 1984), with εNd values <-6 to the north and >-6 the the south.

Xenolith data appear to confirm these observations. Calculated Sm-Nd model ages for both granulite and peridotite xenoliths echo the Caledonian granite trend, and increase towards the north-west (Halliday *et al*, 1985). The peridotite xenolith data are particularly important since they attest to a similarity in age between the lithospheric mantle and crust.

It is now accepted that the continental crust is underlain by heterogeneous lithospheric mantle (Menzies & Halliday, 1988). The extent of these heterogeneities in the Scottish lithospheric mantle has been tested by Menzies & Halliday (1988). Xenoliths from the Outer Hebrides (Loch Roag) are extremely heterogeneous, with respect to Nd isotopes with εNd=-32 to -2.6, indicating the enriched nature of the sub-Archaean mantle in Scotland (Menzies *et al*, 1987; Menzies & Halliday, 1988). The sub-Proterozoic mantle represented by xenoliths from Streap Comlaidh in the Highlands is variably enriched in ^{87}Sr with εSr=-15 to +88. The xenoliths appear to have been modified by the influx of Ba, Rb and LREE possibly due to subduction processes (Menzies & Halliday, 1984, 1988). Midland Valley lithospheric mantle sampled by the Black Rocks vent is similar to the source for OIB. Menzies & Halliday (1988) suggested that this might indicate considerable thinning and modification of the lithospheric mantle by upwelling asthenospheric melts.

The presence of old enriched mantle at Loch Roag, and mantle enriched in ^{87}Sr

at Steap Comlaidh is compatible with an observed increase in Ba, Sr, LREE, P and Nb towards the north-west in ORS subduction-related magmas (Thirlwall, 1982, 1986). REE and isotopic compositions ruled out significant crustal contamination of these rocks, therefore suggesting a variably enriched mantle source deep in the lithosphere or in the asthenosphere (Thirlwall, 1986). ORS lavas in the Midland Valley appear to have been derived from a long-term LREE-depleted mantle source modified by interaction with subducted oceanic lithosphere (Thirlwall, 1981).

All these observations imply that there is no basis for advocating the presence of highly enriched mantle as a magma source beneath the Midland Valley. The composition of the lithospheric mantle may be largely indistinguishable from asthenospheric reservoirs (Smedley, 1986b) making it difficult to discriminate between the two as possible sources, or to identify the lithospheric mantle as a possible contaminant.

The possible importance of lithospheric mantle and continental assimilation processes on the trace element geochemistry of the post-Dinantian igneous suite has been assessed by comparison with the OIB data set of J.G. Fitton & D.E. James (pers. comm., 1989). Plots involving K_2O, Rb, Sr, Ba and TiO_2 (Figs. 6.3 & 6.4) indicate that Ba is the only element to deviate significantly from the OIB field, and then only for a few samples. The cause of high Ba concentrations in these samples was discussed in section 5.1 and is thought to represent the combined influences of partial melting and alteration.

Thompson *et al.* (1983, 1984) suggested that the ratio La/Nb might be a useful index of contamination in magmas, since OIB, continental alkali basalts and kimberlites all have La/Nb <1 and continental flood basalts range between 0.5-7. La/Nb ratios have been determined for the 38 samples analysed for REE by ICP (section 5.5.2). Fig 6.5 compares the ratios for these samples with La/Nb for OIB, continental alkaline basalts (and kimberlites) and continental flood basalts (data from Thompson *et al.*, 1983, 1984 and Fitton *et al.*, 1988). It shows that all the Midland Valley samples (including the quartz dolerites) fall entirely within the fields of OIB and continental alkaline basalts. The two quartz dolerite samples have the highest La/Nb ratios, a reflection of their derivation by larger degrees of melting.

Fig 6.6 compares εNd and εSr for the post-Dinantian samples, Southern

(a)

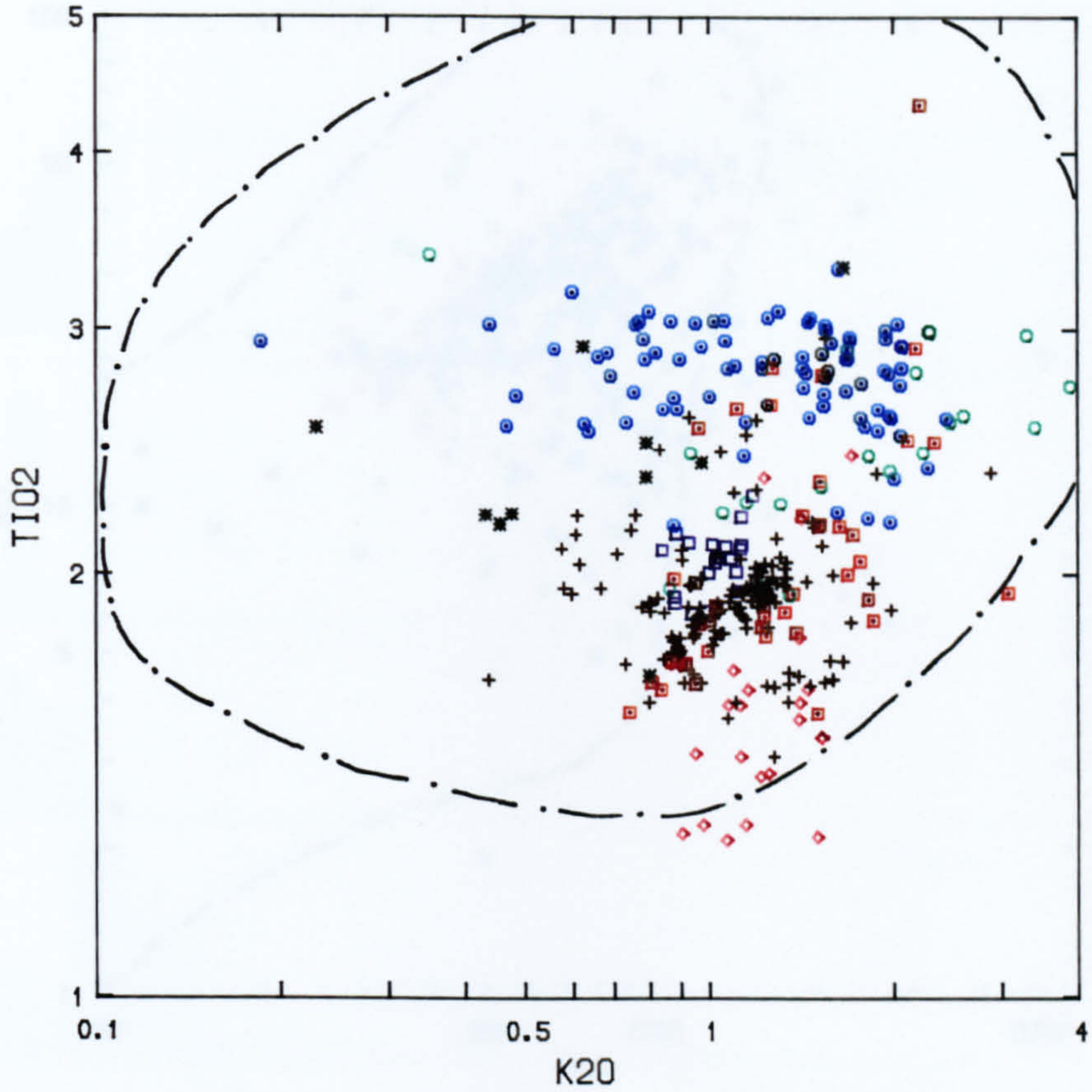

(b)

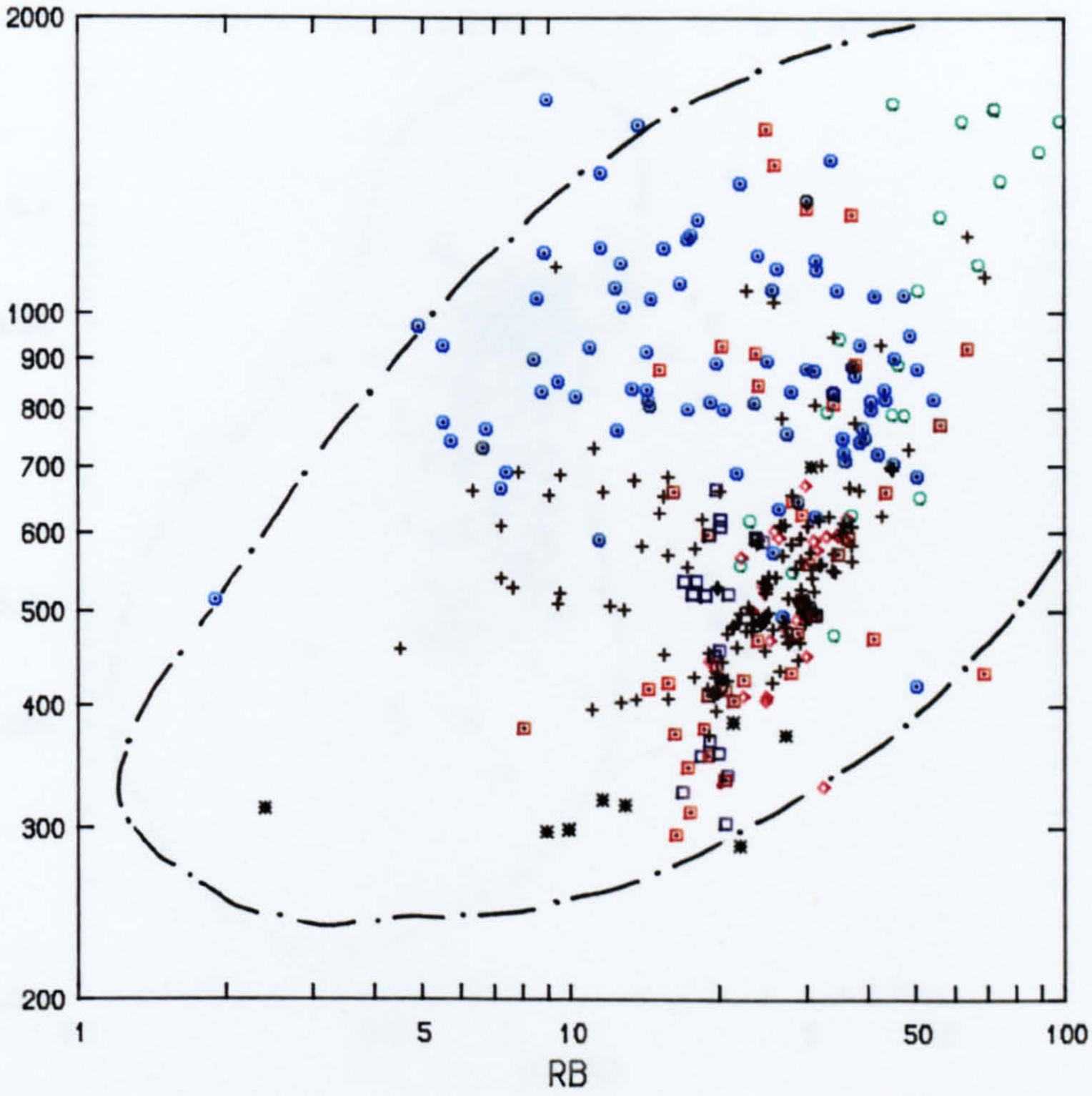

Fig. 6.3 TiO_2 v K_2O (a) and Sr v Rb (b) for basic samples from all groups.
Superimposed OIB fields from J.G. Fitton & D.E. James (pers. comm., 1989).

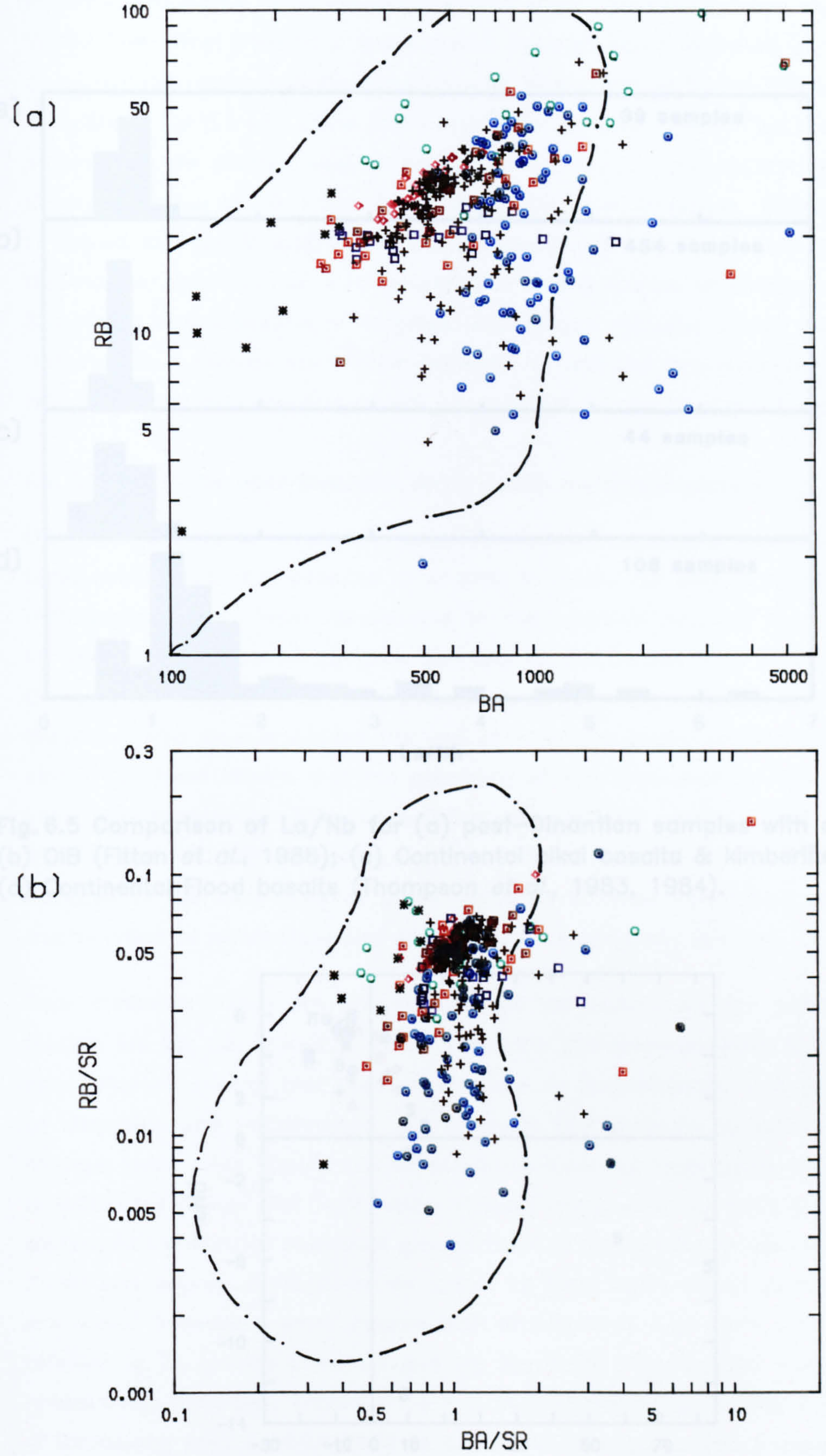

Fig. 6.4 Rb v Ba (a) and Rb/Sr v Ba/Sr (b) for basic samples from all groups Superimposed OIB fields from J.G. Fitton & D.E. James (pers. comm., 1989).

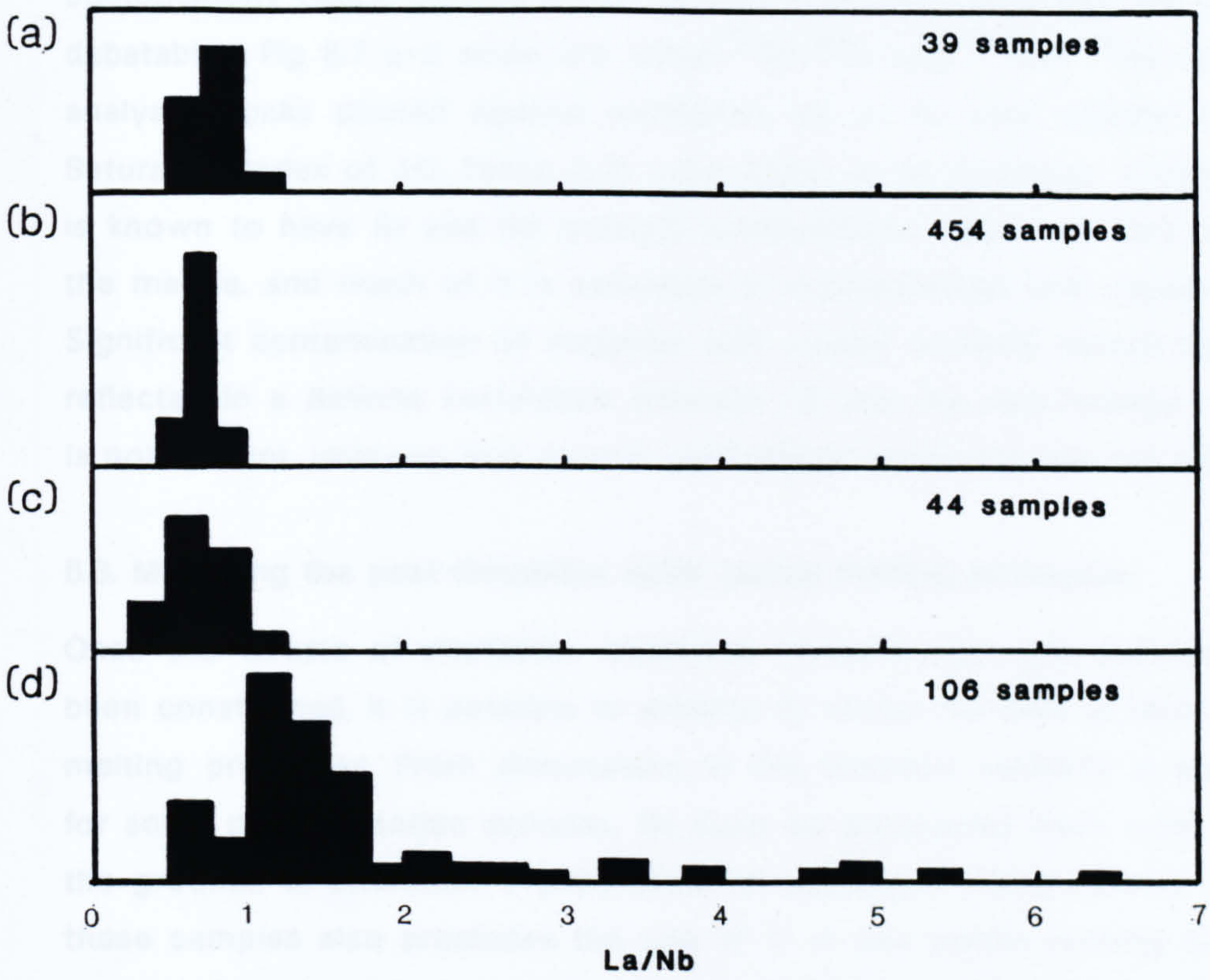

Fig. 6.5 Comparison of La/Nb for (a) post–Dinantian samples with data from (b) OIB (Fitton *et al.*, 1988); (c) Continental alkai basalts & kimberlites and (d) Continental Flood basalts (Thompson *et al.*, 1983, 1984).

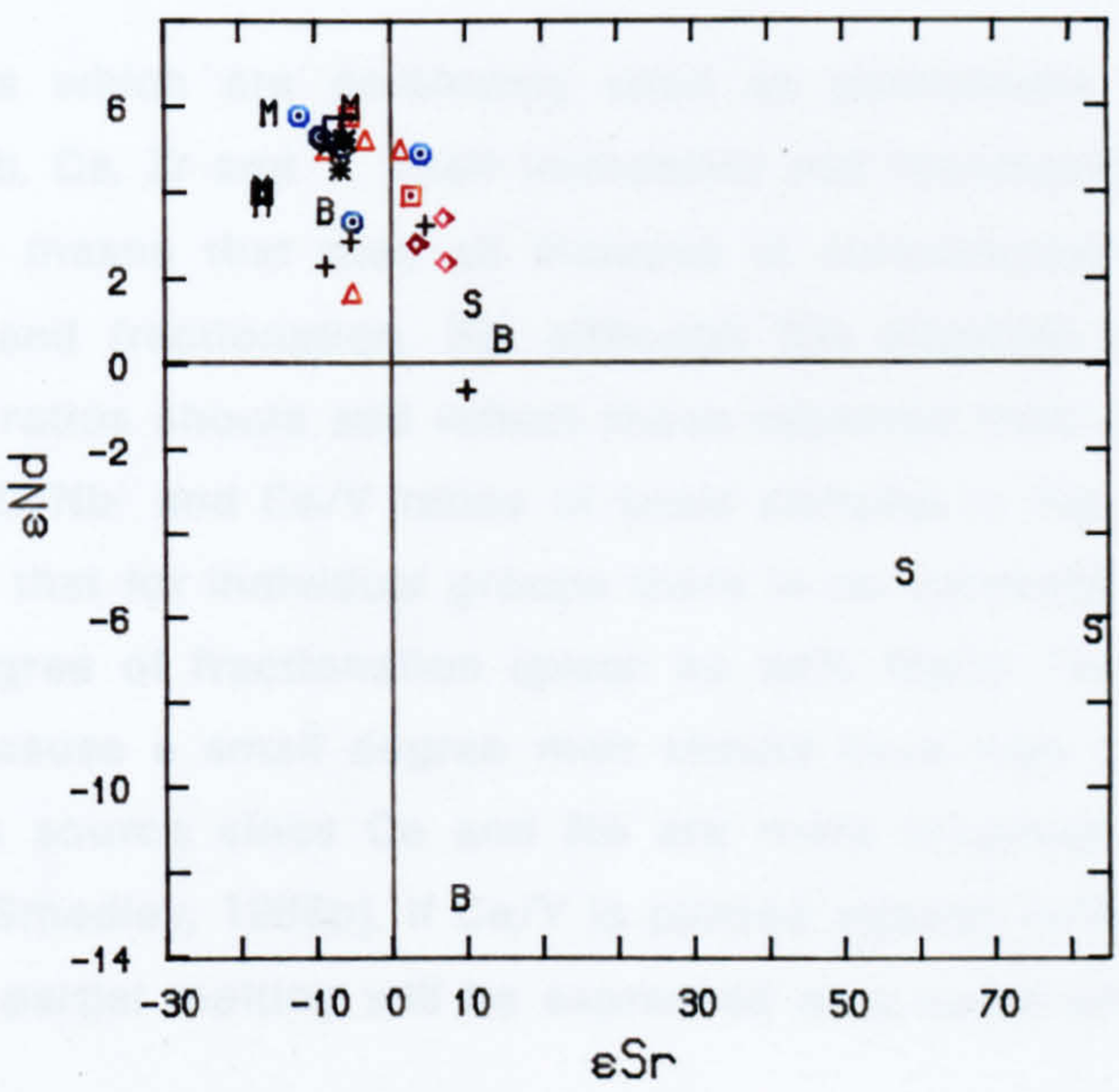

Fig. 6.6 Comparison of εNd and εSr for post–Dinantian samples and Megacrysts **(M)** (Menzies & Halliday, 1988; Smedley, 1986a, fig 7.8); Basic Granulites **(B)** (Smedley, 1986a, fig 7.8) and Southern Uplands sediments **(S)** (Halliday, 1984).

Uplands sediments, and megacrysts and basic granulites from the Midland Valley. The offset trend of a few samples towards some sediment and granulite compositions might indicate minor crustal interaction, although the evidence is debatable. Fig 6.7 a-d show the initial $^{87}Sr/^{86}Sr$ and $^{143}Nd/^{144}Nd$ ratios for all analysed rocks plotted against normative ne or 'Q' (see chapter 5) and the Saturation Index of J.G. Fitton & D. Latin (Latin *et al*, in press). Crustal material is known to have Sr and Nd isotopic compositions which are very different to the mantle, and much of it is saturated or oversaturated with respect to silica. Significant contamination of magmas with crustal material should therefore be reflected in a definite correlation between 'Q' and the two isotope ratios. This is not evident, implying that crustal assimilation processes are not significant.

6.3. Modelling the post-Dinantian suite: partial melting processes

Once the effects of alteration, fractional crystallisation and assimilation have been constrained, it is possible to attempt to model the data in terms of partial melting processes. From discussions in the previous sections it appears that for some post-Dinantian samples, Ba must be discounted from such models on the grounds of alteration. Fractionation of significant clinopyroxene in many of these samples also precludes the use of Ti in any partial melting calculations; and it has been shown that the precision of XRF-measured La is not good at low concentrations. The post-Dinantian samples appear not to have fractionated feldspar or apatite, so it should be possible to use Sr and P, but because of the sensitivity of these elements to even very small amounts of fractionation of plagioclase and apatite they are generally avoided.

Four elements which are commonly used as parameters for partial melting models are Nb, Ce, Zr and Y. Their immobility and incompatibility in olivine and clinopyroxene means that they all increase in concentration during processes of alteration and fractionation. So, although the absolute concentrations may change, their ratios should still reflect those inherited from partial melting. This is tested for Zr/Nb and Ce/Y ratios of basic samples in Fig. 6.8 a & b. The two plots indicate that for individual groups there is no correlation between Ce/Y or Zr/Nb and degree of fractionation (given by wt% MgO). These particular ratios are useful because a small degree melt should have high Ce/Y and low Zr/Nb relative to its source since Ce and Nb are more incompatible than Y and Zr respectively (Smedley, 1986b). If Ce/Y is plotted against Zr/Nb (Fig. 6.9a) a trend of increasing partial melting will be expressed as a curve with a negative slope

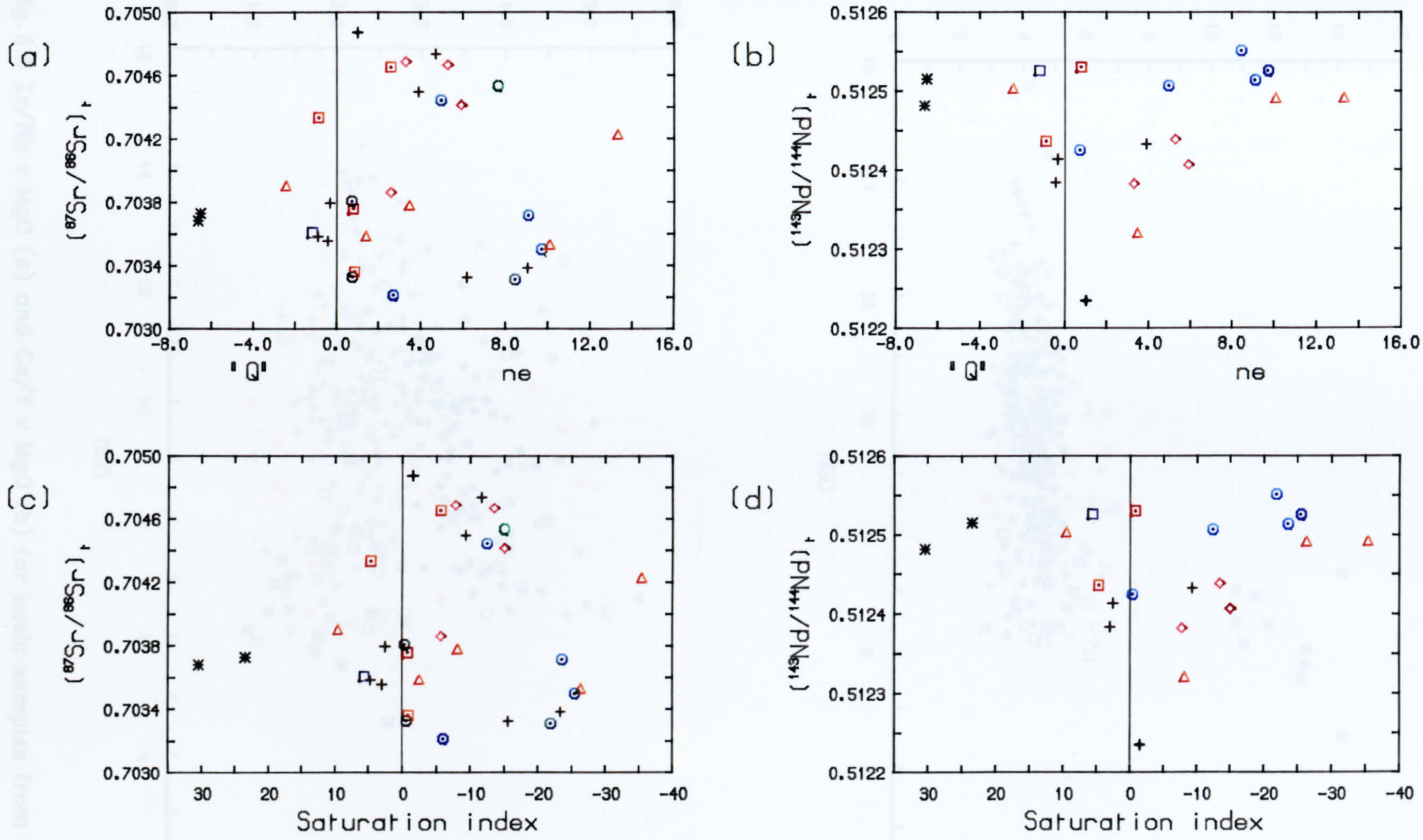

Fig.6.7 $^{87}Sr/^{86}Sr$ and $^{143}Nd/^{144}Nd$ plotted against normative ne and 'Q' (a & b), (see chapter 5 for definition), and the Saturation index of J.G. Fitton & D. Latin (Latin *et al.*, in press a) (c & d).

$$SI = 2Si - (11(Na+K) + 3Ca + Al + Fe'' + Mg)$$

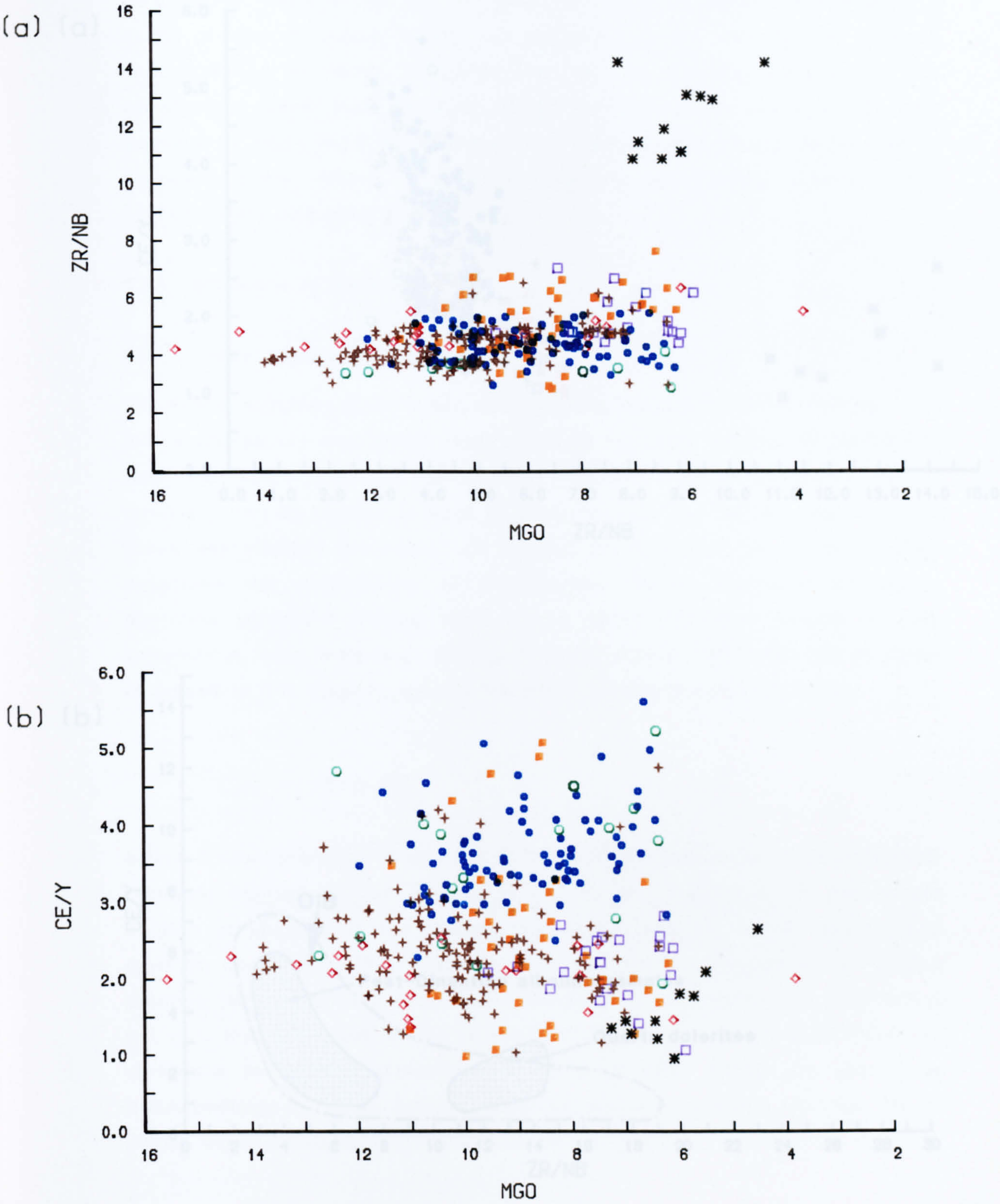

Fig.6.8 Zr/Nb v MgO (a) and Ce/Y v MgO (b) for basic samples from all groups.

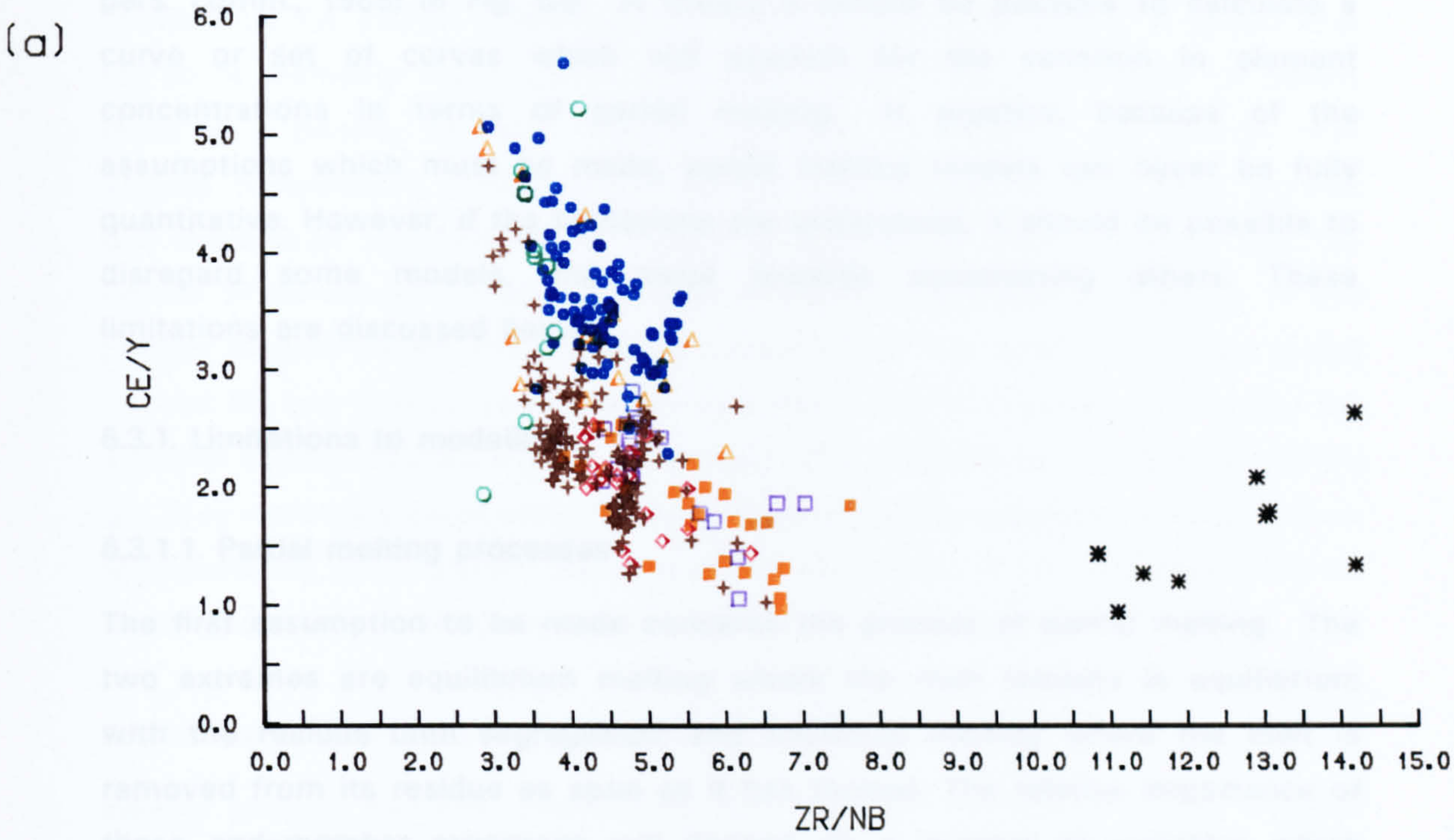

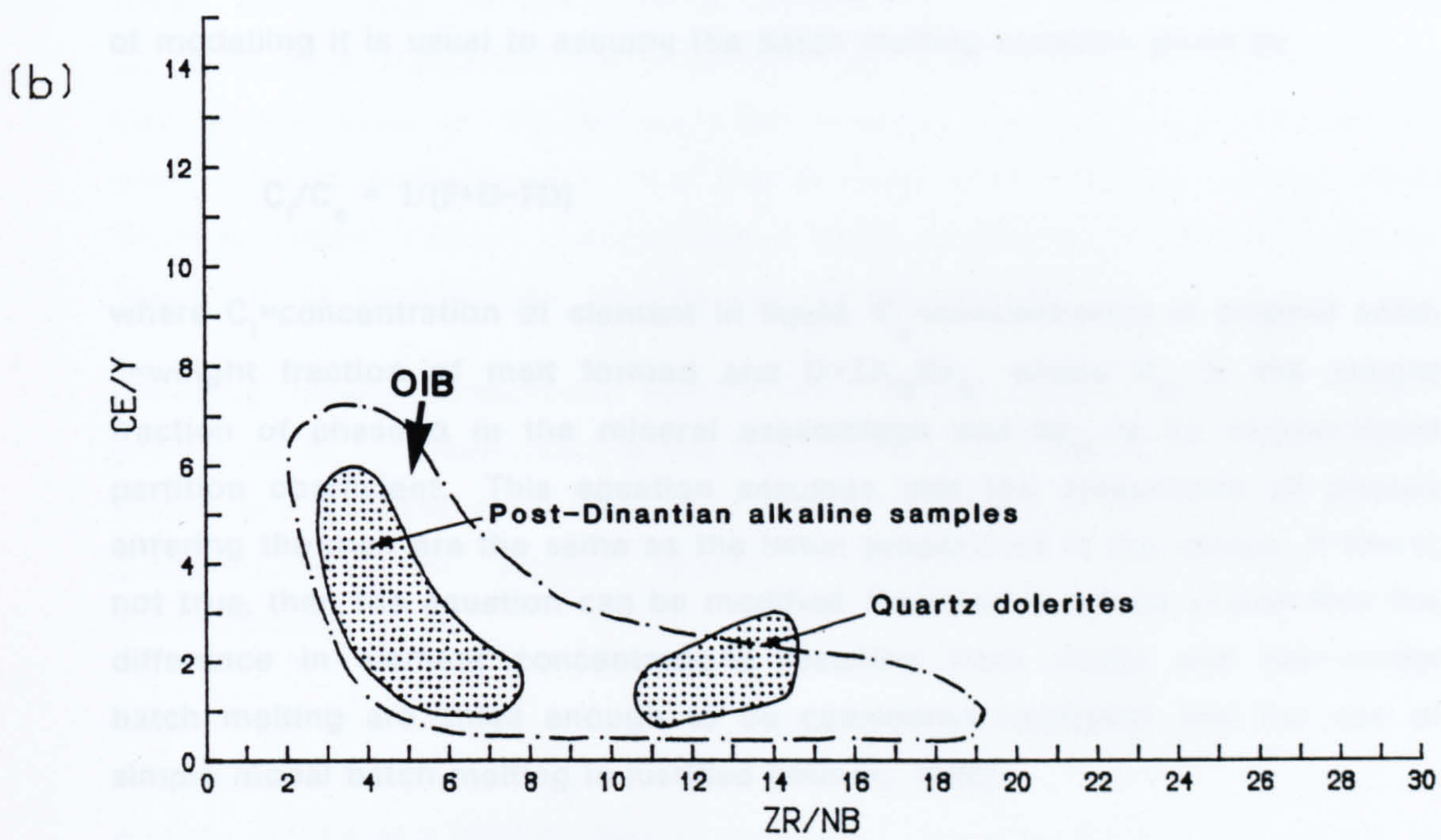

Fig. 6.9 Ce/Y v Zr/Nb for basic samples from all groups (a), and comparison with the field for OIB (b).

from high Ce/Y, low Zr/Nb to low Ce/Y, high Zr/Nb. Ce/Y and Zr/Nb variations for the alkaline suite are compared with the OIB field (J.G. Fitton & D.E. James, pers. comm., 1988) in Fig. 6.9. In theory it should be possible to calculate a curve or set of curves which will account for the variation in element concentrations in terms of partial melting. In practice, because of the assumptions which must be made, partial melting models can never be fully quantitative. However, if the limitations are understood, it should be possible to disregard some models, and move towards constraining others. These limitations are discussed below.

6.3.1. Limitations to modelling

6.3.1.1. Partial melting processes

The first assumption to be made concerns the process of partial melting. The two extremes are equilibrium melting where the melt remains in equilibrium with the residue until segregation; and fractional melting where the melt is removed from its residue as soon as it has formed. The relative importance of these end-member processes will depend on a number of variables which determine the permeability of the mantle. Perfect fractional melting is physically unrealistic (Wilson, 1989) and in reality a process between the two extremes is more likely (e.g. Critical melting (Maaloe, 1982)). For the purposes of modelling it is usual to assume the batch melting equation given by

$$C_l/C_o = 1/(F+D-FD)$$

where C_l=concentration of element in liquid, C_o=concentration in original solid, F=weight fraction of melt formed and $D=\Sigma X_\alpha Kd_\alpha$, where X_α is the weight fraction of phase α in the mineral assemblage and Kd_α is its crystal-liquid partition coefficient. This equation assumes that the proportions of phases entering the melt are the same as the initial proportions in the source. If this is not true, then the equation can be modified. However it can be shown that the difference in element concentrations resulting from modal and non-modal batch melting are small enough to be considered negligible and the use of simple modal batch melting is justified (Wilson, 1989).

6.3.1.2. Choice of Kd-values

Appendix VII summarises some of the published crystal-liquid partition coefficients for olivine, orthopyroxene, clinopyroxene and garnet. It shows that for some elements the range in measured values is large, whereas for others there is a paucity of data. Although partition coefficients will change with varying temperature, pressure, composition and oxygen fugacity, (see section 5.1) there is at the moment no means of quantifying these changes, and the choice of Kd-values remains a matter of personal preference. Because of the paucity of data for Nb and Zr, values calculated by interpolation between K and La, and Nd and Ti have been used in this study. Fig 6.10 shows two curves for a MORB source (section 6.3.1.5) containing 63% ol, 22.5% opx, 9.5% cpx and 5% gt. They were calculated using the minimum and maximum published Kd-values (Appendix VII) and highlight the effects that the choice of Kd-value can have on the shape of the melting curve generated.

6.3.1.3. Calculation of bulk distribution coefficients

Having chosen partition coefficients, the mineral proportions of the residue must be estimated to allow the calculation of bulk distribution coefficients. Melting experiments and xenolith data go some way towards constraining this. Such experiments (e.g. Green & Ringwood, 1967; Green & Hibberson, 1970; Green, 1970, 1973a, 1973b; Green & Liebermann, 1976; summarised by Frey *et al*, 1978), have suggested that undersaturated liquids are the result of melting through the range 4-11%. Although this is larger than the range indicated by trace element concentrations (e.g. Kay & Gast, 1973; Fitton & Dunlop, 1985; Fitton & James, 1986) it does provide a range of residue mineral proportions. These are: ol: 56-63%; opx: 18-30%; cpx: 7-14%; gt:2-4%.

Changing mineral proportions within these limits suggests that the biggest control on Ce concentrations is the abundance of clinopyroxene in the source. Garnet provides the most effective buffer of Y; orthopyroxene of Zr; and Nb concentrations are almost equally controlled by orthopyroxene and clinopyroxene.

A partial solution to the problem of calculating distribution coefficients is to calculate the D-values needed to generate a liquid of a given composition from a given source at a specific degree of melting. The plausibility of the values so calculated can then be checked against the range of measured values (e.g.

Minimum Kd values

%	0	1	2	5	10	20	100
Ce	411	127	75	34	18	9	1 8
Y	80	71	64	50	36	24	6 2
Zr	323	275	240	173	118	72	17 7
Nb	228	50	28	12	6	3	0 6
Ce/Y	5 2	1 8	1.2	0 7	0 5	0 4	0.3
Zr/Nb	1 4	5.5	8 5	14 3	19 0	22.9	27 6

Maximum Kd values

%	0	1	2	5	10	20	100
Ce	39	32	28	19	13	8	1 8
Y	36	35	33	29	25	18	6 2
Zr	87	84	81	73	63	49	17.7
Nb	15	13	11	7	5	3	0 6
Ce/Y	1 1	0 9	0 8	0 7	0.5	0.4	0 3
Zr/Nb	5.7	6.7	7 7	10 2	13.5	17 8	27 6

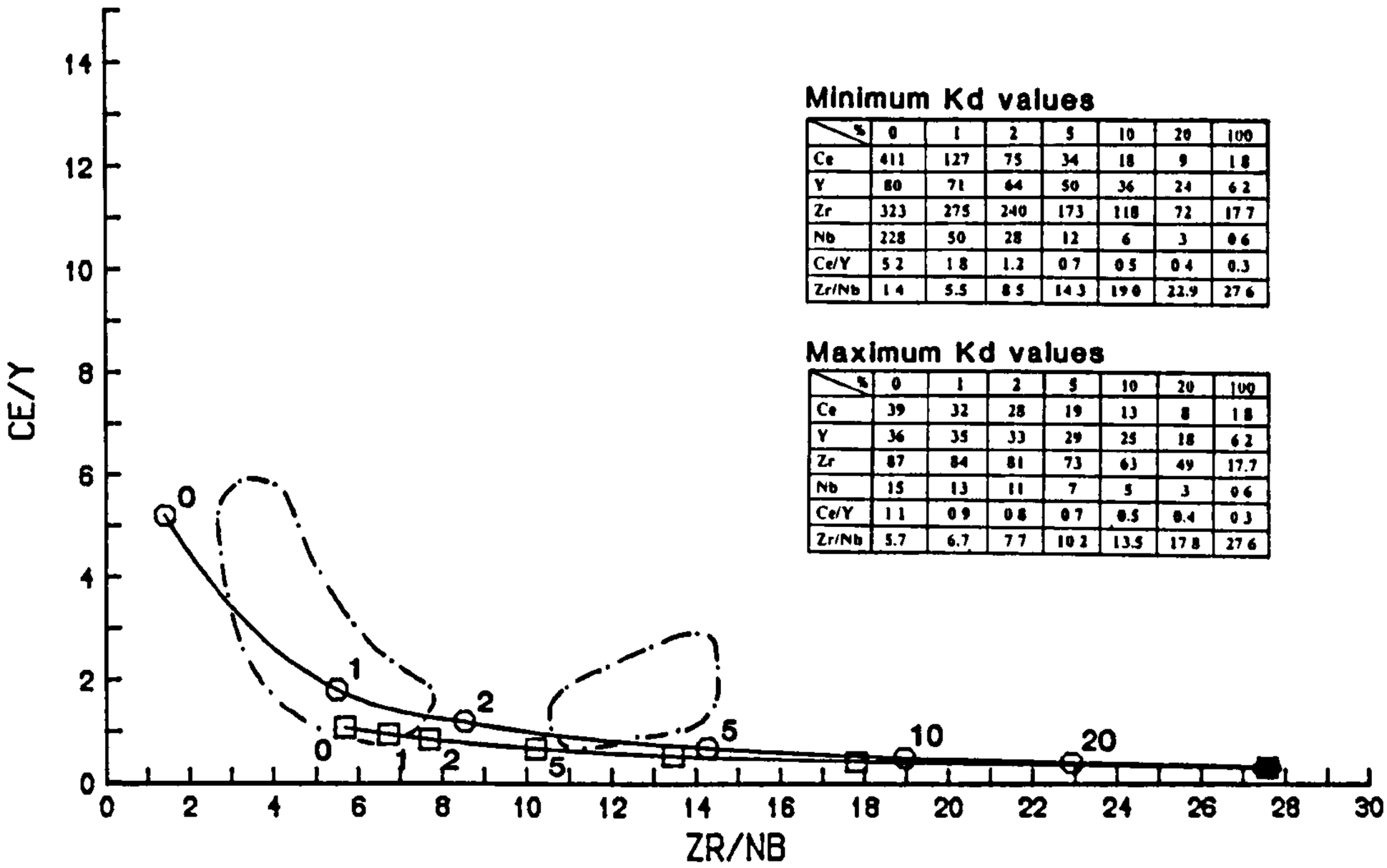

Fig 6.10 Ce/Y v Zr/Nb field for post–Dinantian basic samples. Melting curves are calculated using the minimum (squares) and maximum (circles) K_d–values of Appendix VII for a MORB20 source containing 63% ol, 22.5% opx, 9.5% cpx and 5% gt (Frey *et al.*, 1978).

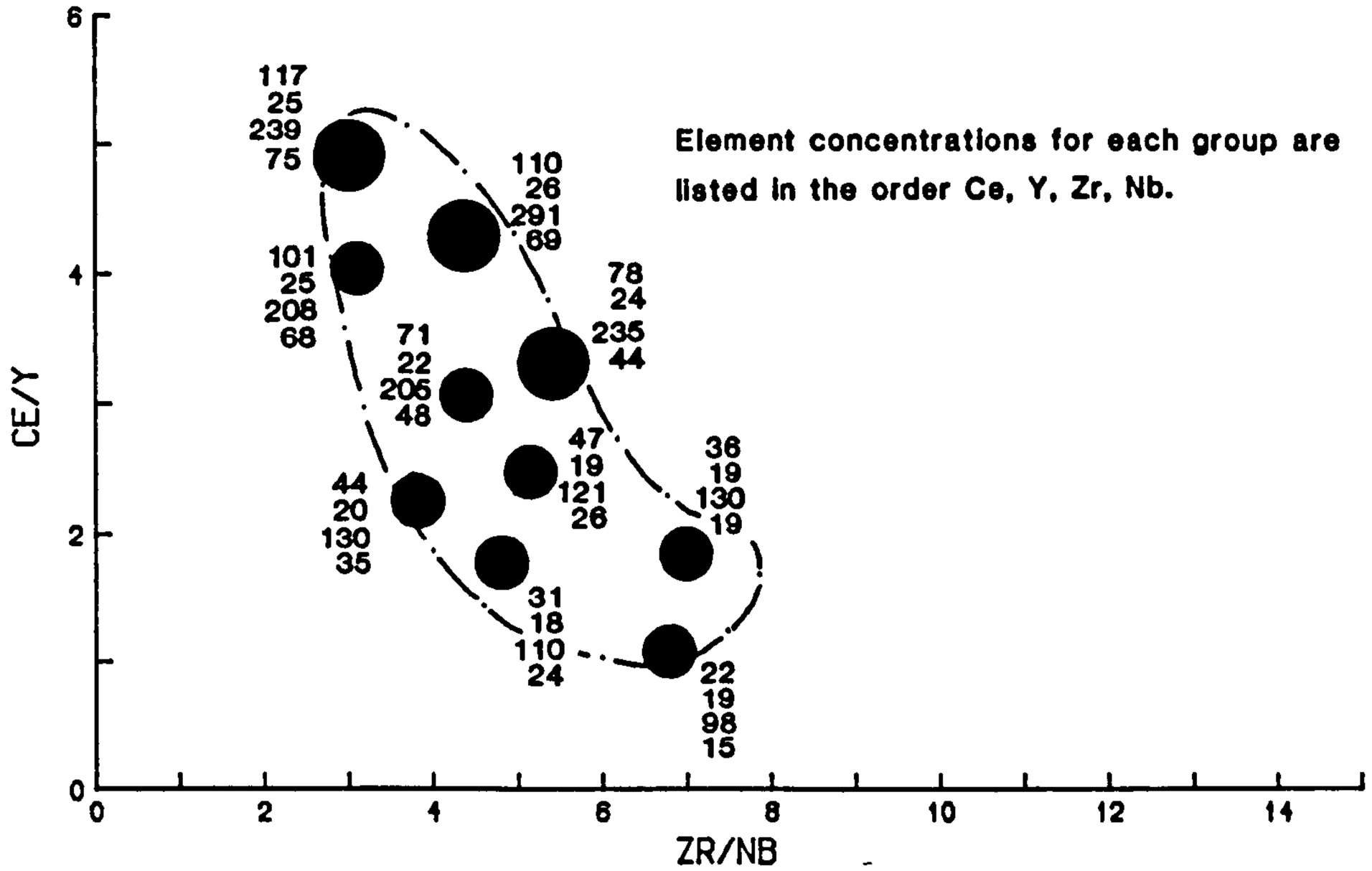

Fig 6.11 Averaged recalculated primary compositions for selected basic samples spanning the post–Dinantian alkaline range of Ce/Y & Zr/Nb concentrations.

Fitton & Dunlop, 1985). This has the advantage of accounting for melting dominated by accessory phases, but its disadvantages are that the degree of melting and the composition of the liquid must be assumed.

6.3.1.4. Composition of melt

The test of any melting model is that it not only generates reasonable element ratios but that the absolute values are also reasonable. By assuming that olivine was the major fractionating phase it is possible to calculate plausible primary magma compositions. This has been done by adding 0.1% increments of equilibrium olivine iteratively (using Kd=0.3; Roeder & Emslie, 1970) until the equilibrium olivine reached Fo_{90} (e.g. Fitton & James, 1986). The problems associated with this calculation have been discussed in section 5.1. However, it provides a means of normalising the composition of each sample, so providing a common base for comparison. The assumption that only minor clinopyroxene has fractionated is a fair one for the Ayrshire samples (see section 5.4.1) but not so for many of the Fife & Lothian and Highland dyke samples. The greater compatibility of trace elements in clinopyroxene than in olivine will result in their relative depletion in magmas crystallising clinopyroxene. It is possible therefore that the recalculated trace element abundances for the cpx-phyric samples are too low. Despite this they still provide a means of assessing the plausibility of values produced through modelling

Fig 6.11 shows the average recalculated primary compositions for various parts of the Ce/Y, Zr/Nb plot. These are used in later sections as a credibility check for the various models tested.

6.3.1.5. Source composition

The composition of the source is one of the least easily constrained variables. The commonest approach is to assume a composition and then determine the conditions (i.e. F and D) under which it could melt to produce the required liquid composition. Commonly used sources include the MORB source (Fitton & Dunlop, 1985; Roex, 1987), Bulk Silicate Earth (James, 1988) and 2x chondrite (Frey *et al*, 1978). This study uses chondrite and MORB sources for the basis of discussions. Values for chondrite are taken from Sun (1980) and the composition of the MORB source is calculated by assuming that N-type MORB (Sun, 1980) is the result of 20% melting of its source, leaving a residue

composed of 70% ol, 23% opx and 7% cpx (Frey *et al*, 1978; Fitton & Dunlop, 1985). This is referred to as MORB20. Compositions for the MORB20 and chondrite sources are listed in Table 6.1.

One approach to the determination of source compositions is to use the $C_{l\alpha}/C_{l\beta}$ vs $C_{l\alpha}$ discrimination plots adapted from Treuil (1973) and Treuil & Joron (1975). The batch melting equation predicts that at similar F, the concentration of two elements $C_{l\alpha}$ and $C_{l\beta}$ in a liquid are given by:

$$(C_{o\alpha}-C_{l\alpha}D_{\alpha})/(C_{l\alpha}(1-D_{\alpha}))=(C_{o\beta}-C_{l\beta}D_{\beta}/(C_{l\beta}(1-D_{\beta}))$$

This equation can be rearranged to give:

$$C_{l\alpha}/C_{l\beta}=(C_{o\alpha}/C_{o\beta})((1-D_{\alpha})/(1-D_{\beta}))+C_{l\alpha}((D_{\alpha}-D_{\beta})/C_{o\beta}(1-D_{\alpha}))$$

such that a graph of $C_{l\alpha}/C_{l\beta}$ vs $C_{l\alpha}$ produces a straight line with a gradient of $(D_{\alpha}-D_{\beta})/(C_{o\beta}(1-D_{\alpha}))$ which intercepts the $C_{l\alpha}/C_{l\beta}$ axis at a value given by $(C_{o\alpha}/C_{o\beta})(1-D_{\alpha}/1-D_{\beta})$. If elements $C_{l\alpha}$ and $C_{l\beta}$ are equally incompatible then $(1-D_{\alpha}/1-D_{\beta}) = 1$, so the intercept will give the source ratio of the two elements α and β

This approach can only be used effectively if it can be shown that the simple batch melting model is appropriate. It appears from the previous discussions that this is probably not the case for the post-Dinantian suite. However, on the assumption that the Fife & Lothian basanites were dominated by melts from one source, and the Mauchline group by melts from a separate source, such modelling was attempted. Unfortunately, the standard deviations of the values calculated are large, so that statistically the two sources are indistinguishable. Therefore this has not been pursued further.

6.3.2. Melting models

Fig 6.12 shows the post-Dinantian data plotted in the Ce/Y-Zr/Nb diagram with two superimposed melting curves (for MORB20 and chondrite sources) calculated using D-values from Fitton & James (1986). It shows that unless systematic changes in partition coefficients can be appealed to for all four elements, the range in compositions cannot be the result of variable degree

	1	2	3
Ce	9.0	1.83	0.82
Y	29.0	6.2	2.0
Zr	85.0	17.7	5.6
Nb	3.1	0.64	0.35

Table 6.1 Ce, Y, Zr & Nb concentrations for:

1. N-type MORB (Sun, 1980).

2. MORB20: The composition of a MORB-source assuming that MORB is the result of 20% melting, leaving a residue comprising 70% ol, 23% opx, 7% cpx. (Partition coefficients used in this calculation were taken from Frey *et al*, 1978)

3. Chondrite (Sun, 1980).

	Ol	Opx	Cpx	Gt
Ce	0.00048	0.0009	0.04	0.0029
Y	0.002	0.009	0.05	1.4
Zr	0.0116	0.673	0.23	0.206
Nb	0.00259	0.0005	0.0107	0.001

Table 6.2 Mineral-melt partition coefficients used in the calculation of magma compositions.

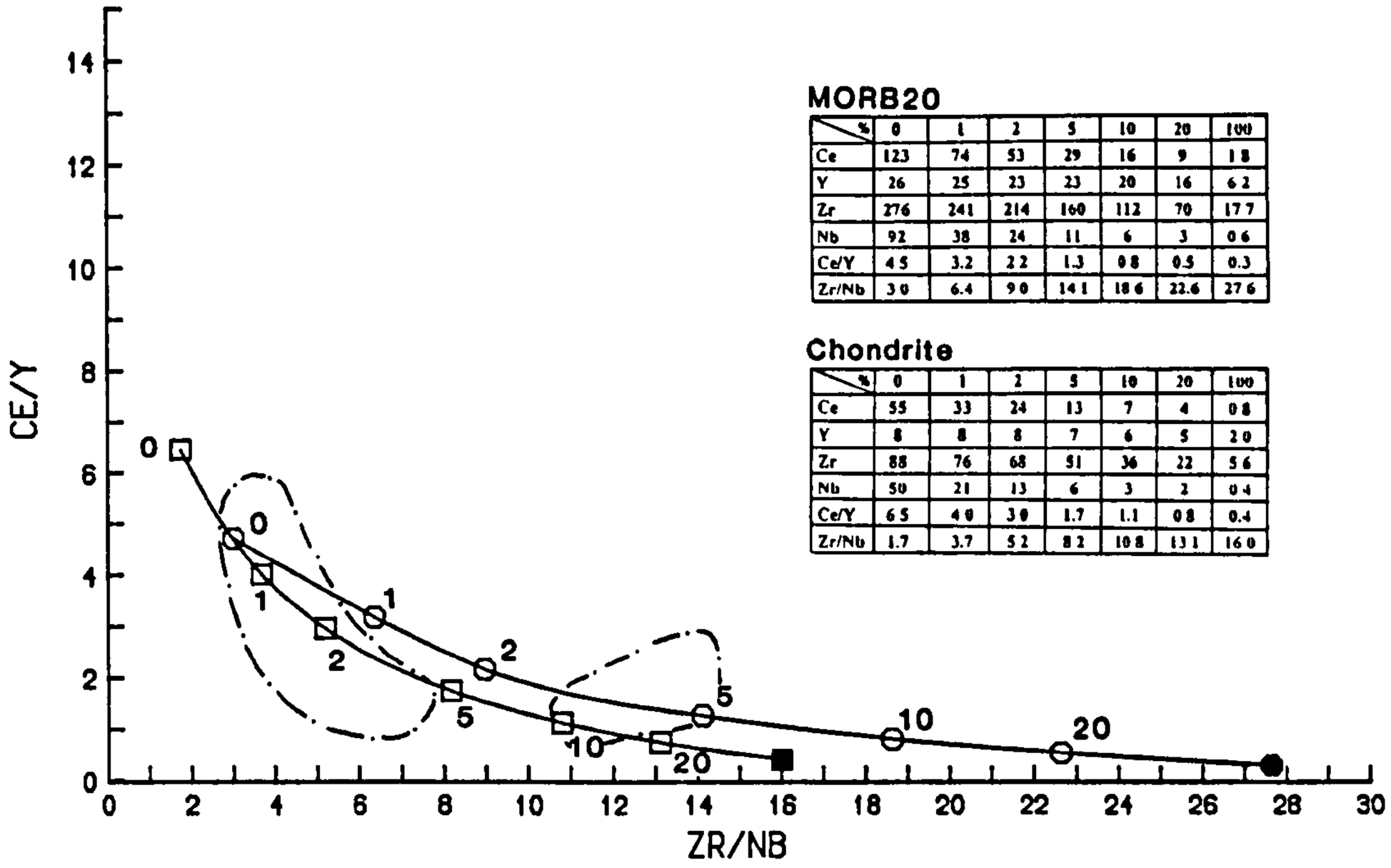

MORB20

%	0	1	2	5	10	20	100
Ce	123	74	53	29	16	9	1 8
Y	26	25	23	23	20	16	6 2
Zr	276	241	214	160	112	70	17 7
Nb	92	38	24	11	6	3	0 6
Ce/Y	4 5	3.2	2 2	1.3	0 8	0.5	0.3
Zr/Nb	3 0	6.4	9 0	14 1	18 6	22.6	27 6

Chondrite

%	0	1	2	5	10	20	100
Ce	55	33	24	13	7	4	0 8
Y	8	8	8	7	6	5	2 0
Zr	88	76	68	51	36	22	5 6
Nb	50	21	13	6	3	2	0 4
Ce/Y	6 5	4 0	3 0	1.7	1.1	0 8	0.4
Zr/Nb	1.7	3.7	5 2	8 2	10 8	13 1	16 0

Fig 6.12 Ce/Y v Zr/Nb field for post-Dinantian basic samples. Melting curves for a MORB20 source (circles) and a chondrite source (squares) are calculated assuming the partition coefficients of Fitton & James (1986): D_{Ce}=0.0149, D_{Y}=0.237, D_{Zr}=0.0640 and D_{Nb}=0.00696.

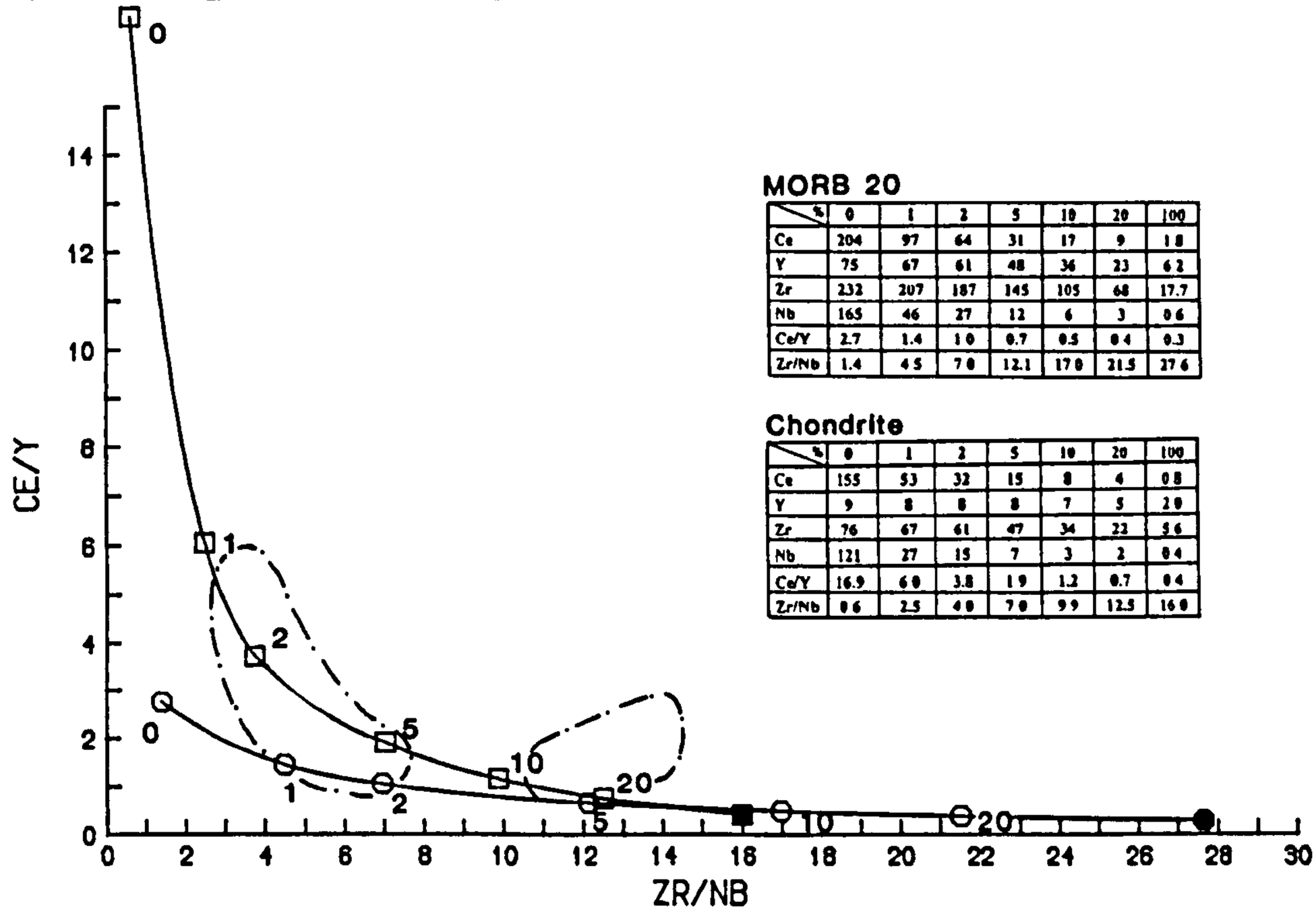

MORB 20

%	0	1	2	5	10	20	100
Ce	204	97	64	31	17	9	1 8
Y	75	67	61	48	36	23	6 2
Zr	232	207	187	145	105	68	17.7
Nb	165	46	27	12	6	3	0 6
Ce/Y	2.7	1.4	1 0	0.7	0.5	0 4	0.3
Zr/Nb	1.4	4 5	7 0	12.1	17 0	21.5	27 6

Chondrite

%	0	1	2	5	10	20	100
Ce	155	53	32	15	8	4	0 8
Y	9	8	8	8	7	5	2 0
Zr	76	67	61	47	34	22	5 6
Nb	121	27	15	7	3	2	0 4
Ce/Y	16.9	6 0	3.8	1 9	1.2	0.7	0 4
Zr/Nb	0 6	2.5	4 0	7 0	9 9	12.5	16 0

Fig 6.13 Ce/Y v Zr/Nb field for post-Dinantian basic samples with melting curves for a MORB20 source (circles) and a chondrite source (squares), calculated assuming respective source mineralogies of 58% ol, 16% opx, 23% cpx and 5% gt; and 58% ol, 16% opx, 11% cpx and 15% gt. K_d-values from table 6.2.

melting of a single homogeneous source.

Section 6.1.2 summarised three models developed to account for the composition of alkalic magmas. They appeal alternatively to stratified, heterogeneous (streaky), or metasomatised mantle. Each of these is discussed below for the genesis of the post-Dinantian alkaline suite, using the Ce/Y-Zr/Nb diagram as a basis for discussion. Modelling has assumed batch melting of a source containing residual garnet. It appears from the spiderdiagram plots of chapter 5 that this is a fair assumption for all the groups. However, the Ce/Y ratios of the quartz dolerites (Fig. 6.9a) generally increase with increasing Zr/Nb, suggesting that these melts were not in equilibrium with garnet (contrary to the evidence suggested by Y and HREE concentrations; chapter 5). This should be borne in mind throughout the following discussions.

6.3.2.1. Stratified mantle

At its simplest the stratified mantle model places the initial source for OIB-like magmas deep within the mantle, and attributes to it characteristics of undifferentiated mantle, possibly of chondrite composition. OIB-source melts mix with MORB-source melts as they ascend through the mantle. At small degrees of melting the OIB-source melts are dominant, but with increasing degrees of melting they are swamped by MORB-source melts, (although a vigorous plume might be expected to produce large-degree melts dominated by the lower mantle, with small degree MORB-like melts at the edges c.f. Chen & Frey, 1985).

On this basis the more undersaturated samples should be expected to show the more pronounced OIB signature, which is less apparent in larger degree melts. Examination of Fig. 6.12 shows that the range in compositions cannot be explained by mixing between melts from MORB20 and chondrite sources if source-melt distribution coefficients for both sources are the same. Bulk distribution coefficients are influenced by variations in the individual partition coefficients and modal mineralogy. Since the former cannot be constrained, the model must rely on changing the latter. Fig 6.13 shows two curves calculated for chondrite and MORB20 sources using Kd values from Table 6.2 and assuming a residual mineralogy of 58% ol: 16% opx: 11% cpx: 15% gt and 58% ol: 16% opx :23% cpx: 5% gt respectively. It assumes that the garnet content of

the mantle increases with depth from the cpx-gt phase transition zone (Kay & Gast, 1973; Alibert *et al*, 1983), and that this is compensated for by decreasing cpx contents. Garnet acts as a buffer to Y, so the greater the amount of this mineral in a source, the lower the Y content of the initial liquid from that source. Reduction of source clinopyroxene will increase the Ce content and reduce the Nb content of the liquid. Hence the overall effect is one of substantial increase in the Ce/Y ratio accompanying a much smaller increase in the Zr/Nb ratio. Fig 6.13 shows that given a variation in modal mineralogy, the range in Ce/Y, Zr/Nb values could be accounted for by mixing between melts from a chondritic and a MORB20 source. However, agreement of the absolute Ce, Y, Zr and Nb values with the recalculated values of Fig. 6.11 is poor. Values of the correct order of magnitude would require an undepleted source with a composition of c.3-4x chondrite and a depleted source with a composition c.0.25-0.5x MORB20. The difficulty of melting such a depleted source makes this an unattractive model. However, it must be emphasised that for both this and the other models, much is dependent on the choice of distribution coefficients (controlled by mineral-melt partition coefficients and mineral proportions of the source). An alternative approach would have been to assume MORB20 and chondrite sources, and calculate the distibution coefficients needed to produce the liquid compositions at specific degrees of melting. The resulting distribution coefficients fall within a credible range of values.

Smedley (1986b) modelled Ce/Y-Zr/Nb variations in the Dinantian alkaline and transitional suite on the basis of similar variations in modal mineralogy for a single source. This model is tested for the post-Dinantian suite in Fig. 6.14 using a MORB20 source and the partition coefficients of Table 6.2. The diagram shows that for the partition coefficients used, the whole range in Ce/Y and Zr/Nb values could be accounted for by variable small degree melting of a source heterogeneous in garnet. However, at low garnet concentrations the agreement with the recalculated values is poor, and if this model is used the source must again become increasingly depleted at shallower levels. A garnet content of 15% is possibly high for the MORB source. However, if the partition coefficient of Y in garnet is closer to some of the values measured for the HREE, a less garnet-rich source would be required.

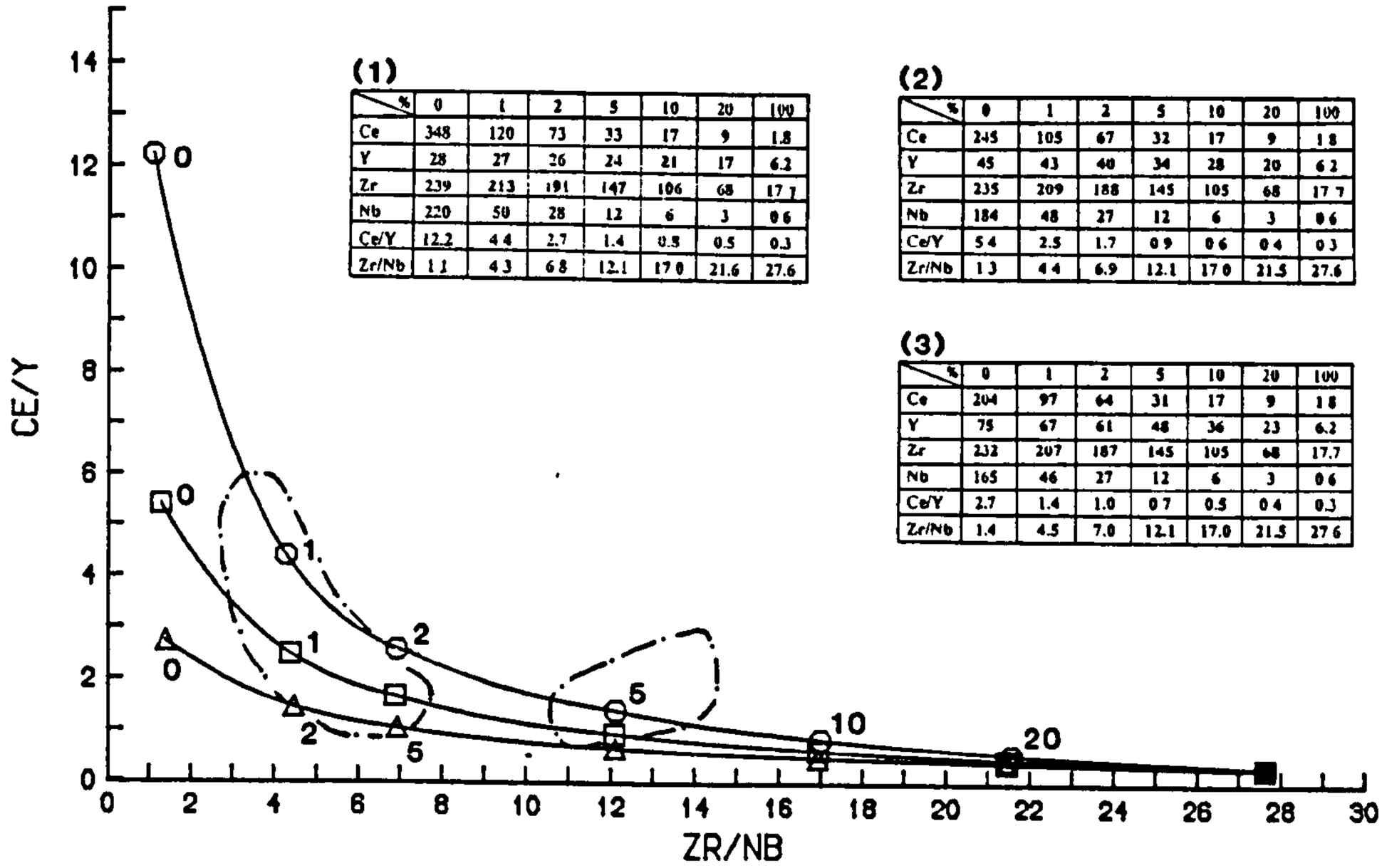

(1)

%	0	1	2	5	10	20	100
Ce	348	120	73	33	17	9	1.8
Y	28	27	26	24	21	17	6.2
Zr	239	213	191	147	106	68	17.7
Nb	220	58	28	12	6	3	0.6
Ce/Y	12.2	4.4	2.7	1.4	0.8	0.5	0.3
Zr/Nb	1.1	4.3	6.8	12.1	17.0	21.6	27.6

(2)

%	0	1	2	5	10	20	100
Ce	245	105	67	32	17	9	1.8
Y	45	43	40	34	28	20	6.2
Zr	235	209	188	145	105	68	17.7
Nb	184	48	27	12	6	3	0.6
Ce/Y	5.4	2.5	1.7	0.9	0.6	0.4	0.3
Zr/Nb	1.3	4.4	6.9	12.1	17.0	21.5	27.6

(3)

%	0	1	2	5	10	20	100
Ce	204	97	64	31	17	9	1.8
Y	75	67	61	48	36	23	6.2
Zr	232	207	187	145	105	68	17.7
Nb	165	46	27	12	6	3	0.6
Ce/Y	2.7	1.4	1.0	0.7	0.5	0.4	0.3
Zr/Nb	1.4	4.5	7.0	12.1	17.0	21.5	27.6

Fig 6.14 Ce/Y v Zr/Nb field for post-Dinantian basic samples. Melting curves for a MORB20 source assuming three mineralogies: (1) 58% ol, 16% opx, 11% cpx, 15% gt (circles); (2) 58% ol, 16% opx, 17% cpx, 9% gt (squares); (3) 58% ol, 16% opx, 21% cpx, 5% gt (triangles). K_d-values are taken from table 6.2.

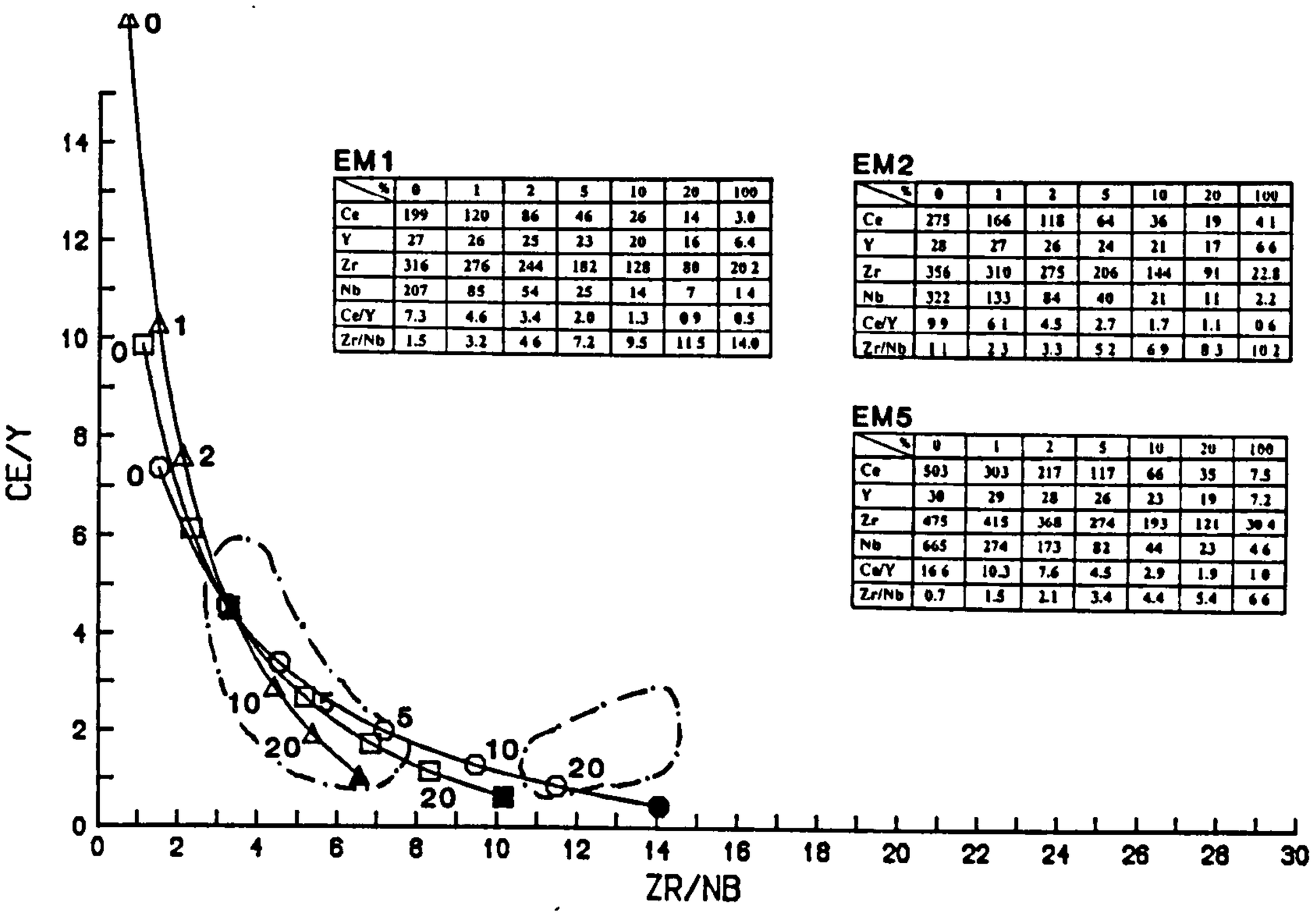

EM1

%	0	1	2	5	10	20	100
Ce	199	120	86	46	26	14	3.0
Y	27	26	25	23	20	16	6.4
Zr	316	276	244	182	128	80	20.2
Nb	207	85	54	25	14	7	1.4
Ce/Y	7.3	4.6	3.4	2.0	1.3	0.9	0.5
Zr/Nb	1.5	3.2	4.6	7.2	9.5	11.5	14.0

EM2

%	0	1	2	5	10	20	100
Ce	275	166	118	64	36	19	4.1
Y	28	27	26	24	21	17	6.6
Zr	356	310	275	206	144	91	22.8
Nb	322	133	84	40	21	11	2.2
Ce/Y	9.9	6.1	4.5	2.7	1.7	1.1	0.6
Zr/Nb	1.1	2.3	3.3	5.2	6.9	8.3	10.2

EM5

%	0	1	2	5	10	20	100
Ce	503	303	217	117	66	35	7.5
Y	30	29	28	26	23	19	7.2
Zr	475	415	368	274	193	121	30.4
Nb	665	274	173	82	44	23	4.6
Ce/Y	16.6	10.3	7.6	4.5	2.9	1.9	1.0
Zr/Nb	0.7	1.5	2.1	3.4	4.4	5.4	6.6

Fig 6.15 Ce/Y v Zr/Nb field for post-Dinantian basic samples with melting curves for enriched MORB sources EM1 (circles), EM2 (squares) and EM5 (triangles). Compositions calculated assuming mixing between a source with the composition of a 0.1% MORB20 melt and MORB20 in the proportions 1:99, 2:98 and 5:95 respectively. (D-values from Fitton & James, 1986).

6.3.2.2. Streaky mantle

Xenolith studies have indicated that many parts of the lithospheric mantle are enriched in accessory phases such as amphibole, mica, apatite and zircon. The streaky mantle model of Fitton & Dunlop (1985) and Fitton & James (1986) implied that geochemically enriched streaks in the asthenosphere are similarly concentrated in accessory phases. Their presence will significantly affect the composition of small degree melts, and it is possible that initial melting is dominated by these phases. Fig 6.11 indicates that Y is buffered over all ranges of melting, and therefore that garnet was a significant source phase. However, if Y is as compatible in amphibole as measurements suggest for the HREE (Irving & Frey, 1984) then it is possible for Y to be buffered during melting of assemblages where garnet is absent but amphibole present. Table 6.3 shows the concentrations of Ce, Y, Zr and Nb produced at various degrees of partial melting of a source with the bulk composition of MORB20, composed of 50% amphibole and 50% mica. It shows that within the assumptions made, sources greatly enriched in amphibole might provide a possible alternative means of buffering Y concentrations. However this is considered unlikely since amphibolite sources would produce H_2O-rich initial melts. As melting progresses enriched pockets will be consumed and subsequent melts will be more depleted in composition. MORB must therefore represent an average of the initial and subsequent melts. These considerations indicate the problems of modelling initial (small degree) melts assuming a MORB20 source composition: a more enriched composition would be more realistic. Table 6.4 shows the calculated compositions of melts from a source with the composition of a 0.1% MORB20 melt (0.1MM). Only the more undersaturated samples could result from melting of such a source, and then only at extreme degrees of melting (>90%). Fig 6.15 shows melting curves for enriched MORB sources EM1, EM2 and EM5. Their compositions were calculated by assuming mixing between 0.1MM and MORB20 in the proportions 1:99, 2:98 and 5:95 repectively (after Latin *et al*, in press,b). Agreement between the calculated and actual absolute values is good for Ce/Y > 2.5 and Zr/Nb < 5. It is unlikely that all accessory phases will be consumed at once, and modelling of these initial very small degree melts should really assume non-modal batch, or fractional melting processes.

Disequilibrium melting of accessory phases has been advocated by Campbell & Gorton (1980) to account for the generation of LREE-enriched basalts. They

%	0	1	2	5	10	20
Ce	13	12	12	10	8	6
Y	24	23	23	21	18	15
Zr	78	75	73	66	58	46
Nb	7	6	6	5	3	3

Table 6.3 Compositions of melt from a MORB20 source comprising equal proportions of amphibole and mica Partition coefficients for Ce from Irving & Frey (1984); Lu, Nd and La values assumed for Y, Zr and Nb respectively.

%	0	2	10	20	50	70	100
Ce	7732	3329	1016	544	227	164	115
Y	110	104	83	67	42	34	26
Zr	4254	3291	1728	1084	512	379	272
Nb	11562	3000	757	391	160	115	80
Ce/Y	70.3	32.0	12.2	8.1	5.4	4.8	4.4
Zr/Nb	0.4	1.1	2.3	2.8	3.2	3.3	3.4

Table 6.4 Calculated melt compositions from a source with the composition of a 0.1% MORB20 melt, (partition coefficients taken from table 6.2).

assumed that accessory phases present in the mantle at the 0.001% level would be completely consumed by 0.1% partial melting, producing a melt extract rich in incompatible elements. This liquid would be diluted by later mixing with the melting products of the major phases. Modelling of alkali basalt REE patterns on this basis requires a moderate degree of re-equilibration with a garnet-free assemblage such as ol-opx-cpx (Campbell & Gorton, 1980).

6.3.2.3. Mantle metasomatism

In many respects the streaky mantle and mantle metasomatism models are similar. Both assume the enrichment of an initially depleted source by the infiltration of small-degree partial melts, and much of the discussion of the previous section is relevant. Since metasomatic processes are so variable in their consequences it is virtually impossible to constrain source compositions for modelling. However, Tables 6.5 a & b show calculated melt compositions assuming sources with the same mean compositions as those measured for garnet and garnet phlogopite peridotite xenoliths from the Kimberley Pipes, South Africa (Erlank *et al*, 1987). The post-Dinantian samples could not have been derived from such sources. Unfortunately there are no recorded examples of garnet peridotite from the Midland Valley xenolith set which can be used to constrain possible source compositions.

6.3.2.4. Discussion

Consideration of incompatible trace element compositions has shown that the post-Dinantian suite cannot be modelled by simple batch melting of a homogeneous source. Mixing between melts from at least two sources is required. It is not clear whether these sources are distinct from one another in terms of a vertical zonation within the mantle (i.e. mesosphere v asthenosphere v lithosphere) or whether one is present as more fusible heterogeneities within the other (streaky mantle). Buffering of Y throughout the range of melting places possible sources within the stability field of garnet, and as such magmas are unlikely to represent partial melts of mantle shallower than the lower lithosphere. A large lithospheric and/or crustal component has been discounted on three accounts: (1) the inter-group similarities in incompatible trace element and REE profile patterns which do not suggest derivation from a grossly heterogeneous source, (2) the overall similarity of magma compositions to OIB and (3) the impossibly large degrees of melting required to produce

%	0	1	2	5	10	20	100
Ce	322	194	139	75	42	23	4.8
Y	8	8	8	7	6	5	2.0
Zr	114	100	88	66	46	29	7.3
Nb	273	112	71	34	18	9	1.9
Ce/Y	38.2	23.7	17.5	10.3	6.6	4.4	2.4
Zr/Nb	0.4	0.9	1.2	2.0	2.6	3.2	3.8

%	0	1	2	5	10	20	100
Ce	1725	1038	743	401	227	121	25.7
Y	12	11	11	10	9	7	2.8
Zr	219	191	169	126	89	56	14.0
Nb	661	272	172	81	43	22	4.6
Ce/Y	146.0	90.7	66.9	39.4	25.4	16.9	9.1
Zr/Nb	0.3	0.7	1.0	1.6	2.1	2.5	3.0

Table 6.5 Calculated melt compositions assuming sources with the same mean compositions as those analysed for (a) garnet peridotite and (b) garnet phlogopite peridotite xenoliths from the Kimberley Pipes, South Africa (Erlank *et al*, 1987).

incompatible element concentrations consistent with values for the post-Dinantian suite. This does not however preclude minor lithosphere and/or crustal involvement. Isotope variations are examined below in an attempt to differentiate between possible models.

6.3.2.5. Isotopes

The stratified and streaky mantle models predict decreasing $^{87}Sr/^{86}Sr$ and increasing $^{143}Nd/^{144}Nd$ ratios with increasing degrees of partial melting as MORB-like melts begin to dominate the melt composition. It is difficult to predict patterns for the metasomatised mantle model because of the range of possible types of mantle enrichment. However, with the exception of a vigorous plume (Chen & Frey, 1985), this is the only model which could account for increasing $^{87}Sr/^{86}Sr$ and decreasing $^{143}Nd/^{144}Nd$ with degree of melting, as increasing lithosphere-melt interaction accompanies the through-flux of larger volumes of asthenospheric melt.

Initial $^{87}Sr/^{86}Sr$ and $^{143}Nd/^{144}Nd$ ratios have been plotted against a variety of trace element ratios in Figs. 6.16-6.21. A cursory inspection does not identify any obvious trends on these graphs, and they could be interpreted in terms of variable degree melting of a heterogeneous mantle. However if the Mauchline group samples are considered in isolation from the other samples, some trends can be identified. The following discussion is concerned mainly with $^{87}Sr/^{86}Sr$, since data are more abundant than for $^{143}Nd/^{144}Nd$. However, the Nd isotope plots are included for reference. Figs 6.16 a & b show $^{87}Sr/^{86}Sr$ and $^{143}Nd/^{144}Nd$ against Ce/Y. The Mauchline group as a whole displays the greatest of all intra-group ranges in Ce/Y ratio (1-5). Isotope compositions have been determined for part of this range (c. 1-3). Examination of Fig. 6.16a suggests a general trend of increasing $^{87}Sr/^{86}Sr$ with decreasing Ce/Y and, therefore increasing degrees of partial melting. If this is so, $^{87}Sr/^{86}Sr$ would be expected to increase with Zr/Nb. Such a correlation might be argued from Fig. 6.16c, however it is unlikely to be as clear as for Ce/Y variations because of the relative insensitivity of the Zr/Nb ratio to small changes in degree of melting.

Mixing between two sources with distinct $^{87}Sr/^{86}Sr$ and $^{143}Nd/^{144}Nd$ concentrations has often been demonstrated by considering the relationship between isotope-element compositions of Nd and Sr. Figs 6.17 a & b show $^{87}Sr/^{86}Sr$ and $^{143}Nd/^{144}Nd$ plotted against 1000/Sr and 100/Nd respectively. It

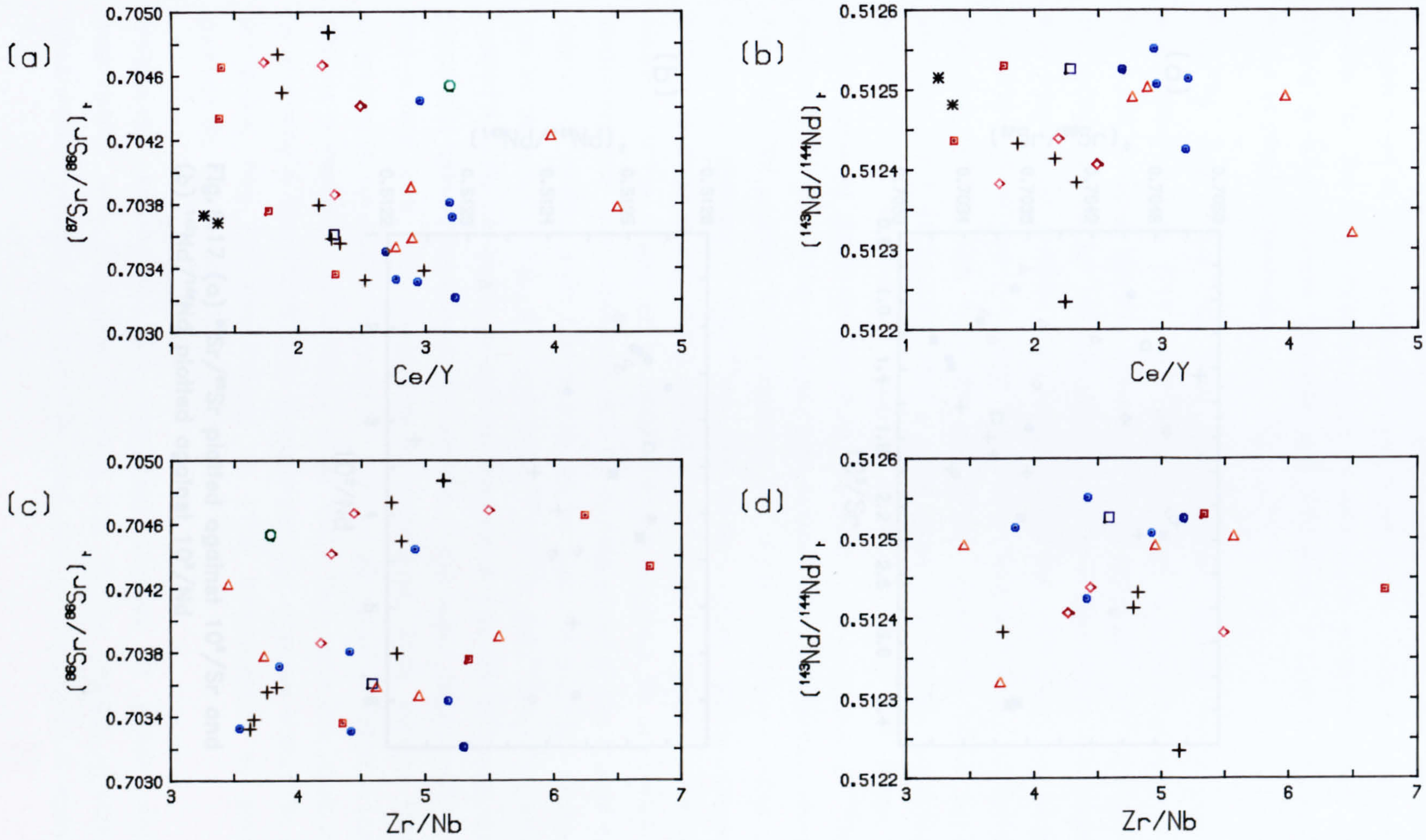

Fig. 6.16a–d $^{87}Sr/^{86}Sr$ and $^{143}Nd/^{144}Nd$ plotted against Ce/Y and Zr/Nb.

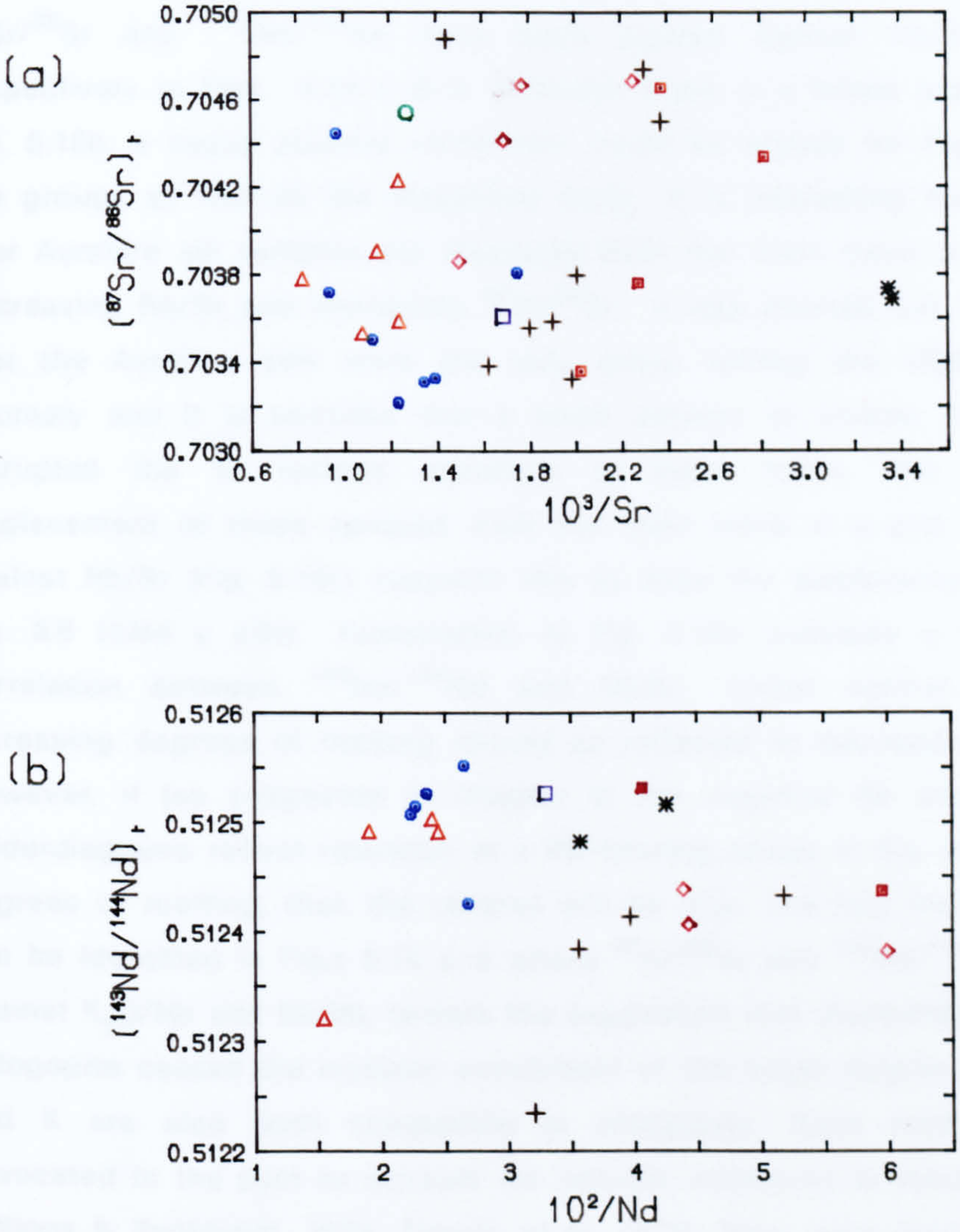

Fig. 6.17 (a) $^{87}Sr/^{86}Sr$ plotted against $10^3/Sr$ and
(b) $^{143}Nd/^{144}Nd$ plotted against $10^2/Nd$

has been shown that simple mixing between two distinct components should produce linear trends on these diagrams, provided that the end-member compositions are constant and no other processes (e.g. AFC) have operated (Langmuir *et al*, 1978; Chauvel & Jahn, 1984; Faure, 1986). No such trends are visible for the post-Dinantian suite. It cannot be concluded from this that mixing was unimportant, however if it did occur, it cannot be explained in terms of simple processes.

$^{87}Sr/^{86}Sr$ and $^{143}Nd/^{144}Nd$ have been plotted against Rb/Sr and Sm/Nd respectively in Figs. 6.18 a & b. Although there is a broad scatter of data in Fig. 6.18b, a vague positive correlation could be argued for Fig. 6.18a (for all the groups as well as the Mauchline data). It is interesting that three of the four Ayrshire sill samples are displaced from the main trend in a direction of decreasing Rb/Sr and increasing $^{87}Sr/^{86}Sr$. It was pointed out in section 5.5.1 that the Ayrshire sills were the only group lacking the slight negative Sr anomaly and it is possible that a small amount of crustal assimilation has disrupted the Sr isotope signature of these rocks. The much smaller displacement of these samples from the main trend in a plot of $^{143}Nd/^{144}Nd$ against Rb/Sr (Fig. 6.18c) supports this as does the displacement identified in Fig. 6.6 (εNd v εSr). Examination of Fig. 6.18c indicates a broad negative correlation between $^{143}Nd/^{144}Nd$ and Rb/Sr. Under normal circumstances increasing degrees of melting should be reflected in decreasing Rb/Sr ratios. However, if (as suggested in chapter 5) the negative Rb anomalies on the spiderdiagrams reflect retention in a Rb-bearing phase in the mantle for small degrees of melting, then the reverse will be true. The fact that similar trends can be identified in Fig.s 6.19 a-d where $^{87}Sr/^{86}Sr$ and $^{143}Nd/^{144}Nd$ are plotted against K_2O/Nb and Ba/Nb, tempts the suggestion that disequilibrium melting of phlogopite caused the isotopic enrichment of the larger degree melts, since Ba and K are also both compatible in phlogopite. Such models have been advocated in the past to account for isotopic variations in volcanic suites (e.g. O'Nions & Pankhurst, 1974; Flower *et al*, 1975). They were discussed at length by Hofmann & Hart (1978), who showed that the diffusion coefficient of Sr in phlogopite was not low enough to allow disequilibrium to persist for geologically significant lengths of time.

Progressive enrichment with increasing degrees of partial melting is inconsistent with both the stratified and streaky mantle models. Since disequilibrium melting of phlogopite must also be discounted, it appears that

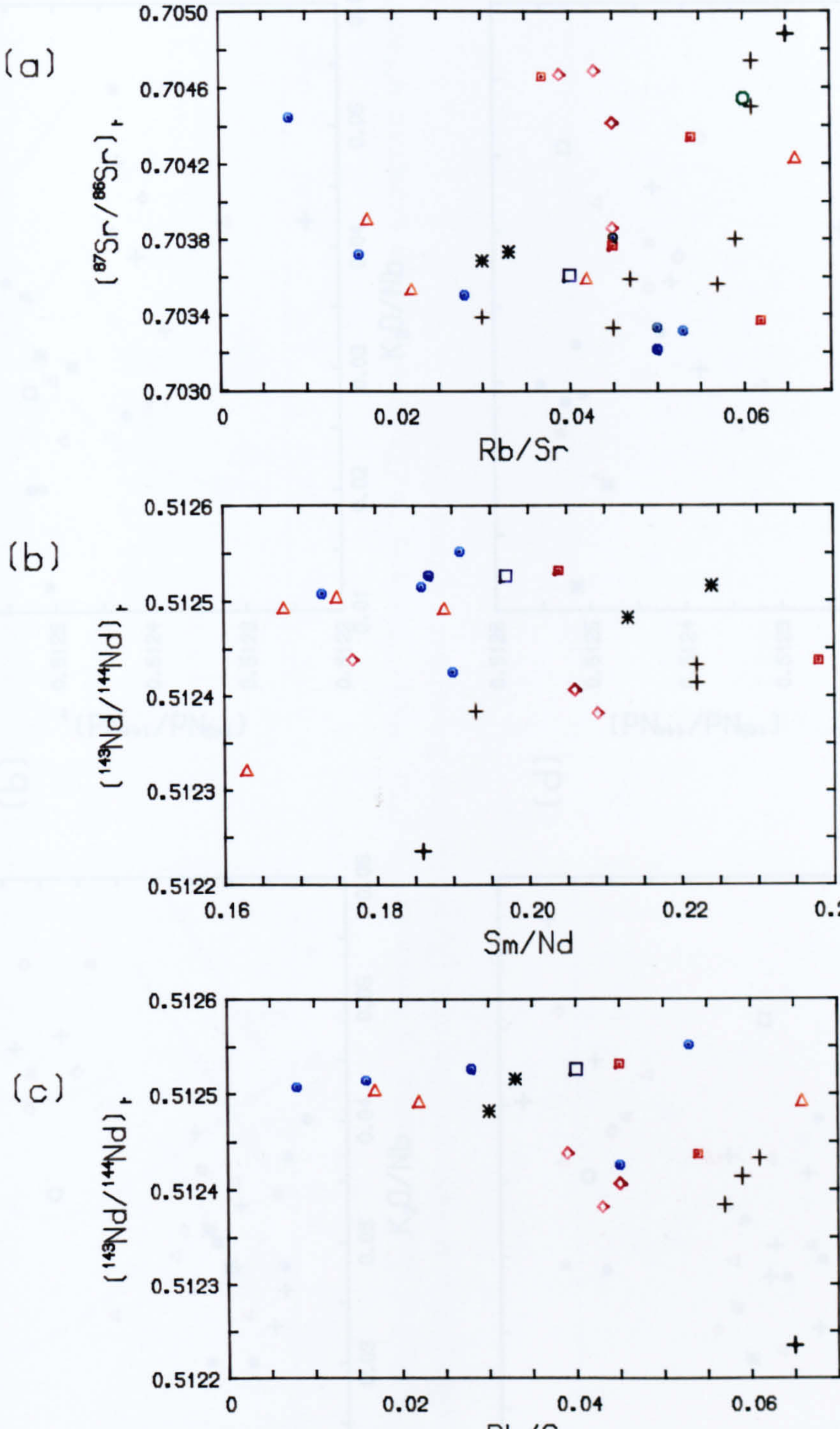

Fig. 6.18 (a) $^{87}Sr/^{86}Sr$ against Rb/Sr; (b) $^{143}Nd/^{144}Nd$ against Sm/Nd; (c) $^{143}Nd/^{144}Nd$ against Rb/Sr

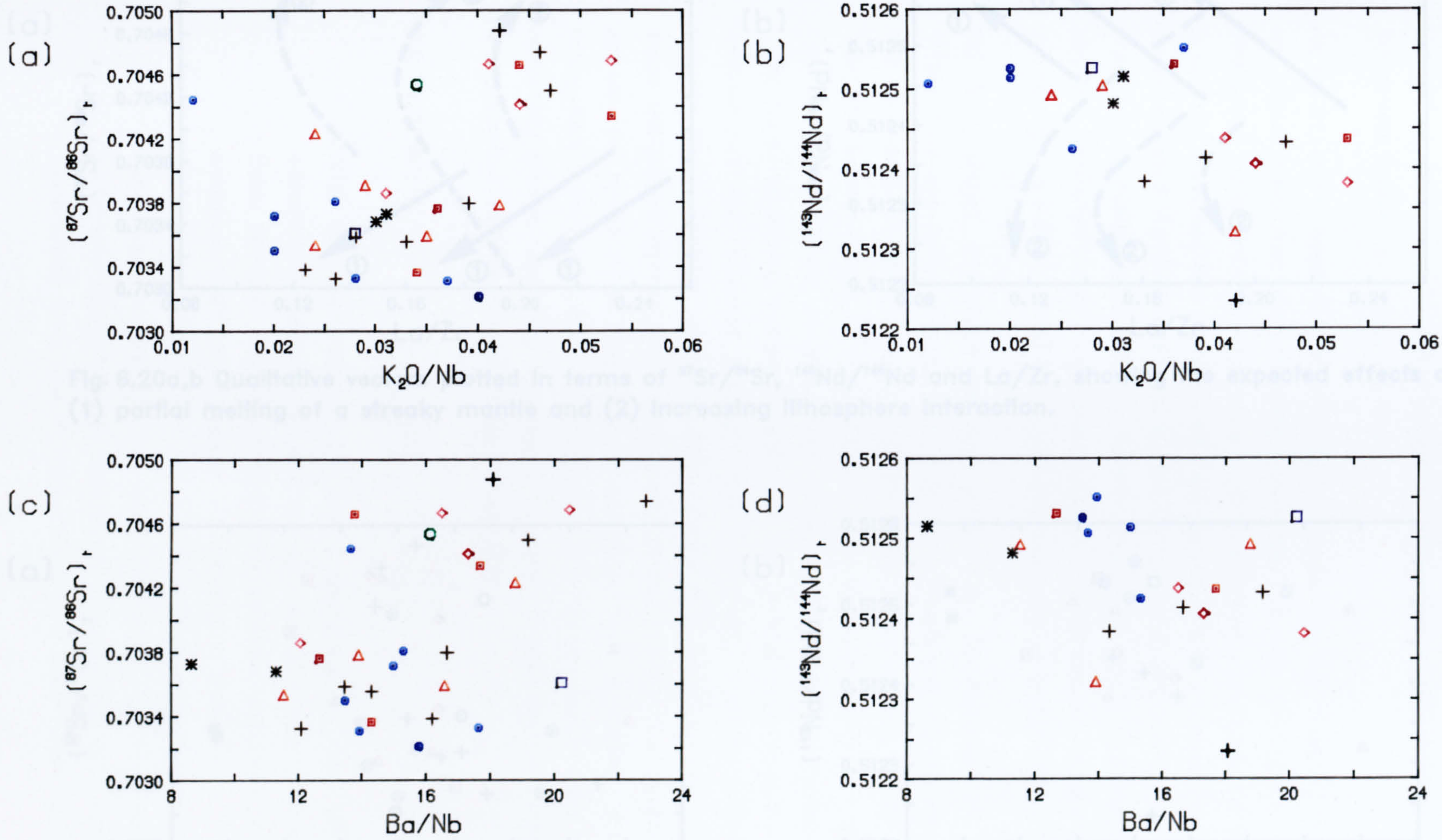

Fig. 6.19a–d $^{87}Sr/^{86}Sr$ and $^{143}Nd/^{144}Nd$ plotted against K_2O/Nb and Ba/Nb.

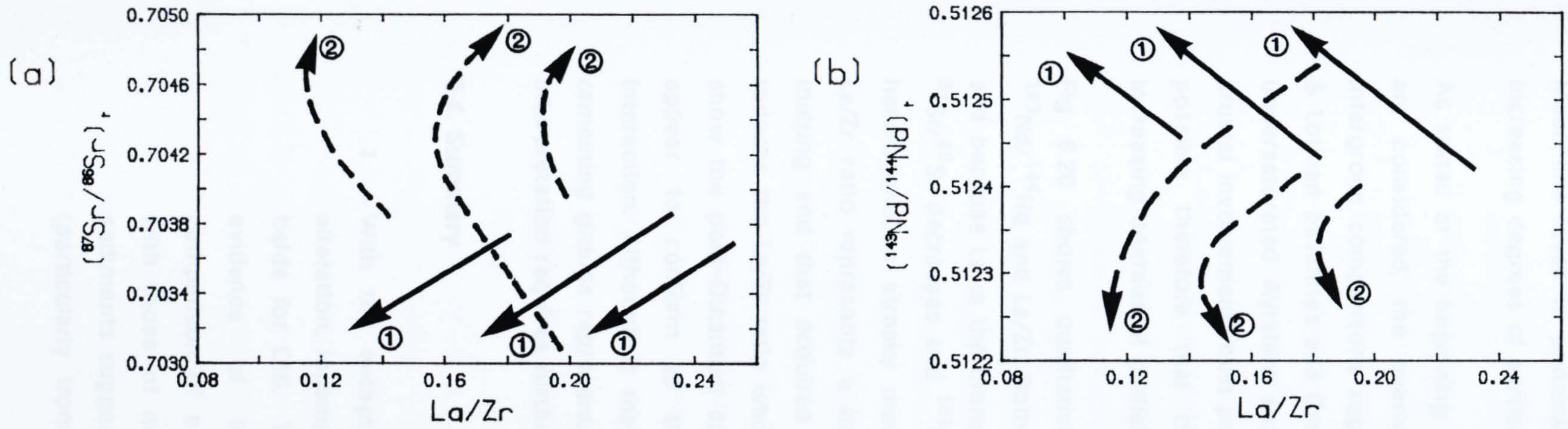

Fig. 6.20a,b Qualitative vectors plotted in terms of $^{87}Sr/^{86}Sr$, $^{143}Nd/^{144}Nd$ and La/Zr, showing the expected effects of (1) partial melting of a streaky mantle and (2) increasing lithosphere interaction.

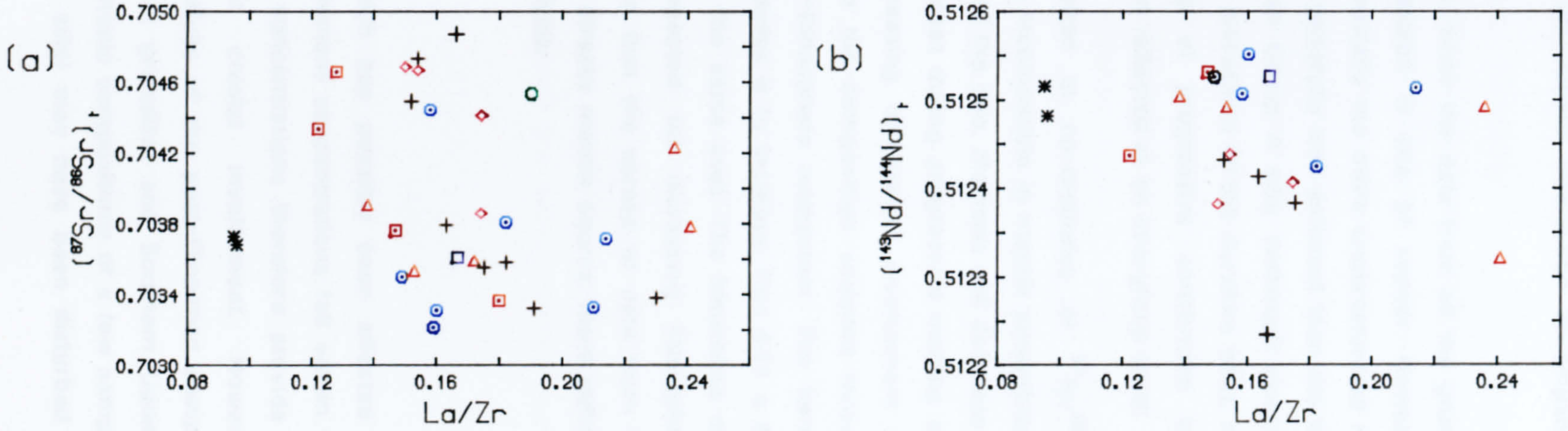

Fig. 6.21a,b $^{87}Sr/^{86}Sr$ and $^{143}Nd/^{144}Nd$ plotted against La/Zr for the post-Dinantian data

the enriched reservoir must be displaced from the initial source melting. The most obvious place is the lithosphere. It therefore appears that for the Mauchline lavas in particular, increasing lithospheric interaction accompanied increasing degrees of partial melting.

As stated at the beginning of this section, when the data from all the groups are considered, the overwhelming impression is one of scatter. However, intergroup comparisons suggest that isotopically the more undersaturated Fife & Lothian basanites and Group B sills are generally less enriched than the less undersaturated Ayrshire and Fife & Lothian Group A sills, (although possible crustal involvement must preclude further discussion of the Ayrshire sills). It is possible therefore that the relationship of progressive enrichment with increasing degrees of partial melting is also reflected at an intergroup level.

Fig 6.20 shows qualitative vectors plotted in co-ordinates of $^{87}Sr/^{86}Sr$, $^{143}Nd/^{144}Nd$ and La/Zr. Both La and Zr are incompatible in mantle assemblages and because La is the more incompatible of the two, the ratio will decrease as $^{87}Sr/^{86}Sr$ decreases and $^{143}Nd/^{144}Nd$ increases during progressive melting of a heterogeneous streaky mantle. With increasing lithosphere involvement the La/Zr ratio represents a balance between the composition acquired through melting and that acquired through melt-lithosphere interaction. The former reduces the La/Zr ratio while the latter causes it to increase. Figs 6.21 a & b show the post-Dinantian data plotted on the same axes. The Mauchline data appear to conform to the pattern expected for increasing lithospheric interaction. Although it may be concluded that the spread of data from the remaining groups represents melting of a streaky mantle source, more definite interpretation requires further isotopic analysis.

6.4. Summary

1. With the exception of Ba which has possibly been affected by alteration, incompatible trace element concentrations fall within the fields for OIB. Trace element concentrations therefore provide no evidence of lithospheric or crustal involvement. However, comparison of εNd and εSr values of the post-Dinantian samples with those of megacrysts, basic granulites and Southern Uplands sediments suggests that the isotopic compositions of a few samples (particularly from the Ayrshire sills) may have been disturbed by

crustal interaction. The extent of this disturbance must be slight since it has not affected the degree of silica saturation of any of the samples.

2. Incompatible trace element ratios (excepting those which include TiO_2) are not fractionated with magma differentiation. Melting models using Ce/Y and Zr/Nb suggest that mixing between magmas from more than one source has produced the range of compositions. However, because of the uncertainties in bulk partition coefficients, residual mantle mineralogy and source compositions, it is not possible to constrain the nature of these sources. Using the distribution coefficients of Fitton & James (1986) (Fig. 6.12) it is possible to constrain the amount of melting required to produce the range of compositions from a MORB20 source. On this basis, the alkaline samples represent partial melts of <2%, and the quartz dolerites c.5%. If the source is more enriched than MORB20, the more undersaturated alkaline samples must be the result of larger (5–15%) degrees of melting.

3. Isotopic and elemental variations could be interpreted in terms of variable degree melting of a heterogeneous source. Alternatively it is suggested that the trends highlighted by the Mauchline group indicate progressive lithosphere interaction with increasing degrees of partial melting. It is suggested that the scatter in the Fife & Lothian basanites and Group B sills reflects variable melting of a streaky mantle, and the effects of lithosphere interaction (as emphasised by the Mauchline samples) are superimposed on this trend.

CHAPTER 7

COMPARISONS

Most of this chapter is devoted to a comparison of Dinantian and post-Dinantian magmatism in the Midland Valley. It concludes with a comparison of both Midland Valley suites with several other continental and oceanic provinces.

7.1. Comparison of the Dinantian and post-Dinantian suites

7.1.1. Introduction

As outlined in chapter 1, the post-Dinantian igneous suite represents the latter part of a longer magmatic event which affected the Midland Valley through the Carboniferous and part of the Permian. A synthesis of Dinantian magmatism (Smedley 1986a,b; 1988a,b) concluded that the Dinantian suite was 'transitional' to mildly alkaline in character, and displayed several distinct magmatic lineages: basic samples ranging from basanite to q-normative tholeiite, and evolved members ranging from trachyte and phonolitic trachyte, to peralkaline rhyolite (Smedley, 1986b). She confirmed and amplified earlier suggestions by Macdonald (1980) that many of the basic members displayed inter-regional variations in incompatible element concentrations, particularly LREE, Zr, Nb, K and Ba. These are less well reflected in Sr, Nd and Pb isotopic compositions (Smedley, 1986a,b; 1988a,b). Smedley (1986a,b; 1988a) modelled Ce/Y and Zr/Nb variations in terms of variable degree melting of slightly heterogeneous asthenosphere.

In the following sections, the two suites are compared in terms of degree of silica saturation (reflecting degree of melting), concentration of incompatible elements (reflecting degree of enrichment), and isotopic composition. Ce/Y and Zr/Nb variations are also compared since these have formed the basis of melting models for both suites (chapter 6 and Smedley, 1986a,b; 1988a). Average compositions for each group have been used for comparisons of degrees of saturation and incompatible element content. The degree of silica saturation of each group has been expressed using the Saturation Index (S.I.) (Latin *et al*, in press). Before calculation of S.I. the mean composition of each group was normalised to mantle olivine (Fo_{90}) to compensate for inter-group

variations in degree of differentiation on the assumption that the principal agency for such variations was olivine fractionation.

7.1.2. Comparisons

The geographical distribution of Carboniferous and Permian igneous rocks in the Midland Valley (Fig. 7.1) shows that throughout the period, magmatism was more productive in the west than in the east. This is confirmed by comparison of the S.I. values of the various groups (Table 7.1). Consideration of S.I. for all the west Midland Valley groups shows that the Clyde Plateau, Kintyre, Firth of Clyde and Passage Group lavas resulted from significantly larger (and similar) degrees of melting than the Mauchline and Ayrshire sill groups. It is therefore surprising that when the incompatible element concentrations of each group are compared (Fig. 7.2), the four saturated groups appear to have incompatible element contents just as high, if not higher, than the undersaturated groups. However, the two most saturated Dinantian groups (Firth of Clyde and Kintyre) lack the characteristic depletion in K, suggesting that melting has proceeded to a stage where phlogopite has been consumed.

Comparison of the east Midland Valley groups allows similar observations to be made. The variably saturated Dinantian compositions (Table 7.1) contrast strongly with the undersaturated post-Dinantian Fife & Lothian basanites and Group B sills. However the contrast is less clearly reflected in their incompatible element compositions (compare Figs. 7.2b and 7.3b).

Comparison of Dinantian and post-Dinantian groups in all parts of the Midland Valley presents a paradox. On the basis of major element chemistry (S.I.) the Dinantian samples represent the larger degree melts. However, their high incompatible trace element concentrations seem to contradict this. It is possible that the source for the Dinantian lavas was more enriched than that of the post-Dinantian magmas. More extensive melting of such an enriched source would have produced magmas with incompatible trace element abundances similar to those of magmas from a less enriched, less extensively melted source. Depending on the time of this supposed enrichment, it might be expected to be reflected in the isotope compositions of the Dinantian samples. Fig 7.4 compares initial $^{87}Sr/^{86}Sr$ and $^{143}Nd/^{144}Nd$ for the Dinantian and post-Dinantian suites and shows that the ranges are very similar despite the fact that a few Dinantian samples have slightly lower $^{87}Sr/^{86}Sr$ and two

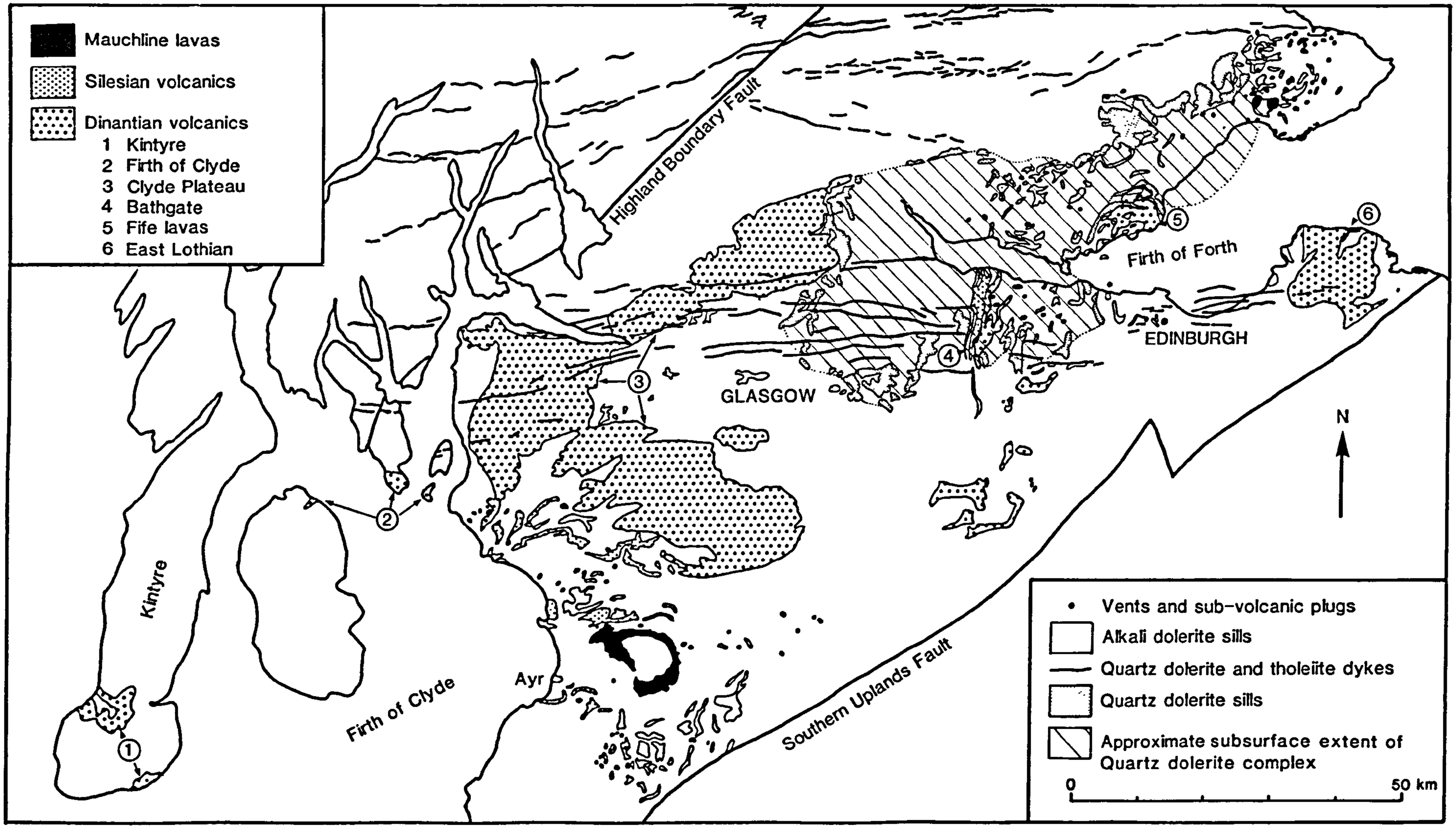

Fig 7.1 Geographical distribution of Carboniferous and Permian igneous rocks in the Midland Valley of Scotland.

West		East	
Dinantian			
Clyde Plateau lavas	6.24	Holyrood lavas	0.46
Firth of Clyde lavas	7.91	Fife lavas	4.37
Kintyre lavas	7.01	East Lothian lavas	0.37
		Bathgate lavas	6.47
Post-Dinantian			
Passage Group lavas	5.01	Fife & Lothian Group A sills	4.09
Ayrshire sills	-10.69	Fife & Lothian Group B sills	-8.68
Mauchline Group	-3.18	Fife & Lothian basanites	-13.07

Table 7.1 Degree of silica-saturation for each of the Midland Valley groups expressed in terms of the Saturation index. The mean composition of each group was first normalised to mantle olivine (Fo_{90}) to compensate for inter-group variations in degree of differentiation.

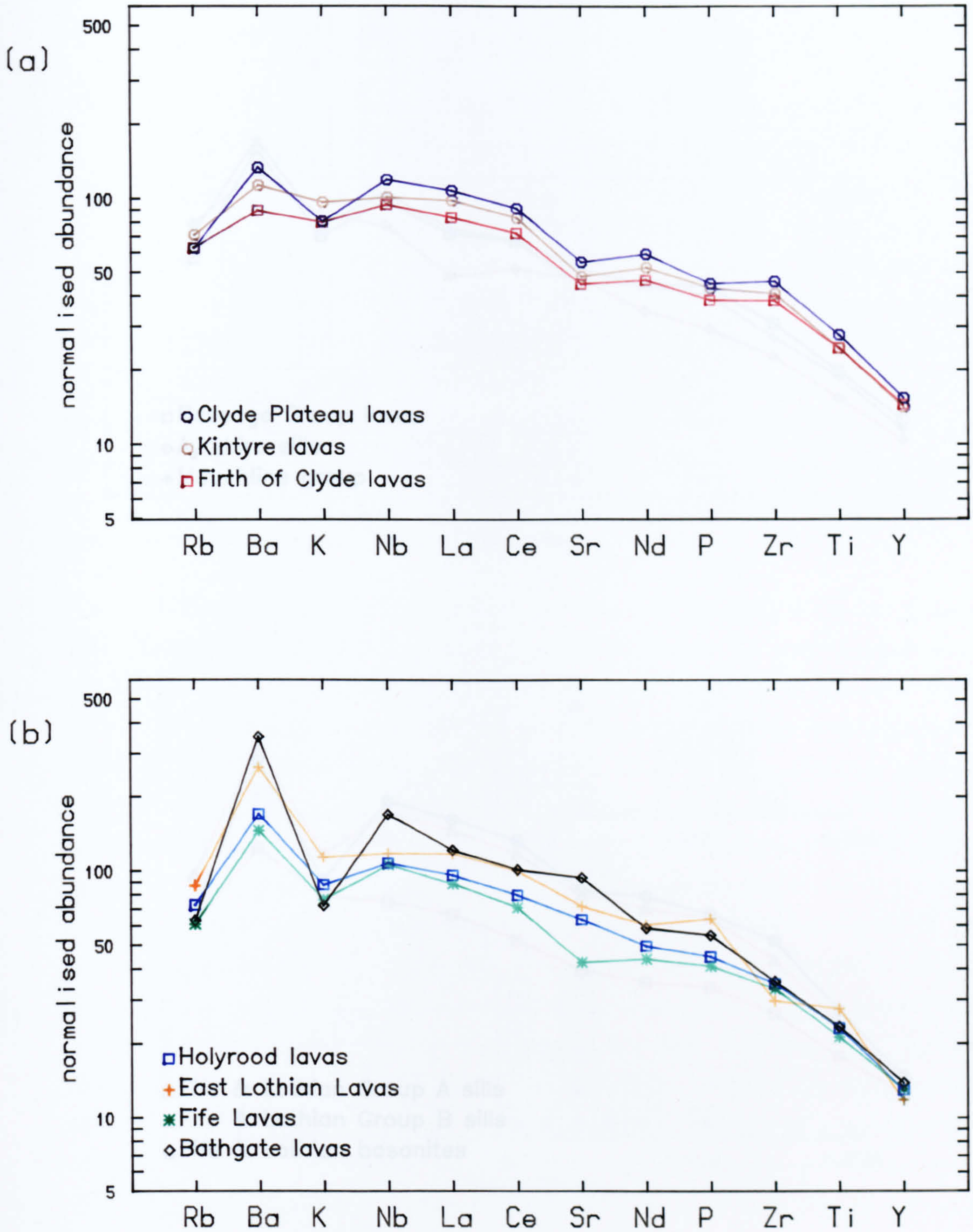

Fig.7.2 Mean chondrite–normalised spiderdiagram plots for basic samples from Dinantian Suite: (a) west Midland Valley, (b) east Midland Valley. Data from Smedley (1986b).

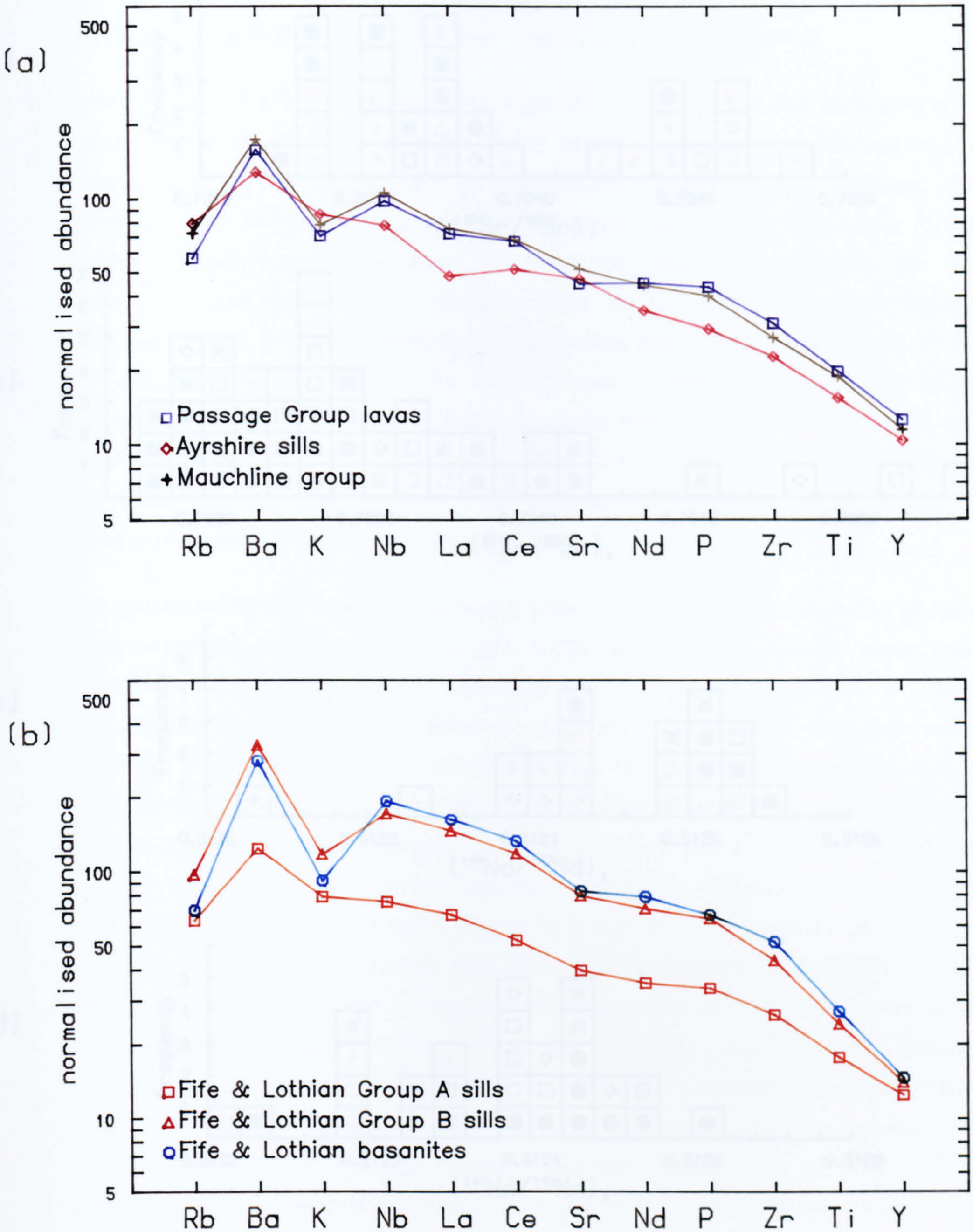

Fig.7.3 Mean chondrite–normalised spiderdiagram plots for basic samples from post–Dinantian Suite: (a) west Midland Valley, (b) east Midland Valley.
(Duplicate copy on overlay in back pocket of thesis)

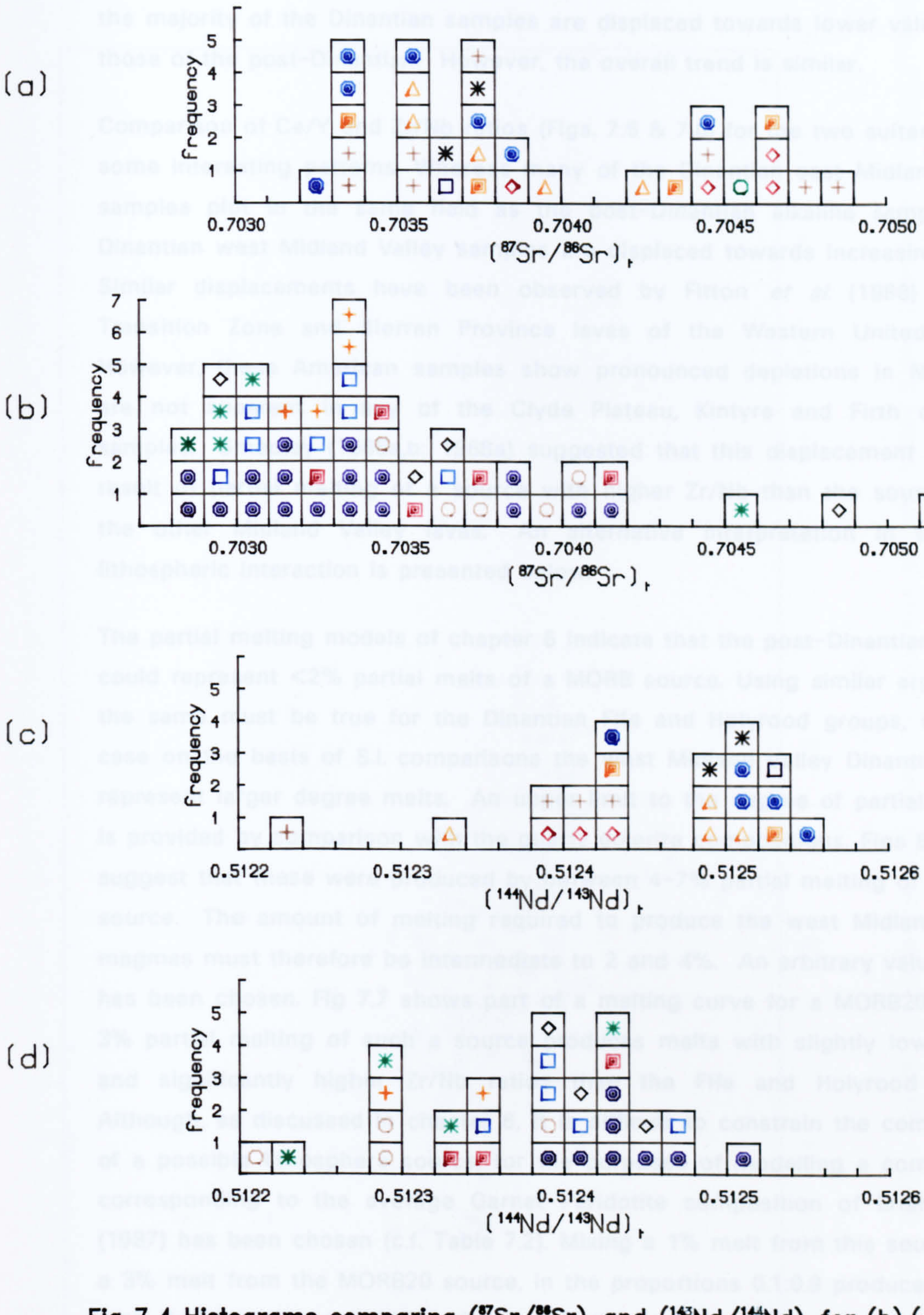

Fig. 7.4 Histograms comparing $(^{87}Sr/^{86}Sr)_t$ and $(^{143}Nd/^{144}Nd)_t$ for (b),(d) Dinantian and (a),(c) post–Dinantian suites. Dinantian data from Smedley (1986b).

samples have higher ratios, (with $^{87}Sr/^{86}Sr > 0.7050$). In terms of $^{143}Nd/^{144}Nd$ the majority of the Dinantian samples are displaced towards lower values than those of the post-Dinantian. However, the overall trend is similar.

Comparison of Ce/Y and Zr/Nb ratios (Figs. 7.5 & 7.6) for the two suites reveals some interesting patterns. Whereas many of the Dinantian east Midland Valley samples plot in the same field as the post-Dinantian alkaline samples, the Dinantian west Midland Valley samples are displaced towards increasing Zr/Nb. Similar displacements have been observed by Fitton *et al.* (1988) for the Transition Zone and Sierran Province lavas of the Western United States. However, these American samples show pronounced depletions in Nb which are not apparent in any of the Clyde Plateau, Kintyre and Firth of Clyde samples. Smedley (1986a,b; 1988a) suggested that this displacement was the result of partial melting of a source with higher Zr/Nb than the source(s) for the other Midland Valley lavas. An alternative interpretation in terms of lithospheric interaction is presented below.

The partial melting models of chapter 6 indicate that the post-Dinantian groups could represent <2% partial melts of a MORB source. Using similar arguments the same must be true for the Dinantian Fife and Holyrood groups, in which case on the basis of S.I. comparisons the west Midland Valley Dinantian lavas represent larger degree melts. An upper limit to the degree of partial melting is provided by comparison with the quartz dolerite compositions. Figs 6.12-6.15 suggest that these were produced by between 4-7% partial melting of a MORB source. The amount of melting required to produce the west Midland Valley magmas must therefore be intermediate to 2 and 4%. An arbitrary value of 3% has been chosen. Fig 7.7 shows part of a melting curve for a MORB20 source. 3% partial melting of such a source produces melts with slightly lower Ce/Y and significantly higher Zr/Nb ratios than the Fife and Holyrood groups. Although, as discussed in chapter 6, it is difficult to constrain the composition of a possible lithosphere source, for the purposes of modelling a composition corresponding to the average Garnet Peridotite composition of Erlank *et al.* (1987) has been chosen (c.f. Table 7.2). Mixing a 1% melt from this source with a 3% melt from the MORB20 source, in the proportions 0.1:0.9 produces a melt with Ce/Y of c.2 and Zr/Nb c.8: very similar to ratios for some of the Clyde Plateau lavas. Table 7.2 shows that the calculated absolute concentrations of Ce, Y, Zr and Nb agree well with the mean recalculated primary concentrations for the Clyde Plateau lavas. This model of mixing magmas from contrasted

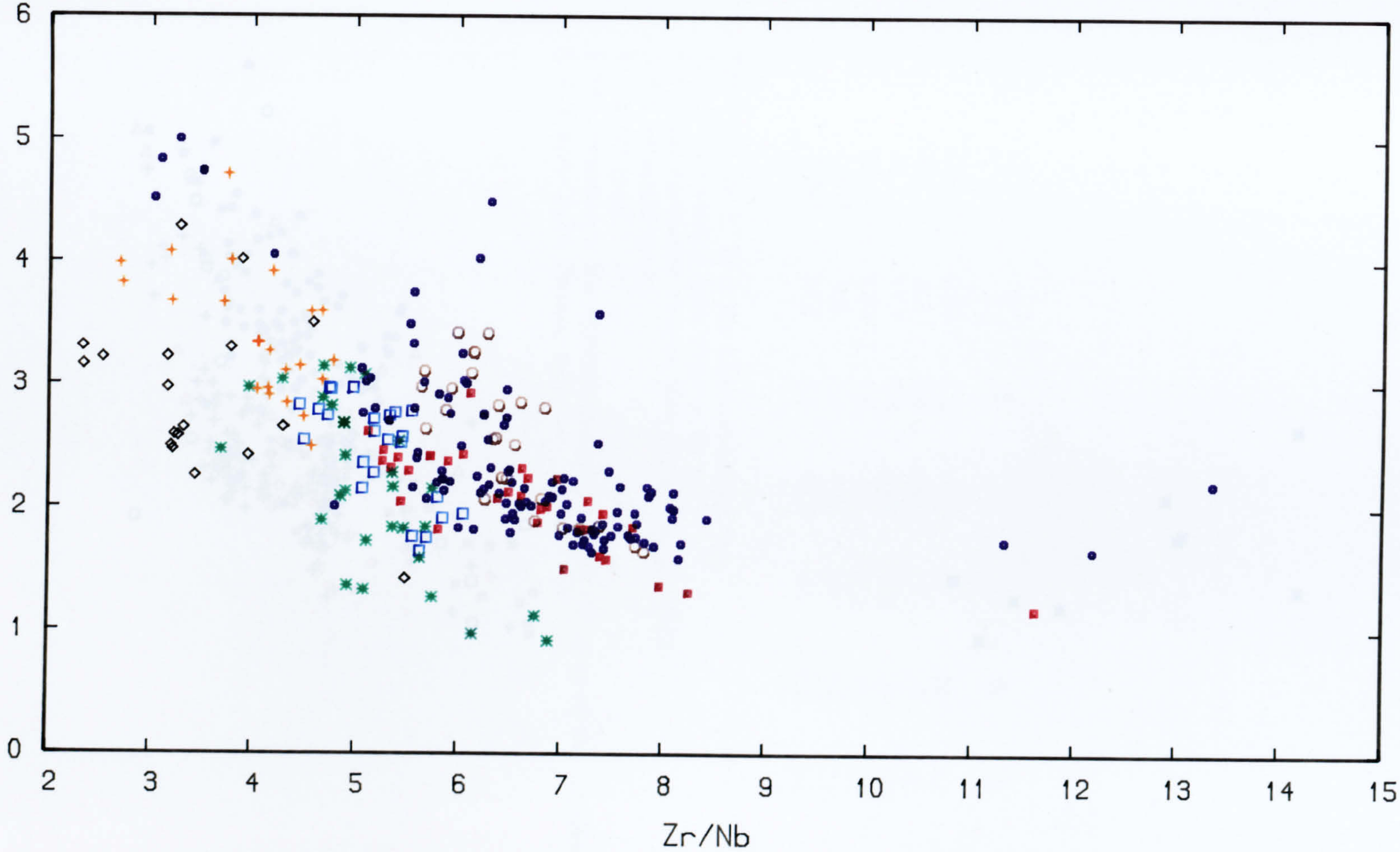

Fig. 7.5 Ce/Y v Zr/Nb for basic samples from the Dinantian Midland Valley Suite. Data from Smedley (1986b).

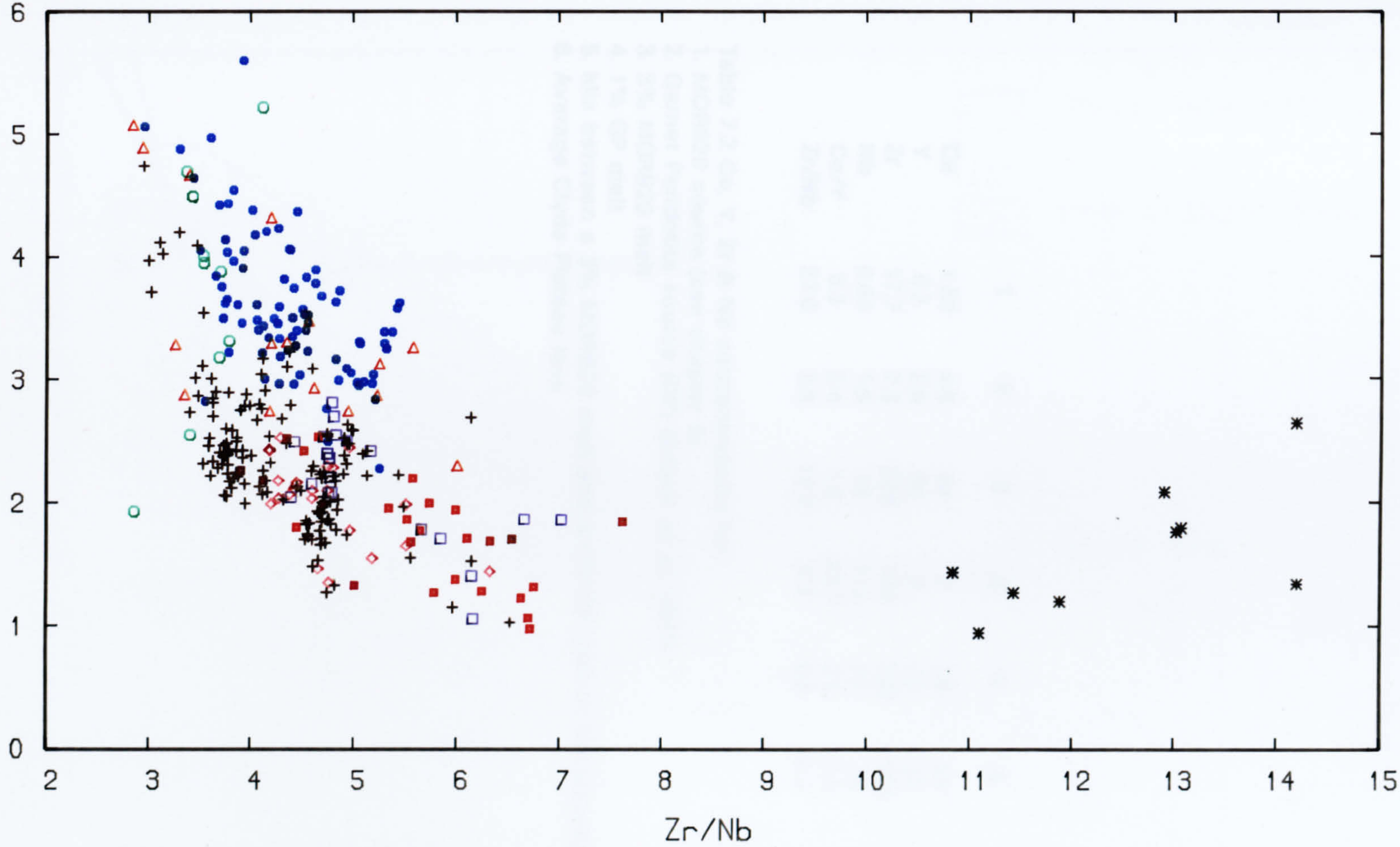

Fig. 7.6 Ce/Y v Zr/Nb for basic samples from the post–Dinantian Midland Valley Suite. (Duplicate copy on overlay in back pocket of thesis).

	1	2	3	4	5	6
Ce	1.83	4.8	44	2	56	53
Y	6.2	2.0	30	8	22	22
Zr	17.7	7.3	228	100	183	183
Nb	0.64	1.9	18	112	27	30
Ce/Y	0.3	2.4	1.5	23.7	2.5	2.4
Zr/Nb	27.6	3.8	12.7	0.9	6.8	6.2

Table 7.2 Ce, Y, Zr & Nb concentrations for:
1. MORB20 source (see chapter 6)
2. Garnet Peridotite source (GP) (Erlank *et al*, 1987)
3. 3% MORB20 melt
4. 1% GP melt
5. Mix between a 3% MORB20 melt and a 1% GP melt in the proportions 0.9:0.1
6. Average Clyde Plateau lava

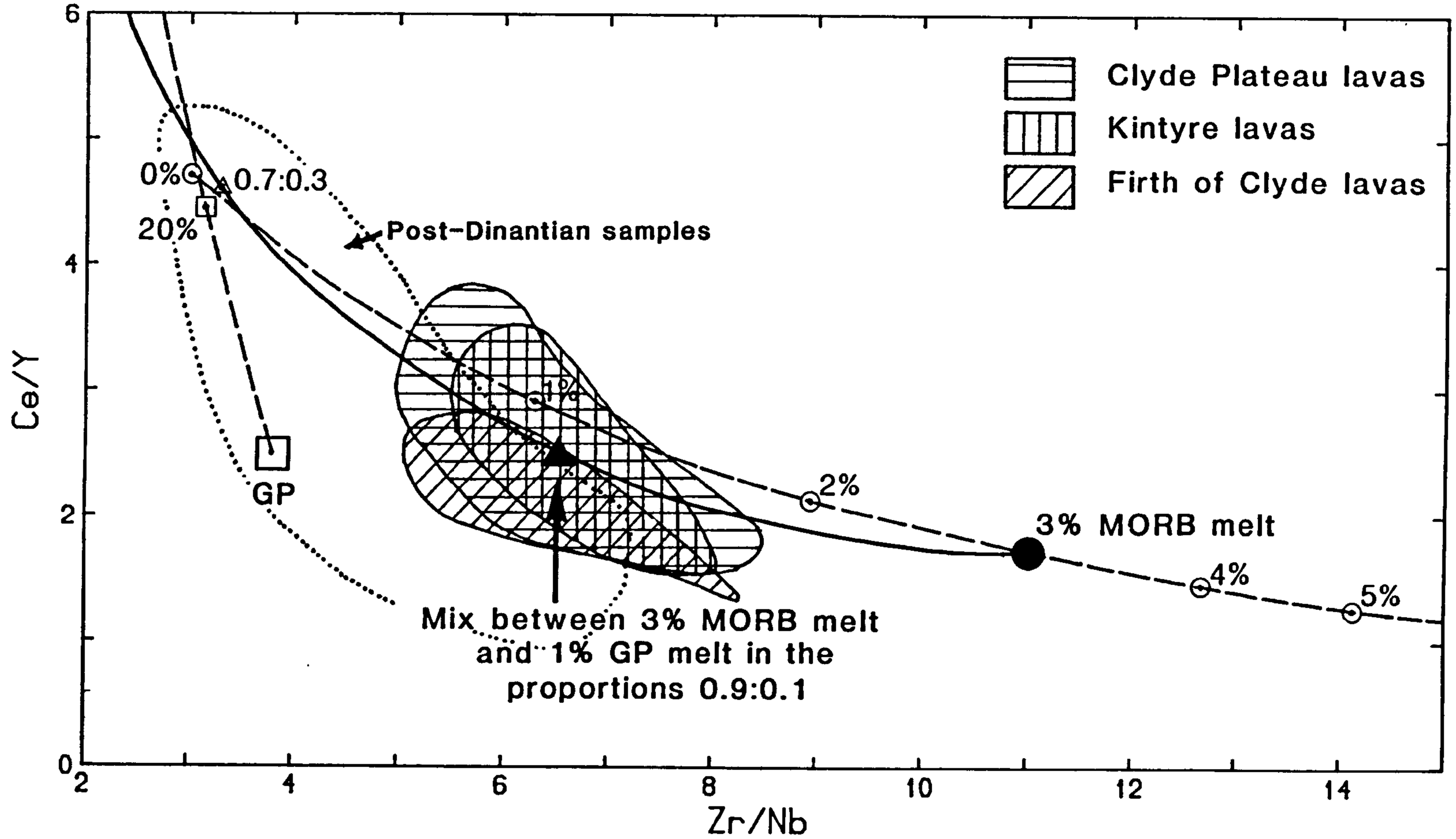

Fig. 7.7 Regional variations in Ce/Y and Zr/Nb for west Midland Valley Dinantian samples with MgO > 4wt%. Melting curves for a MORB20 source (circles) and a lithosphere mantle (GP) source (squares) are calculated using the partition coefficients of Fitton & Dunlop (1986): D_{Ce}=0.0149, D_{Y}=0.237, D_{Zr}=0.064 and D_{Nb}=0.00696. The mixing curve (triangles) between a 3% MORB20 melt and a 1% GP (Ce/Y=23.7,Zr/Nb=0.88) is also shown.

sources therefore provides a possible means of producing saturated magmas with anomalously high incompatible element concentrations.

Examination of Figs. 7.5 & 7.7 shows that three of the Clyde Plateau lavas and one Firth of Clyde sample plot close to the calculated composition of a 3% MORB20 melt (which is just within the field of the post-Dinantian quartz dolerites). Their recalculated primary Ce, Y, Zr and Nb concentrations are similar to those calculated for the melt, and it is suggested that they represent magmas which have escaped significant lithosphere interaction (although it is possible that these samples are mis-identified quartz dolerites).

The modified composition of an asthenospheric melt after interaction with the mantle lithosphere will depend on a variety of factors. The most obvious are: the degree of melting of the asthenospheric source, the degree of lithospheric melting and/or leaching, and the original compositions of both sources. These effects are discussed in the following section.

7.1.3. Melting and enrichment processes.

Melt is generated in the mantle when the mantle geotherm intersects the solidus. Under normal conditions (Fig. 7.8), the geotherm is a long way below the solidus for dry peridotite and melting does not occur unless the temperature is raised (mantle plume), or upwelling occurs (in response to lithosphere attenuation), or the solidus is depressed (e.g. by hydration during subduction). However, Latin *et al.* (in press,a) have suggested that instead of representing the initiation of melting, the solidus of Fig. 7.8 represents the line of significant (or experimentally visible) melt generation (5-10%) and at a given pressure, small melt fractions could be present at substantially lower temperatures. Minor volatile concentrations in the mantle can notably modify the position of the solidus, and the varying effects of H_2O-CO_2 enrichment are shown in Fig. 7.9. The volatile content of the upper part of the asthenosphere is influenced by indigenous amphibole, mica and carbonate (Latin *et al.*, in press,b) and by the ascent of melts generated at greater depths. The crystallisation of anhydrous phases from such melts will enrich the remaining fluids in volatiles, not all of which are scavenged by later crystallisation of volatile-bearing phases (Spera, 1984, 1987). Recently, the process of redox melting has been proposed for the generation of melts (Taylor, 1985; Green *et al.*, 1987; Foley, 1988). Green *et al.* (1987) suggested that the mantle beneath

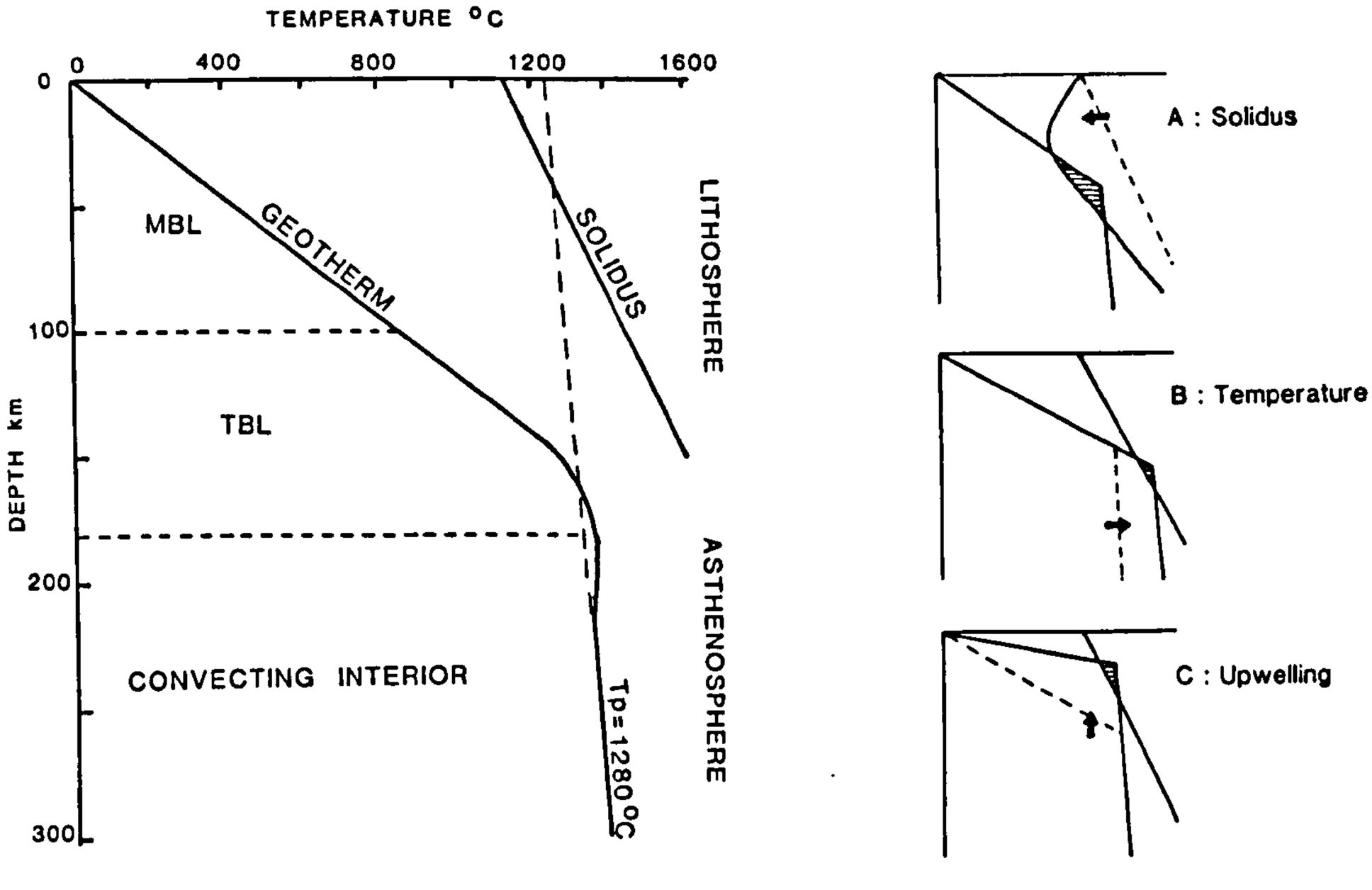

Fig. 7.8 from Latin *et al.* (in press, b). The horizontally averaged thermal structure of the lithosphere for a potential temperature of 1280°C, a mechanical boundary layer thickness of 100km, and an interior viscosity of $2x10^{17}m^2s^{-1}$ following McKenzie & Bickle (1988). The corresponding adiabatic upwelling curve (assuming no melting) is shown dashed. The solidus position for dry peridotite is also indicated. **MBL**= mechanical boundary layer (the upper rigid part of the lithosphere, where heat is transported by conduction only); **TBL**= thermal boundary layer (the sandwich layer between MBL and asthenosphere in which heat is transported by conduction and convection, and which is inferred to be periodically incorporated into the asthenosphere circulation). The cartoons to the right of the main diagram show three mechanisms for producing melt: (a) melting due to a change in solidus position, (b) melting by raising the potential temperature, and (c) melting by adiabatic upwelling. The potential temperature is the temperature of the adiabatic gradient projected to the surface.

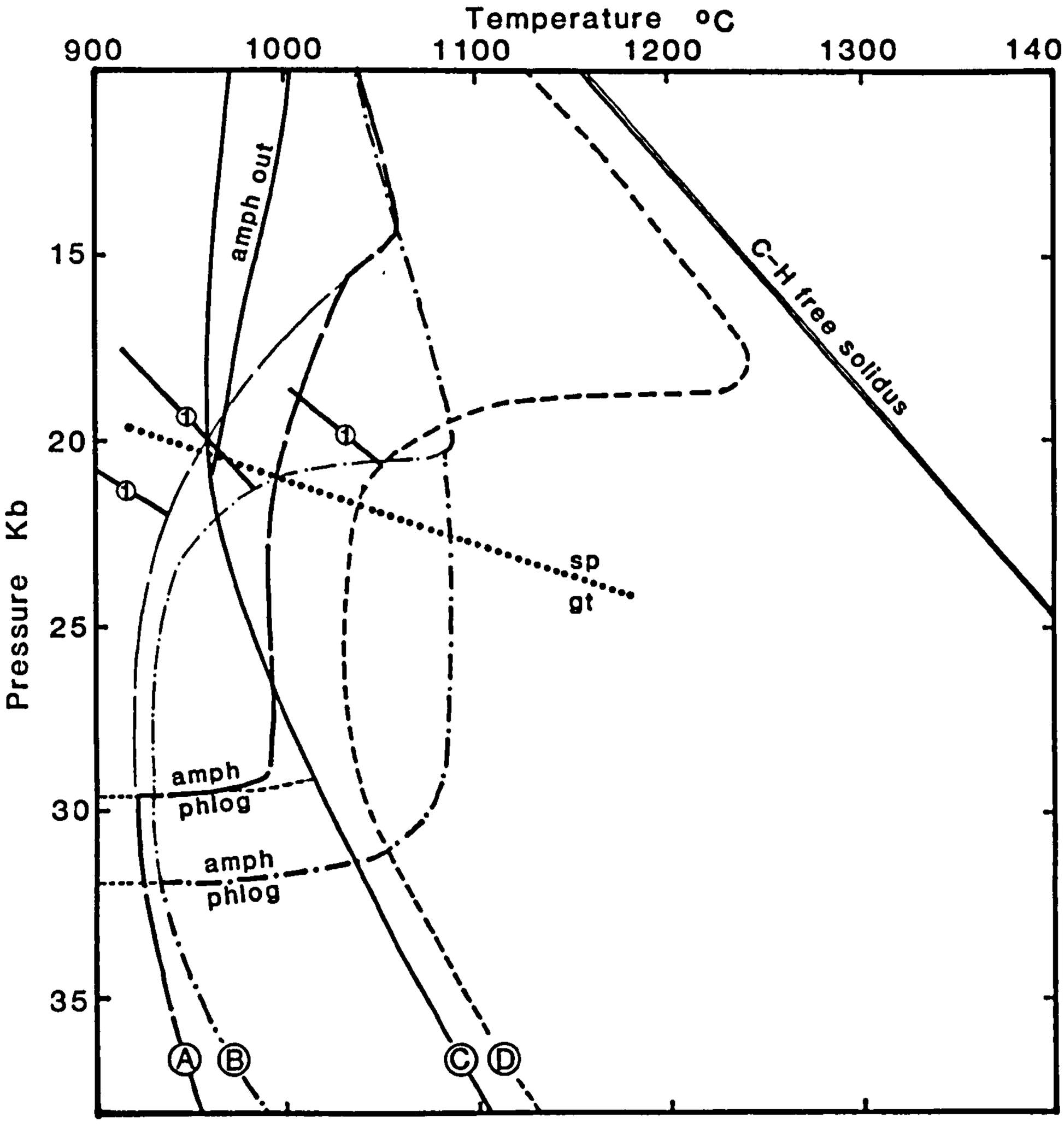

Fig. 7.9 Solidi for peridotite-C-H-O. (A) H_2O-CO_2: (Falloon & Green, in press); (B) H_2O-CO_2: (Wallace & Green, 1988); (C) H_2O: (Green, 1973); (D) CO_2. (Falloon & Green, 1989). The dotted line shows the approximate position of the spinel-garnet transition. (1) marks the lower boundary of the decarbonation reaction for the solidus curves A, B & D. Melts above this boundary will be in equilibrium with a vapour phase.

the asthenosphere is a region of reduced volatile species containing C-H-O fluids. The transition from these supposed reduced conditions to the more oxidised environment of the lithosphere encourages an increase in the H_2O:CH_4 ratio of the fluid, so depressing the mantle solidus. In this way, at pressures >30kb (above the stability field of amphibole), the geothermal gradient will lie within a field of partial melting, and minor melting can be considered to be part of the steady state regime.

The volatile composition and concentration of a melt or fluid is influenced by oxygen fugacity and the buffering capacity of peridotite. Fluids which are CH_4-H_2O rich under reducing conditions will oxidise to CO_2-H_2O with increasing fO_2. At present there is no concensus on the oxidation state of the mantle. The involvement of reduced C-O-H fluids has been inferred for parts of the lower lithosphere in cratonic regions (Deines, 1980; Taylor, 1987; Foley, 1988), but the presence of primary carbonate in some alkaline magmas has suggested a more oxidised source (Eggler, 1987).

At sub-solidus temperatures, the stability of carbonate at pressures >16-21 kb, and its effectiveness at buffering CO_2, ensures that in the garnet lherzolite stability field, any fluid/vapour in excess of that needed to fully hydrate phlogopite (>25-30 kb) or amphibole (<25-30 kb) will be H_2O-rich (Eggler, 1987; Menzies *et al*, 1987). The breakdown of carbonate at pressures <16-21 kb (Eggler, 1987) and the partitioning of water into silicate melt (Menzies *et al*, 1987) enhance the CO_2 content of fluids at low pressures.

The temperature of the mantle solidus at a given pressure is therefore dependent on a number of factors, including the composition of volatile species, and whether they can be effectively buffered by hydrous or carbonate accessory minerals and also by the capacity of any melt present to accommodate volatiles.

Steady-state melting in the upper asthenosphere (>30 kb) appears to be the natural response to minor volatile concentrations. If fluid concentrations in the source region are low they will be accommodated by the melt and the region of partial melting will be vapour-free. However, the stability field of amphibole at pressures <25-30 kb provides a lid to this partially molten layer since any interstitial melt migration upwards will crystallise to amphibole lherzolite (Green *et al*, 1987). McKenzie (1989) has suggested that intersection of a

volatile-dependent solidus by the steady-state geotherm might cause the movement of melt fractions as low as 0.001%. Such small-degree melts are unlikely to be heat carriers, and will migrate upwards along the geotherm, fractionally crystallising from the 'knee' of the geotherm to the point where they again intersect their solidus. (e.g. Fig. 7.10).

Hydrous fluids are capable of leaching and transporting large concentrations of incompatible elements. The addition of small amounts of CO_2 to such a liquid will greatly reduce their capacity as solvents (Eggler, 1987; Menzies *et al*, 1987). However carbonate melts are very effective at fractionating the LILE and P, and carbonatites in general are known to be greatly enriched in Na, K, Sr, Rb and LREE (Green & Wallace, 1988). Recent experimental studies (Wallace & Green, 1988; Green & Wallace, 1988) have emphasised the importance of carbonatite melts in mantle metasomatism. Infiltration of lherzolite at pressures <16-21 kb (at 950-1050°C) triggers decarbonation reactions with the release of CO_2 vapour. The net effect of such reactions is the replacement of opx with cpx+ol$^{+}_{-}$sp, altering lherzolite or harzburgite towards wehrlitic compositions (Green & Wallace, 1988). The composition and CO_2/H_2O ratio of the fluid released in this reaction will influence the stability of amphibole and phlogopite, moving the solidus to higher temperatures. The base of the mechanical boundary layer will therefore become increasingly enriched in incompatible elements hosted in amphibole, phlogopite, apatite and carbonate (Green *et al*, 1987). Fractional crystallisation will ensure that the more fusible phases are concentrated at deeper levels. These enrichments may well pass down into the thermal boundary layer. However, the lower part of the thermal boundary layer and the asthenosphere will become relatively depleted as they lose repeated melt fractions. Long term replenishment of both will be achieved by mantle convection processes.

The significance of amphibole in the petrogenesis of alkaline rocks has been discussed by many authors (e.g. Kesson & Prince, 1972; Vinx & Jung, 1977; Wilshire *et al*, 1980; Witt & Seck, 1989). Calculated REE profiles of melts which may have coexisted with mantle vein amphibole are remarkably similar to those for alkaline magmas (Menzies *et al*, 1987). Recently Francis & Ludden (1989, in press) identified a population gap along a mixing line between transitional alkaline basalt and olivine nephelinite (for the Fort Selkirk lavas of the central Yukon). The gap coincides with the compositions of amphibole and amphibole-garnet-clinopyroxene assemblages observed in mantle xenoliths,

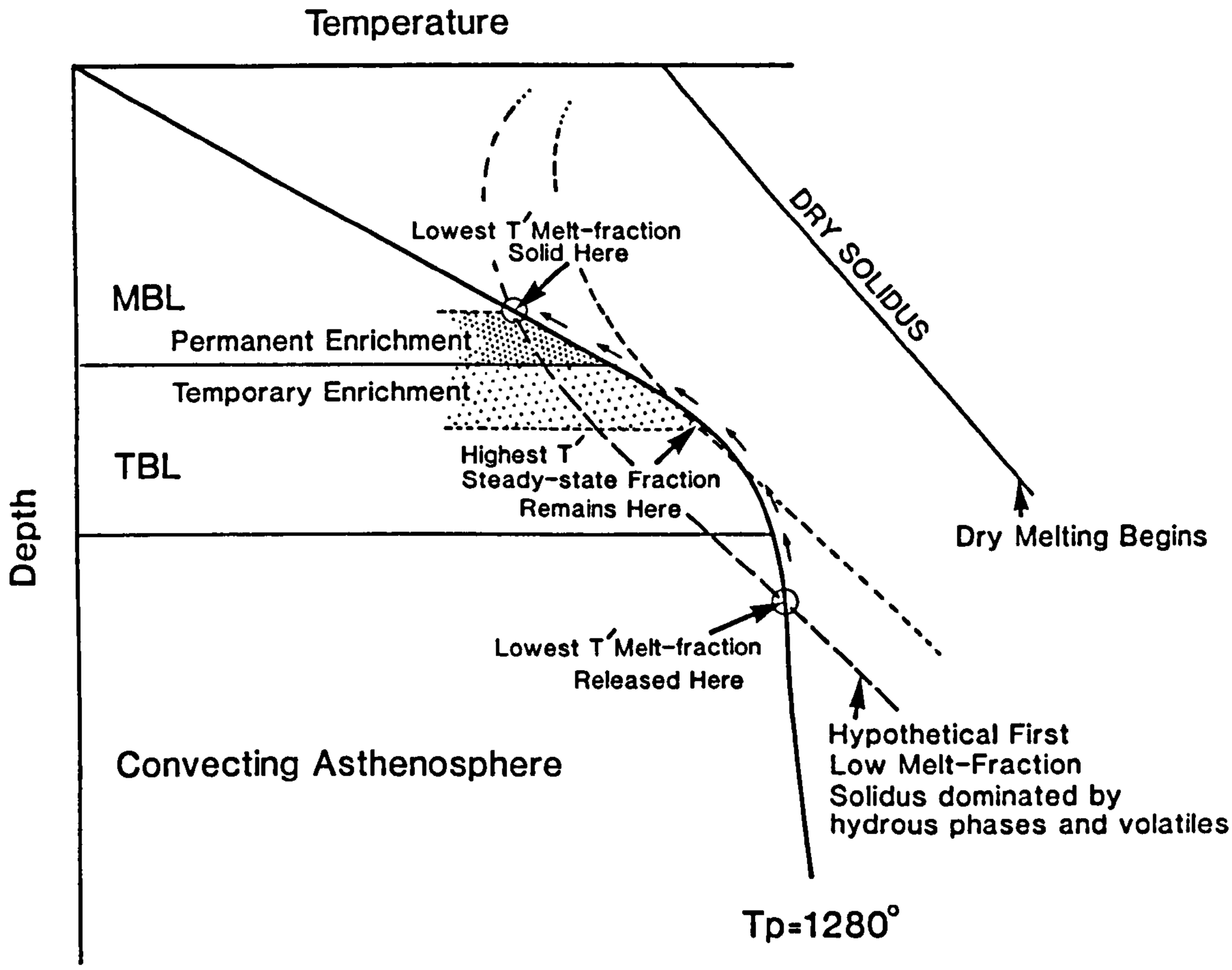

Fig 7.10 from Latin *et al.* (in press, a). The steady-state production of ultra-low melt fractions from a hypothetical mantle with a solidus (bold dashed line) dominated by hydrous phases and volatiles. The first melts are produced when this solidus intersects the geotherm. After upward migration these melt fractions freeze at the lowest temperatures as an enriched layer in the mechanical boundary layer (MBL) where the geotherm re-intersects their solidus. The largest steady-state melt fractions are those produced by the largest amount of upwelling over the hypothetical solidus. They will crystallise at the highest temperatures where their respective solidi (fine dashed line) intersects the geotherm. T is the temperature above the solidus at a given pressure. Arrows show the path taken (in P-T space) by the migrating melt fractions which carry no heat. Any melts which solidify in the thermal boundary layer (TBL) will only reside there temporarily because of its periodic overturn. Melts reaching the MBL will reside permanently in steady state conditions and will be remobilised if the geotherm is perturbed. Also marked on the diagram is the dry peridotite solidus which must be intersected in order for large scale melt production to occur. **NOTE**: the hypothetical solidi (dashed lines) are highly schematic, they may not have this shape in reality, they may not be parallel to each other or to the dry solidus, and they will not necessarily intersect the geotherm at the depths indicated.

and it may represent a thermal divide separating two minimum-melt compositions. Francis & Ludden (1989, in press) have suggested that the olivine nephelinite end-member may have been derived by early melting of the amphibole-garnet-clinopyroxenite veins, while the transitional alkaline basalt would represent more extensive melting of the (lithospheric) host lherzolite.

Since it therefore appears to be possible to derive alkaline magmas from the lithosphere, it should also be possible to contaminate asthenospherically derived magmas with lithospheric melts without destroying the characteristic 'alkaline signature'

7.1.4. Melting the Midland Valley mantle

The Midland Valley was a region of tension during much of the Carboniferous and part of the Permian. The absence of any clear temporal-spatial relationships makes plume-generated melting unlikely. However, from comparisons with Mesozoic lavas of similar composition from the North Sea, and by analogy with melting calculations for these rocks (Latin *et al*, in press a,b), it appears that melting at the dry solidus is unlikely for many of the samples. Latin *et al.* (in press, b) have shown that if the 0.01-0.45 wt% H_2O content of MORB (Michael & Chase, 1987) represents the total H_2O content of the asthenospheric source, then alkali basalts might be expected to contain up to 1 wt% H_2O. Melting would therefore take place at a volatile dependent solidus. Metasomatic enrichment of the base of the lithosphere has been proposed as a result of steady-state mantle conditions. Dehydration of the subducted Iapetus slab during the Siluro-Devonian would have further enhanced the H_2O content of the overlying asthenosphere at this time. Magmatism associated with this event is represented by the ORS lavas which outcrop within, and to the north and south of the Midland Valley. Given these enhanced hydrous conditions, it is unlikely that the base of the Midland Valley lithosphere could have escaped the volatile-induced enrichment events described in the previous section. Indeed, the hydrous nature of many of the Dinantian magmas (indicated by very calcic plagioclase phenocrysts, general lack of Fe enrichment trends, abundance of hornblende phenocrysts in some intermediate and evolved samples, and the lack of negative Eu anomalies (despite plagioclase fractionation)) has been emphasised by Smedley (1986b).

The earliest Dinantian magmatism in the Midland Valley is represented by the

Holyrood and East Lothian lavas in the east, and the Clyde Plateau lavas in the west. There is no obvious reason for suggesting lithosphere involvement for the Holyrood lavas, since (compared to the post-Dinantian suite) they have incompatible element concentrations consistent with their degree of saturation. The same is not true of the Clyde Plateau and East Lothian lavas, although the effect of lithosphere interaction on these two groups appears to be different. In the Clyde Plateau lavas there is a general enrichment in all elements except P; in the East Lothian lavas selective enrichment (P) and depletion (Zr) appears to have taken place. Whereas these differences might indicate differences in lithosphere enrichment they might also reflect variations in degree of melting. Although lithosphere involvement should be expected to be greater at higher temperatures, the lithosphere component will be more highly diluted in larger degree melts. It is suggested that the more irregular spiderdiagram profiles for the East Lothian and Bathgate groups (compared to those for the three west Midland Valley Dinantian groups) are a reflection of smaller degrees of melting and therefore more selective lithosphere input.

Turning back to the isotopes (Fig. 7.4) and examining the data in terms of inferred degree of melting, it is apparent that three of the four Dinantian samples with $^{87}Sr/^{86}Sr > 0.7045$ are from the smaller melt groups: Bathgate, Holyrood and Fife (implying therefore that some of the Holyrood and Fife samples have possibly experienced some lithospheric contamination). Consideration of the main data range (i.e. $^{87}Sr/^{86}Sr$ between 0.7028-0.7042) shows that the majority of samples in the higher part of the range are from the Clyde Plateau, Kintyre, Firth of Clyde and Bathgate lavas. Given the susceptibility of Sr to alteration processes, it is possible that some of the more extreme $^{87}Sr/^{86}Sr$ compositions do not reflect magma ratios. However, Nd is much less likely to have been affected by alteration. Because of the time dependence of $^{144}Nd/^{143}Nd$ ratios, Fig. 7.11 a & b show histograms for εNd for the post-Dinantian and Dinantian samples. The data show the same shift towards more depleted values for the post-Dinantian suite compared to the Dinantian suite.

These observations by no means provide unequivocal evidence for lithosphere contributions to these magmas and an explanation in terms of variable degree melting of a heterogeneous mantle source is equally tenable. However, the observations do not contradict the lithosphere contamination model.

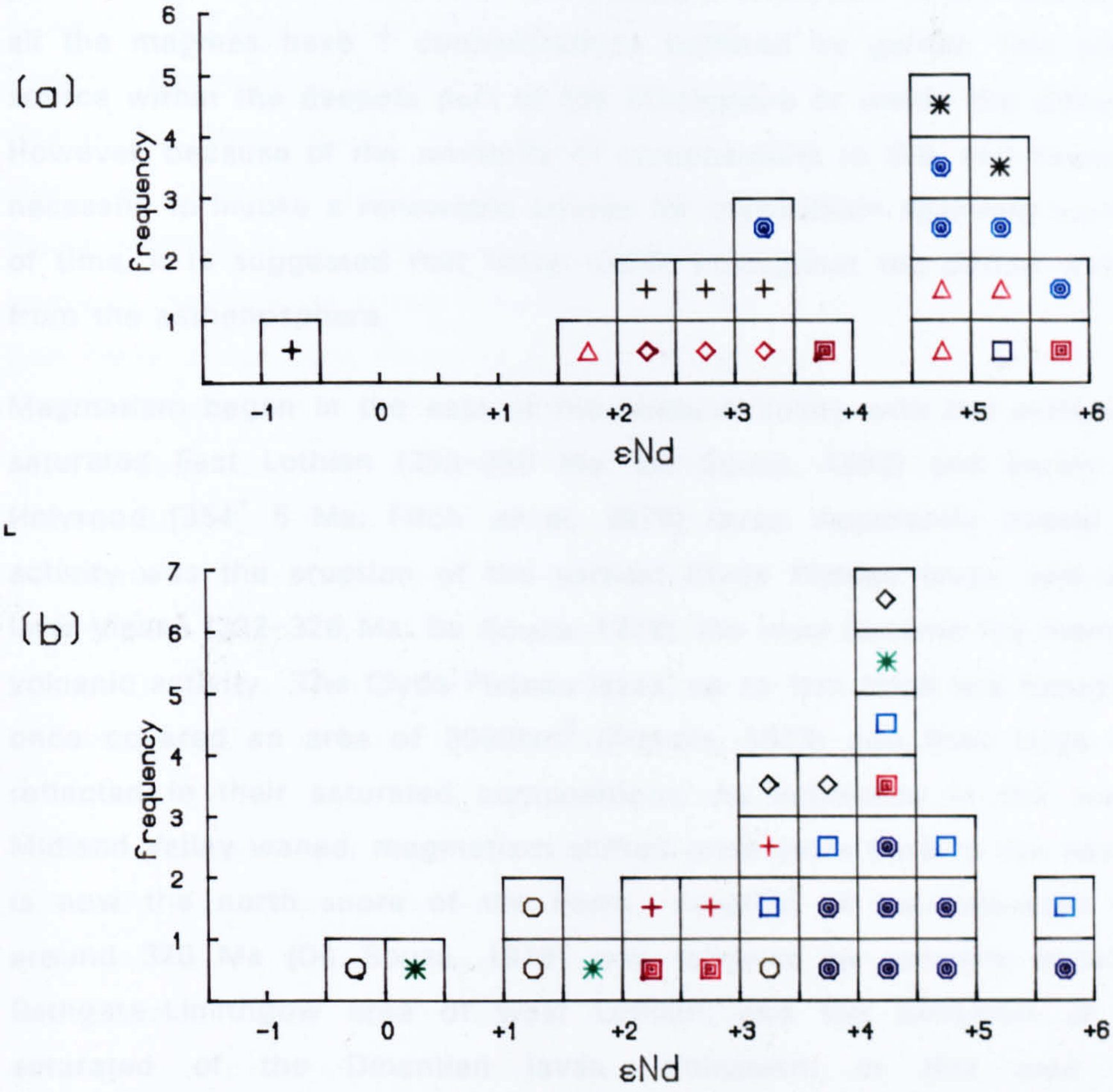

Fig. 7.11 εNd histograms for (a) post–Dinantian and (b) Dinantian samples.

7.1.5. Synthesis

The Midland Valley provided a focus for magmatism through most of the Carboniferous and possibly a significant part of the Permian (spanning a time period of at least 70 Ma). With the possible exception of the quartz dolerites, all the magmas have Y concentrations buffered by garnet. This places their source within the deepest part of the lithosphere or within the asthenosphere. However, because of the similarity of compositions to OIB, and because of the necessity to invoke a renewable source for magmatism spanning such a length of time, it is suggested that initial melts throughout the period were derived from the asthenosphere.

Magmatism began in the east of the Midland Valley with the extrusion of the saturated East Lothian (355–350 Ma: De Souza, 1982) and barely saturated Holyrood (354^{+}_{-} 5 Ma: Fitch *et al*, 1970) lavas. Apparently coeval with this activity was the eruption of the earliest Clyde Plateau lavas, and during the later Visean (332–326 Ma: De Souza, 1979), the west became the main focus for volcanic activity. The Clyde Plateau lavas, up to 1km thick, are thought to have once covered an area of 3000km^2 (Francis, 1973) and their large volume is reflected in their saturated compositions. As volcanism in the west of the Midland Valley waned, magmatism shifted once more back to the east, to what is now the north shore of the Forth. Eruption of the saturated Fife lavas around 320 Ma (De Souza, 1979) was followed by volcanic activity in the Bathgate–Linlithgow area of west Lothian, and the extrusion of the least saturated of the Dinantian lavas. Volcanism in this area continued intermittently into the Namurian until c.310 Ma.

The contradictory evidence of major and trace elements and the patterns observed in terms of Ce/Y and Zr/Nb imply that these magmas encountered and interacted with enriched lithosphere during their ascent, so that their compositions were variably modified. This is most obvious for the Clyde Plateau, Kintyre and Firth of Clyde lavas, and to a lesser extent, the Bathgate and East Lothian lavas. It is less clear for the Holyrood and Fife lavas, and it might be argued that these magmas escaped significant lithosphere contamination. Alternatively, and perhaps less probably, (given the evidence from included xenoliths) the lithosphere under this part of the Midland Valley escaped significant enrichment.

The division between Dinantian and post-Dinantian magmatism is an artificial

one born of the need to categorise for descriptive purposes, and does not reflect the identification of new volcano-tectonic influences. Through much of the Namurian, volcanic activity in the west of the Midland Valley was spasmodic (tuffs in the Dalry area), until the extrusion of the Passage Group lavas (c. 310 Ma). These outcrop in a broad belt to the south of the Clyde Plateau. On the Ce/Y-Zr/Nb diagram most of the Passage Group lavas plot within the main alkaline field, although two samples (SW274 & SW276) are displaced towards higher Zr/Nb values, and sit within the same field as the Clyde Plateau lavas. Lithospheric interactions may therefore be inferred for some of the Passage Group magmas. With the exception of the Bathgate lavas and other minor lava flows (e.g. Saline, Westfield and the Blindwells Quarry lavas), magmatism in the eastern Midland Valley through the Namurian and early Westphalian was confined to intrusive activity. The clear geochemical division of these intrusions into less and more enriched samples (Groups A and B respectively) suggests an explanation in terms of differing ages of magmatism. However, K-Ar ages for the two groups are not distinct (313-262 Ma for Group A and 319-235 Ma for Group B). In terms of degree of saturation and incompatible element abundances, the Group A sills compare closely with the Dinantian Fife lavas. Some of these sills intrude Calciferous Sandstone and Lower Limestone sediments and thus, they are possibly also of Dinantian age. Given the possibility of Ar-loss in many samples, it is plausible that the more saturated Group A sills represent the Namurian continuation of magmatism in the Midland Valley. Interpretation of the Group B sills is less clear. Their geochemical resemblance to the Fife & Lothian basanites was emphasised in chapter 5. The discussion in chapter 2 suggested that although some of the Fife & Lothian basanite group were possibly Namurian to Westphalian in age, the majority were late Stephanian - early Permian (<295 Ma). A similar age might therefore be inferred for the Group B sills, and the distinction that has been made between Group B sills and the Fife & Lothian basanites may be wholly artificial. However, the older K-Ar age determinations of 319-302 Ma contradict this assumption for at least some of the samples. It is possible therefore that they correlate with both the Bathgate and the Fife & Lothian basanite magmatic activity.

The post-Passage Group quiescence of the west Midland Valley was brought to an end in the late Westphalian by the intrusion of the earliest Ayrshire sills. Alkaline magmatism then continued here throughout the Stephanian and into

the Permian, and this area (lying some 30km south of the quartz dolerite swarms) appears to have escaped the effects of the 'tholeiitic event'. The outcrop of the quartz dolerite dykes and sills is shown in Fig. 7.1. The nature of the event which gave rise to this suite remains unclear, although the increased degrees of melting imply increased lithosphere thinning and stretching. After this brief event, alkaline magmatism recommenced in the east and is represented by numerous vents and minor intrusions, and possibly many of the Group B sills. In the west Midland Valley, similar vents and minor intrusions acted as feeders for the Mauchline lavas.

On the basis of inter-element and isotope relationships, minor mantle lithosphere involvement was advocated in chapter 6 for some of the Mauchline group samples. Comparisons suggest that some of the Fife & Lothian sill samples (particularly Group A) have been similarly affected, and several of them plot within the Clyde Plateau field on the Ce/Y-Zr/Nb diagram. The fact that no notable lithosphere involvement has been inferred for the majority of the Fife & Lothian Group B sills and basanites is not surprising given that most of them are thought to post-date the quartz dolerites. It is suggested that the large-scale melting event that produced the quartz dolerites effectively exhausted the enrichments at the base of the lithosphere, leaving only refractory phases, less likely to contribute to the late Silesian-Permian melts. Recognition of a lithospheric mantle signature in some of the Mauchline group samples is also not surprising given that enriched lithosphere contributed to the Passage Group magmas, but was not swept clean by the quartz dolerite melts (which do not intrude this area). Because the most incompatible elements would have been lost to the Passage Group magmas, later lithosphere interaction with Mauchline magmas did not noticeably affect incompatible element compositions of the melts. However, a record of such interaction is provided by the Sr (and to a lesser extent, Nd) isotope patterns.

7.2. Comparisons with suites from other areas

Figs 7.12-7.14 show normalised incompatible element concentrations for basalts from a variety of continental and oceanic settings. They emphasise the similarity between the Midland Valley samples and many other intra-continental alkaline suites (e.g. Kisingeri (Kenya), Jos Plateau (Nigeria), Basin & Range, Cameroon and various Kenyan lavas; Norry & Fitton, 1983; Fitton & James, 1986; Fitton *et al*, 1988). There is also a marked similarity between the Midland

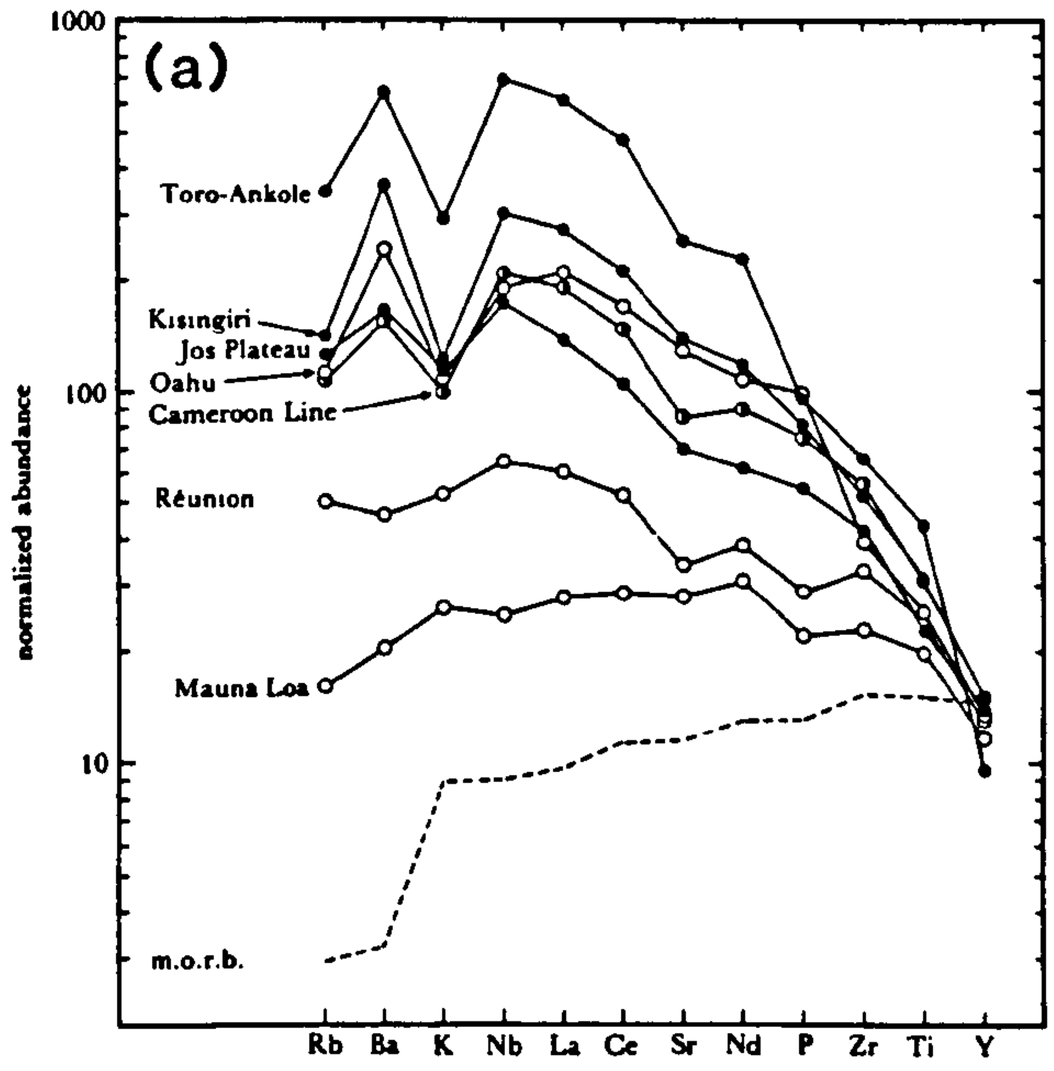

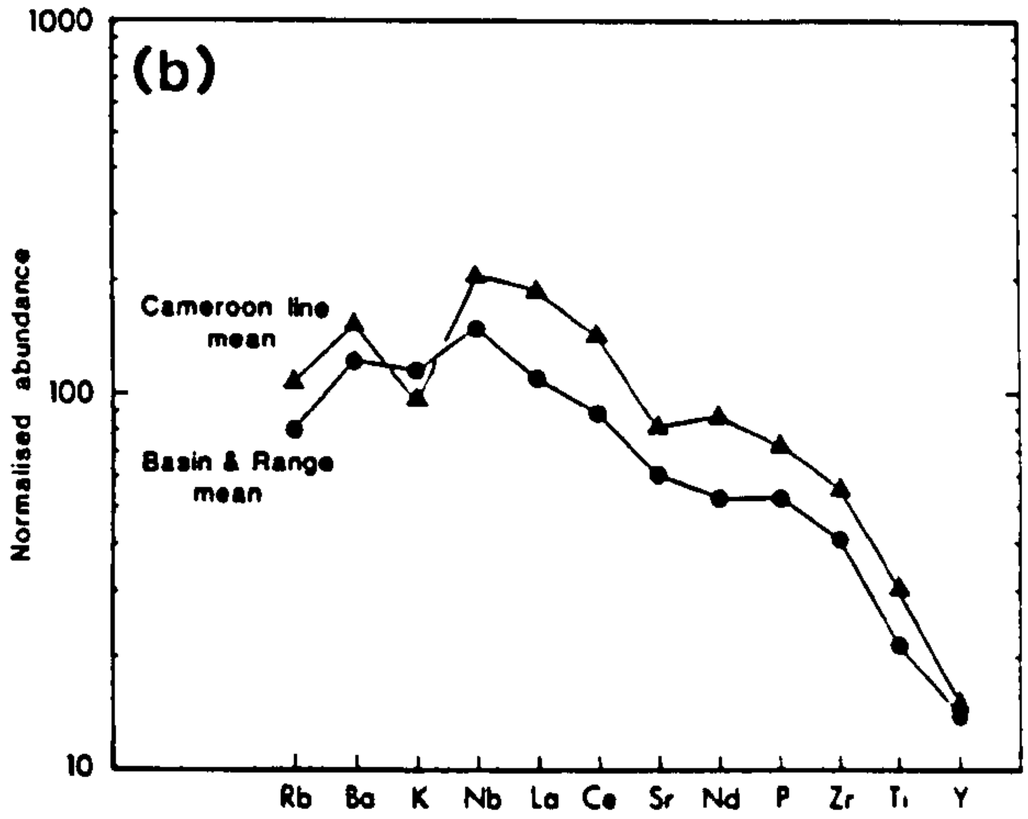

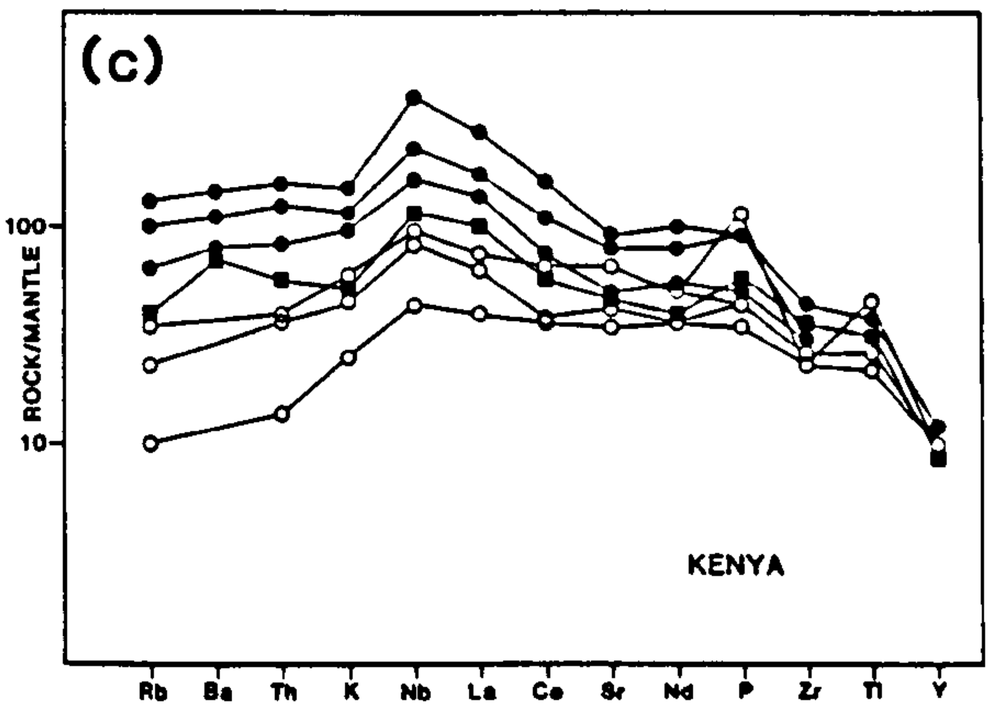

Fig. 7.12a From Fitton & James (1986). A comparison of normalised incompatible element abundances in several suites of intraplate basic volcanic rocks. Open and solid symbols represent oceanic and continental suites respectively. The Cameroon Line data include analyses from both the oceanic and continental sectors. Typical MORB abundances (Sun, 1980) are shown for comparison.

Fig. 7.12b From Fitton *et al.* (1988). A comparison of normalised incompatible element abundances in average Basin & Range basalt with average oceanic and continental Cameroon Line basalts.

Fig. 7.12c From Norry & Fitton (1983). Normalised incompatible element abundances for Kenyan alkaline lavas of varying age: Miocene (solid circles); Pliocene (solid squares); Pleistocene (open circles).

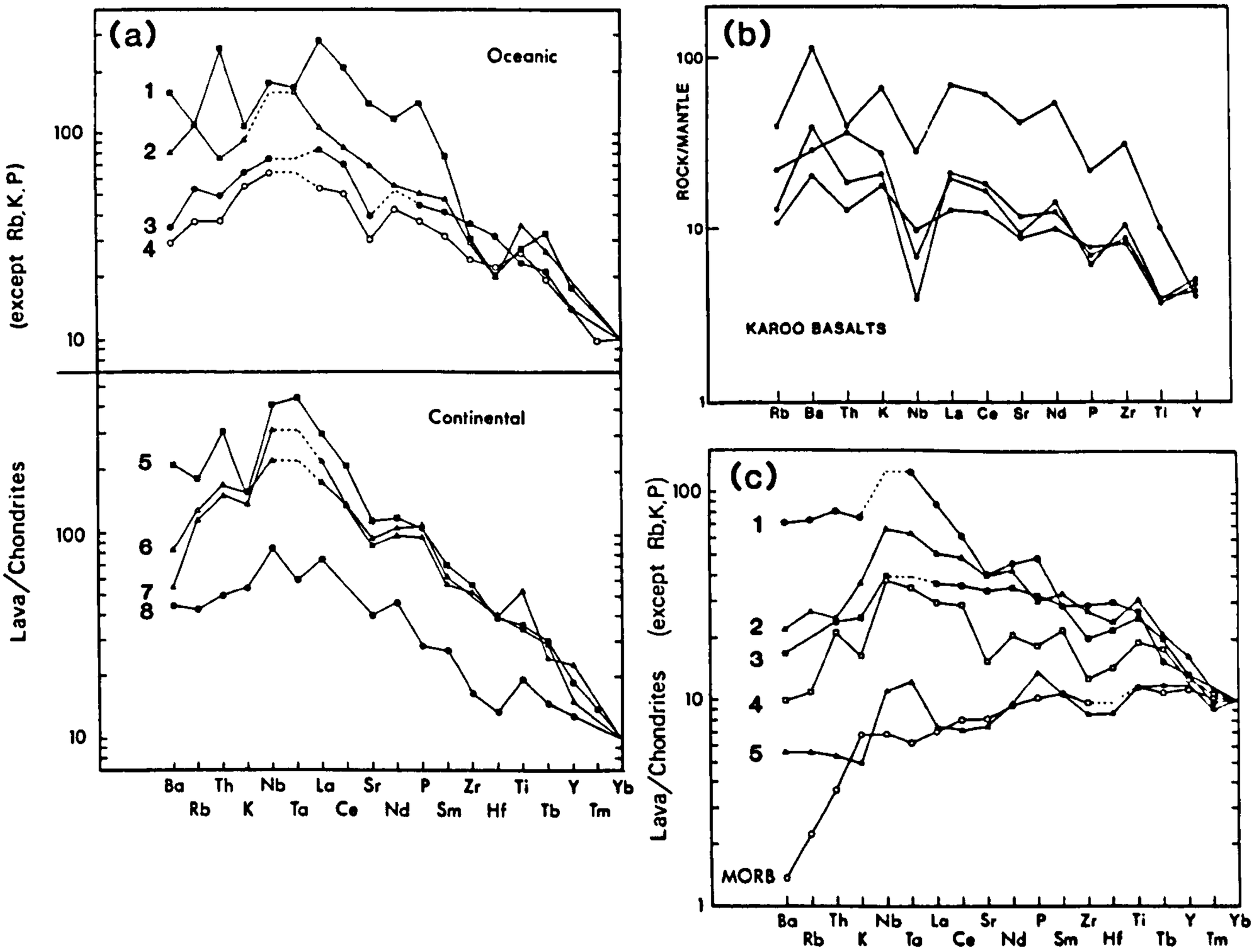

Fig. 7.13a From Thompson *et al.* (1983). Normalised incompatible element abundances of representative oceanic and continental alkali and strongly-alkalic lavas from: Oahu, Hawaii (1,2); Kohala, Hawaii (3); Suiko, Emperor seamounts (4); Hegau, Germany (5); Mt Shadwell, Australia (6); Dry Valley, Antarctica (7); Gregory Rift, East Africa (8). (See reference for sources of data).

Fig. 7.13b From Norry & Fitton (1983). Normalised incompatible element abundances for continental flood basalts from the Karoo province.

Fig. 7.13c From Thompson *et al.* (1983). Normalised incompatible element abundances of basalts from: Boina, Ethiopia (1); Kilauea, Hawaii (2); Ojin, Emperor seamounts (3); Iceland (4); Reykjanes Ridge (5). (See reference for sources of data).

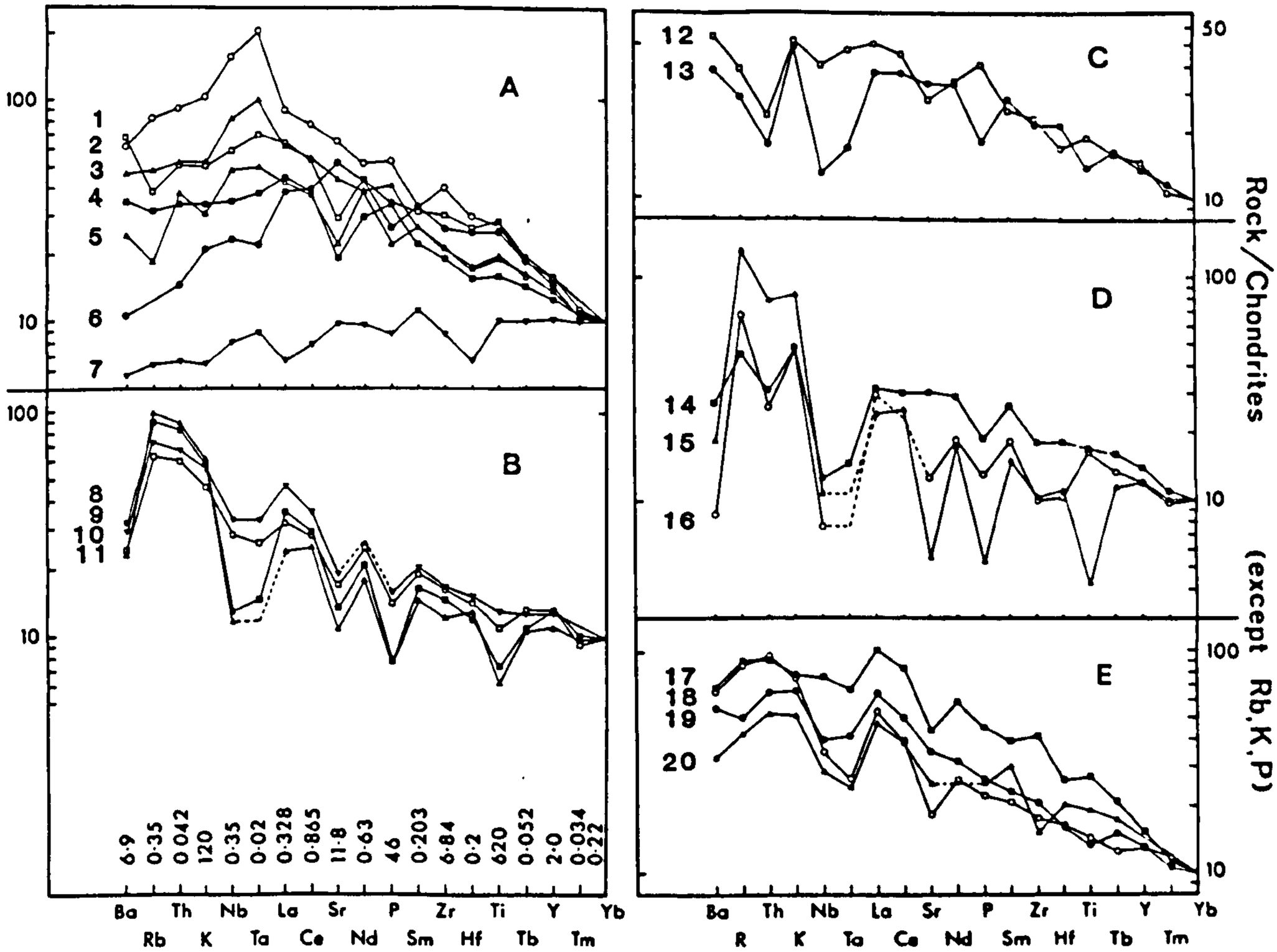

Fig. 7.14 From Thompson *et al.* (1983). Normalised incompatible element abundances for representative continental flood basalts and hypabyssal intrusions. Samples from: Ubekendt Ejland, West Greenland (1, 16); Adis Ababa, Ethiopia (2, 3); Snake River Plain, Idaho (4, 12); Midland Valley, Scotland (5); Skye Main Lava series (6, 13); Preshal Mhor basalts, Skye (7); Mull (8); High Atlas, Morocco (9); Virginia, eastern USA (10); Antarctica (11, 20); Mull Plateau Group (14); Sierra di Tinguia, Brazil (15); Parana Basin, Brazil (17); Columbia River Plateau (18); Rio Grande Rift, New Mexico (19). (See reference for sources of data).

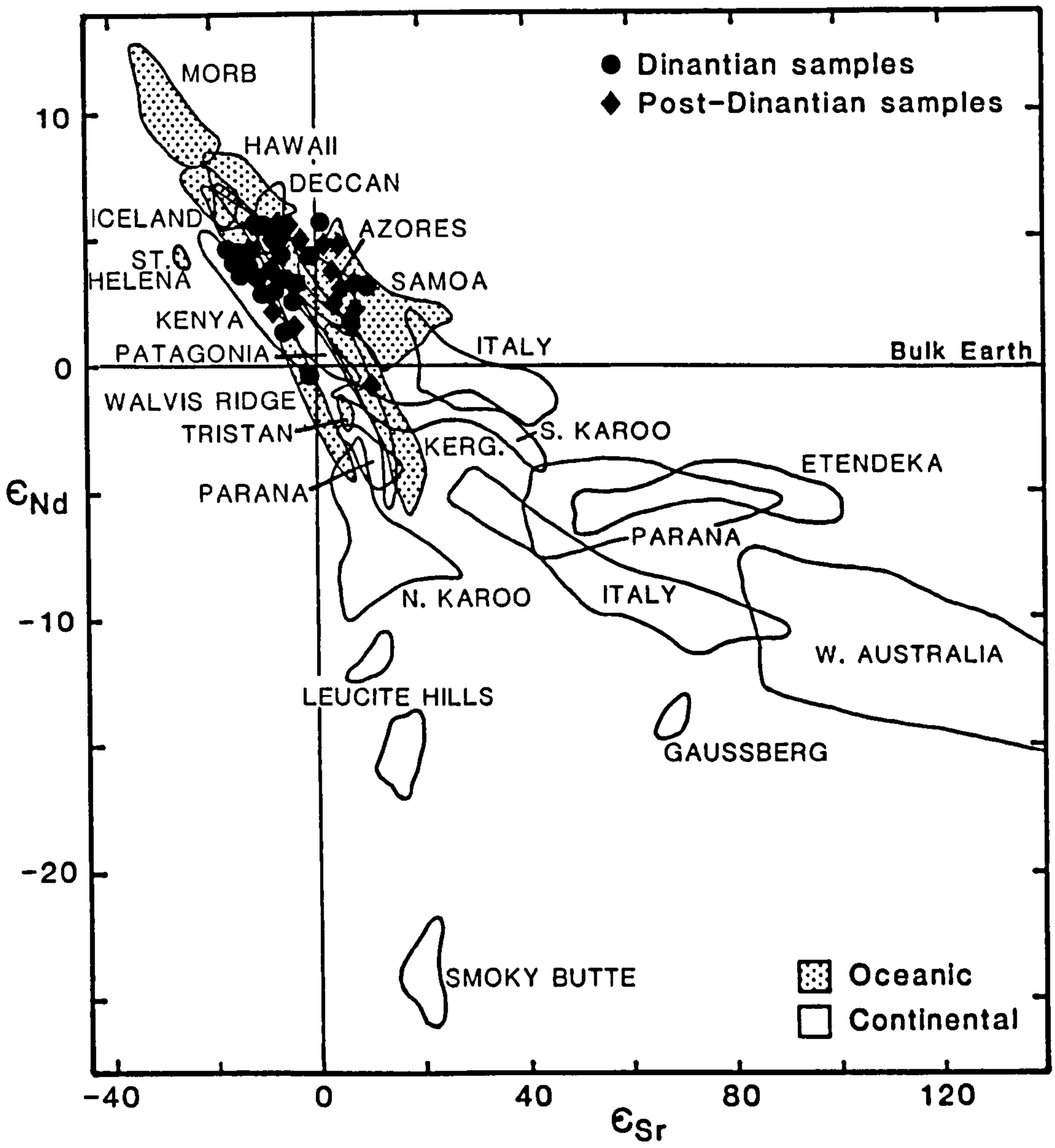

Fig. 7.15 εNd – εSr correlation diagram for Scottish Carboniferous – Permian igneous rocks compared with MORB, OIB and other continental rift lavas after Hawkesworth *et al.* (1987). (See reference for sources of data).

Valley province rocks and OIB (Thompson *et al*, 1983; Fig. 7.13a), which was shown for Ce/Y-Zr/Nb in chapter 6 (Fig. 6.9) and by Smedley (1986b). Figs 7.13b,c and 7.14 display normalised incompatible element concentrations for various continental flood basalts and for some oceanic tholeiites (Norry & Fitton, 1983; Thompson *et al*, 1983). Many of the samples show depletions in P and Sr similar to those of the Midland Valley quartz dolerites. Samples 8-12 of Fig. 7.14 are all believed to have been significantly affected by crustal contamination (Thompson *et al*, 1983), and many have pronounced depletions in Nb and Ti which are not shared by the quartz dolerites. Fig 7.15 compares εNd-εSr for the Midland Valley Suites with values for MORB, OIB and other continental rift lavas, all of which are thought not to have been affected significantly by contamination with crustal material *en route* to the surface (Hawkesworth *et al*, 1987). The diagram emphasises once more the similarity between the Midland Valley samples and OIB.

CHAPTER 8

SUMMARY AND CONCLUSIONS

The main theatre for late Palaeozoic igneous activity in northern Britain was provided by the Midland Valley, and it is the rocks of this region which have formed the basis of this thesis. They outcrop in two main areas within the Midland Valley: Fife & Lothian in the east and Ayrshire in the west. Magmatism during the late Silesian and early Permian also affected areas to the north and south of the Midland Valley producing a series of lavas and minor intrusions in the Southern Uplands and a suite of dykes in the Scottish Highlands. Volcanic activity was often phreatic, and centred on numerous short-lived vents producing abundant pyroclastic deposits. Relatively large volumes of magma were intruded as sills, and the only lava flows of any consequence outcrop in Ayrshire. Magmatism throughout the late Palaeozoic was dominated by alkaline-transitional compositions, with a short tholeiite period in the late Stephanian-early Permian. Both groups are relatively unevolved: the alkaline samples range from basalt and basanite to hawaiite, and the tholeiitic quartz dolerites span the range basalt to basaltic andesite (with local internal differentiation to granophyre).

All fine- to medium-grained samples are (micro)porphyritic. Phenocryst assemblages are limited to olivine$^{+}_{-}$clinopyroxene with the rare occurrence of plagioclase. Olivine phenocrysts are generally euhedral or subhedral and have core compositions in the range Fo_{90-65}. They display trends of increasing Fe and Mn with decreasing Mg and Ni. Compositions of olivine cores from the larger sills are generally more evolved than those from lavas and minor intrusions. This probably reflects slower cooling and longer equilibration times for the sills. Ranges in Ca content suggest that olivines in the Fife & Lothian basanites began growing at higher pressures than those of the Mauchline lavas and Ayrshire and Fife & Lothian sills.

Clinopyroxene phenocrysts are diopsidic salites or augites and many show appreciable Tschermak's-molecule substitution reflecting the degree of magma undersaturation. Variations in Al and Ti reflect both initial melt composition and the effects of fractionation. Both increase with fractionation in all but the transitional Passage Group lavas where Al decreases. Al^{iv}/Al^{vi} ratios show that pyroxenes crystallised over a range of pressures, and all groups contain

examples of low pressure clinopyroxenes. The highest crystallisation pressures (10–20kb) are indicated by clinopyroxenes from the Highland dykes and the Fife basanites. Petrographically these are represented by euhedral crystals with amoeboid cores, where partially resorbed high pressure phenocrysts have acted as nucleation sites for later crystallisation.

Xenoliths and xenocrysts are common in the small intrusions and diatremes of Fife & Lothian and have been found in several vent intrusions and one lava flow in the Mauchline Basin. In fresh samples it is possible to distinguish between phenocrysts and possible xenocrysts of olivine on the basis of the larger size and fragmental shape of the latter. Some of the xenocrysts show distinct reversed zoning and have Fe-rich cores similar in composition to olivines from the Fidra wehrlite-clinopyroxenite suite. However, many of the xenocrysts are geochemically indistinguishable from the phenocrysts. The morphological distinction between phenocrysts and xenocrysts is not always so clear for clinopyroxene. Glomeroporphyritic and xenolithic fragments of clinopyroxene are easily confused. Individual anhedral clinopyroxenes with strained extinction and sieve-textured cores have been identified as clinopyroxenite fragments on the basis of their similarity to those in xenoliths. Partially resorbed Cr-diopside and fassaitic augite xenocrysts have been identified as irregular cores to phenocrysts and are probably derived from disaggregated spinel lherzolite and metasomatised mantle rocks. The presence of high-pressure phenocrysts and xenolith fragments indicates high rates of ascent for many of these magmas, with little or no residence time in magma chambers.

The post-Dinantian alkaline suite forms a remarkably coherent group in terms of whole-rock geochemistry. Variations in major and compatible trace elements have been controlled by fractional crystallisation of ol$^{+}_{-}$cpx. Simple lever-rule calculations using Al_2O_3 and MgO whole-rock and phenocryst compositions have constrained fractional crystallisation to <36%, and indicate the dominance of olivine fractionation in the Ayrshire samples. Clinopyroxene fractionation was increasingly important in the Fife & Lothian samples and the Highland dykes. CMAS and ne-di-ol projections confirm the importance of polybaric fractionation and suggest that crystal fractionation occurred at pressures between 0–10kb, and exceptionally at pressures as high as 20kb for some of the Fife basanites.

Incompatible trace element and REE concentrations indicate a narrow range of melting for the alkaline samples. Both Y and HREE concentrations suggest that these elements were buffered by residual garnet in their mantle source; and pronounced negative K and Rb chondrite-normalised anomalies imply that phlogopite was also a minor residual phase. Flatter chondrite-normalised profiles for the quartz dolerites indicate a higher degree of melting for these magmas, however, average Y and HREE contents are very similar to those of the alkaline samples, suggesting that melting had not proceeded to a point at which garnet was consumed. However a trend of increasing Ce/Y with increasing Zr/Nb for these samples apparently contradicts this observation. Negative chondrite-normalised P and Sr anomalies could be interpreted in terms of fractional crystallisation of apatite and plagioclase respectively. This hypothesis however, recieves little petrographic support, and alternatively the magmas may have been derived from a source which was deficient in these elements or which retained accessory buffering phases for significant degrees of melting. Evolution of the magmas under oxidising (high pH_2O) conditions could account for depletions in Sr without similar depletions in Eu.

Ce/Y and Zr/Nb ratios have been used to model partial melting. They show that the post-Dinantian suite cannot represent the result of simple batch melting of a homogeneous source, and mixing between melts from at least two sources is required. It is not clear whether these sources are distinct from one another in terms of a vertical zonation or layering in the mantle (i.e. mesosphere v asthenosphere v lithosphere) or whether one source is present as irregularly distributed more fusible patches or streaks within the other (streaky mantle). The absence of a hot-spot trail across the Midland Valley despite a long period of intraplate volcanism and rapid plate movements sugests that alkali basalt magmatism was not the product of a deep-seated mantle plume. Lithospheric mantle sources require impossibly large degrees of melting to produce incompatible element concentrations consistent with values for the post-Dinantian suite. By elimination it is therefore suggested that the post-Dinantian basalts represent partial melts from a heterogeneous (streaky) asthenospheric source. In this case fractional melting should more closely model partial melting. However, given poorly constrained source compositions and partition coefficient values, this has not been rigorously tested.

Initial $^{87}Sr/^{86}Sr$ and $^{143}Nd/^{144}Nd$ ratios are in the range 0.7032-0.7049 and 0.5122-0.5126 respectively. Relatively high $^{87}Sr/^{86}Sr$ ratios for the Ayrshire sills

suggest a possible crustal influence in the evolution of some of these samples. However, close similarities of incompatible element concentrations to those of O.I.B. indicate that this is of minor importance. Isotopic comparisons with data for Midland Valley spinel lherzolites and megacrysts of presumed lithospheric origin show an overlap between the igneous rocks and mantle inclusions, with the former tending to higher εSr and lower εNd values. However since it is possible that the xenoliths and megacrysts represent mid-mantle lithosphere compositions, more enriched compositions may exist at the base of the lithosphere.

Isotopic and elemental variations for post-Dinantian samples have been interpreted in terms of variable degree melting of a heterogeneous (streaky) asthenospheric mantle. However, consideration of the Mauchline group samples in isolation from the other groups indicates a trend of increasing $^{87}Sr/^{86}Sr$ and decreasing $^{143}Nd/^{144}Nd$ with progressive melting. This has been interpreted in terms of lithospheric interaction. The quartz dolerites are isotopically indistinguishable from the alkaline samples and an asthenospheric source has also been proposed for them.

Comparison of the post-Dinantian compositions with data for the Dinantian lavas allows the following observations. Major element compositions (saturation index) imply that the Dinantian lavas are the products of larger degree melting than most of the post-Dinantian volcanics. However they have incompatible element contents just as high as, and sometimes higher than many of the post-Dinantian groups. It is possible that the source for Dinantian lavas was more enriched than that of the post-Dinantian magmas. However modelling of Ce/Y and Zr/Nb variations allows the identification of a lithospheric component in many of the Dinantian lavas. It has been suggested that they represent the result of mixing between small degree partial melts (<3%) from the asthenosphere and even smaller degree melts (<1%) from the lithospheric mantle. If this is so then similar variations in Zr/Nb for a few of the Passage Group lavas and some of the Fife & Lothian sills may indicate lithosphere interaction for these samples. A synthesis of magmatism in the Midland Valley through the Carboniferous and Permian suggests that during the Dinantian asthenospheric melts were affected by significant mantle lithosphere interaction. The younger larger-scale melting event which produced the quartz dolerites would effectively exhaust any remaining enrichments at the base of the lithosphere leaving only refractory phases less likely to contribute to the

late Stephanian - Permian melts. The lithospheric mantle beneath Ayrshire interacted with some of the Passage Group lava melts but was not affected by the quartz dolerites which intrude an area some 30km to the north. Lithosphere interaction with the Mauchline melts is therefore reflected in higher $^{87}Sr/^{86}Sr$ and lower $^{143}Nd/^{144}Nd$ ratios.

K-Ar age determinations for the post-Dinantian samples have suggested that the Fife & Lothian sills were intruded during the Namurian and Westphalian and that many of the minor intrusions and diatremes are the result of volcanic activity in late Silesian and early Permian times. Geochemical comparisons suggest that the division is not quite so clear and that many of the sills may be coeval with the Fife & Lothian basanites. The fact that an $^{40}Ar/^{39}Ar$ age for a kaersutite separate from the Lugar sill (Henderson *et al.*, 1987) was c.10 Ma younger than a K-Ar whole-rock age determination for the same sill implies that K-Ar age determined ages for other sills may also be too old. Younger ages might be expected from $^{40}Ar/^{39}Ar$ analysis. K-Ar ages of 270-250 Ma for nine of the Midland Valley minor intrusions suggests that magmatism continued on a small scale into the mid- late-Lower Permian and could therefore have been coeval with volcanic activity in Orkney and the Oslo Graben.

It is clear that the Midland Valley was a region of passive rifting throughout the Carboniferous and early Permian. Magmatism in the Dinantian has been attributed to N-S back-arc tension associated with subduction of the Proto-Tethys Ocean several hundred kilometres to the south. This tension reactivated Caledonian NE/SW faults and created new E-W faults. The quartz dolerite dykes and sills have been associated with initiation of rifting in the northern North Atlantic during the latter part of the Palaeozoic, and it is possible that the subsequent alkaline magmatism was also influenced by these stresses.

REFERENCES

Abbey S. 1980, Studies in 'standard samples' for use in the general analysis of silicate rocks and minerals. Part 6: 1979 edition of 'usable values'. *Geol. Surv. Canad. Paper*, 80–14.

Aftalion M., Van Breeman O. & Bowes D.R. 1984, Age constraints on basement of the Midland Valley of Scotland. *Trans. R. Soc. Edin: Earth Sci.*, **75**, 53–64.

Akella J. & Boyd F.R. 1973, Partitioning of Ti and Al between coexisting silicates, oxides and liquids. *Proceedings of the 4th Lunar Science Conference*, **4** pp 1049–1059.

Allan D.A. 1924, The igneous geology of the Burntisland district. *Trans. R. Soc. Edin.*, **53**, 479–501.

Alibert C., Michard A. & Albarède F. 1983, The transition from alkali basalts to kimberlites: isotope and trace element evidence from melilitites. *Contrib. Mineral. Petrol.*, **82**, 176–186.

Allègre C.J. 1982, Chemical geodynamics. *Tectonophysics*, **81**, 109–132.

Allègre C.J., Dupre B., Lambret B. & Richard P. 1981, The subcontinental versus suboceanic debate; I. Lead–neodymium–strontium isotopes in primary alkali basalts from a shield area; the Ahaggar volcanic suite. *Earth Planet. Sci. Lett.*, **52**, 85–92.

Allègre C.J., Dupre B., Richard P., Rousseau D., & Brooks C. 1982, The subcontinental versus suboceanic debate II Nd–Sr–Pb isotopic comparison of continental tholeiites with mid-ocean ridge tholeiites, and the structure of continental lithosphere. *Earth Planet. Sci. Lett.*, **57**, 25–34.

Allègre C.J. & Turcotte D.L. 1985, Geodynamic mixing in the mesosphere boundary layer and the origin of oceanic islands. *Geophys. Res. Lett.*, **12**, 207–210.

Almond D.C. 1988, Chemical fractionation in titaniferous clinopyroxene from Bayuda, Sudan. *Can. Min.*, **26**, 1027–1035.

Anastasiou P. & Seifert F. 1972, Solid solubility of Al_2O_3 in enstatite at high temperatures and 1–5 kb water pressure. *Contrib. Mineral. Petrol.*, **34**, 272–287.

Anderson A.T. & Greenland L.P. 1969, Phosphorous fractionation diagram as a quantitative indicator of crystallisation differentiation of basaltic liquids. *Geochim. Cosmochim. Acta*, **33**, 493–505.

Anderson D.L. 1982a, Isotopic evolution of the mantle: the role of magma

mixing. *Earth Planet. Sci. Lett*, 57, 1-12.

Anderson D.L. 1982b, Isotopic evolution of the mantle: a model. *Earth Planet. Sci. Lett*, 57, 13-24.

Aoki K. & Kushiro I. 1968, Some clinopyroxenes from ultramafic inclusions in Dreiser Weiher, Eifel. *Contrib. Mineral. Petrol*, 18, 326-337.

Aoki K. & Shiba I. 1973, Pyroxenes from lherzolite inclusions of Itinome-gata, Japan. *Lithos*, 6, 41-51.

Armstrong D. 1957, Dating of some minor intrusions of Ayrshire. *Nature*, 180, 1277.

Arthaud F. & Matte P. 1977, Late Palaeozoic strike-slip faulting in southern Europe and northern Africa: result of a right lateral shear zone between the Apalachians and the Urals. *Bull. geol. Soc. Am*, 88, 1305-1320.

Aspen P., Upton B.G.J. & Dickin A.P. (submitted), Anorthoclase, sanidine and associated megacrysts in Scottish alkali basalts: their parageneses and possible origins.

Badham J.P.N. 1982, Strike-slip orogens- an explanation for the Hercynides. *J. geol. Soc. Lond*, 139, 493-504.

Bailey D.K. 1987, Mantle metasomatism - perspective and prospect. *In: Alkaline Igneous Rocks*, eds: Fitton J.G. & Upton B.G.J. *Geol. Soc. Spec. Publ*, 30, 1-14.

Balsillie D. 1923, Further observations on the volcanic geology of east Fife. *Geol. Mag*, 60, 530-545.

Balsillie D. 1927, Contemporaneous volcanic activity in east Fife. *Geol. Mag*, 64, 481-494.

Bamford D., Falser S., Jacob B., Kaminski W., Nunn K., Prodehl C. Fuchs K., King R. & Willmore P. 1976, A lithosphere seismic profile in Britain-I. Preliminary results. *Geophys. J. R. astr. Soc*, 44, 145-160.

Bamford D., Nunn K., Prodehl C. & Jacob B. 1977, LISPB - III. Upper crustal structure of northern Britain. *J. geol. Soc. Lond*, 133, 481-488.

Bamford D., Nunn K., Prodehl C. & Jacob B. 1978, LISB - IV. Crustal structure of northern Britain. *Geophys. J. R. astr. Soc*, 54, 43-60.

Barton M. & van Bergen M.J. 1981, Green clinopyroxenes and associated phases in a potassium-rich lava from the Leucite hills, Wyoming. *Contrib. Mineral. Petrol*, 77, 101-114.

Barton M., Varekamp J.C. & vanBergman M.J. 1982, Complex zoning of clinopyroxenes in the lavas of Vulsini, Latium, Italy: evidence for magma mixing. *J. Volcanol. Geotherm. Res*, 14, 361-388.

Basaltic Volcanism Study Project 1981, Basaltic Volcanism on the Terrestial Planets. *Pergamon Press Inc., New York*, 1286pp.

Basu A.R. & Murthy V.R. 1977, Ancient lithospheric lherzolite xenoliths in alkali basalt from Baja California. *Earth Planet. Sci. Lett.*, **34**, 246-253.

Bates R.L. & Jackson J.A. (eds) 2nd edition 1980, *Glossary of geology*. American Geological Institute.

Baxter A.N. 1986, Petrochemistry of late Palaeozoic alkali lamprophyre dykes from N. Scotland. *Trans. R. Soc. Edin: Earth Sci.*, **77**, 267-278.

Baxter A.N. & Mitchell J.G. 1984, Camptonite - Monchiquite dyke swarms of northern Scotland; age relationships and their implications. *Scott. J. Geol.*, **20**, 297-308.

Bedard J.H., Francis D.M. & Ludden J. 1988, Petrology and pyroxene chemistry of Monteregian dykes: the origin of concentric zoning and green cores in clinopyroxenes from alkali basalts and lamprophyres. *Can. J. Earth Sci.*, **25**, 2041-2058.

Bender J.F., Hodges F.N. & Bence A.E. 1978, Petrogenesis of basalts from the Project Famous area: experimental study from 0 to 15 kbars. *Earth Planet. Sci. Lett.*, **41**, 277-302.

Best M.G. 1974, Contrasting types of chromium-spinel peridotite xenoliths in basanitic lavas, western Grand Canyon, Arizona. *Earth Planet. Sci. Lett.*, **23**, 229-237.

Binns R.A., Duggan M.B. & Wilkinson J.F.G. 1970, High pressure megacrysts in alkaline lavas from northeastern New South Wales. *Am. J. Sci.*, **269**, 132-168.

Blaxland A.B., Aftalion M. & Van Breemen O. 1979, Pb isotopic composition of feldspar from Scottish Caledonian Granites, and the nature of the underlying crust. *Scott. J. Geol.*, **15**, 139-151.

Bluck B.J. 1978, Sedimentation in a late orogenic basin: The O.R.S. of the Midland Valley of Scotland. *In: Crustal Evolution in Northwest Britain and Adjacent Regions*, eds: Bowes D.R. & Leake B.E. *Geol. J. Spec. Issue*, **10**, 247-278.

Bluck B.J. 1980, Evolution of a strike-slip fault-controlled basin, Upper O.R.S., Scotland. *In: Sedimentation in Oblique-slip Mobile Zones*, eds: Ballance P.F. & Reading H.E. *Spec. Publ. Int. Assoc. Sedimentol.*, **4**, 63-78.

Boettcher A.L. & O'Neil J.R. 1980, Stable isotope, chemical, and petrographic studies of high-pressure amphiboles and micas: evidence for metasomatism in the mantle source regions of alkali basalts and

kimberlites. *Am. J. Sci*, 280a, 594-621.

Borley G.D., Suddaby P. & Scott P. 1971, Some xenoliths from the alkalic rocks of Tenerife, Canary Islands. *Contrib. Mineral. Petrol*, **31**, 102-114.

Brooks C.K. 1976, The Fe_2O_3/FeO ratio of basalt analyses: an appeal for a standardised procedure. *Bull. geol. Soc. Denmark*, **25**, 117-120.

Brooks C.K. & Printzlau I. 1978, Magma mixing in mafic alkaline volcanic rocks: the evidence from relict phenocryst phases and other inclusions. *J. Volcanol. Geotherm. Res*, **4**, 315-331.

Cameron I.B. & Stephenson D. 1985, **British Regional Geology: the Midland Valley of Scotland.** 3rd edition, HMSO, London.

Campbell I.H. & Borley G.D. 1974, The geochemistry of pyroxenes from the lower layered series of the Jimberlana Intrusion, western Australia. *Contrib. Mineral. Petrol*, **47**, 281-297.

Campbell I. H. & Gorton M. P. 1980, Accessory phases and the generation of LREE-Enriched basalts - a test for disequilibrium melting. *Contrib. Mineral. Petrol*, **72**, 157-163.

Campbell R., Day T.C. & Stenhouse A.G. 1932, The Braefoot Outer Sill, Part I: The Braefoot Promontory. *Trans. Edin. geol. Soc*, **12**, 342-375.

Campbell R., Day T.C. & Stenhouse A.G. 1934, The Braefoot Outer Sill, Fife, part II. *Trans. Edin. geol. Soc*, **13**, 148-173.

Cawthorn R.G. & Collerson K.D. 1974, The recalculation of pyroxene end-member paramaters and the estimation of ferrous and ferric iron content from electron microprobe analysis. *Am. Mineralogist*, **59**, 1203-1208.

Chapman N.A. 1974, *Petrology of inclusions from some late Palaeozoic British volcanic rocks*. Unpubl. Ph.D. thesis, Univ. Edinburgh.

Chapman N.A. 1975, An experimental study of spinel clinopyroxenite xenoliths from Duncansby Ness vent, Caithness, Scotland. *Contrib. Mineral. Petrol*, **51**, 223-230.

Chapman N.A. 1976, Inclusions and megacrysts from undersaturated tuffs and basanites, east Fife, Scotland. *J. Petrol.* **17**, 472-498.

Chapman N.A. & Powell R. 1976, Origin of anorthoclase megacrysts in alkali basalts. *Contrib. Mineral. Petrol*, **58**, 29-35.

Chase C. G. 1981, Ocean island Pb: two-stage histories and mantle evolution. *Earth Planet. Sci. Lett*, **52**, 277-284.

Chauvel C. & Jahn B. M. 1984, Nd-Sr isotope and REE geochemistry of alkali basalts from the Massif Central, France. *Geochim. Cosmochim. Acta*, **48**,

93-110.

Chen C-Y. & Frey F. A. 1985, Trace element and isotope geochemistry of lavas from Haleakala volcano, East Maui, Hawaii: implications for the origin of Hawaiian basalts. *J. Gephys. Res*, **90**, 8743-8768.

Clough C.T., Barrow G., Crampton C.B., Mauff H.B., Bailey E.B. and Anderson E.M. 1910, *The geology of East Lothian*. Mem. geol. Surv., Scotland.

Cohen R. S. & O'Nions R. K. 1982, Identification of recycled continental material in the mantle from Sr, Nd and Pb isotope investigations. *Earth Planet. Sci. Lett*, **61**, 73-84.

Cohen R.S., O'Nions R.K. & Dawson J.B. 1984, Isotope geochemistry of xenoliths from East Africa: implications for development of mantle reservoirs and their interaction. *Earth Planet. Sci. Lett*, **68**, 209-220.

Coombs D.S. & Wilkinson J.F.G. 1969, Lineages and fractionation trends in undersaturated volcanic rocks from the East Otago Volcanic Province (New Zealand) and related rocks. *J. Petrol*, **10**, 440-501.

Cox K.G. & Bell J.D. 1972, A crystal fractionation model for the basaltic rocks of the New Georgia Group, British Solomon Islands. *Contrib. Mineral. Petrol*, **37**, 1-13.

Cox K.G., Bell J.D. & Pankhurst R.J. 1979, *The Interpretation of Igneous Rocks*. Allen & Unwin, London.

Craig P.M. & Hall I.H.S. 1975, The Lower Carboniferous rocks of the Campsie-Kilpatrick area. *Scott. J. Geol*, **11**, 171-174.

Cullers R. L. & Graf J. L. 1983, Rare Earth Elements in igneous rocks of the continental crust: predominantly basic and ultrabasic rocks. *In: Rare Earth Element Chemistry*, ed: Henderson P., pp. 237-274. Elsevier.

Cundari A. & Ferguson A.K. 1982, Significance of the pyroxene chemistry from leucite-bearing and related assemblages. *Tschermaks Mineral. Petrogr. Mitt*, **30**, 189-204.

Cundari A. & Salviulo G. 1989, Ti solubility in diopsidic pyroxene from a suite of New South Wales leucities (Australia). *Lithos*. **22**, 191-198.

Davies A., McAdam A.D. & Cameron I.B. 1986, *Geology of the Dunbar district*. Mem. geol. Surv..

Davies G.R., Upton B. G. J. & Strogen P. 1984, Sr & Nd isotope evidence for age and origin of crustal xenoliths from the Midland Valley of Scotland and Central Ireland (abstract). *Trans. R. Soc. Edin. : E S*, **75**, 297.

De Paolo D. J. 1980, Crustal growth and mantle evolution: inferences from models of element transport and Nd and Sr isotopes. *Geochim.*

Cosmochim. Acta, 44, 1185-1196.

De Paolo D.J. & Wasserburg G. J. 1976, Nd isotopic variations and petrogenetic models. *Geophys. Res. Lett.*, 3, 249-252.

De Souza H.A.F. 1974, *Potassium-argon ages of Carboniferous igneous rocks from east Lothian and the south of Scotland* Unpubl. M.Sc. thesis, Univ. Leeds.

De Souza H.A.F. 1979, *The geochronology of Scottish Carboniferous volcanism* Unpubl. Ph.D. thesis, Univ. Edinb.

De Souza H.A.F. 1982, Age data from Scotland and the Carboniferous time scale. *In: Numerical Dating in Stratigraphy* ed: Odin G.S., John Wiley & Sons.

Deines P. 1980, The carbon isotopic composition of diamonds: relationship to diamond shape, colour, occurence and vapour composition. *Geochim. Cosmochim. Acta*, 44, 943-961.

Dewey J.F. 1982, Plate tectonics and the evolution of the British Isles. *J. geol. Soc. Lond.*, 139, 371-412.

Dixon J.E., Fitton J.G. & Frost R.T.C. 1981, The tectonic significance of post-Carboniferous igneous activity in the North Sea Basin. *In: Petroleum Geology of the Continental Shelf of North-west Europe*, pp121-137, Institute of Petroleum, London.

Dobosi G. 1989, Clinopyroxene zoning patterns in the young alkali basalts of Hungary and their petrogenetic significance. *Contrib. Mineral. Petrol.*, 101, 112-121.

Dolfi D. & Trigila R. 1983, Clinopyroxene solid solutions and water in magmas: results in the system phonolitic tephrite - H_2O. *Min. Mag.*, 47, 347-351.

Donaldson C.H. 1976, An experimental investigation of olivine morphology. *Contrib. Mineral. Petrol.*, 57, 187-213.

Downes M.J. 1974, Sector and oscillatory zoning in calcic augites from Mount Etna, Sicily. *Contrib. Mineral. Petrol.*, 47, 187-196.

Drever H.I. & Johnston R. 1957, Crystal growth of forsteritic olivine in magmas and melts. *Trans. R. Soc. Edin.*, 63, 289-315.

Droop G.T.R. 1987, A general equation for estimating Fe^{3+} concentrations in ferromagnesian silicates and oxides from microprobe analyses, using stoichiometric criteria. *Min. Mag.*, 51, 431-435.

Duda A. & Schmincke H.U. 1985, Polybaric differentiation of alkali basaltic magmas: evidence from green-core clinopyroxenes (Eifle, F.R.G.). *Contrib. Mineral. Petrol.*, 91, 340-353.

Dunn T. 1987, Partitioning of Hf, Lu, Ti and Mn between olivine, clinopyroxene and basaltic liquid. *Contrib. Mineral. Petrol*, 96, 476-484.

Dupré B. & Allègre C. J. 1980, Pb-Sr-Nd isotopic correlation and the chemistry of the North Atlantic mantle. *Nature*, 286, 17-22.

Edgar A.D., Condliffe E., Barnett R.L. & Shirran R.J. 1980, An experimental study of an olivine ugandite magma and mechanisms for the formation of its K-enriched derivatives. *J. Petrol*, 21, 475-497.

Eggler D. H. 1987, Solubility of Major and Trace Elements in Mantle Metasomatic Fluids: Experimental Constraints. *In: Mantle Metasomatism* eds: Menzies M.A. & Hawkesworth C.J., pp21-39. Academic Press.

Erlank A.J., Waters F.G., Hawkesworth C.J., Haggerty S.E., Allsopp H.L., Rickard R.S. & Menzies M. 1987, Evidence for mantle metasomatism in peridotite nodules from the Kimberley Pipes, South Africa. *In: Mantle Metasomatism* eds: Menzies M.A. & Hawkesworth C.J. pp221-311. Academic Press.

Eyles V.A., Simpson J.B. & Macgregor A.G. 1949, *Geology of Central Ayrshire*. Mem. geol. Surv., Scotland.

Falloon T.J. & Green D.H. 1989, The solidus of carbonated, fertile peridotite. *Earth Planet. Sci. Lett.* (submitted).

Falloon T.J. & Green D.H., The solidus of carbonated fertile peridotite under fluid saturated conditions. *Geology*, (in press).

Farone D., Molin G. & Zanazzi P.F. 1988, Clinopyroxenes from Vulcano (Aeolian Islands, Italy): Crystal chemistry and cooling history. *Lithos*, 22, 113-126.

Faure G. 1986, *Principles of isotope geology*. John Wiley & Sons Ltd.

Faure G. & Hurley P.M. 1963, The isotopic composition of strontium in oceanic and continental basalts: application to the origin of igneous rocks. *J. Petrol*, 4, 31-50.

Fitch F.J., Miller J.A. & Williams S.C. 1970, Isotopic ages of British Carboniferous rocks. *C R 6e Congr. Int. Stratigr. Geol. Carboniferous*, 2, 771-790.

Fitton J.G. 1987, The Cameroon line, West Africa: a comparison between oceanic and continental alkaline volcanism. *In: Alkaline Igneous Rocks*, eds: Fitton J.G. & Upton B.G.J. *Geol. Soc. Spec. Publ.* 30 273-292. Blackwell.

Fitton J. G. & Dunlop H. M. 1985, The Cameroon line, West Africa, and its bearing on the origin of oceanic and continental alkali basalt. *Earth Planet. Sci. Lett.*, 72, 23-38.

Fitton J. G. & James D.J. 1986, Basic volcanism associated with intraplate linear feature. *Phil. Trans. R. Soc. Lond.*, A317, 253-266.

Fitton J. G., James D., Kempton P. D., Ormerod D. S. & Leeman W. P. 1988, The role of lithospheric mantle in the generation of late Cenozoic basic magmas in the western United States. *J. Petrol. Special Lithosphere Issue*, 331-349.

Fitton J.G., James D.E. & Thirlwall M.F. 1984, *A user's guide to the X-ray fluoresence analysis of rock samples*, Upubl. report, 2nd edition, Univ. of Edinburgh.

Fitton J.G. & Upton B.G.J. (eds) 1987, *Alkaline igneous rocks. Geol. Soc. Spec. Publ*, **30**. Blackwell.

Flower M. F. J., Schmince H. U. & Thompson R. N. 1975, Phlogopite stability and the $^{87}Sr/^{86}Sr$ step in basalts along the Reykjanes Ridge. *Nature*, **254**, 404.

Floyd P. A. & Winchester J. A. 1975, Magma type and tectonic setting discrimination using immobile elements. *Earth Planet. Sci. Lett.*, **27**, 211-218.

Fodor R.V., Keil K. & Bunch T.E. 1975, Contributions to the mineral chemistry of Hawaiian rocks, IV Pyroxenes in rocks from Haleakala and west Maui volcanoes, Maui, Hawaii. *Contrib. Mineral. Petrol.*, **50**, 173-195.

Foley S. F. 1988, The genesis of continental basic alkaline magmas - an interpretation in terms of redox melting. *J. Petrol. Special Lithosphere Issue*, 139-161.

Forster S.C. & Warrington G. 1985, Geochronology of the Carboniferous, Permian and Triassic. *In: The Chronology of the Geological Record*, ed: Snelling N.J., *Mem. geol. Soc. Lond.*, **10** pp 99-113.

Forsyth I.H. & Chisholm J.I. 1977, *Geology of east Fife*. Mem. geol. Surv., Scotland.

Forsyth I.H. & Rundle C.C. 1978, The age of the volcanic and hypabyssal rocks of east Fife. *Bull. geol. Surv. Scotland*, **60**, 23-29.

Francis D. & Ludden J. 1989, The mantle sources for quaternary alkaline volcanism in the northern Canadian Cordillera. (abstract) *Continental magmatism abstracts, International Association of Volcanology & Chemistry of the Earth's interior*, **97**.

Francis D. & Ludden J. in press, The mantle source for olivine nephelinite, basanite, and alkaline olivine basalt at Fort Selkirk, Yukon, Canada. *J. Petrol.*

Francis E.H. 1961, Volcanism in relation to sedimentation in the Carboniferous rocks of the Saline district, Fife. *Bull. Geol. Surv. U.K.* **17**, 116-144.

Francis E.H. 1968, Effect of sedimentation on volcanic processes, including

neck-sill relationships, in the British Carboniferous. *23d Sess. Int. geol. Congr.* Czechoslovakia, sect. 2, 163-174.

Francis E.H. 1978a, Igneous activity in a fractured craton: Carboniferous volcanism in northern Britain. *In: Crustal Evolution in Northwestern Britain and Adjacent Regions*, eds: Bowes D.R. & Leake B.E., *Geol. J. Spec. Issue* 10, 279-296.

Francis E.H. 1978b, The Midland Valley as a rift, seen in connection with the late Palaeozoic European rift system. *In: Tectonics and Geophysics of Continental Rifts*, eds: Ramberg I.B. & Neuman E.R., pp 133-147, D. Reidel, Holland.

Francis E.H 1983, Carboniferous - Permian igneous rocks. *In: The Geology of Scotland*, ed: Craig G.Y., pp 297-324, Edinburgh.

Francis E.H. 1988, Mid-Devonian to early Permian volcanism: old world. *The Caledonian - Appalachian Orogen*, eds: Harris A.L. & Fettes D.J., *Geol. Soc. Spec. Publ.* 38, 573-584.

Francis E.H., Forsyth I.H., Read W.A. & Armstrong M. 1970, *The geology of the Stirling district.* Mem. geol. Surv. Scotland

Francis E.H. & Hopgood A.M. 1970, Volcanism and the Ardross Fault, Fife, Scotland. *Scott. J. Geol*, 6, 162-185.

Francis E.H. & Walker B.H. 1987, Emplacement of alkali-dolerite sills relative to extrusive volcanism and sedimentary basins in the Carboniferous of Fife, Scotland. *Trans. R. Soc. Edin*, 77, 309-323.

Frisch T. & Schmincke H.U. 1969, Petrology of clinopyroxene - amphibole inclusions from the Roque Nublo Volcanics, Gran Canaria, Canary Islands (Petrology of Roque Nublo Volcanics I). *Bull. Volcanol*, 33, 1073-1088.

Frey F.A. & Green D.H. 1974, The mineralogy, geochemistry and origin of lherzolite inclusions in Victorian basanites. *Geochim. Cosmochim. Acta* 38, 1023-1059.

Frey F.A., Green D.H. & Roy S.D. 1978, Integrated models of Basalt petrogenesis: A study of quartz tholeiites to olivine melilitites from south eastern Australia utilizing geochemical and experimental petrological data. *J. Petrol*, 19, 463-513.

Fugii T. & Scarfe C.M. 1985, Compositions of liquids coexisting with spinel lherzolite at 10kbar and the genesis of MORBS. *Contrib. Mineral. Petrol*, 90, 18-29.

Futa K. & Le Masurier W.E. 1983, Nd and Sr isotopic studies on Cenozoic mafic lavas from west Antartica: another source for continental alkali basalts.

Contrib. Mineral. Petrol., **83**, 38–44.

Gamble R.P. & Taylor L.A. 1980, Crystal/liquid partitioning in augite: effects of cooling rate. *Earth Planet. Sci. Lett.*, **47**, 21–33.

Gast P.W. 1968, Trace element fractionation and the origin of tholeiitic and alkaline magma types. *Geochim. Cosmochim. Acta*, **32**, 1057–1086.

Geikie A. 1866, Traces of a group of Permian volcanoes in the south west of Scotland. *Geol. Mag.*, **3**, 243–248.

Geikie A. 1880, On the Carboniferous volcanic rocks in the basin of the Firth of Forth – their structure in the field and under the microscope. *Trans. R. Soc. Edin.*, **29**, 437–518.

Geikie A. 1892, Volcanic action in the British Isles between Silurian and Tertiary. *Q. J. geol. Soc. Lond.*, **48**, 104–162.

Geikie A. 1897, *The ancient volcanoes of Great Britain*, 2 vols., Macmillan & Co., London.

Geikie A. 1900, *The geology of central and western Fife and Kinross*. Mem. geol. Surv., Scotland.

George T.N. 1960, The stratigraphical evolution of the Midland Valley. *Trans. geol. Soc. Glasg.*, **24**, 32–107.

Gibb F.G.F. 1973, The zoned clinopyroxenes of the Shiant Isles Sill, Scotland. *J. Petrol.*, **14**, 203–230.

Green D.H. 1973a, Conditions of melting of basanitic magma from garnet peridotite. *Earth Planet. Sci. Lett.*, **17**, 456–465.

Green D.H. 1973b, Experimental melting studies on a model upper mantle composition at high pressure under water-saturated and water-undersaturated conditions. *Earth Planet. Sci. Lett.*, **19**, 37–53.

Green D.H. 1970, A review of experimental evidence on the origin of basaltic and nephelintic magmas. *Phys. Earth planet. Interiors*, **3**, 221–235.

Green D.H. 1971, Compositions of basaltic magmas as indicators of conditions of origin: application to oceanic volcanism. *Phil. Trans. R. Soc. Lond.*, **A268**, 707–725.

Green D.H., Fallon T.J. & Taylor W.R. 1987, Mantle-derived magmas– roles of variable source peridotite and variable C–H–O fluid compositions. *In: Magmatic Processes: Physicochemical Principles*, ed: Mysen B.O. *The Geochemical Society, Spec. Publ.*, **1**, 139–154.

Green D.H. & Hibberson W. 1970, Experimental duplication of conditions of precipitation of high-pressure phenocrysts in a basaltic magma. *Phys. Earth Planet. Interiors*, **3**, 247–254.

Green D.H. & Liebermann R.C. 1976, Phase equilibria and elastic properties of a pyrolite model for the oceanic upper mantle. *Tectonophysics*, 32, 61-92.

Green D.H. & Ringwood A.E. 1967, Crystallisation of basalt and andesite under high pressure hydrous conditions. *Earth Planet. Sci. Lett.*, 3, 481-489.

Green D.H. & Ringwood A.E. 1967, The genesis of basaltic magmas. *Contrib. Mineral. Petrol.*, 15, 103-190.

Green D.H. & Wallace M.E. 1988, Mantle metasomatism by ephemeral carbonite melts. *Nature*, 336, 459-461.

Hall J. 1974, A seismic reflection survey of the Clyde Plateau lavas in north Ayrshire and Renfrewshire. *Scott. J. Geol.*, 9, 253-279.

Halliday A.N. 1984, Coupled Sm-Nd and U-Pb systematics in late Caledonian granites and the basement under northern Britain. *Nature*, 307, 229-233.

Halliday A.N., Aftalion M., Van Breeman O. & Jocelyn J. 1979, Petrogenetic significance of Rb-Sr and U-Pb isotopic systems in the 400 Ma old British Isles granitoids and their hosts. *In: The Caledonides of the British Isles - Reviewed*, eds: Harris A.L., Holland C.H. & Leake B.E., *Geol. Soc. Lond. Spec. Publ.*, 8, 653-681.

Halliday A.N., Fallick A.E., Dickin A.P., Mackenzie A.B., Stephens W.E. & Hildreth W. 1983, The isotopic and chemical evolution of Mount St. Helens. *Earth Planet. Sci. Lett.*, 63, 241-256.

Halliday A.N., Fallick A.E., Hutchinson J. & Hildreth W. 1984, A Nd, Sr and O isotopic investigation into the causes of chemical and isotopic zonation in the Bishop Tuff California]. *Earth. Planet. Sci. Lett.*, 68, 379-391.

Halliday A.N., Stephens W.E., Hunter R.H., Menzies M.A., Dicken A.P. & Hamilton P.J. 1985, Isotopic and chemical constraints on the building of the deep Scottish lithosphere. *Scott. J. Geol.*, 21, 465-91.

Hanson G.N. 1977, Geochemical evolution of the suboceanic mantle. *J. geol. Soc. Lond.*, 134, 235-253.

Hanson G.N. 1980, Rare earth elements in petrogenetic studies of igneous systems. *Ann. Rev. Earth Planet. Sci.*, 8, 371-406.

Harland W.B., Cox A.V., Llewellyn P.G., Pickton C.A.G., Smith A.G. & Walters R. 1982. *A geologic time scale*, Cambridge University Press.

Harmon R.S. & Halliday A.N. 1980, Oxygen and strontium isotope relationships in the British late Caledonian granites. *Nature*, 283, 21-25.

Hart S. 1988, Heterogeneous mantle domains: signatures, genesis and mixing chronologies. *Earth Planet. Sci. Lett.*, 90, 273-296.

Hart S.R. & Brooks C. 1974, Clinopyroxene-matrix partitioning of K, Rb, Cr, Sr

and Ba. *Geochim. Cosmochim. Acta*, 38, 1799-1806.

Hart S.R. & Brooks C. 1977, The geochemistry and evolution of the early Precambrian mantle . *Contrib. Mineral. Petrol*, 61, 109.

Hart S.R., Gerlach D.C. & White W.M. 1986, A possible new Sr-Nd-Pb mantle array and consequences for mantle-mixing. *Geochim. Cosmochim. Acta* 50, 1551-1557.

Hartman P. 1969, Can Ti^{4+} replace Si^{4+} in silicates? *Min. Mag.*, 37, 366-369.

Haszeldine R.S. 1984, Carboniferous North Atlantic palaeogeography: stratigraphic evidence for rifting not megashear or subduction. *Geol. Mag.*, 121, 443-463.

Hawkesworth C.J., Norry M.J., Roddick J.C. & Vollmer R. 1979, $^{143}Nd/^{144}Nd$ and $^{87}Sr/^{86}Sr$ ratios from the Azores and their significance in LIL-element enriched mantle. *Nature*, 280, 28-31.

Hawkesworth C.J., vanCalsteren P., Rogers N.W. & Menzies M.A. 1987, Isotope variations in Recent Volcanics: a trace element perspective. *In: Mantle Metasomatism*, eds: Menzies M.A. & Hawkesworth C. J. pp365-388. Academic Press.

Hays J.F. 1967, Lime-alumina-silica. *Carnegie Inst. Wash. Yrbk.*, 65, 234-239.

Henderson C.M.B., Foland K.A. & Gibb F.G.F 1987, The age of the Lugar Sill and a discussion of the late-Carboniferous / Early Permian sill complex of SW Scotland. *Geol. J.*,22, 43-52.

Henderson C.M.B. & Gibb F.G.F. 1983, Felsic mineral crystallization trends in differentiating alkaline basic magmas. *Contrib. Mineral. Petrol.*, 84, 355-364.

Henderson C.M.B. & Gibb F.G.F. 1987, The petrology of the Lugar Sill, SW Scotland. *Trans. R. Soc. Edin.*, 77, 325-347.

Henderson P. *Inorganic geochemistry* pp353. Pergamon Press.

Henderson P. 1984, General geochemical properties and abundances of the rare earth elements. *In: Rare Earth Element Geochemistry*, ed: Henderson P. pp 1-32. Elsevier.

Herzberg C. T. 1974, *Phase assemblages of the system* $CaO-Na_2O-MgO-Al_2O_3-SiO_2$ *in the plagioclase and spinel-lherzolite mineral facies.* Unpubl. Ph.D. thesis, Univ of Edinburgh.

Hess J.C., Lippolt H.J., Holub V.M. & Pesek 1985, Isotopic ages of two Westphalian C tuffs- a contribution to the Upper Carboniferous time-scale. *(Abstr.) Eur. Geophys. Ass.*, Cambridge U.K.

Hofmann A.W. & Hart S.R. 1978, An assessment of local and regional isotopic

equilibrium in the mantle. *Earth Planet. Sci. Lett.*, 38, 44-62.

Hofman A.W., Jochum K.P., Seufert M. & White W.M. 1986, Nb and Pb in oceanic basalts: new constraints on mantle evolution. *Earth Planet. Sci. Lett.*, 79, 33-45.

Hofman A.W. & White W.M. 1982, Mantle plumes from ancient oceanic crust. *Earth Planet. Sci. Lett.*, 57, 421-436.

Hole M.J. 1988, Post-subduction alkaline volcanism along the Antartic Peninsula. *J. geol. Soc. Lond.*, 145, 985-998.

Hunter R.H., Upton B.G.J. & Aspen P. 1984, Meta-igneous granulite and ultramafic xenoliths from basalts of the Midland Valley of Scotland: petrology and mineralogy of the lower crust and upper mantle. *Trans. R. Soc. Edin: Earth Sci.*, 75, 75-84.

Hunter R.H. & Upton B.G.J. 1987, The British Isles - a Palaeozoic mantle sample. *In: Mantle Xenoliths*, ed: Nixon P.H., pp 107-118. John Wiley & Sons.

Huppert H.E. & Sparks R.S.J. 1985, Cooling and contamination of mafic and ultramafic magmas during ascent through continental crust. *Earth Planet. Sci. Lett.*, 74, 371-386.

Hutchison R., Chambers A.L., Paul D.K. & Harris P.G. 1975, Chemical variation among French ultramafic Xenoliths - evidence for a heterogeneous mantle. *Min. Mag.*, 40, 153-170.

Irving A.J. 1974a, Pyroxene-rich ultramafic xenoliths in the Newer Basalts of Victoria, Australia. *Neues Jahrb. Mineral. Abhandl.* 120, 147-167.

Irving A.J. 1974b, Megacrysts from the Newer Basalts and other basaltic rocks of southeastern Australia. *Geol. Soc. Am. Bull.*, 85, 1503-1514.

Irving A.J. 1978, A review of experimental studies of crystal/liquid trace element partitioning. *Geochim. Cosmochim. Acta*, 42, 743-770.

Irving A.J. & Frey F.A. 1984, Trace element abundances in megacrysts and host basalts: Constraints on partition coefficients and megacrust genesis. *Geochim. Cosmochim. Acta*, 48, 1201-1221.

Jacobsen S.B. & Wasserburg G.J. 1979, The mean age of mantle and crustal reservoirs. *J. Geophys. Res.*, 84, 7411-7428.

James S.D. 1988, *Volcanism in sedimentary basins and its implications for mineralization*. Unpubl. Ph.D. thesis, Univ. of Newcastle upon Tyne.

Jaques A.L. & Green D.H. 1980, Anhydrous melting of peridotite at 0-15 kb pressure and the genesis of tholeiitic basalts. *Contrib. Mineral. Petrol.*, 73, 287-310.

Jurewicz A.J.G. & Watson E.B. 1988, Cations in olivine: part 1: calcium

partitioning between olivines and coexisting melts, with petrologic applications. *Contrib. Mineral. Petrol*, *99* 176-185.

Kay R.W. & Gast P.W. 1973, The rare earth content and origin of alkali- rich basalts. *J. Geol*, 81, 653-682.

Keller W.D. 1957, *The principles of chemical weathering*. 2nd edition 1957, 111pp. Columbia, Mo. Lucas Bros.

Kennedy W.Q. 1958, The tectonic evolution of the Midland Valley of Scotland. *Trans. geol. Soc. Glasg*, 23, 106-133.

Kesson S, & Price R.C. 1972, The major and trace element chemistry of Kaersutite and its bearing on the petrogenesis of alkaline rocks. *Contrib. Mineral. Petrol*, 35, 119-124.

Kirton S.R. 1984, Carboniferous volcanicity in England with special reference to the Westphalian of the E and W Midlands. *J. geol. Soc. Lond*, 141, 161-170.

Kleeman J.D., Green D.H. & Lovering J.F. 1969, Uranium distribution in ultramafic inclusions from Victoria basalts. *Earth Planet. Sci. Lett*, 5, 449-458.

Klein E.M. & Langmuir C.H. 1987, Global Correlations of Ocean Ridge Basalt Chemistry with axial depth and crustal thickness. *J. Gephys. Res*, 92, 8089-8115.

Kurz M.D., Jenkins W.J., Shilling J.G. & Hart S.R. 1982, Helium isotopic systematics of ocean islands and mantle heterogeneity. *Nature*, 297, 43-46.

Kushiro I. 1960, Si-Al relation in clinopyroxenes from igneous rocks. *Am. J. Sci*, 258, 548-554.

Kuno H. 1964, Aluminian augite and bronzite in alkali olivine basalt from Taka-sima, northern Kyushu, Japan. *In: Advancing Frontiers in Geology and Geophysics* eds:-*-, pp205-220, Osmania Univ. Press, Hyderabad.

Kutolin V.A. & Frolova V.M. 1970, Petrology of ultrabasic inclusions from basalts of Minusa and Transbaikalian regions (Siberia, USSR). *Contrib. Mineral. Petrol*, 29, 163-170.

Langmuir C.H., Vocke R.D.jr, Hanson G.N. & Hart S.R. 1978, A general mixing equation with applications to Icelandic basalts. *Earth Planet. Sci. Lett*, 37, 380-392.

Latin D.M., Dixon J.E. & Fitton J.G. 1989 in press a, Rift-related magmatism in the North Sea basin. *In: Tectonic Evolution of the North Sea Rifts*, eds: Blundell D.J. & Gibbs A. Oxford University Press.

Latin D.M., Dixon J.E., Fitton J.G. & White N. 1989 in press b, Mesozoic

magmatic activity in the North Sea Basin: implications for stretching history. *In: Tectonic Movements Responsible for Britain's Oil and Gas Reserves*, eds: Hardman R.F.P. & Brooks J.R.V. *Geol. Soc. Spec. Publ.*

Larsen L. M. 1976, Clinopyroxenes and coexisting mafic minerals from the alkaline Ilimaussq intrusion, south Greenland. *J. Petrol.*, **17**, 258-290.

Le Bas M. 1962, The role of aluminium in igneous clinopyroxenes with relation to their parentage. *Am. J. Sci.*, **260**, 267-288.

Le Bas M. 1989 in press, Nephelinitic and basanitic rocks. *J Petrol., in press*

Le Bas M.J., Le Maitre R.W., Streckeisen A. & Zanettin B. 1986, A chemical classification of volcanic rocks based on the total alkali-silica diagram. *J. Petrol.*, **27**, 745-750.

Le Roex A.P. 1987, Source regions of mid-ocean ridge basalts: Evidence for enrichment processes. *In: Mantle Metasomatism*, eds: Menzies M.A. & Hawkesworth C.J. Academic Press.

Leeder M.R. 1974, The origin of the Northumberland Basin. *Scott. J. Geol.*, **10**, 283-296.

Leeder M.R. 1976, Sedimentary facies and the origins of basin subsidence along the northern margin of the supposed Hercynian Ocean. *Tectonophysics*, **36**, 167-179.

Leeder M.R. 1982, Upper Palaeozoic basins of the British Isles- Caledonide inheritance versus Hercynian plate margin processes. *J. geol. Soc. Lond.*, **139**, 479-491.

Leeder M.R. 1987, Plate tectonics , palaeogeography and sedimentation in Lower Carboniferous Europe. *In: European Dinantian Environments*, eds: Miller J., Adams A.E. & Wright V.P., pp 1-20, Wiley, London.

Leeder M.R. 1988a, Devono- Carboniferous river systems and sediment dispersal from the orogenic belts and cratons of NW Europe. *In: The Caledonian - Appalachian Orogen*, eds: Harris A.L. & Fettes D.J., *Geol. Soc. Spec. Publ.*, **38**, 549-558.

Leeder M.R. 1988b, Recent developments in Carboniferous geology: a critical review with implications for the British Isles and N.W. Europe. *Proc. Geol. Ass.*, **99**, 73-100.

Leeder M.R. & McMahon A.H. 1988, Upper Carboniferous (Silesian) basin evolution in northern Britain. *In: Sedimentation in a Synorogenic Basin Complex* eds: Besley B.M. & Kelling G. pp43-52. Blackie & Sons.

Leung I.S. 1974, Sector-zoned titanaugites: morphology, crystal chemistry and growth. *Am. Mineralogist*, **59**, 127-138.

Lippolt H.J., Hess J.C. & Burger K. 1984, Isotopische alter Pyroklastischen Sanidinen aus Kaolin – Kohlentonsteinen als Korrelationsmarken fur das Mitteleuropisch Oberkarbon]. *Fortschr. Geol. Rheinld. Westf.*, 32, 119–150.

Littlejohn A.L. & Greenwood H.J. 1974, Lherzolite nodules in basalts from British Columbia, Canada. *Can. J. Earth Sci.*, 11, 1288–1308.

Lloyd F.E. & Bailey D.K. 1975, Light element metasomatism of the continental mantle: the evidence and the consequence. *In: Physics & Chemistry of the Earth*, 9, eds: Ahrens L.H., Dawson J.B., Duncan A.R. & Erlank A.J. pp 389–416.

Longhi J., Walker D., Grove T.L. Stolper E.H. & Hays J.F. 1974, The petrology of Apollo 17 mare basalts. *Proc. Lunar. Sci. Conf.*, 5th, 447–469.

Lorenz V. & Nicholls I.A. 1976, The Permocarboniferous basin and range province of Europe. An application of plate tectonics. *In: The Continental Permian in Central, West and South Europe*, ed: Falke –*–., pp 313–342, Reidel Dordrecht, Holland.

Maaloe S. 1982, Geochemical aspects of permeability controlled partial melting and fractional crystallisation. *Geochim. Cosmochim. Acta*, 46, 43–57.

McAdam A.D. 1974, The petrography of the igneous rocks in the Lower Carboniferous (Dinantian) at Spilmersford, east Lothian, Scotland. *Bull. geol. Surv. Scotland*, 45, 39–46.

McAdam A.D. & Tulloch W. 1985, Geology of the Haddington district. *Mem. geol. Surv. G.B.*

Macdonald G.A. & Katsura T. 1964, Chemical composition of Hawaiian lavas. *J. Petrol.*, 5, 82–133.

Macdonald R. 1975, Petrochemistry of the Early Carboniferous (Dinantian) lavas of Scotland. *Scott. J. Geol.*, 11, 269–314.

Macdonald R. 1980, Trace element evidence for mantle heterogeneity beneath the Scottish Midland Valley in the Carboniferous and Permian. *Phil. Trans. R. Soc. Lond.*, A297, 245–257.

Macdonald R., Gass K.N., Thorpe R.S. & Gass I.G. 1984, Geochemistry and petrogenesis of Derbyshire Carboniferous basalts. *J. geol. Soc. Lond.*, 141, 147–159.

Macdonald R., Gottfried D., Farrington M.J., Brown F.W. & Skinner N.G. 1981, Geochemistry of a continental tholeiite suite: late Palaeozoic quartz dolerite dykes of Scotland. *Trans. R. Soc. Edin.*, 72, 57–74.

Macdonald R., Thomas J.E. & Rizello S.A. 1977, Variations in basalt chemistry with time in the Midland Valley province during the Carboniferous and

Permian. *Scott. J. Geol*, 13, 11-22.

Macgregor A.G. 1948, Problems of Carboniferous - Permian volcanicity in Scotland. *Q. J. Geol. Soc. Lond*, 104, 133-153.

Macintyre R.M., Cliff R.A. & Chapman N.A. 1981, Geochronological evidence for phased volcanic activity in Fife and Caithness necks, Scotland. *Trans. R. Soc. Edin., Earth Sci*, 72, 1-7.

McKenzie D.P. 1984, The Generation and Compaction of Partially Molten Rock. *J. Petrol*, 25, 713-765.

McKenzie D.P. 1985, The extraction of magma from the crust and mantle. *Earth Planet. Sci. Lett*, 74, 81-91.

McKenzie D.P. 1987, The compaction of igneous and sedimentary rocks. *J. geol. Soc. Lond*, 144, 299-307.

McKenzie D. & O'Nions R.K. 1983, Mantle reservoirs and ocean island basalts. *Nature*, 301, 229-231.

McLean A.C. 1978, Evolution of fault-controlled ensialic basins in north-western Britain. *In: Crustal Evolution in North-western Britain and Adjacent Regions*, eds: Bowes D.R. & Leake B.E. *Geol. J. Spec.Issue*, 10, 279-296.

Martin N.R. 1955, Lower Carboniferous volcanism near North Berwick. *Bull. geol. Surv. Scotland*, 7, 90-100.

Menzies M. 1987, Alkaline rocks and their inclusions: a window on the earth's interior. *In: Alkaline Igneous Rocks*, eds: Fitton J.G. & Upton B.G.J. *Geol. Soc. Spec. Publ.* 30 15-28. Blackwell.

Menzies M.A. & Halliday A.N. 1984, Isotopic evidence for mantle heterogeneity beneath the Midland Valley and adjacent regions from studies of inclusion suites.(abstract). *Trans. R. Soc. Edin: Earth Sci*, 75, 298-299.

Menzies M. & Halliday A. 1988, Lithospheric mantle domains beneath the Archean and Proterozoic crust of Scotland. *J. Petrol. Special Lithosphere Issue*, 275-302.

Menzies M.A., Halliday A.N., Palacz Z., Hunter R., Upton B.G.J., Aspen P. & Hawkesworth C.J. 1987, Evidence from mantle xenoliths for an enriched lithospheric keel under rhe Outer Hebrides. *Nature*, 325, 44-47.

Menzies M.A. & Hawkesworth C.J. 1987, Upper mantle processes and composition. *In: Mantle Xenoliths*, ed: Nixon P.H. pp725-738. John Wiley & Sons Ltd.

Menzies M. & Murthy V.R. 1980, Mantle Metasomatism as a precursor to the genesis of alkaline magmas - isotopic evidence. *Am. J. Sci*, 280a, 622-638.

Menzies M.A. & Murthy V.R. 1980, Nd and Sr isotope geochemistry of hydrous mantle nodules and their host alkali basalts: implications for local heterogeneities in a metasomatically veined mantle. *Earth Planet. Sci. Lett.* 46, 323-324.

Menzies M.A., Rogers N., Tindle A. & Hawkesworth C. 1987, Metasomatic and enrichment processes in lithospheric peridotites, an effect of asthenosphere-lithosphere interaction. *In: Mantle Metasomatism*, eds: Menzies M.A. & Hawkesworth C. pp 313-361. Academic Press.

Michael P.J. & Chase R.L. 1987, The influence of primary magma composition, H_2O and pressure on mid-ocean ridge basalt differentiation. *Contrib. Mineral. Petrol.* 96, 245-263.

Morrison M.A., Hendry G.L. & Leat P.T. 1986, Regional and tectonic implications of parallel Caledonian and Permo-Carboniferous lamprophyre dyke swarms from Lismore, Ardgour. *Trans. R. Soc. Edin: Earth Sci.* 77, 279-288.

Murata K.J. & Richter D.H. 1966, Chemistry of the lavas of the 1959-60 eruption of the Kilauea Volcano, Hawaii. *U.S. Geol. Surv. Prof. Paper, 537-A* 26pp.

Mykura W. 1965, The age of the lower part of the New Red Sandstone of south-west Scotland. *Scott. J. Geol.* 1, 9-18.

Mykura W. 1967, The Upper Carboniferous rocks of south-west Ayrshire. *Bull. geol. Surv. Scotland*, 26, 23-98.

Mysen B.O. 1975, Partitioning of iron and magnesium between crystals and partial melts in peridotite upper mantle. *Contrib. Mineral. Petrol.* 52, 69-76.

Nakamura N. 1974, Determination of REE, Ba, Fe, Mg, Na and K in carbonaceous and ordinary chondrites. *Geochim. Cosmochim. Acta* 38, 757-775.

Nakamura N., Tatsumoto M., Nunes P.D. Unruh D.M., Schwab A.P. & Wildeman P.D. 1976, 4.4 by-old clast in boulder 7, Apollo 17: a comprehensive chronological study by U-Pb, Rb-Sr and Sm-Nd methods. *Proc. 7th Lunar Sci. Conf.* 2309.

Nakamura Y. 1973, Origin of sector zoning of igneous clinopyroxenes. *Am. Mineralogist* 58, 986-990.

Nicholls I.A. 1974, Liquids in equilibrium with peridotitic mineral assemblages at high water pressure. *Contrib. Mineral. Petrol.* 45, 289-316.

Nicholls I.A. & Lorenz V. 1973, Origin and crystallisation history of Permian tholeiites from the Sarr-Nahe trough, SW Germany. *Contrib. Mineral. Petrol.* 40, 327-344.

Norry M.J. & Fitton J.G. 1983, Compositional differences between oceanic and continental basic lavas and their significance. *In: Continental Basalts and Mantle Xenoliths*, eds: Hawkesworth C.J. & Norry M.J. pp 5-19. Shiva, Nantwich.

Oftedahl C. 1978, Origin of the magmas of the Vestfold Lava Plateau. *In: Petrology and Geochemistry of Continental Rifts*, eds: Neuman E.R. & Ramberg I.B. pp 193-208. D. Reidel, Holland.

O'Hara M.J. 1968, The bearing of phase equilibria studies in synthetic and natural systems on the origin and evolution of basic and ultrabasic rocks. *Earth Sci. Reviews*, 4, 69-133.

Oslen P., Yuen D.A. & Balsiger D. 1984, Mixing of passive heterogeneities by mantle convection. *J. Gephys. Res.*, 89, 425-436.

O'Nions R.K., Evensen J.N. & Hamilton P.J. 1979, Geochemical modelling of mantle differentiation and crustal growth. J G R , 84, 6091-6101.

O'Nions R.K. & Pankhurst R.J. 1974, Petrogenetic significance of isotope and trace element variation in volcanic rocks from the Mid-Atlantic. *J. Petrol.*, 15, 603-634.

Peach B.N., Clough C.T., Hinxman L.W., Grant Wilson J.S.,Crampton C.B., Maufe H.B. & Bailey B.A. 1910, *Geology of the neighbourhood of Edinburgh*. Mem. geol. Surv., Scotland.

Pearce J.A. 1983, Role of the sub-continental lithosphere in magma genesis at active continental margins. *In: Continental Basalts and Mantle Xenoliths*, eds: Hawkesworth C.J. & Norry M.J. pp230-249. Shiva.

Pearce J.A. & Cann J.R. 1973, Tectonic setting of basic volcanic rocks determined using trace element analysis. *Earth Planet. Sci. Lett.*, 19, 290-300.

Pearce J.A. & Norry M.J. 1979, Petrogenetic implications of Ti, Zr, Y and Nb variations in volcanic rocks. *Contrib. Mineral. Petrol.*, 69, 33-47.

Pidgeon R.T. & Aftalion M. 1978, Cogenetic and inherited zircon U-Pb systems in granites: Palaeozoic granites of Scotland and England. *In: Crustal Evolution in Northwestern Britain and Adjacent Regions*, eds: Bowes D.R. & Leake B.E. *Geol. J. Spec. Iss.* 10, 183-248.

Read W.A. 1988, Controls on Silesian sedimentation in the Midland Valley of Scotland. *In: Sedimentation in a Synorogenic Basin Complex*, eds: Besley B.M. & Kelling G. pp222-241. Blackie.

Richey J.E., Anderson E.M. & MacGregor A.G. 1930, *The geology of North Ayrshire*. Mem. geol. Surv. Scotland.

Ringwood A.E. 1975, *Composition and Petrology of the Earth's Mantle.* McGraw-Hill, New York.

Ringwood A.E. 1982, Phase transformations and differentiation in subducted lithosphere: implications for mantle dynamics, basalt petrogenesis, and crustal evolution. *J. Geol*, 90, 611-643.

Robinson P. 1980, The composition space of terrestrial pyroxenes - internal and external limits. *In: Reviews in Mineralogy, vol. 7, Pyroxenes*, ed: Prewitt C.T. , pp419-476. Min. Soc. Am.

Rock N.M.S. 1977, The nature and origin of lamprophyres: some definitions, distinctions and derivations. *Earth Sci. Rev*, 13, 123-169.

Rock N.M.S. 1983, The Permo-Carboniferous camptonite - monchiquite dyke suite of the Scottish Highlands and Islands: distribution, field and petrological aspects. *Report 82/14, Institute of Geological Sciences.*

Roden M.K., Hart S.R., Frey F.A. & Melson W.G. 1984, Sr, Nd & Pb isotopic and REE geochemistry of St. Paul's Rocks: the metamorphic and metasomatic development of an alkali basalt mantle source. *Contrib. Mineral. Petrol*, 85, 376-390.

Roeder P.L. & Emslie R.F. 1970, Olivine-liquid equilibrium. *Contrib. Mineral. Petrol*, 29, 275-289.

Russell D.G. 1985, *Experimental and petrological studies of phenocryst assemblages in Scottish Permo-Carboniferous basaltic rocks.* Unpubl. Ph.D. thesis, Univ. Edinburgh.

Russell M.J. 1976, A possible Lower Permian age for the onset of ocean floor spreading in the northern North Atlantic. *Scott. J. Geol*, 12, 315-323.

Russell M.J. & Smythe D.K. 1983, Origin of the Oslo Graben in relation to the Hercynian - Alleghenian orogeny and lithospheric rifting in the north Atlantic. *Tectonophysics*, 94, 457-472.

Sack R.O. & Carmichael I.S.E. 1984, Fe=Mg and $TiAL_2$=$MgSi_2$ exchange reactions between clinopyroxenes and silicate melts. *Contrib. Mineral. Petrol*, 85, 103-115.

Sack R.O., Walker D. & Carmichael I.S.E. 1987, Experimental petrology of alkalic lavas: constraints on cotectics of multiple saturation in natural basic liquids. *Contrib. Mineral. Petrol*, 96, 1-23.

Schilling J.G. 1973, Iceland mantle plume. Geochemical study of Reykjanes Ridge. *Nature*, 242, 565-571.

Shimizu N. 1981, Trace element incorporation into growing augite phenocryst. *Nature*, 289, 575-577.

Simkin T. & Smith J.V. 1970, Minor element distribution in olivine. *J. Geol.*, 78, 304–325.

Sleep N.H. 1984, Tapping of magmas from ubiquitous mantle heterogeneities: an alternative to mantle plumes? *J. Geophys. Res.*, 89, 10029–10041.

Smedley P.L. 1986a, The relationship between calc-alkaline volcanism and within-plate continental rift volcanism: evidence from Scottish Palaezoic lavas. *Earth Planet. Sci. Lett.*, 76, 113–128.

Smedley P.L. 1986b, *Petrochemistry of Dinantian volcanism in northern Britain* Unpubl. Ph.D. thesis, Univ. Edinburgh.

Smedley P.L. 1988a, Trace element and isotopic variations in Scottish and Irish Dinantian volanism: evidence for an OIB-like mantle source. *J. Petrol.*, 29, 413–445.

Smedley P.L. 1988b, The geochemistry of Dinantian volcanism in south Kintyre and the evidence for provincialism in the southern Scottish mantle. *Contrib. Mineral. Petrol.*, 99, 374–384.

Snelling & Chan 1976, I.G.S. internal report *In: Geology of the Haddington District* Mem. geol. Surv. Scotland., McAdam A.D. & Tulloch W.

Sørensen H. (ed.) 1974, *The Alkaline Rocks* 622pp Wiley.

Speight J.M. & Mitchell J.G. 1979, The Permo-Carboniferous dyke swarm of northern Argyll and its bearing on the dextral displacement on the Great Glen Fault. *J. Geol. Soc. Lond.*, 136, 3–11.

Spera F.J. 1984, Carbon dioxide in petrogenesis III: role of volatiles in the ascent of alkaline magma with special reference to xenolith-bearing mafic lavas. *Contrib. Mineral. Petrol.*, 88, 217–232.

Spera F.J. 1987, Dynamics of translithic migration of metasomatic fluid and alkaline magma. *In: Mantle Metasomatism*, eds: Menzies M.A. & Hawkesworth C.J. pp 1–20. Academic Press.

Steiger R.H. & Jager E. 1977, Subcommission on geochronology: convention on the use of decay constants in geo- and cosmochronology. *Earth Planet. Sci. Lett.*, 36, 359–362.

Stolper E.M. 1980, A phase diagram for mid-ocean ridge basalts: preliminary results and implications for petrogenesis. *Contrib. Mineral. Petrol.*, 74, 13–27.

Stormer J.C. 1973, Calcium zoning in olivine and its relationship to silica activity and pressure. *Geochim. Cosmochim. Acta* 37, 1815–1821.

Stosch H.G. & Seck H.A. 1980, Geochemistry and mineralogy of two spinel peridotite suites from Dreiser Weiher, West Germany. *Geochim.*

Cosmochim. Acta 44, 457-470.

Strekeisen A. 1979, Classification and nomenclature of volcanic rocks, lamprophyres, carbonatites and melilitic rocks: recommendations and suggestions of the IUGS subcomission on the systematics of igneous rocks. *Geology*, 7, 331-335.

Strong D.F. 1969, Formation of the hour-glass structure in augite. *Min. Mag*, 37, 472-479.

Sun S-S 1980, Lead isotopic study of young volcanic rocks from mid-ocean ridges, ocean islands and island arcs. *Phil. Trans. R. Soc. Lond*, A297, 409-445.

Sun S-S & Hanson G.N. 1975, Evolution of the mantle: geochemical evidence from alkali basalt. *Geology*, 3, 297-302.

Sundvoll B. 1978, Rb/Sr - relationship in the Oslo igneous rocks. *In: Petrology & Geochemistry of Continental Rifts*, eds: Neuman E.R. & Ramberg I.B. pp181-184. D. Reidel, Holland.

Sweatman T.R. & Long J.V.P. 1969, Quantitative electron probe micranalysis of rock-forming minerals. *J. Petrol*, 10, 332-379.

Takahashi E. & Kushiro I. 1983, Melting of dry perdotite at high pressures and basalt magma genesis. *Am. Mineralogist*, 68, 859-879.

Tatsumoto M. 1978, Isotopic composition of lead in oceanic basalt and its implication to mantle evolution. *Earth Planet. Sci. Lett*, 38, 63-87.

Taylor W.R. 1985, *The role of COH fluids in upper mantle processes: a theoretical, experimental and spectroscopic study.* Unpubl. Ph.D. thesis, Univ. of Tasmania, Hobart.

Taylor W.R. 1987, A reappraisal of the nature of fluids included in diamonds: a window to deep-seated mantle fluids and redox conditions. *Geol. Soc. Australia Spec. Publ*, 12.

Thirlwall M.F. 1979, *The petrochemistry of the British Old Red Sandstone volcanic province.* Unpubl. Ph.D. thesis Univ. Edinburgh.

Thirlwall M.F. 1981, Implications for Caledonian plate tectonic models of chemical data from volcanic rocks of the British Old Red Sandstone. *J. geol. Soc. Lond*, 138, 123-138.

Thirlwall M.F. 1982, Systematic variation in chemistry and Nd-Sr isotopes across a Caledonian calc-alkaline volcanic arc: implications for source materials. *Earth Planet. Sci. Lett*, 58, 27-50.

Thirlwall M.F, 1986, Lead isotope evidence for the nature of the mantle beneath Caledonian Scotland. *Earth Planet. Sci. Lett*, 80, 55-70.

Thompson R.N. 1974, Some high-pressure pyroxenes. *Min. Mag*, **39**, 768-787.

Thompson R.N. 1977, Primary basalts and magma genesis. III Alban Hills, Roman comagmatic province, Central Italy. *Contrib. Mineral. Petrol*, **60**, 91-108.

Thompson R.N. 1982, Magmatism of the British Tertiary Volcanic province. *Scott. J. Geol*, **18**, 49-107.

Thompson R.N., Esson J. & Dunham A.C. 1972, Major element chemical variation in the Eocene lavas of the Isle of Skye, Scotland. *J. Petrol*, **13**, 219-253.

Thompson R.N., Morrison M.A., Dickin A.P. & Hendry G.L 1983, Continental flood basalts ... arachnids rule OK? *In: Continental Basalts and Mantle Xenoliths*, eds: Hawkesworth C.J. & Norry M.J. pp158-185. Shiva.

Thompson R.N., Morrison M.A., Hendry G.L & Parry S.J. 1984, An assessment of the relative roles of crust and mantle in magma genesis: an elemental approach. *Phil. Trans. Roy. Soc.* **A310**, 541-590.

Thornton C.P. & Tuttle O.F. 1960, Chemistry of igneous rocks I. Differentiation Index. *Am. J. Sci*, **258**, 664-684.

Tomkeieff S.I. 1937, Petrochemistry of the Scottish Permian igneous rocks. *Bull. Volcanol*, **1**, 59-87.

Treuil M. 1973, *Criteres petrologiques, geochemiques et structuraux de la genese et de la differenciation des magmas basaltiques: exemple de l'Afar.* Unpubl. Ph.D. thesis, Univ. of Orleans.

Treuil M. & Joron J.M. 1975, Utilisation des elements hygromagmatophiles pour la simplification de la modelisation quantitative des processus magmatiques. Exemples de l'Afar et de la dorsade medioatlantique. *Soc. It. Mineral. Petrol*, **31**, 125.

Tyrrell G.W. 1909, The classification of the post - Carboniferous intrusive igneous rocks of the west of Scotland. *Trans. geol. Soc. Glasg*, **13**, 298-317.

Upton B.G.J. 1982, Carboniferous to Permian volcanism in the stable foreland. *In: Igneous rocks of the British Isles*, ed: Sutherland D.S., pp255-275. Wiley.

Upton B.G.J., Aspen P. & Chapman N.A. 1983, The upper mantle and deep crust beneath the British Isles: evidence from inclusions in volcanic rocks. *J. geol. Soc. Lond*, **140**, 105-121.

Upton B.G.J., Aspen P. & Hunter R.H. 1984, Xenoliths and their implications for the deep geology of the Midland Valley of Scotland and adjacent regions. *Trans. R. Soc. Edin*, **75**, 65-70.

Upton B.G.J., Fitton J.G. & Macintyre R.M. 1987, The Glas Eilean lavas: evidence

of a Lower Permian volcano-tectonic basin between Islay and Jura, Inner Hebrides. *Trans. R. Soc. Edin.*, **77**, 289-293.

Varne R. 1977, On the origin of spinel lherzolite inclusions in basaltic rocks from Tasmania and elsewhere. *J. Petrol.*, **18**, 1-23.

Velde B. & Kushiro I. 1978, Structure of sodium alumino-silicate melts quenched at high pressure; infrared and aluminium K-radiation data. *Earth Planet. Sci. Lett.*, **40**, 137-140.

Vidal P. & Dosso L. 1978, Core formation: catastrophic or continuous? Sr and Pb isotope geochemistry constraints. *Geophys. Res. Lett.*, **5**, 169-172.

Vinx R. & Jung D. 1977, Pargasitic-kaersutitic amphibole from a basanitic diatreme at the Rosenburg, North of Kassel (North Germany). *Contrib. Mineral. Petrol.*, **65**, 135-142.

Vollmer R. 1977, Terrestrial lead evolution and formation time of the Earth's Core. *Nature*, **270**, 144-147.

Vollmer R. 1983, Earth degassing, mantle metasomatism, and isotopic evolution of the mantle. *Geology*, **11**, 452-454.

Wagner R.H. 1966, On the presence of probable Upper Stephanian beds in Ayrshire, Scotland. *Scott. J. Geol.*, **2**, 122-123.

Wagner R.H. 1983, A lower Rotliegend flora from Ayrshire. *Scott. J. Geol.*, **19**, 135-155.

Wakita H.,Rey P. & Schmitt R.A. 1971, Abundances of the 14 rare-earth elements and 12 other trace elements in Apollo 12 samples: Five igneous and one breccia rocks and four soils. **P 2nd L S C**, pp1319-1329.

Walker B.H. 1986, *Emplacement mechanism of high-level dolerite sills and related eruptions in sedimentary basins, Fife, Scotland* Unpubl. Ph.D. thesis, Univ. Leeds.

Walker G.P.L. & Croasdale R. 1972, Characteristics of some basaltic pyroclastics. *Bull. Volcanol.*, **35**, 303-317.

Wallace M.E. & Green D.H. 1988, An experimental determination of primary carbonatite magma composition. *Nature*, **335**, 343-346.

Walsh J.N., Buckley F. & Barker J. 1981, The simultaneous determination of the rare-earth elements in rocks using inductively coupled plasma source spectrometry. *Chem. Geol.*, **33**, 141-153.

Wass S.Y. 1973, The origin and petrogenetic significance of hour-glass zoning in titaniferous clinopyroxenes. *Min. Mag.*, **39**, 133-144.

Wass S.Y. 1979, Multiple origin of clinopyroxenes in alkali basaltic rocks. *Lithos*, **12**, 115-132.

Wass S.Y. 1980, Geochemistry and origin of Xenolith-bearing and related alkali Basaltic rocks from the Southern Highlands, New South Wales, Australia. *Am. J. Sci*, **280a**, 639-666.

Wass S.Y., Henderson P. & Elliot C.J. 1980, Chemical heterogeneity and metasomatism in the upper mantle: evidence from rare earth elements in apatite-rich xenoliths n basaltic rocks from eastern Australia. *Phil. Trans. R. Soc. Lond*, **A297**, 222-246.

Wass S.Y. & Irving A. J. 1976, *XENMEG: a catalogue of occurrences of xenoliths and megacrysts in volcanic rocks of eastern Australia* 441pp Australian Museum, Sydney.

Watson E.B. 1977, Partitioning of manganese between forsterite and silicate liquid. *Geochim. Cosmochim. Acta*, **41**, 1363-1374.

Watson E.B., 1979, Calcium content of forsterite coexisting with silicate liquid in the system Na_2O-CaO-MgO-Al_2O_3-SiO_2. *Am. Mineralogist*, **64**, 824-829.

Weaver B.L., Wood D.A., Tarney J. & Joron J.L 1987, Geochemistry of ocean island basalts from the South Atlantic: Ascension, Bouvet, St. Helena, Gough and Tristan da Cunha. *In: Alkaline Igneous Rocks*, eds: Fitton J.G. & Upton B.G.J., *Geol. Soc. Spec. Publ*, **30**, 253-268. Blackwell.

White R.W. 1966, Ultramafic inclusions in basaltic rocks from Hawaii. *Contrib. Mineral. Petrol*, **12**, 245-314.

White W.M. 1985, Sources of oceanic basalts: radiogenic isotope evidence. *Geology*, **13**, 115-118.

White W.M. & Hoffmann A.W. 1982, Sr and Nd isotope geochemistry of oceanic basalts and mantle evolution. *Nature*, **296**, 821-825.

Whyte F. & Macdonald J.G. 1974, Lower Carboniferous vulcanicity in the northern part of the Clyde Plateau. *Scott. J. Geol*, **10**, 187-198.

Wilkinson J.G.F. 1974, The mineralogy and petrography of alkali basaltic rocks. *In: The Alkaline Rocks*, ed:Sorensen H., pp 67-95, John Wiley & Sons.

Wilkinson J.G.F. 1975, Ultramafic inclusions and high-pressure megacrysts from a nephelinite sill, Nandewar Mountains, north-eastern New South Wales, and their bearing on the origin of certain ultramafic inclusions in alkaline volcanic rocks. *Contrib. Mineral. Petrol*, **51**, 235-262.

Wilkinson J.F.G. 1986, Classification and average chemical compositions of common basalts and andesites. *J. Petrol*, **27**, 31-62.

Wilkinson J.F.G. & Le Maitre R.W. 1987, Upper Mantle Amphiboles and Micas and TiO_2, K_2O, and P_2O_5 abundances and 100 Mg/(Mg+Fe^{2+}) ratios of common basalts and andesites: implications for modal mantle metasomatism and

undepleted mantle compositions. *J. Petrol*, 28, 37-73.

Wilshire H.G., Nielson Pike J.E., Meyer C.E. & Schwarzman E.C. 1980, Amphibole-rich veins in lherzolite xenoliths, Dish Hill and Deadman Lake, California. *Am. J. Sci*, 280A, 576-593.

Wilson G.V. 1916, Preliminary notes on volcanic necks in north-west Ayrshire. *Trans. geol. Soc. Glasg*, **16**, 86-99.

Wilson M. 1989, *Igneous Petrogenesis: A global tectonic approach*. Unwin Hyman, London. pp466.

Witt G. & Seck H.A. 1989, Origin of amphibole in recrystallized and porphyroclastic mantle xenoliths from the Rhenish Massif: implications for the nature of mantle metasomatism. *Earth Planet. Sci. Lett*, 91, 327-340.

Yagi K. & Onuma K. 1967, The join $CaMgSi_2O_6$ - $CaTiAl_2$ and its bearing on the titanaugites. *J. Fac. Sci. Hokkaido Univ. Ser iv*, 13, 113-138.

Yoder H.S. & Tilley C.E. 1962, Origin of basaltic magmas: An experimental study of natural and synthetic rock systms. *J. Petrol*, 3, 342-532.

Ziegler P.A. 1978, North western Europe: tectonics and basement development. *Geol. Mijnbouw*, 57, 589-626.

Ziegler P.A. 1981, Evolution of sedimentary basins in north-west Europe. *In: Petroleum Geology of the Continental Shelf of North-west Europe*, eds: Illing L.V. & Hobson G.D., pp3-39, Institute of Petroleum, London.

Ziegler P.A. 1982, *Geological atlas of western and central Europe* -*-pp. Shell International Petroleum, Maatschappij. B.V.

Ziegler P.A. 1984, Caledonian and Hercynian crustal consolidation of western and central Europe - a working hypothesis. *Geol. Mijnbouw*, 63, 93-108.

Zindler A. & Hart S. 1986, Chemical geodynamics. *Ann. Rev. Earth Planet. Sci*, 14, 493-571.

Zindler A., Hart S. R. & Frey F.A. 1979, Nd and Sr isotope ratios and rare earth element abundances in Reykjanes Peninsular basalts: evidence for mantle heterogeneity beneath Iceland. *Earth Planet. Sci Lett*, 45, 249-262.

Zindler A., Jagoutz E. & Goldstein S. 1982, Nd, Sr and Pb isotopic systematics in a three-components mantle: a new perspective. *Nature*, 58, 519-523.

Zindler A., Staudigel H. & Batiza R. 1984, Isotope and trace element geochemistry of young Pacific Seamounts: implications for the scale of upper mantle heterogeneity. *Earth Planet. Sci. Lett*, 70, 175-195.

APPENDIX I

LIST OF ANALYSED SAMPLES, LITHOLOGIES AND LOCALITIES

Sample	Gp	Lithology	Grid. Ref.	Locality	Phenocrysts
SW2	5	B intrusion	NT 678793	Castle, Dunbar Harbour	ol cpx
SW3	5	B intrusion	NT 519858	Yellow Craig Plantation.	ol (cpx)
SW4A	5	BH intrusion	NT 519859	100m N. Yellow Craig Plant.	ol
SW5	5	B sill	NT 519862	Longskelly Point.	ol (cpx)
SW6	5	B sill	NT 509861	Brigs of Fidra.	ol
SW7	5	B sill	NT 495859	Cheese Bay.	ol
SW8	5	B sill	NT 513868	Fidra drift, Long Skelly rks.	ol
SW9	5	B intrusion	NO 455006	Ruddon's Point.	ol cpx
SW12	5	B dyke	NO 523013	St. Monance vent	ol (cpx)
SW19	5	B dyke	NO 514010	Coalyard Hill Vent.	ol cpx
SW20	5	B block	NO 505004	Ardross vent.	ol cpx
SW22	5	BH dyke	NO 505004	Ardross vent.	ol cpx
SW23	5	BH block	NT 498993	Elie Ness vent.	ol cpx plag
SW25	5	B sill	NT 737706	Oldham stocks.	ol cpx
SW26	5	H intrusion	NT 693785	Coast, Dunbar, 1.5 km E. of station.	ol cpx plag
SW27	5	BH sill	NT 583708	Chester's Quarry, Garvald Mains	ol cpx
SW28	5	BH intrusion	NT 507643	Kidlaw Quarry	(ol)
SW31C	5	B sill	NT 572857	The Leithies.	(ol)
SW32	5	B dyke	NT 574855	Nr. Partan Craig vent.	ol cpx plag
SW34	5	H dyke	NT 574855	Nr. Partan Craig Vent	ol cpx plag
SW36	4	H sill	NT 631814	Frances Craig Sill	ol
SW38A	5	B intrusion	NT 602847	Seacliff	ol cpx plag
SW39	5	B intrusion	NO 435049	Craig Rock Largo Law	ol cpx
SW40	5	BH intrusion	NO 427050	Trig Point Largo Law	ol cpx
SW41	5	BH intrusion	NO 428055	Largo Law	ol cpx
SW42	5	B intrusion	NO 427049	SW of Trig Point Largo Law	ol cpx
SW43	5	B intrusion	NO 427047	Largo Law	ol cpx
SW44	5	B intrusion	NO 426046	Largo Law	ol cpx
SW45	5	B intrusion	NO 432046	Largo Law	ol cpx
SW47	5	BH bomb	NO 501147	Wester Balrymonth Hill	
SW48	4	H sill	NO 460132	Drumcarrow Craig	ol
SW49	4	B sill	NO 501120	Cameron Burn	ol cpx
SW53A	5	H intrusion	NO 511101	Kinaldy vent	ol cpx
SW56	4	BH sill	NO 509099	Kinaldy sill	ol
SW57	5	B bomb	NO 521067	Kellie Law vent	ol cpx
SW59	5	B bomb	NO 521067	Kellie Law vent	ol cpx
SW66	3	B block	NS 443089	Greenhill vent Waterside	ol cpx
SW70	2	B sill	NS 443151	Craigs of Kyle	ol cpx
SW76	3	H block	NS 394099	Carclout Hill	ol cpx
SW84	2	B sill	NS 432115	Polnessan Burn (east)	ol
SW89	2	B sill	NS 459088	Corbie Craigs - Dunaskin Glen	ol cpx
SW91	2	B sill	NS 497082	Benbeoch	ol cpx
SW93	2	B sill	NS 532138	High Mount Sill	ol cpx
SW94	2	B sill	NS 536144	High Mount Sill	ol cpx
SW100	2	B sill	NS 467103	Benquhat - Kilmein sill	ol cpx
SW102	3	B block	NS 486117	Brown Rig Vent	ol (cpx)
SW103	3	B block	NS 486117	Brown Rig Vent	ol (cpx)
SW105	2	B sill	NS 533128	Tappet Hill	ol cpx
SW109	3	B block	NS 534137	Ashentree vent Carline Knowe	ol cpx
SW111	6	B dyke	NM 645773	Smearisary, 3km W Glen Uig Hotel	ol (cpx)
SW112	6	B dyke	NM 645773	Smearisary	ol (cpx)
SW113	6	B dyke	NM 645770	Smearisary	ol (cpx)
SW114	6	B dyke	NM 950858	Streap Comhlaidh	ol (cpx)
SW115	6	B dyke	NN 095848	Achnanellan Glen Loy	ol cpx
SW116	6	B dyke	NN 070849	Brian Choille	ol
SW124	3	BH lava	NS 452452	River Ayr nr.Stair east bank	ol
SW125	3	BH lava	NS 452452	River Ayr nr.Stair east bank	ol (cpx)
SW126	3	H lava	NS 452452	River Ayr nr.Stair east bank	ol
SW127	3	B lava	NS 452452	River Ayr nr.Stair east bank	ol (cpx)
SW128	3	BH lava	NS 452452	River Ayr nr.Stair east bank	ol (cpx)
SW129	3	BH lava	NS 452452	River Ayr nr.Stair east bank	ol (cpx)
SW130	3	BH lava	NS 452452	River Ayr nr.Stair east bank	ol (cpx)
SW131	3	BH lava	NS 452452	River Ayr nr.Stair east bank	ol (cpx)
SW132	3	H lava	NS 455243	Stairhill Burn	ol cpx

SW133	3	H lava	NS 455243	Stairhill Burn	ol cpx
SW134	3	BH lava	NS 455243	Stairhill Burn	ol cpx
SW135	3	H lava	NS 455243	Stairhill Burn	ol cpx
SW136	3	H lava	NS 455243	Stairhill Burn	ol cpx
SW137	3	H lava	NS 455243	Stairhill Burn	ol cpx
SW138	3	H lava	NS 455243	Stairhill Burn	ol cpx
SW139	3	BH lava	NS 455243	Stairhill Burn	ol cpx
SW140	3	H lava	NS 455243	Stairhill Burn	ol cpx
SW141	3	H lava	NS 455243	Stairhill Burn	ol cpx
SW142	3	BH lava	NS 455243	Stairhill Burn	ol cpx
SW143	3	H lava	NS 455243	Stairhill Burn	ol cpx
SW144	3	H lava	NS 455243	Stairhill Burn	ol cpx
SW145	3	BH lava	NS 452452	Stairhill Burn	ol cpx
SW146	3	B lava	NS 452242	River Ayr west bank nr. Stair	ol
SW147	3	B lava	NS 452242	River Ayr west bank nr. Stair	ol
SW148	3	BH lava	NS 452242	River Ayr west bank nr. Stair	ol (cpx)
SW149	3	B lava	NS 452242	River Ayr west bank nr. Stair	ol (cpx)
SW150	3	BH lava	NS 452242	River Ayr west bank nr. Stair	ol (cpx)
SW151	3	B lava	NS 452242	River Ayr west bank nr. Stair	ol cpx
SW152	3	BH lava	NS 452242	River Ayr west bank nr. Stair	ol
SW153	3	BH lava	NS 452242	River Ayr west bank nr. Stair	ol (cpx)
SW154	3	BH lava	NS 452242	River Ayr west bank nr. Stair	ol (cpx)
SW155	3	BH lava	NS 453243	River Ayr west bank nr. Stair	ol (cpx)
SW156	3	BH lava	NS 453243	River Ayr west bank nr. Stair	ol
SW157	3	BH lava	NS 454245	River Ayr west bank nr. Stair	ol cpx
SW158	3	BH lava	NS 454245	River Ayr west bank nr. Stair	ol cpx
SW159	3	BH lava	NS 454245	River Ayr west bank nr. Stair	ol cpx
SW160	3	BH lava	NS 454245	River Ayr west bank nr. Stair	ol
SW161A	3	BH lava	NS 454245	River Ayr west bank nr. Stair	ol
SW161B	3	BH lava	NS 454245	River Ayr west bank nr. Stair	ol
SW161C	3	BH lava	NS 453243	River Ayr west bank nr. Stair	ol
SW162	3	B lava	NS 514252	River Ayr north bank nr. Catrine	ol
SW163	3	B lava	NS 514252	River Ayr north bank nr. Catrine	ol
SW170	3	B lava	NS 514252	River Ayr north bank nr. Catrine	ol cpx
SW172	3	B lava	NS 514252	River Ayr north bank nr. Catrine	ol cpx
SW173	3	B lava	NS 519256	River Ayr east bank nr. Catrine	ol cpx
SW174	3	B lava	NS 519256	River Ayr east bank nr. Catrine	ol cpx
SW175	3	B lava	NS 519256	River Ayr east bank nr. Catrine	ol cpx
SW177	3	B lava	NS 519256	River Ayr east bank nr. Catrine	ol cpx
SW178	3	B lava	NS 519257	River Ayr east bank nr. Catrine	ol cpx
SW179	3	B lava	NS 519258	River Ayr east bank nr. Catrine	ol cpx
SW180	3	B lava	NS 514252	River Ayr south bank nr. Catrine	ol cpx
SW181	3	B lava	NS 514252	River Ayr south bank nr. Catrine	ol cpx
SW182	3	B lava	NS 514252	River Ayr south bank nr. Catrine	ol cpx
SW185	3	B lava	NS 514252	River Ayr south bank nr. Catrine	ol
SW186	3	B lava	NS 514252	River Ayr south bank nr. Catrine	ol
SW187	3	B lava	NS 514252	River Ayr south bank nr. Catrine	ol
SW188	3	B lava	NS 514252	River Ayr south bank nr. Catrine	ol
SW189	3	B lava	NS 514252	River Ayr south bank nr. Catrine	ol
SW190A	3	B lava	NS 514252	River Ayr south bank nr. Catrine	ol
SW190C	3	B lava	NS 514252	River Ayr south bank nr. Catrine	ol (cpx)
SW190D	3	B lava	NS 514252	River Ayr south bank nr. Catrine	ol (cpx)
SW190E	3	B lava	NS 514252	River Ayr south bank nr. Catrine	ol (cpx)
SW194	3	B lava	NS 498225	Lugar Water west bank	ol cpx
SW195	3	BH lava	NS 498225	Lugar Water west bank	ol cpx
SW196	3	B lava	NS 498225	Lugar Water west bank	ol cpx
SW197	3	B lava	NS 498225	Lugar Water west bank	ol cpx
SW198	3	B lava	NS 498225	Lugar Water west bank	ol cpx
SW199	3	B lava	NS 498225	Lugar Water west bank	ol cpx
SW200	3	B lava	NS 498225	Lugar Water west bank	ol cpx
SW201	3	B lava	NS 498225	Lugar Water west bank	ol cpx
SW202	3	B lava	NS 500225	Lugar Water east bank	ol (cpx)
SW204	3	B lava	NS 500225	Lugar Water east bank	ol cpx
SW206	3	B lava	NS 500225	Lugar Water east bank	ol (cpx)
SW207	3	B lava	NS 500225	Lugar Water east bank	ol cpx
SW208	3	B lava	NS 500225	Lugar Water east bank	ol cpx
SW209	3	B lava	NS 500225	Lugar Water east bank	ol cpx
SW210	3	B lava	NS 500225	Lugar Water east bank	ol cpx
SW213	3	B lava	NS 500225	Lugar Water east bank	ol cpx
SW214	3	B lava	NS 500225	Lugar Water east bank	ol cpx
SW217	3	B lava	NS 500225	Lugar Water east bank	ol

SW218	2	H sill	NS 601214	Lugar Water south bank	cpx
SW222	3	B lava	NS 456222	Trabboch Mains	ol
SW223	3	B lava	NS 456222	Trabboch Mains	ol
SW224	3	B lava	NS 456222	Trabboch Mains	ol cpx
SW226	3	B lava	NS 443252	Outmains rail cutting	ol
SW227	3	B lava	NS 443252	Outmains rail cutting	ol
SW229	3	B lava	NS 406301	East of Underhills	ol (cpx)
SW230	3	B lava	NS 409297	Quarry at Hall of Barnweill junction	ol
SW231	3	B lava	NS 406295	Monument Hill	ol (cpx)
SW232	3	B lava	NS 406295	Monument Hill	ol
SW235	1	B lava	NS 318486	Cleeves Stream	ol
SW241	1	B lava	NS 328485	Trig point near Pencot Farm	ol
SW243A	1	B lava	NS 327486	Trig point near Pencot Farm	ol
SW243B	1	B lava	NS 327486	Trig point near Pencot Farm	ol
SW246	1	B lava	NS 329494	OBO 083° Bowertrapping Farm	ol
SW247	1	B lava	NS 326492	Old Mine	ol
SW248	1	B lava	NS 332500	West Middlebank	ol
SW249	1	B lava	NS 341500	Bank Head	ol
SW250	1	B lava	NS 337499	Field cutting near road	ol
SW254	1	BH lava	NS 279459	High Smithstone Copse	ol
SW256	1	B lava	NS 277450	Lochwood Road	ol
SW261	1	BH lava	NS 383438	Annick Water	ol cpx
SW262	1	B lava	NS 383438	Annick Water	ol
SW264	1	B lava	NS 384432	Rashillhouse Quarry	ol
SW265	1	B lava	NS 379424	Annick Water, south bank	ol cpx
SW266	1	B lava	NS 381425	Annick Water, south bank	ol cpx
SW267	1	B lava	NS 382424	Annick Water	ol
SW269	1	B lava	NS 426417	Distributary - Burnfoot Reservoir	ol
SW270	1	B lava	NS 426417	Distributary - Burnfoot Reservoir	ol cpx
SW274	1	BH lava	NS 471422	Craufurdland Water	ol
SW276	1	B lava	NS 486429	Pockinan Burn	ol
SW277	1	B lava	NS 456417	Fenwick Water	ol cpx
SW280	1	B lava	NS 445409	Fenwick Water	ol cpx
SW286	3	B lava	NS 455294	Mossbog Ridge	
SW297	2	B sill	NS 348343	Hillhouse Quarry	ol
SW298	2	B sill	NS 348343	Hillhouse Quarry	ol
SW299	2	B sill	NS 353340	Hillhouse Quarry	ol
SW300	2	B sill	NS 353340	Hillhouse Quarry	ol cpx
SW301	2	B sill	NS 360328	Hillhouse Quarry	ol
SW303	3	B block	NS 373337	Broomhill Vent	ol cpx
SW304	3	B block	NS 373337	Broomhill Vent	ol cpx
SW305	2	B sill	NS 377334	Hillhouse Quarry sill Craigs Farm	ol
SW306	2	B sill	NS 372330	Road cutting	ol
SW307	1	BH lava	NS 378315	Towend nr. Symington	ol cpx plag
SW308	3	BH intrusion	NS 395345	Templeton plug	ol cpx plag
SW309	2	BH sill	NS 423328	Craigie Hill	ol cpx
SW310	2	BH sill	NS 427316	Craigie Hill sill Catcraig Quarry	ol
SW316A	3	B block	NS 418418	Bellsland Vent	ol (cpx)
SW316B	3	B block	NS 418418	Bellsland Vent	ol
SW319	3	B block	NS 418418	Bellsland Vent	ol
SW320	3	B block	NS 418418	Bellsland Vent	
SW322	3	B block	NS 418418	Bellsland Vent	
SW323	3	B block	NS 436427	Rowellan Vent	
SW324	3	B block'	NS 436427	Rowellan Vent	
SW325	3	B block	NS 436427	Rowellan Vent	
SW326	3	B block	NS 436427	Rowellan Vent	
SW330	3	B lava	NS 470205	Rail cutting Killoch Colliery	
SW331B	3	B block	NS 539267	Sorn Hill vent	
SW331C	3	B block	NS 539267	Sorn Hill vent	
SW331D	3	BH block	NS 539267	Sorn Hill vent	
SW331E	3	B block	NS 539267	Sorn Hill vent	ol
SW332A	3	H block	NS 542266	Sorn Hill vent	ol
SW332B	3	B block	NS 542266	Sorn Hill vent	ol (cpx)
SW332C	3	BH block	NS 542266	Sorn Hill vent	ol cpx
SW332D	3	B block	NS 542266	Sorn Hill vent	ol cpx
SW332E	3	H block	NS 542266	Sorn Hill vent	ol cpx
SW333	3	B block	NS 542266	Sorn Hill vent	ol
SW334	3	B block	NS 542266	Sorn Hill vent	ol (cpx)
SW335	3	B block	NS 542266	Sorn Hill vent	
SW336	3	B block	NS 470305	Little Hill (East)	ol
SW337	3	B block	NS 469306		ol

SW338	3	B block	NS 469306		ol
SW339	3	B block	NS 469306		ol
SW342	3	B block	NS 469306		ol (cpx)
SW345	3	B block	NS 426218	Raithill Vent	ol cpx
SW358	3	B intrusion	NS 227485	Blackshaw Hill	ol (cpx)
SW363B	2	BH sill	NS 242411	Ardrossan-saltcoats sill	ol cpx
SW365	3	B intrusion	NS 391305	Helenton Mains Vent	ol (cpx)
SW366	3	B intrusion	NS 391305	Helenton Mains Vent	ol
SW367	3	B block	NS 391305	Helenton Mains Vent	ol (cpx)
SW368	3	B intrusion	NS 391305	Helenton Mains Vent	plag (ol cpx)
SW369	3	B block	NS 391305	Helenton Mains Vent	ol (cpx)
SW370	3	B intrusion	NS 391305	Helenton Mains Vent	ol (cpx)
SW371	3	B intrusion	NS 404303	Heughmill Vent	ol (cpx)
SW372	3	B intrusion	NS 395228	Colvinston Vent	ol
SW374	2	BH sill	NS 377374	Craig Sill, Newhouse intrusion	ol cpx
SW376	2	B block	NS 375375	Craig Sill, Newhouse intrusion	ol cpx
SW377	3	B block	NS 342372	Shewalton Mill vent	ol
SW378	3	B block	NS 342372	Shewalton Mill vent	ol cpx
SW379	3	B block	NS 342372	Shewalton Mill vent	ol
SW380	3	B block	NS 342372	Shewalton Mill vent	ol
SW381	3	B block	NS 342372	Shewalton Mill vent	-
SW382	2	H sill	NS 364374	Capington Castle sill, Dundonald	ol
SW383	2	B sill	NS 364374	Capington Castle sill, Dundonald	ol
SW391	2	B sill	NS 469080	Benbeoch sill, Craigmark Hill	ol cpx
SW392	2	B sill	NS 473080	Benbeoch sill, Craigmark Hill	ol cpx
SW393	2	B sill	NS 476095	2km OBO 078° From Burnhead Farm	ol cpx
SW397	2	B sill	NS 545182	Knockterra Farm quarry	ol cpx
SW402	4	BH sill	NO 444131	Drumcarrow intrusion	ol
SW403	5	B intrusion	NO 443132	Ladeddie vent	ol cpx
SW404	5	B intrusion	NO 442132	Ladeddie vent	ol cpx
SW405	4	B int	NO 444132	Ladeddie vent	ol cpx
SW406	4	H sill	NO 456137	Denork Craig intrusion	ol
SW408	4	BH sill	NO 452120	Wilkieston sill	ol
SW409	4	BH sill	NO 446110	Greigston sill	ol
SW413	4	BH sill	NO 430098	Bruntshiels sill	ol
SW414	4	BH sill	NO 423090	Newbiggin of Craighall-Gathercauld	ol
SW415	4	BH sill	NO 452083	Dunicher Law, Falfield hill	ol cpx
SW416	5	B block	NO 515075	Lochty Station vent	ol cpx
SW417	5	B block	NO 515075	Lochty Station vent	ol cpx
SW420	4	B sill	NO 518076	Lochty sill	ol cpx
SW421	4	H sill	NO 496067	Lingo sill, North Baldutho	ol
SW422	4	H sill	NO 499064	South Baldutho quarry	ol
SW423	5	B intrusion	NO 512063	Gillingshill vent	ol cpx
SW424	5	B intrusion	NO 512063	Gillingshill vent	ol cpx
SW426	5	B block	NO 486078	South Cassingray vent	ol cpx
SW427	5	B block	NO 486078	South Cassingray vent	ol cpx
SW428	5	B block	NO 486078	South Cassingray vent	ol cpx
SW429	5	B block	NO 486078	South Cassingray vent	ol cpx
SW434	4	H sill	NO 437074	Gilston sill	ol cpx
SW435	5	B intrusion	NO 423064	Balhousie vent	ol cpx
SW436	5	B intrusion	NO 345036	Langside Hill Quarry	ol cpx
SW437	5	B intrusion	NO 345036	Langside Hill Quarry	ol cpx
SW438	5	BH intrusion	NO 245062	East Lomond Hill	ol cpx plag
SW439	5	B intrusion	NO 198066	West Lomond Hill	ol cpx
SW440	5	B sill	NO 222068	Greenhill	ol cpx
SW442	5	H intrusion	NO 439034	Drumelarie intrusion	ol cpx
SW443	5	B dyke	NO 457039	Rosebank dyke Rires vent	ol cpx
SW444	5	BH intrusion	NO 456042	Coates intrusion Rires vent	
SW445	5	B intrusion	NO 453047	Blinkbonny wood Rires vent	ol cpx
SW446	5	B intrusion	NO 448048	Blinkbonny ruin Rires vent	ol cpx
SW448	5	BH block	NT 464997	Kincraig vent	ol cpx
SW449	5	B dyke	NT 464997	Kincraig vent	ol cpx
SW450	5	B intrusion	NT 465996	Cave Kincraig vent	ol cpx
SW451	5	B block	NT 465996	Kincraig vent	ol cpx
SW452	5	B intrusion	NT 467998	Kincraig vent	ol cpx
SW453	5	B intrusion	NT 480992	Chapel Ness	ol cpx
SW454	5	B intrusion	NT 475996	Chapel Ness intrusion, Earlsferry Links	ol cpx
SW455	5	B intrusion	NT 475996	Chapel Ness intrusion, Earlsferry Links	ol cpx
SW456	5	B intrusion	NT 475996	Chapel Ness intrusion, Earlsferry Links	ol cpx
SW457	5	B intrusion	NT 483022	Clubhouse intrusion	ol cpx
SW458	4	B sill	NT 228907	Raith - Galliston sill	ol cpx

SW459	4	B sill	NT 243923	Raith – Galliston sill, Raith Park	ol cpx plag
SW462	4	BH sill	NT 168937	Lumphinnans Farm	ol
SW463	4	BH sill	NT 168937	Harren Hill sill	
SW465	4	BH sill	NT 149908	Cowdenbeath	ol
SW467	4	BH sill	NT 128944	Drumnagoil sill	ol
SW468	4	B sill	NT 119942	Blairenbothie sill	ol cpx
SW469	4	H sill	NT 120949	Blairenbothie sill	ol
SW470	4	B sill	NT 122955	Blairadam sill	ol
SW471	4	B sill	NT 122958	Blairadam sill	ol cpx
SW472	4	B intrusion	NT 112964	Cowden Hill vent	ol
SW473	4	H sill	NT 102953	Craigencrow sill	ol cpx
SW474	4	BH sill	NT 104944	Lochorinie sill	ol cpx
SW475	4	BH sill	NT 084925	Roscobie sill	ol cpx
SW476	4	BH sill	NT 089951	Roscobiemuir sill	ol cpx
SW477	4	B sill	NT 054955	North Lethans hill	ol cpx
SW478	4	B sill	NT 060929	Dunnygask sill	ol cpx
SW479	4	B intrusion	NT 054934	Knock Hill	ol cpx
SW480	4	B intrusion	NT 054938	OBO 354° Dunnygask farm Knock hill	ol cpx
SW482	4	B intrusion	NT 047946	Saline hills	ol
SW484	4	B intrusion	NT 044933	Easter Cairn, Saline hills	ol cpx
SW487	5	H block	NT 493995	Elie Harbour vent	ol cpx
SW488	5	H block	NT 493995	Elie Harbour vent	ol cpx
SW491	5	H block	NT 493995	Elie Harbour vent	ol cpx
SW494	5	BH block	NT 495994	Elie Ness vent	
SW496	5	H block	NT 495994	Lighthouse, Elie Ness vent	
SW498	5	B dyke	NT 499993	~30m N Ladies ower, Elie Ness	
SW505	5	B block	NO 511006	Ardross Vent	ol cpx
SW507	5	B block	NO 511006	Ardross Vent	ol cpx
SW509	5	H block	NO 511006	Ardross Vent	ol cpx
SW514	4	B sill	NT 032888	Carneil Hill	ol
SW515	4	H sill	NT 012869	High Valley Field	ol
SW517	4	H sill	NT 155761	Mons Hill	ol (cpx)
SW518	4	H sill	NT 155761	Mons Hill	ol
SW519	4	H sill	NT 148792	Mons Hill sill, Dalmeny Park	ol
SW520	4	H sill	NT 196785	Cramond Island	
SW521	4	B sill	NT 223857	Ross Point, Burntisland	
SW522	5	B intrusion	NT 239889	Stoneyhall Hill, Burntisland	ol (plag)
SW523	5	B intrusion	NT 239888	Stoneyhall Hill, Burntisland	ol (plag)
SW524	5	B intrusion	NT 218887	Orrock Quarry	ol
SW525	4	BH intrusion	NT 219889	Linhead	ol
SW526	5	B intrusion	NT 211883	Stenhouse Farm	ol cpx plag
SW527	5	B intrusion	NT 203876	Montquey intrusion	ol cpx plag
SW531	5	B intrusion	NT 222872	OBO 227° old ruin	ol
SW532	5	B intrusion	NT 233873	T.V. Station The Binns	ol
SW534	5	B intrusion	NT 211872		ol
SW535	5	B intrusion	NT 213873	Dunearn intrusion	ol cpx plag
SW536	5	B intrusion	NT 205871	Glenshee vent	
SW537	4	B sill	NT 186884	Cullaloe Sill	ol cpx
SW538	4	B sill	NT 188872	Cullaloe Reservoir sill	ol cpx
SW540	4	B sill	NT 177834	Braefoot Point	ol
SW545	4	B intrusion	NT 053786	Trig Point The Binns	ol cpx plag
SW555	3	B lava	NX 893992	Murton Loch nr. Thornhill	ol cpx
SW556B	5	H intrusion	NT 602845	Sea cliff nr. Aldhame castle	ol cpx
SW560	5	B dyke	NT 592852	Gin Head Vent	cpx
SW562	5	H dyke	NT 574854	Yellow Man vent (west of)	ol cpx plag
SW564	5	BH sill	NT 482842	Black Rocks sill	ol
SW566	4	BH sill	NT 440776	Gosford Bay	ol
SW567A	3	B dyke	NS 775113	Bridge End Cleugh	ol
SW571	4	B lava	NO 418040	Blindwell's Quarry	ol
SW572	4	B lava	NO 419038		ol
SW576	4	B sill	NT 202751	Corstorphine Hill	
SW581	4	B sill		Salisbury Crags	

Lithological abbreviations: B: basalt/basanite; BH: basaltic hawaiite; H: hawaiite.
Mineralogical abbreviations: ol: olivine; cpx: clinopyroxene; pl: plag. Parentheses indicate phenocryst present in minor amounts.
Groups: 1 Passage Group lavas; 2 Ayrshire sills; 3 Mauchline group; 4 Fife & Lothian sills; 5 Fife & Lothian basanites; 6 Highland dykes; 7 Quartz dolerites.

N.B. Details for BC and PA samples are available from the Grant Institute of Geology, Edinburgh.. AB samples can be found in Baxter (1986); MM samples in Morrison *et al.* (1986) and RM samples in Macdonald *et al.* (1981).

APPENDIX II

TABLES OF MINERAL DATA

CLINOPYROXENE

Passage Group lavas

	1	2	3	4	5	6	7	8	9
SiO2	49.71	50.30	49.09	47.96	49.45	49.65	50.52	49.13	49.22
TiO2	1.82	1.17	1.82	2.82	1.82	1.65	1.67	1.15	2.81
Al2O3	2.92	3.36	3.28	3.81	3.30	3.95	2.21	4.57	2.99
Cr2O3	0.01	0.55	0.02	0.01	0.03	0.36	nd	0.86	nd
FeO	8.62	6.89	8.34	9.38	8.52	7.76	9.07	6.78	9.91
MnO	0.19	0.19	0.16	0.21	0.18	0.18	0.22	0.15	0.24
MgO	13.62	14.87	13.62	12.24	13.71	14.14	13.52	14.57	12.22
CaO	22.08	22.03	22.11	21.92	22.25	21.56	21.90	21.12	21.91
Na2O	0.50	0.41	0.50	0.65	0.52	0.44	0.55	0.44	0.70
total=	99.47	99.77	98.94	99.00	99.78	99.69	99.66	98.77	99.60
Si	1.86	1.86	1.85	1.82	1.84	1.85	1.89	1.84	1.86
Ti	0.05	0.03	0.05	0.08	0.05	0.05	0.05	0.03	0.07
Al	0.13	0.15	0.15	0.17	0.14	0.17	0.10	0.20	0.13
Fe3	0.08	0.08	0.10	0.08	0.10	0.06	0.07	0.07	0.07
Cr	-	0.02	-	-	-	0.01	-	0.03	-
Fe2	0.19	0.14	0.17	0.21	0.16	0.18	0.22	0.14	0.24
Mg	0.76	0.82	0.76	0.69	0.76	0.78	0.75	0.81	0.69
Ca	0.89	0.87	0.89	0.89	0.89	0.86	0.88	0.85	0.89
Na	0.04	0.03	0.04	0.05	0.04	0.03	0.04	0.03	0.05
total=	4.00	4.00	4.00	4.00	4.00	4.00	4.00	4.00	4.00
oxygens=	[6]	[6]	[6]	[6]	[6]	[6]	[6]	[6]	[6]
Mg*	0.80	0.85	0.82	0.76	0.82	0.81	0.77	0.85	0.73
Al4	0.14	0.14	0.15	0.18	0.16	0.15	0.11	0.16	0.14
Al6	-0.01	0.01	-0.01	-0.01	-0.01	0.02	-0.01	0.04	-0.01

1 SW265 PR 3 SW265 G 5 SW265 G 7 SW265 PR 9 SW265 PR
2 SW265 PC 4 SW265 G 6 SW265 PC 8 SW265 PC

	10	11	12	13	14	15	16	17	18
SiO2	50.47	49.54	49.51	50.29	51.42	50.35	51.99	51.10	50.63
TiO2	1.11	1.28	1.82	1.04	1.14	1.21	1.16	0.88	0.99
Al2O3	2.90	3.35	3.26	1.88	2.28	2.96	1.57	3.07	1.43
Cr2O3	0.48	0.61	nd	0.02	0.18	0.48	0.14	0.54	nd
FeO	6.90	6.82	8.62	14.57	8.29	8.15	9.75	7.67	12.77
MnO	0.17	0.16	0.19	0.32	0.18	0.19	0.23	0.20	0.30
MgO	14.69	14.43	13.45	11.46	14.80	14.89	15.00	16.18	13.11
CaO	21.88	22.18	21.95	18.56	20.46	19.99	20.17	19.88	19.61
Na2O	0.39	0.41	0.53	0.46	0.33	0.34	0.35	0.33	0.39
total=	98.99	98.78	99.33	98.60	99.08	98.56	100.36	99.85	99.23
Si	1.88	1.85	1.86	1.94	1.93	1.89	1.93	1.88	1.92
Ti	0.03	0.04	0.05	0.03	0.03	0.03	0.03	0.02	0.03
Al	0.13	0.15	0.14	0.09	0.10	0.13	0.07	0.13	0.06
Fe3	0.05	0.08	0.08	-	-	0.02	0.03	0.06	0.06
Cr	0.01	0.02	-	-	-	0.01	-	0.02	-
Fe2	0.16	0.13	0.19	0.47	0.26	0.23	0.27	0.18	0.34
Mn	-	-	-	0.01	-	-	-	-	-
Mg	0.82	0.81	0.75	0.66	0.83	0.83	0.83	0.89	0.74
Ca	0.88	0.89	0.88	0.77	0.82	0.81	0.80	0.79	0.80
Na	0.03	0.03	0.04	0.03	0.02	0.02	0.03	0.02	0.03
total=	4.00	4.00	4.00	4.00	4.00	4.00	4.00	4.00	4.00
oxygens=	[6]	[6]	[6]	[6]	[6]	[6]	[6]	[6]	[6]
Mg*	0.83	0.86	0.79	0.58	0.76	0.78	0.75	0.83	0.68
Al4	0.12	0.15	0.14	0.06	0.07	0.11	0.07	0.12	0.08
Al6	0.01	0.00	-	0.03	0.03	0.02	0.00	0.02	-0.01

10 SW265 PC 12 SW265 PR 14 SW270 G 16 SW270 G 18 SW270 PR
11 SW265 PC 13 SW270 G 15 SW270 G 17 SW270 PC

PC: Phenocryst core PR: Phenocryst rim XC: Xenocryst core XR: Xenocryst rim
G: Groundmass

Mg*: $Mg/(Mg+Fe^{2+}+Mn)$

	19	20	21	22	23	24	25	26	27
SiO2	50.11	51.49	51.68	50.38	49.58	50.48	49.40	50.36	50.49
TiO2	1.14	0.87	0.70	1.13	0.98	1.28	1.04	1.33	1.60
Al2O3	3.89	1.69	2.53	2.07	3.78	1.69	3.86	2.20	2.48
Cr2O3	0.41	0.18	0.27	0.15	1.02	0.01	0.71	0.04	0.02
FeO	7.87	8.39	7.83	8.55	6.92	10.51	7.42	9.58	12.55
MnO	0.17	0.21	0.19	0.21	0.15	0.28	0.17	0.21	0.29
MgO	15.28	15.60	16.61	15.00	15.28	14.28	15.06	14.40	12.10
CaO	20.08	20.42	19.26	20.83	20.78	20.06	20.67	20.32	19.46
Na2O	0.39	0.30	0.36	0.33	0.36	0.36	0.40	0.36	0.43
total=	99.30	99.15	99.43	98.65	98.69	98.87	98.73	98.76	99.42
Si	1.86	1.92	1.91	1.89	1.85	1.91	1.85	1.90	1.92
Ti	0.03	0.02	0.02	0.03	0.03	0.04	0.03	0.04	0.05
Al	0.17	0.07	0.11	0.09	0.16	0.08	0.17	0.10	0.11
Fe3	0.06	0.05	0.05	0.08	0.08	0.07	0.09	0.05	-0.02
Cr	0.01	-	-	-	0.03	-	0.02	-	-
Fe2	0.19	0.21	0.19	0.19	0.18	0.27	0.15	0.25	0.41
Mg	0.84	0.87	0.92	0.84	0.85	0.80	0.84	0.81	0.69
Ca	0.80	0.82	0.76	0.84	0.83	0.81	0.83	0.82	0.79
Na	0.03	0.02	0.03	0.02	0.03	0.03	0.03	0.03	0.03
total=	4.00	4.00	4.00	4.00	4.00	4.00	4.00	4.00	4.00
oxygens=	[6]	[6]	[6]	[6]	[6]	[6]	[6]	[6]	[6]
Mg*	0.81	0.80	0.82	0.81	0.86	0.75	0.85	0.76	0.62
Al4	0.14	0.08	0.09	0.11	0.15	0.09	0.15	0.10	0.08
Al6	0.03	0.00	0.02	-0.01	0.02	-0.02	0.02	0.00	0.03

19 SW270 PC 21 SW270 PC 23 SW270 PC 25 SW270 PC 27 SW277 PR
20 SW270 PR 22 SW270 PR 24 SW270 PR 26 SW270 PR

	28	29	30	31	32	33	34	35	36
SiO2	50.16	51.31	51.47	51.56	50.48	51.48	51.91	50.89	51.39
TiO2	1.73	0.68	0.84	0.98	1.01	0.86	0.59	0.66	0.71
Al2O3	2.50	2.46	2.31	2.25	2.71	1.73	2.47	3.19	2.62
Cr2O3	0.01	0.47	0.62	0.33	0.60	0.28	0.63	0.75	0.53
FeO	11.55	7.06	7.68	7.93	7.83	8.05	7.06	6.85	7.18
MnO	0.26	0.20	0.21	0.18	0.17	0.20	0.19	0.15	0.18
MgO	13.16	16.43	15.81	15.28	15.28	15.56	16.84	16.06	16.34
CaO	19.62	20.27	20.48	21.00	20.32	20.19	19.48	19.66	19.98
Na2O	0.45	0.36	0.32	0.33	0.38	0.32	0.35	0.40	0.36
total=	99.48	99.28	99.78	99.80	98.70	98.67	99.48	98.61	99.21
Si	1.90	1.90	1.91	1.91	1.89	1.93	1.91	1.90	1.90
Ti	0.05	0.02	0.02	0.03	0.03	0.02	0.02	0.02	0.02
Al	0.11	0.11	0.10	0.10	0.12	0.08	0.11	0.18	0.11
Fe3	0.03	0.07	0.05	0.04	0.05	0.03	0.04	0.04	0.05
Cr	-	0.01	0.02	-	0.02	-	0.02	0.02	0.02
Fe2	0.33	0.15	0.19	0.21	0.20	0.22	0.18	0.18	0.17
Mg	0.74	0.91	0.87	0.84	0.85	0.87	0.93	0.89	0.90
Ca	0.79	0.80	0.81	0.83	0.82	0.81	0.77	0.78	0.79
Na	0.03	0.03	0.02	0.02	0.02	0.02	0.03	0.03	0.03
total=	4.00	4.00	4.00	4.00	4.00	4.00	4.00	4.00	4.00
oxygens=	[6]	[6]	[6]	[6]	[6]	[6]	[6]	[6]	[6]
Mg*	0.68	0.85	0.81	0.80	0.81	0.79	0.83	0.83	0.84
Al4	0.10	0.10	0.09	0.09	0.11	0.07	0.09	0.10	0.10
Al6	0.01	0.01	0.01	0.01	0.01	0.01	0.02	0.04	0.02

28 SW277 PR 30 SW277 G 32 SW277 PR 34 SW277 PC 36 SW277 PC
29 SW277 PC 31 SW277 G 33 SW277 PR 35 SW277 PR

	37	38	39	40	41	42	43	44	45
SiO2	51.58	49.36	51.60	48.87	51.27	49.56	50.52	48.87	49.85
TiO2	0.95	1.95	0.99	1.69	0.93	1.97	1.17	2.07	1.88
Al2O3	3.06	3.47	3.41	5.97	3.75	4.46	4.11	4.46	3.84
Cr2O3	0.59	0.02	0.08	0.12	0.14	0.15	0.05	0.11	nd
FeO	7.73	8.63	6.99	7.79	6.74	8.43	7.38	8.14	9.63
MnO	0.20	0.17	0.17	0.16	0.16	0.19	0.18	0.17	0.21
MgO	15.76	12.87	15.43	13.61	15.34	12.81	14.63	12.98	12.55
CaO	20.62	22.44	21.40	21.73	21.33	22.48	21.57	22.57	21.59
Na2O	0.35	0.51	0.45	0.60	0.47	0.57	0.52	0.50	0.58
total=	100.84	99.42	100.52	100.54	100.13	100.62	100.13	99.87	100.13
Si	1.89	1.85	1.89	1.80	1.88	1.84	1.86	1.82	1.86
Ti	0.03	0.06	0.03	0.05	0.03	0.05	0.03	0.06	0.05
Al	0.13	0.15	0.15	0.26	0.16	0.19	0.18	0.20	0.17
Fe3	0.05	0.07	0.05	0.09	0.05	0.06	0.07	0.07	0.08
Cr	0.02	-	-	-	-	-	-	-	-
Fe2	0.19	0.21	0.17	0.15	0.16	0.20	0.16	0.18	0.26
Mg	0.86	0.72	0.84	0.75	0.84	0.71	0.80	0.72	0.70
Ca	0.81	0.90	0.84	0.86	0.84	0.89	0.85	0.90	0.86
Na	0.02	0.04	0.03	0.04	0.03	0.04	0.04	0.04	0.04
total=	4.00	4.00	4.00	4.00	4.00	4.00	4.00	4.00	4.00
oxygens=	[6]	[6]	[6]	[6]	[6]	[6]	[6]	[6]	[6]
Mg*	0.81	0.77	0.83	0.83	0.84	0.77	0.83	0.80	0.72
Al4	0.11	0.15	0.11	0.20	0.12	0.16	0.14	0.18	0.14
Al6	0.02	0.01	0.04	0.06	0.05	0.03	0.04	0.02	0.03

37 SW277 PR 39 SW307 PC 41 SW307 PC 43 SW307 PC 45 SW307 G
38 SW307 G 40 SW307 PR 42 SW307 PR 44 SW307 PR

	46	47	48	49	50	51	52	53	54
SiO2	49.36	49.69	52.76	47.72	50.44	49.36	49.67	49.02	49.29
TiO2	1.69	1.76	0.72	2.32	1.32	1.86	2.15	2.31	1.81
Al2O3	2.91	2.62	8.69	6.97	4.74	5.59	4.26	4.49	4.58
Cr2O3	nd	0.01	0.91	0.08	0.06	0.03	0.07	0.02	0.11
FeO	8.77	9.43	5.38	8.47	7.64	10.62	8.40	8.62	8.74
MnO	0.19	0.25	0.14	0.16	0.16	0.21	0.19	0.18	0.19
MgO	13.63	12.33	12.42	12.78	14.56	11.67	13.03	12.86	12.58
CaO	21.83	22.47	16.85	21.12	21.25	20.37	22.00	22.12	21.93
Na2O	0.47	0.54	2.41	0.52	0.50	0.78	0.47	0.47	0.51
total=	98.85	99.10	100.28	100.14	100.67	100.49	100.24	100.09	99.74
Si	1.86	1.88	1.92	1.77	1.85	1.84	1.85	1.83	1.85
Ti	0.05	0.05	0.02	0.06	0.04	0.05	0.06	0.06	0.05
Al	0.13	0.12	0.37	0.31	0.20	0.25	0.19	0.20	0.20
Fe3	0.09	0.06	-0.10	0.05	0.06	0.02	0.03	0.05	0.04
Cr	-	-	0.03	-	-	-	-	-	-
Fe2	0.19	0.24	0.26	0.21	0.18	0.31	0.23	0.22	0.23
Mg	0.77	0.70	0.67	0.71	0.80	0.65	0.72	0.72	0.70
Ca	0.88	0.91	0.66	0.84	0.84	0.81	0.88	0.88	0.88
Na	0.03	0.04	0.17	0.04	0.04	0.06	0.03	0.03	0.04
total=	4.00	4.00	4.00	4.00	4.00	4.00	4.00	4.00	4.00
oxygens=	[6]	[6]	[6]	[6]	[6]	[6]	[6]	[6]	[6]
Mg*	0.80	0.74	0.71	0.77	0.81	0.67	0.75	0.76	0.74
Al4	0.14	0.12	0.08	0.23	0.15	0.16	0.15	0.17	0.15
Al6	-0.01	0.00	0.29	0.08	0.06	0.09	0.04	0.03	0.05

46 SW307 G 48 SW307 PC 50 SW307 PC 52 SW307 PC 54 SW307 PC
47 SW307 G 49 SW307 PR 51 SW307 PR 53 SW307 PR

	55
SiO2	47.93
TiO2	2.07
Al2O3	5.70
Cr2O3	0.05
FeO	8.52
MnO	0.16
MgO	12.81
CaO	22.12
Na2O	0.48
total=	99.80
Si	1.79
Ti	0.06
Al	0.25
Fe3	0.08
Fe2	0.18
Mg	0.71
Ca	0.88
Na	0.03
total=	8.00
oxygens=	[6]
Mg*	0.79
Al4	0.21
Al6	0.08

55 SW307 PR

Ayrshire sills

	56	57	58	59	60	61	62	63	64
SiO2	48.22	46.49	48.33	46.81	50.74	47.49	50.69	48.03	50.49
TiO2	1.43	3.08	1.45	2.94	0.85	2.62	0.87	2.40	0.88
Al2O3	6.58	5.94	6.42	6.34	3.83	5.72	4.13	6.06	4.23
Cr2O3	0.89	0.02	0.63	0.03	0.36	0.02	0.42	0.09	0.59
FeO	5.57	7.41	5.68	7.48	5.42	7.48	5.29	7.11	5.05
MnO	0.09	0.15	0.08	0.13	0.12	0.13	0.10	0.13	0.08
MgO	13.70	12.21	13.66	12.36	15.34	12.82	15.22	13.01	14.99
CaO	22.69	22.62	22.57	22.62	22.52	22.63	22.71	22.98	22.77
Na2O	0.47	0.69	0.42	0.58	0.38	0.56	0.38	0.53	0.41
total=	99.64	98.61	99.24	99.29	99.56	99.47	99.81	100.34	99.49
Si	1.78	1.76	1.80	1.76	1.87	1.77	1.86	1.78	1.86
Ti	0.04	0.09	0.04	0.08	0.02	0.07	0.02	0.07	0.02
Al	0.29	0.26	0.28	0.28	0.17	0.25	0.18	0.26	0.18
Fe3	0.07	0.10	0.06	0.08	0.06	0.09	0.06	0.08	0.05
Cr	0.03	-	0.02	-	0.01	-	0.01	-	0.02
Fe2	0.10	0.13	0.12	0.15	0.10	0.14	0.10	0.14	0.10
Mg	0.76	0.69	0.76	0.69	0.84	0.71	0.83	0.72	0.82
Ca	0.90	0.92	0.90	0.91	0.89	0.91	0.89	0.91	0.90
Na	0.03	0.05	0.03	0.04	0.03	0.04	0.03	0.04	0.03
total=	8.00	8.00	8.00	8.00	8.00	8.00	8.00	8.00	8.00
oxygens=	[6]	[6]	[6]	[6]	[6]	[6]	[6]	[6]	[6]
Mg*	0.88	0.83	0.86	0.82	0.89	0.83	0.89	0.84	0.89
Al4	0.22	0.24	0.20	0.24	0.13	0.23	0.14	0.22	0.14
Al6	0.07	0.02	0.08	0.04	0.04	0.03	0.04	0.04	0.05

56 SW70 PC 58 SW70 PR 60 SW70 PR 62 SW70 PR 64 SW70 PR
57 SW70 PC 59 SW70 PC 61 SW70 PC 63 SW70 PC

	65	66	67	68	69	70	71	72	73
SiO2	48.80	49.36	45.72	48.64	48.90	51.15	46.68	49.37	48.41
TiO2	2.57	1.89	3.67	1.80	1.55	1.01	3.29	1.36	2.64
Al2O3	5.07	4.57	6.77	6.09	5.55	3.52	5.99	4.99	4.57
Cr2O3	0.02	0.03	0.03	1.06	0.63	0.57	0.02	0.79	0.03
FeO	7.30	6.60	8.01	5.32	5.40	5.12	7.87	5.37	7.36
MnO	0.15	0.11	0.16	0.11	0.11	0.11	0.16	0.11	0.16
MgO	12.74	13.97	11.87	13.87	14.00	15.14	12.04	14.33	12.79
CaO	22.68	22.96	22.52	22.75	22.98	22.86	22.60	23.11	22.74
Na2O	0.65	0.45	0.61	0.45	0.39	0.37	0.65	0.39	0.63
total=	99.58	99.94	99.36	99.69	99.51	99.85	99.30	99.82	99.33
Si	1.81	1.83	1.72	1.80	1.81	1.88	1.76	1.82	1.81
Ti	0.07	0.05	0.10	0.04	0.04	0.03	0.09	0.04	0.07
Al	0.22	0.20	0.30	0.27	0.24	0.15	0.27	0.22	0.20
Fe3	0.06	0.07	0.10	0.06	0.06	0.04	0.08	0.07	0.07
Cr	-	-	-	0.03	0.02	0.02	-	0.02	-
Fe2	0.16	0.13	0.16	0.10	0.11	0.12	0.16	0.10	0.16
Mg	0.71	0.77	0.67	0.76	0.77	0.83	0.67	0.79	0.71
Ca	0.91	0.91	0.91	0.90	0.91	0.90	0.91	0.91	0.91
Na	0.05	0.03	0.04	0.03	0.03	0.03	0.05	0.03	0.05
total=	4.00	4.00	4.00	4.00	4.00	4.00	4.00	4.00	4.00
oxygens=	[6]	[6]	[6]	[6]	[6]	[6]	[6]	[6]	[6]
Mg*	0.81	0.85	0.80	0.88	0.87	0.87	0.80	0.89	0.81
Al4	0.19	0.17	0.28	0.20	0.19	0.12	0.28	0.18	0.19
Al6	0.03	0.03	0.02	0.06	0.05	0.04	0.02	0.04	0.02

65 SW70 PC 67 SW89 PC 69 SW89 PC 71 SW89 PC 73 SW89 PC
66 SW89 PR 68 SW89 PR 70 SW89 PR 72 SW89 PR

	74	75	76	77	78	79	80	81	82
SiO2	48.80	49.48	48.58	50.48	47.76	49.83	49.51	51.13	48.53
TiO2	2.50	1.80	3.00	1.67	2.84	1.51	2.45	0.93	3.08
Al2O3	5.75	5.03	8.90	4.18	6.14	4.55	4.21	4.23	5.25
Cr2O3	0.04	0.18	nd	nd	nd	0.24	nd	0.72	nd
FeO	7.29	5.66	8.00	6.25	7.25	5.51	7.65	5.17	7.87
MnO	0.14	0.10	0.16	0.10	0.13	0.11	0.16	0.10	0.16
MgO	13.27	14.82	12.67	14.89	13.16	14.99	13.34	15.80	12.73
CaO	23.16	23.44	23.13	23.47	23.10	23.58	23.27	22.84	23.07
Na2O	0.53	0.41	0.75	0.43	0.56	0.39	0.66	0.39	0.72
total=	101.48	100.92	101.15	101.47	100.94	100.71	101.25	101.31	101.41
Si	1.79	1.80	1.79	1.83	1.76	1.82	1.82	1.85	1.78
Ti	0.07	0.05	0.08	0.05	0.08	0.04	0.07	0.03	0.09
Al	0.25	0.22	0.21	0.18	0.27	0.20	0.18	0.18	0.23
Fe3	0.08	0.10	0.10	0.09	0.10	0.10	0.09	0.08	0.09
Cr	-	-	-	-	-	-	-	0.02	-
Fe2	0.14	0.07	0.15	0.10	0.12	0.06	0.14	0.08	0.16
Mg	0.72	0.81	0.70	0.81	0.72	0.82	0.73	0.85	0.70
Ca	0.91	0.92	0.91	0.91	0.91	0.92	0.92	0.89	0.91
Na	0.04	0.03	0.05	0.03	0.04	0.03	0.05	0.03	0.05
total=	4.00	4.00	4.00	4.00	4.00	4.00	4.00	4.00	4.00
oxygens=	[6]	[6]	[6]	[6]	[6]	[6]	[6]	[6]	[6]
Mg*	0.83	0.92	0.82	0.89	0.85	0.92	0.83	0.91	0.81
Al4	0.21	0.20	0.21	0.17	0.24	0.18	0.18	0.15	0.22
Al6	0.03	0.02	0.00	0.01	0.02	0.01	-	0.03	0.01

74 SW89 PR 76 SW105 PC 78 SW105 PC 80 SW105 PC 82 SW105 PC
75 SW105 G 77 SW105 PR 79 SW105 PR 81 SW105 PR

	83	84	85	86	87	88	89	90	91
SiO2	48.97	47.93	50.49	46.58	50.03	51.18	47.81	50.78	49.51
TiO2	1.31	3.03	1.46	3.53	1.60	0.97	2.73	1.06	2.02
Al2O3	6.20	5.30	3.90	6.52	3.99	3.88	6.21	3.59	5.28
Cr2O3	0.89	0.03	0.04	0.02	0.04	0.52	0.04	0.62	0.18
FeO	5.50	7.87	5.94	8.00	6.50	5.63	7.29	5.63	6.89
MnO	0.08	0.15	0.11	0.15	0.09	0.11	0.16	0.12	0.12
MgO	13.99	12.01	14.11	11.93	14.28	15.26	12.63	15.06	13.84
CaO	22.63	22.89	22.94	22.82	22.90	22.68	22.34	22.75	22.84
Na2O	0.43	0.67	0.80	0.65	0.43	0.37	0.67	0.89	0.63
K2O	nd	nd	nd	nd	nd	nd	nd	nd	0.03
total=	100.00	99.88	99.39	99.80	99.86	100.60	99.88	100.10	100.90
Si	1.80	1.80	1.88	1.74	1.85	1.87	1.78	1.87	1.81
Ti	0.04	0.09	0.04	0.10	0.04	0.03	0.08	0.03	0.06
Al	0.27	0.23	0.17	0.29	0.17	0.17	0.27	0.16	0.23
Fe3	0.05	0.04	0.02	0.07	0.07	0.05	0.06	0.07	0.08
Cr	0.03	-	-	-	-	0.02	-	0.02	-
Fe2	0.12	0.21	0.16	0.18	0.14	0.12	0.16	0.10	0.12
Mg	0.77	0.67	0.78	0.67	0.79	0.83	0.70	0.82	0.76
Ca	0.89	0.91	0.91	0.90	0.91	0.89	0.89	0.90	0.90
Na	0.03	0.05	0.03	0.05	0.03	0.03	0.05	0.03	0.04
total=	4.00	4.00	4.00	4.00	4.00	4.00	4.00	4.00	4.00
oxygens=	[6]	[6]	[6]	[6]	[6]	[6]	[6]	[6]	[6]
Mg*	0.87	0.76	0.83	0.78	0.85	0.87	0.81	0.89	0.86
Al4	0.20	0.20	0.12	0.26	0.15	0.13	0.22	0.13	0.19
Al6	0.07	0.04	0.05	0.03	0.02	0.04	0.05	0.02	0.04

83 SW105 PR 85 SW105 PR 87 SW383 PR 89 SW383 G 91 SW383 G
84 SW105 PC 86 SW105 PC 88 SW383 PC 90 SW383 G

	92	93
SiO2	49.78	47.57
TiO2	2.08	3.33
Al2O3	4.49	5.88
Cr2O3	0.01	0.02
FeO	7.17	7.50
MnO	0.14	0.13
MgO	13.66	12.52
CaO	22.87	22.51
Na2O	0.57	0.74
total=	100.77	100.20
Si	1.83	1.77
Ti	0.06	0.09
Al	0.19	0.26
Fe3	0.07	0.07
Fe2	0.15	0.16
Mg	0.75	0.69
Ca	0.90	0.90
Na	0.04	0.05
total=	4.00	4.00
oxygens=	[6]	[6]
Mg*	0.83	0.81
Al4	0.17	0.23
Al6	0.03	0.03

92 SW383 G
93 SW383 G

Mauchline group

	94	95	96	97	98	99	100	101	102
SiO2	44.36	42.30	49.14	46.68	43.77	45.46	46.67	49.15	47.32
TiO2	4.19	4.93	1.33	2.72	4.51	3.71	2.70	1.32	1.87
Al2O3	6.93	9.09	5.27	6.73	7.84	6.34	6.59	5.36	6.12
Cr2O3	nd	nd	0.16	0.12	0.01	0.01	0.12	0.17	0.28
FeO	11.54	9.72	6.34	7.69	9.92	12.20	7.66	6.23	6.71
MnO	0.22	0.15	0.12	0.11	0.17	0.23	0.10	0.12	0.11
MgO	8.96	9.67	14.05	12.04	9.93	8.73	12.11	14.02	13.36
CaO	21.96	22.02	21.94	22.70	21.96	22.25	22.53	21.85	22.71
Na2O	0.73	0.65	0.49	0.49	0.64	0.77	0.49	0.48	0.46
total=	98.89	98.53	98.84	99.28	98.75	99.70	98.97	98.70	98.94
Si	1.71	1.62	1.83	1.75	1.68	1.74	1.76	1.83	1.77
Ti	0.12	0.14	0.04	0.08	0.13	0.11	0.08	0.04	0.05
Al	0.31	0.41	0.23	0.30	0.35	0.29	0.29	0.24	0.27
Fe3	0.08	0.11	0.06	0.07	0.08	0.08	0.07	0.05	0.11
Fe2	0.29	0.21	0.14	0.17	0.24	0.31	0.17	0.14	0.10
Mg	0.51	0.55	0.78	0.67	0.57	0.50	0.68	0.78	0.74
Ca	0.91	0.91	0.88	0.91	0.90	0.91	0.91	0.87	0.91
Na	0.05	0.05	0.04	0.04	0.05	0.06	0.04	0.03	0.03
total=	4.00	4.00	4.00	4.00	4.00	4.00	4.00	4.00	4.00
oxygens=	[6]	[6]	[6]	[6]	[6]	[6]	[6]	[6]	[6]
Mg#	0.63	0.72	0.85	0.80	0.70	0.61	0.80	0.84	0.88
Al4	0.29	0.38	0.17	0.25	0.32	0.26	0.24	0.17	0.23
Al6	0.02	0.03	0.06	0.05	0.03	0.03	0.05	0.07	0.04

94 SW66 PR 96 SW66 PC 98 SW66 G 100 SW66 PR 102 SW66 G
95 SW66 PR 97 SW66 G 99 SW66 PR 101 SW66 PC

	103	104	105	106	107	108	109	110	111
SiO2	48.31	49.00	46.84	45.73	46.46	45.87	45.48	45.60	50.62
TiO2	2.13	1.35	1.89	2.65	2.08	2.61	2.35	2.20	1.90
Al2O3	4.45	5.98	7.46	7.03	7.65	7.72	8.34	8.03	3.60
Cr2O3	0.02	0.17	0.17	0.18	0.31	0.29	0.27	0.27	nd
FeO	8.18	6.33	6.67	7.91	6.78	7.32	7.30	6.99	8.71
MnO	0.17	0.12	0.11	0.14	0.12	0.12	0.14	0.13	0.18
MgO	12.89	14.04	12.85	12.60	12.67	12.16	12.35	12.52	13.24
CaO	22.66	22.30	22.44	21.99	22.55	22.71	22.31	22.60	22.61
Na2O	0.45	0.51	0.49	0.46	0.50	0.45	0.54	0.51	0.46
total=	99.26	99.80	98.92	98.69	99.12	98.85	99.08	98.85	101.32
Si	1.81	1.81	1.75	1.72	1.74	1.71	1.70	1.71	1.86
Ti	0.06	0.04	0.05	0.08	0.06	0.07	0.07	0.06	0.05
Al	0.20	0.26	0.33	0.31	0.34	0.34	0.37	0.35	0.16
Fe3	0.09	0.08	0.09	0.12	0.10	0.11	0.13	0.13	0.04
Fe2	0.17	0.12	0.11	0.13	0.11	0.12	0.10	0.09	0.23
Mg	0.72	0.77	0.72	0.71	0.71	0.68	0.69	0.70	0.73
Ca	0.91	0.88	0.90	0.89	0.90	0.92	0.89	0.91	0.89
Na	0.03	0.04	0.04	0.03	0.04	0.03	0.04	0.04	0.03
total=	4.00	4.00	4.00	4.00	4.00	4.00	4.00	4.00	4.00
oxygens=	[6]	[6]	[6]	[6]	[6]	[6]	[6]	[6]	[6]
Mg#	0.80	0.87	0.86	0.84	0.86	0.85	0.87	0.89	0.76
Al4	0.19	0.19	0.25	0.28	0.26	0.29	0.30	0.29	0.14
Al6	0.01	0.07	0.08	0.04	0.07	0.05	0.07	0.06	0.02

103 SW66 PR 105 SW66 PC 107 SW66 PC 109 SW66 PR 111 SW67 PR
104 SW66 PC 106 SW66 PR 108 SW66 PC 110 SW66 PC

	112	113	114	115	116	117	118	119	120
SiO2	48.34	48.17	50.54	49.94	50.91	48.62	50.23	49.77	49.89
TiO2	2.34	2.85	1.40	1.24	1.56	2.78	1.76	1.71	1.59
Al2O3	6.39	5.80	3.86	5.90	4.07	5.36	3.01	2.91	4.85
Cr2O3	0.19	nd	0.09	0.51	0.15	nd	nd	nd	0.17
FeO	7.71	9.26	7.37	5.87	7.24	9.54	9.34	9.20	7.13
MnO	0.13	0.26	0.15	0.12	0.15	0.20	0.21	0.20	0.13
MgO	13.13	11.73	14.74	14.71	14.20	11.83	12.79	12.73	14.12
CaO	22.41	22.21	21.98	21.95	22.28	22.13	22.54	22.74	22.43
Na2O	0.45	0.53	0.39	0.40	0.40	0.64	0.48	0.50	0.76
K2O	nd	nd	nd	nd	nd	0.03	nd	nd	nd
total=	101.09	100.81	100.52	100.64	100.96	101.13	100.36	99.76	100.67
Si	1.78	1.79	1.86	1.82	1.87	1.80	1.87	1.87	1.81
Ti	0.06	0.08	0.04	0.03	0.04	0.08	0.05	0.05	0.04
Al	0.28	0.25	0.17	0.25	0.18	0.23	0.13	0.13	0.21
Fe3	0.07	0.04	0.06	0.04	0.03	0.05	0.06	0.08	0.13
Cr	-	-	-	0.01	-	-	-	-	-
Fe2	0.17	0.25	0.16	0.14	0.20	0.25	0.24	0.21	0.09
Mg	0.72	0.65	0.81	0.80	0.78	0.65	0.71	0.71	0.77
Ca	0.88	0.89	0.87	0.86	0.88	0.88	0.90	0.91	0.88
Na	0.03	0.04	0.03	0.03	0.03	0.05	0.03	0.04	0.05
total=	4.00	4.00	4.00	4.00	4.00	4.00	4.00	4.00	4.00
oxygens=	[6]	[6]	[6]	[6]	[6]	[6]	[6]	[6]	[6]
Mg#	0.80	0.71	0.83	0.85	0.79	0.72	0.75	0.77	0.89
Al4	0.22	0.21	0.14	0.18	0.13	0.20	0.13	0.13	0.19
Al6	0.05	0.05	0.03	0.08	0.04	0.04	0.01	0.00	0.02

112 SW67 PC 114 SW67 PC 116 SW67 PC 118 SW67 G 120 SW67 PC
113 SW67 PR 115 SW67 PC 117 SW67 G 119 SW67 G

	121	122	123	124	125	126	127	128	129
SiO2	47.87	50.34	51.61	51.91	49.69	51.36	51.81	49.63	51.35
TiO2	2.40	1.28	0.88	0.72	1.22	1.06	0.77	1.23	1.05
Al2O3	6.17	5.16	3.54	2.91	4.94	2.97	2.88	4.79	7.47
Cr2O3	0.15	0.86	0.60	0.77	0.79	0.13	0.56	0.78	0.15
FeO	7.70	6.03	5.77	5.45	5.83	7.43	5.83	6.13	6.46
MnO	0.14	0.12	0.12	0.13	0.13	0.15	0.12	0.10	0.14
MgO	12.96	14.77	15.99	16.40	14.85	15.46	16.10	14.69	12.74
CaO	22.51	22.09	21.13	21.36	21.91	21.35	21.43	22.03	19.60
Na2O	0.51	0.50	0.40	0.77	0.47	0.41	0.39	0.44	1.12
K2O	nd	nd	0.01	0.05	0.01	nd	nd	nd	0.04
total=	100.81	101.15	100.05	100.47	99.84	100.32	99.89	99.82	100.12
Si	1.77	1.83	1.89	1.89	1.83	1.89	1.90	1.83	1.89
Ti	0.07	0.04	0.02	0.02	0.03	0.03	0.02	0.03	0.03
Al	0.27	0.22	0.15	0.12	0.21	0.13	0.12	0.21	0.32
Fe3	0.08	0.05	0.03	0.10	0.07	0.06	0.04	0.07	-0.08
Cr	-	0.02	0.02	0.02	0.02	-	0.02	0.02	-
Fe2	0.15	0.13	0.15	0.07	0.11	0.17	0.14	0.12	0.28
Mg	0.72	0.80	0.87	0.89	0.82	0.85	0.88	0.81	0.70
Ca	0.89	0.86	0.83	0.83	0.86	0.84	0.84	0.87	0.77
Na	0.04	0.04	0.03	0.05	0.03	0.03	0.03	0.03	0.08
total=	4.00	4.00	4.00	4.00	4.00	4.00	4.00	4.00	4.00
oxygens=	[6]	[6]	[6]	[6]	[6]	[6]	[6]	[6]	[6]
Mg#	0.82	0.86	0.85	0.92	0.88	0.83	0.86	0.87	0.71
Al4	0.23	0.17	0.11	0.11	0.17	0.11	0.10	0.17	0.11
Al6	0.04	0.05	0.05	0.01	0.05	0.02	0.03	0.04	0.21

121 SW67 PC 123 SW159 PC 125 SW159 PR 127 SW159 PR 129 SW159 G
122 SW159 PC 124 SW159 PC 126 SW159 PR 128 SW159 PC

	130	131	132	133	134	135	136	137	138
SiO2	51.64	50.85	48.59	48.42	48.93	50.57	49.15	47.25	48.16
TiO2	0.74	0.85	1.16	1.23	1.11	0.63	1.10	1.49	2.05
Al2O3	2.98	3.50	4.93	4.90	4.39	3.76	4.77	6.10	5.22
Cr2O3	0.50	0.67	0.94	0.67	0.76	0.14	0.85	0.88	0.13
FeO	5.89	5.88	5.91	6.09	5.97	8.05	5.97	5.69	7.05
MnO	0.15	0.15	0.15	0.14	0.14	0.24	0.13	0.10	0.13
MgO	16.32	16.21	15.04	15.47	15.25	14.51	15.31	13.79	13.49
CaO	21.33	21.71	21.83	21.59	22.01	19.88	21.92	22.94	22.94
Na2O	0.42	0.43	0.50	0.45	0.44	0.98	0.49	0.41	0.45
K2O	nd	nd	nd	nd	nd	nd	nd	0.01	nd
total=	99.97	100.25	99.05	98.96	99.00	98.76	99.69	98.66	99.62
Si	1.89	1.86	1.80	1.79	1.82	1.88	1.81	1.77	1.79
Ti	0.02	0.02	0.03	0.03	0.03	0.02	0.03	0.04	0.06
Al	0.13	0.15	0.22	0.21	0.19	0.17	0.21	0.27	0.23
Fe3	0.06	0.10	0.12	0.14	0.12	0.10	0.12	0.12	0.10
Cr	0.01	0.02	0.03	0.02	0.02	-	0.02	0.03	-
Fe2	0.12	0.08	0.06	0.05	0.06	0.15	0.06	0.06	0.12
Mg	0.89	0.88	0.83	0.85	0.84	0.81	0.84	0.77	0.75
Ca	0.84	0.85	0.87	0.86	0.87	0.79	0.86	0.92	0.91
Na	0.03	0.03	0.04	0.03	0.03	0.07	0.03	0.03	0.03
total=	4.00	4.00	4.00	4.00	4.00	4.00	4.00	4.00	4.00
oxygens=	[6]	[6]	[6]	[6]	[6]	[6]	[6]	[6]	[6]
Mg*	0.88	0.91	0.93	0.94	0.93	0.83	0.93	0.93	0.86
Al4	0.11	0.14	0.20	0.21	0.18	0.12	0.19	0.23	0.21
Al6	0.02	0.01	0.02	0.01	0.01	0.05	0.02	0.03	0.02

130 SW159 G 132 SW159 PR 134 SW159 PR 136 SW159 PR 138 SW173 PR
131 SW159 PC 133 SW159 PC 135 SW159 PC 137 SW173 PC

	139	140	141	142	143	144	145	146	147
SiO2	47.86	50.06	48.41	47.77	49.38	48.72	47.16	48.78	50.61
TiO2	1.48	1.13	1.30	1.41	1.09	2.39	2.74	3.94	1.33
Al2O3	6.14	4.70	6.09	6.42	4.13	4.53	6.35	7.34	3.79
Cr2O3	0.80	0.68	0.81	0.85	0.20	0.02	0.02	0.02	0.25
FeO	5.69	5.72	5.78	5.78	5.98	8.83	8.31	9.61	6.63
MnO	0.11	0.11	0.11	0.08	0.11	0.19	0.14	0.15	0.13
MgO	14.13	14.67	13.94	14.01	15.25	12.67	12.14	10.91	14.62
CaO	22.82	22.53	22.59	22.55	22.22	22.35	22.42	22.27	22.60
Na2O	0.42	0.40	0.44	0.43	0.32	0.54	0.58	0.66	0.38
K2O	nd	nd	0.02	nd	nd	0.01	nd	nd	nd
total=	99.45	100.00	99.49	99.30	98.68	100.25	99.86	99.68	100.34
Si	1.77	1.84	1.79	1.77	1.84	1.82	1.76	1.69	1.86
Ti	0.04	0.03	0.04	0.04	0.03	0.07	0.08	0.11	0.04
Al	0.27	0.20	0.27	0.28	0.18	0.20	0.28	0.33	0.16
Fe3	0.11	0.06	0.08	0.10	0.10	0.07	0.08	0.12	0.06
Cr	0.02	0.02	0.02	0.02	-	-	-	-	-
Fe2	0.06	0.12	0.09	0.08	0.09	0.20	0.18	0.19	0.15
Mg	0.78	0.81	0.77	0.77	0.85	0.70	0.68	0.61	0.80
Ca	0.91	0.89	0.90	0.90	0.89	0.89	0.90	0.90	0.89
Na	0.03	0.03	0.03	0.03	0.02	0.04	0.04	0.05	0.03
total=	4.00	4.00	4.00	4.00	4.00	4.00	4.00	4.00	4.00
oxygens=	[6]	[6]	[6]	[6]	[6]	[6]	[6]	[6]	[6]
Mg*	0.92	0.87	0.89	0.91	0.90	0.77	0.79	0.76	0.84
Al4	0.23	0.16	0.21	0.23	0.16	0.18	0.24	0.31	0.14
Al6	0.04	0.05	0.06	0.05	0.02	0.02	0.04	0.02	0.03

139 SW173 PC 141 SW173 PC 143 SW173 PC 145 SW173 PC 147 SW173 G
140 SW173 PC 142 SW173 PC 144 SW173 PR 146 SW173 PR

	148	149	150	151	152	153	154	155	156
SiO2	49.79	50.32	49.56	46.18	48.06	45.30	49.08	48.23	48.86
TiO2	1.74	1.56	1.20	2.17	1.37	4.09	1.06	2.25	1.27
Al2O3	4.06	4.00	5.03	6.45	6.84	6.59	4.63	4.57	6.17
Cr2O3	0.02	0.05	0.87	0.35	0.51	0.02	0.62	0.02	0.68
FeO	7.50	7.03	5.54	6.86	5.67	11.35	5.51	8.46	5.66
MnO	0.14	0.13	0.09	0.14	0.11	0.27	0.11	0.18	0.11
MgO	13.96	14.29	14.95	13.38	14.35	9.75	15.21	13.13	14.41
CaO	22.90	22.96	23.06	22.88	22.61	21.98	22.95	23.04	21.95
Na2O	0.48	0.45	0.36	0.42	0.48	0.79	0.36	0.52	0.43
K2O	0.01	0.02	nd	nd	nd	nd	nd	nd	0.04
total=	100.60	100.81	100.66	98.79	100.00	100.14	99.53	100.40	99.58
Si	1.83	1.85	1.81	1.73	1.76	1.72	1.81	1.79	1.80
Ti	0.05	0.04	0.03	0.06	0.04	0.12	0.03	0.06	0.04
Al	0.18	0.17	0.22	0.28	0.30	0.29	0.20	0.20	0.27
Fe3	0.09	0.08	0.10	0.16	0.12	0.09	0.13	0.13	0.07
Cr	-	-	0.03	0.01	0.01	-	0.02	-	0.02
Fe2	0.14	0.14	0.07	0.06	0.06	0.27	0.04	0.13	0.11
Mg	0.77	0.78	0.81	0.75	0.79	0.55	0.84	0.73	0.79
Ca	0.90	0.90	0.90	0.92	0.89	0.89	0.91	0.92	0.87
Na	0.03	0.03	0.03	0.03	0.03	0.06	0.03	0.04	0.03
total=	4.00	4.00	4.00	4.00	4.00	4.00	4.00	4.00	4.00
oxygens=	[6]	[6]	[6]	[6]	[6]	[6]	[6]	[6]	[6]
Mg*	0.84	0.85	0.91	0.92	0.93	0.67	0.95	0.84	0.88
Al4	0.17	0.15	0.19	0.27	0.24	0.28	0.19	0.21	0.20
Al6	0.01	0.02	0.03	0.01	0.06	0.01	0.01	-0.01	0.07

148 SW173 G 150 SW173 PC 152 SW173 PC 154 SW173 PC 156 SW179 PC
149 SW173 G 151 SW173 PR 153 SW173 PR 155 SW173 PR

	157	158	159	160	161	162	163	164	165
SiO2	50.58	48.76	48.50	48.87	46.84	48.70	53.76	49.24	49.50
TiO2	0.96	1.29	2.35	1.21	3.04	0.98	0.20	1.39	1.28
Al2O3	4.95	5.83	4.85	6.49	6.76	6.45	0.23	6.20	6.57
Cr2O3	0.77	0.83	0.01	0.98	0.03	1.23	nd	0.76	0.98
FeO	5.27	5.63	9.02	5.42	8.89	5.13	6.86	5.94	5.56
MnO	0.10	0.09	0.16	0.10	0.16	0.10	0.16	0.12	0.11
MgO	14.88	14.17	12.38	13.95	11.60	14.36	15.53	13.88	14.15
CaO	22.50	22.83	22.82	22.12	22.62	21.68	22.41	22.35	22.15
Na2O	0.52	0.43	0.55	0.53	0.59	0.64	0.40	0.42	0.54
K2O	0.03	nd	0.02	0.01	0.02	0.01	0.02	0.03	0.01
total=	100.56	99.86	99.86	99.68	100.55	99.28	99.57	100.33	100.85
Si	1.85	1.80	1.82	1.80	1.74	1.80	1.99	1.81	1.81
Ti	0.03	0.04	0.07	0.03	0.09	0.03	-	0.04	0.04
Al	0.21	0.25	0.20	0.28	0.30	0.28	0.01	0.27	0.28
Fe3	0.06	0.08	0.08	0.05	0.09	0.08	0.03	0.04	0.04
Cr	0.02	0.02	-	0.03	-	0.04	-	0.02	0.03
Fe2	0.10	0.09	0.21	0.12	0.19	0.08	0.19	0.14	0.13
Mg	0.81	0.78	0.69	0.77	0.64	0.79	0.86	0.76	0.77
Ca	0.88	0.90	0.90	0.87	0.90	0.86	0.89	0.88	0.87
Na	0.04	0.03	0.04	0.04	0.04	0.05	0.03	0.03	0.04
total=	4.00	4.00	4.00	4.00	4.00	4.00	4.00	4.00	4.00
oxygens=	[6]	[6]	[6]	[6]	[6]	[6]	[6]	[6]	[6]
Mg*	0.88	0.89	0.77	0.87	0.77	0.90	0.82	0.84	0.86
Al4	0.15	0.20	0.18	0.20	0.26	0.20	0.01	0.19	0.19
Al6	0.06	0.05	0.01	0.09	0.04	0.08	-	0.08	0.09

157 SW179 PC 159 SW179 PR 161 SW179 PR 163 SW179 G 165 SW179 PC
158 SW179 PC 160 SW179 PC 162 SW179 PC 164 SW179 G

	166	167	168	169	170	171	172	173	174
SiO2	46.52	48.65	50.67	47.59	50.39	47.23	44.68	46.69	48.16
TiO2	3.07	1.99	1.36	2.35	1.68	1.41	3.94	1.59	2.30
Al2O3	7.28	5.11	3.47	6.09	3.79	6.26	6.98	7.49	3.87
Cr2O3	0.01	0.12	0.17	0.13	0.03	0.78	0.01	0.61	0.01
FeO	8.86	7.21	6.59	7.40	7.40	5.91	10.23	6.09	9.95
MnO	0.16	0.14	0.12	0.13	0.15	0.12	0.19	0.13	0.22
MgO	11.45	13.19	14.28	12.63	13.58	14.36	10.70	14.01	12.09
CaO	21.81	22.66	22.48	22.61	22.67	23.02	21.90	21.99	22.32
Na2O	0.59	0.45	0.38	0.47	0.44	0.43	0.67	0.46	0.53
K2O	0.03	0.01	0.01	0.02	0.02	nd	nd	nd	nd
total=	99.78	99.53	99.53	99.42	100.15	99.52	99.30	99.06	99.45
Si	1.75	1.81	1.88	1.78	1.87	1.75	1.70	1.73	1.82
Ti	0.09	0.06	0.04	0.07	0.05	0.04	0.11	0.04	0.07
Al	0.32	0.22	0.15	0.27	0.17	0.27	0.31	0.33	0.17
Fe3	0.06	0.06	0.03	0.07	0.04	0.17	0.12	0.13	0.10
Cr	-	-	-	-	-	0.02	-	0.02	-
Fe2	0.22	0.16	0.18	0.16	0.19	0.02	0.21	0.06	0.22
Mg	0.64	0.73	0.79	0.70	0.75	0.79	0.61	0.78	0.68
Ca	0.88	0.91	0.89	0.91	0.90	0.91	0.89	0.87	0.90
Na	0.04	0.03	0.03	0.03	0.03	0.03	0.05	0.03	0.04
total=	4.00	4.00	4.00	4.00	4.00	4.00	4.00	4.00	4.00
oxygens=	[6]	[6]	[6]	[6]	[6]	[6]	[6]	[6]	[6]
Mg#	0.74	0.82	0.82	0.81	0.79	0.97	0.74	0.93	0.75
Al4	0.25	0.19	0.12	0.22	0.13	0.25	0.30	0.27	0.18
Al6	0.07	0.04	0.03	0.05	0.03	0.02	0.01	0.06	-0.01

166 SW179 PR 168 SW179 G 170 SW179 G 172 SW179 PR 174 SW179 PR
167 SW179 G 169 SW179 G 171 SW179 PC 173 SW179 PC

	175	176	177	178	179
SiO2	47.43	48.30	45.56	46.72	47.15
TiO2	2.12	1.07	2.52	1.49	1.56
Al2O3	5.97	6.76	7.63	8.61	8.81
Cr2O3	0.05	0.06	0.02	0.02	0.01
FeO	7.76	7.71	8.58	7.33	7.61
MnO	0.17	0.07	0.16	0.16	0.16
MgO	12.77	12.16	11.60	12.18	11.79
CaO	22.74	21.22	22.60	21.08	21.02
Na2O	0.60	1.50	0.55	1.36	1.48
total=	99.61	98.85	99.22	98.91	99.59
Si	1.77	1.80	1.71	1.74	1.74
Ti	0.06	0.03	0.07	0.04	0.04
Al	0.26	0.30	0.34	0.38	0.38
Fe3	0.12	0.15	0.13	0.16	0.15
Fe2	0.12	0.09	0.14	0.07	0.09
Mg	0.71	0.68	0.65	0.67	0.65
Ca	0.91	0.85	0.91	0.84	0.83
Na	0.04	0.11	0.04	0.10	0.11
total=	4.00	4.00	4.00	4.00	4.00
oxygens=	[6]	[6]	[6]	[6]	[6]
Mg#	0.85	0.88	0.82	0.91	0.88
Al4	0.23	0.20	0.29	0.26	0.26
Al6	0.03	0.10	0.05	0.11	0.13

175 PA01 PC 177 PA01 PR 179 PA01 XC
176 PA02 PC 178 PA01 XC

Fife & Lothian sills

	180	181	182	183	184	185	186	187	188
SiO2	50.55	50.87	50.53	51.43	50.95	49.57	48.95	50.72	48.83
TiO2	1.40	1.35	1.46	1.08	1.03	1.52	1.88	1.08	2.02
Al2O3	2.92	1.81	2.78	1.72	1.45	3.82	3.77	1.91	4.10
Cr2O3	0.08	nd	0.02	0.03	0.01	0.07	0.03	0.02	0.04
FeO	8.04	10.21	8.46	8.28	13.10	7.54	8.68	8.11	7.94
MnO	0.19	0.23	0.18	0.20	0.33	0.18	0.19	0.20	0.19
MgO	14.86	14.05	14.84	15.46	12.45	14.80	14.24	15.78	14.47
CaO	21.08	20.70	21.16	21.07	20.30	21.28	21.11	20.44	21.20
Na2O	0.37	0.41	0.40	0.35	0.42	0.37	0.39	0.29	0.39
K2O	nd	nd	nd	nd	0.02	0.01	nd	0.01	0.01
total=	99.49	99.63	99.83	99.58	100.06	99.16	99.24	98.56	98.79
Si	1.88	1.91	1.88	1.91	1.93	1.85	1.83	1.90	1.82
Ti	0.04	0.04	0.04	0.03	0.03	0.04	0.05	0.03	0.06
Al	0.13	0.08	0.12	0.08	0.06	0.17	0.17	0.08	0.18
Fe3	0.05	0.06	0.07	0.07	0.06	0.08	0.09	0.07	0.10
Fe2	0.20	0.26	0.19	0.19	0.36	0.16	0.18	0.18	0.15
Mn	-	-	-	-	0.01	-	-	-	-
Mg	0.82	0.79	0.82	0.86	0.70	0.82	0.79	0.88	0.81
Ca	0.84	0.83	0.84	0.84	0.82	0.85	0.85	0.82	0.85
Na	0.03	0.03	0.03	0.03	0.03	0.03	0.03	0.02	0.03
total=	4.00	4.00	4.00	4.00	4.00	4.00	4.00	4.00	4.00
oxygens=	[6]	[6]	[6]	[6]	[6]	[6]	[6]	[6]	[6]
Mg*	0.80	0.78	0.81	0.81	0.66	0.83	0.81	0.83	0.84
Al4	0.12	0.09	0.12	0.09	0.07	0.15	0.17	0.10	0.18
Al6	0.01	-0.01	0.00	-0.01	-0.01	0.02	0.00	-0.02	0.00

180 SW48 G 182 SW48 G 184 SW48 G 186 SW49 G 188 SW49 G
181 SW48 G 183 SW48 G 185 SW49 G 187 SW49 G

	189	190	191	192	193	194	195	196	197
SiO2	51.40	50.28	50.47	50.58	50.00	49.61	50.81	51.35	51.43
TiO2	1.03	1.45	1.25	1.42	1.56	1.77	1.29	0.98	0.98
Al2O3	2.18	2.42	3.65	3.32	3.10	3.14	2.26	2.38	2.35
Cr2O3	0.14	0.07	0.87	0.31	0.11	0.02	0.02	0.26	0.26
FeO	6.69	7.59	6.24	6.69	7.25	8.38	8.15	6.31	6.43
MnO	0.16	0.17	0.14	0.15	0.14	0.21	0.21	0.16	0.17
MgO	15.69	14.83	15.23	15.23	14.92	14.40	15.17	16.29	16.17
CaO	21.52	21.53	21.73	22.06	21.78	21.83	22.13	22.22	22.07
Na2O	0.14	0.18	0.16	0.16	0.17	0.48	0.43	0.34	0.33
total=	98.95	98.52	99.74	99.92	99.03	99.84	100.47	100.29	100.19
Si	1.92	1.89	1.87	1.87	1.87	1.84	1.87	1.88	1.89
Ti	0.03	0.04	0.03	0.04	0.04	0.05	0.04	0.03	0.03
Al	0.10	0.11	0.16	0.14	0.14	0.14	0.10	0.10	0.10
Fe3	0.02	0.04	0.02	0.04	0.05	0.11	0.12	0.10	0.09
Cr	-	-	0.03	-	-	-	-	-	-
Fe2	0.19	0.20	0.17	0.17	0.18	0.15	0.13	0.09	0.11
Mg	0.87	0.83	0.84	0.84	0.83	0.80	0.83	0.89	0.88
Ca	0.86	0.87	0.86	0.87	0.87	0.87	0.87	0.87	0.87
Na	0.01	0.01	0.01	0.01	0.01	0.03	0.03	0.02	0.02
total=	4.00	4.00	4.00	4.00	4.00	4.00	4.00	4.00	4.00
oxygens=	[6]	[6]	[6]	[6]	[6]	[6]	[6]	[6]	[6]
Mg*	0.82	0.80	0.83	0.83	0.82	0.84	0.86	0.90	0.88
Al4	0.08	0.11	0.13	0.13	0.13	0.16	0.13	0.12	0.11
Al6	0.01	-	0.03	0.02	0.01	-0.02	-0.03	-0.02	-0.01

189 SW56 G 191 SW56 G 193 SW56 G 195 SW56 G 197 SW56 G
190 SW56 G 192 SW56 G 194 SW56 G 196 SW56 G

	198	199	200	201	202	203	204	205	206
SiO2	48.38	50.59	47.88	50.46	51.07	50.44	50.56	48.23	48.93
TiO2	2.40	1.34	2.88	1.44	1.53	1.30	1.49	2.36	2.18
Al2O3	3.09	2.06	3.49	1.98	1.15	2.00	1.82	5.02	5.16
Cr2O3	nd	nd	nd	nd	nd	nd	nd	0.13	0.02
FeO	9.00	7.08	9.23	7.70	9.07	7.04	7.60	7.74	7.68
MnO	0.19	0.17	0.20	0.15	0.21	0.14	0.15	0.14	0.16
MgO	12.66	14.50	12.05	14.35	13.45	14.73	14.19	13.86	13.88
CaO	21.95	22.58	22.17	22.09	22.04	22.47	22.27	22.77	22.65
Na2O	0.63	0.47	0.68	0.49	0.58	0.46	0.45	0.41	0.49
K2O	0.01	nd	nd	nd	nd	0.01	0.01	0.03	0.02
total=	98.31	98.79	98.58	98.62	99.06	98.59	98.54	100.69	101.17
Si	1.84	1.89	1.82	1.90	1.93	1.89	1.90	1.78	1.79
Ti	0.07	0.04	0.08	0.04	0.04	0.04	0.04	0.07	0.06
Al	0.16	0.09	0.16	0.09	0.05	0.09	0.08	0.22	0.22
Fe3	0.09	0.08	0.08	0.07	0.05	0.09	0.06	0.12	0.11
Fe2	0.20	0.14	0.21	0.17	0.24	0.13	0.18	0.12	0.13
Mg	0.72	0.81	0.68	0.80	0.76	0.82	0.80	0.76	0.76
Ca	0.89	0.91	0.90	0.89	0.89	0.90	0.90	0.90	0.89
Na	0.05	0.03	0.05	0.04	0.04	0.03	0.03	0.03	0.03
total=	4.00	4.00	4.00	4.00	4.00	4.00	4.00	4.00	4.00
oxygens=	[6]	[6]	[6]	[6]	[6]	[6]	[6]	[6]	[6]
Mg*	0.78	0.84	0.76	0.82	0.76	0.86	0.81	0.86	0.85
Al8	0.16	0.11	0.18	0.10	0.07	0.11	0.10	0.22	0.21
Al6	-0.02	-0.01	-0.02	-0.02	-0.02	-0.02	-0.02	0.00	0.02

198 SW415 PR 200 SW415 PR 202 SW415 G 204 SW415 G 206 SW472 PR
199 SW415 PC 201 SW415 PC 203 SW415 G 205 SW472 PC

	207	208	209	210	211	212	213	214	215
SiO2	50.44	50.62	50.78	50.49	50.68	51.04	50.56	51.35	51.54
TiO2	1.20	0.96	1.04	1.16	1.14	0.89	1.14	1.38	1.56
Al2O3	2.27	3.09	2.51	2.44	2.63	2.50	2.58	3.66	3.08
Cr2O3	0.01	0.43	0.06	0.02	0.04	0.12	0.04	0.17	nd
FeO	13.04	8.50	9.94	11.00	10.37	9.16	10.74	6.42	7.92
MnO	0.34	0.21	0.25	0.21	0.21	0.20	0.21	0.12	0.17
MgO	13.78	15.35	14.38	14.23	14.78	15.28	14.71	14.82	14.26
CaO	18.23	20.25	20.46	20.33	20.68	20.97	20.62	22.82	22.46
Na2O	0.38	0.36	0.36	0.34	0.35	0.33	0.36	0.38	0.44
total=	99.69	99.77	99.78	100.22	100.88	100.49	100.96	101.12	101.43
Si	1.90	1.88	1.90	1.88	1.87	1.88	1.87	1.87	1.89
Ti	0.03	0.03	0.03	0.03	0.03	0.02	0.03	0.04	0.04
Al	0.10	0.14	0.11	0.11	0.11	0.11	0.11	0.16	0.13
Fe3	0.05	0.07	0.06	0.09	0.11	0.10	0.12	0.04	0.04
Cr	-	0.01	-	-	-	-	-	-	-
Fe2	0.36	0.19	0.25	0.26	0.21	0.19	0.22	0.16	0.20
Mn	0.01	-	-	-	-	-	-	-	-
Mg	0.77	0.85	0.80	0.79	0.81	0.84	0.81	0.81	0.78
Ca	0.74	0.80	0.82	0.81	0.82	0.83	0.82	0.89	0.88
Na	0.03	0.03	0.03	0.02	0.03	0.02	0.03	0.03	0.03
total=	4.00	4.00	4.00	4.00	4.00	4.00	4.00	4.00	4.00
oxygens=	[6]	[6]	[6]	[6]	[6]	[6]	[6]	[6]	[6]
Mg*	0.68	0.81	0.76	0.75	0.79	0.81	0.79	0.83	0.79
Al8	0.10	0.12	0.10	0.12	0.13	0.12	0.13	0.13	0.11
Al6	0.00	0.01	0.01	-0.01	-0.02	-0.01	-0.02	0.03	0.02

207 SW521 PC 209 SW521 G 211 SW521 G 213 SW521 G 215 SW538 G
208 SW521 G 210 SW521 G 212 SW521 G 214 SW538 G

	216	217	218	219	220	221	222	223	224
SiO2	49.10	51.07	49.29	50.21	49.77	48.41	50.19	46.32	47.24
TiO2	2.26	1.57	2.23	1.63	2.13	1.91	1.61	2.73	2.16
Al2O3	5.23	3.12	4.35	4.76	4.96	5.10	3.17	7.41	5.92
Cr2O3	0.04	0.01	0.01	0.51	nd	0.22	nd	nd	0.10
FeO	7.66	7.98	9.22	6.40	7.66	6.76	10.11	7.20	7.32
MnO	0.14	0.19	0.21	0.14	0.14	0.13	0.27	0.13	0.13
MgO	13.68	14.23	12.89	14.39	13.72	14.18	13.15	13.06	13.59
CaO	22.43	22.54	21.48	22.59	22.59	23.00	21.94	21.64	22.29
Na2O	0.46	0.48	0.55	0.38	0.44	0.38	0.57	0.68	0.55
K2O	nd	nd	nd	nd	nd	nd	nd	0.01	nd
total=	101.00	101.19	100.23	101.01	101.41	100.09	101.01	99.18	99.30
Si	1.80	1.87	1.84	1.84	1.82	1.79	1.86	1.73	1.76
Ti	0.06	0.04	0.06	0.04	0.06	0.05	0.04	0.08	0.06
Al	0.23	0.13	0.19	0.21	0.21	0.22	0.14	0.33	0.26
Fe3	0.07	0.07	0.05	0.04	0.06	0.12	0.10	0.11	0.14
Cr	-	-	-	0.01	-	-	-	-	-
Fe2	0.16	0.18	0.24	0.15	0.18	0.09	0.22	0.11	0.09
Mg	0.75	0.78	0.72	0.78	0.75	0.78	0.73	0.73	0.75
Ca	0.88	0.89	0.86	0.89	0.89	0.91	0.87	0.86	0.89
Na	0.03	0.03	0.04	0.03	0.03	0.03	0.04	0.05	0.04
total=	4.00	4.00	4.00	4.00	4.00	4.00	4.00	4.00	4.00
oxygens=	[6]	[6]	[6]	[6]	[6]	[6]	[6]	[6]	[6]
Mg*	0.82	0.81	0.74	0.83	0.80	0.89	0.76	0.86	0.89
Al4	0.20	0.13	0.16	0.16	0.18	0.21	0.14	0.27	0.24
Al6	0.03	0.01	0.03	0.04	0.04	0.01	0.00	0.05	0.02

216 SW538 G 218 SW538 G 220 SW538 G 222 SW538 G 224 SW545 PC
217 SW538 G 219 SW538 G 221 SW538 G 223 SW545 PR

	225	226	227	228	229	230	231	232	233
SiO2	47.09	45.18	46.41	48.59	49.12	47.57	46.69	46.50	48.59
TiO2	2.30	3.23	2.42	1.97	2.14	1.96	2.48	2.49	1.85
Al2O3	6.84	7.78	7.10	5.59	5.15	5.90	7.11	7.20	6.47
Cr2O3	0.57	0.16	0.52	0.34	0.17	0.50	0.05	0.06	0.48
FeO	7.06	7.62	6.94	7.07	7.21	7.00	8.11	8.04	6.84
MnO	0.13	0.13	0.12	0.15	0.12	0.14	0.17	0.14	0.14
MgO	13.37	12.48	13.48	14.05	14.10	14.08	12.88	12.98	14.60
CaO	21.63	22.08	21.66	21.83	22.23	21.19	21.42	21.35	20.86
Na2O	0.64	0.57	0.64	0.63	0.47	0.67	0.69	0.70	0.65
K2O	0.01	0.02	nd	nd	0.01	nd	0.01	nd	nd
total=	99.64	99.25	99.29	100.22	100.72	99.01	99.61	99.46	100.48
Si	1.75	1.69	1.73	1.79	1.81	1.77	1.74	1.73	1.78
Ti	0.06	0.09	0.07	0.05	0.06	0.05	0.07	0.07	0.05
Al	0.30	0.34	0.31	0.24	0.22	0.26	0.31	0.32	0.28
Fe3	0.10	0.13	0.13	0.10	0.08	0.12	0.12	0.13	0.09
Cr	0.02	-	0.02	-	-	0.01	-	-	0.01
Fe2	0.12	0.11	0.09	0.12	0.15	0.10	0.13	0.12	0.12
Mg	0.74	0.70	0.75	0.77	0.77	0.78	0.72	0.72	0.80
Ca	0.86	0.89	0.86	0.86	0.88	0.85	0.85	0.85	0.82
Na	0.05	0.04	0.05	0.05	0.03	0.05	0.05	0.05	0.05
total=	4.00	4.00	4.00	4.00	4.00	4.00	4.00	4.00	4.00
oxygens=	[6]	[6]	[6]	[6]	[6]	[6]	[6]	[6]	[6]
Mg*	0.86	0.86	0.89	0.86	0.84	0.88	0.84	0.85	0.87
Al4	0.25	0.31	0.27	0.21	0.19	0.23	0.26	0.27	0.22
Al6	0.05	0.04	0.04	0.03	0.03	0.03	0.05	0.05	0.06

225 SW545 PC 227 SW545 PC 229 SW545 G 231 SW545 G 233 SW545 PC
226 SW545 PR 228 SW545 PC 230 SW545 G 232 SW545 G

	234	235	236	237	238	239	240	241	242
SiO2	49.88	49.07	45.06	48.23	47.98	49.08	48.28	51.56	50.30
TiO2	2.08	1.48	3.40	2.10	2.69	1.62	1.81	1.68	1.87
Al2O3	4.22	6.90	8.38	5.88	5.84	5.33	6.42	2.39	2.91
Cr2O3	0.01	0.15	0.12	0.56	0.03	0.57	0.65	0.05	0.03
FeO	7.57	7.96	7.93	7.05	7.67	6.56	6.58	8.34	9.70
MnO	0.18	0.17	0.13	0.16	0.14	0.14	0.12	0.17	0.19
MgO	14.28	13.74	12.47	13.83	13.38	14.52	14.41	14.58	13.39
CaO	22.64	20.88	22.72	22.02	22.91	21.87	21.58	21.85	21.77
Na2O	0.44	0.76	0.58	0.64	0.49	0.63	0.70	0.45	0.55
K2O	nd	nd	nd	nd	nd	nd	nd	0.01	0.02
total=	100.90	101.11	100.79	100.47	101.13	100.32	100.51	101.04	100.73
Si	1.82	1.79	1.66	1.78	1.76	1.80	1.77	1.90	1.87
Ti	0.06	0.04	0.09	0.06	0.07	0.04	0.05	0.05	0.05
Al	0.18	0.30	0.36	0.26	0.25	0.23	0.28	0.10	0.13
Fe3	0.10	0.09	0.16	0.11	0.11	0.10	0.12	0.05	0.08
Cr	-	-	-	0.02	-	0.02	0.02	-	-
Fe2	0.13	0.15	0.09	0.11	0.13	0.10	0.08	0.21	0.23
Mg	0.78	0.75	0.69	0.76	0.73	0.79	0.79	0.80	0.78
Ca	0.89	0.82	0.90	0.87	0.90	0.86	0.85	0.86	0.87
Na	0.03	0.05	0.04	0.05	0.03	0.04	0.05	0.03	0.04
total=	4.00	4.00	4.00	4.00	4.00	4.00	4.00	4.00	4.00
oxygens=	[6]	[6]	[6]	[6]	[6]	[6]	[6]	[6]	[6]
Mg*	0.85	0.82	0.88	0.87	0.85	0.89	0.90	0.79	0.76
Al4	0.18	0.21	0.34	0.22	0.24	0.20	0.23	0.10	0.13
Al6	-	0.09	0.03	0.03	0.02	0.03	0.04	-	-0.01

234 SW545 PR
235 SW545 PC
236 SW545 PR
237 SW545 PC
238 SW545 PR
239 SW545 PC
240 SW545 PR
241 SW566 G
242 SW566 G

	243	244	245	246	247	248
SiO2	52.16	51.47	49.98	51.63	51.21	51.86
TiO2	1.24	1.46	2.10	1.16	1.39	1.25
Al2O3	2.31	2.29	3.02	1.44	1.98	2.28
Cr2O3	0.10	0.06	0.02	0.02	0.04	0.11
FeO	7.14	7.88	9.92	11.02	9.76	7.24
MnO	0.14	0.13	0.21	0.25	0.20	0.14
MgO	15.50	15.02	13.27	12.82	13.72	15.71
CaO	22.11	21.76	21.71	21.63	21.66	21.98
Na2O	0.37	0.48	0.62	0.60	0.51	0.39
K2O	nd	0.02	nd	0.03	nd	0.01
total=	101.07	100.57	100.85	100.60	100.87	100.97
Si	1.91	1.89	1.85	1.93	1.90	1.89
Ti	0.03	0.04	0.06	0.03	0.04	0.03
Al	0.10	0.10	0.13	0.06	0.09	0.10
Fe3	0.04	0.06	0.09	0.06	0.06	0.07
Fe2	0.17	0.18	0.22	0.28	0.24	0.15
Mg	0.84	0.82	0.73	0.71	0.76	0.86
Ca	0.87	0.86	0.86	0.87	0.86	0.86
Na	0.03	0.03	0.04	0.04	0.04	0.03
total=	4.00	4.00	4.00	4.00	4.00	4.00
oxygens=	[6]	[6]	[6]	[6]	[6]	[6]
Mg*	0.83	0.82	0.76	0.71	0.76	0.85
Al4	0.09	0.11	0.15	0.07	0.10	0.11
Al6	0.00	-0.01	-0.01	-0.01	-0.01	-0.01

243 SW566 G
244 SW566 G
245 SW566 G
246 SW566 G
247 SW566 G
248 SW566 G

Fife & Lothian basanites

	249	250	251	252	253	254	255	256	257
SiO2	50.45	51.03	44.76	50.03	48.36	47.52	40.18	45.25	46.23
TiO2	0.35	0.66	4.14	0.73	2.59	1.77	6.01	3.20	2.64
Al2O3	4.07	5.61	7.87	4.68	4.84	8.41	11.14	7.02	6.45
FeO	10.97	8.53	7.66	11.18	7.08	9.38	8.35	7.90	7.65
MnO	0.40	0.27	0.11	0.36	0.11	0.17	0.11	0.11	0.10
MgO	12.99	13.08	11.69	10.60	13.60	11.66	10.32	12.77	12.66
CaO	18.54	19.89	23.07	20.75	22.91	20.86	22.38	22.16	22.33
Na2O	1.29	1.33	0.60	1.50	0.40	0.95	0.52	0.41	0.47
total=	99.06	100.40	99.90	99.83	99.89	100.32	99.01	98.82	98.53
Si	1.89	1.87	1.67	1.88	1.80	1.76	1.53	1.70	1.74
Ti	-	0.02	0.12	0.02	0.07	0.05	0.17	0.09	0.07
Al	0.18	0.24	0.35	0.21	0.21	0.37	0.50	0.31	0.29
Fe3	0.11	0.07	0.12	0.11	0.08	0.08	0.14	0.13	0.11
Fe2	0.23	0.20	0.12	0.24	0.14	0.21	0.12	0.12	0.13
Mn	0.01	-	-	0.01	-	-	-	-	-
Mg	0.73	0.72	0.65	0.59	0.75	0.64	0.58	0.72	0.71
Ca	0.74	0.78	0.92	0.83	0.91	0.81	0.91	0.89	0.90
Na	0.09	0.09	0.04	0.11	0.03	0.07	0.04	0.03	0.03
total=	4.00	4.00	4.00	4.00	4.00	4.00	4.00	4.00	4.00
oxygens=	[6]	[6]	[6]	[6]	[6]	[6]	[6]	[6]	[6]
Mg*	0.75	0.78	0.84	0.70	0.84	0.75	0.82	0.85	0.84
Al4	0.11	0.13	0.33	0.12	0.20	0.24	0.47	0.30	0.26
Al6	0.07	0.12	0.02	0.08	0.01	0.13	0.03	0.02	0.03

249 SW6 XC
250 SW6 XC
251 SW6 XR
252 SW6 XC
253 SW6 XR
254 SW6 XC
255 SW6 XR
256 SW6 XR
257 SW6 XC

	258	259	260	261	262	263	264	265	266
SiO2	42.28	47.95	48.55	45.97	48.16	48.07	46.38	43.63	44.75
TiO2	5.15	2.42	2.42	3.16	2.34	1.55	3.72	4.36	4.09
Al2O3	10.03	5.57	4.63	6.29	5.33	5.86	6.83	8.86	8.19
FeO	7.95	7.32	7.14	7.92	6.34	8.43	7.13	8.01	7.70
MnO	0.12	0.13	0.12	0.13	0.11	0.20	0.10	0.10	0.12
MgO	10.76	13.95	13.66	12.79	13.93	12.63	12.53	11.65	11.91
CaO	22.78	21.89	22.81	22.14	22.59	22.57	23.16	22.20	22.64
Na2O	0.51	0.37	0.40	0.52	0.33	0.50	0.58	0.62	0.63
total=	99.58	99.60	99.73	98.92	99.13	99.81	100.43	99.43	100.03
Si	1.59	1.78	1.81	1.73	1.80	1.79	1.72	1.64	1.67
Ti	0.15	0.07	0.07	0.09	0.07	0.04	0.10	0.12	0.11
Al	0.45	0.24	0.20	0.28	0.23	0.26	0.30	0.39	0.36
Fe3	0.11	0.08	0.08	0.12	0.06	0.11	0.10	0.13	0.12
Fe2	0.14	0.15	0.15	0.13	0.13	0.15	0.12	0.12	0.12
Mg	0.60	0.77	0.76	0.72	0.77	0.70	0.69	0.65	0.66
Ca	0.92	0.87	0.91	0.89	0.90	0.90	0.92	0.89	0.90
Na	0.04	0.03	0.03	0.04	0.02	0.04	0.04	0.05	0.05
total=	4.00	4.00	4.00	4.00	4.00	4.00	4.00	4.00	4.00
oxygens=	[6]	[6]	[6]	[6]	[6]	[6]	[6]	[6]	[6]
Mg*	0.81	0.84	0.84	0.84	0.85	0.81	0.84	0.84	0.84
Al4	0.41	0.22	0.19	0.27	0.20	0.21	0.28	0.36	0.33
Al6	0.04	0.03	0.01	0.01	0.03	0.05	0.02	0.03	0.03

258 SW6 G
259 SW6 G
260 SW6 G
261 SW6 XC
262 SW8 PR
263 SW8 PC
264 SW8 G
265 SW8 G
266 SW8 G

	267	268	269	270	271	272	273	274	275
SiO2	49.28	46.67	48.36	50.37	49.78	49.81	48.53	47.39	47.28
TiO2	1.27	2.68	1.53	1.28	1.36	1.21	1.43	2.48	2.71
Al2O3	5.90	5.96	6.96	4.55	4.72	5.30	6.51	6.00	5.23
FeO	6.25	8.23	6.04	5.37	6.10	6.54	6.28	7.78	7.79
MnO	0.11	0.18	0.11	0.11	0.12	0.13	0.12	0.15	0.15
MgO	14.53	12.91	14.17	14.65	14.85	15.34	14.74	12.45	13.11
CaO	20.81	22.20	20.91	22.76	21.45	20.18	20.47	22.53	22.64
Na2O	0.73	0.51	0.78	0.55	0.60	0.77	0.79	0.69	0.46
total=	98.84	99.30	98.86	99.60	98.94	99.28	98.87	99.43	99.33
Si	1.83	1.75	1.79	1.86	1.85	1.84	1.80	1.77	1.77
Ti	0.04	0.08	0.04	0.03	0.04	0.03	0.04	0.07	0.08
Al	0.26	0.26	0.30	0.20	0.21	0.23	0.28	0.26	0.23
Fe3	0.07	0.12	0.08	0.06	0.07	0.09	0.10	0.10	0.11
Fe2	0.12	0.13	0.11	0.11	0.12	0.12	0.09	0.14	0.13
Mg	0.80	0.72	0.78	0.80	0.82	0.84	0.81	0.69	0.73
Ca	0.83	0.89	0.83	0.90	0.85	0.80	0.81	0.90	0.91
Na	0.05	0.04	0.06	0.04	0.04	0.06	0.06	0.05	0.03
total=	4.00	4.00	4.00	4.00	4.00	4.00	4.00	4.00	4.00
oxygens=	[6]	[6]	[6]	[6]	[6]	[6]	[6]	[6]	[6]
Mg*	0.86	0.84	0.88	0.88	0.87	0.88	0.89	0.83	0.84
Al4	0.17	0.25	0.21	0.18	0.15	0.16	0.20	0.23	0.23
Al6	0.08	0.01	0.10	0.05	0.05	0.07	0.08	0.04	-

267 SW9 XC 269 SW9 XC 271 SW9 XC 273 SW9 XR 275 SW9 G
268 SW9 XR 270 SW9 XC 272 SW9 XC 274 SW9 G

	276	277	278	279	280	281	282	283	284
SiO2	47.38	48.05	47.09	47.26	43.98	50.29	48.29	49.16	47.53
TiO2	1.56	2.06	1.15	1.55	2.87	0.62	1.50	1.05	2.23
Al2O3	7.06	5.85	5.95	5.63	10.18	5.47	5.01	4.95	5.31
Cr2O3	nd	nd	nd	nd	0.03	0.29	0.45	0.74	nd
FeO	8.36	6.79	12.95	10.28	9.08	5.55	6.33	5.71	7.50
MnO	0.18	0.13	0.31	0.28	0.18	0.12	0.11	0.10	0.15
MgO	13.17	13.80	9.26	11.15	10.57	18.02	14.81	15.75	13.62
CaO	19.98	21.68	21.30	20.83	21.35	17.73	21.64	20.98	22.43
Na2O	0.83	0.65	1.29	1.58	1.15	0.78	0.62	0.70	0.55
total=	98.52	99.01	99.30	98.56	99.39	98.87	98.76	99.14	99.32
Si	1.78	1.79	1.79	1.79	1.65	1.84	1.80	1.81	1.77
Ti	0.04	0.06	0.03	0.04	0.08	0.02	0.04	0.03	0.06
Al	0.31	0.26	0.27	0.25	0.45	0.24	0.22	0.21	0.23
Fe3	0.11	0.09	0.18	0.21	0.18	0.10	0.14	0.13	0.14
Cr	-	-	-	-	-	-	0.01	0.02	-
Fe2	0.16	0.12	0.23	0.12	0.11	0.06	0.06	0.04	0.10
Mg	0.74	0.77	0.52	0.63	0.59	0.98	0.82	0.87	0.76
Ca	0.80	0.87	0.87	0.84	0.86	0.69	0.86	0.83	0.90
Na	0.06	0.05	0.10	0.12	0.08	0.06	0.04	0.05	0.04
total=	4.00	4.00	4.00	4.00	4.00	4.00	4.00	4.00	4.00
oxygens=	[6]	[6]	[6]	[6]	[6]	[6]	[6]	[6]	[6]
Mg*	0.82	0.86	0.69	0.83	0.84	0.93	0.93	0.95	0.88
Al4	0.22	0.21	0.21	0.21	0.35	0.16	0.20	0.19	0.23
Al6	0.09	0.05	0.06	0.04	0.10	0.07	0.02	0.03	0.01

276 SW9 XC 278 SW9 XC 280 SW9 PC 282 SW9 PR 284 SW9 PR
277 SW9 PC 279 SW9 XR 281 SW9 PC 283 SW9 PC

	285	286	287	288	289	290	291	292	293
SiO2	45.79	43.69	47.61	49.16	42.87	49.46	47.90	45.85	49.25
TiO2	3.21	4.06	2.10	1.54	4.92	1.41	1.91	2.48	1.36
Al2O3	8.51	9.01	6.82	5.56	9.81	5.66	7.44	9.08	5.37
Cr2O3	0.13	0.23	0.40	0.88	0.03	0.81	0.84	0.09	0.01
FeO	7.43	7.39	6.68	5.61	8.26	5.66	6.02	8.48	11.32
MnO	0.09	0.10	0.12	0.08	0.11	0.10	0.11	0.15	0.30
MgO	12.03	11.84	13.07	14.46	10.63	14.88	13.61	11.46	12.16
CaO	22.04	22.36	22.15	21.95	22.28	21.49	21.41	21.89	19.36
Na2O	0.77	0.61	0.72	0.64	0.67	0.69	0.79	0.58	1.13
K2O	nd	nd	0.05	nd	0.04	nd	0.01	nd	nd
total=	100.00	99.29	99.72	99.88	99.62	100.16	100.04	100.06	100.26
Si	1.70	1.64	1.76	1.81	1.61	1.81	1.76	1.71	1.83
Ti	0.09	0.11	0.06	0.04	0.14	0.04	0.05	0.07	0.04
Al	0.37	0.40	0.30	0.24	0.44	0.24	0.32	0.40	0.24
Fe3	0.10	0.13	0.10	0.07	0.11	0.08	0.08	0.09	0.10
Cr	-	-	0.01	0.03	-	0.02	0.02	-	-
Fe2	0.13	0.10	0.11	0.10	0.15	0.09	0.11	0.18	0.25
Mg	0.67	0.66	0.72	0.79	0.60	0.81	0.75	0.64	0.68
Ca	0.88	0.90	0.88	0.87	0.90	0.88	0.88	0.87	0.77
Na	0.06	0.04	0.05	0.05	0.05	0.05	0.06	0.04	0.08
total=	4.00	4.00	4.00	4.00	4.00	4.00	4.00	4.00	4.00
oxygens=	[6]	[6]	[6]	[6]	[6]	[6]	[6]	[6]	[6]
Mg#	0.83	0.86	0.86	0.89	0.79	0.89	0.87	0.78	0.72
Al4	0.30	0.36	0.24	0.19	0.39	0.19	0.24	0.29	0.17
Al6	0.07	0.04	0.06	0.05	0.05	0.06	0.09	0.11	0.07

285 SW20 PR 287 SW20 PC 289 SW20 PR 291 SW20 XC 293 SW20 G
286 SW20 PR 288 SW20 PC 290 SW20 XC 292 SW20 G

	294	295	296	297	298	299	300	301	302
SiO2	47.45	50.84	48.33	51.22	48.45	48.27	45.60	49.23	48.03
TiO2	2.27	0.38	1.66	0.42	1.47	1.19	2.33	0.80	1.68
Al2O3	7.68	5.78	8.88	6.30	8.86	5.83	7.46	8.90	6.05
Cr2O3	0.09	1.33	0.28	1.27	0.82	0.76	0.69	1.07	0.89
FeO	7.93	2.91	6.33	3.53	6.20	5.07	6.36	8.87	5.79
MnO	0.18	0.11	0.16	0.12	0.15	0.15	0.14	0.17	0.15
MgO	12.83	16.31	14.73	15.52	15.10	15.27	13.44	15.71	14.44
CaO	21.82	19.64	21.73	19.09	21.82	21.53	21.92	21.27	21.98
Na2O	0.89	1.66	0.59	1.85	0.60	0.78	0.68	0.73	0.65
K2O	0.11	nd	nd	nd	nd	nd	nd	nd	nd
total=	100.45	98.96	98.69	99.32	98.67	98.85	98.62	98.75	99.66
Si	1.75	1.85	1.80	1.86	1.80	1.78	1.71	1.82	1.77
Ti	0.06	0.01	0.05	0.01	0.04	0.03	0.07	0.02	0.05
Al	0.33	0.25	0.21	0.27	0.21	0.25	0.33	0.21	0.26
Fe3	0.10	0.12	0.13	0.08	0.13	0.15	0.16	0.13	0.12
Cr	-	0.04	-	0.04	0.01	0.02	0.02	0.03	0.03
Fe2	0.14	-0.03	0.07	0.02	0.06	-	0.04	0.02	0.06
Mg	0.68	0.88	0.82	0.84	0.84	0.84	0.75	0.86	0.79
Ca	0.85	0.76	0.87	0.74	0.85	0.85	0.88	0.84	0.87
Na	0.06	0.12	0.04	0.13	0.04	0.06	0.05	0.05	0.05
total=	4.00	4.00	4.00	4.00	4.00	4.00	4.00	4.00	4.00
oxygens=	[6]	[6]	[6]	[6]	[6]	[6]	[6]	[6]	[6]
Mg#	0.82	1.03	0.91	0.97	0.93	0.99	0.94	0.97	0.93
Al4	0.25	0.15	0.20	0.14	0.20	0.22	0.29	0.18	0.23
Al6	0.08	0.09	0.01	0.13	0.02	0.04	0.03	0.03	0.03

294 SW20 G 296 SW20 PR 298 SW20 PR 300 SW20 PR 302 SW20 PR
295 SW20 PC 297 SW20 PC 299 SW20 PC 301 SW20 PC

	303	304	305	306	307	308	309	310	311
SiO2	48.28	47.87	46.98	48.32	50.12	47.48	47.93	46.07	48.59
TiO2	1.65	2.85	2.71	2.68	0.65	2.95	2.53	3.43	2.20
Al2O3	5.90	5.30	5.27	4.95	4.09	5.61	4.26	6.38	3.25
Cr2O3	0.06	nd	nd	nd	nd	nd	nd	nd	nd
FeO	9.40	7.58	7.68	7.61	11.28	7.68	8.55	7.73	7.39
MnO	0.35	0.11	0.11	0.11	0.38	0.11	0.13	0.12	0.15
MgO	11.71	13.35	13.10	13.33	12.18	12.82	13.20	12.17	13.69
CaO	20.60	23.02	22.82	22.95	20.62	22.80	22.25	22.81	22.65
Na2O	1.52	0.52	0.58	0.48	0.80	0.52	0.50	0.52	0.57
total=	99.47	100.60	99.13	100.39	100.08	99.89	99.35	99.19	98.49
Si	1.80	1.77	1.76	1.79	1.87	1.77	1.80	1.73	1.83
Ti	0.05	0.08	0.08	0.07	0.02	0.08	0.07	0.10	0.06
Al	0.26	0.23	0.23	0.22	0.18	0.25	0.19	0.28	0.14
Fe3	0.15	0.11	0.13	0.09	0.09	0.09	0.11	0.09	0.11
Fe2	0.14	0.12	0.11	0.14	0.26	0.15	0.16	0.15	0.12
Mn	0.01	-	-	-	0.01	-	-	-	-
Mg	0.65	0.74	0.73	0.74	0.68	0.71	0.74	0.68	0.77
Ca	0.82	0.91	0.92	0.91	0.83	0.91	0.89	0.92	0.91
Na	0.11	0.04	0.04	0.03	0.06	0.04	0.04	0.04	0.04
total=	4.00	4.00	4.00	4.00	4.00	4.00	4.00	4.00	4.00
oxygens=	[6]	[6]	[6]	[6]	[6]	[6]	[6]	[6]	[6]
Mg*	0.81	0.85	0.87	0.83	0.71	0.82	0.82	0.82	0.86
Al4	0.20	0.23	0.24	0.21	0.13	0.23	0.20	0.27	0.17
Al6	0.06	-	-0.01	0.01	0.05	0.02	-0.01	0.02	-0.02

303 SW20 XR 305 SW25 XC 307 SW25 XC 309 SW25 XC 311 SW25 G
304 SW25 XC 306 SW25 XR 308 SW25 XC 310 SW25 XC

	312	313	314	315	316	317	318	319	320
SiO2	47.91	48.00	47.76	47.38	50.90	47.81	47.35	47.82	48.50
TiO2	2.41	2.57	2.29	2.70	0.60	2.70	2.87	2.11	2.32
Al2O3	3.87	5.12	4.65	5.20	3.21	5.22	5.57	5.87	4.26
Cr2O3	nd	0.08	0.32	0.11	0.03	0.12	0.12	0.63	0.03
FeO	7.26	7.71	7.70	7.81	10.73	7.65	7.66	6.36	7.56
MnO	0.13	0.13	0.14	0.13	0.36	0.10	0.14	0.10	0.11
MgO	14.03	13.49	13.85	13.49	13.25	13.67	13.81	14.18	14.02
CaO	22.50	22.25	21.95	22.21	20.83	22.32	22.31	22.19	22.07
Na2O	0.50	0.53	0.48	0.54	0.84	0.52	0.53	0.53	0.49
total=	98.61	99.88	99.14	99.17	100.35	100.11	99.96	99.79	99.36
Si	1.80	1.79	1.79	1.77	1.89	1.77	1.76	1.77	1.81
Ti	0.07	0.07	0.06	0.08	0.02	0.08	0.08	0.06	0.07
Al	0.17	0.22	0.21	0.23	0.14	0.23	0.24	0.26	0.19
Fe3	0.13	0.10	0.12	0.11	0.10	0.11	0.11	0.11	0.10
Cr	-	-	-	-	-	-	-	0.02	-
Fe2	0.10	0.14	0.13	0.12	0.23	0.13	0.13	0.09	0.14
Mn	-	-	-	-	0.01	-	-	-	-
Mg	0.79	0.75	0.77	0.75	0.73	0.76	0.74	0.78	0.78
Ca	0.91	0.89	0.88	0.89	0.81	0.89	0.89	0.88	0.88
Na	0.04	0.04	0.03	0.04	0.06	0.04	0.04	0.04	0.04
total=	4.00	4.00	4.00	4.00	4.00	4.00	4.00	4.00	4.00
oxygens=	[6]	[6]	[6]	[6]	[6]	[6]	[6]	[6]	[6]
Mg*	0.88	0.84	0.86	0.85	0.75	0.85	0.85	0.90	0.85
Al4	0.20	0.21	0.21	0.23	0.11	0.23	0.24	0.23	0.19
Al6	-0.03	0.01	-0.01	0.00	0.03	-	0.00	0.02	0.00

312 SW25 G 314 SW25 PC 316 SW25 XC 318 SW25 PR 320 SW25 PR
313 SW25 PR 315 SW25 PR 317 SW25 PC 319 SW25 PC

	321	322	323	324	325	326	327	328	329
SiO2	47.45	47.29	48.61	48.17	51.67	46.08	47.73	49.19	50.07
TiO2	2.63	2.81	1.83	2.04	0.70	2.38	2.05	1.35	1.12
Al2O3	5.52	5.52	5.30	5.89	3.00	7.44	7.03	5.19	5.41
Cr2O3	0.11	0.09	nd	nd	nd	nd	nd	nd	nd
FeO	7.85	7.54	8.29	8.43	6.79	8.61	6.94	6.50	6.91
MnO	0.14	0.13	0.21	0.20	0.17	0.17	0.13	0.14	0.14
MgO	13.48	13.27	13.93	13.07	17.33	12.17	13.40	14.93	15.42
CaO	21.97	22.39	20.30	20.94	18.18	21.00	21.68	20.99	19.75
Na2O	0.54	0.53	0.66	0.79	0.80	0.91	0.73	0.63	0.70
total=	99.69	99.57	99.13	99.53	98.68	98.72	99.69	98.92	99.52
Si	1.77	1.76	1.81	1.80	1.91	1.73	1.77	1.82	1.84
Ti	0.07	0.08	0.05	0.06	0.02	0.07	0.06	0.04	0.03
Al	0.24	0.24	0.23	0.26	0.13	0.33	0.31	0.23	0.23
Fe3	0.11	0.11	0.08	0.09	0.08	0.14	0.10	0.09	0.07
Fe2	0.13	0.13	0.18	0.17	0.13	0.13	0.12	0.11	0.14
Mg	0.75	0.74	0.78	0.73	0.95	0.68	0.74	0.83	0.85
Ca	0.88	0.90	0.81	0.84	0.72	0.85	0.86	0.83	0.78
Na	0.04	0.04	0.05	0.06	0.06	0.07	0.05	0.05	0.05
total=	4.00	4.00	4.00	4.00	4.00	4.00	4.00	4.00	4.00
oxygens=	[6]	[6]	[6]	[6]	[6]	[6]	[6]	[6]	[6]
Mg*	0.84	0.85	0.81	0.80	0.87	0.83	0.86	0.88	0.85
Al4	0.23	0.24	0.19	0.20	0.09	0.27	0.23	0.18	0.16
Al6	0.01	0.01	0.05	0.05	0.04	0.06	0.07	0.05	0.08

321 SW25 XC 323 SW40 XC 325 SW40 XC 327 SW40 XC 329 SW40 XC
322 SW25 XR 324 SW40 XC 326 SW40 XC 328 SW40 XC

	330	331	332	333	334	335	336	337	338
SiO2	49.52	50.07	53.54	48.18	51.40	47.30	47.74	47.10	46.90
TiO2	1.34	0.83	0.29	1.92	1.00	2.19	1.73	2.22	2.09
Al2O3	4.16	4.41	0.71	5.24	4.02	5.83	6.66	7.12	7.87
Cr2O3	nd	nd	0.09	0.15	0.06	0.09	0.03	0.02	0.03
FeO	11.46	9.15	8.92	8.03	8.17	7.97	9.04	8.68	10.47
MnO	0.39	0.29	0.51	0.14	0.25	0.14	0.18	0.15	0.25
MgO	9.57	11.63	13.92	14.28	11.82	13.71	12.73	12.74	11.74
CaO	21.89	21.58	21.91	20.87	21.13	21.20	20.77	21.11	19.69
Na2O	1.34	1.13	1.28	0.63	2.03	0.64	1.00	0.94	1.26
total=	99.67	99.09	101.17	99.44	99.88	99.07	99.88	100.08	100.30
Si	1.87	1.88	1.96	1.79	1.90	1.77	1.77	1.74	1.74
Ti	0.04	0.02	-	0.05	0.03	0.06	0.05	0.06	0.06
Al	0.19	0.20	0.03	0.23	0.18	0.26	0.29	0.31	0.34
Fe3	0.09	0.08	0.12	0.12	0.11	0.13	0.14	0.14	0.15
Fe2	0.28	0.21	0.15	0.13	0.14	0.12	0.14	0.13	0.18
Mn	0.01	-	0.02	-	-	-	-	-	-
Mg	0.54	0.65	0.76	0.79	0.65	0.76	0.70	0.70	0.65
Ca	0.89	0.87	0.86	0.83	0.84	0.85	0.83	0.84	0.78
Na	0.10	0.08	0.09	0.05	0.15	0.05	0.07	0.07	0.09
total=	4.00	4.00	4.00	4.00	4.00	4.00	4.00	4.00	4.00
oxygens=	[6]	[6]	[6]	[6]	[6]	[6]	[6]	[6]	[6]
Mg*	0.65	0.75	0.82	0.86	0.81	0.86	0.83	0.84	0.78
Al4	0.13	0.12	0.04	0.21	0.10	0.23	0.23	0.26	0.26
Al6	0.06	0.08	-0.01	0.02	0.08	0.02	0.06	0.06	0.08

330 SW40 G 332 SW40 PC 334 SW40 PC 336 SW40 XC 338 SW40 PC
331 SW40 G 333 SW40 PR 335 SW40 PR 337 SW40 XR

	339	340	341	342	343	344	345	346	347
SiO2	48.68	48.02	47.70	47.61	47.19	46.64	47.01	49.75	50.09
TiO2	1.47	2.89	2.40	3.03	3.14	3.14	3.19	2.04	1.40
Al2O3	6.50	5.30	5.29	6.79	6.52	12.30	6.43	4.24	5.46
Cr2O3	0.17	0.03	0.02	0.02	0.31	0.06	0.08	0.37	0.41
FeO	8.03	7.55	8.83	7.93	6.86	6.64	7.33	6.24	5.72
MnO	0.16	0.14	0.18	0.16	0.11	0.09	0.12	0.13	0.11
MgO	15.22	13.62	12.33	11.99	12.87	10.12	13.08	14.77	15.04
CaO	19.13	22.28	22.99	21.55	22.97	19.21	22.77	22.80	21.48
Na2O	0.76	0.52	0.58	0.93	0.54	1.30	0.51	0.45	0.73
K2O	nd	nd	nd	0.20	nd	0.61	nd	nd	nd
total=	100.12	100.35	100.32	100.21	100.51	100.11	100.52	100.79	100.44
Si	1.78	1.78	1.78	1.77	1.75	1.73	1.74	1.82	1.83
Ti	0.04	0.08	0.07	0.08	0.09	0.09	0.09	0.06	0.04
Al	0.28	0.23	0.23	0.30	0.28	0.54	0.28	0.18	0.23
Fe3	0.12	0.09	0.12	0.07	0.08	-0.04	0.10	0.08	0.07
Cr	-	-	-	-	-	-	-	0.01	0.01
Fe2	0.13	0.18	0.15	0.17	0.13	0.25	0.13	0.11	0.10
Mg	0.83	0.75	0.68	0.66	0.71	0.56	0.72	0.81	0.82
Ca	0.75	0.88	0.92	0.86	0.91	0.76	0.90	0.89	0.84
Na	0.05	0.04	0.04	0.07	0.04	0.09	0.04	0.03	0.05
K	-	-	-	-	-	0.03	-	-	-
total=	4.00	4.00	4.00	4.00	4.00	4.00	4.00	4.00	4.00
oxygens=	[6]	[6]	[6]	[6]	[6]	[6]	[6]	[6]	[6]
Mg*	0.86	0.84	0.81	0.79	0.84	0.69	0.85	0.88	0.89
Al4	0.21	0.22	0.22	0.23	0.25	0.27	0.26	0.18	0.17
Al6	0.07	0.01	0.01	0.07	0.03	0.26	0.02	0.00	0.06

339 SW40 PR
340 SW436 PC
341 SW436 PC
342 SW436 PR
343 SW436 PC
344 SW436 PR
345 SW436 G
346 SW436 G
347 SW442 XC

	348	349	350	351	352	353	354	355	356
SiO2	49.11	49.77	47.88	50.17	49.45	47.06	49.64	50.06	49.04
TiO2	1.61	1.37	1.85	1.36	1.46	2.26	1.33	1.14	1.54
Al2O3	5.88	5.02	7.21	4.95	5.70	7.74	6.37	4.62	6.04
Cr2O3	0.25	0.63	0.05	0.34	0.95	0.27	0.42	0.68	1.12
FeO	5.84	5.93	8.54	5.63	5.62	7.71	6.18	5.59	5.70
MnO	0.09	0.13	0.18	0.11	0.11	0.14	0.12	0.13	0.12
MgO	14.46	14.66	12.70	14.84	14.51	12.95	14.22	15.09	14.19
CaO	21.89	21.54	20.36	21.84	21.49	20.74	20.50	21.51	21.69
Na2O	0.70	0.75	0.98	0.70	0.79	0.90	0.79	0.71	0.78
K2O	nd	nd	nd	nd	nd	0.01	0.17	nd	nd
total=	99.83	99.80	99.75	99.94	100.17	99.78	99.74	99.53	100.22
Si	1.81	1.83	1.78	1.84	1.81	1.74	1.83	1.84	1.80
Ti	0.04	0.04	0.05	0.04	0.04	0.06	0.04	0.03	0.04
Al	0.25	0.22	0.32	0.21	0.25	0.34	0.28	0.20	0.26
Fe3	0.09	0.08	0.10	0.07	0.07	0.11	0.05	0.08	0.08
Cr	-	0.02	-	-	0.03	-	0.01	0.02	0.03
Fe2	0.09	0.11	0.17	0.11	0.10	0.13	0.14	0.09	0.10
Mg	0.79	0.80	0.70	0.81	0.79	0.72	0.78	0.83	0.78
Ca	0.86	0.85	0.81	0.86	0.84	0.82	0.81	0.85	0.85
Na	0.05	0.05	0.07	0.05	0.06	0.06	0.06	0.05	0.06
total=	4.00	4.00	4.00	4.00	4.00	4.00	4.00	4.00	4.00
oxygens=	[6]	[6]	[6]	[6]	[6]	[6]	[6]	[6]	[6]
Mg*	0.89	0.88	0.80	0.88	0.88	0.84	0.84	0.90	0.88
Al4	0.19	0.17	0.22	0.16	0.19	0.26	0.17	0.16	0.20
Al6	0.06	0.05	0.09	0.06	0.06	0.08	0.10	0.04	0.06

348 SW442 XC
349 SW442 XR
350 SW442 XC
351 SW442 XC
352 SW442 XR
353 SW442 XC
354 SW442 XR
355 SW442 PC
356 SW442 PR

	357	358	359	360	361	362	363	364	365
SiO2	48.22	48.51	45.17	48.75	46.29	50.86	45.35	48.71	46.95
TiO2	1.87	1.40	3.74	1.62	2.90	1.27	4.08	2.02	2.38
Al2O3	5.97	5.75	7.50	6.21	9.23	4.45	7.17	5.52	6.92
Cr2O3	nd	0.89	0.01	0.89	0.17	0.37	0.01	0.14	0.35
FeO	8.80	5.64	8.88	5.53	7.08	5.42	9.86	7.22	6.85
MnO	0.17	0.12	0.17	0.11	0.13	0.14	0.19	0.16	0.10
MgO	13.22	14.93	12.14	14.39	11.92	15.74	11.09	14.44	13.88
CaO	20.56	21.30	21.79	22.72	22.39	22.65	22.11	21.80	22.47
Na2O	0.96	0.74	0.63	0.53	0.83	0.44	0.66	0.44	0.48
K2O	nd	nd	0.01	nd	0.03	nd	nd	nd	nd
total=	99.77	99.28	100.04	100.75	100.97	101.34	100.52	100.45	100.38
Si	1.79	1.79	1.69	1.78	1.70	1.84	1.70	1.79	1.73
Ti	0.05	0.04	0.11	0.04	0.08	0.03	0.11	0.06	0.07
Al	0.26	0.25	0.33	0.27	0.40	0.19	0.32	0.24	0.30
Fe3	0.12	0.12	0.13	0.09	0.10	0.08	0.10	0.09	0.14
Cr	-	0.03	-	0.03	-	0.01	-	-	0.01
Fe2	0.15	0.06	0.15	0.07	0.12	0.08	0.21	0.13	0.07
Mg	0.73	0.82	0.68	0.78	0.65	0.85	0.62	0.79	0.76
Ca	0.82	0.84	0.87	0.89	0.88	0.88	0.89	0.86	0.89
Na	0.07	0.05	0.05	0.04	0.06	0.03	0.05	0.03	0.03
total=	4.00	4.00	4.00	4.00	4.00	4.00	4.00	4.00	4.00
oxygens=	[6]	[6]	[6]	[6]	[6]	[6]	[6]	[6]	[6]
Mg*	0.83	0.93	0.82	0.91	0.84	0.91	0.75	0.86	0.91
Al4	0.21	0.21	0.31	0.22	0.30	0.16	0.30	0.21	0.27
Al6	0.05	0.04	0.02	0.05	0.10	0.03	0.02	0.03	0.03

357 SW442 PC
358 SW442 PR
359 SW526 PR
360 SW526 PC
361 SW526 PR
362 SW526 PC
363 SW526 PR
364 SW526 G
365 SW526 G

	366	367	368	369	370
SiO2	47.99	48.28	46.71	44.85	43.28
TiO2	2.10	1.96	2.31	3.17	3.64
Al2O3	6.63	6.57	7.74	8.74	9.98
Cr2O3	0.50	0.32	0.47	0.13	0.16
FeO	6.42	6.05	6.45	7.52	8.03
MnO	0.12	0.11	0.11	0.11	0.11
MgO	13.87	14.26	13.32	12.37	11.96
CaO	22.62	22.59	22.47	22.56	22.04
Na2O	0.49	0.49	0.54	0.52	0.53
total=	100.74	100.59	100.12	99.97	99.73
Si	1.76	1.77	1.72	1.67	1.62
Ti	0.06	0.05	0.06	0.09	0.10
Al	0.29	0.28	0.34	0.38	0.44
Fe3	0.10	0.10	0.11	0.14	0.16
Cr	0.01	-	0.01	-	-
Fe2	0.10	0.08	0.09	0.09	0.09
Mg	0.76	0.78	0.73	0.69	0.67
Ca	0.89	0.89	0.89	0.90	0.88
Na	0.03	0.03	0.04	0.04	0.04
total=	4.00	4.00	4.00	4.00	4.00
oxygens=	[6]	[6]	[6]	[6]	[6]
Mg*	0.88	0.90	0.89	0.88	0.88
Al4	0.24	0.23	0.28	0.33	0.38
Al6	0.05	0.05	0.06	0.05	0.05

366 SW526 G
367 SW526 PC
368 SW526 PR
369 SW526 XC
370 SW526 XC

Highland dykes

	371	372	373	374	375	376	377	378	379
SiO2	48.75	42.74	51.28	47.68	49.00	40.61	49.09	42.28	51.71
TiO2	1.32	3.96	0.58	2.30	1.60	4.82	1.41	4.30	0.28
Al2O3	5.95	9.97	4.52	5.83	5.64	11.43	5.45	10.40	4.57
Cr2O3	0.79	0.03	0.05	0.03	0.07	0.06	0.76	0.04	nd
FeO	4.93	7.85	9.95	6.69	5.54	8.24	4.85	7.87	3.99
MnO	0.10	0.12	0.14	0.14	0.09	0.11	0.10	0.12	0.21
MgO	14.23	10.89	12.01	13.22	14.22	10.47	14.17	10.61	14.50
CaO	22.24	23.04	20.01	23.15	22.70	22.32	22.33	22.93	22.10
Na2O	0.55	0.47	1.39	0.37	0.55	0.46	0.43	0.46	1.17
total=	98.86	99.07	99.93	99.41	99.41	98.52	98.59	99.01	98.53
Si	1.81	1.61	1.91	1.78	1.81	1.58	1.83	1.60	1.91
Ti	0.04	0.11	0.02	0.06	0.04	0.14	0.04	0.12	-
Al	0.26	0.44	0.20	0.26	0.25	0.51	0.24	0.46	0.20
Fe3	0.06	0.14	0.05	0.08	0.08	0.15	0.03	0.13	0.05
Cr	0.02	-	-	-	-	-	0.02	-	-
Fe2	0.09	0.11	0.26	0.12	0.09	0.11	0.13	0.12	0.07
Mg	0.79	0.61	0.67	0.73	0.78	0.59	0.79	0.60	0.80
Ca	0.89	0.93	0.80	0.93	0.90	0.91	0.89	0.93	0.87
Na	0.04	0.03	0.10	0.03	0.04	0.03	0.03	0.03	0.08
total=	4.00	4.00	4.00	4.00	4.00	4.00	4.00	4.00	4.00
oxygens=	[6]	[6]	[6]	[6]	[6]	[6]	[6]	[6]	[6]
Mg*	0.89	0.84	0.72	0.85	0.89	0.84	0.86	0.83	0.91
Al4	0.19	0.39	0.09	0.22	0.19	0.46	0.17	0.40	0.09
Al6	0.07	0.06	0.11	0.03	0.06	0.06	0.07	0.06	0.11

371 SW115 XC
372 SW115 XR
373 SW115 PC
374 SW115 PR
375 SW115 PC
376 SW115 PR
377 SW115 PC
378 SW115 PR
379 SW115 PC

	380	381	382
SiO2	46.86	49.36	48.07
TiO2	2.51	1.71	2.17
Al2O3	6.16	4.44	5.36
Cr2O3	0.01	0.31	0.10
FeO	7.12	5.69	6.45
MnO	0.11	0.12	0.14
MgO	13.25	14.32	13.62
CaO	22.16	23.10	22.78
Na2O	0.38	0.32	0.32
total=	98.56	99.37	99.01
Si	1.76	1.83	1.80
Ti	0.07	0.05	0.06
Al	0.27	0.19	0.24
Fe3	0.09	0.06	0.07
Fe2	0.14	0.12	0.14
Mg	0.74	0.79	0.76
Ca	0.89	0.92	0.91
Na	0.03	0.02	0.02
total=	4.00	4.00	4.00
oxygens=	[6]	[6]	[6]
Mg*	0.84	0.87	0.84
Al4	0.24	0.17	0.20
Al6	0.04	0.03	0.03

380 SW115 PR
381 SW115 G
382 SW115 G

Ayrshire sills

	1	2	3	4	5	6	7	8	9
SiO2	37.15	37.21	38.47	39.21	38.60	39.63	39.61	38.89	40.07
Al2O3	0.03	0.05	0.04	0.07	0.06	0.07	0.07	0.05	0.05
FeO	28.07	27.93	24.78	24.98	28.84	22.87	20.86	28.58	22.80
MnO	0.57	0.54	0.45	0.44	0.61	0.40	0.36	0.57	0.38
NiO	0.17	0.16	0.14	0.10	0.08	0.13	0.15	0.07	0.14
MgO	32.53	32.38	36.34	35.46	32.10	37.00	38.92	32.43	37.32
CaO	0.43	0.45	0.43	0.37	0.43	0.36	0.38	0.45	0.36
total=	98.95	98.72	100.65	100.63	100.72	100.46	100.35	101.04	101.12
Si	1.01	1.01	1.01	1.02	1.03	1.03	1.02	1.03	1.03
Fe2	0.64	0.63	0.54	0.55	0.64	0.50	0.45	0.63	0.49
Mn	0.01	0.01	-	-	0.01	-	-	0.01	-
Mg	1.32	1.31	1.42	1.38	1.27	1.43	1.49	1.28	1.43
Ca	0.01	0.01	0.01	0.01	0.01	-	0.01	0.01	-
total=	2.99	2.99	2.99	2.97	2.97	2.97	2.98	2.97	2.97
oxygens=	[4]	[4]	[4]	[4]	[4]	[4]	[4]	[4]	[4]
Fo	67.38	67.39	72.33	71.67	66.49	74.25	76.88	66.91	74.47

1 SW70 G
2 SW70 G
3 SW70 PC
4 SW70 XC
5 SW70 XR
6 SW70 PC
7 SW70 PC
8 SW70 PC
9 SW70 PR

	10	11	12	13	14	15	16	17	18
SiO2	39.15	40.38	39.20	41.01	38.77	39.56	39.61	39.19	36.38
Al2O3	0.08	0.06	0.05	0.03	0.06	0.06	0.05	0.07	0.04
FeO	27.77	21.90	27.76	17.32	29.43	23.75	25.12	17.82	31.72
MnO	0.53	0.37	0.51	0.27	0.60	0.41	0.44	0.27	0.60
NiO	0.09	0.13	0.09	0.26	0.07	0.14	0.10	0.19	0.11
MgO	33.39	37.45	32.63	41.02	31.49	36.33	34.98	42.36	31.17
CaO	0.41	0.30	0.43	0.06	0.40	0.39	0.42	0.29	0.48
total=	101.42	100.59	100.67	99.97	100.82	100.64	100.72	100.19	100.50
Si	1.03	1.04	1.04	1.04	1.03	1.03	1.03	1.00	0.99
Fe2	0.61	0.47	0.61	0.37	0.66	0.52	0.55	0.38	0.72
Mn	0.01	-	0.01	-	0.01	-	-	-	0.01
Mg	1.31	1.43	1.29	1.55	1.25	1.41	1.36	1.61	1.26
Ca	0.01	-	0.01	-	0.01	0.01	0.01	-	0.01
total=	2.97	2.96	2.96	2.96	2.97	2.97	2.97	3.00	3.01
oxygens=	[4]	[4]	[4]	[4]	[4]	[4]	[4]	[4]	[4]
Fo	68.18	75.30	67.69	80.85	65.60	73.16	71.28	80.90	63.65

10 SW70 PR
11 SW70 PC
12 SW70 PR
13 SW70 PC
14 SW70 PR
15 SW70 PC
16 SW70 PR
17 SW89 PC
18 SW89 PR

	19	20	21	22	23	24	25	26	27
SiO2	40.06	36.15	38.76	36.86	39.28	38.28	37.77	35.99	37.33
Al2O3	0.04	0.05	0.08	0.05	0.08	0.08	0.07	0.08	0.20
FeO	13.27	35.03	19.23	30.53	17.35	22.84	20.16	30.96	24.69
MnO	0.17	0.69	0.28	0.58	0.26	0.40	0.32	0.64	0.38
NiO	0.32	0.11	0.20	0.11	0.21	0.12	0.20	0.14	0.18
MgO	46.87	28.51	41.91	32.21	42.57	38.67	40.62	31.79	37.12
CaO	0.05	0.44	0.32	0.44	0.27	0.36	0.27	0.47	0.36
total=	100.38	100.98	100.78	100.78	100.02	100.75	99.41	100.07	100.26
Si	1.00	1.00	0.99	0.99	1.00	0.99	0.98	0.98	0.98
Fe2	0.28	0.81	0.41	0.69	0.37	0.50	0.44	0.71	0.54
Mn	-	0.02	-	0.01	-	-	-	0.01	-
Mg	1.72	1.17	1.59	1.29	1.61	1.49	1.57	1.29	1.46
Ca	-	0.01	-	0.01	-	0.01	-	0.01	0.01
total=	3.00	3.00	3.01	3.01	3.00	3.01	3.02	3.02	3.01
oxygens=	[4]	[4]	[4]	[4]	[4]	[4]	[4]	[4]	[4]
Fo	86.19	59.19	79.52	65.28	81.39	75.11	78.22	68.66	72.82

19 SW89 PC
20 SW89 PR
21 SW89 PC
22 SW89 PR
23 SW89 PC
24 SW89 PR
25 SW105 PC
26 SW105 PR
27 SW105 PC

	28	29	30	31	32	33	34	35	36
SiO2	34.02	36.33	34.78	38.84	35.74	41.27	38.62	40.18	37.83
Al2O3	0.08	0.06	0.07	0.06	0.08	0.04	0.06	0.07	0.05
FeO	39.39	27.79	37.29	18.53	35.56	17.70	28.20	20.14	35.76
MnO	0.90	0.50	0.80	0.29	0.79	0.26	0.53	0.31	0.75
NiO	0.09	0.15	0.09	0.19	0.10	0.33	0.18	0.26	0.14
MgO	24.99	33.99	26.86	42.18	28.13	40.72	32.06	38.19	25.31
CaO	0.40	0.45	0.48	0.24	0.46	0.11	0.44	0.25	0.43
total=	99.87	99.27	100.37	99.93	100.86	100.43	100.09	99.40	100.27
Si	0.97	0.98	0.98	0.99	0.99	1.04	1.03	1.04	1.05
Fe2	0.94	0.63	0.88	0.40	0.82	0.37	0.63	0.43	0.83
Mn	0.02	0.01	0.02	-	0.02	-	0.01	-	0.02
Mg	1.07	1.37	1.13	1.61	1.16	1.53	1.28	1.47	1.04
Ca	0.01	0.01	0.01	-	0.01	-	0.01	-	0.01
total=	3.02	3.02	3.02	3.01	3.01	2.96	2.97	2.96	2.95
oxygens=	[4]	[4]	[4]	[4]	[4]	[4]	[4]	[4]	[4]
Fo	53.07	68.55	56.21	80.23	58.51	80.39	66.96	77.17	55.78

28 SW105 PR 30 SW105 PR 32 SW105 PR 34 SW105 PR 36 SW105 PR
29 SW105 PC 31 SW105 PC 33 SW105 PC 35 SW105 PC

	37	38	39	40	41	42	43	44	45
SiO2	38.97	37.45	38.98	37.75	38.19	37.69	38.00	36.19	40.35
Al2O3	0.04	0.06	0.08	0.07	0.08	0.10	0.05	0.07	0.07
FeO	21.93	29.74	20.77	26.64	22.25	27.62	25.81	29.80	19.52
MnO	0.34	0.60	0.33	0.49	0.34	0.50	0.45	0.60	0.28
NiO	0.22	0.16	0.20	0.15	0.19	0.17	0.20	0.17	0.21
MgO	39.41	32.51	40.40	35.48	39.38	34.80	36.49	33.52	40.39
CaO	0.26	0.43	0.42	0.43	0.26	0.45	0.41	0.43	0.29
total=	101.17	100.95	101.18	101.01	100.69	101.33	101.41	100.78	101.11
Si	1.00	1.00	1.00	0.99	0.99	0.99	0.99	0.97	1.02
Fe2	0.47	0.67	0.44	0.59	0.48	0.61	0.56	0.67	0.41
Mn	-	0.01	-	0.01	-	0.01	-	0.01	-
Mg	1.51	1.30	1.54	1.39	1.52	1.37	1.42	1.35	1.52
Ca	-	0.01	0.01	0.01	-	0.01	0.01	0.01	-
total=	3.00	3.00	3.00	3.00	3.01	3.00	3.01	3.02	2.98
oxygens=	[4]	[4]	[4]	[4]	[4]	[4]	[4]	[4]	[4]
Fo	76.21	66.08	77.61	70.36	75.93	69.19	71.59	66.72	78.67

37 SW383 PC 39 SW383 PC 41 SW383 PC 43 SW383 PC 45 SW383 PC
38 SW383 PR 40 SW383 PR 42 SW383 PR 44 SW385 PR

	46
SiO2	39.74
Al2O3	0.05
FeO	23.62
MnO	0.42
NiO	0.18
MgO	36.21
CaO	0.42
total=	100.64
Si	1.03
Fe2	0.51
Mg	1.40
Ca	0.01
total=	2.97
oxygens=	[4]
Fo	73.20

46 SW383 PR

Mauchline group

	47	48	49	50	51	52	53	54	55
SiO2	39.35	38.76	39.57	37.84	40.05	37.72	39.50	36.80	38.63
Al2O3	0.09	0.08	0.09	0.09	0.03	0.05	0.20	0.09	0.08
FeO	15.99	17.76	15.07	23.45	11.24	25.35	18.25	26.69	18.08
MnO	0.28	0.26	0.24	0.38	0.20	0.38	0.18	0.45	0.27
NiO	0.25	0.18	0.24	0.16	0.33	0.19	0.28	0.15	0.19
MgO	44.06	42.84	44.99	38.46	47.90	36.59	45.16	35.93	42.62
CaO	0.21	0.28	0.25	0.36	0.04	0.38	0.26	0.37	0.35
total=	100.23	100.16	100.45	100.74	99.79	100.66	99.83	100.48	100.22
Si	0.99	0.99	0.99	0.99	0.99	0.99	0.99	0.98	0.99
Fe2	0.34	0.38	0.32	0.51	0.23	0.56	0.30	0.59	0.39
Mn	-	-	-	-	-	-	-	0.01	-
Mg	1.66	1.63	1.68	1.49	1.77	1.43	1.69	1.42	1.62
Ca	-	-	-	0.01	-	0.01	-	0.01	-
total=	3.01	3.01	3.01	3.01	3.01	3.01	3.00	3.02	3.01
oxygens=	[4]	[4]	[4]	[4]	[4]	[4]	[4]	[4]	[4]
Fo	83.08	81.13	84.18	74.51	88.37	72.01	84.96	70.58	80.77

47 SW152 PC
48 SW152 PC
49 SW152 PC
50 SW152 PR
51 SW152 PC
52 SW152 PR
53 SW152 PC
54 SW152 PR
55 SW152 PR

	56	57	58	59	60	61	62	63	64
SiO2	39.85	38.89	39.19	38.59	38.35	39.56	37.94	40.29	38.54
Al2O3	0.11	0.08	0.04	0.06	0.05	0.03	0.06	0.03	0.04
FeO	13.96	18.57	17.35	22.31	21.50	14.89	24.73	11.78	20.45
MnO	0.18	0.27	0.24	0.35	0.34	0.22	0.45	0.15	0.33
NiO	0.32	0.22	0.25	0.22	0.21	0.35	0.17	0.37	0.24
MgO	45.44	41.72	42.87	39.31	39.77	45.34	37.31	47.73	40.78
CaO	0.30	0.30	0.24	0.27	0.26	0.21	0.34	0.09	0.24
total=	100.16	100.05	100.18	101.11	100.48	100.60	101.00	100.44	100.62
Si	1.00	0.99	1.00	0.99	0.99	0.99	0.99	0.99	0.99
Fe2	0.29	0.40	0.37	0.48	0.46	0.31	0.54	0.24	0.44
Mg	1.69	1.59	1.62	1.51	1.53	1.69	1.45	1.75	1.56
total=	3.00	3.00	3.00	3.01	3.01	3.01	3.01	3.01	3.01
oxygens=	[4]	[4]	[4]	[4]	[4]	[4]	[4]	[4]	[4]
Fo	85.30	80.02	81.49	75.85	76.73	84.44	72.89	87.84	78.04

56 SW152 PC
57 SW152 PR
58 SW161C PC
59 SW161C PC
60 SW161C PC
61 SW161C XC
62 SW161C XR
63 SW616CXC
64 SW161C XR

	65	66	67	68	69	70	71	72	73
SiO2	37.36	37.37	37.80	36.53	35.60	37.00	38.80	37.81	38.37
Al2O3	0.06	0.05	0.06	0.07	0.09	0.04	0.25	0.05	0.09
FeO	23.55	26.24	25.83	27.39	28.23	21.02	12.91	17.29	13.14
MnO	0.41	0.50	0.45	0.51	0.53	0.30	0.17	0.29	0.18
NiO	0.15	0.15	0.12	0.11	0.08	0.14	0.33	0.25	0.33
MgO	38.04	36.41	36.07	35.63	34.27	40.27	46.51	43.33	46.88
CaO	0.31	0.33	0.31	0.40	0.44	0.37	0.24	0.28	0.26
total=	99.88	101.05	100.64	100.64	99.24	99.14	99.21	99.30	99.25
Si	0.98	0.98	1.00	0.97	0.97	0.97	0.98	0.97	0.97
Fe2	0.52	0.58	0.57	0.61	0.64	0.46	0.27	0.37	0.28
Mn	-	0.01	0.01	0.01	0.01	-	-	-	-
Mg	1.49	1.43	1.42	1.41	1.39	1.58	1.75	1.66	1.76
Ca	-	-	-	0.01	0.01	0.01	-	-	-
total=	3.02	3.02	3.00	3.03	3.03	3.03	3.02	3.03	3.03
oxygens=	[4]	[4]	[4]	[4]	[4]	[4]	[4]	[4]	[4]
Fo	74.22	71.21	71.38	69.87	68.39	77.35	86.52	81.70	86.41

65 SW161C PC
66 SW161C PR
67 SW161C PR
68 SW161C PC
69 SW161C PR
70 SW161C PC
71 PA01 PC
72 PA01 PR
73 PA01 PC

	74	75	76	77	78
SiO2	37.21	38.61	36.33	38.50	37.43
Al2O3	0.08	0.04	0.07	0.05	0.08
FeO	20.01	14.06	24.46	11.30	23.20
MnO	0.38	0.22	0.50	0.15	0.45
NiO	0.23	0.31	0.17	0.32	0.19
MgO	40.73	46.26	37.50	48.10	38.63
CaO	0.30	0.08	0.43	0.09	0.32
total=	98.94	99.58	99.46	98.51	100.30
Si	0.97	0.97	0.97	0.97	0.98
Fe2	0.44	0.30	0.54	0.24	0.51
Mn	-	-	0.01	-	-
Mg	1.59	1.74	1.49	1.81	1.51
Ca	-	-	0.01	-	-
total=	3.02	3.03	3.03	3.03	3.02
oxygens=	[4]	[4]	[4]	[4]	[4]
Fo	78.39	85.43	73.21	88.35	74.80

74 PA01 PR 76 PA01 PR 78 PA01 XR
75 PA01 PC 77 PA01 XC

Fife & Lothian sills

	78a	79	80	81	82	83	84	85	86
SiO2	35.07	36.63	37.21	37.59	38.85	37.04	38.16	39.18	37.94
Al2O3	nd	nd	nd	nd	0.05	0.05	0.06	0.04	0.05
FeO	40.74	29.64	28.20	27.08	22.13	28.67	27.70	22.51	30.10
MnO	0.69	0.45	0.43	0.38	0.35	0.43	0.41	0.35	0.46
NiO	0.05	0.13	0.13	0.12	0.17	0.14	0.12	0.13	0.07
MgO	23.29	32.85	33.81	34.85	39.60	34.11	34.17	38.54	32.45
CaO	0.42	0.41	0.40	0.39	0.29	0.37	0.32	0.36	0.39
total=	100.26	100.11	100.18	100.41	101.44	100.81	100.94	101.11	101.46
Si	1.00	0.99	1.00	1.00	1.00	0.99	1.01	1.01	1.01
Fe2	0.97	0.67	0.63	0.60	0.47	0.64	0.61	0.48	0.67
Mn	0.02	0.01	-	-	-	-	-	-	0.01
Mg	0.99	1.32	1.35	1.38	1.51	1.36	1.35	1.48	1.29
Ca	0.01	0.01	0.01	0.01	-	0.01	-	-	0.01
total=	3.00	3.01	3.00	3.00	3.00	3.01	2.99	2.99	2.99
oxygens=	[4]	[4]	[4]	[4]	[4]	[4]	[4]	[4]	[4]
Fo	50.47	66.39	68.12	69.64	76.13	67.95	68.78	75.32	65.77

78a SW48 G 80 SW48 G 82 SW48 PC 84 SW48 PR 86 SW48 PR
79 SW48 G 81 SW48 G 83 SW48 PR 85 SW48 PC

	87	88	89	90	91	92	93	94	95
SiO2	39.46	38.11	38.35	39.48	38.58	38.90	39.22	38.79	38.22
Al2O3	0.04	0.04	0.06	0.04	0.02	0.05	nd	0.01	0.01
FeO	21.50	26.71	27.33	21.81	25.27	20.25	16.58	18.94	18.55
MnO	0.31	0.36	0.39	0.31	0.38	0.30	0.22	0.26	0.25
NiO	0.13	0.09	0.10	0.15	0.11	0.21	0.21	0.21	0.22
MgO	39.55	35.17	34.53	39.02	36.01	40.79	43.59	42.10	41.99
CaO	0.30	0.39	0.36	0.29	0.34	0.29	0.27	0.30	0.28
total=	101.29	100.87	101.12	101.10	100.67	100.79	100.05	100.61	99.52
Si	1.01	1.00	1.01	1.01	1.01	1.00	0.99	0.99	0.98
Fe2	0.46	0.59	0.60	0.47	0.55	0.43	0.35	0.40	0.40
Mg	1.51	1.38	1.36	1.49	1.41	1.56	1.65	1.60	1.61
Ca	-	0.01	0.01	-	-	-	-	-	-
total=	2.99	3.00	2.99	2.99	2.99	3.00	3.01	3.01	3.02
oxygens=	[4]	[4]	[4]	[4]	[4]	[4]	[4]	[4]	[4]
Fo	76.63	70.12	69.25	76.13	71.75	78.22	82.45	79.85	80.14

87 SW48 PC 89 SW48 PR 91 SW48 PR 93 SW415 PC 95 SW415 PC
88 SW48 PC 90 SW48 PC 92 SW415 PC 94 SW415 PR

	96	97	98	99	100	101	102	103	104
SiO2	36.48	38.68	36.33	37.89	40.11	38.79	38.73	38.57	38.39
Al2O3	0.01	nd	0.02	0.02	0.05	0.06	0.07	0.07	0.07
FeO	31.95	21.38	33.39	27.63	17.63	20.80	19.57	19.96	22.22
MnO	0.58	0.32	0.58	0.48	0.29	0.45	0.36	0.38	0.47
NiO	0.11	0.18	0.11	0.15	0.22	0.15	0.16	0.17	0.18
MgO	31.30	39.78	29.80	34.93	42.16	39.97	41.22	40.89	39.13
CaO	0.45	0.29	0.42	0.31	0.31	0.29	0.29	0.27	0.38
total=	100.88	100.87	100.65	101.37	100.77	100.51	100.40	100.27	100.76
Si	0.99	1.00	0.99	1.00	1.01	1.00	0.99	0.99	0.99
Fe2	0.73	0.46	0.76	0.61	0.37	0.45	0.42	0.43	0.48
Mn	0.01	-	0.01	-	-	-	-	-	0.01
Mg	1.27	1.53	1.22	1.37	1.58	1.53	1.57	1.57	1.51
Ca	0.01	-	0.01	-	-	-	-	-	-
total=	3.01	3.00	3.00	3.00	2.99	3.00	3.01	3.01	3.01
oxygens=	[4]	[4]	[4]	[4]	[4]	[4]	[4]	[4]	[4]
Fo	63.58	76.85	61.40	69.26	81.00	77.40	78.96	78.50	75.84

96 SW815 PR
97 SW815 PC
98 SW815 PR
99 SW815 PC
100 SW815 PC
101 SW872 PC
102 SW872 PR
103 SW872 PC
104 SW872 PR

	105	106	107	108	109	110	111	112	113
SiO2	38.83	37.81	38.80	38.19	37.98	37.78	37.02	38.88	38.11
Al2O3	0.06	0.07	0.01	0.05	0.11	0.06	0.06	0.07	0.06
FeO	17.61	21.08	15.71	22.17	22.86	24.03	29.71	20.87	25.26
MnO	0.27	0.41	0.21	0.45	0.50	0.53	0.47	0.33	0.40
NiO	0.20	0.19	0.32	0.19	0.14	0.13	0.11	0.13	0.11
MgO	42.72	39.95	44.81	39.56	38.64	37.74	33.59	40.59	37.01
CaO	0.30	0.26	0.19	0.25	0.27	0.33	0.34	0.30	0.29
total=	99.99	99.73	100.05	100.86	100.50	100.60	101.30	101.17	101.24
Si	0.99	0.98	0.98	0.99	0.99	0.99	0.99	0.99	0.99
Fe2	0.38	0.46	0.33	0.48	0.50	0.53	0.66	0.45	0.55
Mn	-	-	-	-	0.01	0.01	0.01	-	-
Mg	1.62	1.55	1.69	1.52	1.50	1.47	1.34	1.55	1.48
total=	3.01	3.01	3.02	3.01	3.01	3.01	3.01	3.01	3.01
oxygens=	[4]	[4]	[4]	[4]	[4]	[4]	[4]	[4]	[4]
Fo	81.22	77.19	83.56	76.08	75.08	73.68	66.83	77.61	72.31

105 SW872 PC
106 SW872 PR
107 SW872 PC
108 SW872 PR
109 SW872 PC
110 SW872 PR
111 SW566 PC
112 SW566 PR
113 SW566 PC

	114	115	116	117	118	119	120	121	122
SiO2	38.62	40.40	40.63	39.26	38.89	40.79	40.18	39.96	38.95
Al2O3	0.05	1.47	0.04	0.08	0.06	0.06	0.07	0.04	0.08
FeO	22.80	15.76	18.49	24.37	28.59	17.29	21.65	21.03	27.22
MnO	0.30	0.18	0.23	0.34	0.47	0.24	0.32	0.26	0.38
NiO	0.16	0.23	0.24	0.19	0.16	0.19	0.18	0.12	0.16
MgO	38.99	42.02	41.66	36.63	32.92	41.13	38.65	39.45	34.15
CaO	0.21	0.13	0.15	0.28	0.32	0.28	0.30	0.08	0.31
total=	101.13	100.19	101.44	101.15	101.41	99.98	101.31	100.94	101.25
Si	1.00	1.01	1.02	1.02	1.03	1.03	1.02	1.02	1.02
Al	-	0.04	-	-	-	-	-	-	-
Fe2	0.49	0.33	0.39	0.53	0.63	0.37	0.46	0.45	0.60
Mn	-	-	-	-	0.01	-	-	-	-
Mg	1.50	1.57	1.56	1.41	1.29	1.55	1.47	1.50	1.34
total=	3.00	2.97	2.98	2.98	2.97	2.97	2.98	2.98	2.98
oxygens=	[4]	[4]	[4]	[4]	[4]	[4]	[4]	[4]	[4]
Fo	75.30	82.62	80.06	72.82	67.28	80.92	76.09	76.98	69.10

114 SW566 PC
115 SW566 PC
116 SW566 PR
117 SW566 PC
118 SW566 PR
119 SW566 PC
120 SW566 PR
121 SW566 PC
122 SW566 PR

Fife & Lothian basanites

	122a	123	124	125	126	127	128	129	130
SiO2	38.70	37.94	38.78	38.80	38.38	38.58	39.08	40.79	39.46
Al2O3	0.04	0.07	0.07	0.07	0.07	0.07	0.07	0.09	0.07
FeO	10.10	16.15	15.45	13.53	17.07	13.48	12.19	13.31	18.41
MnO	0.17	0.26	0.23	0.21	0.28	0.20	0.16	0.19	0.30
NiO	0.38	0.29	0.28	0.33	0.22	0.31	0.32	0.28	0.19
MgO	50.19	44.88	44.47	45.96	43.07	46.24	47.02	46.33	42.25
CaO	0.06	0.23	0.21	0.17	0.24	0.21	0.18	0.15	0.20
total=	99.64	99.82	99.49	99.07	99.33	99.09	99.02	101.14	100.88
Si	0.96	0.97	0.98	0.98	0.98	0.98	0.98	1.00	1.00
Fe2	0.21	0.34	0.33	0.29	0.37	0.29	0.26	0.27	0.39
Mg	1.86	1.70	1.68	1.73	1.65	1.74	1.76	1.70	1.59
total=	3.04	3.03	3.01	3.02	3.02	3.02	3.02	2.99	3.00
oxygens=	[4]	[4]	[4]	[4]	[4]	[4]	[4]	[4]	[4]
Fo	0.90	0.83	0.84	0.86	0.82	0.86	0.87	0.86	0.80

122A SW4A PR 124 SW4A PR 126 SW4A PR 128 SW4A PC 130 SW4A PR
123 SW4A PR 125 SW4A PC 127 SW4A PR 129 SW4A PC

	131	132	133	134	135	136	137	138	139
SiO2	37.86	39.02	39.05	39.43	38.38	39.23	38.84	39.30	40.54
Al2O3	0.06	0.07	0.07	0.05	0.08	0.07	0.07	0.11	0.08
FeO	13.53	15.33	13.09	14.22	17.62	15.04	16.33	16.08	15.20
MnO	0.23	0.25	0.21	0.21	0.25	0.24	0.28	0.22	0.19
NiO	0.31	0.26	0.32	0.27	0.20	0.24	0.20	0.14	0.19
MgO	46.74	45.01	46.84	45.24	43.07	45.13	43.57	43.40	44.35
CaO	0.24	0.26	0.21	0.26	0.19	0.25	0.30	0.30	0.23
total=	98.97	100.20	99.79	99.68	99.79	100.20	99.59	99.55	100.78
Si	0.96	0.98	0.98	0.99	0.98	0.99	0.99	1.00	1.01
Fe2	0.29	0.32	0.27	0.30	0.38	0.32	0.35	0.34	0.32
Mg	1.77	1.69	1.75	1.70	1.64	1.69	1.65	1.64	1.65
total=	3.04	3.02	3.02	3.01	3.02	3.01	3.01	3.00	2.99
oxygens=	[4]	[4]	[4]	[4]	[4]	[4]	[4]	[4]	[4]
Fo	0.86	0.84	0.86	0.85	0.81	0.84	0.83	0.83	0.84

131 SW6 PC 133 SW6 PC 135 SW6 PR 137 SW6 PR 139 SW6 PC
132 SW6 PR 134 SW6 PR 136 SW6 PR 138 SW6 PC

	140	141	142	143	144	145	146	147	148
SiO2	40.06	39.44	38.69	37.44	37.55	38.25	38.68	38.26	37.78
Al2O3	0.08	0.09	0.09	0.09	0.11	0.08	0.09	0.10	0.10
FeO	16.07	18.72	23.83	23.28	25.76	21.26	24.19	21.29	22.43
MnO	0.20	0.33	0.47	0.44	0.57	0.37	0.49	0.38	0.42
NiO	0.16	0.18	0.09	0.09	0.06	0.18	0.08	0.16	0.13
MgO	43.80	41.65	37.84	37.52	35.43	39.80	37.36	40.20	38.28
CaO	0.27	0.25	0.43	0.42	0.48	0.25	0.43	0.26	0.36
total=	100.64	100.66	101.44	99.28	99.96	100.19	101.32	100.65	99.50
Si	1.00	1.00	1.00	0.99	1.00	0.99	1.00	0.99	0.99
Fe2	0.34	0.40	0.51	0.51	0.57	0.46	0.52	0.46	0.49
Mn	-	-	0.01	-	0.01	-	0.01	-	-
Mg	1.64	1.58	1.46	1.48	1.40	1.54	1.44	1.54	1.50
Ca	-	-	0.01	0.01	0.01	-	0.01	-	0.01
total=	2.99	3.00	3.00	3.01	3.00	3.01	3.00	3.01	3.01
oxygens=	[4]	[4]	[4]	[4]	[4]	[4]	[4]	[4]	[4]
Fo	0.83	0.80	0.74	0.74	0.71	0.77	0.73	0.77	0.75

140 SW6 PR 142 SW8 PR 144 SW8 PR 146 SW8 PR 148 SW8 PR
141 SW8 PC 143 SW8 PC 145 SW8 PC 147 SW8 PC

	149	150	151	152	153	154	155	156	157
SiO2	37.20	39.41	38.88	38.92	39.39	39.25	39.21	40.17	40.26
Al2O3	0.08	0.08	0.08	0.09	0.08	0.08	0.08	0.07	0.08
FeO	25.53	17.87	23.24	22.95	17.88	19.33	19.95	17.04	14.88
MnO	0.58	0.31	0.46	0.43	0.26	0.31	0.27	0.23	0.20
NiO	0.07	0.21	0.09	0.10	0.20	0.20	0.12	0.22	0.26
MgO	35.92	42.01	37.95	38.10	41.76	41.19	40.58	42.87	44.47
CaO	0.46	0.23	0.43	0.42	0.26	0.27	0.17	0.24	0.24
total=	99.80	100.12	101.13	101.01	99.83	100.63	100.34	100.84	100.39
Si	0.99	1.00	1.00	1.01	1.00	1.00	1.00	1.01	1.01
Fe2	0.57	0.38	0.50	0.50	0.38	0.41	0.43	0.36	0.31
Mn	0.01	-	0.01	-	-	-	-	-	-
Mg	1.42	1.59	1.46	1.47	1.59	1.57	1.55	1.61	1.66
Ca	0.01	-	0.01	0.01	-	-	-	-	-
total=	3.01	3.00	2.99	2.99	2.99	3.00	2.99	2.99	2.99
oxygens=	[4]	[4]	[4]	[4]	[4]	[4]	[4]	[4]	[4]
Fo	0.71	0.81	0.74	0.75	0.81	0.79	0.78	0.82	0.84

149 SW8 PC
150 SW8 PC
151 SW8 PR
152 SW8 XC
153 SW8 XC
154 SW9 PR
155 SW9 PR
156 SW9 PR
157 SW9 PC

	158	159	160	161	162	163	164	165	166
SiO2	39.27	40.25	39.85	40.10	40.06	38.22	38.36	38.46	36.87
Al2O3	0.08	0.07	0.06	0.08	0.07	0.09	0.18	0.06	0.02
FeO	17.83	15.30	16.04	12.86	15.62	22.71	22.64	16.94	27.30
MnO	0.31	0.21	0.25	0.14	0.24	0.45	0.44	0.21	0.47
NiO	0.23	0.28	0.25	0.36	0.25	0.15	0.16	0.22	0.17
MgO	41.50	44.36	43.52	45.87	43.44	37.74	37.61	43.63	35.23
CaO	0.22	0.22	0.25	0.22	0.26	0.32	0.37	0.22	0.38
total=	99.44	100.69	100.22	99.63	99.94	99.68	99.76	99.74	100.44
Si	1.01	1.01	1.00	1.00	1.01	1.00	1.00	0.98	0.98
Fe2	0.38	0.32	0.34	0.27	0.33	0.50	0.50	0.36	0.61
Mn	-	-	-	-	-	-	-	-	0.01
Mg	1.58	1.65	1.63	1.71	1.63	1.47	1.47	1.66	1.40
Ca	-	-	-	-	-	-	0.01	-	0.01
total=	2.99	2.99	3.00	3.00	2.99	3.00	2.99	3.02	3.02
oxygens=	[4]	[4]	[4]	[4]	[4]	[4]	[4]	[4]	[4]
Fo	0.81	0.84	0.83	0.86	0.83	0.75	0.75	0.82	0.70

158 SW9 PR
159 SW9 PC
160 SW9 PR
161 SW9 PC
162 SW9 PR
163 SW9 PC
164 SW9 PR
165 SW25 PC
166 SW25 PR

	167	168	169	170	171	172	173	174	175
SiO2	37.54	36.23	38.24	35.83	40.17	37.25	38.35	41.25	40.93
Al2O3	0.01	0.03	0.04	0.05	nd	0.01	0.08	0.03	0.03
FeO	25.84	29.31	18.61	27.93	8.28	23.03	26.84	12.18	11.90
MnO	0.41	0.55	0.26	0.52	0.11	0.35	0.44	0.17	0.15
NiO	0.15	0.13	0.27	0.13	0.35	0.21	0.15	0.36	0.33
MgO	36.65	33.46	42.00	34.00	49.89	38.26	34.72	46.74	46.42
CaO	0.17	0.46	0.19	0.42	0.05	0.25	0.42	0.05	0.06
total=	100.77	100.17	99.61	98.88	98.85	99.36	101.00	100.78	99.82
Si	0.99	0.98	0.98	0.98	0.99	0.98	1.01	1.01	1.01
Fe2	0.57	0.66	0.40	0.64	0.17	0.51	0.59	0.25	0.25
Mn	-	0.01	-	0.01	-	-	-	-	-
Mg	1.44	1.35	1.61	1.38	1.84	1.51	1.36	1.71	1.71
Ca	-	0.01	-	0.01	-	-	0.01	-	-
total=	3.01	3.02	3.01	3.02	3.01	3.02	2.99	2.99	2.99
oxygens=	[4]	[4]	[4]	[4]	[4]	[4]	[4]	[4]	[4]
Fo	0.72	0.67	0.80	0.68	0.91	0.75	0.70	0.87	0.87

167 SW25 PC
168 SW25 PR
169 SW25 PC
170 SW25 PR
171 SW25 PC
172 SW25 PR
173 SW25 PR
174 SW25 XC
175 SW25 XC

	176	177	178	179	180	181	182	183	184
SiO2	38.42	37.48	37.62	37.94	37.66	38.37	38.02	38.91	38.67
Al2O3	0.06	0.05	0.07	0.07	0.07	0.05	0.07	0.10	0.06
FeO	26.74	19.42	19.05	17.65	19.21	17.43	17.70	15.42	19.19
MnO	0.45	0.23	0.23	0.22	0.23	0.19	0.21	0.16	0.23
NiO	0.15	0.17	0.20	0.17	0.17	0.20	0.17	0.19	0.18
MgO	35.17	41.43	42.16	42.76	41.71	42.73	42.29	42.59	41.68
CaO	0.41	0.22	0.25	0.22	0.24	0.24	0.24	0.20	0.27
total=	101.40	99.00	99.58	99.03	99.31	99.21	98.70	99.57	100.28
Si	1.01	0.98	0.97	0.98	0.98	0.99	0.98	0.99	0.99
Fe2	0.59	0.42	0.41	0.38	0.42	0.37	0.38	0.33	0.41
Mg	1.37	1.61	1.62	1.64	1.61	1.64	1.63	1.68	1.59
Ca	0.01	-	-	-	-	-	-	-	-
total=	2.99	3.02	3.03	3.02	3.02	3.01	3.02	3.01	3.01
oxygens=	[4]	[4]	[4]	[4]	[4]	[4]	[4]	[4]	[4]
Fo	0.70	0.79	0.80	0.81	0.79	0.81	0.81	0.84	0.79

176 SW25 PR 178 SW40 PR 180 SW40 PR 182 SW40 PR 184 SW40 PR
177 SW40 PC 179 SW40 PC 181 SW40 PC 183 SW40 PC

	185	186	187	188	189	190	191	192	193
SiO2	39.06	38.74	37.41	37.88	38.87	39.42	38.44	36.67	40.04
Al2O3	0.10	0.07	0.08	0.07	0.39	0.08	0.06	0.05	0.07
FeO	16.83	20.42	28.11	26.03	20.71	12.61	19.43	23.34	12.72
MnO	0.20	0.27	0.47	0.41	0.36	0.17	0.30	0.43	0.17
NiO	0.23	0.10	0.09	0.09	0.26	0.03	0.23	0.14	0.35
MgO	43.21	40.30	34.83	36.11	39.88	46.80	41.55	38.27	46.92
CaO	0.21	0.31	0.31	0.29	0.35	0.22	0.26	0.43	0.21
total=	99.84	100.21	101.30	100.88	100.82	99.33	100.27	99.33	100.48
Si	0.99	1.00	0.99	1.00	1.00	0.99	0.99	0.97	0.99
Al	-	-	-	-	0.01	-	-	-	-
Fe2	0.36	0.44	0.62	0.57	0.44	0.26	0.42	0.52	0.26
Mn	-	-	0.01	-	-	-	-	-	-
Mg	1.64	1.55	1.37	1.41	1.52	1.75	1.59	1.51	1.73
Ca	-	-	-	-	-	-	-	0.01	-
total=	3.01	3.00	3.01	3.00	3.00	3.01	3.01	3.03	3.01
oxygens=	[4]	[4]	[4]	[4]	[4]	[4]	[4]	[4]	[4]
Fo	0.82	0.78	0.69	0.71	0.77	0.87	0.79	0.75	0.87

185 SW40 PC 187 SW40 PC 189 SW436 PC 191 SW436 PR 193 SW436 PC
186 SW40 PR 188 SW40 PR 190 SW436 PC 192 SW436 PC

	194	195	196	197	198	199	200	201	202
SiO2	38.39	39.24	39.11	38.00	38.98	39.97	40.17	39.51	39.51
Al2O3	0.05	0.04	0.05	0.07	0.06	0.07	0.07	0.07	0.07
FeO	22.68	17.47	17.00	24.35	18.36	12.46	12.79	15.54	16.70
MnO	0.39	0.23	0.28	0.37	0.31	0.20	0.20	0.24	0.29
NiO	0.15	0.24	0.17	0.18	0.18	0.33	0.28	0.25	0.21
MgO	39.08	43.04	43.08	37.27	42.15	46.97	46.48	44.56	43.59
CaO	0.30	0.24	0.34	0.22	0.35	0.21	0.26	0.28	0.31
total=	101.04	100.50	100.03	100.46	100.39	100.21	100.25	100.45	100.68
Si	0.99	0.99	0.99	1.00	0.99	0.99	1.00	0.99	1.00
Fe2	0.49	0.37	0.36	0.53	0.39	0.26	0.27	0.33	0.35
Mg	1.50	1.62	1.63	1.45	1.60	1.78	1.72	1.67	1.64
total=	3.01	3.01	3.01	3.00	3.01	3.01	3.00	3.01	3.00
oxygens=	[4]	[4]	[4]	[4]	[4]	[4]	[4]	[4]	[4]
Fo	0.75	0.81	0.82	0.73	0.80	0.87	0.87	0.84	0.82

194 SW436 PR 196 SW442 XR 198 SW442 XR 200 SW442 PR 202 SW442 PR
195 SW442 XC 197 SW442 XC 199 SW442 PC 201 SW442 PC

	203	204	205	206	207	208	209	210	211
SiO2	38.90	38.85	39.39	38.87	39.29	38.74	36.79	37.76	38.45
Al2O3	0.05	0.06	0.07	0.08	0.08	0.05	0.04	0.07	0.05
FeO	21.87	18.81	14.42	16.94	13.37	15.72	23.00	19.27	16.60
MnO	0.35	0.34	0.21	0.27	0.19	0.21	0.33	0.28	0.26
NiO	0.19	0.18	0.27	0.21	0.28	0.20	0.11	0.17	0.22
MgO	39.75	41.91	45.29	43.01	45.61	44.30	38.90	41.51	44.55
CaO	0.23	0.32	0.20	0.31	0.26	0.29	0.21	0.34	0.14
total=	101.34	100.47	99.85	99.69	99.08	99.51	99.38	99.40	100.27
Si	1.00	0.99	0.99	0.99	0.99	0.98	0.97	0.98	0.97
Fe2	0.47	0.40	0.30	0.36	0.28	0.33	0.51	0.42	0.35
Mg	1.52	1.59	1.70	1.63	1.72	1.68	1.53	1.60	1.68
total=	3.00	3.01	3.01	3.01	3.01	3.01	3.03	3.02	3.02
oxygens=	[4]	[4]	[4]	[4]	[4]	[4]	[4]	[4]	[4]
Fo	0.76	0.80	0.85	0.82	0.86	0.83	0.75	0.79	0.83

203 SW442 XC 205 SW442 PC 207 SW442 PC 209 SW442 PC 211 SW526 XC
204 SW442 XR 206 SW442 PR 208 SW442 PR 210 SW442 PR

	212	213	214	215	216	217	218	219	220
SiO2	39.18	39.42	38.87	38.49	39.10	39.16	38.37	39.93	40.36
Al2O3	0.07	0.09	0.09	0.07	0.08	0.08	0.10	0.07	0.08
FeO	15.77	15.47	18.00	20.86	18.19	16.48	17.06	16.87	15.39
MnO	0.25	0.24	0.27	0.31	0.29	0.25	0.28	0.25	0.22
NiO	0.20	0.21	0.20	0.17	0.18	0.23	0.18	0.25	0.25
MgO	44.13	44.44	42.08	40.23	42.09	43.10	42.96	43.73	44.78
CaO	0.22	0.28	0.32	0.10	0.33	0.21	0.35	0.22	0.27
total=	99.82	100.15	99.83	100.23	100.26	99.51	99.30	101.32	101.31
Si	0.99	0.99	0.99	0.99	1.00	1.00	0.98	1.00	1.00
Fe2	0.33	0.33	0.38	0.45	0.39	0.35	0.37	0.35	0.32
Mg	1.66	1.67	1.60	1.55	1.60	1.64	1.64	1.63	1.66
total=	3.01	3.01	3.00	3.01	3.00	3.00	3.01	3.00	3.00
oxygens=	[4]	[4]	[4]	[4]	[4]	[4]	[4]	[4]	[4]
Fo	0.83	0.84	0.81	0.77	0.80	0.82	0.82	0.82	0.84

212 SW526 XR 214 SW526 PR 216 SW526 XR 218 SW526 PR 220 SW526 XR
213 SW526 PC 215 SW526 XC 217 SW526 PC 219 SW526 XC

	221	222	223	224
SiO2	39.82	40.00	39.59	39.50
Al2O3	0.10	0.07	0.08	0.09
FeO	15.81	16.52	15.77	15.78
MnO	0.24	0.27	0.20	0.24
NiO	0.17	0.19	0.18	0.21
MgO	44.56	43.46	44.38	43.98
CaO	0.26	0.35	0.26	0.32
total=	100.96	100.86	100.46	100.12
Si	1.00	1.00	0.99	1.00
Fe2	0.33	0.35	0.33	0.33
Mg	1.66	1.62	1.66	1.65
total=	3.00	3.00	3.00	3.00
oxygens=	[4]	[4]	[4]	[4]
Fo	0.83	0.82	0.83	0.83

221 SW526 PC 223 SW526 PC
222 SW526 PR 224 SW526 PR

Passage Group lavas

	1	2	3	4	5	6	7	8	9
SiO2	51.45	51.82	53.89	53.17	52.98	53.04	53.07	51.50	53.17
Al2O3	30.10	29.05	28.60	28.68	29.50	28.93	29.08	29.27	28.77
FeO	0.61	1.15	0.63	0.59	0.56	0.55	0.57	0.58	0.31
MgO	0.06	0.48	0.13	0.12	0.15	0.15	0.16	0.18	0.08
CaO	13.02	12.29	12.09	12.10	12.81	12.53	12.23	12.89	11.50
Na2O	4.15	4.25	4.66	4.62	4.28	4.43	4.59	4.10	4.93
K2O	0.27	0.26	0.26	0.29	0.23	0.23	0.25	0.20	0.37
BaO	0.08	0.08	0.03	0.03	0.03	0.01	nd	0.01	0.03
total=	99.70	99.31	100.28	99.61	100.49	99.87	99.91	98.78	99.12
Si	9.41	9.53	9.76	9.70	9.58	9.66	9.65	9.50	9.73
Al	6.49	6.29	6.10	6.17	6.29	6.21	6.23	6.37	6.20
Fe2	0.09	0.18	0.09	0.09	0.08	0.08	0.09	0.09	0.05
Mg	0.02	0.12	0.03	0.03	0.04	0.04	0.04	0.05	0.01
Ca	2.55	2.42	2.35	2.37	2.49	2.48	2.38	2.55	2.25
Na	1.47	1.51	1.64	1.63	1.50	1.56	1.62	1.47	1.75
K	0.06	0.06	0.06	0.07	0.05	0.05	0.06	0.05	0.09
total=	20.11	20.12	20.04	20.06	20.04	20.05	20.07	20.07	20.09
oxygens=	[32]	[32]	[32]	[32]	[32]	[32]	[32]	[32]	[32]

1 SW265 G
2 SW265 G
3 SW270 G
4 SW270 G
5 SW270 G
6 SW270 G
7 SW277 G
8 SW277 G
9 SW307 PC

	10	11	12	13	14	15	16	17	18
SiO2	53.72	53.41	50.93	50.35	58.49	54.60	55.15	51.85	52.36
Al2O3	28.20	28.14	30.37	30.15	24.98	27.42	27.90	30.42	30.82
FeO	0.32	0.45	0.36	0.36	0.33	1.17	0.32	0.38	0.32
MgO	0.04	0.04	0.03	0.02	0.05	0.39	0.03	0.04	0.02
CaO	11.46	10.92	13.78	13.73	7.70	9.88	10.58	13.39	13.62
Na2O	4.94	5.26	3.73	3.64	6.76	5.40	5.52	3.76	3.81
K2O	0.36	0.40	0.23	0.27	0.71	0.45	0.44	0.25	0.25
BaO	0.03	0.07	0.03	0.13	0.17	0.08	0.06	0.03	0.01
total=	99.07	98.69	99.46	98.65	99.19	99.40	100.00	100.11	101.21
Si	9.83	9.82	9.34	9.32	10.59	9.96	9.98	9.43	9.42
Al	6.08	6.10	6.57	6.58	5.33	5.90	5.95	6.52	6.53
Fe2	0.05	0.07	0.06	0.06	0.05	0.18	0.05	0.06	0.05
Mg	0.01	0.01	-	-	0.01	0.11	-	0.01	-
Ca	2.25	2.15	2.71	2.72	1.49	1.93	2.05	2.61	2.62
Na	1.75	1.87	1.33	1.31	2.37	1.91	1.98	1.32	1.33
K	0.08	0.09	0.05	0.06	0.16	0.10	0.10	0.06	0.06
Ba	-	-	-	-	0.01	-	-	-	-
total=	20.05	20.12	20.06	20.07	20.02	20.10	20.07	20.01	20.01
oxygens=	[32]	[32]	[32]	[32]	[32]	[32]	[32]	[32]	[32]

10 SW307 PR
11 SW307 G
12 SW307 G
13 SW307 G
14 SW307 G
15 SW307 G
16 SW307 G
17 SW307 PC
18 SW307 PR

	19	20	21	22
SiO2	51.38	50.78	51.92	55.03
Al2O3	30.29	30.22	30.88	26.42
FeO	0.33	0.30	0.31	1.22
MgO	0.04	0.02	0.02	0.63
CaO	13.80	13.52	13.37	9.22
Na2O	3.57	3.61	3.78	5.06
K2O	0.22	0.20	0.24	1.20
BaO	0.04	0.01	0.03	0.09
total=	99.67	98.62	100.07	98.88
Si	9.39	9.37	9.48	10.10
Al	6.53	6.58	6.52	5.72
Fe2	0.05	0.05	0.05	0.19
Mg	0.01	-	-	0.17
Ca	2.70	2.67	2.60	1.81
Na	1.27	1.29	1.32	1.80
K	0.05	0.05	0.06	0.28
total=	20.00	20.01	19.99	20.08
oxygens=	[32]	[32]	[32]	[32]

19 SW307 PC
20 SW307 PR
21 SW307 PC
22 SW307 PR

Ayrshire sills

	23	24	25	26	27	28	29	30	31
SiO2	50.79	50.70	51.23	52.29	65.77	51.37	51.19	51.28	50.34
Al2O3	31.94	31.51	31.35	29.89	19.75	30.40	30.94	31.00	31.68
FeO	0.22	0.22	0.25	0.28	0.18	0.39	0.41	0.23	0.38
MgO	0.02	0.03	0.03	0.03	0.01	0.02	0.02	0.04	0.06
CaO	14.77	14.72	14.59	13.14	0.65	13.81	13.91	13.98	14.78
Na2O	3.28	3.40	3.44	4.42	5.57	3.86	3.96	3.78	3.44
K2O	0.22	0.18	0.19	0.24	8.82	0.19	0.18	0.26	0.23
BaO	0.03	0.03	0.02	0.04	0.05	nd	0.02	nd	0.01
total=	101.27	100.79	101.10	100.33	100.80	100.04	100.63	100.57	100.92
Si	9.16	9.19	9.25	9.49	11.80	9.37	9.29	9.30	9.13
Al	6.79	6.73	6.67	6.40	4.18	6.53	6.62	6.63	6.77
Fe2	0.03	0.03	0.04	0.04	0.03	0.06	0.06	0.03	0.06
Mg	-	-	-	-	-	-	-	0.01	0.02
Ca	2.85	2.86	2.82	2.56	0.12	2.70	2.70	2.72	2.87
Na	1.15	1.19	1.20	1.56	1.94	1.36	1.39	1.33	1.21
K	0.05	0.04	0.04	0.06	2.02	0.04	0.04	0.06	0.05
total=	20.04	20.06	20.04	20.11	20.09	20.07	20.12	20.08	20.11
oxygens=	[32]	[32]	[32]	[32]	[32]	[32]	[32]	[32]	[32]

23 SW89 G 25 SW89 G 27 SW105 G 29 SW105 G 31 SW383 G
24 SW89 G 26 SW105 G 28 SW105 G 30 SW383 G

	32	33
SiO2	50.60	51.11
Al2O3	31.03	31.03
FeO	0.31	0.45
MgO	0.04	0.03
CaO	14.42	14.20
Na2O	3.70	3.81
K2O	0.17	0.17
BaO	0.01	0.01
total=	100.28	100.81
Si	9.22	9.27
Al	6.67	6.63
Fe2	0.05	0.07
Mg	0.01	-
Ca	2.82	2.76
Na	1.31	1.34
K	0.04	0.04
total=	20.12	20.11
oxygens=	[32]	[32]

32 SW383 G
33 SW383 G

Mauchline group

	34	35	36	37	38	39	40	41	42
SiO2	64.97	50.68	50.25	50.50	50.76	51.00	52.51	56.95	53.12
Al2O3	17.48	30.06	30.19	29.85	30.07	30.00	30.08	27.15	30.05
FeO	0.44	0.51	0.48	0.54	0.51	0.52	0.62	0.51	0.58
MgO	0.01	0.10	0.10	0.37	0.09	0.10	0.43	0.10	0.14
CaO	nd	13.78	13.87	13.50	13.80	13.54	12.99	9.50	12.96
Na2O	1.11	3.60	3.50	3.53	3.63	3.77	3.89	6.12	4.20
K2O	15.26	0.32	0.28	0.45	0.25	0.23	0.26	0.67	0.37
BaO	0.11	0.05	0.05	0.04	nd	0.04	0.05	0.21	0.08
total=	99.38	99.10	98.72	98.78	99.11	99.20	100.83	101.21	101.50
Si	12.08	9.34	9.30	9.34	9.35	9.38	9.48	10.18	9.53
Al	3.83	6.53	6.59	6.51	6.53	6.50	6.40	5.72	6.36
Fe2	0.07	0.08	0.07	0.08	0.08	0.08	0.09	0.08	0.09
Mg	-	0.03	0.03	0.10	0.02	0.03	0.12	0.03	0.04
Ca	-	2.72	2.75	2.68	2.72	2.67	2.51	1.82	2.49
Na	0.40	1.29	1.26	1.27	1.30	1.34	1.36	2.12	1.46
K	3.62	0.08	0.07	0.11	0.06	0.05	0.06	0.15	0.08
Ba	-	-	-	-	-	-	-	0.01	-
total=	20.01	20.07	20.07	20.09	20.06	20.06	20.03	20.10	20.06
oxygens=	[32]	[32]	[32]	[32]	[32]	[32]	[32]	[32]	[32]

34 SW66 PC 36 SW66 G 38 SW66 G 40 SW67 G 42 SW67 G
35 SW66 G 37 SW66 G 39 SW66 G 41 SW67 G

	43	44	45	46	47	48	49	50	51
SiO2	52.77	53.42	53.65	52.49	63.50	51.47	51.00	50.43	54.23
Al2O3	30.33	29.63	29.73	28.90	20.32	30.21	30.31	30.30	28.46
FeO	0.48	0.58	0.45	0.73	0.23	0.50	0.54	0.53	0.36
MgO	0.09	0.43	0.10	0.06	0.02	0.11	0.14	0.22	0.08
CaO	13.32	12.43	12.50	11.68	1.60	13.84	14.03	13.87	11.15
Na2O	4.00	4.28	4.51	4.94	7.26	3.81	3.62	3.71	5.13
K2O	0.35	0.42	0.34	0.29	5.62	0.33	0.31	0.30	0.55
BaO	0.01	0.07	0.06	0.01	0.25	0.06	0.04	0.05	0.14
total=	101.35	101.26	101.34	99.10	98.80	100.33	99.99	99.41	100.10
Si	9.48	9.60	9.62	9.64	11.57	9.37	9.33	9.28	9.83
Al	6.42	6.27	6.29	6.25	4.36	6.49	6.53	6.57	6.08
Fe2	0.07	0.09	0.07	0.11	0.04	0.08	0.08	0.08	0.05
Mg	0.02	0.12	0.03	0.02	-	0.03	0.04	0.06	0.02
Ca	2.56	2.39	2.40	2.30	0.31	2.70	2.75	2.74	2.17
Na	1.39	1.49	1.57	1.76	2.57	1.35	1.28	1.32	1.80
K	0.08	0.10	0.08	0.07	1.31	0.08	0.07	0.07	0.13
Ba	-	-	-	-	0.02	-	-	-	-
total=	20.04	20.06	20.06	20.15	20.18	20.09	20.09	20.13	20.09
oxygens=	[32]	[32]	[32]	[32]	[32]	[32]	[32]	[32]	[32]

43 SW67 G 45 SW67 G 47 SW159 G 49 SW173 G 51 SW173 G
44 SW67 G 46 SW159 G 48 SW173 G 50 SW173 G

	52	53	54	55	56	57
SiO2	50.39	51.22	51.76	51.24	52.80	51.42
Al2O3	30.95	30.47	30.71	30.75	28.10	28.98
FeO	0.48	0.49	0.52	0.55	0.71	0.66
MgO	0.17	0.09	0.10	0.10	0.06	0.06
CaO	14.12	13.73	13.68	13.93	9.66	12.24
Na2O	3.65	3.89	3.98	3.74	5.34	4.43
K2O	0.28	0.33	0.36	0.31	1.60	0.31
BaO	0.03	0.05	0.02	0.02	0.22	0.07
total=	100.07	100.27	101.13	100.64	98.49	98.17
Si	9.21	9.34	9.35	9.31	9.79	9.55
Al	6.67	6.55	6.54	6.58	6.14	6.34
Fe2	0.07	0.07	0.08	0.08	0.11	0.10
Mg	0.05	0.02	0.03	0.03	0.02	0.02
Ca	2.77	2.68	2.65	2.71	1.92	2.43
Na	1.29	1.37	1.39	1.32	1.92	1.59
K	0.07	0.08	0.08	0.07	0.38	0.07
Ba	-	-	-	-	0.02	-
total=	20.13	20.12	20.12	20.10	20.29	20.12
oxygens=	[32]	[32]	[32]	[32]	[32]	[32]

52 SW179 G 54 SW179 G 56 PA01 G
53 SW179 G 55 SW179 G 57 PA01 G

Fife & Lothian sills

	58	59	60	61	62	63	64	65	66
SiO2	52.43	52.98	53.07	57.36	56.30	67.13	65.19	53.51	55.88
Al2O3	29.21	28.97	29.92	26.23	27.11	18.62	21.15	25.63	27.05
FeO	0.52	0.53	0.43	0.50	0.49	0.36	0.33	4.05	0.55
MgO	0.19	0.17	0.19	0.10	0.07	0.01	nd	1.49	0.08
CaO	12.52	12.53	12.93	8.67	9.60	0.67	2.45	8.24	9.97
Na2O	4.41	4.52	4.22	6.34	5.98	6.89	7.91	5.32	5.53
K2O	0.28	0.27	0.23	0.58	0.51	6.70	3.17	0.48	0.41
BaO	nd	nd	nd	0.03	0.09	0.04	0.33	0.08	0.04
total=	99.56	99.97	100.99	99.81	100.15	100.42	100.53	98.80	99.51
Si	9.58	9.64	9.55	10.34	10.15	11.99	11.56	9.94	10.13
Al	6.29	6.21	6.35	5.57	5.76	3.92	4.42	5.61	5.78
Fe2	0.08	0.08	0.06	0.08	0.07	0.05	0.05	0.63	0.08
Mg	0.05	0.05	0.05	0.03	0.02	-	-	0.41	0.02
Ca	2.45	2.44	2.49	1.67	1.85	0.13	0.47	1.64	1.94
Na	1.56	1.59	1.47	2.22	2.09	2.39	2.72	1.92	1.94
K	0.07	0.06	0.05	0.13	0.12	1.53	0.72	0.11	0.09
Ba	-	-	-	-	-	-	0.02	-	-
total=	20.09	20.08	20.04	20.05	20.07	20.01	19.95	20.27	20.00
oxygens=	[32]	[32]	[32]	[32]	[32]	[32]	[32]	[32]	[32]

58 SW48 G 60 SW48 G 62 SW49 G 64 SW49 G 66 SW49 G
59 SW48 G 61 SW48 G 63 SW48 G 65 SW49 G

	67	68	69	70	71	72	73	74	75
SiO2	55.52	52.14	65.67	52.45	63.78	54.94	52.67	53.59	53.32
Al2O3	27.14	29.23	19.19	29.23	18.67	28.09	29.42	28.54	28.83
FeO	0.54	0.54	0.34	0.55	0.65	0.57	0.89	0.76	0.66
MgO	0.08	0.15	nd	0.11	0.61	0.10	0.29	0.08	0.08
CaO	10.09	12.81	0.58	12.28	0.54	10.78	12.87	11.49	11.83
Na2O	5.60	4.15	6.35	4.36	4.68	5.18	4.10	4.87	4.84
K2O	0.44	0.28	7.75	0.27	9.53	0.39	0.67	0.72	0.46
BaO	0.05	0.05	0.02	0.04	0.18	0.03	nd	0.07	0.09
total=	99.46	99.35	99.90	99.29	98.64	100.08	100.91	100.12	100.11
Si	10.09	9.56	11.85	9.60	11.78	9.93	9.54	9.75	9.70
Al	5.81	6.31	4.08	6.31	4.06	5.99	6.28	6.12	6.18
Fe2	0.08	0.08	0.05	0.08	0.10	0.09	0.13	0.12	0.10
Mg	0.02	0.04	-	0.03	0.17	0.03	0.08	0.02	0.02
Ca	1.96	2.52	0.11	2.41	0.11	2.09	2.50	2.24	2.30
Na	1.97	1.47	2.22	1.55	1.68	1.82	1.44	1.72	1.71
K	0.10	0.07	1.78	0.06	2.24	0.09	0.15	0.17	0.11
Ba	-	-	-	-	0.01	-	-	-	-
total=	20.04	20.06	20.11	20.05	20.15	20.03	20.12	20.13	20.12
oxygens=	[32]	[32]	[32]	[32]	[32]	[32]	[32]	[32]	[32]

67 SW49 G 69 SW56 G 71 SW56 G 73 SW472 G 75 SW472 G
68 SW49 G 70 SW56 G 72 SW56 G 74 SW472 G

	76	77	78	79	80	81	82	83	84
SiO2	55.72	53.82	53.47	55.95	51.48	51.27	49.90	51.16	51.21
Al2O3	27.59	28.52	29.18	27.54	29.84	30.32	31.43	29.60	30.17
FeO	0.60	0.72	0.77	0.56	1.16	0.59	0.54	0.63	0.60
MgO	0.12	0.12	0.12	0.21	0.40	0.16	0.09	0.11	0.11
CaO	10.15	11.61	12.29	10.06	13.71	14.08	15.25	13.13	13.29
Na2O	6.06	5.13	4.75	6.05	3.68	3.72	3.11	4.13	3.95
K2O	0.21	0.17	0.15	0.22	0.09	0.08	0.14	0.41	0.36
BaO	0.04	nd	nd	nd	nd	0.02	nd	0.04	0.03
total=	100.49	100.09	100.73	100.59	100.36	100.28	100.46	99.21	99.72
Si	10.03	9.77	9.66	10.05	9.38	9.34	9.10	9.43	9.38
Al	5.85	6.10	6.21	5.83	6.41	6.51	6.76	6.43	6.51
Fe2	0.09	0.11	0.12	0.08	0.18	0.09	0.08	0.10	0.09
Mg	0.03	0.03	0.03	0.06	0.11	0.04	0.02	0.03	0.03
Ca	1.96	2.26	2.38	1.94	2.68	2.75	2.98	2.59	2.61
Na	2.11	1.80	1.66	2.11	1.30	1.31	1.10	1.48	1.40
K	0.05	0.04	0.03	0.05	0.02	0.02	0.03	0.10	0.08
total=	20.13	20.11	20.09	20.11	20.07	20.07	20.08	20.15	20.11
oxygens=	[32]	[32]	[32]	[32]	[32]	[32]	[32]	[32]	[32]

76 SW521 G 78 SW521 G 80 SW521 G 82 SW538 G 84 SW585 G
77 SW521 G 79 SW521 G 81 SW521 G 83 SW585 G

	85	86	87	88	89
SiO2	50.88	64.48	52.26	53.04	52.09
Al2O3	29.54	19.43	29.65	29.37	29.84
FeO	0.58	0.56	0.55	0.60	0.52
MgO	0.10	0.40	0.12	0.08	0.12
CaO	13.33	0.89	12.74	12.64	12.93
Na2O	4.02	4.51	4.23	4.37	4.17
K2O	0.39	9.29	0.20	0.24	0.25
BaO	0.05	0.07	0.07	0.07	0.04
total=	98.89	99.63	99.82	100.41	99.96
Si	9.41	11.75	9.53	9.61	9.49
Al	6.44	4.17	6.37	6.27	6.41
Fe2	0.09	0.09	0.08	0.09	0.08
Mg	0.03	0.11	0.03	0.02	0.03
Ca	2.64	0.17	2.49	2.45	2.52
Na	1.44	1.59	1.50	1.54	1.47
K	0.09	2.16	0.05	0.06	0.06
total=	20.14	20.04	20.05	20.05	20.07
oxygens=	[32]	[32]	[32]	[32]	[32]

85 SW585 G 87 SW566 G 89 SW566 G
86 SW566 G 88 SW566 G

Fife & Lothian basanites

	90	91	92	93	94	95	96	97	98
SiO2	53.78	58.84	53.53	52.25	50.71	56.67	68.51	52.20	51.57
Al2O3	29.50	25.16	27.57	29.70	30.83	27.18	19.73	29.57	29.37
FeO	0.53	0.43	1.29	0.43	0.60	0.44	0.17	0.69	0.65
MgO	nd	nd	0.07	0.12	0.18	0.11	0.09	0.16	0.18
CaO	11.99	6.67	10.16	12.65	14.27	9.02	0.47	12.66	12.96
Na2O	4.85	6.36	5.57	4.27	3.36	5.93	8.62	4.13	3.94
K2O	0.57	1.90	0.90	0.47	0.33	0.91	3.47	0.51	0.49
BaO	0.12	0.55	0.09	0.10	0.08	0.21	0.33	0.07	0.04
total=	101.30	99.91	99.18	99.99	100.32	100.47	101.39	99.99	99.20
Si	9.66	10.62	9.85	9.52	9.25	10.19	11.96	9.52	9.49
Al	6.25	5.35	5.98	6.38	6.63	5.76	4.06	6.36	6.37
Fe2	0.08	0.06	0.20	0.07	0.09	0.07	0.02	0.11	0.10
Mg	-	-	0.02	0.03	0.04	0.03	0.02	0.04	0.05
Ca	2.31	1.29	2.00	2.47	2.79	1.74	0.09	2.47	2.56
Na	1.69	2.23	1.99	1.51	1.19	2.07	2.92	1.46	1.41
K	0.13	0.44	0.21	0.11	0.08	0.21	0.77	0.12	0.12
Ba	-	0.04	-	-	-	0.01	0.02	-	-
total=	20.13	20.03	20.26	20.10	20.07	20.07	19.86	20.09	20.09
oxygens=	[32]	[32]	[32]	[32]	[32]	[32]	[32]	[32]	[32]

90 SW32 G 92 SW32 G 94 SW32 XR 96 SW40 XC 98 SW436 G
91 SW32 G 93 SW32 PC 95 SW32 XC 97 SW436 G

	99	100	101	102
SiO2	52.16	50.38	49.66	50.49
Al2O3	29.20	31.01	30.07	31.07
FeO	1.01	0.73	1.41	0.52
MgO	0.37	0.18	0.80	0.15
CaO	12.21	14.96	13.91	14.89
Na2O	4.26	3.11	3.21	3.21
K2O	0.55	0.26	0.26	0.26
BaO	0.06	0.03	0.02	0.02
total=	99.82	100.58	99.34	100.61
Si	9.58	9.18	9.18	9.19
Al	6.30	6.66	6.55	6.67
Fe2	0.15	0.11	0.22	0.08
Mg	0.10	0.08	0.22	0.08
Ca	2.39	2.92	2.76	2.90
Na	1.51	1.10	1.15	1.13
K	0.13	0.06	0.06	0.06
total=	20.13	20.07	20.15	20.07
oxygens=	[32]	[32]	[32]	[32]

99 SW436 G 101 SW526 G
100 SW526 G 102 SW526 G

APPENDIX III

TABLES OF WHOLE-ROCK DATA

	SW2 (5)	SW3 (5)	SW4A (5)	SW5 (5)	SW6 (5)	SW7 (5)	SW8 (5)	SW9 (5)	SW12 (5)
SiO2	44.66	46.58	46.84	45.38	48.59	46.09	44.57	44.87	43.56
Al2O3	12.56	15.50	15.62	14.70	15.78	14.31	14.38	13.30	13.61
Fe2O3	13.69	12.03	11.95	13.05	13.86	11.97	12.66	12.96	12.70
MgO	10.82	8.13	7.27	9.41	10.18	9.85	9.65	10.06	9.78
CaO	10.21	8.44	7.83	10.89	10.41	10.91	10.13	10.30	11.06
Na2O	1.95	3.01	3.86	2.30	3.05	2.26	3.69	3.49	3.16
K2O	2.06	2.05	1.97	0.60	1.62	0.81	1.06	1.15	1.69
TiO2	2.91	2.73	2.60	3.19	3.31	2.88	2.94	2.57	2.94
MnO	0.16	0.17	0.18	0.26	0.21	0.15	0.18	0.19	0.23
P2O5	0.66	0.65	0.79	0.62	0.69	0.65	0.63	0.62	0.93
TOTAL	99.68	99.28	98.89	100.38	107.70	99.88	99.90	99.49	99.66
LOI	3.4	1.4	1.7	3.5	9.8	4.4	1.3	1.2	3.4
Ni	338	231	144	241	209	273	168	233	227
Cr	596	211	221	437	287	417	228	283	311
V	282	209	189	277	268	253	246	244	263
Sc	29	20	19	31	29	28	26	21	22
Cu	32	89	45	51	59	57	49	65	54
Zn	94	93	101	102	107	96	85	114	115
Sr	828	813	863	969	876	1151	893	1070	1432
Rb	34	41	38	5	30	9	25	17	34
Zr	236	270	317	281	298	276	274	220	277
Nb	63	51	59	53	59	57	53	57	76
Ba	951	806	873	790	1385	900	718	855	935
Pb	8	2	2	2	2	1	0	*	3
Th	6	2	3	4	4	2	0	*	3
La	49	37	47	36	42	40	42	48	47
Ce	112	91	100	98	93	105	89	99	113
Nd	49	42	41	43	44	46	41	45	49
Y	27	28	28	30	31	29	30	27	29
Q	-	-	-	-	-	-	-	-	-
or	12.34	12.30	11.87	3.55	9.00	4.87	6.36	6.89	10.15
ab	10.23	20.99	23.66	19.57	16.03	19.33	13.70	13.30	6.66
an	19.73	23.16	19.92	28.25	23.09	26.81	19.79	17.55	18.23
ne	3.53	2.66	5.26	-	4.43	-	9.68	9.04	11.07
lct	-	-	-	-	-	-	-	-	-
di	22.15	12.31	11.82	17.95	17.15	19.13	21.82	24.57	25.33
hy	-	-	-	2.04	-	2.87	-	-	-
ol	22.43	19.64	18.43	18.82	20.62	17.83	19.29	19.94	18.45
mt	2.39	2.10	2.10	2.26	2.24	2.08	2.20	2.26	2.21
il	5.61	5.28	5.04	6.10	5.89	5.53	5.65	4.96	5.67
ap	1.58	1.57	1.92	1.47	1.54	1.55	1.51	1.49	2.23
cort	-	-	-	-	-	-	-	-	-

(1) Passage Group lavas (2) Ayrshire sills (3) Mauchline group (4) Fife & Lothian sills
(5) Fife & Lothian basanites (6) Highland dykes (7) Quartz dolerites

	SW19 (5)	SW20 (5)	SW22 (5)	SW23 (5)	SW25 (5)	SW26 (5)	SW27 (5)	SW28 (5)	SW31C (5)
SiO2	43.61	45.66	45.26	45.67	45.59	47.45	46.16	45.55	42.96
Al2O3	14.52	14.67	13.97	14.44	12.81	15.54	13.96	14.79	13.04
Fe2O3	13.91	10.77	14.02	13.02	13.76	11.28	12.73	12.56	11.98
MgO	8.94	7.14	10.61	7.08	11.01	6.87	8.22	6.66	11.53
CaO	9.96	12.11	6.87	10.01	9.41	9.13	10.09	9.03	12.92
Na2O	2.67	3.66	3.35	3.56	2.33	3.56	3.45	4.36	3.25
K2O	1.96	1.22	1.76	1.07	1.24	1.53	1.02	1.94	0.19
TiO2	2.78	2.81	2.59	2.81	2.64	2.88	3.04	2.99	2.93
MnO	0.14	0.12	0.28	0.59	0.18	0.18	0.18	0.16	0.13
P2O5	0.85	0.66	0.76	0.79	0.51	1.20	0.64	1.16	0.71
TOTAL	99.36	98.81	99.46	99.04	99.49	99.62	99.48	99.21	99.64
LOI	3.9	3.4	4.4	2.8	2.1	2.7	2.3	3.3	6.6
Ni	242	190	175	338	267	116	204	105	280
Cr	331	315	258	301	312	266	312	147	548
V	255	262	221	246	254	229	254	202	300
Sc	19	27	18	18	20	16	25	15	28
Cu	55	62	57	59	69	44	55	32	65
Zn	476	245	124	161	109	105	109	143	109
Sr	875	797	419	914	573	874	923	1243	511
Rb	50	20	50	14	26	31	11	18	2
Zr	281	259	216	293	208	174	225	469	265
Nb	75	64	58	60	47	46	60	120	72
Ba	1044	5155	1394	1040	724	661	1025	1482	497
Pb	6	29	2	2	2	4	3	31	4
Th	5	4	6	3	3	2	3	13	7
La	57	42	46	47	37	52	50	100	58
Ce	123	100	96	105	84	106	89	201	120
Nd	51	53	39	42	35	50	41	76	51
Y	30	29	27	28	22	27	25	36	27
Q	-	-	-	-	-	-	-	-	-
or	11.81	7.35	10.61	6.47	7.48	9.15	6.11	11.69	1.11
ab	9.67	13.45	20.62	21.34	18.80	27.83	21.25	18.18	7.12
an	22.22	20.41	18.20	20.69	21.18	22.17	19.91	15.32	20.74
ne	7.24	9.86	4.43	5.09	0.68	1.48	4.58	10.53	11.24
lc	-	-	-	-	-	-	-	-	-
di	18.36	29.70	9.26	20.29	18.59	12.85	21.79	18.53	31.87
hy	-	-	-	-	-	-	-	-	-
ol	20.83	10.29	27.59	16.47	24.53	16.12	16.75	14.97	18.49
mt	2.44	1.89	2.45	2.28	2.40	1.96	2.22	2.20	2.09
il	5.38	5.44	5.00	5.45	5.11	5.54	5.86	5.78	5.64
ap	2.04	1.60	1.84	1.92	1.22	2.89	1.53	2.79	1.70
cort	-	-	-	-	-	-	-	-	-

	SW32 (5)	SW34 (5)	SW36 (4)	SW38A (5)	SW39 (5)	SW40 (5)	SW41 (5)	SW42 (5)	SW43 (5)
SiO2	41.24	47.26	48.96	47.71	43.82	46.01	45.51	45.61	43.29
Al2O3	12.61	16.34	16.81	16.97	13.64	14.60	14.39	14.52	13.60
Fe2O3	14.13	12.53	12.45	10.46	12.43	13.53	13.76	13.74	13.06
MgO	10.73	4.24	3.74	7.45	10.43	8.03	8.15	8.27	10.03
CaO	13.22	8.99	6.05	7.88	10.75	9.86	9.65	9.59	10.56
Na2O	3.15	5.28	3.86	3.35	3.35	3.18	3.23	2.95	4.05
K2O	0.44	1.72	3.58	2.27	1.22	0.78	0.76	0.87	0.89
TiO2	3.02	2.31	3.11	2.38	2.84	2.95	3.02	3.04	2.62
MnO	0.13	0.21	0.20	0.23	0.19.	0.19	0.19	0.19	0.22
P2O5	0.69	0.57	0.73	0.60	0.83	0.64	0.69	0.71	0.70
TOTAL	99.35	99.46	99.49	99.31	99.50	99.76	99.34	99.47	99.02
LOI	5.0	4.3	2.0	3.7	2.3	2.3	2.6	2.4	1.6
Ni	322	172	6	55	216	135	145	141	205
Cr	507	296	4	121	388	147	144	146	277
V	295	187	145	199	264	227	228	229	248
Sc	25	19	8	16	21	18	19	17	26
Cu	29	42	13	15	62	54	53	54	58
Zn	388	405	108	427	103	120	124	123	113
Sr	664	1024	1217	1186	834	1649	1165	1388	850
Rb	7	25	83	24	14	9	12	12	9
Zr	274	271	315	299	273	228	228	228	279
Nb	72	79	84	91	73	53	54	54	76
Ba	767	1200	1173	1416	761	884	835	878	1399
Pb	2	5	3	2	3	*	1	*	3
Th	5	5	5	6	4	*	1	*	6
La	61	57	76	61	51	38	44	40	59
Ce	126	125	154	134	107	100	99	98	123
Nd	51	45	62	50	48	42	45	41	54
Y	28	.26	32	28	29	28	28	28	33
Q	-	-	-	-	-	-	-	-	-
or	2.64	10.31	21.50	13.65	7.31	4.67	4.56	5.21	5.35
ab	0.80	20.53	26.81	23.22	9.98	23.72	23.58	23.83	9.31
an	19.36	16.08	18.24	24.96	18.89	23.61	22.98	24.23	16.65
ne	14.26	13.47	3.45	3.02	10.19	1.91	2.30	0.85	13.93
let	-	-	-	-	-	-	-	-	-
di	34.75	21.26	6.19	8.78	24.10	17.80	17.31	15.91	26.12
hy	-	-	-	-	-	-	-	-	-
ol	18.20	10.33	13.87	18.51	19.89	18.71	19.37	20.00	19.56
mt	2.87	2.19	2.17	1.83	2.17	2.36	2.41	2.40	2.29
il	5.84	4.47	5.99	4.59	5.47	5.68	5.84	5.87	5.09
ap	1.68	1.37	1.76	1.44	1.99	1.54	1.67	1.71	1.70
cort	-	-	-	-	-	-	-	-	-

	SW48 (5)	SW45 (5)	SW47 (5)	SW48 (4)	SW49 (4)	SW53A (5)	SW56 (4)	SW57 (5)	SW59 (5)
SiO2	48.95	43.31	48.19	49.48	51.25	49.67	50.49	45.11	45.65
Al2O3	13.61	13.50	14.97	15.15	16.65	13.86	15.50	14.64	14.70
Fe2O3	13.13	13.14	12.12	11.65	11.16	11.34	10.74	12.79	13.05
MgO	10.00	10.36	6.25	7.44	6.86	7.18	10.18	7.66	7.51
CaO	9.68	10.98	10.05	9.28	6.59	8.60	6.72	10.27	9.15
Na2O	2.97	3.86	2.96	3.64	3.00	3.40	2.97	4.08	3.85
K2O	1.42	0.75	1.61	1.03	1.81	2.44	1.50	1.25	1.68
TiO2	2.72	2.70	2.21	1.89	1.92	2.59	1.59	3.05	2.90
MnO	0.25	0.20	0.81	0.16	0.10	0.21	0.11	0.32	0.25
P2O5	0.69	0.68	0.54	0.37	0.44	0.58	0.31	0.67	0.68
TOTAL	99.43	99.49	99.72	100.09	99.78	99.85	100.11	99.84	99.42
LOI	4.2	1.9	2.0	1.3	2.8	2.2	3.6	2.6	2.8
Ni	199	204	218	132	52	196	222	171	150
Cr	223	284	362	229	172	240	551	219	200
V	239	260	251	195	213	238	163	270	253
Sc	20	27	25	21	27	23	19	25	21
Cu	50	59	63	56	36	45	32	57	46
Zn	111	108	227	98	180	116	67	120	120
Sr	893	822	721	440	469	817	496	1107	1055
Rb	27	10	36	20	41	54	31	31	35
Zr	282	259	203	150	174	313	156	323	359
Nb	72	69	57	28	30	69	26	83	92
Ba	930	934	1009	357	810	944	456	1099	1258
Pb	3	2	2	1	3	3	3	2	2
Th	7	4	3	0	1	5	2	5	6
La	56	55	40	22	28	53	25	59	66
Ce	107	99	83	49	44	104	38	132	145
Nd	49	48	37	25	24	44	18	56	63
Y	31	31	29	25	22	31	22	34	36
Q	-	-	-	-	-	-	-	-	-
or	8.56	4.52	9.67	6.13	10.84	14.56	8.91	7.46	10.09
ab	15.39	8.90	24.05	29.68	25.72	25.46	25.37	14.92	17.58
an	19.96	17.57	23.11	22.18	26.90	15.55	24.72	18.17	18.19
ne	5.49	13.18	0.71	0.75	-	1.95	-	10.88	8.42
lct	-	-	-	-	-	-	-	-	-
di	19.73	27.00	19.69	17.88	2.69	19.36	5.55	23.66	19.20
hy	-	-	-	-	24.08	-	15.74	-	-
ol	21.65	19.69	15.11	16.85	3.10	14.78	14.06	15.21	17.00
mt	2.29	2.30	2.11	2.02	1.94	1.97	1.86	2.23	2.28
il	5.26	5.22	4.25	3.63	3.68	4.96	3.04	5.87	5.59
ap	1.67	1.63	1.29	0.88	1.04	1.40	0.73	1.61	1.64
cort	-	-	-	-	-	-	-	-	-

	SW66 (3)	SW70 (2)	SW76 (3)	SW84 (2)	SW89 (2)	SW91 (2)	SW93 (2)	SW94 (2)	SW100 (2)
SiO2	45.78	46.10	49.94	43.30	46.27	44.26	47.11	47.43	43.98
Al2O3	15.12	13.83	16.00	16.70	14.43	10.29	14.51	15.82	9.23
Fe2O3	12.48	11.44	10.86	17.97	10.86	13.03	10.63	10.19	13.12
MgO	8.58	11.93	6.40	8.74	11.05	18.52	11.49	9.25	20.26
CaO	11.12	10.24	8.69	7.18	10.87	8.62	10.83	11.03	8.77
Na2O	2.19	2.86	3.84	3.82	2.76	2.13	2.91	3.26	1.90
K2O	1.85	1.52	1.35	0.71	1.21	0.97	0.98	1.13	0.64
TiO2	1.97	1.52	1.66	1.15	1.43	1.13	1.32	1.48	1.08
MnO	0.16	0.18	0.31	0.19	0.16	0.18	0.16	0.15	0.18
P2O5	0.39	0.34	0.35	0.18	0.31	0.24	0.25	0.29	0.20
TOTAL	99.64	99.97	99.39	99.94	99.34	99.37	100.18	99.62	99.33
LOI	2.3	1.1	1.4	8.5	0.7	1.2	0.8	1.1	1.8
Ni	133	260	75	286	255	530	240	169	590
Cr	262	491	140	381	559	847	585	461	893
V	250	238	261	189	221	194	206	217	183
Sc	24	27	23	33	25	23	27	25	26
Cu	58	66	5	29	62	45	48	53	38
Zn	59	84	53	127	77	90	75	78	88
Sr	697	598	692	152	591	404	565	601	346
Rb	44	35	45	18	26	20	22	26	15
Zr	141	136	164	79	118	92	106	121	81
Nb	39	33	32	12	28	21	24	26	17
Ba	1297	607	578	159	479	405	394	462	330
Pb	2	2	2	10	1	1	2	1	1
Th	1	1	*	*	*	*	*	*	*
La	30	23	27	13	18	5	16	18	13
Ce	63	48	58	19	36	32	36	39	19
Nd	30	26	29	7	18	13	18	20	10
Y	22	20	24	18	18	18	17	19	13
Q	-	-	-	-	-	-	-	-	-
or	11.07	9.10	8.07	4.24	7.28	5.85	5.82	6.75	3.87
ab	11.16	10.70	31.20	16.56	12.90	8.66	15.12	16.61	8.27
an	26.36	20.60	22.79	26.76	23.81	15.96	23.83	28.82	15.01
ne	4.13	7.45	0.98	8.84	5.85	5.23	5.23	6.13	4.41
lct	-	-	-	-	-	-	-	-	-
di	22.04	22.98	15.30	6.87	23.40	20.85	23.15	23.56	22.41
hy	-	-	-	-	-	-	-	-	-
ol	18.34	23.43	15.70	30.98	21.38	38.42	21.90	17.22	41.25
mt	2.18	1.99	1.90	3.18	1.90	2.28	1.84	1.77	2.30
il	3.79	2.93	3.21	2.23	2.76	2.19	2.53	2.85	2.01
ap	0.94	0.82	0.85	0.43	0.73	0.57	0.59	0.69	0.49
cort	-	-	-	-	-	-	-	-	-

	SW102 (3)	SW103 (3)	SW105 (2)	SW109 (3)	SW111 (6)	SW112 (6)	SW113 (6)	SW114 (6)	SW115 (6)
SiO2	43.79	45.52	46.26	46.68	42.68	44.59	44.31	41.32	44.00
Al2O3	13.48	13.46	14.24	16.32	14.00	14.49	14.71	12.49	12.27
Fe2O3	12.78	12.40	11.57	11.79	13.35	12.21	13.10	12.43	11.90
MgO	11.41	10.41	10.46	11.30	7.97	10.04	7.31	12.40	10.78
CaO	10.72	11.08	10.51	7.24	10.91	11.67	10.25	12.96	14.01
Na2O	2.96	3.44	3.17	2.03	3.58	2.05	3.09	1.13	1.93
K2O	0.60	0.57	1.41	1.98	2.28	1.82	2.60	2.18	1.31
TiO2	2.13	2.08	1.62	1.88	2.98	2.43	2.60	2.79	2.24
MnO	0.20	0.22	0.17	0.12	0.25	0.15	0.21	0.19	0.18
P2O5	0.57	0.49	0.35	0.32	1.00	0.59	0.83	0.90	0.76
TOTAL	98.68	99.68	99.75	99.61	98.96	100.05	99.00	98.76	99.37
LOI	4.0	3.2	1.0	5.1	4.6	4.4	5.1	6.7	6.2
Ni	320	386	224	219	127	222	128	289	437
Cr	490	495	438	490	196	509	267	482	611
V	262	268	227	310	262	315	263	252	249
Sc	22	24	23	33	19	30	19	25	24
Cu	22	59	71	35	35	73	53	51	64
Zn	217	90	83	123	120	96	102	105	97
Sr	683	607	593	622	1607	786	1118	1053	787
Rb	10	7	33	43	72	47	67	50	45
Zr	197	175	137	157	402	201	304	282	220
Nb	56	51	32	32	118	53	86	84	62
Ba	1633	1777	548	756	1694	857	4996	1136	1656
Pb	6	3	2	12	3	2	1	2	4
Th	5	1	*	*	5	0	1	4	3
La	43	25	17	17	78	38	58	53	51
Ce	84	66	50	50	168	79	125	124	100
Nd	36	33	26	23	68	38	58	52	49
Y	24	22	20	19	37	24	32	26	25
Q	-	-	-	-	-	-	-	-	-
or	3.66	3.43	8.41	11.85	13.79	10.84	15.68	0.48	7.85
ab	12.62	15.23	12.23	17.41	1.85	6.73	6.76	-	2.56
an	22.29	19.87	20.75	30.00	15.70	25.22	19.01	23.11	21.31
ne	7.05	7.74	8.07	-	15.79	5.85	10.79	5.31	7.59
lct	-	-	-	-	-	-	-	9.93	-
di	23.00	26.45	24.10	3.49	26.91	23.77	22.50	29.53	35.82
hy	-	-	-	6.27	-	-	-	-	-
ol	23.60	19.93	20.47	24.54	15.41	19.39	15.92	21.85	16.63
mt	2.25	2.16	2.01	2.05	2.38	2.12	2.30	2.19	2.08
il	4.15	4.01	3.11	3.62	5.79	4.66	5.04	5.42	4.33
ap	1.38	1.18	0.84	0.77	2.42	1.42	2.00	2.17	1.83
cort	-	-	-	-	-	-	-	-	-

	SW116 (6)	SW124 (3)	SW125 (3)	SW126 (3)	SW127 (3)	SW128 (3)	SW129 (3)	SW130 (3)	SW131 (3)
SiO2	42.70	46.96	47.62	47.56	47.01	48.23	47.53	47.65	47.69
Al2O3	14.68	13.67	14.04	13.85	13.91	16.91	13.84	13.92	14.04
Fe2O3	13.28	12.43	12.71	12.67	12.96	11.91	12.82	12.89	12.65
MgO	6.43	11.41	10.69	9.92	9.69	4.66	10.23	10.06	10.69
CaO	11.90	8.55	8.95	8.87	9.87	9.45	9.12	9.00	8.78
Na2O	2.95	3.77	3.07	3.43	2.82	3.37	3.05	3.29	3.36
K2O	3.30	0.87	0.89	0.90	0.96	1.58	0.89	0.89	0.87
TiO2	2.97	1.75	1.75	1.76	1.86	2.32	1.80	1.77	1.75
MnO	0.17	0.18	0.17	0.18	0.16	0.20	0.23	0.22	0.21
P2O5	1.09	0.30	0.31	0.31	0.33	0.67	0.31	0.30	0.30
TOTAL	99.47	99.89	100.20	99.48	99.16	99.31	99.82	99.98	100.33
LOI	5.5	3.2	4.0	3.9	3.5	3.2	4.0	4.2	4.2
Ni	78	277	299	295	293	282	302	306	299
Cr	214	468	477	475	470	473	477	486	480
V	259	238	243	243	259	273	246	245	250
Sc	19	26	25	21	23	23	25	22	24
Cu	49	56	20	25	20	17	27	18	25
Zn	115	93	100	106	116	98	108	109	121
Sr	1459	415	431	443	473	469	408	423	411
Rb	89	19	20	20	21	20	20	21	20
Zr	457	123	128	127	133	131	126	126	126
Nb	111	27	27	27	30	29	27	27	27
Ba	1537	417	412	426	532	475	443	399	377
Pb	1	3	17	17	24	20	12	14	13
Th	7	*	*	*	*	*	*	*	*
La	86	13	19	14	17	9	14	9	18
Ce	174	34	38	46	37	35	34	33	39
Nd	73	18	19	19	21	18	20	17	20
Y	33	20	21	21	22	21	20	20	20
Q	-	-	-	-	-	-	-	-	-
or	9.63	5.18	5.32	5.38	5.79	9.51	5.35	5.31	5.17
ab	-	21.04	23.88	24.87	20.87	28.11	24.00	24.11	23.84
an	17.35	18.01	22.06	20.11	24.76	26.79	21.71	20.85	20.83
ne	13.74	6.11	1.29	2.72	-	0.50	1.17	2.18	2.59
lct	8.01	-	-	-	-	-	-	-	-
di	29.12	18.58	16.80	18.37	18.72	13.65	17.98	18.15	17.11
hy	-	-	-	-	3.33	-	-	-	-
ol	11.46	24.82	24.36	22.60	19.86	13.26	23.37	23.04	24.19
mt	2.32	2.16	2.20	2.21	2.27	2.08	2.23	2.24	2.19
il	5.73	3.36	3.35	3.40	3.61	4.48	3.46	3.40	3.36
ap	2.63	0.72	0.74	0.75	0.79	1.62	0.74	0.72	0.71
cort	-	-	-	-	-	-	-	-	-

	SW132 (3)	SW133 (3)	SW134 (3)	SW135 (3)	SW136 (3)	SW137 (3)	SW138 (3)	SW139 (3)	SW140 (3)
SiO2	49.51	48.88	49.93	49.45	49.61	49.34	49.13	49.05	48.69
Al2O3	14.85	14.81	14.73	14.54	14.65	14.82	14.83	14.80	14.30
Fe2O3	11.60	12.16	11.42	11.59	10.81	11.48	11.28	11.22	11.65
MgO	7.65	7.21	7.94	7.25	7.17	7.36	7.56	7.84	7.91
CaO	9.23	9.68	9.45	9.49	9.88	9.70	9.73	9.72	9.80
Na2O	3.32	3.34	3.18	3.61	3.36	3.43	3.15	3.12	3.19
K2O	1.24	1.20	1.21	1.20	1.22	1.26	1.23	1.20	1.20
TiO2	1.97	1.95	1.94	1.93	1.93	1.93	1.93	1.94	1.94
MnO	0.15	0.36	0.12	0.20	0.39	0.24	0.28	0.37	0.14
P2O5	0.37	0.37	0.37	0.37	0.36	0.37	0.36	0.37	0.37
TOTAL	99.90	99.55	100.28	99.63	99.39	99.51	99.07	99.23	99.19
LOI	2.1	1.6	2.1	1.8	1.4	1.4	1.4	1.6	1.9
Ni	103	109	120	118	117	116	116	118	115
Cr	272	268	283	280	279	274	268	273	268
V	247	241	243	265	249	240	243	244	248
Sc	24	23	24	25	23	21	22	25	25
Cu	11	42	31	26	68	55	50	63	18
Zn	90	105	98	75	101	95	96	96	117
Sr	511	499	485	510	511	500	499	503	511
Rb	30	30	30	29	29	31	29	30	30
Zr	153	151	149	154	151	149	150	151	152
Nb	31	31	31	32	32	32	32	31	32
Ba	616	592	514	577	512	535	524	525	545
Pb	10	4	4	8	3	3	2	3	9
Th	1	1	*	*	0	1	0	*	*
La	19	18	12	18	22	16	16	18	18
Ce	43	47	60	46	55	61	43	49	48
Nd	23	24	23	24	24	23	23	22	22
Y	25	24	24	25	24	24	24	24	24
Q	-	-	-	-	-	-	-	-	-
or	7.39	7.18	7.22	7.20	7.33	7.54	7.39	7.25	7.20
ab	28.38	27.12	27.13	28.47	28.54	27.62	27.19	26.88	26.31
an	22.23	21.11	22.48	20.20	21.61	20.56	22.03	22.12	21.57
ne	-	0.85	-	1.35	0.18	0.97	-	-	0.62
lct	-	-	-	-	-	-	-	-	-
di	17.69	20.68	18.19	20.56	21.07	21.15	20.23	20.02	20.82
hy	1.58	-	4.39	-	-	-	1.45	1.31	-
ol	16.04	16.31	14.03	15.60	14.78	15.55	15.14	15.84	16.78
mt	2.02	2.12	1.98	2.02	1.89	2.00	1.98	1.96	2.04
il	3.78	3.76	3.71	3.71	3.73	3.72	3.74	3.75	3.76
ap	0.88	0.88	0.88	0.88	0.87	0.88	0.87	0.88	0.89
cort	-	-	-	-	-	-	-	-	-

	SW181 (3)	SW182 (3)	SW183 (3)	SW188 (3)	SW185 (3)	SW186 (3)	SW187 (3)	SW188 (3)	SW189 (3)
SiO2	49.15	47.85	49.20	47.67	49.32	44.41	44.85	47.15	46.57
Al2O3	14.44	13.86	14.60	13.86	14.48	13.80	13.66	13.93	13.87
Fe2O3	11.45	12.34	11.68	12.44	11.22	12.73	12.54	12.81	12.76
MgO	7.78	9.78	7.53	10.05	7.50	11.81	11.58	10.17	11.63
CaO	9.57	9.69	9.58	9.35	9.79	11.50	11.19	9.27	9.48
Na2O	3.16	2.70	3.17	2.56	3.09	1.29	1.84	2.80	2.07
K2O	1.24	1.15	1.25	1.09	1.24	1.24	1.28	0.94	0.87
TiO2	1.92	1.95	1.97	1.95	1.95	1.94	1.91	1.80	1.80
MnO	0.37	0.15	0.16	0.15	0.37	0.19	0.18	0.18	0.16
P2O5	0.36	0.36	0.37	0.35	0.37	0.41	0.41	0.31	0.31
TOTAL	99.44	99.81	99.51	99.47	99.33	99.32	99.44	99.36	99.51
LOI	1.8	2.6	1.9	2.7	1.6	4.6	3.9	4.0	3.8
Ni	115	230	111	229	123	356	351	310	305
Cr	265	335	291	342	276	576	573	499	487
V	239	240	267	253	244	281	272	259	258
Sc	24	25	26	24	21	25	26	26	24
Cu	68	13	28	13	65	22	26	35	21
Zn	98	82	160	74	99	116	96	139	137
Sr	494	494	503	490	505	569	550	458	427
Rb	30	25	30	24	30	27	31	22	18
Zr	151	146	155	146	152	147	147	127	127
Nb	31	31	33	31	32	37	38	28	28
Ba	589	519	575	504	682	820	726	519	488
Pb	3	4	7	2	1	26	20	16	20
Th	2	1	*	*	*	*	*	*	*
La	21	18	21	15	18	20	18	14	17
Ce	54	53	51	41	48	59	49	36	39
Nd	22	28	25	26	24	30	27	17	19
Y	25	24	26	25	26	21	21	20	21
Q	-	-	-	-	-	-	-	-	-
or	7.42	6.86	7.49	6.55	7.44	7.46	7.68	5.65	5.20
ab	27.18	23.10	27.24	22.01	26.62	9.81	10.35	23.31	17.83
an	21.90	22.61	22.25	23.48	22.33	28.72	25.64	23.08	26.41
ne	-	-	-	-	-	0.69	2.98	0.41	-
lct	-	-	-	-	-	-	-	-	-
di	19.57	19.27	19.26	17.30	20.10	21.56	22.75	17.64	15.66
hy	1.11	0.43	1.66	4.35	2.92	-	-	-	6.68
ol	16.25	20.97	15.38	19.53	13.98	24.81	23.73	23.44	21.78
mt	2.00	2.15	2.04	2.17	1.96	2.23	2.19	2.24	2.23
il	3.71	3.76	3.80	3.76	3.76	3.75	3.68	3.47	3.47
ap	0.87	0.86	0.89	0.85	0.88	0.98	0.98	0.74	0.74
cort	-	-	-	-	-	-	-	-	-

	SW150 (3)	SW151 (3)	SW152 (3)	SW153 (3)	SW154 (3)	SW155 (3)	SW156 (3)	SW157 (3)	SW158 (3)
SiO2	47.02	47.98	46.87	47.66	46.86	47.24	46.67	47.74	47.95
Al2O3	13.81	13.89	13.74	14.08	14.01	13.92	13.57	13.87	13.73
Fe2O3	12.83	11.74	12.86	13.06	12.80	12.84	12.50	12.04	12.20
MgO	10.31	9.48	9.90	9.50	9.68	9.95	11.82	10.06	9.38
CaO	9.18	9.75	9.25	9.35	9.35	9.02	8.66	9.68	9.65
Na2O	2.81	2.66	3.33	3.31	3.03	3.29	3.27	2.75	2.98
K2O	0.95	1.13	0.96	0.95	0.94	0.87	0.84	1.03	1.04
TiO2	1.81	1.93	1.85	1.85	1.83	1.79	1.73	1.90	1.88
MnO	0.22	0.40	0.17	0.17	0.16	0.27	0.18	0.18	0.33
P2O5	0.31	0.35	0.32	0.32	0.32	0.30	0.29	0.35	0.35
TOTAL	99.23	99.31	99.28	100.26	98.97	99.48	99.53	99.61	99.49
LOI	4.1	2.4	2.8	4.6	3.8	3.8	3.3	2.7	2.4
Ni	310	227	294	307	293	306	288	235	243
Cr	470	339	472	490	471	480	469	339	349
V	230	256	248	268	268	245	238	241	248
Sc	21	23	23	24	23	21	20	25	24
Cu	27	59	51	37	23	34	45	29	63
Zn	107	212	98	123	115	100	94	122	98
Sr	483	486	486	531	480	426	372	476	477
Rb	21	23	22	25	21	20	19	23	23
Zr	123	146	130	130	133	124	122	142	144
Nb	27	31	29	28	29	27	26	30	31
Ba	453	499	455	459	431	379	409	504	439
Pb	15	2	10	25	24	11	1	3	0
Th	*	0	*	*	*	*	*	1	*
La	13	11	13	14	18	16	20	18	15
Ce	36	37	37	40	38	29	36	46	43
Nd	16	23	17	24	19	20	19	22	23
Y	20	25	21	21	21	20	20	23	22
Q	-	-	-	-	-	-	-	-	-
or	5.70	6.82	5.77	5.67	5.65	5.25	5.08	6.18	6.26
ab	23.09	22.92	21.51	23.11	22.65	23.48	21.22	23.53	24.24
an	22.70	22.99	20.08	20.93	22.35	20.96	20.20	22.79	21.37
ne	0.61	-	3.92	2.79	1.91	2.62	3.71	0.04	0.72
lct	-	-	-	-	-	-	-	-	-
di	17.62	19.41	20.01	19.39	18.65	18.35	17.42	19.16	20.34
hy	-	2.39	-	-	-	-	-	-	-
ol	23.79	18.83	22.12	21.52	22.22	22.92	26.18	21.69	20.46
mt	2.25	2.05	2.25	2.26	2.25	2.24	2.18	2.10	2.13
il	3.50	3.73	3.57	3.55	3.56	3.45	3.34	3.67	3.63
ap	0.75	0.84	0.76	0.76	0.77	0.72	0.70	0.84	0.83
cort	-	-	-	-	-	-	-	-	-

	SW159 (3)	SW160 (3)	SW161A (3)	SW161B (3)	SW161C (3)	SW162 (3)	SW163 (3)	SW170 (3)	SW172 (3)
SiO2	48.01	46.52	46.54	46.70	46.61	46.80	46.69	46.30	46.61
Al2O3	13.84	13.69	13.73	13.79	13.78	14.45	14.73	14.99	14.65
Fe2O3	12.23	12.23	12.18	12.28	12.37	11.98	12.03	12.17	12.14
MgO	9.00	10.15	10.18	10.02	9.75	11.46	10.84	10.38	9.92
CaO	9.78	9.34	9.21	8.95	9.05	9.64	9.32	10.18	10.93
Na2O	2.95	3.55	3.60	3.68	3.76	2.14	2.94	1.70	1.84
K2O	1.08	1.13	1.21	1.20	1.19	1.13	0.80	1.46	1.23
TiO2	1.91	1.94	1.95	1.99	2.02	1.86	1.90	1.66	1.66
MnO	0.39	0.18	0.17	0.19	0.19	0.17	0.17	0.12	0.15
P2O5	0.35	0.46	0.46	0.48	0.50	0.41	0.42	0.31	0.31
TOTAL	99.54	99.18	99.21	99.28	99.21	99.63	99.83	99.27	99.46
LOI	2.1	2.0	2.1	2.3	2.3	3.7	3.7	3.4	3.9
Ni	234	232	220	233	226	299	290	194	188
Cr	335	339	329	345	333	440	440	450	476
V	246	231	227	237	240	233	247	276	281
Sc	26	23	23	24	22	28	25	26	30
Cu	65	60	57	56	59	54	38	6	21
Zn	95	98	92	101	101	87	90	122	104
Sr	498	504	497	485	466	535	500	616	585
Rb	25	23	23	29	28	24	13	32	24
Zr	146	159	158	159	164	138	144	142	137
Nb	30	44	44	45	47	37	38	29	27
Ba	448	529	523	515	562	515	527	687	1186
Pb	3	2	3	3	3	3	4	17	11
Th	*	*	2	3	0	*	2	*	*
La	17	32	18	26	27	20	20	21	12
Ce	51	63	50	53	66	49	52	53	45
Nd	24	28	24	28	34	21	23	28	24
Y	23	22	22	23	23	21	21	20	20
Q	-	-	-	-	-	-	-	-	-
or	6.47	6.81	7.28	7.20	7.14	6.77	4.77	8.77	7.42
ab	24.26	19.21	18.89	20.24	20.04	18.34	22.17	14.67	15.84
an	21.66	18.42	18.08	17.92	17.52	26.87	24.92	29.48	28.53
ne	0.59	6.16	6.56	6.20	6.72	-	1.64	-	-
lct	-	-	-	-	-	-	-	-	-
di	20.59	20.88	20.64	19.60	20.23	15.30	15.46	16.13	19.95
hy	-	-	-	-	-	1.96	-	3.95	2.35
ol	19.77	21.51	21.55	21.71	21.07	24.11	24.29	20.91	19.86
mt	2.13	2.14	2.13	2.15	2.17	2.09	2.09	2.13	2.12
il	3.68	3.75	3.77	3.85	3.90	3.59	3.65	3.21	3.20
ap	0.85	1.12	1.10	1.15	1.20	0.98	1.01	0.75	0.74
cort	-	-	-	-	-	-	-	-	-

	SW173 (3)	SW174 (3)	SW175 (3)	SW177 (3)	SW178 (3)	SW179 (3)	SW180 (3)	SW181 (3)	SW182 (3)
SiO2	46.80	46.59	46.87	46.93	46.68	46.80	46.32	46.29	46.75
Al2O3	14.93	15.03	14.72	14.89	14.74	14.88	14.56	14.45	14.75
Fe2O3	12.13	12.16	12.00	12.15	11.95	12.12	11.65	11.89	11.91
MgO	9.15	8.77	11.18	9.63	8.99	9.05	10.68	10.36	9.98
CaO	10.65	10.54	10.42	10.44	10.66	10.50	10.31	10.29	10.00
Na2O	2.14	2.31	1.84	1.90	2.50	2.17	2.20	2.02	2.38
K2O	1.57	1.65	1.27	1.40	1.58	1.59	1.16	1.20	1.27
TiO2	1.73	1.73	1.66	1.69	1.67	1.68	1.96	1.95	1.98
MnO	0.19	0.21	0.18	0.15	0.19	0.20	0.18	0.16	0.15
P2O5	0.33	0.34	0.31	0.32	0.32	0.32	0.45	0.45	0.46
TOTAL	99.61	99.32	100.46	99.49	99.24	99.31	99.49	99.07	99.63
LOI	3.1	2.8	3.9	3.5	2.7	3.1	3.5	3.3	3.2
Ni	183	182	208	190	187	187	290	305	296
Cr	469	481	485	428	446	449	436	423	443
V	290	279	264	284	242	240	235	244	251
Sc	25	24	24	20	25	24	28	26	27
Cu	35	52	34	24	40	40	27	9	17
Zn	134	126	127	117	112	113	81	84	87
Sr	612	608	610	622	596	600	591	608	608
Rb	36	37	27	33	35	35	29	27	30
Zr	145	147	143	142	142	144	152	151	154
Nb	29	30	29	28	29	29	42	42	43
Ba	833	833	748	808	686	719	616	562	565
Pb	15	12	8	23	12	12	2	2	1
Th	*	*	0	*	*	*	1	0	1
La	19	16	17	17	17	16	24	20	31
Ce	54	49	52	53	46	52	56	55	60
Nd	25	30	25	28	28	24	25	28	26
Y	22	21	21	20	20	20	22	23	22
q	-	-	-	-	-	-	-	-	-
or	9.42	9.93	7.57	8.37	9.28	9.56	6.99	7.24	7.59
ab	16.33	15.64	15.67	16.34	15.54	16.73	18.26	17.47	19.84
an	26.89	26.21	28.31	28.41	24.90	26.60	26.83	27.34	26.20
ne	1.09	2.33	-	-	3.23	1.08	0.35	-	0.31
lct	-	-	-	-	-	-	-	-	-
di	19.96	20.18	17.50	17.99	21.85	19.79	17.86	17.57	17.08
hy	-	-	2.84	3.89	-	-	-	2.70	-
ol	20.07	19.44	22.52	18.86	19.09	20.10	22.81	20.72	21.98
mt	2.11	2.13	2.07	2.12	2.09	2.12	2.03	2.08	2.08
il	3.33	3.34	3.17	3.25	3.23	3.24	3.78	3.78	3.82
ap	0.79	0.81	0.75	0.76	0.78	0.77	1.09	1.10	1.11
cort	-	-	-	-	-	-	-	-	-

	SW173 (3)	SW174 (3)	SW175 (3)	SW177 (3)	SW178 (3)	SW179 (3)	SW180 (3)	SW181 (3)	SW182 (3)
SiO2	46.80	46.59	46.87	46.93	46.68	46.80	46.32	46.29	46.75
Al2O3	14.93	15.03	14.72	14.89	14.74	14.88	14.56	14.45	14.75
Fe2O3	12.13	12.16	12.00	12.15	11.95	12.12	11.65	11.89	11.91
MgO	9.15	8.77	11.18	9.63	8.99	9.05	10.68	10.36	9.98
CaO	10.65	10.54	10.42	10.44	10.66	10.50	10.31	10.29	10.00
Na2O	2.14	2.31	1.84	1.90	2.50	2.17	2.20	2.02	2.38
K2O	1.57	1.65	1.27	1.40	1.54	1.59	1.16	1.20	1.27
TiO2	1.73	1.73	1.66	1.69	1.67	1.68	1.96	1.95	1.98
MnO	0.19	0.21	0.18	0.15	0.19	0.20	0.18	0.16	0.15
P2O5	0.33	0.34	0.31	0.32	0.32	0.32	0.45	0.45	0.46
TOTAL	99.61	99.32	100.46	99.49	99.24	99.31	99.49	99.07	99.63
LOI	3.1	2.8	3.9	3.5	2.7	3.1	3.5	3.3	3.2
Ni	183	182	208	190	187	187	290	305	296
Cr	469	481	445	428	446	489	436	423	443
V	290	279	264	284	282	280	235	284	251
Sc	25	24	24	20	25	24	28	26	27
Cu	35	52	34	24	40	40	27	9	17
Zn	134	126	127	117	112	113	81	84	87
Sr	612	608	610	622	596	600	591	608	608
Rb	36	37	27	33	35	35	29	27	30
Zr	145	147	143	142	142	144	152	151	154
Nb	29	30	29	28	29	29	42	42	43
Ba	833	833	748	808	686	719	616	562	565
Pb	15	12	8	23	12	12	2	2	1
Th	*	*	0	*	*	*	1	0	1
La	19	16	17	17	17	16	24	20	31
Ce	54	49	52	53	46	52	56	55	60
Nd	25	30	25	28	28	24	25	28	26
Y	22	21	21	20	20	20	22	23	22
Q	-	-	-	-	-	-	-	-	-
or	9.42	9.93	7.57	8.37	9.28	9.56	6.99	7.24	7.59
ab	16.33	15.64	15.67	16.34	15.54	16.73	18.26	17.47	19.84
an	26.89	26.21	28.31	28.41	28.90	26.60	26.83	27.34	26.20
ne	1.09	2.33	-	-	3.23	1.08	0.35	-	0.31
lct	-	-	-	-	-	-	-	-	-
di	19.96	20.18	17.50	17.99	21.85	19.79	17.86	17.57	17.08
hy	-	-	2.44	3.89	-	-	-	2.70	-
ol	20.07	19.44	22.52	18.86	19.09	20.10	22.81	20.72	21.98
mt	2.11	2.13	2.07	2.12	2.09	2.12	2.03	2.08	2.08
il	3.33	3.34	3.17	3.25	3.23	3.24	3.78	3.78	3.82
ap	0.79	0.81	0.75	0.76	0.78	0.77	1.09	1.10	1.11
cort	-	-	-	-	-	-	-	-	-

	SW185 (3)	SW186 (3)	SW187 (3)	SW188 (3)	SW189 (3)	SW190A (3)	SW190C (3)	SW190D (3)	SW190E (3)
SiO2	47.22	47.07	46.86	46.88	47.11	47.06	48.23	45.07	48.03
Al2O3	14.77	14.66	14.66	14.87	14.51	14.62	14.30	14.60	14.17
Fe2O3	12.03	12.08	12.01	12.26	12.53	12.18	12.82	12.73	13.19
MgO	9.43	9.93	10.32	10.55	9.62	9.97	10.68	10.17	11.03
CaO	10.09	9.91	9.96	9.83	9.83	9.78	10.84	10.84	10.85
Na2O	2.39	2.36	2.20	2.30	2.42	2.51	2.30	1.93	2.23
K2O	1.22	1.19	1.17	1.11	1.03	1.12	0.93	1.19	0.83
TiO2	1.90	1.89	1.91	1.89	1.87	1.89	2.59	2.30	2.45
MnO	0.17	0.17	0.18	0.17	0.16	0.17	0.16	0.18	0.16
P2O5	0.42	0.42	0.42	0.41	0.41	0.40	0.46	0.41	0.45
TOTAL	99.65	99.68	99.68	99.81	99.48	99.70	99.32	99.41	99.40
LOI	2.7	3.0	3.1	3.4	2.7	2.9	3.6	2.8	3.4
Ni	287	290	285	283	283	297	265	253	278
Cr	436	445	461	480	431	434	350	386	368
V	247	250	243	233	245	239	300	286	290
Sc	28	28	25	27	26	26	20	26	23
Cu	19	21	73	24	86	17	17	33	22
Zn	91	95	86	86	98	90	163	112	97
Sr	573	562	584	580	527	521	676	658	658
Rb	31	29	28	26	25	25	13	28	12
Zr	147	144	146	143	139	139	171	160	173
Nb	39	39	39	38	36	37	49	42	48
Ba	538	494	521	516	489	480	635	572	597
Pb	4	3	2	4	2	4	3	2	2
Th	1	0	1	*	0	0	*	*	*
La	23	24	18	21	21	19	22	24	23
Ce	53	53	54	56	48	51	65	50	66
Nd	26	22	23	21	21	22	32	27	27
Y	22	22	23	22	22	21	21	23	22
Q	-	-	-	-	-	-	-	-	-
or	7.33	7.16	7.00	6.67	6.21	6.70	5.57	7.16	4.97
ab	20.47	20.29	18.85	19.77	20.78	21.49	19.24	14.44	12.88
an	26.33	26.23	27.05	26.33	26.10	25.69	26.42	28.12	26.67
ne	-	-	-	-	-	-	3.58	1.17	3.42
lct	-	-	-	-	-	-	-	-	-
di	17.62	16.93	16.42	16.63	16.88	16.92	20.45	19.34	20.32
hy	1.53	1.57	3.10	0.35	3.66	0.16	-	-	-
ol	19.95	21.07	20.80	23.48	19.59	22.31	22.37	22.11	23.59
mt	2.10	2.10	2.09	2.14	2.19	2.12	2.24	2.22	2.31
il	3.67	3.64	3.68	3.64	3.61	3.64	5.01	4.44	4.74
ap	1.00	1.00	1.01	0.99	0.98	0.97	1.12	1.00	1.10
cort	-	-	-	-	-	-	-	-	-

	SW194 (3)	SW195 (3)	SW196 (3)	SW197 (3)	SW198 (3)	SW199 (3)	SW200 (3)	SW201 (3)	SW202 (3)
SiO2	46.59	46.79	46.19	45.74	46.52	45.94	46.43	46.44	43.52
Al2O3	14.59	13.70	13.85	13.76	13.99	14.02	14.21	13.99	13.43
Fe2O3	11.32	12.53	12.02	12.14	11.99	12.02	11.84	11.91	12.65
MgO	11.53	10.14	12.24	13.91	11.69	13.79	10.99	11.98	12.65
CaO	9.22	9.26	9.62	8.69	9.93	8.40	9.90	9.89	10.44
Na2O	2.01	2.63	2.05	1.86	2.36	2.06	2.60	2.22	2.38
K2O	1.23	1.22	1.10	1.02	0.58	0.82	0.66	0.59	1.30
TiO2	2.03	2.00	1.89	1.82	1.95	1.92	1.95	1.93	2.03
MnO	0.16	0.18	0.17	0.16	0.18	0.16	0.19	0.18	0.19
P2O5	0.43	0.50	0.40	0.40	0.42	0.42	0.42	0.42	0.73
TOTAL	99.09	99.00	99.53	99.49	99.61	99.56	99.20	99.56	99.39
LOI	3.7	2.9	3.9	4.6	3.7	4.9	3.4	3.9	4.1
Ni	355	411	395	427	380	371	357	373	316
Cr	515	572	532	578	528	543	486	505	438
V	434	215	244	306	264	263	246	253	248
Sc	31	23	28	26	23	27	24	22	23
Cu	30	31	51	41	23	14	26	23	25
Zn	92	94	85	93	92	85	88	87	110
Sr	558	525	515	485	527	508	539	520	807
Rb	32	29	27	23	8	9	7	10	31
Zr	144	156	136	130	137	140	142	138	193
Nb	38	43	36	35	36	36	37	35	64
Ba	592	578	494	490	507	540	497	497	784
Pb	2	3	2	2	2	2	1	2	3
Th	*	*	0	1	*	*	*	*	1
La	25	29	18	19	17	22	24	24	45
Ce	57	56	48	43	58	52	50	45	94
Nd	28	22	21	24	28	24	23	25	42
Y	24	24	21	21	23	22	23	23	25
Q	-	-	-	-	-	-	-	-	-
or	7.40	7.34	6.63	6.11	3.45	4.92	3.98	3.56	7.84
ab	17.33	22.42	17.62	16.01	20.29	17.73	22.05	19.09	7.93
an	27.69	22.46	25.70	26.59	26.24	26.97	25.63	26.82	22.48
ne	-	0.17	-	-	-	-	0.17	-	6.81
lct	-	-	-	-	-	-	-	-	-
di	12.95	17.14	16.22	11.71	16.92	10.06	17.48	16.32	20.64
hy	7.19	-	1.76	5.65	3.45	7.21	-	5.14	-
ol	20.49	23.18	25.37	27.35	22.80	26.29	23.82	22.26	26.37
mt	1.98	2.20	2.10	2.12	2.09	2.10	2.07	2.08	2.21
il	3.93	3.89	3.64	3.51	3.76	3.70	3.78	3.73	3.97
ap	1.04	1.22	0.96	0.96	1.00	1.02	1.02	1.00	1.75
cort	-	-	-	-	-	-	-	-	-

	SW204 (3)	SW206 (3)	SW207 (3)	SW208 (3)	SW209 (3)	SW210 (3)	SW213 (3)	SW214 (3)	SW217 (3)
SiO2	45.72	46.06	47.29	46.62	46.70	46.13	46.26	46.26	46.12
Al2O3	13.90	13.55	14.19	14.26	14.29	13.97	13.51	13.51	13.99
Fe2O3	11.80	12.40	12.11	12.08	12.06	11.99	12.15	12.23	11.86
MgO	13.73	12.48	9.58	10.07	9.89	12.88	13.75	12.85	12.25
CaO	8.49	9.27	9.89	9.82	9.88	8.77	8.81	9.04	9.19
Na2O	2.71	2.39	2.43	2.38	2.27	2.08	1.97	2.02	2.17
K2O	0.80	0.80	1.28	1.32	1.33	1.10	1.02	0.99	1.14
TiO2	1.88	1.91	1.97	1.96	1.98	1.89	1.80	1.82	1.85
MnO	0.16	0.19	0.17	0.17	0.17	0.17	0.20	0.16	0.18
P2O5	0.40	0.43	0.44	0.43	0.43	0.40	0.39	0.39	0.39
TOTAL	99.59	99.47	99.35	99.08	99.01	99.38	99.85	99.27	99.14
LOI	4.9	3.9	2.6	3.0	2.8	4.2	4.5	4.0	4.2
Ni	378	424	360	356	346	384	441	477	368
Cr	509	563	505	500	517	544	625	574	529
V	238	270	252	248	291	275	259	269	235
Sc	24	21	23	25	25	27	29	25	25
Cu	65	28	45	55	52	48	49	35	21
Zn	90	84	87	92	83	95	91	93	87
Sr	405	505	556	547	549	488	455	491	479
Rb	14	12	32	34	34	27	25	20	26
Zr	135	137	146	146	146	138	130	131	133
Nb	36	35	39	39	39	37	34	33	34
Ba	441	564	555	578	664	504	470	496	431
Pb	2	3	2	2	2	3	2	2	2
Th	0	1	*	0	*	*	*	*	*
La	21	22	21	19	18	19	20	20	16
Ce	44	56	44	53	54	49	45	44	48
Nd	23	26	23	22	25	25	21	19	21
Y	21	22	22	21	22	22	20	21	20
Q	-	-	-	-	-	-	-	-	-
or	4.78	4.77	7.72	7.97	8.03	6.61	6.11	5.98	6.88
ab	19.57	20.58	20.87	19.88	19.58	17.91	16.90	17.80	18.71
an	23.72	24.28	24.46	24.99	25.41	25.95	25.29	25.32	25.54
ne	2.01	-	-	0.17	-	-	-	-	-
lct	-	-	-	-	-	-	-	-	-
di	13.15	15.86	18.30	17.69	17.62	12.59	13.18	14.29	14.82
hy	-	0.07	1.81	-	1.32	4.16	5.17	5.79	1.07
ol	30.12	27.57	19.85	22.33	21.04	26.07	26.86	24.60	26.40
mt	2.06	2.16	2.12	2.12	2.12	2.10	2.11	2.14	2.08
il	3.62	3.68	3.80	3.80	3.85	3.65	3.45	3.52	3.59
ap	0.97	1.03	1.06	1.04	1.05	0.96	0.93	0.94	0.94
cort	-	r	-	-	-	-	-	-	-

	SW218 (2)	SW222 (3)	SW223 (3)	SW228 (3)	SW227 (3)	SW229 (3)	SW230 (3)	SW231 (3)	SW232 (3)
SiO2	49.22	45.53	45.85	46.84	48.25	43.94	44.32	44.00	44.84
Al2O3	17.29	12.44	14.12	13.95	15.22	14.19	13.41	14.13	13.40
Fe2O3	10.86	12.21	11.82	12.24	12.45	12.44	12.35	12.24	12.44
MgO	5.18	15.55	13.58	10.15	9.07	11.42	12.01	12.23	12.39
CaO	7.86	8.35	8.63	10.11	8.68	11.75	11.10	11.63	11.86
Na2O	4.84	1.96	1.70	2.28	2.82	1.88	1.61	1.60	1.44
K2O	2.33	0.74	1.05	0.97	0.73	0.70	0.97	0.61	0.92
TiO2	1.83	1.70	1.81	1.86	1.72	2.07	1.98	2.03	1.89
MnO	0.15	0.22	0.34	0.20	0.15	0.19	0.18	0.21	0.25
P2O5	0.43	0.34	0.41	0.32	0.23	0.56	0.41	0.54	0.42
TOTAL	100.00	99.05	99.31	98.92	99.32	99.14	98.32	99.22	99.45
LOI	3.7	5.5	4.6	2.8	4.5	4.7	4.3	5.2	4.9
Ni	40	340	334	235	251	302	312	291	375
Cr	29	544	506	394	508	513	537	478	584
V	250	207	268	239	254	282	272	284	268
Sc	14	22	27	24	31	26	22	26	23
Cu	58	37	25	39	6	34	25	27	26
Zn	100	78	112	114	125	95	87	105	85
Sr	559	384	488	484	395	689	553	660	577
Rb	59	19	25	24	11	8	17	6	18
Zr	184	114	133	127	122	165	145	158	150
Nb	46	29	34	30	19	41	35	40	37
Ba	914	313	746	447	324	863	667	928	803
Pb	4	1	23	1	21	10	2	20	6
Th	1	*	*	*	*	*	*	*	*
La	25	15	21	20	8	28	21	20	21
Ce	61	32	46	43	24	63	53	61	57
Nd	31	16	26	19	14	27	27	26	27
Y	24	18	22	21	23	23	21	22	20
Q	-	-	-	-	-	-	-	-	-
or	13.92	4.48	6.32	5.86	4.37	4.25	5.88	3.68	5.53
ab	23.32	16.94	14.63	19.75	24.27	11.51	12.49	12.45	12.32
an	18.74	23.41	28.27	25.49	27.21	28.72	27.25	30.14	27.83
ne	9.75	-	-	-	-	2.57	0.82	0.70	0.04
lct	-	-	-	-	-	-	-	-	-
di	14.71	13.33	10.11	19.15	12.33	21.86	21.50	20.20	21.98
hy	-	8.66	9.86	3.18	10.06	-	-	-	-
ol	13.15	30.92	24.27	20.03	15.69	23.56	25.01	25.45	25.47
mt	1.88	2.14	2.07	2.15	2.18	2.18	2.18	2.14	2.17
il	3.51	3.30	3.50	3.61	3.33	4.00	3.87	3.93	3.65
ap	1.03	0.82	0.99	0.78	0.55	1.35	0.99	1.30	1.00
cort	-	-	-	-	-	-	-	-	-

	SW235 (1)	SW241 (1)	SW243A (1)	SW243B (1)	SW246 (1)	SW247 (1)	SW248 (1)	SW249 (1)	SW250 (1)
SiO2	47.34	45.39	43.01	46.69	47.18	47.45	47.56	47.82	48.59
Al2O3	15.14	15.03	14.64	14.92	16.13	15.28	14.76	14.78	14.68
Fe2O3	12.89	13.85	12.39	12.52	11.40	11.68	11.72	12.79	12.12
MgO	7.49	7.77	6.13	6.37	5.77	7.14	6.29	8.23	7.45
CaO	10.63	11.76	12.41	12.95	13.02	12.00	12.03	9.63	10.43
Na2O	2.58	2.18	2.50	2.73	2.83	2.56	2.91	2.44	2.57
K2O	1.03	1.11	1.10	1.12	1.10	1.04	1.13	1.02	1.08
TiO2	2.05	1.94	2.01	2.08	2.16	2.05	2.10	2.03	2.05
MnO	0.14	0.14	0.15	0.18	0.11	0.16	0.14	0.13	0.13
P2O5	0.54	0.52	0.56	0.57	0.54	0.52	0.59	0.54	0.56
TOTAL	99.79	99.70	94.90	100.16	100.23	99.88	99.24	99.43	99.66
LOI	4.0	6.0	5.3	5.6	5.9	4.2	3.4	2.9	3.0
Ni	192	197	182	176	187	177	183	194	210
Cr	261	279	237	253	286	263	247	255	258
V	227	229	217	224	250	227	218	223	208
Sc	25	28	20	25	29	27	20	25	21
Cu	58	51	57	59	68	60	69	60	57
Zn	126	158	260	347	429	338	122	114	97
Sr	518	519	596	608	572	535	617	535	662
Rb	19	18	19	20	19	17	20	18	20
Zr	179	182	190	199	194	183	201	189	192
Nb	38	38	40	41	39	37	42	39	41
Ba	407	685	1704	748	449	420	476	416	557
Pb	3	4	2	0	37	29	2	97	3
Th	0	1	*	*	*	*	*	2	*
La	27	26	21	31	24	31	27	29	30
Ce	55	62	61	68	63	67	76	68	66
Nd	25	30	33	35	32	34	35	32	31
Y	25	26	26	27	28	27	27	25	26
Q	-	-	-	-	-	-	-	-	-
or	6.15	6.65	6.96	6.69	6.55	6.20	6.77	6.14	6.48
ab	21.75	18.84	10.93	15.12	16.74	20.22	20.78	21.00	22.09
an	27.25	28.37	27.12	25.37	28.27	27.48	24.30	26.82	25.65
ne	-	2.12	6.30	4.46	4.00	0.89	2.33	-	-
lct	-	-	-	-	-	-	-	-	-
di	18.56	22.52	28.54	29.42	27.36	24.01	26.74	14.87	18.93
hy	3.60	-	-	-	-	-	-	11.90	9.68
ol	15.21	18.09	12.41	11.42	9.69	13.99	11.55	11.81	9.78
mt	2.25	2.42	2.27	2.17	1.97	2.03	2.05	2.23	2.11
il	3.95	3.74	4.06	3.99	4.13	3.94	4.05	3.93	3.94
ap	1.30	1.25	1.41	1.37	1.28	1.24	1.43	1.30	1.34
cort	-	-	-	-	-	-	-	-	-

	SW254 (1)	SW256 (1)	SW261 (1)	SW262 (1)	SW264 (1)	SW265 (1)	SW266 (1)	SW267 (1)	SW269 (1)
SiO2	49.11	46.94	49.83	46.69	47.72	47.98	47.82	47.12	50.62
Al2O3	14.41	15.61	14.95	14.39	15.08	14.69	14.81	14.26	15.50
Fe2O3	12.78	11.63	12.24	13.50	11.97	12.75	12.15	13.31	13.29
MgO	7.50	6.38	6.98	9.60	6.18	8.17	7.55	9.04	6.78
CaO	9.10	12.15	9.47	9.21	11.91	9.74	10.32	9.66	8.05
Na2O	2.86	2.53	3.10	2.17	2.49	2.69	2.51	2.48	2.61
K2O	0.92	1.01	0.88	1.00	1.17	0.98	1.13	1.06	0.93
TiO2	2.11	2.10	1.90	2.00	2.28	1.88	2.20	2.09	1.87
MnO	0.15	0.23	0.11	0.16	0.13	0.17	0.16	0.18	0.10
P2O5	0.36	0.50	0.38	0.39	0.50	0.41	0.49	0.48	0.30
TOTAL	99.26	99.06	99.81	99.10	99.42	99.48	99.13	99.65	100.04
LOI	2.3	9.4	2.1	3.4	3.1	2.2	2.3	1.8	3.2
Ni	209	170	177	197	178	182	198	188	160
Cr	248	321	248	228	218	231	226	218	285
V	196	249	195	208	221	200	238	221	219
Sc	17	32	28	21	25	21	24	24	26
Cu	81	52	33	57	72	52	83	67	68
Zn	135	383	91	96	100	104	107	103	155
Sr	355	456	367	451	588	520	591	593	303
Rb	18	20	19	20	25	21	24	24	21
Zr	155	185	143	155	189	163	186	173	133
Nb	27	36	25	33	43	38	42	38	22
Ba	329	355	361	1071	660	609	887	761	298
Pb	2	4	1	2	3	2	2	2	2
Th	*	1	*	*	1	1	0	0	*
La	17	28	17	13	29	15	26	29	11
Ce	42	62	44	48	54	48	66	53	30
Nd	23	31	20	23	29	26	28	24	15
Y	25	26	25	23	26	23	26	25	21
q	-	-	-	-	-	-	-	-	0.66
or	5.56	6.08	5.24	6.02	7.05	5.88	6.78	6.37	5.58
ab	24.64	20.04	26.59	18.71	21.39	23.16	21.61	21.35	22.33
an	24.20	28.83	24.58	27.16	26.95	25.53	26.35	25.00	28.14
ne	-	0.95	-	-	-	-	-	-	-
lct	-	-	-	-	-	-	-	-	-
di	15.94	24.07	17.05	13.77	24.88	17.07	18.45	16.91	8.48
hy	14.08	-	11.29	10.51	1.20	6.37	7.52	4.53	28.21
ol	8.43	12.72	8.65	16.63	11.25	15.15	11.73	18.43	-
mt	2.23	2.08	2.13	2.37	2.09	2.23	2.13	2.32	2.31
il	4.07	4.06	3.66	3.88	4.39	3.63	4.25	4.03	3.59
ap	0.86	1.21	0.82	0.95	1.20	0.99	1.18	1.06	0.71
cort	-	-	-	-	-	-	-	-	-

	SW270 (1)	SW274 (1)	SW276 (1)	SW277 (1)	SW280 (1)	SW286 (3)	SW297 (2)	SW298 (2)	SW299 (2)
SiO2	48.91	48.68	49.71	49.69	51.96	44.83	46.68	46.92	45.40
Al2O3	15.09	14.50	14.18	15.06	15.17	14.04	15.63	14.71	13.93
Fe2O3	11.13	12.44	12.55	13.03	10.96	12.43	11.09	11.88	12.25
MgO	5.90	7.37	8.43	5.39	5.72	10.69	9.06	11.17	12.50
CaO	12.92	9.87	8.37	11.06	9.73	11.85	10.51	9.59	10.35
Na2O	3.01	3.11	2.77	2.75	2.61	1.22	3.25	2.92	2.55
K2O	0.87	0.88	0.83	0.85	1.09	1.70	1.40	0.90	1.16
TiO2	1.93	2.14	2.08	1.79	1.83	1.84	1.57	1.30	1.65
MnO	0.13	0.16	0.15	0.13	0.10	0.18	0.17	0.18	0.18
P2O5	0.30	0.37	0.33	0.28	0.29	0.48	0.28	0.21	0.31
TOTAL	100.19	99.53	99.41	100.02	99.45	99.24	99.66	99.78	100.28
LOI	4.7	4.6	4.0	4.5	3.6	4.6	1.2	0.6	0.8
Ni	138	224	222	160	152	334	191	282	282
Cr	260	290	260	250	244	548	338	472	465
V	193	216	192	208	190	251	229	211	265
Sc	23	23	20	28	27	24	22	24	31
Cu	15	56	53	39	22	37	76	57	65
Zn	91	134	101	197	72	99	77	83	82
Sr	357	339	326	343	328	662	588	484	481
Rb	20	21	17	16	30	38	31	19	27
Zr	137	171	155	128	131	156	123	93	122
Nb	22	26	22	21	21	38	26	17	28
Ba	303	642	330	336	339	1788	508	348	502
Pb	2	1	5	1	1	2	1	2	2
Th	*	*	*	*	*	*	*	*	*
La	13	18	15	17	12	21	14	7	11
Ce	27	46	44	32	26	58	44	30	43
Nd	17	27	21	15	16	26	23	18	22
Y	26	25	23	22	21	20	21	18	21
Q	-	-	-	-	2.89	-	-	-	-
or	5.21	5.28	5.02	5.06	6.55	10.21	8.38	5.41	6.90
ab	21.40	26.76	23.86	23.55	22.43	8.32	14.33	19.04	11.00
an	25.26	23.35	24.20	26.53	26.86	28.36	24.24	24.65	23.29
ne	2.33	-	-	-	-	1.16	7.34	3.26	5.84
lct	-	-	-	-	-	-	-	-	-
di	30.69	19.61	12.92	22.51	16.64	22.99	21.70	17.92	21.30
hy	-	3.87	21.13	11.61	18.51	-	-	-	-
ol	8.78	13.94	5.88	4.37	-	22.07	18.38	24.65	25.64
mt	1.93	2.17	2.19	2.26	1.91	2.18	1.93	2.07	2.12
il	3.69	4.12	4.02	3.44	3.52	3.57	3.02	2.51	3.16
ap	0.73	0.90	0.80	0.67	0.69	1.15	0.68	0.51	0.75
cort	-	-	-	-	-	-	-	-	-

	SW300 (2)	SW301 (2)	SW303 (3)	SW304 (3)	SW305 (2)	SW306 (2)	SW307 (1)	SW308 (3)	SW309 (2)
SiO2	45.40	49.04	45.87	46.03	45.89	45.93	48.94	49.12	47.97
Al2O3	13.17	15.85	14.25	14.25	14.19	14.19	16.95	15.53	14.59
Fe2O3	12.23	10.52	12.45	12.53	12.53	12.58	11.87	11.99	12.14
MgO	14.39	6.13	11.45	11.18	11.09	11.04	4.75	7.67	7.92
CaO	9.30	11.30	9.78	9.87	9.92	9.83	9.53	7.87	9.19
Na2O	2.61	3.95	2.65	2.81	2.80	2.80	3.58	3.23	3.42
K2O	1.07	1.10	1.07	1.10	1.12	1.08	1.59	1.53	1.41
TiO2	1.29	1.70	1.57	1.62	1.61	1.61	2.33	2.09	2.19
MnO	0.18	0.16	0.18	0.19	0.18	0.18	0.19	0.18	0.18
P2O5	0.23	0.22	0.27	0.29	0.28	0.29	0.67	0.46	0.51
TOTAL	99.86	99.98	99.55	99.86	99.61	99.52	100.40	99.67	99.52
LOI	0.7	1.7	1.5	0.7	1.5	1.4	1.6	2.9	1.5
Ni	371	72	267	252	257	260	36	186	112
Cr	582	59	435	409	421	421	27	214	166
V	205	319	238	244	244	253	242	177	219
Sc	25	34	23	25	26	25	19	18	20
Cu	56	76	66	71	67	68	38	48	46
Zn	85	79	88	90	88	88	102	98	97
Sr	500	521	421	434	407	404	815	471	669
Rb	23	25	26	26	25	25	32	27	30
Zr	100	126	109	114	112	112	224	236	188
Nb	21	20	23	24	24	24	57	38	45
Ba	422	337	435	549	414	421	919	541	542
Pb	1	1	1	2	2	2	3	3	2
Th	*	0	*	*	*	*	2	0	*
La	9	13	8	17	10	15	39	35	30
Ce	38	33	26	27	30	29	98	71	66
Nd	18	16	18	17	15	12	44	29	29
Y	17	23	20	21	21	21	30	26	27
Q	-	-	-	-	-	-	-	-	-
or	6.40	6.58	6.42	6.59	6.74	6.46	9.45	9.14	8.47
ab	11.95	21.63	15.61	15.38	14.89	15.80	28.18	27.73	24.70
an	21.29	22.47	24.20	23.30	23.16	23.32	25.65	23.69	20.60
ne	5.65	6.58	3.87	4.70	4.97	4.48	1.24	-	2.54
lct	-	-	-	-	-	-	-	-	-
di	19.25	26.80	18.86	19.72	20.24	19.72	14.53	10.49	18.23
hy	-	-	-	-	-	-	-	5.88	-
ol	30.30	10.35	25.17	24.30	24.05	24.22	12.85	15.84	17.90
mt	2.13	1.83	2.17	2.18	2.19	2.20	2.05	2.09	2.12
il	2.48	3.27	3.08	3.11	3.10	3.11	4.45	4.03	4.23
ap	0.55	0.53	0.66	0.70	0.67	0.69	1.59	1.10	1.23
cort	-	-	-	-	-	-	-	-	-

	SW310 (2)	SW316A (3)	SW316B (3)	SW319 (3)	SW320 (3)	SW322 (3)	SW323 (3)	SW328 (3)	SW325 (3)
SiO2	49.34	42.58	43.85	44.66	42.76	45.72	44.05	44.47	46.74
Al2O3	16.04	14.67	14.58	14.99	15.26	14.75	13.70	14.46	15.80
Fe2O3	11.24	12.25	13.14	13.45	12.22	12.39	14.16	12.79	9.34
MgO	7.52	8.60	10.96	11.61	8.47	10.42	12.16	10.73	9.04
CaO	7.99	15.35	11.32	9.88	13.91	10.97	9.98	11.20	11.33
Na2O	3.17	2.74	1.72	1.43	3.53	1.84	1.40	1.82	3.16
K2O	1.23	0.90	1.02	1.38	0.61	1.25	1.44	1.26	1.59
TiO2	2.35	2.04	2.06	1.62	2.20	1.83	1.97	2.03	1.99
MnO	0.15	0.19	0.18	0.25	0.27	0.18	0.13	0.34	0.34
P2O5	0.44	0.42	0.42	0.30	0.46	0.33	0.40	0.43	0.39
TOTAL	99.46	99.70	99.26	99.53	99.68	99.67	99.39	99.53	99.74
LOI	3.4	6.2	4.1	4.2	6.1	3.9	4.0	3.4	4.7
Ni	82	268	295	286	279	288	318	308	311
Cr	137	521	497	520	483	511	470	513	615
V	221	291	300	285	302	263	279	293	288
Sc	23	27	29	33	30	29	29	27	30
Cu	51	72	55	70	48	51	43	44	78
Zn	81	125	103	201	106	56	73	86	176
Sr	449	681	568	551	1112	581	464	589	665
Rb	30	16	16	28	9	25	29	24	37
Zr	187	145	145	122	164	122	139	145	151
Nb	38	35	35	27	40	27	34	36	35
Ba	454	869	801	653	1142	684	757	779	930
Pb	4	6	8	6	6	4	2	1	1
Th	2	*	*	*	*	*	0	*	*
La	27	15	22	19	17	24	23	18	29
Ce	68	51	48	43	51	50	44	52	71
Nd	30	27	25	21	31	27	23	23	31
Y	28	22	23	20	22	22	20	22	22
Q	-	-	-	-	-	-	-	-	-
or	7.36	-	6.17	8.07	3.64	7.47	8.65	7.58	9.48
ab	27.22	-	10.29	12.30	0.54	14.15	11.07	10.44	12.18
an	26.31	25.39	29.61	31.02	28.31	28.70	27.35	27.98	24.49
ne	-	12.75	2.44	-	16.14	0.88	0.54	2.83	8.05
lct	-	4.23	/-	-	-	-	-	-	-
di	8.97	35.87	20.16	13.65	34.71	19.76	16.58	20.79	23.97
hy	12.09	-	-	1.32	-	-	-	-	-
ol	10.50	13.12	24.02	27.44	13.19	22.56	28.54	23.19	15.42
mt	1.96	2.13	2.30	2.35	2.13	2.16	2.48	2.23	1.62
il	4.52	3.93	3.99	3.12	4.24	3.52	3.82	3.91	3.83
ap	1.07	1.00	1.02	0.73	1.11	0.79	0.97	1.04	0.95
cort	-	1.57	-	-	-	-	-	-	-

	SW326 (3)	SW330 (3)	SW331B (3)	SW331C (3)	SW331D (3)	SW331E (3)	SW332A (3)	SW332B (3)	SW332C (3)
SiO2	51.34	44.22	44.60	41.83	46.10	45.02	45.76	42.21	47.51
Al2O3	15.45	14.10	12.83	12.79	16.45	13.33	15.77	12.94	13.73
Fe2O3	10.45	12.61	13.52	14.18	11.13	11.90	11.74	14.31	12.36
MgO	7.26	10.87	10.86	10.50	6.38	12.74	7.10	10.38	9.33
CaO	11.51	11.60	10.75	10.85	7.44	10.67	8.29	10.69	10.15
Na2O	2.06	2.36	3.00	3.84	4.45	2.18	4.93	3.61	2.78
K2O	0.52	1.04	0.75	1.15	2.87	0.97	1.87	1.19	1.12
TiO2	0.80	1.81	2.20	2.52	2.36	1.98	2.36	2.58	2.05
MnO	0.19	0.17	0.19	0.23	0.18	0.21	0.21	0.24	0.19
P2O5	0.09	0.49	0.63	0.98	1.21	0.46	1.01	0.83	0.39
TOTAL	99.66	99.27	99.33	98.86	98.56	99.47	99.04	98.98	99.60
LOI	1.3	3.9	3.1	2.9	4.5	3.5	3.2	2.9	2.4
Ni	85	312	291	189	248	292	118	167	266
Cr	316	518	395	227	62	500	128	203	417
V	243	249	263	241	169	273	207	252	267
Sc	46	23	27	18	8	23	11	17	22
Cu	129	25	22	20	46	38	46	29	34
Zn	72	91	118	189	78	84	79	127	87
Sr	190	728	782	1054	1087	726	928	945	570
Rb	11	11	27	23	69	48	42	34	34
Zr	89	158	209	268	272	168	246	267	150
Nb	4	38	55	82	93	49	83	77	35
Ba	246	905	798	1136	1363	925	1217	1168	668
Pb	5	5	4	3	5	6	4	2	3
Th	*	*	5	3	8	1	5	3	1
La	6	26	62	62	80	31	57	51	29
Ce	21	68	82	126	185	63	118	112	61
Nd	11	26	39	55	58	31	50	89	27
Y	28	21	28	30	31	23	30	27	28
Q	1.58	-	-	-	-	-	-	-	-
or	3.11	6.28	4.54	6.93	17.39	5.81	11.29	7.19	6.72
ab	17.61	8.80	14.09	3.84	17.73	12.90	17.92	5.03	21.97
an	31.80	25.23	19.67	18.63	16.83	24.10	15.66	15.92	22.02
ne	-	6.27	6.36	15.92	11.27	3.17	13.34	14.22	1.01
lct	-	-	-	-	-	-	-	-	-
di	20.86	24.44	24.72	27.65	10.51	21.46	16.01	26.67	21.55
hy	21.49	-	-	-	-	-	-	-	-
ol	-	22.10	22.45	21.26	16.77	25.56	16.72	21.43	19.68
mt	1.82	2.21	2.37	2.50	1.96	2.08	2.06	2.52	2.16
il	1.54	3.50	4.26	4.90	4.60	3.82	4.57	5.01	3.95
ap	0.21	1.17	1.53	2.36	2.94	1.10	2.44	2.02	0.94
cort	-	-	-	-	-	-	-	-	-

	SW332D (3)	SW332E (3)	SW333 (3)	SW334 (3)	SW335 (3)	SW336 (3)	SW337 (3)	SW338 (3)	SW339 (3)
SiO2	46.78	48.73	45.64	44.06	42.40	45.86	46.12	47.00	46.63
Al2O3	12.02	14.64	14.31	11.90	11.24	14.34	14.80	15.55	16.01
Fe2O3	12.81	12.17	12.56	14.24	13.68	12.95	12.51	12.44	14.17
MgO	11.49	7.87	9.65	11.27	16.22	9.96	8.98	10.02	7.47
CaO	10.40	9.25	10.07	11.36	10.04	9.65	10.60	9.79	9.29
Na2O	2.30	3.30	2.63	2.91	1.48	3.07	2.78	2.34	2.63
K2O	0.96	0.84	1.48	0.74	0.93	1.08	1.32	0.80	0.97
TiO2	1.89	1.87	2.16	2.15	2.31	1.93	2.02	1.62	1.67
MnO	0.21	0.19	0.22	0.22	0.21	0.18	0.16	0.18	0.18
P2O5	0.35	0.32	0.67	0.53	0.85	0.36	0.38	0.21	0.22
TOTAL	99.20	99.18	99.39	99.38	99.35	99.37	99.66	99.95	99.22
LOI	3.6	2.5	2.6	2.6	5.7	3.9	4.1	3.5	2.5
Ni	394	235	248	315	519	296	291	298	289
Cr	556	398	353	467	681	505	527	450	450
V	258	230	322	277	229	346	227	225	270
Sc	20	25	25	24	18	25	27	27	27
Cu	33	16	34	16	42	21	47	43	16
Zn	100	68	95	101	137	115	53	77	55
Sr	502	450	773	701	830	482	561	406	394
Rb	30	15	38	32	31	27	37	16	20
Zr	135	136	191	188	278	128	137	103	101
Nb	32	25	44	46	86	29	30	17	17
Ba	661	389	872	730	1143	598	687	439	427
Pb	2	3	3	2	*	31	7	6	7
Th	*	*	*	2	4	*	1	0	*
La	21	23	26	34	61	15	28	28	15
Ce	45	52	85	75	120	43	53	40	25
Nd	23	26	37	35	50	21	25	19	16
Y	22	24	28	24	25	20	24	26	22
Q	-	-	-	-	-	-	-	-	-
or	5.79	5.07	8.88	4.47	5.61	6.52	7.94	4.75	5.84
ab	19.27	28.43	16.16	10.03	8.43	17.44	15.43	19.99	22.75
an	20.04	23.10	23.25	17.54	21.67	22.53	24.34	29.94	29.59
ne	0.29	-	3.51	8.15	2.32	4.87	4.55	-	-
lct	-	-	-	-	-	-	-	-	-
di	24.49	17.61	18.80	29.51	18.79	19.33	21.58	14.50	13.18
hy	-	2.60	-	-	-	-	-	4.04	2.49
ol	23.38	16.66	21.41	22.36	34.25	22.44	19.19	21.01	19.92
mt	2.24	2.13	2.20	2.49	2.39	2.26	2.18	2.16	2.48
il	3.66	3.62	4.17	4.16	4.47	3.73	3.88	3.11	3.23
ap	0.84	0.77	1.61	1.29	2.05	0.88	0.91	0.50	0.53
cort	-	-	-	-	-	-	-	-	-

	SW342 (3)	SW345 (3)	SW358 (3)	SW3638 (2)	SW365 (3)	SW366 (3)	SW367 (3)	SW368 (3)	SW369 (3)
SiO2	44.38	47.50	49.95	48.02	44.88	44.29	45.87	47.31	44.71
Al2O3	14.36	16.97	15.50	16.84	14.94	13.99	15.07	17.02	14.63
Fe2O3	12.46	13.07	10.50	10.92	12.47	12.30	12.36	11.79	12.77
MgO	11.25	7.97	5.80	5.52	12.17	12.59	9.41	5.36	10.84
CaO	11.31	7.81	11.84	8.42	9.84	10.49	9.98	12.20	10.43
Na2O	1.34	3.13	3.03	4.91	1.63	2.49	2.96	3.15	2.27
K2O	1.29	1.35	0.88	2.64	1.15	0.77	1.19	0.25	1.01
TiO2	2.12	1.70	1.76	1.93	1.83	1.89	1.99	2.07	1.78
MnO	0.18	0.13	0.18	0.18	0.15	0.20	0.15	0.27	0.18
P2O5	0.34	0.31	0.27	0.52	0.41	0.52	0.44	0.22	0.39
TOTAL	99.01	99.94	99.66	99.86	99.87	99.54	99.42	99.65	98.99
LOI	4.4	4.3	3.3	4.6	5.1	4.5	3.7	2.9	4.2
Ni	262	275	155	38	405	333	378	102	412
Cr	457	558	313	58	549	517	750	126	506
V	266	251	199	232	272	242	317	316	281
Sc	27	33	25	16	28	21	27	32	28
Cu	26	15	57	71	37	51	46	111	53
Zn	55	89	112	77	96	82	84	102	86
Sr	539	463	398	540	660	653	580	401	651
Rb	31	27	21	37	20	9	14	4	15
Zr	154	137	130	180	153	175	152	159	151
Nb	35	27	20	38	38	38	37	5	35
Ba	654	474	303	1181	821	835	671	100	686
Pb	11	15	2	1	10	6	11	5	5
Th	0	1	2	2	*	3	*	*	1
La	30	42	23	26	28	45	25	3	40
Ce	63	63	32	62	50	65	58	22	67
Nd	24	35	15	28	23	31	30	19	33
Y	23	26	23	23	24	21	22	31	25
Q	-	-	-	-	-	-	-	-	-
or	7.77	8.06	5.30	15.75	6.88	4.64	7.12	1.49	6.09
ab	10.52	26.32	25.96	16.34	18.05	12.24	17.12	23.70	13.79
an	29.97	28.61	26.40	16.31	30.55	25.09	24.76	32.02	27.30
ne	0.58	0.27	-	13.90	-	4.96	4.50	1.80	3.17
lct	-	-	-	-	-	-	-	-	-
di	20.25	7.04	25.71	18.52	13.20	19.62	18.42	23.09	18.63
hy	-	-	2.67	-	1.85	-	-	-	-
ol	23.80	23.43	8.11	12.35	26.79	26.41	21.01	11.33	24.39
mt	2.19	2.27	1.83	1.90	2.18	2.15	2.16	2.05	2.24
il	4.11	3.26	3.38	3.70	3.53	3.65	3.85	3.99	3.45
ap	0.82	0.74	0.64	1.24	0.98	1.26	1.06	0.52	0.94
cort	-	-	-	-	-	-	-	-	-

	SW370 (3)	SW371 (3)	SW372 (3)	SW374 (2)	SW376 (2)	SW377 (3)	SW378 (3)	SW379 (3)	SW380 (3)
SiO2	43.70	43.37	47.65	48.28	47.61	43.13	48.38	44.04	46.08
Al2O3	13.92	12.43	15.18	17.63	17.03	14.49	14.73	14.35	15.08
Fe2O3	12.20	11.56	12.68	10.07	10.22	15.71	11.24	14.65	12.16
MgO	11.27	15.70	9.55	7.73	7.27	9.78	8.58	11.83	9.75
CaO	11.06	10.30	9.17	7.59	10.59	12.05	9.65	10.22	11.20
Na2O	3.26	3.05	2.96	4.66	4.42	1.67	3.05	1.86	1.66
K2O	1.10	0.55	1.03	1.45	0.83	0.91	0.90	0.44	1.01
TiO2	2.29	1.84	1.26	1.65	1.61	1.67	2.08	1.68	1.87
MnO	0.18	0.19	0.19	0.14	0.17	0.26	0.50	0.24	0.38
P2O5	0.50	0.58	0.18	0.25	0.26	0.29	0.46	0.28	0.33
TOTAL	99.48	99.57	99.85	99.45	100.02	99.95	99.56	99.58	99.51
LOI	2.0	2.2	0.5	5.0	4.5	4.5	3.5	4.2	3.0
Ni	275	500	206	67	86	261	137	295	301
Cr	460	891	367	77	322	406	281	525	477
V	312	266	229	257	239	272	195	273	272
Sc	31	29	25	23	32	25	20	30	29
Cu	60	77	85	133	51	55	61	59	74
Zn	79	69	91	58	65	76	190	57	145
Sr	626	649	328	329	757	452	412	456	497
Rb	15	7	23	33	17	19	19	5	22
Zr	178	163	88	104	101	114	173	112	129
Nb	49	42	16	20	19	23	32	23	28
Ba	792	755	362	655	412	568	389	516	628
Pb	0	1	3	5	1	1	1	5	2
Th	*	*	*	*	*	*	1	*	*
La	25	26	8	6	9	26	22	30	18
Ce	53	60	19	30	27	54	51	43	53
Nd	29	33	8	17	17	23	26	24	27
Y	23	22	20	20	20	24	26	24	26
Q	-	-	-	-	-	-	-	-	-
or	6.58	3.28	6.18	8.67	4.95	5.44	5.39	2.61	6.07
ab	6.45	7.42	22.66	24.88	19.20	6.32	26.18	15.39	14.30
an	20.42	18.87	25.40	23.23	24.37	29.80	24.18	30.05	31.17
ne	11.70	10.18	1.47	8.19	10.05	4.32	-	0.32	-
lct	-	-	-	-	-	-	-	-	-
di	25.84	23.34	15.88	10.84	21.95	23.76	17.35	16.01	18.77
hy	-	-	-	-	-	-	2.92	-	5.33
ol	21.25	29.96	23.35	18.65	14.00	23.71	16.91	29.14	17.86
mt	2.13	2.02	2.21	1.76	1.77	2.74	1.96	2.56	2.12
il	4.41	3.54	2.42	3.18	3.08	3.22	4.01	3.24	3.60
ap	1.21	1.39	0.44	0.59	0.62	0.69	1.10	0.67	0.79
cort	-	-	-	-	-	-	-	-	-

	SW381 (3)	SW382 (2)	SW383 (2)	SW391 (2)	SW392 (2)	SW393 (2)	SW396 (2)	SW397 (2)	SW402 (4)
SiO2	49.85	49.44	46.10	45.59	45.66	48.45	46.36	48.46	48.87
Al2O3	15.02	16.23	14.15	12.16	13.13	10.27	14.06	15.12	13.58
Fe2O3	10.82	11.69	11.71	12.77	12.58	13.74	12.58	11.17	12.98
MgO	7.04	3.85	12.38	15.59	13.16	19.17	11.04	7.87	10.52
CaO	9.63	9.58	9.64	8.48	9.22	7.33	9.55	9.91	8.53
Na2O	3.15	4.55	2.84	1.94	2.62	1.96	2.95	3.53	2.97
K2O	1.04	1.70	1.15	1.50	1.25	0.82	0.95	1.40	0.91
TiO2	2.45	2.43	1.32	1.30	1.44	1.15	1.49	1.80	1.72
MnO	0.40	0.17	0.17	0.19	0.18	0.19	0.18	0.17	0.17
P2O5	0.46	0.39	0.24	0.29	0.33	0.24	0.30	0.36	0.34
TOTAL	99.87	100.03	99.69	99.82	99.56	99.31	99.45	99.79	100.60
LOI	1.6	1.6	0.6	2.3	0.8	2.1	0.3	1.6	3.1
Ni	68	30	300	422	323	560	269	131	242
Cr	81	10	498	650	493	808	389	290	337
V	235	313	209	191	212	189	242	240	184
Sc	27	18	22	21	23	22	23	22	19
Cu	75	98	58	54	68	50	76	66	46
Zn	143	92	82	92	89	98	93	88	104
Sr	402	620	529	466	491	329	408	576	409
Rb	13	36	24	25	29	19	22	32	19
Zr	191	175	104	111	119	89	113	146	141
Nb	35	32	22	26	28	18	23	32	25
Ba	431	739	479	445	485	323	380	581	339
Pb	0	2	*	1	1	2	2	2	2
Th	*	*	*	*	*	0	*	*	*
La	18	19	14	15	18	8	11	15	18
Ce	51	62	40	34	39	25	34	46	38
Nd	27	32	20	14	22	13	18	22	21
Y	33	31	17	17	18	15	19	23	21
Q	-	-	-	-	-	-	-	-	-
or	6.24	10.17	6.86	8.99	7.50	8.94	5.70	8.38	5.82
ab	26.92	26.10	18.09	12.66	13.80	13.87	18.31	22.22	25.28
an	24.02	19.03	22.77	20.28	20.70	17.13	22.69	21.58	21.13
ne	-	6.92	5.57	2.17	4.71	1.63	3.84	4.33	-
lct	-	-	-	-	-	-	-	-	-
di	17.29	22.03	19.86	16.84	19.07	18.74	19.05	21.08	15.55
hy	9.85	-	-	-	-	-	-	-	5.77
ol	7.99	8.13	26.09	34.03	28.86	42.89	28.62	16.19	20.51
mt	1.88	2.03	2.04	2.22	2.19	2.41	2.20	1.94	2.28
il	4.70	4.67	2.54	2.50	2.78	2.23	2.87	3.46	3.28
ap	1.11	0.93	0.57	0.70	0.78	0.58	0.72	0.85	0.82
cort	-	-	-	-	-	-	-	-	-

	SW803 (5)	SW804 (5)	SW805 (4)	SW806 (4)	SW808 (4)	SW809 (4)	SW813 (4)	SW814 (4)	SW815 (4)
SiO2	46.00	45.90	45.16	48.68	48.46	48.87	48.45	48.37	47.20
Al2O3	14.72	14.26	14.32	14.19	14.20	14.79	14.39	14.32	14.30
Fe2O3	12.08	12.10	12.11	12.07	13.56	13.14	13.16	13.27	12.61
MgO	7.17	9.29	9.36	9.31	10.00	8.35	9.45	9.32	8.54
CaO	11.28	9.92	9.47	8.92	8.09	8.30	8.50	8.28	9.06
Na2O	2.47	3.03	2.94	3.37	2.82	3.20	2.91	3.11	3.60
K2O	1.94	0.89	2.17	0.91	0.83	0.87	0.80	0.95	1.37
TiO2	2.95	2.85	2.91	1.72	1.65	1.73	1.67	1.67	1.94
MnO	0.19	0.19	0.20	0.17	0.18	0.17	0.18	0.19	0.20
P2O5	0.55	0.53	0.55	0.34	0.25	0.27	0.26	0.26	0.57
TOTAL	99.35	98.97	99.18	99.69	100.03	99.68	99.77	99.74	99.37
LOI	3.6	3.5	2.0	1.1	2.5	2.2	1.9	1.3	1.7
Ni	205	199	213	191	231	205	203	207	151
Cr	282	269	280	297	295	296	295	293	245
V	258	246	255	186	189	197	191	189	205
Sc	18	21	20	23	19	21	24	22	20
Cu	49	46	49	46	50	53	51	52	44
Zn	97	96	95	99	111	110	109	107	104
Sr	817	1014	771	424	311	346	295	355	686
Rb	43	13	56	22	17	17	16	19	28
Zr	313	309	304	142	116	122	118	120	204
Nb	70	69	70	26	17	18	18	18	44
Ba	858	1040	881	282	296	350	264	315	591
Pb	3	3	3	2	1	2	1	1	3
Th	4	1	3	*	*	*	*	*	1
La	39	40	38	15	9	16	12	8	34
Ce	85	98	90	42	21	28	24	31	73
Nd	45	41	43	22	14	16	13	17	37
Y	28	27	27	22	22	23	23	23	29
Q	-	-	-	-	-	-	-	-	-
or	11.67	5.39	13.08	5.46	4.98	5.20	4.82	5.69	8.22
ab	13.81	21.53	11.75	28.07	24.13	27.49	24.93	26.72	22.16
an	23.75	23.13	19.84	21.20	23.89	23.77	24.18	22.61	19.14
ne	4.03	2.53	7.35	0.45	-	-	-	-	4.79
lct	-	-	-	-	-	-	-	-	-
di	24.13	19.12	19.74	17.41	12.25	13.33	13.75	14.16	18.63
hy	-	-	-	-	10.31	7.23	8.30	3.60	-
ol	13.48	19.36	19.17	21.16	18.31	16.72	17.89	21.07	19.75
mt	2.11	2.12	2.12	2.10	2.36	2.29	2.29	2.31	2.20
il	5.70	5.53	5.63	3.32	3.17	3.33	3.22	3.21	3.74
ap	1.32	1.28	1.32	0.82	0.60	0.64	0.62	0.63	1.37
cort	-	-	-	-	-	-	-	-	-

	SW816 (5)	SW817 (5)	SW820 (4)	SW821 (4)	SW822 (4)	SW823 (5)	SW824 (5)	SW826 (5)	SW827 (5)
SiO2	44.12	44.78	47.65	49.51	48.27	44.88	45.28	44.38	44.93
Al2O3	14.01	14.23	15.74	16.99	14.34	15.17	15.42	14.27	14.37
Fe2O3	13.74	13.66	10.90	10.55	12.62	13.45	12.73	13.47	13.13
MgO	8.91	7.92	9.06	5.81	9.02	8.91	8.43	7.86	8.10
CaO	9.87	9.41	8.42	7.35	8.33	10.05	9.51	10.48	10.39
Na2O	4.25	3.81	3.44	4.43	3.32	2.74	3.16	3.61	3.25
K2O	0.80	1.67	1.56	2.18	1.21	0.77	0.58	1.46	1.45
TiO2	3.09	2.85	1.99	2.01	1.83	3.03	3.11	3.05	3.03
MnO	0.26	0.54	0.19	0.21	0.18	0.22	0.22	0.26	0.33
P2O5	0.73	0.91	0.35	0.53	0.37	0.61	0.63	0.64	0.67
TOTAL	99.75	99.77	99.30	99.57	99.49	99.85	99.08	99.49	99.64
LOI	2.8	3.2	3.7	3.5	0.9	4.2	4.1	2.9	2.8
Ni	157	98	102	37	194	177	159	290	299
Cr	219	113	823	52	278	188	183	377	450
V	258	194	239	205	198	254	268	290	290
Sc	18	15	22	18	22	15	18	26	30
Cu	49	33	70	26	45	51	33	113	79
Zn	116	127	87	104	106	161	247	102	111
Sr	926	1355	679	565	466	1163	1127	703	708
Rb	6	22	30	44	24	15	13	45	36
Zr	360	492	146	251	154	342	349	278	278
Nb	87	123	24	56	28	77	81	64	63
Ba	1394	2153	937	769	391	1260	1213	793	728
Pb	3	0	2	2	3	1	1	2	3
Th	6	5	1	2	*	3	1	5	2
La	71	88	29	37	24	66	101	52	57
Ce	139	184	37	82	42	138	256	96	96
Nd	57	80	20	35	21	59	92	46	41
Y	33	42	24	29	25	32	34	30	29
Q	-	-	-	-	-	-	-	-	-
or	4.77	10.02	9.39	13.07	7.28	4.59	3.51	8.79	8.69
ab	15.19	14.87	22.85	28.28	27.37	20.16	28.50	11.77	14.42
an	17.06	17.01	23.30	20.29	20.98	27.16	26.71	18.71	20.65
ne	11.52	9.66	3.63	5.26	0.65	1.83	1.50	10.46	7.31
lct	-	-	-	-	-	-	-	-	-
di	22.67	19.88	13.64	10.80	15.16	15.73	14.06	24.50	22.25
hy	-	-	-	-	-	-	-	-	-
ol	18.72	18.50	20.59	15.32	21.96	20.87	19.94	15.99	16.94
mt	2.39	2.38	1.90	1.84	2.20	2.34	2.23	2.35	2.29
il	5.94	5.49	3.85	3.87	3.53	5.84	6.04	5.89	5.85
ap	1.74	2.20	0.85	1.26	0.88	1.47	1.51	1.53	1.61
cort	-	-	-	-	-	-	-	-	-

	SW428 (5)	SW429 (5)	SW434 (4)	SW435 (5)	SW436 (5)	SW437 (5)	SW438 (5)	SW439 (5)	SW440 (5)
SiO2	44.08	43.95	50.08	46.07	45.45	45.24	47.58	44.20	42.68
Al2O3	14.31	14.16	15.25	13.24	14.39	14.41	14.60	13.74	13.10
Fe2O3	13.36	13.22	11.63	12.43	12.46	12.17	11.56	13.01	13.35
MgO	8.47	9.17	7.89	11.98	9.28	8.56	7.76	9.02	9.65
CaO	10.58	9.87	8.24	9.77	9.64	10.01	9.47	9.70	10.45
Na2O	3.26	3.33	3.88	2.89	3.11	2.96	3.58	3.97	4.86
K2O	1.30	1.93	0.84	0.63	1.06	2.03	1.81	1.88	1.14
TiO2	3.09	2.80	1.63	2.53	3.04	3.02	2.19	2.53	2.43
MnO	0.25	0.51	0.16	0.19	0.18	0.17	0.18	0.21	0.23
P2O5	0.66	0.84	0.31	0.57	0.69	0.69	0.74	0.81	1.10
TOTAL	99.33	99.78	99.91	100.29	99.28	99.26	99.47	99.08	98.99
LOI	3.0	4.2	3.7	3.6	2.6	2.1	1.1	2.1	1.2
Ni	297	138	103	353	198	206	138	164	201
Cr	380	179	206	451	269	284	194	197	254
V	294	227	175	237	255	263	197	217	209
Sc	26	19	18	20	19	19	18	20	15
Cu	95	85	33	62	52	54	47	49	50
Zn	116	139	80	101	98	97	100	104	114
Sr	755	1043	386	831	1199	949	928	1132	1302
Rb	27	47	15	9	18	49	38	31	30
Zr	280	425	140	278	302	299	284	300	327
Nb	64	106	21	61	67	66	70	88	111
Ba	821	1268	228	661	812	1122	754	811	1074
Pb	2	0	1	1	1	3	3	3	3
Th	4	9	2	1	*	1	2	4	6
La	48	84	30	35	34	42	50	63	85
Ce	101	156	64	87	97	87	116	136	170
Nd	40	62	16	40	45	38	47	57	67
Y	29	37	25	25	28	27	29	29	34
Q	-	-	-	-	-	-	-	-	-
or	7.79	11.57	5.04	3.77	6.37	12.20	10.86	11.35	6.86
ab	12.40	8.82	33.16	20.57	20.55	13.05	20.94	9.00	6.21
an	20.96	18.22	21.96	21.45	22.58	20.82	18.70	18.41	10.80
ne	8.50	10.69	-	2.20	3.37	6.73	5.33	13.69	19.39
lct	-	-	-	-	-	-	-	-	-
di	22.93	21.08	14.16	19.06	17.45	20.75	19.65	23.84	28.36
hy	-	-	1.64	-	-	-	-	-	-
ol	17.53	19.92	18.15	24.59	19.96	17.23	16.50	18.56	18.65
mt	2.38	2.30	2.02	2.15	2.18	2.13	2.02	2.28	2.38
il	5.97	5.39	3.13	4.84	5.88	5.84	4.22	4.91	4.71
ap	1.58	2.02	0.74	1.36	1.65	1.66	1.77	1.97	2.67
cort	-	-	-	-	-	-	-	-	-

	SW482 (5)	SW483 (5)	SW484 (5)	SW485 (5)	SW486 (5)	SW488 (5)	SW489 (5)	SW490 (5)	SW491 (5)
SiO2	44.95	44.87	38.58	44.93	45.41	46.16	45.20	45.76	42.55
Al2O3	13.06	13.94	11.53	14.51	14.09	14.85	14.23	14.47	13.51
Fe2O3	12.60	12.03	8.45	13.50	12.21	11.82	12.31	11.75	11.97
MgO	10.99	10.01	5.61	8.30	8.81	8.08	9.02	8.53	8.33
CaO	9.76	9.34	5.56	10.19	9.73	9.24	10.55	10.79	9.90
Na2O	2.99	3.59	2.21	3.49	4.06	3.66	3.53	3.50	2.61
K2O	1.89	1.79	1.49	0.56	1.45	1.55	1.10	1.28	1.00
TiO2	2.62	2.55	1.76	2.90	2.59	3.02	2.82	2.85	2.68
MnO	0.18	0.19	0.30	0.26	0.20	0.58	0.58	0.44	0.56
P2O5	0.61	0.70	0.50	0.73	0.73	0.63	0.60	0.60	0.50
TOTAL	99.65	99.01	75.98	99.38	99.28	99.57	99.95	99.96	93.62
LOI	1.1	2.1	2.6	5.2	4.2	3.4	2.7	2.6	3.1
Ni	249	233	150	171	237	211	253	244	253
Cr	378	312	198	172	319	351	388	376	401
V	248	225	163	226	226	265	263	274	266
Sc	25	20	15	15	17	22	25	20	22
Cu	60	47	19	47	42	50	57	55	58
Zn	102	101	78	127	102	672	103	104	527
Sr	746	763	505	1061	812	644	803	811	589
Rb	80	39	29	12	19	29	14	24	11
Zr	224	325	258	408	340	346	314	306	219
Nb	51	70	53	94	74	78	76	76	46
Ba	707	736	493	994	771	857	960	955	561
Pb	1	4	7	4	5	3	15	3	2
Th	*	4	8	8	5	3	6	3	4
La	28	45	52	77	46	49	63	49	43
Ce	71	109	81	135	110	102	108	108	66
Nd	32	46	33	54	48	43	45	49	31
Y	24	29	23	33	28	30	31	30	26
Q	-	-	-	-	-	-	-	-	-
or	11.31	10.78	11.67	3.35	8.75	9.27	6.57	7.63	6.38
ab	10.11	12.08	24.85	20.88	18.87	19.36	18.60	18.91	17.11
an	16.91	16.97	22.78	22.67	16.19	19.81	19.95	20.22	23.95
ne	8.42	10.27	-	5.00	10.91	6.52	8.45	8.12	3.67
lct	-	-	-	-	-	-	-	-	-
di	22.77	20.81	7.83	19.57	22.85	18.32	23.58	24.29	20.84
hy	-	-	19.75	-	-	-	-	-	-
ol	21.77	20.36	5.20	18.80	17.54	17.34	17.84	15.88	19.05
mt	2.20	2.11	1.93	2.36	2.14	2.06	2.18	2.08	2.22
il	5.06	4.95	4.44	5.61	5.00	5.81	5.41	5.47	5.50
ap	1.47	1.68	1.56	1.76	1.75	1.52	1.85	1.88	1.28
cort	-	-	-	-	-	-	-	-	-

	SW452 (5)	SW453 (5)	SW454 (5)	SW455 (5)	SW456 (5)	SW457 (5)	SW458 (4)	SW459 (4)	SW462 (4)
SiO2	45.18	43.57	45.06	44.56	45.11	43.89	44.78	46.24	48.35
Al2O3	14.08	13.66	13.25	13.31	13.29	14.13	14.45	15.08	14.47
Fe2O3	12.37	12.06	12.87	12.45	12.58	12.96	14.04	12.94	12.37
MgO	10.04	9.83	10.68	10.02	10.77	9.60	9.86	8.43	9.02
CaO	10.18	10.42	10.07	10.11	9.85	9.83	9.89	9.99	8.42
Na2O	2.89	4.35	2.39	3.35	3.72	3.50	2.11	2.26	2.65
K2O	0.68	1.42	1.69	1.68	1.42	1.55	0.96	1.11	1.85
TiO2	2.88	2.86	2.96	2.85	2.81	2.99	2.55	2.63	1.85
MnO	0.20	0.19	0.18	0.18	0.18	0.20	0.34	0.21	0.13
P2O5	0.61	0.85	0.56	0.74	0.75	0.66	0.55	0.59	0.56
TOTAL	99.06	99.21	99.71	99.27	100.44	99.31	99.52	99.47	99.66
LOI	3.2	1.8	2.4	1.6	1.3	2.3	3.6	2.9	4.1
Ni	201	171	243	218	246	178	241	165	187
Cr	306	342	296	315	344	249	376	269	283
V	243	256	244	242	245	270	242	239	212
Sc	18	22	19	19	21	20	23	16	20
Cu	50	55	59	55	56	45	39	45	55
Zn	103	95	106	102	105	101	212	143	96
Sr	1553	1056	719	889	814	832	597	659	571
Rb	14	26	42	20	14	28	19	16	35
Zr	338	282	212	260	258	295	225	244	141
Nb	75	69	51	61	60	73	43	47	34
Ba	1151	773	946	687	1032	907	513	588	1161
Pb	*	2	1	2	1	0	2	2	2
Th	1	*	*	*	*	1	4	1	*
La	43	39	33	35	36	45	43	45	29
Ce	100	91	75	78	81	98	76	89	54
Nd	46	46	35	38	41	43	37	39	27
Y	28	27	25	25	25	29	26	28	25
Q	-	-	-	-	-	-	-	-	-
or	4.10	8.58	10.15	10.11	8.42	9.32	5.76	6.66	11.08
ab	20.23	7.15	12.92	10.81	12.39	10.41	18.17	19.42	22.70
an	23.79	13.80	20.70	16.60	15.46	18.60	27.59	28.21	22.46
ne	2.56	16.46	4.11	9.80	10.47	10.69	-	-	-
lct	-	-	-	-	-	-	-	-	-
di	19.14	26.89	21.23	23.92	23.27	21.64	15.23	18.89	13.16
hy	-	-	-	-	-	-	1.10	6.28	4.68
ol	20.95	17.48	21.59	19.27	20.67	19.69	23.46	15.77	18.85
mt	2.17	2.11	2.24	2.18	2.17	2.27	2.45	2.26	2.16
il	5.59	5.54	5.70	5.52	5.37	5.79	4.92	5.08	3.56
ap	1.48	2.04	1.35	1.79	1.79	1.59	1.32	1.42	1.35
cort	-	-	-	-	-	-	-	-	-

	SW463 (A)	SW465 (A)	SW467 (A)	SW468 (A)	SW469 (A)	SW470 (A)	SW471 (A)	SW472 (A)	SW473 (A)
SiO2	48.11	51.74	47.57	47.27	49.04	45.69	45.47	45.27	49.66
Al2O3	14.10	15.04	14.25	14.08	14.12	13.05	13.55	14.64	14.65
Fe2O3	12.33	11.43	12.24	11.26	12.33	12.83	12.57	13.35	11.79
MgO	9.18	6.59	9.01	9.14	8.89	11.37	9.71	8.41	7.44
CaO	9.12	9.03	8.96	9.99	8.10	9.94	9.94	9.06	8.21
Na2O	3.09	3.17	3.07	3.27	3.47	3.17	3.62	4.18	3.91
K2O	1.23	0.74	1.68	1.76	1.23	1.42	1.52	1.26	1.32
TiO2	1.80	1.59	2.00	2.04	1.86	2.20	2.33	2.65	1.88
MnO	0.18	0.15	0.18	0.18	0.18	0.20	0.19	0.19	0.17
P2O5	0.40	0.25	0.47	0.56	0.42	0.73	0.77	0.67	0.42
TOTAL	99.52	99.73	99.43	99.54	99.65	100.59	99.68	99.67	99.45
LOI	0.7	1.9	1.5	1.8	2.2	1.5	1.5	1.1	1.4
Ni	187	134	180	185	186	245	203	138	119
Cr	287	227	329	326	351	382	309	158	279
V	213	167	216	229	196	212	217	228	195
Sc	27	20	21	24	20	21	23	20	20
Cu	57	45	48	56	42	48	49	44	36
Zn	99	109	99	90	103	105	103	108	101
Sr	496	379	594	659	432	912	844	927	513
Rb	31	8	36	43	28	24	24	20	29
Zr	157	134	181	195	169	253	250	256	173
Nb	36	18	47	58	38	56	60	52	37
Ba	519	298	705	926	598	534	559	597	535
Pb	3	3	4	2	3	0	2	2	3
Th	1	3	1	2	*	2	0	*	2
La	26	24	30	36	28	49	39	35	28
Ce	61	47	61	78	57	96	91	76	54
Nd	25	18	28	36	24	40	42	36	26
Y	24	26	27	27	26	28	28	28	27
Q	-	0.03	-	-	-	-	-	-	-
or	7.40	4.42	10.08	10.53	7.34	8.42	9.08	7.56	7.95
ab	25.00	27.13	21.76	17.13	29.78	13.47	13.75	17.34	31.31
an	21.29	24.97	20.49	18.82	19.61	17.29	16.48	17.70	18.80
ne	0.83	-	2.51	5.94	-	7.29	9.38	10.07	1.26
lct	-	-	-	-	-	-	-	-	-
di	17.94	15.38	17.54	22.48	14.98	22.27	23.13	19.17	16.23
hy	-	22.40	-	-	0.52	-	-	-	-
ol	20.96	-	20.49	17.86	21.01	23.12	19.66	19.12	17.78
mt	2.15	1.99	2.14	1.96	2.15	2.22	2.19	2.33	2.06
il	3.48	3.06	3.86	3.93	3.58	4.20	4.49	5.10	3.62
ap	0.96	0.61	1.14	1.36	1.02	1.73	1.84	1.61	1.00
cort	-	-	-	-	-	-	-	-	-

	SW474 (A)	SW475 (A)	SW476 (A)	SW477 (A)	SW478 (A)	SW479 (A)	SW480 (A)	SW482 (A)	SW484 (A)
SiO2	50.38	51.07	47.99	45.50	44.89	44.98	45.09	48.13	47.36
Al2O3	14.56	15.67	14.20	16.03	13.35	13.50	14.17	14.82	14.95
Fe2O3	12.03	10.99	12.16	10.82	12.88	13.23	11.69	10.74	11.66
MgO	7.21	6.38	9.53	8.30	9.52	8.60	8.54	6.85	8.90
CaO	9.53	9.37	8.93	12.30	10.47	10.53	10.71	12.49	9.09
Na2O	3.17	3.22	3.00	1.44	3.51	3.13	3.37	2.98	2.86
K2O	0.99	1.02	1.38	2.33	1.63	1.51	1.27	0.96	1.71
TiO2	1.76	1.90	1.81	2.49	2.16	2.16	2.81	1.84	2.14
MnO	0.18	0.13	0.19	0.14	0.22	0.22	0.43	0.19	0.18
P2O5	0.32	0.34	0.45	0.53	0.94	0.99	0.60	0.31	0.59
TOTAL	100.12	100.10	99.64	99.87	99.57	98.85	98.67	99.31	99.44
LOI	3.6	2.1	1.0	4.4	2.1	2.7	2.4	6.2	1.1
Ni	141	93	198	95	178	179	178	205	171
Cr	317	238	337	147	235	227	232	389	254
V	194	201	210	338	208	196	196	242	200
Sc	23	22	22	28	21	20	20	28	21
Cu	40	43	47	54	51	48	45	47	45
Zn	103	91	95	84	104	113	107	148	89
Sr	414	404	558	921	1277	1540	1258	415	809
Rb	21	21	30	64	30	25	37	14	34
Zr	150	147	177	232	288	285	275	148	227
Nb	23	23	39	71	85	97	97	26	49
Ba	333	439	768	1515	849	898	981	389	815
Pb	3	5	3	3	3	2	4	1	3
Th	2	2	0	5	5	2	6	*	0
La	22	25	29	53	73	74	73	21	29
Ce	43	48	60	94	145	156	156	35	79
Nd	21	23	28	38	60	63	59	18	36
Y	25	26	25	29	31	32	31	28	27
Q	-	-	-	-	-	-	-	-	-
or	5.92	6.10	8.29	13.90	9.75	9.10	7.66	5.78	10.26
ab	27.08	27.51	24.17	7.08	11.02	14.66	14.60	19.56	22.00
an	22.77	25.89	21.50	30.71	16.10	18.79	20.28	24.63	23.29
ne	-	-	0.86	2.85	10.37	6.71	7.88	3.28	1.38
lct	-	-	-	-	-	-	-	-	-
di	18.75	15.68	16.62	22.27	24.72	22.90	24.45	29.67	15.14
hy	9.55	14.46	-	-	-	-	-	-	-
ol	9.72	4.41	21.86	15.27	19.35	18.90	16.13	10.89	20.35
mt	2.09	1.91	2.12	1.88	2.25	2.33	2.06	1.88	2.03
il	3.37	3.63	3.49	4.78	4.17	4.20	5.47	3.55	4.12
ap	0.76	0.82	1.08	1.27	2.27	2.41	1.46	0.76	1.42
cort	-	-	-	-	-	-	-	-	-

	SW487 (5)	SW488 (5)	SW491 (5)	SW494 (5)	SW496 (5)	SW498 (5)	SW505 (5)	SW507 (5)	SW509 (5)
SiO2	45.82	46.81	46.60	47.00	47.66	45.32	44.68	44.58	46.76
Al2O3	15.04	14.90	15.23	14.34	14.45	13.92	14.05	14.48	14.08
Fe2O3	11.07	11.08	10.76	11.92	10.66	12.64	12.93	12.84	12.17
MgO	6.78	6.45	7.18	8.74	8.33	9.16	9.49	9.92	8.24
CaO	9.55	9.39	9.19	8.91	9.04	10.28	10.52	9.65	8.57
Na2O	5.35	4.29	4.65	3.01	4.25	3.33	3.08	1.91	3.76
K2O	0.95	2.06	1.58	1.55	1.56	1.77	0.69	1.67	1.44
TiO2	3.03	2.81	2.93	2.77	2.80	2.74	2.77	2.71	2.79
MnO	0.60	0.61	0.55	0.51	0.35	0.22	0.37	0.33	0.37
P2O5	1.23	1.06	1.14	0.76	0.78	0.65	0.65	0.62	0.77
TOTAL	99.41	99.46	99.81	99.51	99.87	100.03	99.28	98.70	98.94
LOI	3.7	2.8	3.9	3.0	3.7	2.9	2.9	3.1	3.2
Ni	215	236	225	314	298	227	228	161	289
Cr	348	302	335	292	295	296	308	229	315
V	241	229	238	246	231	254	264	254	244
Sc	23	18	20	20	17	20	22	20	21
Cu	51	51	58	53	55	58	51	50	55
Zn	168	106	565	306	256	111	293	926	1295
Sr	1189	1040	1109	798	633	836	773	797	687
Rb	17	41	26	17	26	43	6	41	22
Zr	350	318	351	290	301	274	266	246	291
Nb	82	73	77	57	60	62	62	60	58
Ba	970	840	849	880	813	988	886	2384	848
Pb	1	1	0	1	3	3	*	*	0
Th	0	1	3	0	4	2	1	0	2
La	60	50	62	38	54	54	46	44	40
Ce	133	117	125	100	104	94	91	88	81
Nd	61	52	53	44	46	43	37	40	40
Y	32	29	33	30	32	28	27	28	28
Q	-	-	-	-	-	-	-	-	-
or	5.68	12.34	9.83	9.27	9.33	10.56	4.15	10.11	8.66
ab	22.00	19.24	21.25	24.16	22.61	11.55	17.65	15.61	24.44
an	14.41	15.56	16.21	21.38	15.91	18.01	22.90	26.63	17.67
ne	13.00	9.54	10.04	0.91	7.43	9.17	4.82	0.52	4.35
lct	-	-	-	-	-	-	-	-	-
di	20.85	20.18	18.21	14.96	19.66	23.74	21.07	14.86	16.77
hy	-	-	-	-	-	-	-	-	-
ol	13.35	13.25	14.64	20.05	15.98	17.96	20.18	23.26	18.68
mt	1.93	1.93	1.87	2.08	1.85	2.19	2.26	2.26	2.14
il	5.84	5.41	5.63	5.38	5.37	5.26	5.37	5.27	5.41
ap	2.95	2.55	2.73	1.84	1.86	1.56	1.58	1.49	1.87
cort	-	-	-	-	-	-	-	-	-

	SW514 (4)	SW515 (4)	SW517 (4)	SW518 (4)	SW519 (4)	SW520 (4)	SW521 (4)	SW522 (5)	SW523 (5)
SiO2	45.22	49.77	50.24	49.59	47.04	47.77	49.72	44.96	45.35
Al2O3	13.74	15.43	16.84	17.02	17.13	16.49	15.48	14.62	14.37
Fe2O3	11.84	10.91	9.38	9.90	11.69	12.72	12.07	11.80	11.96
MgO	10.24	9.56	5.31	5.12	4.23	4.07	5.13	10.38	10.90
CaO	9.06	4.91	8.06	8.98	8.34	7.65	12.01	10.04	9.61
Na2O	3.86	3.01	5.43	4.67	5.39	5.27	2.93	3.43	2.37
K2O	2.11	3.07	2.01	1.92	1.94	1.55	0.57	0.87	1.54
TiO2	2.49	1.94	1.82	2.03	2.43	3.01	1.52	2.68	2.69
MnO	0.19	0.14	0.14	0.16	0.20	0.19	0.19	0.19	0.17
P2O5	1.23	0.51	0.51	0.52	0.86	0.44	0.20	0.60	0.49
TOTAL	99.99	99.26	99.73	99.92	99.25	99.17	99.82	99.57	99.46
LOI	1.8	4.6	4.2	4.8	3.3	3.7	4.7	1.9	1.9
Ni	259	90	49	45	29	29	62	213	238
Cr	331	306	185	100	7	3	211	308	325
V	197	212	136	189	233	337	237	255	254
Sc	17	27	19	19	14	15	26	30	29
Cu	38	38	32	51	68	96	57	47	49
Zn	103	61	66	67	109	103	104	76	84
Sr	1416	431	583	802	809	581	258	759	622
Rb	26	69	42	37	53	31	10	12	31
Zr	316	187	246	232	282	244	120	260	217
Nb	75	45	61	58	82	36	13	50	41
Ba	695	5050	795	1037	1533	801	209	719	555
Pb	3	1	3	2	7	2	2	3	3
Th	1	4	3	1	8	*	*	1	*
La	59	33	43	37	60	32	10	29	24
Ce	129	75	91	82	123	73	27	69	63
Nd	59	34	36	35	49	41	12	43	31
Y	30	27	27	27	30	31	26	29	28
Q	-	-	-	-	-	-	-	-	-
or	12.57	18.46	11.99	11.46	11.70	9.33	3.43	5.24	9.24
ab	12.75	25.92	27.01	25.36	21.83	27.90	25.13	16.10	15.45
an	14.10	19.84	15.81	19.99	17.11	17.06	27.72	22.22	24.41
ne	10.96	-	10.53	7.88	13.30	9.54	-	7.24	2.66
lct	-	-	-	-	-	-	-	-	-
di	18.72	1.24	17.37	17.74	16.00	15.56	25.98	19.66	16.78
hy	-	6.47	-	-	-	-	6.07	-	-
ol	21.11	21.18	10.95	10.73	11.24	11.47	6.17	20.88	22.99
mt	2.06	1.91	1.63	1.72	2.04	2.23	2.10	2.06	2.09
il	4.79	3.74	3.49	3.89	4.70	5.84	2.93	5.16	5.20
ap	2.95	1.24	1.23	1.24.	2.08	1.07	0.47	1.45	1.18
cort	-	-	-	-	-	-	-	-	-

	SW524 (5)	SW525 (4)	SW526 (5)	SW527 (5)	SW531 (5)	SW532 (5)	SW534 (5)	SW535 (5)	SW536 (5)
SiO2	48.67	47.46	45.08	46.58	45.00	45.39	45.48	45.35	48.56
Al2O3	13.93	15.06	13.85	15.69	14.90	14.83	14.53	14.32	14.39
Fe2O3	12.35	12.81	12.89	11.78	12.56	12.10	11.53	11.81	12.26
MgO	10.39	8.56	11.09	7.96	9.28	10.68	9.99	10.77	10.27
CaO	10.26	9.16	10.39	9.21	9.78	10.30	10.58	10.51	10.31
Na2O	3.35	3.42	2.45	3.08	4.12	2.10	2.42	3.15	3.00
K2O	0.73	0.87	0.87	1.98	0.66	0.48	1.58	0.62	0.84
TiO2	2.57	1.98	2.55	2.59	2.86	2.68	2.64	2.56	2.63
MnO	0.20	0.18	0.19	0.19	0.20	0.23	0.19	0.18	0.19
P2O5	0.66	0.27	0.55	0.62	0.72	0.57	0.63	0.60	0.61
TOTAL	99.11	99.78	99.50	99.60	100.00	99.38	99.85	99.87	99.05
LOI	1.8	2.7	2.6	3.2	2.1	8.9	2.0	1.8	1.8
Ni	231	162	253	136	207	212	236	288	197
Cr	406	292	367	177	292	319	390	395	386
V	236	288	253	222	260	279	258	254	251
Sc	26	27	25	20	29	25	31	33	25
Cu	51	60	62	43	89	51	58	55	50
Zn	92	93	99	81	91	92	88	86	82
Sr	1128	821	761	900	740	689	746	1035	836
Rb	13	16	7	45	6	7	36	9	13
Zr	285	128	248	304	292	260	257	256	250
Nb	57	20	49	57	60	50	53	52	53
Ba	748	273	638	888	2690	2438	778	708	657
Pb	3	1	1	4	3	2	3	2	1
Th	1	*	*	5	1	3	*	*	*
La	36	9	36	46	46	48	39	37	37
Ce	87	32	80	102	89	82	92	86	78
Nd	40	18	35	40	45	40	39	42	43
Y	28	25	27	30	30	29	29	28	28
Q	-	-	-	-	-	-	-	-	-
or	4.40	5.23	2.80	11.87	3.92	2.90	9.22	3.78	5.06
ab	16.40	24.63	19.75	18.41	18.51	18.06	14.48	17.92	16.02
an	21.28	23.46	25.80	23.48	20.48	30.18	28.62	23.45	23.80
ne	6.77	2.56	0.73	4.36	9.07	-	3.82	4.93	5.35
lct	-	-	-	-	-	-	-	-	-
di	21.28	17.05	18.58	15.32	19.21	14.58	19.68	20.55	19.69
hy	-	-	-	-	-	7.48	-	-	-
ol	21.22	20.39	23.88	18.08	19.45	18.15	20.00	21.02	21.37
mt	2.16	2.23	2.25	2.05	2.18	2.12	2.01	1.99	2.15
il	4.97	3.82	4.92	4.98	5.50	5.18	5.09	4.94	5.09
ap	1.60	0.64	1.33	1.49	1.72	1.39	1.51	1.45	1.47
cort	-	-	-	-	-	-	-	-	-

	SW537 (4)	SW538 (4)	SW540 (5)	SW545 (4)	SW555 (3)	SW556B (5)	SW560 (5)	SW562 (5)	SW568 (5)
SiO2	46.85	48.26	47.58	45.64	47.23	47.52	44.65	47.00	45.66
Al2O3	14.75	17.40	14.38	15.07	14.14	16.67	17.23	15.32	14.10
Fe2O3	12.21	10.76	10.91	12.86	12.20	11.35	11.44	11.15	12.09
MgO	9.35	6.22	6.73	6.65	8.93	6.55	5.01	6.78	9.93
CaO	9.61	9.11	14.21	8.90	10.21	7.34	9.68	7.34	9.82
Na2O	2.16	4.11	2.61	2.30	2.78	4.92	3.78	4.47	3.39
K2O	1.76	1.51	0.88	1.53	1.33	2.00	2.70	1.97	0.78
TiO2	2.34	2.17	2.16	2.78	2.04	2.34	3.15	2.18	2.85
MnO	0.18	0.21	0.13	0.18	0.19	0.19	0.25	0.18	0.17
P2O5	0.58	0.36	0.33	0.52	0.43	0.61	1.07	0.52	0.65
TOTAL	99.78	100.11	99.91	96.43	99.48	99.48	98.98	96.91	99.44
LOI	2.8	3.5	5.0	2.5	2.5	4.0	2.7	2.6	4.3
Ni	202	84	202	172	245	70	42	230	251
Cr	399	178	369	244	317	123	12	301	388
V	218	232	247	218	246	193	255	172	231
Sc	25	20	26	16	24	12	7	13	23
Cu	61	47	56	55	17	41	127	39	46
Zn	69	101	88	88	865	103	106	106	83
Sr	403	625	739	876	582	1033	1756	881	729
Rb	16	29	38	15	37	15	49	37	7
Zr	155	182	277	291	161	318	323	279	289
Nb	23	33	51	52	42	89	111	74	55
Ba	343	1013	951	3532	657	1279	2705	1151	2230
Pb	3	4	4	2	19	3	3	3	1
Th	2	2	5	2	1	6	3	6	2
La	23	27	51	54	23	70	78	62	54
Ce	42	59	102	88	59	137	161	112	98
Nd	24	30	43	44	26	53	62	41	45
Y	26	27	28	27	24	28	32	25	29
Q	-	-	-	-	-	-	-	-	-
or	10.53	9.01	5.22	9.47	8.00	12.00	16.27	12.14	4.70
ab	18.48	23.62	14.81	20.39	20.22	22.88	11.44	24.15	20.62
an	25.71	24.79	25.17	27.58	22.52	17.78	22.52	16.58	21.30
ne	-	6.18	4.08	-	1.98	10.48	11.49	8.29	4.60
lat	-	-	-	-	-	-	-	-	-
di	15.23	15.10	35.86	12.44	21.22	12.43	15.90	14.58	19.30
hy	2.52	-	-	9.55	-	-	-	-	-
ol	19.58	18.82	8.02	11.41	18.96	16.47	11.67	16.68	20.29
mt	2.12	1.86	1.89	2.32	2.13	1.98	2.01	2.00	2.11
il	4.50	4.15	4.15	5.54	3.93	4.51	6.10	4.31	5.50
ap	1.38	0.86	0.79	1.30	1.04	1.46	2.60	1.29	1.57
cort	-	-	-	-	-	-	-	-	-

	SW566 (4)	SW567A (3)	SW571 (4)	SW572 (4)	SW576 (4)	SW581 (4)	ab15 (6)	ab16 (6)	ab17 (6)
SiO2	47.62	40.78	49.71	48.28	49.10	43.68	40.40	44.30	44.40
Al2O3	13.80	12.75	15.70	14.75	17.02	15.08	13.60	11.20	12.70
Fe2O3	12.95	13.92	11.60	13.16	11.00	15.10	12.77	12.33	12.00
MgO	10.65	9.72	7.72	8.43	7.15	7.75	6.40	12.75	9.80
CaO	8.48	12.92	8.78	8.67	9.89	6.50	10.26	9.43	10.06
Na2O	3.08	3.23	2.75	2.78	3.32	3.20	2.70	2.45	2.80
K2O	1.23	1.55	0.94	1.00	0.82	2.21	2.23	1.20	0.86
TiO2	1.90	2.95	1.97	1.85	1.25	4.32	2.48	1.96	1.95
MnO	0.18	0.20	0.11	0.18	0.16	0.18	0.21	0.18	0.18
P2O5	0.36	0.91	0.34	0.33	0.15	0.81	0.83	0.26	0.33
TOTAL	100.23	98.94	99.62	99.82	99.87	98.83	91.84	96.06	95.08
LOI	3.2	7.3	2.7	2.5	3.6	5.6	8.4	4.9	4.8
Ni	278	332	193	181	89	16	92	264	282
Cr	358	428	271	256	325	30	102	360	512
V	208	306	235	225	200	348	267	193	232
Sc	21	26	26	27	30	21	28	20	25
Cu	56	61	54	53	85	15	0	0	0
Zn	104	214	126	108	86	91	0	0	0
Sr	474	1026	374	378	403	888	1361	472	547
Rb	29	26	16	19	17	38	74	34	28
Zr	146	215	147	141	75	186	196	125	130
Nb	33	69	25	24	9	31	0	0	0
Ba	441	1262	331	692	299	1389	1029	351	526
Pb	2	4	2	3	0	1	0	0	0
Th	1	3	0	*	*	*	0	0	0
La	26	44	12	15	11	30	47	21	25
Ce	47	109	50	35	19	63	106	46	52
Nd	19	49	23	19	9	33	55	25	27
Y	26	27	26	25	17	27	28	20	24
Q	-	-	-	-	-	-	-	-	-
or	7.31	-	5.66	6.01	4.92	13.39	14.52	7.47	5.80
ab	23.33	-	23.61	23.98	27.50	20.54	4.86	13.71	17.96
an	20.37	16.07	28.10	25.21	29.41	20.77	20.28	16.86	20.78
ne	1.61	15.16	-	-	0.51	3.91	11.01	4.40	3.92
let	-	7.33	-	-	-	-	-	-	-
di	15.98	33.43	11.27	13.38	15.71	5.66	24.56	24.68	24.35
hy	-	-	18.93	9.87	-	-	-	-	-
ol	24.65	16.89	5.80	14.88	17.26	22.69	15.09	26.09	20.62
mt	2.25	2.45	2.02	2.30	1.91	2.66	2.42	2.23	2.19
il	3.63	5.74	3.80	3.57	2.41	8.42	5.11	3.92	3.94
ap	0.86	2.21	0.81	0.80	0.37	1.95	2.17	0.65	0.83
cort	-	0.71	-	-	-	-	-	-	-

	ab18 (6)	ab19 (6)	ab37 (6)	ab38 (6)	ab39 (6)	ab40 (6)	ab41 (6)	BC02 (3)	BC03 (4)
SiO2	40.00	45.20	39.80	43.20	44.90	42.20	42.00	46.35	47.72
Al2O3	12.60	14.50	11.83	13.00	14.10	12.10	13.90	14.17	13.64
Fe2O3	12.45	9.78	13.45	10.21	8.88	11.11	12.34	11.87	13.12
MgO	7.20	10.45	10.32	11.85	8.35	8.25	6.85	10.88	11.04
CaO	12.36	10.69	11.25	10.08	10.82	10.34	12.19	9.86	7.55
Na2O	2.85	3.15	3.35	0.95	1.65	3.95	3.45	2.73	3.24
K2O	1.15	1.35	0.93	3.40	3.88	0.35	1.68	0.93	0.88
TiO2	2.25	1.93	2.44	2.55	2.73	3.38	2.89	1.96	1.73
MnO	0.24	0.17	0.20	0.22	0.19	0.20	0.20	0.17	0.18
P2O5	0.48	0.33	0.97	0.92	1.16	0.95	1.06	0.43	0.25
TOTAL	91.58	97.55	94.54	96.38	96.66	92.83	96.56	99.35	99.34
LOI	9.6	2.3	5.4	4.6	4.4	7.1	4.6	3.4	4.7
Ni	144	121	290	141	101	160	102	344	278
Cr	248	308	377	169	212	189	243	499	428
V	201	187	223	223	201	232	270	256	221
Sc	19	28	23	31	24	16	23	25	26
Cu	0	0	0	0	0	0	0	34	49
Zn	0	0	0	0	0	0	0	89	101
Sr	624	650	942	1252	1568	615	1633	526	335
Rb	37	51	35	56	98	23	45	20	21
Zr	115	149	244	317	400	293	233	147	108
Nb	0	0	0	0	0	0	0	38	22
Ba	517	453	800	1857	2966	653	1428	515	526
Pb	0	0	0	0	0	0	0	10	3
Th	0	0	0	0	0	0	0	2	3
La	31	29	53	86	115	56	56	30	18
Ce	68	59	0	160	218	118	122	59	29
Nd	32	26	0	67	82	55	62	29	15
Y	23	24	33	26	32	29	29	22	22
Q	-	-	-	-	-	-	-	-	-
or	7.51	8.25	5.88	21.03	23.90	2.25	10.39	5.58	5.31
ab	1.90	11.21	2.65	1.56	4.04	20.55	3.94	19.71	27.89
an	20.10	22.17	15.52	22.16	20.44	15.51	18.30	24.08	20.45
ne	13.41	8.86	15.01	3.71	5.69	8.57	14.42	2.05	-
lct	-	-	-	-	-	-	-	-	-
di	36.23	24.50	30.43	19.16	22.20	27.14	30.91	18.50	13.02
hy	-	-	-	-	-	-	-	-	0.14
ol	12.52	18.68	20.62	23.19	13.67	14.47	11.44	23.20	26.96
mt	2.36	1.74	2.47	1.84	1.59	2.08	2.22	2.07	2.30
il	4.72	3.79	4.96	5.07	5.40	6.98	5.75	3.79	3.34
ap	1.26	0.81	2.46	2.28	2.86	2.45	2.63	1.02	0.61
cort	-	-	-	-	-	-	-	-	-

	GE4 (3)	MM13 (6)	MM65 (6)	MM109 (6)	MM185 (6)	PA01 (3)	PA04 (5)	PA07 (3)	PA08 (3)
SiO2	46.59	44.37	43.94	44.73	47.04	44.41	45.22	42.15	42.73
Al2O3	13.57	13.06	13.40	13.39	15.47	13.54	14.27	13.28	12.60
Fe2O3	11.93	13.98	13.17	12.58	12.20	13.08	13.00	14.62	11.57
MgO	9.92	11.97	10.25	10.46	6.33	11.80	8.22	10.80	14.16
CaO	8.34	9.72	10.90	9.98	7.58	9.69	9.56	10.45	10.65
Na2O	3.46	2.19	2.51	2.86	4.47	3.33	4.47	3.08	3.04
K2O	1.06	1.05	1.52	1.97	2.47	0.94	0.97	1.47	0.50
TiO2	1.76	2.21	2.31	2.37	2.57	1.69	2.91	2.18	1.88
MnO	0.17	0.15	0.16	0.15	0.18	0.20	0.22	0.21	0.18
P2O5	0.38	0.38	0.57	0.76	0.84	0.89	0.71	1.04	0.60
TOTAL	97.18	99.08	98.73	99.21	99.55	99.15	99.55	99.28	97.90
LOI	nd	8.5	6.5	6.8	4.1	1.6	1.9	5.5	2.7
Ni	236	318	209	260	86	296	166	224	460
Cr	356	710	376	426	113	494	212	325	881
V	226	0	0	0	0	230	247	207	270
Sc	21	25	24	22	15	24	22	15	32
Cu	58	0	0	0	0	61	51	48	64
Zn	94	0	0	0	0	92	122	97	70
Sr	590	555	793	886	1567	617	897	1196	708
Rb	23	22	33	46	62	18	8	64	7
Zr	135	112	151	192	225	187	351	311	176
Nb	28	33	41	52	79	40	81	101	44
Ba	569	0	373	437	799	650	1165	1586	754
Pb	0	0	0	0	0	0	4	5	1
Th	0	3	3	5	7	2	4	7	2
La	23	21	31	42	59	39	63	81	31
Ce	49	51	70	97	58	66	125	150	57
Nd	24	28	40	48	54	31	54	64	33
Y	22	20	22	25	28	23	33	37	22
Q	-	-	-	-	-	-	-	-	-
or	6.51	6.34	9.20	11.86	14.82	5.67	5.83	8.85	3.02
ab	24.39	14.18	8.46	9.86	19.34	12.13	17.98	4.83	7.88
an	19.10	23.20	21.32	18.22	13.25	19.59	16.25	18.44	19.89
ne	3.28	2.58	7.20	8.01	12.18	9.01	11.08	11.77	10.09
lct	-	-	-	-	-	-	-	-	-
di	17.33	19.08	24.59	22.02	15.89	21.23	22.19	22.41	24.60
hy	-	-	-	-	-	-	-	-	-
ol	22.83	26.96	21.02	21.41	15.42	25.63	17.07	24.41	27.33
mt	2.13	2.45	2.32	2.20	2.13	2.29	2.27	2.56	2.05
il	3.48	4.29	4.49	4.59	4.95	3.28	5.62	4.22	3.68
ap	0.94	0.92	1.38	1.83	2.02	1.17	1.71	2.51	1.85
cort	-	-	-	-	-	-	-	-	-

	PA13 (3)	PA15 (5)	RM5 (7)	RM24 (7)	RM26 (7)	RM27 (7)	RM30 (7)	RM40 (7)	RM42 (7)
SiO2	45.57	48.80	50.19	49.37	49.62	54.03	49.63	51.45	51.48
Al2O3	13.09	13.31	14.27	13.56	13.89	13.61	14.16	13.78	13.93
Fe2O3	11.56	11.43	13.14	14.32	13.69	10.76	13.57	13.54	14.14
MgO	13.39	8.02	6.12	6.48	6.92	7.29	7.02	5.53	6.01
CaO	10.29	10.40	10.87	9.73	10.58	9.80	9.78	9.19	7.99
Na2O	2.51	2.46	2.41	2.21	2.26	1.91	2.14	2.41	2.35
K2O	1.27	2.05	0.45	0.62	0.48	0.80	0.23	0.97	0.79
TiO2	1.48	2.51	2.17	2.91	2.21	1.69	2.55	2.40	2.49
MnO	0.18	0.13	0.21	0.21	0.19	0.17	0.30	0.17	0.18
P2O5	0.40	0.65	0.20	0.30	0.21	0.17	0.25	0.31	0.31
TOTAL	99.74	99.78	100.04	99.71	100.05	100.22	99.63	99.76	99.61
LOI	2.3	4.5	0.8	1.3	1.4	1.8	1.9	1.4	1.9
Ni	371	166	78	89	88	86	109	47	51
Cr	769	198	84	121	103	268	156	63	71
V	240	233	351	398	376	294	364	399	380
Sc	26	23	31	33	34	32	36	28	29
Cu	71	47	160	174	176	68	170	54	55
Zn	83	112	103	127	96	88	104	116	109
Sr	523	682	299	320	316	287	314	373	426
Rb	31	50	10	12	13	22	2	27	20
Zr	139	336	154	198	141	168	161	200	207
Nb	34	72	14	18	12	12	15	16	16
Ba	537	1198	120	208	120	193	108	284	271
Pb	1	6	2	5	3	5	15	5	4
Th	1	7	1	1	*	2	1	3	4
La	30	61	19	28	31	22	26	40	30
Ce	57	111	26	45	34	39	38	66	55
Nd	28	47	16	27	20	25	24	34	28
Y	21	30	28	32	27	29	26	32	31
Q	-	-	1.48	2.20	0.63	7.60	2.88	4.23	5.33
or	7.61	12.26	2.72	3.73	2.85	4.75	1.37	5.82	4.73
ab	10.69	21.03	20.66	19.03	19.36	16.26	18.43	20.71	20.17
an	20.97	19.48	27.06	25.63	26.66	26.41	28.78	24.24	25.57
ne	5.86	-	-	-	-	-	-	-	-
lct	-	-	-	-	-	-	-	-	-
di	22.62	23.09	21.62	17.65	20.62	17.53	15.52	16.55	10.50
hy	-	2.37	19.54	22.92	22.75	21.96	25.14	20.70	25.70
ol	26.45	13.38	-	-	-	-	-	-	-
mt	2.01	1.99	2.28	2.50	2.38	1.86	2.37	2.36	2.47
il	2.84	4.83	4.17	5.62	4.24	3.23	4.91	4.63	4.80
ap	0.95	1.57	0.48	0.73	0.52	0.39	0.59	0.75	0.74
cort	-	-	-	-	-	-	-	-	-

	RM63 (6)	RM68 (6)	RM72 (6)	RM84 (6)	RM86 (6)
SiO2	49.91	50.80	50.78	48.78	51.65
Al2O3	12.95	13.81	13.86	15.48	14.80
Fe2O3	14.99	13.14	14.60	12.02	12.82
MgO	4.55	6.43	3.69	2.61	5.75
CaO	8.39	10.23	7.62	12.90	9.27
Na2O	2.17	2.33	1.77	2.94	2.41
K2O	1.65	0.43	3.27	1.07	0.79
TiO2	3.32	2.20	2.81	2.66	2.35
MnO	0.17	0.18	0.19	0.28	0.19
P2O5	0.62	0.20	0.42	0.40	0.28
TOTAL	98.73	99.77	99.01	99.10	100.30
LOI	2.4	1.0	8.5	7.7	1.9
Ni	17	101	16	39	58
Cr	8	192	22	53	77
V	356	343	372	330	333
Sc	26	32	28	31	27
Cu	15	155	29	52	65
Zn	141	105	126	321	99
Sr	701	297	226	435	385
Rb	31	9	89	24	21
Zr	289	172	255	252	198
Nb	20	15	22	21	15
Ba	718	168	405	346	297
Pb	4	0	6	127	4
Th	2	0	5	1	3
La	49	25	54	33	26
Ce	110	35	73	71	52
Nd	55	21	38	39	28
Y	42	29	41	39	30
Q	4.79	3.13	3.56	-	4.34
or	10.03	2.58	19.74	6.42	4.69
ab	18.84	20.00	15.28	25.41	20.56
an	21.26	26.32	20.73	26.39	27.45
ne	-	-	-	-	-
lct	-	-	-	-	-
di	14.45	19.64	12.79	30.60	14.11
hy	20.00	21.31	18.88	0.53	21.46
ol	-	-	-	2.42	-
mt	2.64	2.29	2.57	2.11	2.22
il	6.47	4.24	5.46	5.15	4.50
ap	1.52	0.48	1.01	0.97	0.67
cort	-	-	-	-	-

APPENDIX IV

TABLES OF REE DATA

	SW3	SW8	SW9	SW25	SW36	SW47	SW48	SW70	SW76
La	16.60	17.45	32.70	14.70	56.60	36.00	28.40	39.10	75.60
Ce	36.65	38.52	61.90	32.03	103.70	69.70	55.70	76.70	138.70
Pr	4.36	4.56	7.52	3.30	11.81	8.48	6.59	9.27	15.83
Nd	19.30	20.50	33.80	16.80	48.20	37.70	30.10	40.90	62.20
Sm	4.28	4.43	6.48	4.00	8.28	7.20	5.48	7.75	10.02
Eu	1.46	1.50	2.15	1.42	2.67	2.41	1.81	2.56	3.15
Gd	4.51	4.76	6.60	4.72	7.54	6.82	5.72	7.34	8.90
Dy	4.24	4.40	5.58	4.30	5.99	5.15	4.95	6.17	6.59
Ho	0.74	0.77	1.11	0.79	1.10	0.91	1.02	1.15	1.24
Er	1.98	2.06	2.38	2.23	2.86	2.33	1.86	3.22	2.90
Yb	1.76	1.83	2.21	1.99	2.16	1.66	2.05	2.86	2.33
Lu	0.26	0.27	0.36	0.30	0.32	0.24	0.34	0.42	0.35
La	50.5	53.0	99.4	44.7	172.0	109.4	86.3	118.8	229.8
Ce	42.4	44.5	71.6	37.0	119.9	80.6	64.4	88.7	160.3
Pr	36.0	37.7	62.1	27.3	97.6	70.1	54.5	76.6	130.8
Nd	30.6	32.5	53.7	26.7	76.5	59.8	47.8	64.9	98.7
Sm	21.1	21.8	31.9	19.7	40.8	35.5	27.0	38.2	49.4
Eu	19.0	19.5	27.9	18.4	34.7	31.3	23.5	33.2	40.9
Gd	16.3	17.2	23.9	17.1	27.3	24.7	20.7	26.6	32.2
Dy	12.4	12.8	16.3	12.5	17.5	15.0	14.4	18.0	19.2
Ho	9.5	9.9	14.2	10.1	14.1	11.7	13.1	14.7	15.9
Er	8.8	9.2	10.6	9.9	12.7	10.4	8.3	14.3	12.9
Yb	8.0	8.3	10.0	9.0	9.8	7.5	9.3	13.0	10.6
Lu	7.7	8.0	10.6	8.8	9.4	7.1	10.0	12.4	10.3

	SW89	SW93	SW112	SW138	SW160	SW189	SW207	SW267	SW298
La	38.89	66.60	15.79	40.40	37.90	40.00	22.90	24.40	33.76
Ce	77.75	120.00	34.63	81.60	78.60	77.70	44.80	50.00	67.36
Pr	8.43	13.17	4.00	9.94	9.32	9.60	5.25	6.32	7.31
Nd	35.00	52.60	18.30	44.90	43.00	41.70	24.60	28.70	30.60
Sm	6.87	8.83	4.31	7.76	7.46	7.29	4.70	5.49	5.98
Eu	2.26	2.80	1.55	2.51	2.43	2.36	1.62	1.83	1.93
Gd	6.58	7.87	5.06	7.45	7.11	7.00	5.28	5.44	5.73
Dy	5.74	6.39	5.09	6.03	5.83	5.70	4.81	4.55	4.89
Ho	0.99	1.22	0.90	1.25	1.18	1.13	1.00	0.87	0.84
Er	2.49	3.32	2.46	1.71	1.18	2.46	1.75	2.37	2.07
Yb	2.20	2.86	2.18	2.54	2.36	2.23	2.07	2.09	1.77
Lu	0.33	0.43	0.33	0.44	0.39	0.37	0.35	0.32	0.26
La	118.2	202.4	48.0	122.8	115.2	121.6	69.6	74.2	102.6
Ce	89.9	138.7	40.0	94.3	90.9	89.8	51.8	57.8	77.9
Pr	69.7	108.8	33.1	82.1	77.0	79.3	43.4	52.2	60.4
Nd	55.6	83.5	29.0	71.3	68.3	66.2	39.0	45.6	48.6
Sm	33.8	43.5	21.2	38.2	36.7	35.9	23.2	27.0	29.5
Eu	29.4	36.4	20.1	32.6	31.6	30.6	21.0	23.8	25.1
Gd	23.8	28.5	18.3	27.0	25.8	25.4	19.1	19.7	20.8
Dy	16.7	18.6	14.8	17.6	17.0	16.6	14.0	13.3	14.3
Ho	12.7	15.6	11.5	16.0	15.1	14.5	12.8	11.2	10.8
Er	11.1	14.8	10.9	7.6	5.2	10.9	7.8	10.5	9.2
Yb	10.0	13.0	9.9	11.5	10.7	10.1	9.4	9.5	8.0
Lu	9.7	12.7	9.7	13.0	11.5	10.9	10.3	9.4	7.7

Concentrations are in ppm with normalised values below (see Chapter 5 for details of normalising factors.

	SW303	SW304	SW309	SW414	SW438	SW442	SW463	SW472	SW478
La	43.11	40.70	47.00	38.00	75.90	42.50	22.10	23.90	27.30
Ce	89.06	80.30	87.60	71.30	142.50	80.60	43.70	51.87	53.60
Pr	9.80	9.60	10.22	8.42	16.26	9.41	5.31	5.61	6.76
Nd	40.40	42.50	44.10	37.30	64.90	39.70	24.60	26.30	31.20
Sm	8.19	7.93	8.19	7.08	10.60	7.14	5.01	5.30	5.79
Eu	2.63	2.59	2.68	2.30	3.35	2.33	1.77	1.65	1.68
Gd	7.55	7.32	7.54	6.58	9.29	7.05	5.44	5.06	5.69
Dy	6.40	5.80	6.05	5.22	6.70	6.21	4.81	3.87	4.70
Ho	1.09	1.05	1.12	0.95	1.26	1.19	0.91	0.68	0.91
Er	2.79	2.59	2.97	2.52	2.95	3.31	2.47	1.86	2.53
Yb	2.57	1.62	2.45	1.93	2.39	2.72	2.02	1.57	2.10
Lu	0.38	0.21	0.35	0.26	0.36	0.40	0.31	0.23	0.31
La	131.0	123.7	142.9	115.5	230.7	129.2	67.2	72.6	83.0
Ce	103.0	92.8	101.3	82.4	164.7	93.2	50.5	60.0	62.0
Pr	81.0	79.3	84.5	69.6	134.4	77.8	43.9	46.4	55.9
Nd	64.1	67.5	70.0	59.2	103.0	63.0	39.0	41.7	49.5
Sm	40.3	39.1	40.3	34.9	52.2	35.2	24.7	26.1	28.5
Eu	34.2	33.6	34.8	29.9	43.5	30.3	23.0	21.4	21.8
Gd	27.4	26.5	27.3	23.8	33.7	25.5	19.7	18.3	20.6
Dy	18.7	16.9	17.6	15.2	19.5	18.1	14.0	11.3	13.7
Ho	14.0	13.5	14.4	12.2	16.2	15.3	11.7	8.7	11.7
Er	12.4	11.5	13.2	11.2	13.1	14.7	11.0	8.3	11.2
Yb	11.7	7.4	11.1	8.8	10.9	12.4	9.2	7.1	9.5
Lu	11.2	6.2	10.3	7.7	10.6	11.8	9.1	6.8	9.1

	SW484	SW519	SW525	SW535	SW536	SW545	SW566	GE4	PA01
La	20.52	16.30	38.20	24.47	30.30	25.30	25.50	28.90	14.00
Ce	44.21	36.00	76.00	50.96	56.50	48.80	50.10	56.20	31.10
Pr	5.03	4.48	9.32	5.75	6.63	5.78	6.18	6.68	3.28
Nd	22.60	22.80	41.40	25.20	29.60	26.50	28.10	30.30	16.70
Sm	4.65	4.03	7.50	5.59	5.66	5.06	5.41	5.96	3.50
Eu	1.56	1.41	2.40	1.89	1.90	1.72	1.80	2.06	1.26
Gd	4.48	4.13	6.91	5.89	5.70	5.12	5.38	6.16	3.91
Dy	3.87	3.42	5.28	5.18	4.68	4.29	4.41	5.13	3.38
Ho	0.65	0.71	0.97	0.88	0.86	0.80	0.82	0.94	0.63
Er	1.67	0.65	2.45	2.26	2.27	2.20	2.21	2.38	1.76
Yb	1.42	1.31	1.96	1.95	1.75	1.81	1.73	1.91	1.52
Lu	0.22	0.24	0.29	0.29	0.27	0.27	0.26	0.28	0.24
La	62.4	49.5	116.1	74.4	92.1	76.9	77.5	87.8	42.6
Ce	51.1	41.6	87.9	58.9	65.3	56.4	57.9	65.0	36.0
Pr	41.6	37.0	77.0	47.5	54.8	47.8	51.1	55.2	27.1
Nd	35.9	36.2	65.7	40.0	47.0	42.1	44.6	48.1	26.5
Sm	22.9	19.9	36.9	27.5	27.9	24.9	26.7	29.4	17.2
Eu	20.3	18.3	31.2	24.5	24.7	22.3	23.4	26.8	16.4
Gd	16.2	15.0	25.0	21.3	20.7	18.6	19.5	22.3	14.2
Dy	11.3	10.0	15.4	15.1	13.6	12.5	12.9	15.0	9.9
Ho	8.3	9.1	12.4	11.3	11.0	10.3	10.5	12.1	8.1
Er	7.4	2.9	10.9	10.0	10.1	9.8	9.8	10.6	7.8
Yb	6.5	6.0	8.9	8.9	8.0	8.2	7.9	8.7	6.9
Lu	6.5	7.1	8.6	8.6	8.0	8.0	7.7	8.3	7.1

	PA13	RM5	RM68
La	26.50	18.70	16.60
Ce	52.70	34.60	39.70
Pr	6.44	4.63	5.22
Nd	30.00	23.50	28.00
Sm	5.39	5.26	5.95
Eu	1.72	1.82	1.98
Gd	5.22	6.07	6.60
Dy	4.28	5.78	6.09
Ho	0.88	1.13	1.24
Er	1.48	3.28	2.26
Yb	1.67	2.93	2.57
Lu	0.29	0.44	0.41
La	60.5	44.7	50.5
Ce	60.9	40.0	45.9
Pr	53.2	38.3	43.1
Nd	47.6	37.3	44.4
Sm	26.6	25.9	29.3
Eu	22.3	23.6	25.7
Gd	18.9	22.0	23.9
Dy	12.5	16.9	17.8
Ho	11.3	14.5	15.9
Er	6.6	14.6	10.0
Yb	7.6	13.3	11.7
Lu	8.6	13.0	12.1

APPENDIX V

TABLES OF ISOTOPE DATA

TABLE V.I

ND ISOTOPIC DATA FOR SELECTED POST-DINANTIAN ROCKS

Sample	Age Ma	Sm ppm	Nd ppm	$\frac{^{147}Sm}{^{144}Nd}$	$^{143}Nd/^{144}Nd$	2σ	$^{143}Nd/^{144}Nd_t$	εNd_t
SW89	288	4.65	22.6	0.1242	0.512640	103	0.512406	2.72
SW93	288	4.03	22.8	0.1067	0.512639	42	0.512438	3.34
SW298	288	3.50	16.7	0.1265	0.512620	70	0.512381	2.24
SW76	286	5.79	31.2	0.1120	0.512444	64	0.512234	-0.68
SW138	286	5.59	25.2	0.1339	0.512664	50	0.512413	2.81
SW207	286	5.41	28.1	0.1162	0.512601	68	0.512383	2.22
SW303	286	4.28	19.3	0.1338	0.512683	44	0.512432	3.19
SW48	310	5.01	24.6	0.1229	0.512780	58	0.512530	5.70
SW414	310	4.00	16.8	0.1437	0.512728	65	0.512436	3.86
SW36	310	10.60	64.9	0.0986	0.512521	52	0.512320	1.61
SW472	310	7.75	40.9	0.1144	0.512724	39	0.512492	4.95
SW519	310	8.83	52.6	0.1013	0.512698	40	0.512492	4.96
SW545	310	7.29	41.7	0.1055	0.512718	32	0.512504	5.18
SW8	295	7.93	42.5	0.1126	0.512743	65	0.512526	5.23
SW9	295	8.19	44.1	0.1121	0.512730	30	0.512514	4.99
SW25	295	7.08	37.3	0.1146	0.512646	54	0.512425	3.26
SW442	295	7.2	37.7	0.1153	0.512774	43	0.512552	5.73
SW535	295	7.76	44.9	0.1043	0.512708	38	0.512507	4.85
SW267	305	5.96	30.3	0.1187	0.512763	106	0.512526	5.48
RM5	301	5.26	23.5	0.1351	0.512781	32	0.512515	5.17
RM64	301	5.95	28.0	0.1282	0.512734	74	0.512481	4.51

Errors are given as 2σ errors about the mean and refer to the last digit quoted for the measured $^{143}Nd/^{144}Nd$ ratio. Initial ratios and ε values are given at time, t (Ma). Sm and Nd concentrations determined by ICP.

TABLE V.II

SR ISOTOPIC DATA FOR SELECTED POST-DINANTIAN ROCKS

Sample	Age Ma	Rb ppm	Sr ppm	$^{87}Rb/^{86}Sr$	$^{87}Sr/^{86}Sr$	2σ	$^{87}Sr/^{86}Sr_t$	εSr_t
SW112	291	47.2	785.6	0.1739	0.70526	26	0.70454	5.30
SW89	288	26.4	590.9	0.1293	0.70494	29	0.70441	3.48
SW93	288	22.1	564.6	0.1133	0.70513	31	0.70467	7.10
SW298	288	19.1	443.5	0.1247	0.70520	34	0.70469	7.39
SW309	288	29.9	668.8	0.1294	0.70439	36	0.70386	-4.37
SW76	286	44.7	692.4	0.1869	0.70564	36	0.70487	10.03
SW138	286	29.3	498.5	0.1701	0.70449	37	0.70379	-5.32
SW160	286	22.8	504.4	0.1308	0.70386	24	0.70332	-12.01
SW189	286	24.8	526.7	0.1363	0.70414	34	0.70359	-8.27
SW207	286	31.9	556.4	0.1659	0.70423	51	0.70355	-8.71
SW303	286	25.5	421.4	0.1752	0.70521	30	0.70450	4.67
SW304	286	26.4	434.4	0.1759	0.705452	42	0.70474	8.08
PA01	286	18.4	616.6	0.0864	0.70373	32	0.70338	-11.17
SW48	310	19.7	440.4	0.1295	0.70433	53	0.70376	-5.40
SW414	310	19.0	355.0	0.1549	0.70502	38	0.70434	2.78
SW463	310	30.7	495.0	0.1795	0.70415	37	0.70336	-11.05
SW525	310	15.7	420.9	0.1080	0.705133	27	0.70466	7.33
SW36	310	83.3	1217.2	0.1981	0.70466	32	0.70378	-5.08
SW472	310	20.2	926.9	0.0631	0.70381	24	0.70353	-8.63
SW484	310	34.0	808.9	0.1217	0.70413	33	0.70359	-7.79
SW519	310	53.0	809.0	0.1896	0.70507	34	0.70423	1.30
SW545	310	15.1	875.5	0.0499	0.70413	37	0.70391	-3.33
SW3	295	40.6	812.6	0.1446	0.70382	42	0.70321	-13.40
SW8	295	25.0	893.0	0.0810	0.70384	30	0.70350	-9.31
SW9	295	16.6	1070.2	0.0449	0.70391	33	0.70372	-6.25
SW25	295	25.7	573.0	0.1298	0.70435	29	0.70381	-4.95
SW47	295	35.7	721.2	0.1433	0.70393	33	0.70333	-11.80
SW442	295	39.5	746.3	0.1532	0.70395	34	0.70331	-12.04
SW535	295	8.5	1034.8	0.0238	0.70455	36	0.70445	4.09
SW267	305	23.6	592.8	0.1152	0.70411	31	0.70361	-7.63
RM5	301	9.9	298.7	0.0959	0.70414	27	0.70373	-5.99
RM64	301	8.9	297.2	0.0867	0.70405	31	0.70368	-6.66

Errors are given as 2σ errors about the mean and refer to the last digit quoted for the measured $^{87}Sr/^{86}Sr$ ratio. Initial ratios and ε values are given at time, t (Ma). Rb and Sr concentrations determined by XRF.

APPENDIX VI

ANALYTICAL METHODS

adapted from Smedley, 1986b

VI.I. X-Ray Fluorescence Spectrometry (XRF)

Samples were analysed for 10 major and 17 trace elements using a Philips PW1450/20 automatic X-Ray fluorescence spectrometer. Major elements were analysed on glass discs prepared by fusion using a borate flux (Johnson Matthey Spectroflux 105^{R}). Rock powders were ignited prior to fusion and LOI values are reported in Appendix III. Trace elements were analysed on pressed powder pellets with matrix corrections calculated from sample major element compositions.

Details of rock crushing procedure, and preparation of fused glass discs and pressed powder pellets are given by Thirlwall (1979), Fitton *et al.* (1984) and Fitton and Dunlop (1985). Samples were analysed along with USGS and CRPG international standards and standard concentrations given by Abbey (1980) were used to calibrate each element. All sample counts were ratioed to monitor counts in order to correct for instrument drift. Six separate glass discs and pressed powders of basaltic sample SW161C (the sample closest in composition to the mean for the alkaline suite) were analysed and the mean and standard deviation (2σ) of the results, along with an estimate of accuracy (RMSD) are reported in Table V.I.

VI.II. Electron probe microanalysis

Mineral analyses were carried out using the Cambridge Instruments Microscan 5 electron probe at the Grant Institute of Geology. A focussed 1-2 µm beam was used with a sample penetration depth of 3µm. Standards were used for Si, Al, Mg, Fe, Ti, Mn, K, Na, Ca, Ni, Cr and Ba, and corrections were made for dead-time, atomic number, atomic absorption and fluorescence, after the method of Sweatman and Long (1969). Further procedural details are given by Thirlwall (1979) and details of detection limits and precision are outlined by Russell (1985).

	wt% oxide mean (n=6)	2σ	RMSD
SiO_2	46.93	0.20	0.26
Al_2O_3	13.90	0.08	0.18
Fe_2O_3	12.34	0.50	0.05
MgO	9.82	0.07	0.07
CaO	9.09	0.06	0.03
Na_2O	3.78	0.08	0.06
K_2O	1.19	0.01	0.03
TiO_2	2.04	0.02	0.01
MnO	0.19	0.004	0.005
P_2O_5	0.50	0.01	0.01
	ppm		
Ni	226	2.4	4.3
Cr	338	2.9	11.0
V	237	3.8	11.5
Sc	22	1.7	2.4
Cu	64	2.3	5.3
Zn	103	1.6	5.0
Sr	469	2.4	9.6
Rb	28	0.4	3.5
Zr	161	1.5	14.8
Nb	47	0.7	2.4
Ba	554	20.6	39.0
Pb	3	1.3	4.0
Th	3	1.4	2.8
La	23	29.5	5.6
Ce	65	9.9	13.5
Nd	27	2.4	3.6
Y	24	0.6	3.4

Table VI.I Typical accuracy (RMSD) and reproducibility (2σ) of data analysed by X-Ray fluorescence (sample SW161C). RMSD values are from Smedley (1986b) for major elements, and Fitton *et al*, (1984) for trace elements.

La	0.00	0.20	0.20	0.00	0.20	0.50	0.10
Ce	1.30	0.60	0.60	0.08	0.70	0.50	1.30
Pr	0.93	0.22	0.20	0.51	1.12	0.92	0.57
Nd	1.30	0.40	0.40	0.70	1.60	1.40	0.90
Sm				0.14		0.21	
Eu	0.03	0.01	0.01	0.01	0.02	0.02	0.01
Gd	0.85	0.24	0.24	0.49	1.05	0.84	0.53
Dy	0.08	0.05	0.02	0.02	0.17	0.17	0.04
Ho	0.04	0.00	0.01	0.01	0.11	0.12	0.02
Er	1.60	0.68	0.63	1.10	1.63	1.38	1.11
Yb	0.10	0.10	0.03	0.04	0.06	0.06	0.07
Lu	0.05	0.03	0.02	0.02	0.06	0.06	0.03

Table VI.II REE concentrations (ppm) of blanks analysed by ICP during the course of sample analysis.

VI.III. Inductively coupled plasma spectrometry (ICP)

Thirty nine samples were chosen for REE analysis using the Philips PV8210 1.5-m inductively coupled plasma spectrometer at Royal Holloway & Bedford New College,, University of London. The ICP method involves the chromatographic separation of REE from rock powders using cation exchange columns. The analyte solution is injected into a high temperature (6000-10000 K) flame such that spectral lines are excited by ionic as well as atomic species. Details of selected spectral lines and operating parameters used in the analysis are reported by Walsh *et al.* (1981).

VI.III.I. Dissolution procedure

Dissolution of rock powders was performed by weighing 0.5 g of sample into a platinum crucible, to which 15 mls of an $HClO_4$ - HF mix were added. The crucibles were then evaporated to dryness on a hot sandbath. When cool, 5 mls of concentrated HCl were added to each with enough distilled water to half fill the crucible. The samples were then left on a hotplate for a further five minutes until dissolved. The solution was filtered using number 42 filter paper, and rinsed well with distilled water, collecting the filtrate in a 100 ml beaker. Each filter paper was ignited in a silver crucible (starting the furnace from room temperature and taking it up to 250°C then to 400°C and finally to 800°C). The samples were removed from the furnace after 30 minutes at 800°C and 5 pellets of NaOH were added to each. They were returned to the furnace for a further 30 mins (at 800°C) adn then removed, swirling the mixture in each crucible until it solidified. When cool, approximately 5 mls of distilled water was added to each crucible to digest the cake, and approximately 5mls of concentrated HCl to dissolve it (stirring with a rubber policeman). Each solution was added to its respective filtered portion and made up to 100 mls with distilled water.

VI.III.II. REE separation

Chromatographic separation was performed using glass columns of 20 mm internal diameter and 250 mm length, with a glass sinter disc and PTFE burette tap at the base (Walsh *et al*, 1981). Columns were loaded to a settled height of 12 cm with Dowex^R AG50W-X8, 200-400 mesh cation exchange resin and washed with 200 mls of distilled H_2O prior to sample loading. Samples were loaded on the columns and once passed through the resin, were eluted

with 500 mls of 1.7M HCl. A further 600 mls of 4M HCl was then added and this portion was collected in pyrex beakers after being first filtered through a Whatman^{R} No. 42 filter paper to remove particles of resin. The separated aliquots were evaporated to dryness and stored. For ICP analysis, samples were redissolved in 5 cm^3 of 10% HNO_3.

VI.III.III. Standards and blanks

Ion exchange separations were carried out in batches of eight, each batch including a blank and one Royal Holloway and Bedford New College standard. Blanks went through the entire chemical separation procedure to ensure that sample memory on the columns was minimal and that all equipment was clean. Mean blank values for each element are given in Table VI.II. The blank concentrations were negligible.

Analytical precision of the ICP method, based on replicate analyses, has been calculated by Walsh *et al.* (1981) and is presented in Table VI.III.

Standards KC11, KC12 and KC13 were also taken through the dissolution and exchange procedure and are reported in Table VI.IV. Comparison with accepted standard values (Table VI.IV) is generally good.

Table VI.V shows the covariation of the elements La, Ce, Nd and Y between XRF analyses and those determined by ICP. Since Y tends to be readily lost from the analyte in the REE separation process, this element is a useful check on the reliability of the HREE analyses.

A synthetic standard containing all the REE and Y was analysed after every tenth sample to check for instrument drift. Although concentrations increased slightly throughout the run, the drift was considered negligible and has not been corrected for.

In addition, a set of interference standards: Nd (10 ppm), Ce (20 ppm), Zr (50 ppm), Sr (50 ppm), Ba (100 ppm), Ca (100 ppm) and Fe (100 ppm) were analysed between sample analyses in order to determine the interferences from these elements on the RE Pr, Er and Gd analyses have been corrected for interference effects from Ca and Fe, but since the blank, instrument drift and interference effects were negligible for the other REE, no corrections have been applied to them. The overall agreement between analysed and accepted standard values, and between XRF and ICP analyses for the elements La, Ce, Nd and Y indicates the reliability of the analysed data (Table VI.V).

	Mean (n=15)	2σ	RSD(%)
La	5.83	0.75	6.5
Ce	12.30	0.86	3.5
Pr	1.89	0.16	4.3
Nd	9.64	0.67	3.5
Sm	2.48	0.11	2.2
Eu	0.90	0.02	1.1
Gd	2.59	0.14	2.7
Dy	2.96	0.05	0.9
Er	1.75	0.08	2.3
Yb	1.79	0.04	1.8
Lu	0.28	0.01	1.8

Table VI.III. Precision estimates for REE data analysis by ICP, based on replicate analyses (from Walsh *et al*, 1981).

		Accepted	Measured	
KC11	La	23.0	24.9	24.0
	Ce	49.0	52.0	51.4
	Pr	5.9	6.7	7.6
	Nd	26.5	38.1	29.4
	Sm	5.2	5.2	5.2
	Eu	1.4	1.5	1.5
	Gd	5.0	5.5	6.4
	Dy	4.5	5.0	4.8
	Ho	1.0	0.9	1.0
	Er	2.7	3.6	4.5
	Yb	2.2	2.9	2.3
	Lu	0.3	0.4	0.4
KC12	La	37.0	36.7	38.8
	Ce	70.0	66.5	71.4
	Pr	7.2	7.6	7.9
	Nd	27.0	27.0	28.5
	Sm	3.3	3.4	3.6
	Eu	1.1	1.1	1.1
	Gd	2.1	2.7	2.7
	Dy	1.2	1.5	1.3
	Ho	0.3	0.3	0.3
	Er	0.8	1.5	1.2
	Yb	0.5	0.7	0.5
	Lu	0.3	0.1	0.1
KC14	La	59.0	55.1	56.7
	Ce	120.0	120.3	121.2
	Pr	13.0	13.7	15.0
	Nd	58.0	52.7	55.3
	Sm	14.0	12.5	12.8
	Eu	0.57	0.5	0.5
	Gd	15.0	14.3	15.6
	Dy	18.0	18.9	19.3
	Ho	4.0	4.0	4.2
	Er	11.8	13.4	14.8
	Yb	11.2	13.2	13.5
	Lu	1.5	1.8	1.9

Table VI.IV Accepted and measured values for standards KC11, KC12 and KC13 analysed by ICP.

	La	Ce	Nd	Y
SW3	0.854	1.024	1.045	1.099
SW8	1.032	1.108	0.965	1.224
SW9	1.021	1.129	1.009	1.026
SW25	0.979	1.177	0.938	1.018
SW36	0.997	1.082	0.948	1.093
SW47	0.939	1.024	0.932	0.973
SW48	0.986	1.112	0.996	1.088
SW70	0.958	0.931	0.989	1.106
SW76	0.974	1:082	0.913	1.057
SW89	0.697	0.819	0.805	0.989
SW93	1.006	0.992	0.776	1.107
SW112	0.880	1.042	0.908	1.013
SW138	0.662	0.848	0.893	0.856
SW160	1.053	1.115	0.943	1.062
SW189	0.838	0.992	0.789	1.090
SW207	0.808	0.884	0.801	1.069
SW267	0.990	0.943	0.776	1.060
SW298	0.507	0.958	1.066	1.124
SW303	0.464	0.712	0.948	0.980
SW304	0.957	0.693	0.844	1.019
SW309	0.924	1.061	0.849	1.075
SW414	0.524	0.958	0.982	1.131
SW438	0.876	1.119	0.967	1.075
SW442	0.772	1.011	0.857	1.077
SW463	0.912	1.101	0.834	1.070
SW472	0.895	0.996	0.873	0.969
SW478	0.967	1.044	0.961	1.073
SW484	0.756	1.015	1.031	1.055
SW519	0.907	1.028	0.933	1.024
SW525	0.583	0.921	0.787	1.069
SW535	0.911	1.049	0.927	1.022
SW536	0.966	0.991	0.998	1.080
SW545	1.343	1.144	1.060	1.080
SW566	1.131	1.040	0.789	1.151
GE4	0.943	0.980	0.836	1.043
PA01	1.149	0.972	1.003	1.108
PA13	1.113	1.080	0.923	1.084
RM5	1.286	0.751	3.273	0.986
RM64	1.476	0.879	0.746	1.032

Table IV.V Covariation of XRF and ICP data for all analysed samples for the elements La, Ce, Nd and Y (XRF/ICP ratio).

VI.IV. Sr and Nd isotopic analysis

Sr and Nd isotopic analyses were performed at the Scottish Universities Research and Reactor Centre at East Kilbride. Sr isotopic analysis was carried out using the VG MM30B mass spectrometer, and Nd isotopic analyses were performed using the VG Isomass 54E machine. All chemical separations were carried out in clean laboratories installed with HEDA filtered clean air overpressure units. All teflonware was thoroughly cleaned in HNO_3, HCl and distilled H_2O prior to use. Because comparison of Rb and Sr concentrations determined by isotope dilution and XRF has been shown to be good (Smedley, 1986b), all samples were analysed unspiked, and $^{87}Rb/^{86}Sr$ ratios have been calculated from XRF data. Similarly, $^{147}Sm/^{144}Nd$ ratios have been calculated from ICP data.

VI.IV.I. Dissolution procedure

Samples were accurately weighed (0.02 g to 0.1 g) into clean screw-top PFA teflon beakers. Samples were then dissolved in 10 mls of HF with 1 ml of HNO_3 added to prevent the precipitation of insoluble fluorides. Samples were then left on a hotplate for 48 hours at 150°c before being evaporated to dryness. Approximately 20 mls of dilute HNO_3 were then added to each beaker and samples were again left of a hotplate overnight to digest. After again being evaporated to dryness, samples were dissolved in 2 mls of 2.5M HCl and solutions were then centrifuged before being separated by ion exchange.

VI.IV.II. Ion exchange procedure

Sr and REE were separated chromatographically using standard cation exchange columns loaded with Bio Rad^R AG20-50W X8 200-400 mesh cation resin in hydrogen form. Columns were precleaned and backwashed using HCl and distilled H_2O and were pretreated with 2.5M HCl. The elution and collection of Sr and REE aliquots was carried out in 2.5M HCl. Sample solutions were then evaporated to dryness. Nd was separated from the REE using PTFE teflon filled columns, following the method of Fichard *et al.* (1976), Hart & Brooks (1977) and Zindler *et al.* (1978). Columns were pretreated and samples loaded using 0.31M HCl. Elution was carried out using).155M HCl, 0.31M HCl and 0.62M HCl. Nd aliquots were collected in 0.31M HCl.

VI.IV.III. Mass spectrometry

Sr was analysed using outgassed single Ta filament assemblies (Halliday *et al*, 1983, 1984). All isotopic data were subsequently corrected for machine discrimination using an $^{88}Sr^{86}Sr$ ratio of 8.37521 (Faure and Hurley, 1963; Nakamura *et al*, 1976). The average $^{87}Sr/^{86}Sr$ ratio for NBS987 during the course of the analysis was 0.71029 + 3 ($2\sigma_{mean}$, N=10).

Nd samples were all analysed as metal species (Halliday *et al*, 1983, 1984) using standard triple filament assemblages with Ta side filaments and Re centre filaments. Filaments were outgassed previosly at 3A for 15 minutes in a vacuum better than 10^{-5} torr.

APPENDIX VII

TABLE OF PUBLISHED K_D VALUES FOR OLIVINE, ORTHOPYROXENE, CLINOPYROXENE & GARNET

	Olivine	Orthopyroxene	Clinopyroxene	Garnet
Rb	0.00018[7] 0.0002–0.011[9] 0.001[3] 0.0044[4] 0.01[5]	0.0006[7] 0.001[3] 0.02[5,10] 0.03[10] 0.044[6]	0.001[3] 0.001–0.28[10] 0.001–0.041[12] 0.0011[7] 0.0018–0.0032[9] 0.05[5] 0.067[6]	0.0007[7] 0.001[3] 0.02[5] 0.033[6]
Ba	0.0001–0.011[9] 0.00011[7] 0.00021[6] 0.001[3] 0.005±0.003[12]	0.001[3,7] 0.11±0.005[12] 0.83[6] 0.12[10] 0.14[10]	0.00078–0.023[12] 0.001[3] 0.0011[7] 0.0016–0.0023[9] 0.002–0.39[10] 0.083[6] 0.3[12]	0.0015[7] 0.002[3] 0.0417[6]
K	0[5] 0.00018[7] 0.0002–0.008[9] 0.0004[2] 0.001[3] 0.00667[6]	0[5] 0.0005[2] 0.001[7,3] 0.01[10] 0.02[10] 0.1[6]	0[5] 0.0013[2] 0.0013–0.0028[9] 0.0014–0.0026[12] 0.002[7,3] 0.002–0.27[10] 0.1[6]	0[5] 0.001[3,7] 0.003[2] 0.025[6]
Nb	0.01[14]	0.15[13]	0.02[12] 0.1[14]	0.1[14]
Sr	0.0001–0.02[9] 0.00019[7] 0.0005[2] 0.003±0.002[12] 0.001[3] 0.002[5] 0.25[6]	0.0002[2] 0.007[7] 0.009[5] 0.013,10 0.18±0.003[12] 0.02[10] 0.417[6]	0.067[7] 0.07[3] 0.07–0.43[10] 0.072[2] 0.72–0.111[9] 0.2[5] 0.25[6]	0.001[3] 0.0011[7] 0.007[2] 0.0125[6] 0.014[5]
P_2O_5	0[5] 0.019[1] 0.43[1]	0[5] 0.014[1]	0[5] 0.009[1] 0.17[1]	0[5] 0.09–0.29[15]
Zr	0.01[14]	0.03[14]	0.1[14] 0.12[12]	0.3[14]
Ti	0.017[4] 0.02[14] 0.24±0.08[12] 0.07±0.005[12]	0.1[14] 0.11±0.01[12] 0.8[10]	0.3[14] 0.42±0.04[4]	0.3[14]

Y	0.002^{5} 0.01^{14}	0.009^{5} 0.2^{14}	0.20^{5} 0.05^{14}	1.4^{5} 2.0^{14}
La	$0.005^{2,5}$ $0.083-0.011^{6}$	$0.0005^{2,5}$ $0.0278-0.0370^{6}$	$0.02^{2,5}$ $0.069^{7,8}$ $0.08^{10,11}$ $0.167-0.222^{6}$	$0.001^{2,5}$ 0.003^{10} $0.0208-0.0278^{6}$ 0.03^{5} 0.05^{11} 0.08^{10}
Ce	0.00048^{13} $0.0005^{5,7,8}$ $0.0008^{2,5}$ $0.009^{10,11}$	$0.0009^{2,3}$ 0.0014^{5} 0.00145^{13} $0.003^{7,8}$ $0.003-0.004^{10}$ 0.02^{11}	$0.04^{2,3}$ $0.096^{5,13}$ $0.098^{7,8}$ 0.10^{3} $0.17-0.65^{10}$ 0.34^{11}	0.0029^{13} $0.0033^{2,5}$ 0.007^{5} 0.02^{3} $0.021^{7,8}$ $0.05^{10,11}$ 0.096^{5}
Nd	$0.0009^{13,15}$ $0.0010^{7,8}$ $0.0013^{2,5}$ 0.0055^{2} 0.007^{10} 0.009^{11} 0.010^{10}	$0.0019^{5,2}$ 0.0029^{5} 0.00294^{13} $0.0068^{7,8}$ 0.0083^{2} 0.03^{10} 0.005^{11} 0.06^{10}	0.09^{2} 0.182^{13} $0.21^{7,8}$ $0.32-1.3^{10}$ 0.38^{2} 0.6^{11}	$0.0184^{2,5}$ $0.019^{5,13}$ 0.033 $0.087^{7,8}$ 0.10^{2}
Sm	$0.0013^{7,8,13}$ 0.0019^{2} 0.002^{3} $0.003-0.015^{11}$ $0.009^{11,5}$ 0.0098^{2}	$0.0028^{5,2}$ $0.005^{5,13}$ $0.01^{7,8,3}$ $0.01-0.10^{10}$ 0.0147^{2} 0.05^{10}	$0.14^{2,5}$ $0.26^{3,5,6,7,8}$ $0.43-108^{10}$ 0.736^{2} 0.9^{11}	$0.07-1.25^{10}$ $0.08^{2,5}$ $0.107^{5,13}$ 0.161^{5} $0.22^{3,7,8}$ 0.32^{2} 0.6^{11}
Eu	$0.0016^{7,8}$ 0.0019^{5} 0.002^{3} 0.006^{10} 0.008^{11} 0.01^{10}	0.0036^{5} $0.013^{7,8,3}$ 0.02^{10} 0.05^{11} 0.08^{10}	0.16^{5} 0.20^{3} 0.30^{3} $0.31^{7,8,}$ $0.48-2.0^{10}$ 0.9^{11}	0.1333^{5} 0.284^{5} $0.3-1.5^{10}$ $0.32^{3,7,8}$ 0.35^{3} 0.9^{11}
Gd	$0.0015^{7,8}$ $0.012^{10,11}$	$0.16^{7,8}$	$0.30^{7,8}$ 0.82^{10} 0.88^{10} 0.90^{11}	$0.498^{7,8}$ 2.1^{10} 3.7^{11} 0.52^{10}
Tb	0.0016^{5} 0.0019^{5}	0.0059^{5} 0.0106^{5} $0.05^{10,11}$	0.19^{5} 0.31^{5} $1.0^{10,11}$	0.257^{5} 1.2^{10} 1.3^{11} 4.1^{10} 4.1^{10} 5.6^{5} 7.1^{5}

Dy	0.00016[13] 0.0017[7,8] 0.009[10] 0.012[11] 0.014[10]	0.011[13] 0.022[7,8] 0.012[10] 0.20[11] 0.29[10]	0.314[13] 0.33[7,8] 0.56[10] 1.1[11] 1.46[10]	1.06[7,8] 1.269[13]
Ho	0.0014[5] 0.0020[5]	0.0089[5] 0.0136[5]	0.195[5] 0.28[5]	1.0835 3.5[5] 2.57[5] 13.0[10] 19.0[11] 24.0[10]
Er	0.0014[13] 0.0015[7,8] 0.009[10] 0.013[10] 0.017[10]	0.0136[13] 0.030[7,8] 0.16[10] 0.31[11] 0.46[10]	0.278[13] 0.30[7,8] 0.53[10] 1.0[11] 1.3[10]	2.0[7,8] 2.57[13]
Yb	0.0011[5,13] 0.0015[7,8] 0.002[3] 0.0040[5] 0.0667–0.1[6]	0.019[5,13] 0.029[5] 0.049[7,8] 0.05[3] 0.11–1.67[10] 0.33–0.5[6] .034[11]	0.20[5] 0.23[3,5,13] 0.28[7,8] 0.48[10] 0.667–1.0[6] 1.0[11] 1.3[10]	4.0[3,5] 4.03[7,8,] 4.0–5.3[10] 4.2[5,13] 9084[5] 33.0–50.5[6]
Lu	0.0048[5]	0.038[5] 0.11[10,11]	0.19[5] 0.67[10] 0.8[11] 1.0[10]	7.0[5] 5–57[10] 13.0[5] 35.0[11]

Data sources: 1 Anderson & Greenland (1969); 2 Chen & Frey (1985); 3 Cox *et al.* (1979); 4 Dunn (1987); 5 Frey *et al.* (1978); 6 Gast (1968); 7 Hanson (1977); 8 Hanson (1980); 9 Hart & Brooks (1974); 10 Henderson (1982); 11 Henderson (1983); 12 Irving (1978); 13 Kay & Gast (1973); 14 Pearce & Norry (1979).

APPENDIX VIII

BIBLIOGRAPHY FOR MIDLAND VALLEY LOCALITIES

Allan J. K. & Knox J. 1934, *The economic geology of the Fife Coalfields, Area II.* Mem. geol. Surv.

Allport S. 1874, On the microscopic structure and composition of British Carboniferous dolerites. *Q. J. geol. Soc. Lond.* **30**, 529-567.

Anderson E.M. 1925, *The economic geology of the Ayrshire coalfields, Area II, Kilmarnock Basin.* Mem. geol. Surv..

Balsillie D. 1919, Geology of Kinkell Ness, Fifeshire. *Geol. Mag.* **6,19** 498-506.

Balsillie D. 1920, Descriptions of some new volcanic vents in east Fife. *Trans. Edin. geol. Soc*, **11**, 81-85.

Balsillie D. 1920, Descriptions of some volcanic vents near St. Andrews. *Trans. Edin. geol. Soc*, **11**, 69-80.

Balsillie D. 1922, Notes on the doleritic intrusions of east Fife. *Geol. Mag*, *59* 442-452.

Balsillie D. 1927, East Fife: Igneous geology. *In: The geology of the district around Edinburgh, Proc. Geol. Ass*, **38**, 463-469.

Balsillie D. 1936, Leucite-basanite in east Lothian. *Geol. Mag*, **73**, 16-19.

Bennett J.A.E. 1945, Some occurrences of leucite in east Lothian. *Trans. Edin. geol. Soc*, **14**, 34-52.

Boyle R. 1908, The occurence of ultra-basic rocks in the igneous intrusions of the Lugar and Cumnock district. *Trans. geol. Soc. Glasg.* **13**, 202-223.

Cadell H.M. 1923, The geology of the Blackness district, as disclosed by recent borings. *Trans. R. Soc. Edin.* **53**, 189-207.

Campbell R. & Stenhouse A.G. 1908, The geology of Inchcolm. *Trans. Edin. geol. Soc.* **9**, 121-134.

Craig R.M. 1912, Additions to the volcanic geology of east Fife. *Trans. Edin. geol. Soc.* **10**, 83-89.

Cumming G. A. 1928, The Lower Limestone and associated volcanic rocks of a section of the Fifeshire coast. *Trans. Edin. geol. Soc*, **12**, 124-140.

Cumming G.A. 1936, The structural and volcanic geology of the Elie - St. Monance district, Fife. *Trans. Edin. geol. Soc*, **13**, 340-365.

Day T.C. 1914, Notes on the Hummell Rocks, Gullane. *Trans. Edin. geol. Soc*, **10**, 114-119.

Day T.C. 1916, The Cheese Bay Sill, Gullane. *Trans. Edin. geol. Soc*, **10**, 249-260.

Day T.C. 1916, The breccias of Cheese Bay and the 'Yellow Conglomerates' of

Weak Law. *Trans. Edin. geol. Soc*, **10**, 261–275.

Day T.C. 1923, A new volcanic vent and other new geological features on the shore, Weak Law, near Gullane. *Trans. Edin. geol. Soc*, **11**, 185–192.

Day T.C. 1923, The Leithes, North Berwick, a small laccolite with unusual intrusive phenomena. *Trans. Edin. geol. Soc.* **11**, 300–307.

Day T.C. 1925, Two unrecorded volcanic vents on the shore east of North Berwick. *Trans. Edin. geol. Soc*, **11**, 338–345.

Day T.C. 1927, The North Berwick shore from the pier eastward to Tantallon Castle. *In: The geology of the district around Edinburgh, Proc. Geol. Ass* **38**, 446–451.

Day T.C. 1928, The volcanic vents on the shore between North Berwick and Tantallon Castle. *Trans. Edin. geol. Soc*, **12**, 41–52.

Day T.C. 1930, Chemical analyses of white trap from Dalmeny, Granton, Weak Law and North Berwick. *Trans. Edin. geol. Soc*, **12**, 189–194.

Day T.C 1930, Volcanic vents on the coast from Tantallon Castle eastwards to Peffer Sands, and at Witberry Point. *Trans. Edin. geol. Soc*, **12**, 213–223.

Day T.C. 1930, The intrusive rocks of Frances Craig, and the teschenite of Ravensheugh. *Trans. Edin. geol. Soc*, **12**, 260–261.

Day T.C. 1930, Chemical analyses of thirteen igneous rocks of east Lothian. *Trans. Edin. geol. Soc*, **12**, 263–266.

Day T.C. 1932, The teschenite of Point Garry, North Berwick. *Trans. Edin. geol. Soc*, **12**, 334–337.

Day T.C. 1932, Volcanic vents at Longskelly Rocks and at Yellow Craig Plantation, west of North Berwick. *Trans. Edin. geol. Soc*, **12**, 376–381.

Day T.C. & Bailey E.B. 1928, Bombs of nepheline- basanite in the Partan Craig vent, North Berwick. *Trans. Edin. geol. Soc*, **12**, 87–89.

Drever H.I. & Macdonald J.G. 1967, Some new data on 'Kylitic' sills and associated picrites in Ayrshire, Scotland. *Proc. R. Soc. Edin*, **B70**, 31–48.

Eyles V.A., Simpson J.B. & Macgregor M.C. 1929, The igneous geology of central Ayrshire. *Trans. geol. Soc. Glasg*, **18**, 361–387.

Eyles V.A., Simpson J.B. & Macgregor A.G. 1930, *The economic geology of the Ayrshire Coalfields, Area III.* Mem. geol. Surv., Scotland.

Falconer J. D. 1905, The igneous geology of the Bathgate and Linlithgow Hills. *Trans. R. Soc. Edin*, **41**,359–366.

Falconer J.D. 1906, The igneous geology of the Bathgate and Linlithgow Hills, part II, Petrography. *Trans. R. Soc. Edin.* **45**, 133–150.

Flett J.S. 1914, Geology of the district around Edinburgh. *Proc. Geol. Ass* **25**,

1-44.

Flett J. 1931, The Saline no. 1 teschenite. *Summ. prog. geol. Surv.*, **pt II**, 44-51.

Flett J.S. 1931, The Blackness teschenite. *Summ. prog. geol. Surv.* for 1930, **pt 3** 39-45.

Flett J.S. 1932, The Stankards sill. *Summ. prog. geol. Surv.* for 1931, 141-156.

Francis E.H. 1957, New evidence of volcanicity in west Fife. *Trans. Edin. geol. Soc.*, **17**, 71-80.

Francis E.H. 1959, A volcanic vent in the Bogside Mines, Fife. *Geol. Mag.* **96**, 457-469.

Francis E.H. 1960, Intrusive tuffs related to the Firth of Forth volcanoes. *Trans. Edin. geol. Soc.* **18**, 32-50.

Francis E.H. 1961, *The economic geology of the Fife coalfields, Area II Cowdenbeath and central Fife.* Mem. geol. Surv., Scotland, 2nd edition.

Francis E.H. 1962, Volcanic neck emplacement and subsidence structures at Dunbar, south east Scotland. *Trans. R. Soc. Edin.*, **65**, 41-58.

Geikie A. 1902, *Geology of east Fife.* Mem. geol. Surv., Scotland.

Geikie A., Geikie J., Jack R.L. & Etheridge R. 1872, *Explanation of sheet 22.* Mem. geol. Surv.

Geikie A., Geikie j. & Peach B.N. 1869, *Explanation of sheet 14*, Mem. geol. Surv., Scotland.

Gordon W.T. 1927, The coastal strip between North Berwick and Cheese Bay, Gullane. *In: The geology of the district around Edinburgh, Proc. Geol. Ass.* **38**, 441-446.

Haldane D. & Allan J.K. 1931, *The economic geology of the Fife coalfields, Area I, Dunfermline and west Fife.* Mem. geol. Surv..

Howell H.H., Geikie A. & Salter J.W. 1861, *The geology of the neighbourhood of Edinburgh.* Mem. geol. Surv. 1st edition.

Howell H.H., Geikie A. & Young J. 1866, *The geology of east Lothian.* Mem. geol. Surv., 1st edition.

Knox J. 1954, *The economic geology of the Fife coalfields, Area III, Markinch, Dysart and Leven.* Mem. geol. Surv..

Kirk S.R. 1925, The geology of the coast between Kinkell Ness and Kingask, Fifeshire. *Trans. Edin. geol. Soc.*, **11**, 366-382.

Macgregor A.G. 1937, The Carboniferous and Permian volcanoes of Scotland. *Bull. Volc.* **1**, 41-58.

Macnair P. 1907, The intrusive dolerites in the neighbourhood of Glasgow. *Trans. geol. Soc. Glasg.* **13**, 56-85.

Macnair P. 1908, Notes on a dolerite showing ocellar structure, from Craigie Hill, Ayrshire. *Trans. geol. Soc. Glasg*, **13**, 235–239.

McLean A.C. 1966, A gravity survey in Ayrshire and its geological interpretation. *Trans. R. Soc. Edin*, **66**, 239–265.

McLean A.C. & Iftikhar R.Q. 1966, Regional gravity anomalies in the western Midland Valley of Scotland. *Trans. R. Soc. Edin*, **66**, 267–283.

Martin N.R. 1955, Lower Carboniferous volcanism near North Berwick, Scotland. *Bull. geol. Surv. Scotland*, **7**, 90–100.

Monkton H.W. 1895, The Stirling dolerite. *Q. J. geol. Soc. Lond*, **51**, 480–492.

Pringle J. 1944, The Carboniferous rocks of Glas Eilean, Sound of Islay, Argyllshire. *Trans. geol. Soc. Glasg*, **20**, 249–260.

Richey J.E., Wilson G.V. & Anderson E.M. 1925, *The economic geology of the Ayrshire Coalfields, Area I, Kilbirnie, Dalry and Kilmaurs*. Mem. geol. Surv..

Scott A. 1915, The Crawfordjohn essexite and associated rocks. *Geol. Mag*, **6,2**, 455–461; 513–519.

Simpson J.B. 1928, Notes on the geology of the Kidlaw district, east Lothian. *Trans. Edin. geol. Soc*, **12**, 111–113.

Simpson J.B. & Macgregor A.G. 1932, *The economic geology of the Ayrshire coalfields, Area IV*. Mem. geol. Surv..

Tomkeieff S.I. 1948, Nepheline-basnite of Southdean, Roxburghshire. *Trans. Edin. geol. Soc*, **14**, 349–359.

Tyrrell G.W. 1912, The late Palaeozoic alkaline igneous rocks of the west of Scotland. *Geol. Mag*, **5,9**. 69–80; 120–131.

Tyrrell G.W. 1915, The Bekinkinite of Barshaw (Renfrewshire) and the associated rocks. *Geol. Mag*,**6,2**, 304–311; 361–366.

Tyrrell G.W. 1917, The picrite-teschenite sill of Lugar (Ayrshire). *Q. J. geol. Soc. Lond*,**72**, 84–129.

Tyrrell G.W. 1918, The igneous geology of the Ayrshire coast from Doonfoot to the Heads of Ayr. *T G G S*, **16**, 339–363.

Tyrrell G.W. 1923, Classification and age of the analcite-bearing igneous rocks of Scotland. *Geol. Mag*, **60**, 249–260.

Tyrrell G.W. 1924, Correspondence: The volcanic geology of east Fife. *Geol. Mag*, **61**, 142–143.

Tyrrell G.W. 1928, A further contribution to the petrography of the late-Palaeozoic igneous suite of the west of Scotland. *Trans. geol. Soc. Glasg*, **18**, 259–294.

Tyrrell G.W. 1948, A boring through the Lugar Sill. *T G S G* **21**, 157–202.

Tyrrell G.W. 1952, A second boring through the Lugar Sill. *Trans. Edin. geol. Soc.*, **15**, 374–392.

Walker F. 1923, The igneous geology of the Dalmeny district. *Trans. R. Soc. Edin.*, **53**, 361–375.

Walker F. 1926, The teschenite sill of Charlestown, Fife. *Geol. Mag.*, **63**, 343–347.

Walker F. 1935, The late Palaeozoic quartz-dolerites and tholeiites of Scotland. *Min. Mag.*, **24**, 131–159.

Walker F. 1936, The geology of the Isle of May. *Trans. Edin. geol. Soc.*, **13**, 275–285.

Walker F. & Irving J. 1928, The igneous intrusions between St. Andrews and Loch Leven. *Trans. R. Soc. Edin.*, **56**,1–17.

Wallace I.F. 1916, Notes on the petrology of the agglomerate and hypabyssal intrusions between Largo and St. Monans. *Trans. Edin. geol. Soc.*, **10**, 348–362.

Young B.R. 1905, An analcite diabase and other rocks from Gullane Hill. *Trans. Edin. geol. Soc.*, **8**, 326–335.

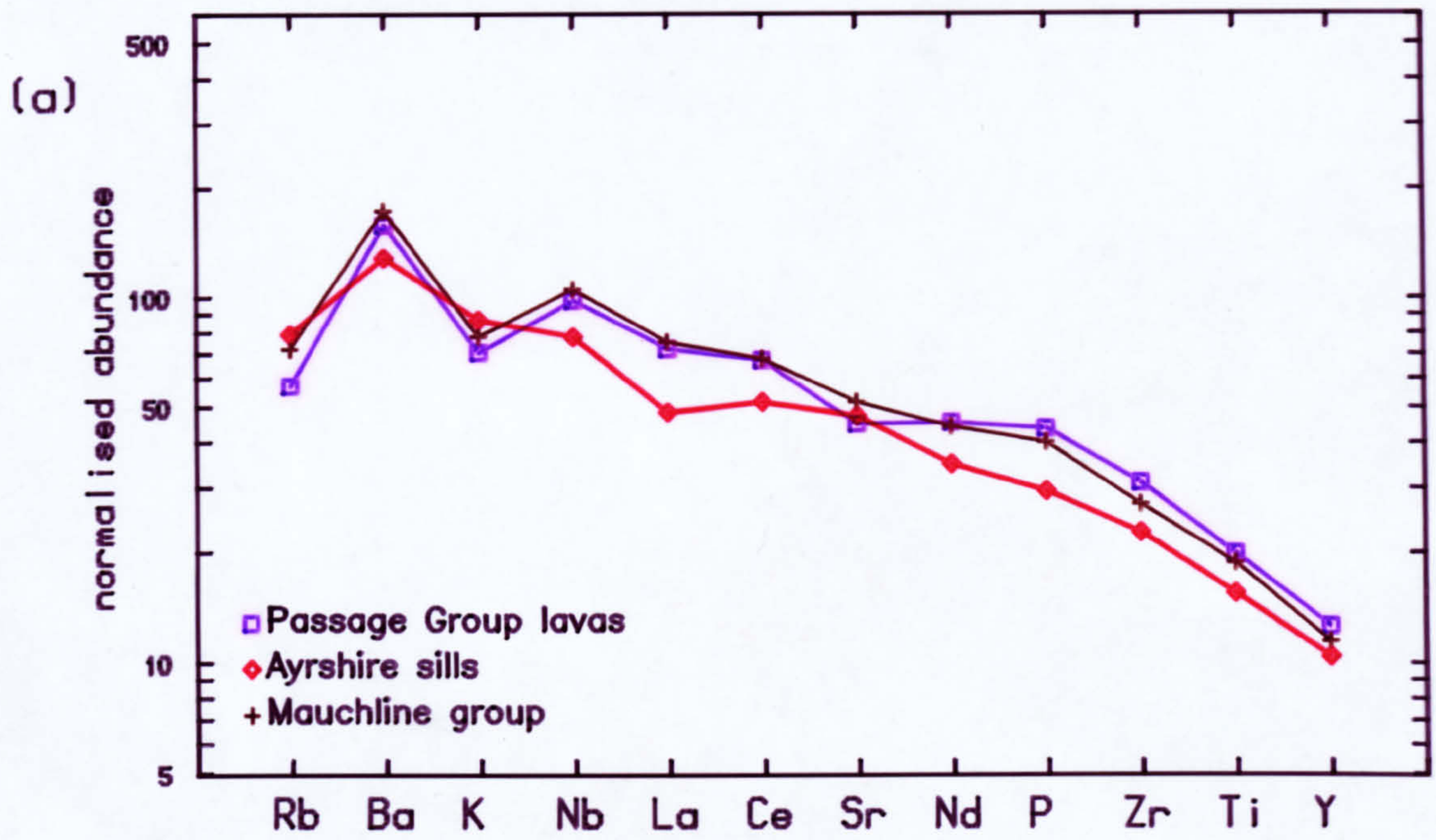

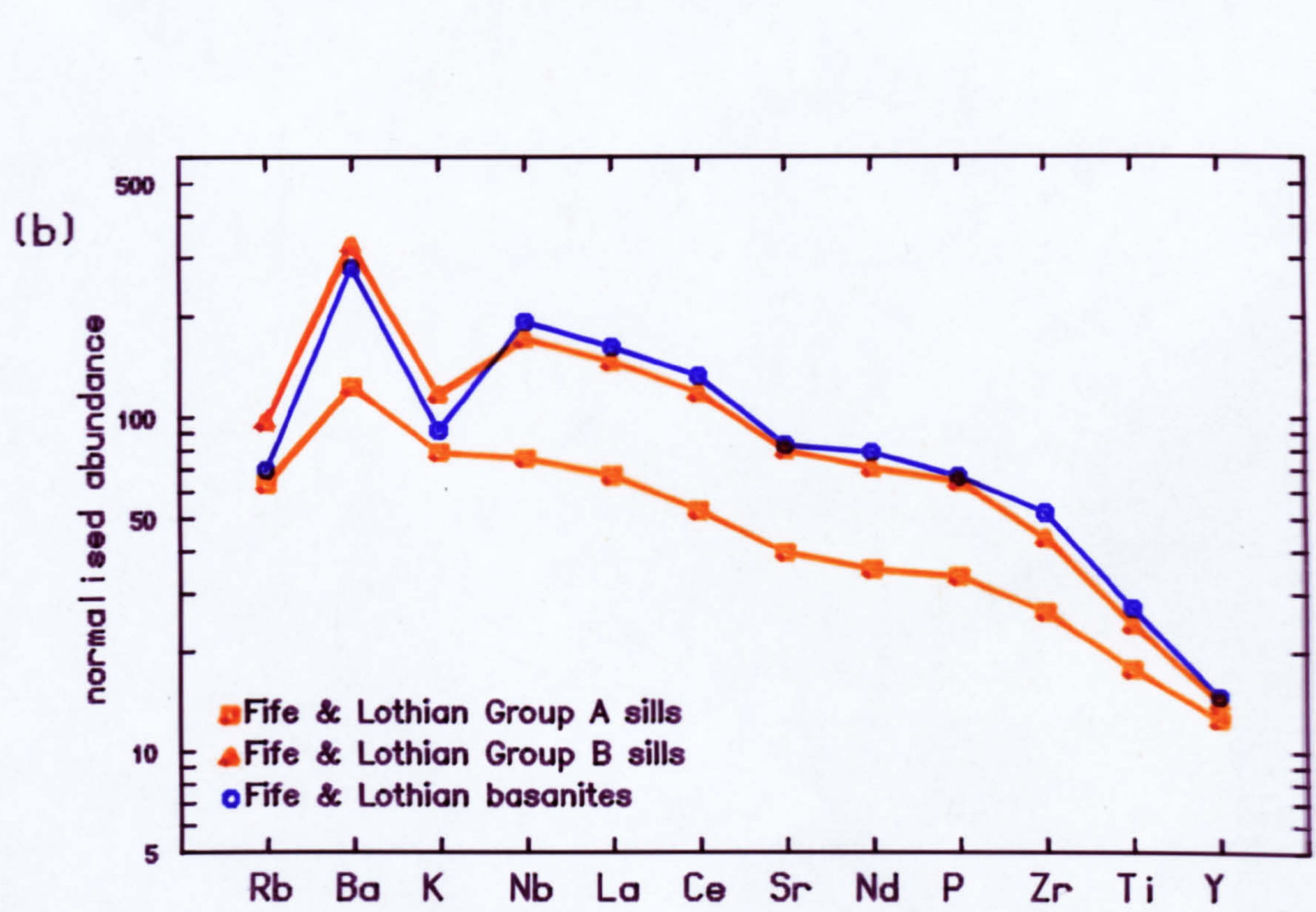

Fig 7.3 Mean chondrite–normalised spiderdiagram plots for basic samples from post–Dinantian Suite: (a) west Midland Valley, (b) east Midland Valley.

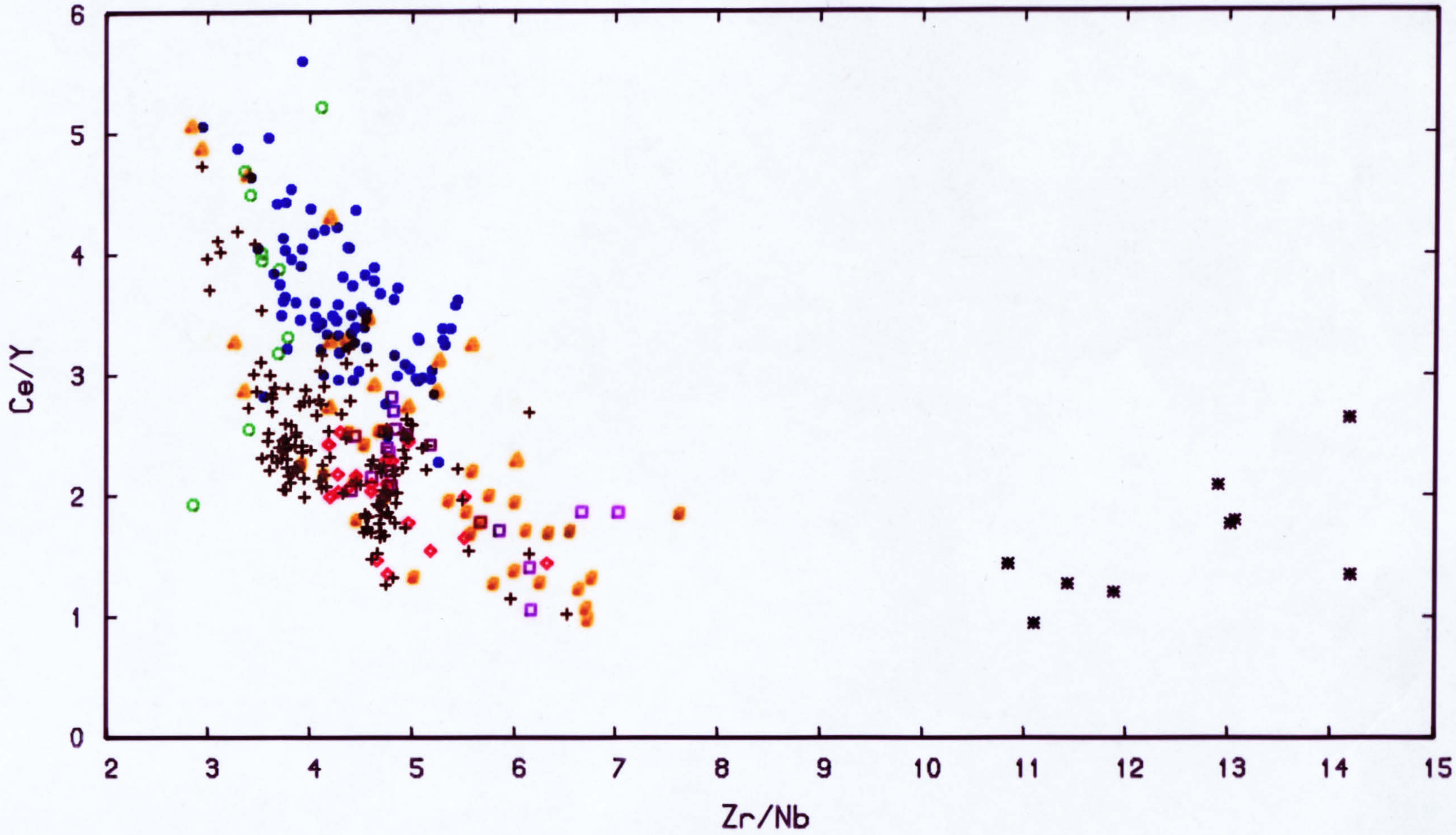

Fig 7.6 Ce/Y v Zr/Nb for basic samples from the post–Dinantian Midland Valley Suite.